frontiers | Research Topics

Key determinants of biodiversity, ecosystem functioning and restoration in climate change sensitive ecosystems

Edited by
Hui Zhang, Xiang Liu and Robert John

Published in
Frontiers in Ecology and Evolution
Frontiers in Environmental Science

ISSN 1664-8714
ISBN 978-2-8325-3997-2
DOI 10.3389/978-2-8325-3997-2

About Frontiers

Frontiers is more than just an open access publisher of scholarly articles: it is a pioneering approach to the world of academia, radically improving the way scholarly research is managed. The grand vision of Frontiers is a world where all people have an equal opportunity to seek, share and generate knowledge. Frontiers provides immediate and permanent online open access to all its publications, but this alone is not enough to realize our grand goals.

Frontiers journal series

The Frontiers journal series is a multi-tier and interdisciplinary set of open-access, online journals, promising a paradigm shift from the current review, selection and dissemination processes in academic publishing. All Frontiers journals are driven by researchers for researchers; therefore, they constitute a service to the scholarly community. At the same time, the *Frontiers journal series* operates on a revolutionary invention, the tiered publishing system, initially addressing specific communities of scholars, and gradually climbing up to broader public understanding, thus serving the interests of the lay society, too.

Dedication to quality

Each Frontiers article is a landmark of the highest quality, thanks to genuinely collaborative interactions between authors and review editors, who include some of the world's best academicians. Research must be certified by peers before entering a stream of knowledge that may eventually reach the public - and shape society; therefore, Frontiers only applies the most rigorous and unbiased reviews. Frontiers revolutionizes research publishing by freely delivering the most outstanding research, evaluated with no bias from both the academic and social point of view. By applying the most advanced information technologies, Frontiers is catapulting scholarly publishing into a new generation.

What are Frontiers Research Topics?

Frontiers Research Topics are very popular trademarks of the *Frontiers journals series*: they are collections of at least ten articles, all centered on a particular subject. With their unique mix of varied contributions from Original Research to Review Articles, Frontiers Research Topics unify the most influential researchers, the latest key findings and historical advances in a hot research area.

Find out more on how to host your own Frontiers Research Topic or contribute to one as an author by contacting the Frontiers editorial office: frontiersin.org/about/contact

Key determinants of biodiversity, ecosystem functioning and restoration in climate change sensitive ecosystems

Topic editors

Hui Zhang — Hainan University, China

Xiang Liu — Lanzhou University, China

Robert John — Indian Institute of Science Education and Research Kolkata, India

Citation

Zhang, H., Liu, X., John, R., eds. (2023). *Key determinants of biodiversity, ecosystem functioning and restoration in climate change sensitive ecosystems*. Lausanne: Frontiers Media SA. doi: 10.3389/978-2-8325-3997-2

Table of contents

frontiers | Frontiers in Ecology and Evolution

TYPE Editorial
PUBLISHED 09 November 2023
DOI 10.3389/fevo.2023.1297617

OPEN ACCESS

EDITED AND REVIEWED BY
Mark A. Elgar,
The University of Melbourne, Australia

*CORRESPONDENCE
Hui Zhang
993781@hainanu.edu.cn
Xiang Liu
lx@lzu.edu.cn
Robert John
robert.john@iiserkol.ac.in

RECEIVED 20 September 2023
ACCEPTED 30 October 2023
PUBLISHED 09 November 2023

CITATION
Zhang H, Liu X and John R (2023) Editorial: Key determinants of biodiversity, ecosystem functioning and restoration in climate change sensitive ecosystems. *Front. Ecol. Evol.* 11:1297617. doi: 10.3389/fevo.2023.1297617

Editorial: Key determinants of biodiversity, ecosystem functioning and restoration in climate change sensitive ecosystems

Hui Zhang [1]*, Xiang Liu [2]* and Robert John [3]*

[1]Key Laboratory of Genetics and Germplasm Innovation of Tropical Special Forest Trees and Ornamental Plants, Ministry of Education, College of Forestry, Hainan University, Haikou, China, [2]State Key Laboratory of Herbage Improvement and Grassland Agro-Ecosystems, College of Ecology, Lanzhou University, Lanzhou, China, [3]Department of Biological Sciences, Indian Institute of Science Education and Research, Kolkata, Mohanpur, West Bengal, India

KEYWORDS

functional traits, ecological restoration, community assembly, life-history strategies, plant diversity, animal diversity, microorganism diversity, ecosystem functioning

Editorial on the Research Topic
Key determinants of biodiversity, ecosystem functioning and restoration in climate change sensitive ecosystems

At the global scale, we are already past the planetary boundary of biodiversity loss (Montoya et al., 2018), and further declines are expected to occur (Tilman et al., 1994; Helm et al., 2006; Vellend et al., 2006). Therefore, ecosystems that contribute greatly to human well-being through the delivery of biodiversity and ecosystem benefits should be the focus of particular concern (Montoya et al., 2012; Seddon et al., 2016). To advance our understanding of biodiversity and ecosystem functioning in the changing world, we organized a Research Topic entitled "*Key Determinants of Biodiversity, Ecosystem Functioning and Restoration in Climate Change Sensitive Ecosystems*". This attracted 23 excellent articles, spanning multiple ecosystems including tropical/subtropical forests and alpine meadows, across several climate change sensitive areas and cover five themes (composition and function of tropical/subtropical forests, forest succession, complex trophic interactions, Biodiversity and ecosystems threats).

Six articles shed light on the composition and function of tropical/subtropical forests. Chai et al. test the influence of vertical structure on beta diversity, while Li et al. show how plant height and soil resources affect carbon gain and plant growth. Tian et al. find that the role of resources is again evident in the habitat preferences of vascular herbaceous plants. Su et al. report a comprehensive study using 1,773 species from 370 sites globally to show how a leaf hydraulic trait (leaf turgor loss point) can serve as a strong predictor of drought-induced tree mortality in a tropical forest. Wang et al. examine the question of sample size and show that the commonly recommended sample size is inadequate in many cases,

particularly when the habitat is heterogenous like the karst forests they studied. Gong et al. report that carbon storage increased with recent land use changes in a river basin in China.

Four articles provide new findings on forest succession. Liu et al. report divergent intraspecific variation and functional strategies in aboveground and belowground functional traits, and Xing et al. report increase in soil organic carbon during succession from plantation to secondary and old-growth forest and that total root biomass was the important factor in predicting soil organic carbon. Yang et al. find that different successional stages show divergent effects on soil arbuscular mycorrhizal fungal communities, and this fungal association with plant roots contributes directly or indirectly to ecosystem functions at different successional stages. Yang et al. also find that species richness and spatial heterogeneity are accompanied by enhanced soil organic carbon in a 60-ha plot of an old-growth tropical montane rainforest.

Five articles describe new results for complex trophic interactions. Hou et al. demonstrate abiotic effects by showing how soil properties primarily drive nematode community assembly by habitat filtering, while Yang and Chen highlight the importance of biotic interactions in reporting that decreasing phylogenetic diversity in tree species led to decreased generalist herbivore richness, abundance and herbivory, while increasing specialist herbivores. Demonstrating higher level trophic interactions Rao et al. report how nest predation in the red jungle fowl, a ground-dwelling bird involves a wide range of predators including rodents, reptiles and bird species. Wang et al. show that resource availability measured in terms of food plant diversity affects home range area and formation of Hainan gibbon with forage plant diversity impacting survival and fitness. Zou et al. detected that gibbon population growth shows a positive relationship with improved habitat quality, however, changes in individual numbers do not show a significant change with improving habitat quality.

Eight articles provide new understandings of biodiversity and ecosystems threats (biological invasion, global change (nitrogen and phosphorus addition) impacts, infectious diseases and energy needs). Das et al. and Jia et al. provide the following new results on biological invasion threats: 1) the evidence for negative spatial dependence between native and invasive plant species and 2) a replacement control method for managing alien species using biological control. Two studies (Du et al. and Qi et al.) point to the contrasting responses of different biological groups (plant, soil microbial and nematode community) to both nitrogen and phosphorus addition in alpine ecosystems. Two new findings on infectious disease threat are attained by Chen et al. and Chen et al. Namely: 1) host community composition determines the direction and strength of the diversity–disease relationship and 2) adding vector preference and interspecific competition into the system altered the direction of diversity–disease relationship, while host competence, interspecific competition, and vector preference interact to determine the spread of infectious diseases for vector-borne diseases. Bonacic et al. and Zhang et al. report three new energy needs threats: (i) the ecological effects of radioactive leaks on both terrestrial and marine ecosystems, (ii) the rapid increase in construction of solar photovoltaic power stations, which is likely to eat into forest and agricultural lands and (iii) how solar photovoltaic power stations decreased the local air temperature but increased air humidity.

In short, all the studies included in this Research Topic undoubtedly contribute to enhancing our understanding of the biodiversity and ecosystem functioning in climate change sensitive areas. In the future, with the advancement of technology, including sequencing, proteomics, metabolomics, and transcriptomics at the molecular level on one hand, and landscape- and regional-scale analyses using developments in drone-based and satellite-based sensing on the other, studies focused on biodiversity and ecosystem function will gain greater power and impact in managing the global biosphere.

Author contributions

HZ: Conceptualization, Formal Analysis, Funding acquisition, Investigation, Methodology, Software, Supervision, Writing – original draft, Writing – review & editing. XL: Conceptualization, Formal Analysis, Investigation, Methodology, Supervision, Validation, Writing – original draft, Writing – review & editing. RJ: Conceptualization, Formal Analysis, Investigation, Methodology, Supervision, Validation, Writing – original draft, Writing – review & editing.

Funding

The author(s) declare financial support was received for the research, authorship, and/or publication of this article. This work was funded by the Hainan Provincial Natural Science Foundation of China (422CXTD508), Research project of Hainan academician innovation platform (YSPTZX202017), and the Hainan Province Science and Technology Special Fund (ZDYF2022SHFZ320).

Conflict of interest

The authors declare that the research was conducted in the absence of any commercial or financial relationships that could be construed as a potential conflict of interest.

Publisher's note

References

Helm, A., Hanski, I., and Pärtel, M. (2006). Slow response of plant species richness to habitat loss and fragmentation. *Ecol. Lett.* 9, 72–77. doi: 10.1111/j.1461-0248.2005.00841.x

Montoya, D., Rogers, L., and Memmott, J. (2012). Emerging perspectives in the restoration of biodiversity-based ecosystem services. *Trends. Ecol. Evol.* 27, 666–672. doi: 10.1016/j.tree.2012.07.004

Montoya, J. M., Donohue, I., and Pimm, S. L. (2018). Planetary boundaries for biodiversity: implausible science, pernicious policies. *Trends. Ecol. Evol.* 33, 71–73. doi: 10.1016/j.tree.2017.10.004

Seddon, A. W. R., Macias-Fauria, M., Long, P. R., Benz, D., and Willis, K. J. (2016). Sensitivity of global terrestrial ecosystems to climate variability. *Nature* 531, 229–232. doi: 10.1038/nature16986

Tilman, D., May, R. M., Lehman, C. L., and Nowak, M. A. (1994). Habitat destruction and the extinction debt. *Nature* 371, 65–66. doi: 10.1038/371065a0

Vellend, M., Verheyen, K., Jacquemyn, H., Kolb, A., Calster, H. V., Peterken, G., et al. (2006). Extinction Debt of Forest Plants Persists for More than a Century following Habitat Fragmentation. *Ecology* 87, 542–548. doi: 10.1890/05-1182

frontiers | Frontiers in Ecology and Evolution

ORIGINAL RESEARCH
published: 14 July 2022
doi: 10.3389/fevo.2022.953637

Recent Recovery of the World's Rarest Primate Is Not Directly Linked to Increasing Habitat Quality

Yike Zou[1†], Samuel T. Turvey[2†], Jie Cui[3], Hui Zhang[1*] and Wenfeng Gong[1*]*

[1] Key Laboratory of Genetics and Germplasm Innovation of Tropical Special Forest Trees and Ornamental Plants, School of Forestry, Hainan University, Haikou, China, [2] Institute of Zoology, Zoological Society of London, London, United Kingdom, [3] Development Research Center of People's Government of Sanya City, Sanya, China

Due to habitat loss and hunting, the Hainan gibbon (*Nomascus hainanus*), the world's rarest primate, was reduced to only two social groups and seven known individuals in 1978. Following the establishment of Bawangling National Natural Reserve (BNNR), gibbon forest habitat increased within this landscape from 56 km^2 in 1980 to 300 km^2, and the species had increased to five groups and 35 individuals by 2021. It is important to assess whether the large increase in habitat area was responsible for gibbon population increase, or whether gibbon recovery was associated with other factors. Here we use a 21-year longitudinal dataset of Hainan gibbon population change and habitat change, combined with vegetation survey plot data for 2021, to establish an accurate distribution baseline for natural tropical broadleaf forest across the BNNR landscape from 400 to 1300 m (the elevational range of gibbons at BNNR) and within the home range for each of the five Hainan gibbon social groups. We then utilized Landsat time-series images and analysis to compute non-linear causal relationships between forest dynamics and gibbon population growth from 2000 to 2021, both across BNNR and within each gibbon group home range. Metrics of forest dynamics include change in total forest area and forest fragmentation, and metrics of gibbon population dynamics include variation in total number of individuals for the entire population and within each social group, and variation in total number of groups. Our results demonstrate that overall gibbon population growth shows a positive relationship with improved habitat quality, with a one-year time lag of population response. However, changes in numbers of individuals within social groups do not show a similar relationship with improving habitat quality, suggesting that increasing forest cover and connectivity within the BNNR landscape are not direct determinants of Hainan gibbon recovery and that other environmental and/or anthropogenic factors are likely to be involved.

Keywords: habitat quality, Hainan gibbon, population dynamics, primate conservation, remote sensing, species recovery

OPEN ACCESS

Edited by:
Xiang Liu,
Lanzhou University, China

Reviewed by:
Mengjiao Huang,
Fudan University, China
Yao Xiao,
Lanzhou University, China

****Correspondence:***
Jie Cui
443464199@qq.com
Wenfeng Gong
gwf101@163.com
Hui Zhang
zhanghuitianxia@126.com

† These authors have contributed equally to this work

Specialty section:
This article was submitted to Conservation and Restoration Ecology, a section of the journal Frontiers in Ecology and Evolution

Received: *26 May 2022*
Accepted: *13 June 2022*
Published: *14 July 2022*

Citation:
Zou Y, Turvey ST, Cui J, Zhang H and Gong W (2022) Recent Recovery of the World's Rarest Primate Is Not Directly Linked to Increasing Habitat Quality. Front. Ecol. Evol. 10:953637. doi: 10.3389/fevo.2022.953637

INTRODUCTION

Effective conservation of tiny threatened populations requires a robust understanding of the factors that regulate population growth and recovery (Carwardine et al., 2012; Crees et al., 2016). However, collection of large datasets for such populations can be challenging, necessitating long-term data to identify possible relationships between population dynamics and available environmental baselines.

One such species in urgent need of evidence-based conservation is the Critically Endangered Hainan gibbon (*Nomascus hainanus*), the world's rarest primate. It is restricted to a single population of 35 individuals within a single protected area, Bawangling National Natural Reserve (BNNR; 109°14′47.35″E, 19°5′45.17″N) in Hainan, China (Fellowes et al., 2008; Turvey et al., 2015a; Deng et al., 2017; Chan et al., 2020a; **Figure 1A**). Various factors have been proposed to limit growth of the Hainan gibbon population at BNNR, including human disturbance, habitat and/or resource limitation, low population density, low genetic diversity, and/or limited availability or suitability of mates (Turvey et al., 2015a). Long-term recovery of the Hainan gibbon is likely to require intensive, carefully planned conservation management, but these different proposed processes require different mitigations, making effective identification of the primary factors limiting gibbon population growth a conservation research priority.

Hainan gibbon population decline during the twentieth century was driven by hunting and habitat loss, resulting from clearance of natural forests and monoculture plantations (Liu et al., 1984; Zhou et al., 2005). BNNR was established in 1980 in a mountainous landscape (elevation 200–1,800 m) that still retained tropical evergreen rainforest, with trees reaching a maximum of 30 m in height (Zhou et al., 2005; Zhang et al., 2020). The reserve was originally 56 km^2, but was later expanded to almost 300 km^2 in total area (Turvey et al., 2015a). Establishment of the reserve aimed to prevent hunting of gibbons and natural forest clearance, and to support recovery of the last remaining Hainan gibbon population. The gibbon population at BNNR consisted of only two social groups (A and B) and seven known individuals at the time of the first survey in 1978. The population has been monitored regularly since 2000 by the reserve's management office, and has increased to five social groups and 31 known individuals in 2021: Group C formed in 2010, Group D in 2015, and Group E in 2019 (Liu et al., 1984; Fellowes et al., 2008; Bryant et al., 2016; Deng et al., 2017; Chan et al., 2020a). This multi-decadal increasing trend suggests that population recovery can be attributed directly to effective protection of gibbons and gibbon habitat within BNNR. Continued increase in natural tropical broadleaf forest habitat (increasing total forest area and decreasing fragmentation) is a primary management policy for the recently established Hainan Tropical Rainforest National Park, which has designated the Hainan gibbon as its flagship species (Chinese National Park Administration, 2019). However, the effectiveness of this policy in recovering the Hainan gibbon population has not yet been evaluated using empirical data.

Remote Sensing (RS) and Geographic Information Systems (GIS) are key tools for detecting and evaluating long-term changes in habitat cover and quality for threatened species management (Jeganathan et al., 2004; McShea et al., 2005; Wang et al., 2008; Zhang et al., 2010). Hainan gibbons are strictly dependent upon natural tropical broadleaf forest habitat (primary or secondary forest, not plantation) from 400 to 1,300 m in BNNR (Bryant et al., 2017; Fan, 2017), so it is necessary to establish a baseline of the changing distribution and quality of this habitat type over time across the BNNR landscape and within the home range of each of the five Hainan gibbon groups. It is also important to recognize that species may not respond instantaneously to environmental change, especially if they have slow life histories, and thus time lags might be expected in population responses to changing habitat conditions. Hainan gibbons require 1 year to birth one infant (Liu et al., 1984; Zhou et al., 2008; Deng et al., 2017), and thus a time lag of this magnitude might be expected in gibbon population response to improving habitat conditions. As such, time-series analyses that can find the most likely time lags in causality between variables (e.g., PCMCI algorithm; Runge et al., 2019) are a suitable methodological choice to investigate whether long-time variation in habitat change is a key determinant in Hainan gibbon population dynamics.

In this study, we first determine the distribution of natural forest habitat (primary and secondary forest) across the BNNR landscape from 400 to 1,300 m and within the home range of all five Hainan gibbon groups. We then use Landsat time-series images to determine natural forest dynamics from 2000 to 2021 across BNNR (400–1,300 m) and within each gibbon home range, and use PCMCI to quantify the relationship between natural forest dynamics and gibbon population dynamics across this 21-year period. In addition, we investigate the relationship between species richness (number of species) of known gibbon food plants and elevation, to provide further insights into environmental factors associated with gibbon dispersal and population growth. Our study provides the first assessment of whether forest dynamics have constituted a key determinant of Hainan gibbon population dynamics during the past two decades, thus identifying how landscape management at BNNR can support gibbon conservation in the future.

MATERIALS AND METHODS

Field-Based Gibbon Home Range and Habitat Data

Hainan gibbon social groups have home ranges with little or no spatial overlap (Bryant et al., 2017; Deng et al., 2017), and have remained in approximately the same locations within the BNNR landscape since 1990 (BNNR Management Office, personal communication, 2021). For the purposes of comparative analysis, we investigated spatial home range locations for each group utilizing unpublished gibbon distribution data provided by the BNNR Management Office (**Figure 1B**).

We investigated the most accurate boundary for natural (primary and secondary forest) and non-natural forest (plantation) across the BNNR landscape from 400 to 1,300 m, by collecting vegetation and land-use data using 395 20 m × 20 m plots distributed across this elevational range over the BNNR landscape in 2021 (**Figure 1B**). The area of this vegetation survey represents 31.6% of the total landscape area of BNNR, and includes some areas outside the existing protected area boundary. We also randomly placed another 20 20 m × 20 m plots inside the home range of each of the five Hainan gibbon social groups in 2021, with plots spaced ≥ 50 m apart, to investigate species richness of gibbon food plants. Species

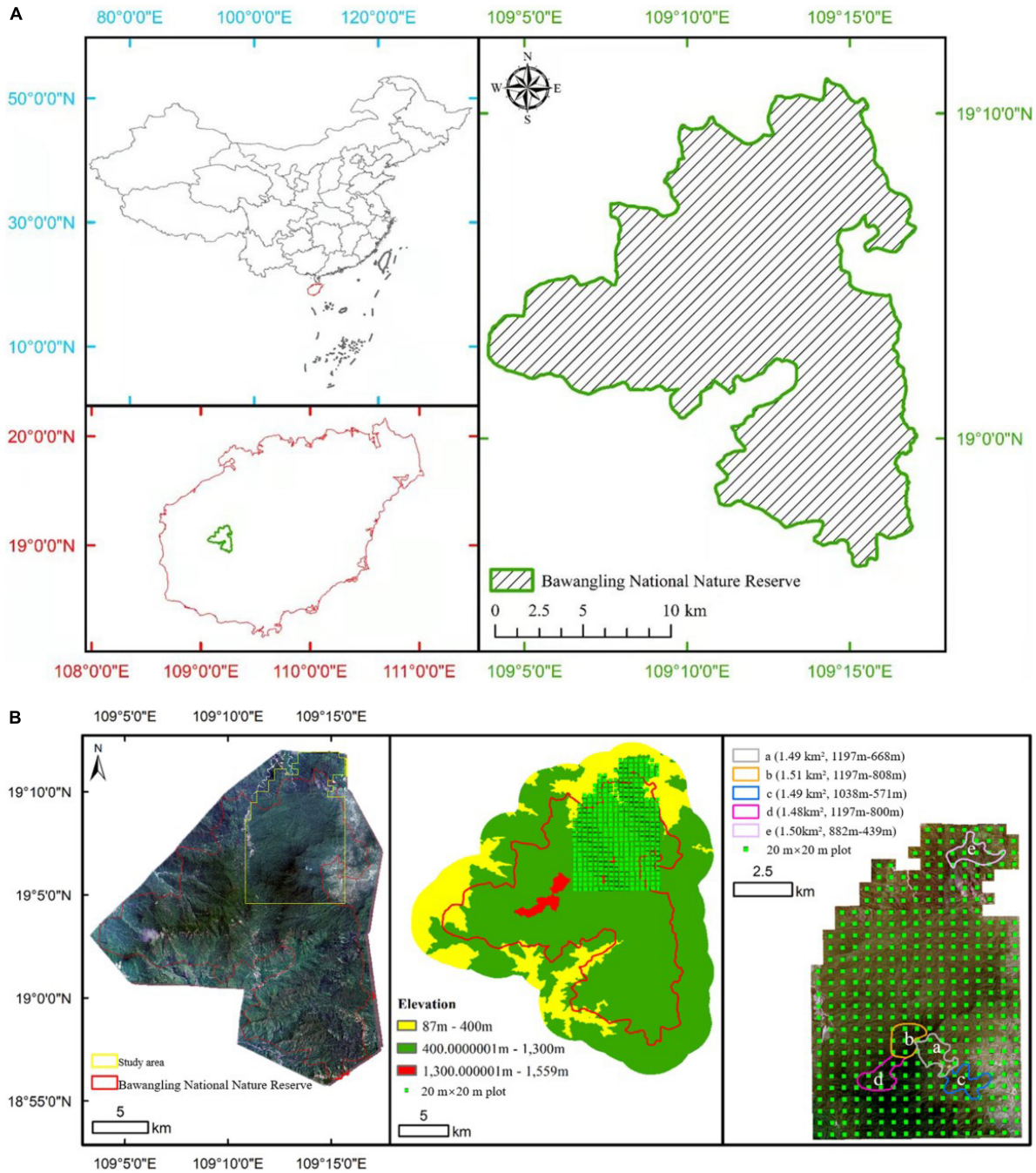

FIGURE 1 | (A) Topographic map of Bawangling National Natural Reserve, Hainan, China; **(B)** location and elevation of our study area, distribution of 395 20 m × 20 m plots, and home ranges and elevations of Hainan gibbon social groups.

were identified as potential gibbon food plants based upon previous published data and unpublished monitoring data (**Supplementary Table 1**).

Remote Sensing Forest Cover Data

The global distribution of all Hainan gibbon social groups in BNNR is contained within Landsat world reference system tile 124/47 (row/column number). We selected annual Landsat images (30 m resolution) for this region for the period 2000–2021 from USGS,[1] selecting images closest to the peak of forest cover (defined as June–September each year) with little to no cloud cover. We performed radiometric calibration and atmospheric correction for each image (Young et al., 2017).

[1]https://earthexplorer.usgs.gov/

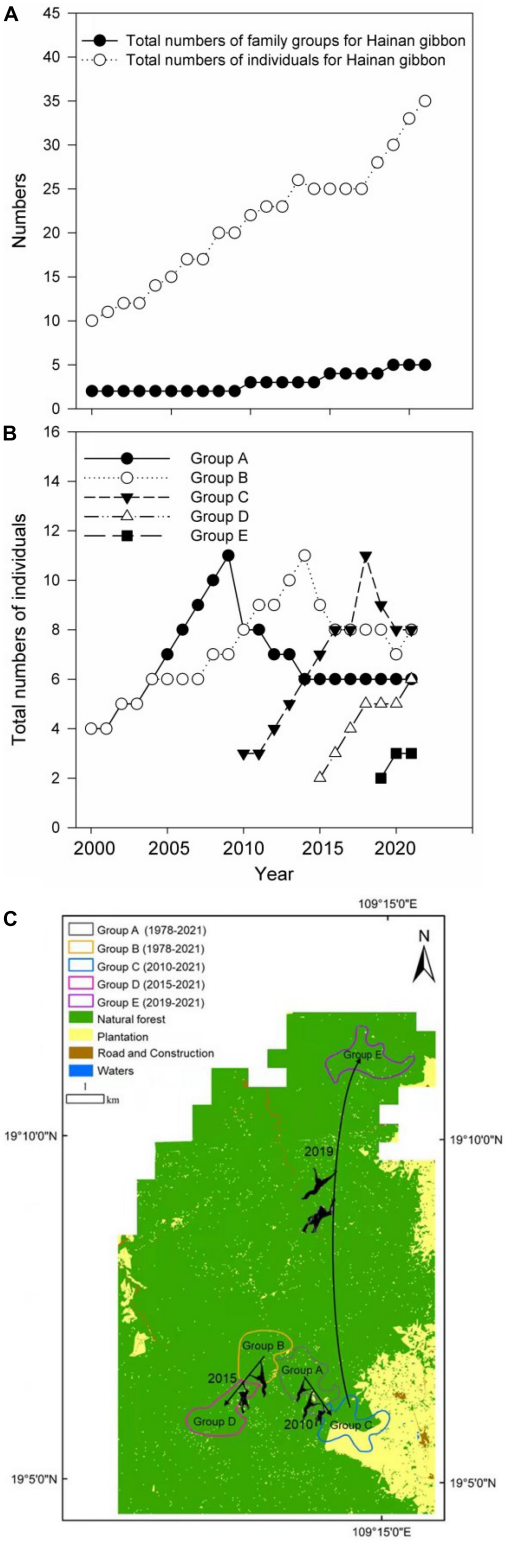

FIGURE 2 | Population change from 2000 to 2021 in: **(A)** total number of Hainan gibbon individuals and social groups, **(B)** individuals in each social group, **(C)** history of formation for groups C, D, and E and boundaries of natural forest and plantation in Bawangling National Natural Reserve from 400 to 1,300 m.

We used specified accurate boundaries for natural and non-natural forest across the BNNR landscape from 400 to 1,300 m, and used the support vector machine method of supervised classification to classify these two land cover types in each image (Phiri and Morgenroth, 2017). Classification requirements were met if separation test values of ROIs (Regions of Interest, selected based on field survey data and representing both land cover types) in each image were greater than 1.9. We manually corrected areas of obvious misclassification based upon field observations. We calculated a confusion matrix by combining classification results and the results of our vegetation survey, with overall classification accuracy for each year greater than 99%. The total area of natural forest across BNNR was then calculated by using the image classification results (number of pixels of each land cover type multiplied by the area of one pixel).

We used FRAGSTATS, a widely used software package for quantifying landscape structure (Ricketts, 2001; Cakir et al., 2007; McGarigal et al., 2012; Lamine et al., 2018), to calculate forest fragmentation across the entirety of BNNR and within the home range of each gibbon group. Fragmentation was calculated according to the formula $F = N/A$, where F is level of forest fragmentation, N is number of forest patches, and A is total forest area within an image.

Time-Series Analysis

We used the PCMCI algorithm (Runge et al., 2019) implemented in Python[2] to compute non-linear causal relationships between changes in forest dynamics (change in total forest area and/or forest fragmentation) across the entirety of BNNR and within the home range of each of the five gibbon groups and Hainan gibbon population dynamics (variation in total number of individuals for the entire gibbon population and within each social group, and variation in total number of social groups) from 2000 to 2021. PCMCI is a two-stage algorithm that includes a PC algorithm and a momentary conditional independence test (MCI; Sun and Bollt, 2014); it can find the most likely time lag of causality between variables, by first running a conditional selection *via* the PC process to find links between variables based on different conditional independence tests, and then applying the MCI process to remove false positive controls and generate a test statistic to measure the strength of the causal relationship between variables. Model selection (data not shown) supported the use of a τ_{max} (maximum time lag) value of 2, thus including three possible time lags (0, 1, and 2 years). The PCMCI method cannot be used for datasets where $n < 7$ (Runge et al., 2019). We therefore only analyzed time-series data using the PCMCI method for groups A, B, C, and D, which have existed for seven or more years across our time-series.

Environmental and Anthropogenic Determinants of Gibbon Distribution

To explore the possible effect of both elevation and human land use activities on gibbon social group distribution and formation, we used a 1.5 m-resolution RS image of the entirety of BNNR from 23 April 2019 obtained from the SPOT-7

[2]https://github.com/jakobrunge/tigramite

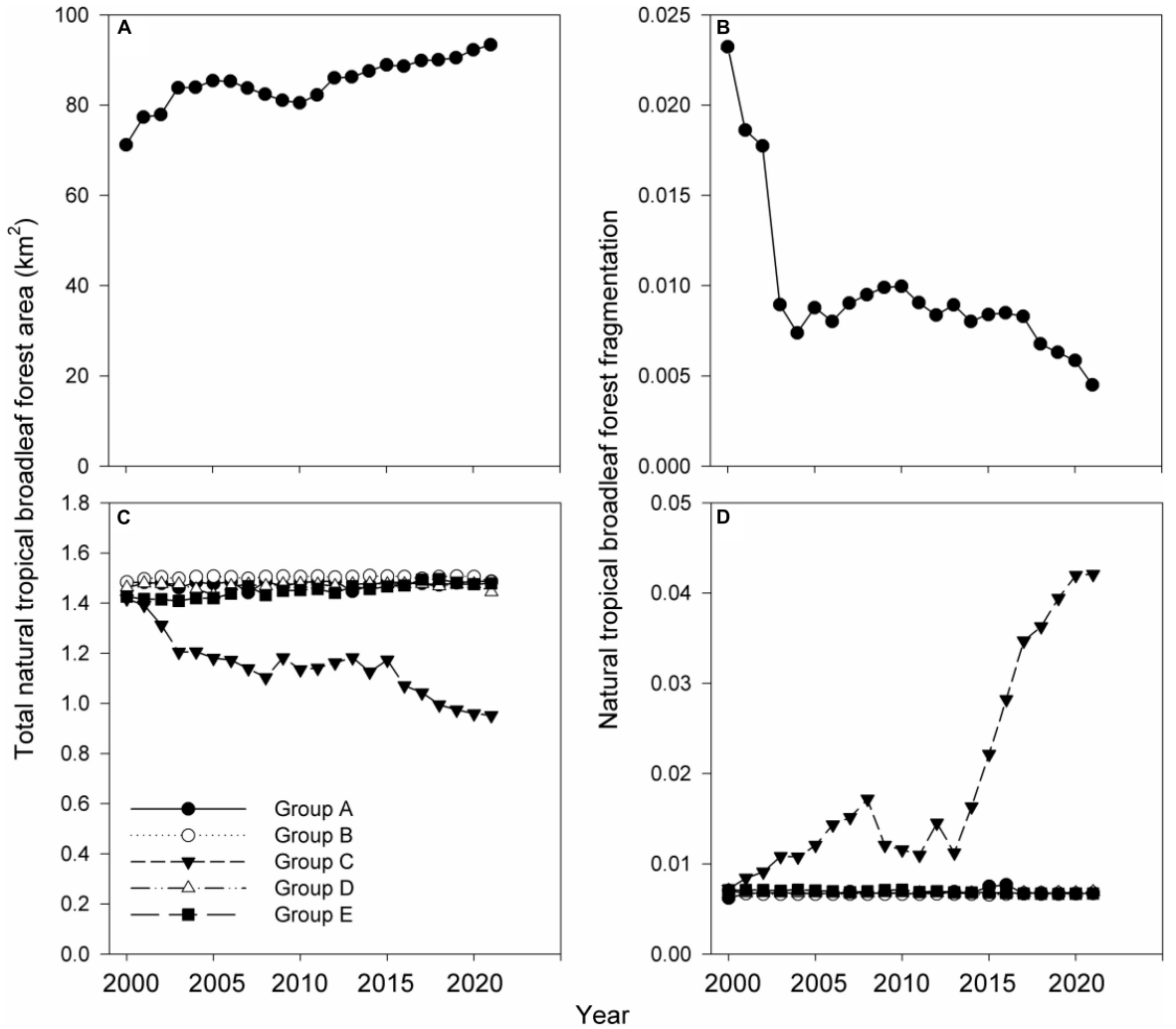

FIGURE 3 | Change from 2000 to 2021 in **(A,B)** total natural forest area and fragmentation across Bawangling National Natural Reserve, **(C,D)** natural forest area and fragmentation within Hainan gibbon social group ranges.

satellite sensor. Following pre-processing, we used the maximum likelihood method of supervised classification to analyze land cover in the image (Phiri and Morgenroth, 2017). Using artificial interpretation of the image and field survey data, we divided land cover into four categories: natural forest, plantation, roads and construction, and water. We extracted the highest and lowest elevations occupied by each gibbon group using digital elevation model (DEM) data.

We investigated the relationship between elevation and gibbon food plant species richness for each gibbon social group using a generalized linear model (GLM), with a Poisson error structure because food plant richness is a discrete random variable (count data).

RESULTS

Between 2000 and 2021, the total number of Hainan gibbon social groups and individuals increased from two groups and 10 individuals in 2000, to five groups and 35 individuals in 2021 (**Figures 2A,B**). Overall, Hainan gibbon habitat (natural tropical broadleaf forest) quality also improved across BNNR during this period, with total area increasing from 71.19 to 93.38 km^2, and fragmentation decreasing from 0.02 to 0.004 (**Figures 3A,B**). Within the range of Group C, total natural forest area decreased from 1.42 to 0.95 km^2, and fragmentation increased from 0.0072 to 0.042. Conversely, natural forest area and fragmentation remained largely unchanged and consistently high within the ranges of other groups (**Figures 3C,D**).

PCMCI results show that variation in total number of gibbon individuals from 2000 to 2021 was determined by both natural forest area and fragmentation when the time lag was 1 year, with a positive correlation between number of individuals and natural forest area, but a negative relationship between number of individuals and forest fragmentation ($p < 0.05$; **Figure 4A**). Variation in both natural forest area and fragmentation could also determine variation in number of individuals within group C when the time lag was 1 year, with a negative

correlation with natural forest area ($p < 0.05$; **Figure 4E**), and a positive correlation with fragmentation ($p < 0.05$; **Figure 4E**). However, natural forest area and fragmentation were not statistically correlated with variation in number of gibbon groups ($p > 0.05$; **Figure 4B**). Similarly neither natural forest area nor fragmentation determined variation in number of individuals within groups A, B, and D ($p > 0.05$; **Figures 4C,D,F**).

Overall, 59–115 different known gibbon food plant species were recorded across different gibbon social group ranges. There was a significant negative relationship between mean elevation and food plant species richness across the five gibbon groups ($p < 0.05$; **Figure 5**), with Group B occupying the highest elevation (mean = 1002.5 m, range = 808–1197 m) and having the lowest food plant species richness, and Group E occupying the lowest elevation (mean = 660.5 m, range = 439–832 m) and having the highest food plant species richness (**Figure 5**).

DISCUSSION

Identifying the factors that have regulated past population dynamics and influenced the rate of recovery are key research goals to inform evidence-based conservation of the world's rarest ape (Turvey et al., 2015a; Qian et al., 2022). Here, we demonstrate that Hainan gibbon habitat quality (as measured by natural forest total area and fragmentation) has improved across the overall BNNR landscape during the past two decades. However, forest dynamics have shown differing patterns within the home ranges of different gibbon groups, with important implications for the likely influence of forest change in promoting gibbon population recovery.

Establishing an accurate understanding of the distribution and long-term change in suitable habitat for threatened species is crucial for evidence-based conservation management, and requires the use of tools such as Landsat time-series images (Oeser et al., 2020). Here we first provide an accurate assessment of the distribution of Hainan gibbon habitat (natural tropical broadleaf forest) within BNNR and within the home range of each gibbon group (**Figure 2C**). This baseline not only provides a key tool to understand gibbon population responses and environmental requirements, but can also be used in future studies to investigate ongoing change in Hainan gibbon habitat and population dynamics.

Our PCMCI results demonstrate that increased natural forest area and decreased forest fragmentation are highly correlated with an increase in total number of Hainan gibbon individuals with a 1-year time-lag (**Figure 4**). This temporal pattern is consistent with Hainan gibbon reproductive biology (Liu et al., 1984; Zhou et al., 2008; Deng et al., 2017), and a time-lag of this scale would thus be expected instead of an instant population response to improving habitat conditions. We recommend that PCMCI should be employed more widely in the future to investigate relationships between long-term dynamics of animal populations and potential determining variables, instead of commonly used linear or non-linear regressions (cf. Mougeot et al., 2003; Koenig and Liebhold, 2016; Hansen et al., 2019).

Conversely, our PCMCI analyses do not demonstrate any positive correlations over time between increased habitat quality (indicated by increased forest total area and decreased fragmentation) and increase in total number of individuals within most gibbon groups (A, B, or D) (**Figure 4**). One potential reason for this lack of signal is that natural forest area has been consistently high and fragmentation has been consistently low within the areas occupied by these groups across the time-series in our study. However, in contrast to the positive relationship between increased habitat quality and increased population growth at BNNR at the total gibbon population level, our PCMCI results also demonstrate an unexpected relationship between growth of Group C and deterioration of local habitat quality within the estimated area of this group's home range. From its formation in 2010, Group C increased to a maximum of 11 individuals, whilst local natural forest area decreased by 1.47 times and local forest fragmentation increased by 5.75 times over the same period. This group is situated close to the reserve boundary adjacent to a village, and the local habitat in this region has been progressively impacted by human disturbance (e.g., encroachment and clearance of forest for conversion to agroforestry and agriculture; Turvey et al., 2015a). We do not suggest that decreasing habitat quality has been a local driver of gibbon population growth; instead, we suggest that this statistical pattern represents an incidental correlation rather than direct causation, with Group C exhibiting resilience to local habitat deterioration with no apparent adverse effect on social group growth. Population recovery of other *Nomascus* gibbon species has also been documented within other degraded forest landscapes (Fan et al., 2013).

These findings indicate that, whereas increased natural forest cover and connectivity is correlated with overall Hainan gibbon population increase over time across BNNR, gibbon social group dynamics are clearly not regulated by changes in these habitat quality metrics. Indeed, it is likely that observed growth of the Hainan gibbon population from 2000 onward is also associated with recovery from recent historical hunting (Fellowes et al., 2008; Deng et al., 2017) rather than solely with improving habitat quality. However, hunting restrictions and forest protection have both been simultaneously enforced by conservation management at BNNR, and their respective contributions to local gibbon recovery are thus difficult to distinguish across the same time-series.

While specific Hainan gibbon habitat requirements are still poorly understood, habitat selection by other *Nomascus* species is determined by local food availability (spatial distribution of food patches and seasonal variation in fruiting; Fan and Jiang, 2008b, 2010; Fan et al., 2009; Ni et al., 2018) as well as local distribution of other key resources such as sleeping sites (Fan and Jiang, 2008a; Fei et al., 2012). We demonstrate a significant negative relationship between elevation and food plant species richness at BNNR (**Figure 5**). These further findings are thus also important for ongoing landscape management and planning for gibbon conservation, and may also help to explain the high growth rate shown by Group C, which occurs at relatively low elevation at the edge of the reserve, despite the progressive decrease in overall forest quality within its home

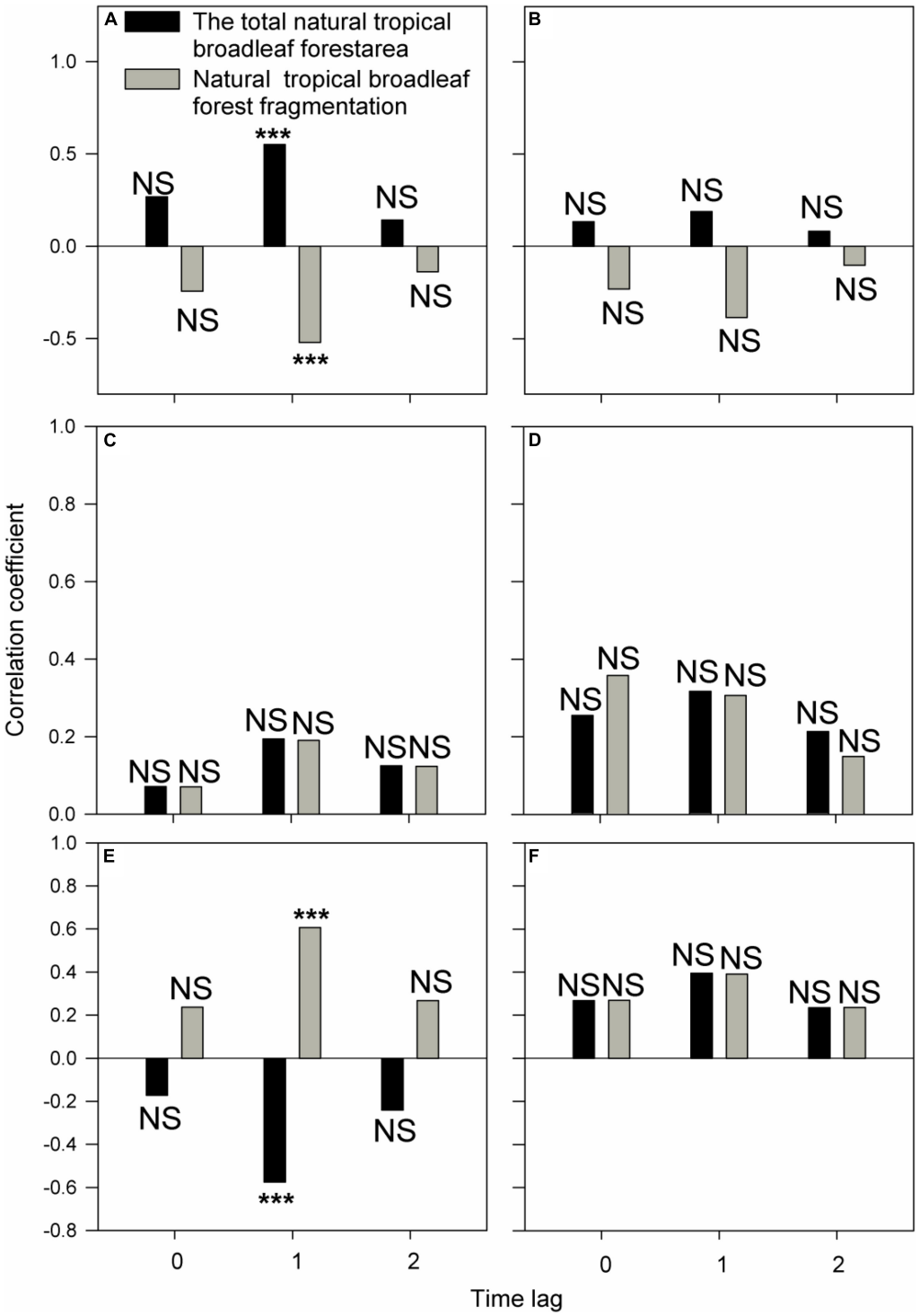

FIGURE 4 | Relationships from 2000 to 2021 between natural forest area and fragmentation, and: **(A)** number of Hainan gibbon social groups, **(B)** total number of Hainan gibbon individuals, and number of individuals in **(C)** Group A, **(D)** Group B, **(E)** Group C, and **(F)** Group D. *** Indicates $p < 0.05$, NS (non-significant) indicates $p > 0.05$, based on PCMCI analysis. Time lag (T) varies between 0 and 2 years.

range. Similarly, although Groups A and B both contained only four individuals in 2000, Group A increased to 11 individuals within 10 years, whereas group B, which occurs at a higher elevation within BNNR, required 15 years to increase to the same group size. These results thus provide further evidence that gibbon social group dynamics at BNNR are regulated

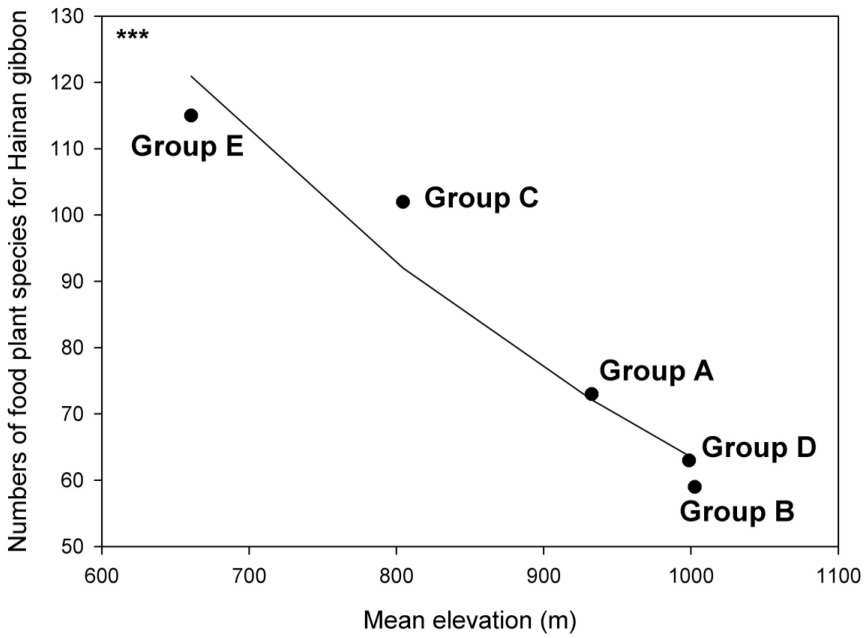

FIGURE 5 | Relationship between Hainan gibbon food plant species richness and mean elevation (m) across five existing Hainan gibbon social groups. *** Indicates $p < 0.05$ based on generalized linear model with Poisson error. Fitted line generated from a generalized linear model with Poisson error structure.

by extrinsic or intrinsic factors other than overall changes in natural forest quality. Two of the three most recently formed gibbon groups (groups C and E) occur at lower elevations than the other groups. However, their expansion to lower-elevation habitats might merely reflect historical survival of gibbons on Hainan and elsewhere across southwestern China in more remote high-elevation refugia, rather than being associated with natural habitat characteristics of lower-elevation sites (Turvey et al., 2015b). We therefore encourage additional research to better understand specific habitat parameters important in home range site selection during new social group formation by dispersing gibbon individuals (Turvey et al., 2015a).

Hainan gibbon population recovery thus exhibits a complex relationship with increased habitat cover and connectivity at BNNR, with a positive correlation at the overall population level but no positive correlation at the social group level. In order to develop maximally effective conservation management strategies to support further Hainan gibbon population growth, we encourage further investigation into more specific metrics of natural tropical broadleaf forest quality and structure at BNNR, and their relationship to gibbon distribution and population dynamics. However, gibbons are obligate canopy-dwellers that are unlikely to cross even small canopy gaps (Chivers et al., 2013). Thus, existing patterns of forest degradation and fragmentation across the BNNR landscape are recognized to constitute a major barrier to Hainan gibbon population growth and dispersal (Zhang et al., 2010; Turvey et al., 2015a). It is therefore essential to continue efforts to restore and connect natural tropical broadleaf forest habitats across BNNR and beyond, in order to facilitate further gibbon population growth and expansion. Improving natural forest cover and quality with both short-term (e.g., canopy bridges; Chan et al., 2020b) and longer-term solutions (replanting activities, establishment of ecological corridors to other reserves) will be essential to support a resilient and increasing gibbon population on Hainan into the future. Further assessment of specific Hainan gibbon habitat requirements is a vital next step for evidence-based conservation of this Critically Endangered species, and we recommend targeted ecological research combined with continuing forest protection and reconnection (e.g., strategic reconnection of isolated major forest patches to facilitate gibbon population expansion) to constitute key components of management plans for the newly established Hainan Tropical Rainforest National Park (Liu et al., 2020).

CONCLUSION

Overall, two important new insights about the influence of habitat quality on Hainan gibbon population dynamics have been revealed by our study. First, due to the species' reproductive behavior (requiring 1 year to birth one infant), the Hainan gibbon population exhibits a one-year time lag instead of an instantaneous response to improving habitat quality. Second, improving habitat quality following the establishment of BNNR is not the sole direct determinant of the observed recovery of the Hainan gibbon population within this landscape, a finding that has hugely important implications for ongoing landscape management and conservation decision-making for this species. Our study has wider implications for conservation science, by providing guidelines to identify factors that determine population

recovery of the world's rarest primate and other Critically Endangered species.

DATA AVAILABILITY STATEMENT

The raw data supporting the conclusions of this article will be made available by the authors, without undue reservation.

AUTHOR CONTRIBUTIONS

JC, HZ, and WG designed the research. YZ, ST, JC, HZ, and WG performed the research and wrote the manuscript. YZ, JC, HZ, and WG analyzed the data. All authors contributed to the article and approved the submitted version.

FUNDING

This research was supported by the specific research fund of the Innovation Platform for Academicians of Hainan Province, a Hainan Academician Innovation Platform Scientific Research Project (YSPTZX202017), the Scientific Research Project of Ecological Restoration of Baopoling (Sanya), a Hainan Province Postgraduate Innovative Research Project (Qhys2021-114), the Arcus Foundation, and Research England.

SUPPLEMENTARY MATERIAL

The Supplementary Material for this article can be found online at: https://www.frontiersin.org/articles/10.3389/fevo.2022.953637/full#supplementary-material

REFERENCES

Bryant, J. V., Brulé, A., Wong, M. H., Hong, X., Zhou, Z., Han, W., et al. (2016). Detection of a new Hainan gibbon (*Nomascus hainanus*) group using acoustic call playback. *Int. J. Primatol.* 37, 534–547. doi: 10.1007/s10764-016-9919-8

Bryant, J. V., Zeng, X., Hong, X., Chatterjee, H. J., and Turvey, S. T. (2017). Spatiotemporal requirements of the Hainan gibbon: does home range constrain recovery of the world's rarest ape? *Am. J. Primatol.* 79:e22617. doi: 10.1002/ajp.22617

Cakir, G., Sivrikaya, F., and Keleş, S. (2007). Forest cover change and fragmentation using Landsat data in Maçka state forest enterprise in Turkey. *Environ. Monit. Assess.* 137, 51–66. doi: 10.1007/s10661-007-9728-9

Carwardine, J., O'Connor, T., Legge, S., Mackey, B., Possingham, H. P., and Martin, T. G. (2012). Prioritizing threat management for biodiversity conservation. *Conserv. Lett.* 5, 196–204. doi: 10.1111/j.1755-263X.2012.00228.x

Chan, B. P. L., Lo, Y. F. P., and Mo, Y. (2020a). New hope for the Hainan gibbon: formation of a new group outside its known range. *Oryx* 54, 296–296. doi: 10.1017/S0030605320000083

Chan, B. P. L., Lo, Y. F. P., Hong, X. J., Mak, C. F., and Ma, Z. (2020b). First use of artificial canopy bridge by the world's most critically endangered primate the Hainan gibbon *Nomascus hainanus*. *Sci. Rep.* 10:15176. doi: 10.1038/s41598-020-72641-z

Chinese National Park Administration (2019). *Using Ecological Corridors to Connect Fragmented Hainan Gibbon Habitats*. Available online at: http://www.forestry.gov.cn/main/5497/20200819/170932364708588.html (Accessed June 23, 2022).

Chivers, D. J., Anandam, M. V., Groves, C. P., Molur, S., Rawson, B. M., Richardson, M. C., et al. (2013). "Family Hylobatidae (gibbons)," in *Handbook of the Mammals of the World*, Vol. 3, eds R. A. Mittermeier, A. B. Rylands, and D. E. Wilson (Barcelona: Lynx Edicions), 754–791.

Crees, J. J., Collins, A. C., Stephenson, P. J., Meredith, H. M., Young, R. P., Howe, C., et al. (2016). A comparative approach to assess drivers of success in mammalian conservation recovery programs. *Conserv. Biol.* 30, 694–705. doi: 10.1111/cobi.12652

Deng, H., Zhang, M., and Zhou, J. (2017). Recovery of the critically endangered Hainan gibbon *Nomascus hainanus*. *Oryx* 51, 161–165. doi: 10.1017/S0030605315000678

Fan, P. (2017). The past, present, and future of gibbons in China. *Biol. Conserv.* 210, 29–39. doi: 10.1159/000342696

Fan, P., and Jiang, X. (2008b). Effects of food and topography on ranging behavior of black crested gibbon (*Nomascus concolor jingdongensis*) in Wuliang Mountain, Yunnan, China. *Am. J. Primatol.* 70, 871–878. doi: 10.1002/ajp.20577

Fan, P., and Jiang, X. (2008a). Sleeping sites, sleeping trees, and sleep-related behaviors of black crested gibbons (*Nomascus concolor jingdongensis*) at Mt. Wuliang, Central Yunnan, China. *Am. J. Primatol.* 70, 153–160. doi: 10.1002/ajp.20470

Fan, P., and Jiang, X. (2010). Altitudinal ranging of black-crested gibbons at Mt. Wuliang, Yunnan: effects of food distribution, temperature and human disturbance. *Folia Primatol.* 81, 1–9. doi: 10.1159/000279465

Fan, P., Jiang, X., and Tian, C. (2009). The critically endangered black crested gibbon *Nomascus concolor* on Wuliang Mountain, Yunnan, China: the role of forest types in the species' conservation. *Oryx* 43, 203–208. doi: 10.1017/S0030605308001907

Fan, P., Ren, G., Wang, W., Scott, M. B., Ma, C., Fei, H., et al. (2013). Habitat evaluation and population viability analysis of the last population of cao vit gibbon (*Nomascus nasutus*): implications for conservation. *Biol. Conserv.* 161, 39–47. doi: 10.1016/j.biocon.2013.02.014

Fei, H., Scott, M. B., Zhang, W., Ma, C., Xiang, Z., and Fan, P. (2012). Sleeping tree selection of cao vit gibbon (*Nomascus nasutus*) living in degraded karst forest in Bangliang, Jingxi, China. *Am. J. Primatol.* 74, 998–1005. doi: 10.1002/ajp.22049

Fellowes, J. R., Chan, B. P. L., Zhou, J., Chen, S., Yang, S., and Ng, S. C. (2008). Current status of the Hainan gibbon (*Nomascus hainanus*): progress of population monitoring and other priority actions. *Asian Primates J.* 1, 2–11.

Hansen, B. B., Gamelon, M., Albon, S. D., Lee, A. M., Stien, A., Irvine, R. J., et al. (2019). More frequent extreme climate events stabilize reindeer population dynamics. *Nat. Commun.* 10:1616. doi: 10.1038/s41467-019-09332-5

Jeganathan, P., Green, R. E., Norris, K., Vogiatzakis, I. N., Bartsch, A., Wotton, S. R., et al. (2004). Modelling habitat selection and distribution of the critically endangered Jerdon's courser *Rhinoptilus bitorquatus* in scrub jungle: an application of a new tracking method. *J. Appl. Ecol.* 41, 224–237. doi: 10.1111/j.0021-8901.2004.00897.x

Koenig, W. D., and Liebhold, A. M. (2016). Temporally increasing spatial synchrony of North American temperature and bird populations. *Nat. Clim. Change* 6, 614–617. doi: 10.1038/nclimate2933

Lamine, S., Petropoulos, G. P., Singh, S. K., Szabó, S., Bachari, N. E. I., Srivastava, P. K., et al. (2018). Quantifying land use/land cover spatio-temporal landscape pattern dynamics from Hyperion using SVMs classifier and FRAGSTATS®. *Geocarto Int.* 33, 862–878. doi: 10.1080/10106049.2017.1307460

Liu, H., Ma, H., Cheyne, S. M., and Turvey, S. T. (2020). Recovery hopes for the world's rarest primate. *Science* 368:1074. doi: 10.1126/science.abc1402

Liu, Z., Yu, S., and Yuan, X. (1984). Resource of the Hainan black crested gibbon and its present situation. *Wild Animals* 6, 1–4.

McGarigal, K., Cushman, S. A., and Ene, E. (2012). *FRAGSTATS v4: Spatial Pattern Analysis Program for Categorical and Continuous Maps. Computer Software Program Produced by the authors at the University of Massachusetts, Amherst*. Amherst, MA: University of Massachusetts.

McShea, W. J., Koy, K., Clements, T., Johnson, A., Vongkhamheng, C., and Aung, M. (2005). Finding a needle in the haystack: regional analysis of suitable Eld's deer (*Cervus eldi*) forest in Southeast Asia. *Biol. Conserv.* 125, 101–111. doi: 10.1016/j.biocon.2005.03.013

Mougeot, F., Redpath, S. M., Leckie, F., and Hudson, P. J. (2003). The effect of aggressiveness on the population dynamics of a territorial bird. *Nature* 421, 737–739. doi: 10.1038/nature01395

Ni, Q., Liang, Z., Xie, M., Xu, H., Yao, Y., Zhang, M., et al. (2018). Microhabitat use of the western black-crested gibbon inhabiting an isolated forest fragment in southern Yunnan, China: implications for conservation of an endangered species. *Primates* 59, 45–54. doi: 10.1007/s10329-017-0634-7

Oeser, J., Heurich, M., Senf, C., Pflugmacher, D., Belotti, E., and Kuemmerle, T. (2020). Habitat metrics based on multi-temporal Landsat imagery for mapping large mammal habitat. *Remote Sens. Ecol. Conserv.* 6, 52–69. doi: 10.1002/rse2.122

Phiri, D., and Morgenroth, J. (2017). Developments in Landsat land cover classification methods: a review. *Remote Sens.* 9:967. doi: 10.3390/rs9090967

Qian, J., Mills, M., Ma, H., and Turvey, S. T. (2022). Assessing the effectiveness of public awareness-raising initiatives for the Hainan gibbon *Nomascus hainanus*. *Oryx* 56, 249–259. doi: 10.1017/S0030605320000599

Ricketts, T. H. (2001). The matrix matters: effective isolation in fragmented landscapes. *Am. Nat.* 158, 87–99. doi: 10.1086/320863

Runge, J., Nowack, P., Kretschmer, M., Flaxman, S., and Sejdinovic, D. (2019). Detecting and quantifying causal associations in large nonlinear time series datasets. *Sci. Adv.* 5:eaau4996. doi: 10.1126/sciadv.aau4996

Sun, J., and Bollt, E. M. (2014). Causation entropy identifies indirect influences, dominance of neighbors and anticipatory couplings. *Physica D* 267, 49–57. doi: 10.1016/j.physd.2013.07.001

Turvey, S. T., Traylor-Holzer, K., Wong, M. H. G., Bryant, J. V., Zeng, X., Hong, X., et al. (2015a). *International Conservation Planning Workshop for the Hainan Gibbon: Final Report*. London: Zoological Society of London.

Turvey, S. T., Crees, J. J., and Di Fonzo, M. M. (2015b). Historical data as a baseline for conservation: reconstructing long-term faunal extinction dynamics in late imperial–modern China. *Proc. R. Soc. B* 282:20151299. doi: 10.1098/rspb.2015.1299

Wang, W., Ren, G., He, Y., and Zhu, J. (2008). Habitat degradation and conservation status assessment of gallinaceous birds in the Trans-Himalayas, China. *J. Wildl. Manage.* 72, 1335–1341. doi: 10.2193/2007-077

Young, N. E., Anderson, R. S., Chignell, S. M., Vorster, A. G., Lawrence, R., and Evangelista, P. H. (2017). A survival guide to Landsat preprocessing. *Ecology* 98, 920–932. doi: 10.1002/ecy.1730

Zhang, H., Wang, C., Turvey, S. T., Sun, Z., Tan, Z., Yang, Q., et al. (2020). Thermal infrared imaging from drones can detect individuals and nocturnal behavior of the world's rarest primate. *Glob. Ecol. Conserv.* 23:e01101. doi: 10.1016/j.gecco.2020.e01101

Zhang, M., Fellowes, J. R., Jiang, X., Wang, W., Chan, B. P., Ren, G., et al. (2010). Degradation of tropical forest in Hainan, China, 1991–2008: conservation implications for Hainan gibbon (*Nomascus hainanus*). *Biol. Conserv.* 143, 1397–1404. doi: 10.1016/j.biocon.2010.03.014

Zhou, J., Wei, F., Li, M., Chan, B. P. L., and Wang, D. (2008). Reproductive characters and mating behaviour of wild *Nomascus hainanus*. *Int. J. Primatol.* 29, 1037–1046. doi: 10.1007/s10764-008-9272-7

Zhou, J., Wei, F., Li, M., Zhang, J., Wang, D., and Pan, R. (2005). Hainan black-crested gibbon is headed for extinction. *Int. J. Primatol.* 26, 453–465.

Conflict of Interest: The authors declare that the research was conducted in the absence of any commercial or financial relationships that could be construed as a potential conflict of interest.

Publisher's Note: All claims expressed in this article are solely those of the authors and do not necessarily represent those of their affiliated organizations, or those of the publisher, the editors and the reviewers. Any product that may be evaluated in this article, or claim that may be made by its manufacturer, is not guaranteed or endorsed by the publisher.

frontiers | Frontiers in Ecology and Evolution

TYPE Original Research
PUBLISHED 15 August 2022
DOI 10.3389/fevo.2022.974004

OPEN ACCESS

EDITED BY
Xiang Liu,
Lanzhou University, China

REVIEWED BY
Yunquan Wang,
Zhejiang Normal University, China
Yao Guangqian,
Lanzhou University, China
Clément Stahl,
INRA Centre Antilles-Guyane, France

*CORRESPONDENCE
Jie Cui
443464199@qq.com
Hui Zhang
zhanghuitianxia@126.com

†These authors have contributed equally to this work

SPECIALTY SECTION
This article was submitted to Conservation and Restoration Ecology, a section of the journal Frontiers in Ecology and Evolution

RECEIVED 20 June 2022
ACCEPTED 28 July 2022
PUBLISHED 15 August 2022

CITATION
Su R, Liu H, Wang C, Zhang H and Cui J (2022) Leaf turgor loss point is one of the best predictors of drought-induced tree mortality in tropical forest.
Front. Ecol. Evol. 10:974004.
doi: 10.3389/fevo.2022.974004

Leaf turgor loss point is one of the best predictors of drought-induced tree mortality in tropical forest

Rui Su[1†], Hui Liu[2†], Chen Wang[2], Hui Zhang[1*] and Jie Cui[3*]

[1]Key Laboratory of Genetics and Germplasm Innovation of Tropical Special Forest Trees and Ornamental Plants (Hainan University), Ministry of Education, School of Forestry, Hainan University, Haikou, China, [2]Key Laboratory of Vegetation Restoration and Management of Degraded Ecosystem, South China Botanical Garden, Chinese Academy of Sciences, Guangzhou, China, [3]Development Research Center of People's Government of Sanya City, Sanya, China

Accurately predicting global drought-induced tree mortality remains a major challenge facing plant science and ecology. Stem hydraulic safety margin (HSM, the difference between water potential at the minimum value and the value that causes xylem vulnerability to embolism) performs as one of the best hydraulic traits in predicting global drought-induced tree mortality, however, HSM is time-consuming and very difficult to measure. We proposed to use leaf turgor loss point (TLP, the water potential at which leaves start to wilt) as a proxy for HSM because HSM may be highly correlated to TLP, as both of them are tightly linked with water potential changes after stomatal closure. Since TLP is more easy and rapid to measure than HSM, if we find strong HSM-TLP relationships at the global scale, TLP can be used in predicting global drought-induced tree mortality. However, no study has quantified the relationships between HSM and TLP at the global scale. Here we draw together published data on HSM and TLP for 1,773 species from 370 sites worldwide to check whether HSM and TLP are highly associated. We found that HSMs and TLPs are merely highly related in tropical forests, thus TLP can be a reliable surrogate of HSM to predict drought-induced tree mortality in tropical forest. Here we are certainly not advocating for the use of TLP instead of HSM to predict drought-induced tree mortality in tropical forests, but simply for predicting drought-induced tree mortality in tropical forests in supplementary of HSM in the future.

KEYWORDS

drought-induced tree mortality, hydraulic failure, physiological trait, stem hydraulic safety margin, turgor loss point, wavelet coherence

Introduction

Climate change is predicted to increase both the frequency and severity of droughts worldwide (Sheffield and Wood, 2008). When the severity of drought increases, water flow in the xylem conduits of trees may be irreversibly disrupted (hydraulic failure), leading to mortality of the roots or branches and even to tree death (Rice et al., 2004; Bréda et al., 2006; Choat et al., 2018). Rapid tree mortality events could convert the world's forest from a net carbon sink into a large carbon source during this century. However, accurately predicting the impact of climate change on plant performance and survival remains a major challenge facing plant science and ecology (Grierson et al., 2011; Bartlett et al., 2014). Recent tree mortality under frequent extreme drought events have led to recognition of the importance of the physiological mechanisms associated with drought-induced tree mortality in different biomes (McDowell et al., 2011; Anderegg et al., 2012).

Stem hydraulic safety margin (HSM) which defines the difference between water potential at the minimum value and the value that causes xylem vulnerability to embolism, is widely assumed the key to understand drought-induced tree mortality (Brodribb and Holbrook, 2003; Choat et al., 2012; Martorell et al., 2014). A meta-analysis of drought-induced mortality rates across 475 species from 33 studies around the globe revealed that HSM is one of the best predictors of drought-induced forest mortality, with lower HSM indicating higher risk of mortality (Anderegg et al., 2016). Thus, quantifying the variations in global patterns of HSM can facilitate to predict how drought-induced forest mortality varies globally. However, it is time-consuming and hard to measure HSM (Zhu et al., 2018), which impeded the possibility to quantify the dynamics of global HSM. As a result, finding a reliable proxy of HSM can be an alternative way to solve this problem.

When facing drought stress, stomatal closure has been assumed to be the vital mechanism for avoiding xylem embolism as it stops transpiration and water loss in leaves and maintains negative Ψ in stems and roots (Brodribb and Holbrook, 2003). Although stomatal closure does not stop the decline of xylem pressure and hydraulic capacity (Choat et al., 2012), it is strongly associated with both TLP (Blackman, 2018) and HSM (Brodribb and Holbrook, 2003; Martorell et al., 2014), that measure plant's ability to keep cell turgor pressure when facing drought stress. Compared to HSM, TLP is more easy and rapid to measure (Zhu et al., 2018) and there are largely available TLP dataset at global scale (Bartlett et al., 2012). Thus, if HSM and TLP are highly associated at the global scale, TLP may be a good proxy for HSM to predict drought-induced tree mortality. However, till now only Zhu et al. (2018) has found a strong relationship between TLP and HSM in China. Blackman (2018) also assumes this association is still uncertain, but emphasizes the high necessity to quantify the relationships between HSM and TLP at the global scale.

Here we draw together previous published data on stem HSM and TLP for 1,773 species at 370 sites worldwide. Aridity index (AI), the ratio of mean annual precipitation (MAP), and potential evapotranspiration (PET) were used to represent the water environment. It is highly possible that there is no strong HSM-TLP relationship at the global scale, as at the global scale, HSM does not vary significantly with water environment (Choat et al., 2012), whereas TLP is significantly positively associated with water availability (Bartlett et al., 2012). However, it is also possible that HSM-TLP may be highly correlated in some special water environment (i.e., moist tropical rainforest). Thus we first used traditional Pearson correlation method to quantify the relationship between HSM and TLP at the global scale. Finally, we applied a novel wavelet coherence method, which can compute how the relationship between stem HSM and TLP differs while considering water availability (indicated by AI) at local scales. Our goal was to quantify whether strong HSM-TLP relationship can also be found in some special water environment.

Methods and methods

Data collection

Three categories of data were collected for each site, including plant hydraulic traits (stem HSM and TLP), AI and biome type. The detailed information is shown below:

(1) plant stem HSM and leaf TLP: We obtained stem HSM and leaf TLP for as many woody species and study sites as possible. Datasets we collected were from the TRY Plant Traits Database (Kattge et al., 2011) and published papers (see **Supplementary Table 1**). We also tried to collect leaf P50, but the largest dataset available was only about 60 species from three different forest types (Zhu et al., 2019), which is not enough for a meta-analysis. Because leaf TLP could be used as a convenient proxy of leaf HSM, we decided to use more available TLP data (298 species in

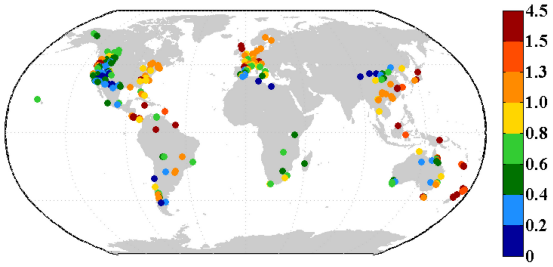

FIGURE 1
Distribution of the study sites (n = 370) and their corresponding AI values.

our dataset) to represent leaf drought tolerance. Collected data were confined to measurements taken on the terminal branches of mature plants. For multiple measures on the same species from the same site, we used average values. In total, our collected dataset included 1,116 stem HSM (198 sites) and 703 TLP (172 sites) values for 1,773 species at 370 sites worldwide. There were matched HSM and TLP data in 105 sites.

(2) Aridity index (AI). AI is defined as the ratio of MAP and PET. AI directly reflects a site's water environment and includes more climatic factors than just precipitation (Maestre et al., 2015). We used AI as a proxy for water availability or drought stress at each site. We extracted AI values for each study site based on the Global Aridity Index database at a 30 arc-s resolution[1] (Trabucco and Zomer, 2009). In this study AI values range from 0.1 to 2.5; we discretized them at intervals of 0.1. The distribution of each site and its corresponding AI value are shown in **Figure 1**.

(3) Biome type for each site. We followed the biome type classification of the geological database of Terrestrial Ecoregions of the World (Olson et al., 2001). The biome type for each site was classified into seven biome types, i.e., deserts, woodland/shrubland, boreal forest, temperate seasonal forest, temperate rain forest, tropical seasonal forest (including savanna), and tropical rain forest. **Supplementary Figure 1** shows the distribution of biome type for each study site in our study.

Statistical methods

Pearson correlation analysis

Pearson correlation is a measure of the strength and direction of the linear relationship between two random variables. We considered correlations strong if the correlation coefficient was greater than 0.8 and weak if the correlation coefficient was less than 0.5 (Bolboacă and Jäntschi, 2006). A student *t*-test was used to determine if the value of the Pearson correlation coefficient was statistically significant. We used a significance level of 5%; a *p*-value less than 0.05 represents evidence to reject the null hypothesis in favor of the alternative hypothesis that there is a linear relationship between the variables. The data length of HSM and TLP are not the same in this study (1,116 stem HSM and 703 TLP values), thus we quantified the HSM-TLP relationship varies with specific water availability levels (classified by AI values). Here we calculated the mean value for stem HSM and TLP at each specific AI interval. The data series relating stem HSM and TLP to AI at a global scale are shown in **Supplementary Figure 2**. We then applied Pearson correlation analysis on the two data series (mean HSM-TLP vs. AI).

Wavelet coherence analysis

The wavelet transform is a useful tool for analyzing localized variations of a data series. It can transform a data series into frequency space where oscillations can be seen in an intuitive way and can show localized intermittent periodicities or relationships (Grinsted et al., 2014). Wavelet coherence can analyze two data series together. It can be thought of as the local correlation between two data series. Following Torrence and Webster (1999), the wavelet coherence of two data series can define as

$$R_n^2(s) = \frac{|S(s^{-1}W_n^{XY}(s))|^2}{S\left(s^{-1}\left|W_n^X(s)\right|^2\right)\cdot S(s^{-1}|W_n^Y(s)|^2)}$$

where S is a smoothing operator, and can be written as

$$S(W) = S_{scale}(S_{time}(W_n(s)))$$

where S_{scale} denotes smoothing along the wavelet scale axis and S_{time} smoothing in time. For the Morlet wavelet used in this study, a suitable smoothing operator is given by Torrence and Webster (1999):

$$S_{time}(W)|_s = \left(W_n(s) * c_1^{\frac{-t^2}{2s^2}}\right)|_s$$

$$S_{scale}(W)|_n = \left(W_n(s) * c_2\Pi(0.6s)\right)|_n$$

where c_1 and c_2 are normalization constants and $\Pi()$ is the rectangle function. The factor of 0.6 is the empirically determined scale decorrelation length for the Morlet wavelet (Torrence and Compo, 1998; Grinsted et al., 2014). The coefficient of wavelet coherence ranges from zero to one and the closer the value approximates one, the more correlated the two series are. The statistical significance levels of the wavelet coherence, which show confidence levels against red noise, were estimated using Monte Carlo methods. The detailed process of calculation and the MATLAB codes for calculating wavelet coherence are provided in Grinsted et al. (2014). Wavelet coherence is most used for time series. Nevertheless, more recently, applications of wavelet coherence have been extended to other data series analysis (He, 2014; Guo et al., 2015; Hu and Si, 2016). Consequently, here we use it to investigate localized intermittent relationships between stem HSM and TLP values in different water environments reflected by AI. Specifically wavelet coherence analysis requires continuous time or spatial variables, so we first calculate the mean HSM and TLP for all species at each of the continuous AI variables (ranging from 0.1 to 2.5 at interval of 0.1). Then we used wavelet coherence analysis to quantify whether strong HSM-TLP relationship can be found in some special AI ranges. Previous studies have found that TLP can be easily affected by

1 https://cgiarcsi.community/

whether the species being sampled are deciduous or evergreen (Bartlett et al., 2012). Moreover, tropical rain forests have the largest proportions of evergreen species, thus we further tested if HSM-TLP relationships might vary when merely considering evergreen species, using both Pearson correlation and wavelet coherence analysis.

Results

Stem HSM and TLP values were not significantly correlated when we averaged them according to AI intervals (r = 0.2296, p = 0.2696) (**Figure 2**), indicating that stem HSM and TLP were not significantly correlated at the global scale. It was possible that the correlation between HSM and TLP was significant only for some particular range of AI. Results of wavelet coherence analysis supported this assertion. The correlation between stem HSM and TLP was significant only for AI values between 1.3 and 1.5 (**Figure 3A**), which represented the environment of tropical seasonal and rain forests (**Supplementary Figure 3**). When repeating the wavelet coherence analysis for just evergreen species, we found further evidence for the strongest relationships between stem HSM and TLP values in tropical woody species (**Figure 3B**).

Discussion

At the global scale, stem HSM values are not significantly correlated to TLP values. This indicates leaf and stem hydraulic failure are decoupled at the global scale, which supports a strong hydraulic segmentation between leaves and stems in hydraulic pathways (Bucci et al., 2013; Pivovaroff et al., 2014). However, when using wavelet coherence to analyze the regional patterns of stem HSM and TLP, we found strong stem HSM-TLP relationships at AI values indicative of tropical seasonal and rain forests. This indicates that stem and leaf hydraulic properties are well coupled only in tropical forests, as has been found in three tropical forest species (Nolf et al., 2015). This finding suggests that TLP is a good proxy of HSM to predict drought-induced tree mortality only in tropical forests.

It is reasonable that we observed strong correlations between stem HSM and TLP values only in tropical forests, given that plants tend to develop different leaf and stem drought adaptation strategies in different water environments. In wet areas, such as tropical rain and seasonal forests, stem and leaf hydraulic connections can be coupled in the absence of selection pressure from drought (Nolf et al., 2015; Zhu et al., 2016). However, other mechanisms may also save plant species from drought stress in non-tropical forest types (Klein et al., 2014).

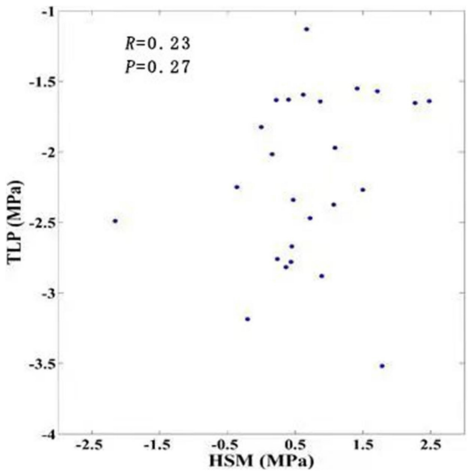

FIGURE 2
Relationship between stem HSM and TLP paired according to AI levels (n = 25). The Pearson correlation coefficient (R) and its corresponding p-value are presented in the upper left.

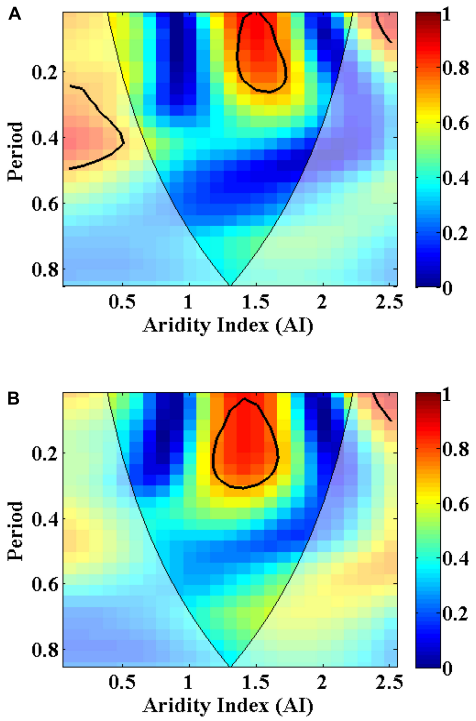

FIGURE 3
Wavelet coherence analysis between stem HSM and TLP for **(A)** all woody species and **(B)** evergreen woody species paired according to AI intervals at global scale. Red reflects perfect correlation while blue reflects a lack of correlation. The thick black contour represents the 95% significance level against red noise. The y label means the period of strong local correlation. In this study, the strong correlation only for AI between 1.3 and 1.5, and the corresponding y label value is about 0.2. It means that the period of strong local correlation is 0.2 (just the interval between 1.3 and 1.5). Because the edge effects cannot be ignored, we only focus on the data inside the Cone of Influence (COI) (darker shade).

For example, in extremely dry areas, such as deserts, some plants are adapted to long-term drought stress and can survive under large stem HSM, because xylem cavitation is not always fatal (Fisher et al., 2006; Klein et al., 2011). On the other hand, leaf TLP is not closely related with tree mortality across the globe (Anderegg et al., 2016), thus it has more flexibility in drought tolerance. In deserts (roughly AI < 1.3), species show both very negative stem HSM and leaf TLP values (through different drought tolerance strategies) and no coordination between the two. Furthermore, in biomes with seasonal drought, plants tend to develop drought avoidance strategies, such as dropping leaves to prevent fatal xylem cavitation (Volaire, 2018). Similar deciduousness strategies are also used by shrub species to avoid drought stress in shrubland biomes (Hacke et al., 2000). In our data, if only considering evergreen woody species, comparable correlations between stem HSM and leaf TLP values are evident (see **Figure 3B**). This confirms that drought avoidance, but not drought stress resistance, prevails in temperate forest and woodland biomes, thereby causing weak HSM-TLP relationships. As a result, except for tropical forests, TLP can act as a safety valve to prevent xylem embolism (low HSM) for global forests.

Our observed HSM-TLP relationships may also explain why HSM does not vary with water environment at the global scale (Choat et al., 2012). In very wet environments, such as tropical rain and seasonal forests, although TLP cannot act as safety valve to prevent xylem embolism, HSM can still persist at safe values to avoid xylem embolism due to the lower probability of drought stress (Nolf et al., 2015) and cavitation-resistant leaves and effective hydraulic compensatory strategies (Zhu et al., 2016). In other biomes, TLP can serve as a safety valve (e.g., shed leaves) to prevent stem xylem embolism even in extreme arid environments such as desert. Thus, HSM can remain at safe values for all biomes. However, there is a possibility that HSM in tropical rain forest could drop under extreme drought stress, as is suggested by high drought-induced tree mortality in tropical rain forests. We noted that our HSM data were not measured during extreme drought stress, which explains why we observed globally similar HSM values (Choat et al., 2012). Future studies should examine HSM during extreme drought stress to better understand how global HSMs response to drought stress.

There are still some gaps in our understanding of the HSM-TLP relationships at the global scale. First, currently, there is a large innovation on the measurements of HSM and TLP and also some difference among them (see Sergent et al., 2020, doi.org/10.1016/j.foreco.2020.118175). Moreover, one single water potential measurement can hardly be considered an estimate of minimum leaf water potential which is the basis for calculating HSM. That is because a proper estimate of minimum water potential is likely to be substantially lower than the values you report for a single date, even if during the dry season. Here for collecting as many HSM and TLP data as possible to perform reliable wavelet coherence analysis, we cannot consider these two potential limitations for our collected HSM and TLP data. Thus, future quantifying the HSM-TLP relationships are still needed to be performed, when many and reliable HSM and TLP data are available. The fifth intergovernmental panel on climate change assessment report (IPCC AR5) indicates that, by the end of the twenty-first century, it is very likely that extreme drought events will be more intense and frequent over the tropical regions (Ipcc, 2013). Indeed, drought has occurred more frequently in tropical regions recently. Examples include the dry extremes over the Amazon in 2005 and 2010 and Northeast Brazil in 2012 (Marengo et al., 2008, 2013; Coelho et al., 2012). Models predict that extreme drought will result in ∼223-million-hectare canopy cover losses by 2050, with the vast majority of losses occurring in the tropics (Cox et al., 2000; Bastin et al., 2019), which in turn could result in large carbon emissions. Given the strong relationship between HSM and TLP in tropical forests, TLP should possibly be used to predict drought induced tree mortality in tropics. Moreover, given the largely available TLP data in tropics, TLP can also be directly incorporated into models forecasting the influence of increased drought-induced tree mortality on carbon emissions in tropical rain forests. Here we are certainly not advocating for the use of TLP instead of HSM to predict drought-induced tree mortality in tropical forests, but simply for the addition of HSM in predicting drought-induced tree mortality in tropical forests in the future.

Data availability statement

The original contributions presented in the study are included in the article/**Supplementary material**, further inquiries can be directed to the corresponding author/s.

Author contributions

RS: conceptualization, methodology, writing—original draft, and review and editing. HL: methodology, data curation, and writing—review and editing. CW: writing—review and editing. HZ and JC: conceptualization, methodology, data curation, and writing—original draft. All authors contributed to the article and approved the submitted version.

Funding

This work was funded by the Hainan Provincial Natural Science Foundation of China (2019RC161 and 422CXTD508),

the specific research fund of the Innovation Platform for Academicians of Hainan Province, Research project of Hainan academician innovation platform (YSPTZX202017), the Scientific Research Project of Ecological Restoration of Baopoling (Sanya), the Pearl River S&T Nova Program of Guangzhou (201806010083), and the Youth Innovation Promotion Association of the Chinese Academy of Sciences (2019339).

Conflict of interest

The authors declare that the research was conducted in the absence of any commercial or financial relationships that could be construed as a potential conflict of interest.

Publisher's note

Supplementary material

The Supplementary Material for this article can be found online at: https://www.frontiersin.org/articles/10.3389/fevo.2022.974004/full#supplementary-material

References

Anderegg, W. R., Berry, J. A., Smith, D. D., Sperry, J. S., Anderegg, L. D., and Field, C. B. (2012). The roles of hydraulic and carbon stress in a widespread climate-induced forest die-off. *Proceedings of the National Academy of Sciences.* 109, 233–237. doi: 10.1073/pnas.1107891109

Anderegg, W. R., Klein, T., Bartlett, M., Sack, L., Pellegrini, A. F., Choat, B., et al. (2016). Meta-analysis reveals that hydraulic traits explain cross-species patterns of drought-induced tree mortality across the globe. *Proceedings of the National Academy of Sciences.* 113, 5024–5029. doi: 10.1073/pnas.1525678113

Bartlett, M. K., Scoffoni, C., and Sack, L. (2012). The determinants of leaf turgor loss point and prediction of drought tolerance of species and biomes: a global meta-analysis. *Ecology Letters.* 15, 393–405. doi: 10.1111/j.1461-0248.2012.01751.x

Bartlett, M. K., Zhang, Y., Kreidler, N., Sun, S., Ardy, R., Cao, K., et al. (2014). Global analysis of plasticity in turgor loss point, a key drought tolerance trait. *Ecol. Lett.* 17, 1580–1590. doi: 10.1111/ele.12374

Bastin, J. F., Finegold, Y., Garcia, C., Mollicone, D., Rezende, M., Routh, D., et al. (2019). The global tree restoration potential. *Science* 365, 76–79. doi: 10.1126/science.aax0848

Blackman, C. J. (2018). Leaf turgor loss as a predictor of plant drought response strategies. *Tree Physiology.* 38, 655–657. doi: 10.1093/treephys/tpy047

Bolboacă, S. D., and Jäntschi, L. (2006). Pearson versus Spearman, Kendall's tau correlation analysis on structure-activity relationships of biologic active compounds. *Leonardo J. Sci.* 5, 179–200.

Bréda, N., Huc, R., Granier, A., and Dreyer, E. (2006). Temperate forest trees and stands under severe drought: A review of ecophysiological responses, adaptation processes and long-term consequences. *Ann. For. Sci.* 63, 625–644. doi: 10.1051/forest:2006042

Brodribb, T. J., and Holbrook, N. M. (2003). Stomatal closure during leaf dehydration, correlation with other leaf physiological traits. *Plant Physiology* 132, 2166–2173. doi: 10.1104/pp.103.023879

Bucci, S. J., Scholz, F. G., Peschiutta, M. L., Arias, N. S., Meinzer, F. C., and Goldstein, G. (2013). The stem xylem of Patagonian shrubs operates far from the point of catastrophic dysfunction and is additionally protected from drought-induced embolism by leaves and roots. *Plant, Cell & Environment.* 36, 2163–2174. doi: 10.1111/pce.12126

Choat, B., Jansen, S., Brodribb, T. J., Cochard, H., Delzon, S., Bhaskar, R., et al. (2012). Global convergence in the vulnerability of forests to drought. *Nature* 491, 752–755. doi: 10.1038/nature11688

Choat, B., Brodribb, T. J., Brodersen, C. R., Duursma, R. A., López, R., and Medlyn, B. E. (2018). Triggers of tree mortality under drought. *Nature* 558, 531–539. doi: 10.1038/s41586-018-0240-x

Coelho, C. A. S., Cavalcanti, I. A., Costa, S., Freitas, S. R., Ito, E. R., Luz, G., et al. (2012). Climate diagnostics of three major drought events in the Amazon and illustrations of their seasonal precipitation predictions. *Meteorol. Appl.* 19, 237–255. doi: 10.1002/met.1324

Cox, P. M., Betts, R. A., Jones, C. D., Spall, S. A., and Totterdell, I. J. (2000). Acceleration of global warming due to carbon-cycle feedbacks in a coupled climate model. *Nature* 408, 184–187. doi: 10.1038/35041539

Fisher, R. A., Williams, M., Do, V., Lobo, R., Costa, A. L. D. A., and Meir, P. (2006). Evidence from Amazonian forests is consistent with isohydric control of leaf water potential. *Plant, Cell & Environment.* 29, 151–165. doi: 10.1111/j.1365-3040.2005.01407.x

Grierson, C. S., Barnes, S. R., Chase, M. W., Clarke, M., Grierson, D., Edwards, K. J., et al. (2011). One hundred important questions facing plant science research. *New Phytol.* 192, 6–12. doi: 10.1111/j.1469-8137.2011.03859.x

Grinsted, A., Moore, J. C., and Jevrejeva, S. (2014). Application of the cross wavelet transform and wavelet coherence to geophysical time series. *Nonlinear Processes in Geophysics.* 11, 561–566. doi: 10.5194/npg-11-561-2004

Guo, J., Wang, L., Liu, X., Kong, Q., Zhao, C., and Guo, B. (2015). Temporal-spatial variation of global gps-derived total electron content, 1999–2013. *PLoS One.* 10:e0133378. doi: 10.1371/journal.pone.0133378

Hacke, U. G., Sperry, J. S., and Pittermann, J. (2000). Drought experience and cavitation resistance in six shrubs from the Great Basin. *Utah. Basic and Applied Ecology.* 1, 31–41. doi: 10.1078/1439-1791-00006

He, Y. (2014). The relationship between an invasive shrub and soil moisture: seasonal interactions and spatially covarying relations. *ISPRS International Journal of Geo-Information.* 3, 1139–1153. doi: 10.3390/ijgi3031139

Hu, W., and Si, B. C. (2016). Technical note: multiple wavelet coherence for untangling scale-specific and localized multivariate relationships in geosciences. *Hydrology & Earth System Sciences.* 20, 3183–3191. doi: 10.5194/hess-20-3183-2016

Ipcc. (2013). "IPCC, 2013," in *climate change 2013: the physical science basis. Contribution of working group I to the fifth assessment report of the intergovernmental panel on climate change*, eds T. F. Stocker, D. Qin, G.-K. Plattner, M. Tignor, S. K. Allen, J. Boschung, et al. (Cambridge: Cambridge University Press), 1535.

Kattge, J., Diaz, S., Lavorel, S. I, Prentice, C., Leadley, P., and Bönisch, G. (2011). TRY–a global database of plant traits. *Global Change Biology.* 17, 2905–2935. doi: 10.1111/j.1365-2486.2011.02451.x

Klein, T., Cohen, S., and Yakir, D. (2011). Hydraulic adjustments underlying drought resistance of Pinus halepensis. *Tree physiology.* 31, 637–648. doi: 10.1093/treephys/tpr047

Klein, T., Yakir, D., Buchmann, N., and Grünzweig, J. M. (2014). Towards an advanced assessment of the hydrological vulnerability of forests to climate change-induced drought. *New Phytologist.* 201, 712–716. doi: 10.1111/nph.12548

Maestre, F. T., Delgado-Baquerizo, M., Jeffries, T. C., Eldridge, D. J., Ochoa, V., Gozalo, B., et al. (2015). Increasing aridity reduces soil microbial diversity and abundance in global drylands. *Proceedings of the National Academy of Sciences.* 112, 15684–15689. doi: 10.1073/pnas.1516684112

Marengo, J. A., Alves, L. M., Soares, W. R., Rodriguez, D. A., Camargo, H., Riveros, M. P., et al. (2013). Two contrasting severe seasonal extremes in tropical South America in (2012). flood in Amazonia and drought in northeast Brazil. *Journal of Climate.* 26, 9137–9154. doi: 10.1175/JCLI-D-12-00642.1

Marengo, J. A., Nobre, C. A., Tomasella, J., Oyama, M. D., de Oliveira, G. Sampaio, Oliveira, R. De, et al. (2008). The drought of Amazonia in 2005. *Journal of Climate* 21, 495–516. doi: 10.1175/2007JCLI1600.1

Martorell, S., Diaz-Espejo, A., Medrano, H., Ball, M. C., and Choat, B. (2014). Rapid hydraulic recovery in Eucalyptus pauciflora after drought: linkages between stem hydraulics and leaf gas exchange. *Plant, Cell and Environment* 37, 617–626. doi: 10.1111/pce.12182

McDowell, N. G., Beerling, D. J., Breshears, D. D., Fisher, R. A., Raffa, K. F., and Stitt, M. (2011). The interdependence of mechanisms underlying climate-driven vegetation mortality. *Trends in Ecology & Evolution* 26, 523–532. doi: 10.1016/j.tree.2011.06.003

Nolf, M., Creek, D., Duursma, R., Holtum, J., Mayr, S., and Choat, B. (2015). Stem and leaf hydraulic properties are finely coordinated in three tropical rain forest tree species. *Plant, Cell & Environment.* 38, 2652–2661. doi: 10.1111/pce.12581

Olson, D. M., Dinerstein, E., Wikramanayake, E. D., Burgess, N. D., Powell, G. V., Underwood, E. C., et al. (2001). Terrestrial eco-regions of the world: A new map of life on earth: A new global map of terrestrial ecoregions provides an innovative tool for conserving biodiversity. *BioScience* 51, 933–938. doi: 10.1641/0006-3568(2001)051[0933:TEOTWA]2.0.CO;2

Pivovaroff, A. L., Sack, L., and Santiago, L. S. (2014). Coordination of stem and leaf hydraulic conductance in southern California shrubs: a test of the hydraulic segmentation hypothesis. *New Phytologist.* 203, 842–850. doi: 10.1111/nph.12850

Rice, K. J., Matzner, S. L., Byer, W., and Brown, J. R. (2004). Patterns of tree dieback in Queensland, Australia: The importance of drought stress and the role of resistance to cavitation. *Oecologia* 139, 190–198. doi: 10.1007/s00442-004-1503-9

Sergent, A. S., Varela, S. A., Barigah, T. S., Badel, E., Cochard, H., Dalla-Salda, G., et al. (2020). A comparison of five methods to assess embolism resistance in trees. *For. Ecol. Manage.* 468:118175. doi: 10.1016/j.foreco.2020.118175

Sheffield, J., and Wood, E. F. (2008). Global trends and variability in soil moisture and drought characteristics, 1950-2000, from observation-driven simulations of the terrestrial hydrologic cycle. *J. Clim.* 21, 432–458. doi: 10.1175/2007JCLI1822.1

Torrence, C., and Compo, G. P. (1998). A practical guide to wavelet analysis. *Bulletin of the American Meteorological Society.* 79, 61–78. doi: 10.1175/1520-0477(1998)079<0061:APGTWA>2.0.CO;2

Torrence, C., and Webster, P. J. (1999). Interdecadal changes in the enso–monsoon system. *Journal of Climate.* 12, 2679–2690. doi: 10.1175/1520-0442(1999)012<2679:ICITEM>2.0.CO;2

Trabucco, A., and Zomer, R. (2009). Global aridity index (global-aridity) and global potential evapo-transpiration (global-PET) geospatial database. *CGIAR Consortium for Spatial Information* 89, 1–2.

Volaire, F. (2018). A unified framework of plant adaptive strategies to drought: crossing scales and disciplines. *Global change biology* 24, 2929–2938. doi: 10.1111/gcb.14062

Zhu, S. D., Chen, Y. J., Ye, Q., He, P. C., Siddiq, Z., and Cao, K. F. (2018). Leaf turgor loss point is correlated with drought tolerance and leaf carbon economics traits. *Tree Physiology* 38, 658–663. doi: 10.1093/treephys/tpy013

Zhu, S. D., Li, R. H., He, P. C., Siddiq, Z., Cao, K. F., and Ye, Q. (2019). Large branch and leaf hydraulic safety margins in subtropical evergreen broadleaved forest. *Tree Physiology.* 39, 1405–1415. doi: 10.1093/treephys/tpz028

Zhu, S. D., Liu, H., Xu, Q. Y., Cao, K. F., and Ye, Q. (2016). Are leaves more vulnerable to cavitation than branches? *Functional Ecology* 30, 1740–1744. doi: 10.1111/1365-2435.12656

frontiers | Frontiers in Ecology and Evolution

TYPE Original Research
PUBLISHED 22 August 2022
DOI 10.3389/fevo.2022.993844

OPEN ACCESS

EDITED BY
Xiang Liu,
Lanzhou University, China

REVIEWED BY
Li Zhang,
Nanjing Forestry University, China
Mu Liu,
Lanzhou University, China
Zechen Peng,
Lanzhou University, China

*CORRESPONDENCE
Lifan Chen
chenlf@sumhs.edu.cn

SPECIALTY SECTION
This article was submitted to Conservation and Restoration Ecology, a section of the journal Frontiers in Ecology and Evolution

RECEIVED 14 July 2022
ACCEPTED 01 August 2022
PUBLISHED 22 August 2022

CITATION
Chen L, Chen S, Kong P and Zhou L (2022) Host competence, interspecific competition and vector preference interact to determine the vector-borne infection ecology.
Front. Ecol. Evol. 10:993844.
doi: 10.3389/fevo.2022.993844

Host competence, interspecific competition and vector preference interact to determine the vector-borne infection ecology

Lifan Chen[1]*, Shiliang Chen[2], Ping Kong[3] and Liang Zhou[3]

[1]Collaborative Innovation Center for Biomedicine, Shanghai University of Medicine and Health Sciences, Shanghai, China, [2]Ministry of Education Key Laboratory for Biodiversity Science and Ecological Engineering, School of Life Sciences, Fudan University, Shanghai, China, [3]Jiading District Central Hospital Affiliated Shanghai University of Medicine and Health Sciences, Shanghai, China

Understanding how ecological interactions affect vector-borne disease dynamics is crucial in the context of rapid biodiversity loss and increased emerging vector-borne diseases. Although there have been many studies on the impact of interspecific competition and host competence on disease dynamics, few of them have addressed the case of a vector-borne disease. Using a simple compartment model with two competing host species and one vector, we investigated the combined effects of vector preference, host competence, and interspecific competition on disease risk in a vector-borne system. Our research demonstrated that disease transmission dynamics in multi-host communities are more complex than anticipated. Vector preference and differences in host competence shifted the direction of the effect of competition on community disease risk, yet interspecific competition quantitatively but not qualitatively changed the effect of vector preference on disease risk. Our work also identified the conditions of the dilution effect and amplification effect in frequency-dependent transmission mode, and we discovered that adding vector preference and interspecific competition into a simple two-host-one-vector model altered the outcomes of how increasing species richness affects disease risk. Our work explains some of the variation in outcomes in previous empirical and theoretical studies on the dilution effect.

KEYWORDS

biodiversity-disease relationship, dilution effect, amplification effect, compartment model, contact heterogeneity

Introduction

Vector-borne diseases refer to the infectious diseases that are transmitted by blood-sucking arthropods such as mosquitoes, fleas, lice, ticks, etc. Most vector-borne diseases are zoonosis, they pose a great threat to human health and wildlife conservation. According to estimates, more than 1.5 million people die from vector-borne diseases

worldwide each year, which accounts for 3/4 of the newly emerging infectious diseases in recent years (World Health Organization [WHO], 2004). The effective prevention and management of vector-borne diseases remains one of the main challenges of current scientific research.

There is an increased likelihood that host diversity and total disease risk are inversely related, i.e., the dilution effect hypothesis (Keesing et al., 2006, 2010; Ostfeld and Keesing, 2012). Ecologists have recently confirmed that the dilution effect does exist in some systems through the study of Lyme disease (Ostfeld and Keesing, 2000; LoGiudice et al., 2003), West Nile virus (Kilpatrick et al., 2006), amphibian trematodes (Johnson et al., 2013), and leaf fungal diseases (Mitchell et al., 2002; Liu et al., 2016). They have also come to the following conclusion about the underlying mechanism of the dilution effect: the order of community (dis)assembly is non-random, the most competent host species (the hosts' ability to obtain and transmit pathogens) have the lowest probability of extinction (Halliday et al., 2019, 2020). As host diversity increases, a large number of low-competent or non-competent hosts (a host can become infected but is unable to transmit pathogens) are added to the community, which decreases the contact rate between highly competent hosts and vectors, a dilution effect occurs (Johnson et al., 2013). If this result holds, then the disease risk is highest when the community contains only the most competent host. However, some studies have questioned the universality of the dilution effect by demonstrating that the highest disease risk occurs when the community consists of several host species (Ostfeld and LoGiudice, 2003; Simpson et al., 2012; Costa et al., 2021). Additionally, several researchers have suggested that amplification and no effects also exist in the natural world (Wood et al., 2014; Halliday et al., 2017; Rohr et al., 2019; Vadell et al., 2019). These debates imply that a variety of ecological factors may affect disease risk, and different factors may play different or even perhaps opposite roles in different systems. Exploring how interspecific interactions (resource competition, transmission between species, and vector-host contact rate) affect vector-borne infection is critical not only for theoretical analysis, but also for vector-borne disease prevention and management.

Most vector-borne diseases are transmitted among a variety of hosts, but each host has its own ability to attract vectors, a phenomenon known as the vector preference (Rivera et al., 2020). Several empirical studies supported the existence of vector feeding preferences. For example, *Anopheles gambiae*, the vector of malaria, prefers to bite humans over cattle (Tirados et al., 2006). *Triatoma* bugs that transmit Chagas disease have a strong feeding preference for dogs over chickens and cats (Gürtler et al., 2009). Vector preference is an important ecological factor contributing to the heterogeneity in contact rates between hosts and vectors (Simpson et al., 2012). Both theoretical and experimental studies have found that vector preference not only affects the likelihood of disease outbreak and prevalence, but also interacts with other factors to influence disease dynamics (Kilpatrick et al., 2006; Simpson et al., 2012; Zeilinger and Daugherty, 2014).

Interspecific competition can alter the host's behavior, abundance, living habits, fitness, etc., which can directly or indirectly increase disease risk. For instance, while increased rodent richness facilitates disease transmission between individuals, it can also result in increased interspecific competition, allowing for a decrease in host density, leading to an overall decrease in the prevalence of Sin Nombre Hantavirus (Cortez and Duffy, 2021). Importantly, accounting for interspecific competition may qualitatively alter predictions of diversity-disease relationships. For example, using a mathematical model of infection dynamics and a high-resolution multisite dataset, Luis et al. (2018) found that the prevalence of hantavirus decreased as small mammal diversity increases. However, competition effects, which cause hosts (deer mice) to congregate in refuges far from their main competitors, leading to increased host-to-host contact and thus increased incidence. Therefore, species diversity concurrently dilutes and amplifies disease transmission through competing mechanisms. Similarly, Strauss et al. (2015) used a general trait-based model and found that varying the relationship between the host's ability to compete and its potential to transmit disease could produced three different outcomes: a dilution effect, an amplification effect, and no significant effect. These findings highlight the need for a better understanding of how interspecific competition affects disease ecology in multi-host communities. Although there have been several studies on the effect of host competition on disease transmission, to the best of our knowledge, few research has examined the situation of a vector-borne system (but see Marini et al., 2017).

The purpose of this paper is twofold. On the one hand, to investigate the combined effects of vector feeding preference and host interspecific competition on vector-borne infection ecology. On the other hand, to explore the exact conditions under which diversity amplification or dilution occurs. To this end, we developed a simple compartment model with two competing host species and one vector, based on the SIS framework, to describe the transmission dynamics of a vector-borne system. The basic reproduction number R_0 is used to quantify disease risk, which has been used to identify the conditions under which disease risk would increase or decrease in a multi-host community (Roberts and Heesterbeek, 2013; O'Regan et al., 2015). We found that the conversion of a disease from being extinct to becoming endemic can be made possible by changing the intensity of competition, and that the direction of the effect of competition on disease risk (increasing or decreasing) can be shifted by a combination of vector preference and host competence. Importantly, incorporating vector preference and interspecific competition into a simple model changes the outcomes of how increasing species richness affects disease risk. These findings underscore the importance

of linking vector preference, interspecific competition, and host competence in describing vector-borne infection ecology.

Materials and methods

Model description

Mathematical models have been widely used to study complicated ecological processes. Many previous studies have used SIS or SIR compartmental models as a theoretical framework to analyze transmission dynamics in multi-host systems (Dobson, 2004; O'Regan et al., 2015). Similar to the models proposed by Lord et al. (1996) and Simpson et al. (2012), we constructed a simple compartment model with two hosts and one vector, both of which were classified according to whether they are susceptible S or infected I. We refer to host species 1 as the focal host that is a permanent community resident and host species 2 as the introduced host. Assuming that host species 1 and species 2 can compete with each other for resources (Kambatuku et al., 2010), and pathogens can only be transmitted indirectly through the vector, not directly through host-to-host transmission. Vectors feed on both host species, but with different feeding preferences. To simplify the model formulation and analysis, we assumed that infected hosts could die from disease or recover as susceptible individuals, but the vector could not recover from infection.

To model interspecific competition between two host species, as in O'Regan et al. (2015) and Marini et al. (2017), we assumed that the growth of both host species follows Lotka–Volterra dynamics. The following set of differential equations can be used to illustrate the model:

$$\begin{aligned}
\frac{dN_1}{dt} &= r_1 N_1\left(1-\frac{N_1+c_{12}N_2}{K_1}\right)-\mu_1 I_1\\
\frac{dN_2}{dt} &= r_2 N_2\left(1-\frac{N_2+c_{21}N_1}{K_2}\right)-\mu_2 I_2\\
\frac{dN_v}{dt} &= r_v N_v-\mu_v I_v\\
\frac{dI_1}{dt} &= \frac{P_{v1}b_1 I_v S_1}{N_1}-d_1 I_1-\delta_1 I_1-\mu_1 I_1\\
\frac{dI_2}{dt} &= \frac{P_{v2}b_2 I_v S_2}{N_2}-d_2 I_2-\delta_2 I_2-\mu_2 I_2\\
\frac{dI_v}{dt} &= \frac{P_{1v}b_1 I_1}{N_1}S_v+\frac{P_{2v}b_2 I_2}{N_2}S_v-d_v I_v-\mu_v I_v
\end{aligned}. \tag{1}$$

Where S_i and I_i represent the number of susceptible and infected individuals of species i, respectively, and $N_i$represents the total population size of species i,$N_i = S_i + I_i$ (i = 1, 2, v). c_{ij} represents the competition coefficient of species j on species i. K_1 and K_2 denote the carrying capacities of hosts 1 and 2, respectively. Previous studies have suggested that the transmission of pathogens in vector-borne systems follows a frequency-dependent mode. That is, the total number of bites per unit time by a single vector is independent of the host density (Dobson, 2004; Cortez and Duffy, 2021), therefore the incidence $\frac{P_{vi}b_i I_v S_i}{N_i}$ and $\frac{P_{iv}b_i I_i S_v}{N_i}$ denote the number of infected individuals per unit time for host species i and vector, respectively. To simplify notation, we let $\Gamma_i = d_i + \delta_i + \mu_i$ and $\Gamma_v = d_v + \mu_v$, which denote the per capita removal rate from the I_i class and I_v class, respectively. All parameters and definitions are listed in **Table 1**.

Model analysis

As mentioned above, we used the basic reproduction number R_0 as a measure of disease risk. It identifies the number of secondary infections induced by an infected host individual during the disease duration and the lifespan of the vector (Roberts and Heesterbeek, 2013). If $R_0 < 1$, the disease eventually disappears, otherwise, the disease will break out and become endemic. The basic reproduction number R_0 of system (1) is calculated by using the next-generation matrix approach, which involves linearizing the system at the disease-free equilibrium (N_1^*, N_2^*, N_v^*) and decomposing the resulting Jacobian matrix into two matrices, F and V, which describe the disease transmission and transitions out of the infection state, respectively. The dominant eigenvalue of the next-generation matrix is the basic reproduction number R_0 (Diekmann et al., 2009; Roberts and Heesterbeek, 2013).

The disease-free non-trivial equilibrium point can be found by setting the first three equations of system (1) to 0:

$$N_1^* = \frac{K_1 - c_{12}K_2}{1 - c_{12}c_{21}}, N_2^* = \frac{K_2 - c_{21}K_1}{1 - c_{12}c_{21}}, N_v^* = K_v.$$

Specifically, if there is no host interspecific competition, i.e., $c_{12} = c_{21} = 0$, then $N_1^* = K_1, N_2^* = K_2, N_v^* = K_v$.

Here the epidemiological transmission matrix F at the disease-free equilibrium point (N_1^*, N_2^*, N_v^*) is,

$$F = \begin{pmatrix} 0 & 0 & P_{v1}b_1 \\ 0 & 0 & P_{v2}b_2 \\ \frac{P_{1v}b_1 N_v^*}{N_1^*} & \frac{P_{2v}b_2 N_v^*}{N_2^*} & 0 \end{pmatrix},$$

and the epidemiological transition matrix V is,

$$V = \begin{pmatrix} d_1+\delta_1+\mu_1 & 0 & 0 \\ 0 & d_2+\delta_2+\mu_2 & 0 \\ 0 & 0 & d_v+\mu_v \end{pmatrix} = \begin{pmatrix} \Gamma_1 & 0 & 0 \\ 0 & \Gamma_2 & 0 \\ 0 & 0 & \Gamma_v \end{pmatrix}$$

Therefore, the next-generation matrix M is,

$$M = FV^{-1} = \begin{pmatrix} 0 & 0 & \frac{P_{v1}b_1}{\Gamma_v} \\ 0 & 0 & \frac{P_{v2}b_2}{\Gamma_v} \\ \frac{P_{1v}b_1 N_v^*}{N_1^*\Gamma_1} & \frac{P_{2v}b_2 N_v^*}{N_2^*\Gamma_2} & 0 \end{pmatrix}.$$

The dominant eigenvalue of M is the basic reproduction number R_0 of system (1),

$$R_0 = \sqrt{\frac{P_{v1}P_{1v}b_1^2 N_v^*}{N_1^*\Gamma_1\Gamma_v} + \frac{P_{v2}P_{2v}b_2^2 N_v^*}{N_2^*\Gamma_2\Gamma_v}}. \tag{2}$$

TABLE 1 Parameters and definitions.

Parameter	Definition
S_i	Number of susceptible individuals of species i (i = 1, 2, v, the same below)
I_i	Number of infected individuals of species i
N_i	Total population size of species i,$N_i = S_i + I_i$
r_i	The growth rate of species i
d_i	Per capita natural death rate of species i
δ_i	Per capita recovery rate of species i (i = 1, 2)
μ_i	Per capita disease-induced death rate of species i
c_{ij}	The effect of competition of species j on species i ($i, j \in \{1, 2\}$, $i \neq j$)
p_{vi}	The efficiency that an infected vector would infect a susceptible individual of host species i during one feeding event
p_{iv}	The efficiency that an infected individual of host species i would infect a susceptible vector during one feeding event
b_i	Biting rate between the vector and host species i
$b_{\max}$	The daily biting rate of the vector to the entire community, $b_{\max} = b_1 + b_2$
K_i	Carrying capacity of species i
Γ_i	Per capita removal rate from the I_i class, $\Gamma_i = d_i + \delta_i + \mu_i$ (i = 1, 2)
Γ_v	Per capita removal rate from the I_v class, $\Gamma_v = d_v + \mu_v$
α	The vector's feeding preference to host species 1 compared to that of species 2
g_i	The transmission ability of the host species i
γ	The transmission ratio of host species 1–2, i.e., $\gamma = g_1/g_2$

Let $g_i = \frac{p_{vi}p_{iv}}{\Gamma_i}$ (i = 1, 2), according to Table 1, this parameter characterizes the transmission efficiency that an infected host species i successfully infects a conspecific individual ($p_{vi}p_{iv}$) *via* the vector during its disease duration ($1/\Gamma_i$), thus representing the competence of host species i. The higher the g_i, the greater the ability of host species i to transmit disease. Substitute g_i into Eq. 2, it can be simplified to

$$R_0 = \sqrt{\frac{g_1 b_1^2 N_v^*}{N_1^* \Gamma_v} + \frac{g_2 b_2^2 N_v^*}{N_2^* \Gamma_v}}. \tag{3}$$

As shown in Eq. 3, one of the key factors to determining disease transmission potential and how R_0 varies with species richness is how the bites are divided between the two host species, b_1 and b_2, representing the biting rates of the vector to species 1 and 2, respectively. Assuming that host density is high enough not to limit the biting rate of the vector so that the vector has a fixed daily biting rate $b_{\max}$ (Rogers, 1988). If a vector has no preference for any hosts, then the biting rate of the vector for a specific host is determined by the density of the host (Marini et al., 2017), therefore $b_i = b_{\max} \cdot \frac{N_i}{N_1+N_2}$, $i = 1, 2$. However, if host species i is preferred, i.e., $\frac{b_i}{b_{\max}} > \frac{N_i}{N_1+N_2}$, as in Simpson et al. (2012) and Miller and Huppert (2013), we introduced a preference parameter α to represent the feeding preference of the vector, which represents the feeding preference of the vector for host species 1 relative to species 2. From this, the biting rate becomes

$$b_1 = b_{\max} \cdot \frac{\alpha N_1}{\alpha N_1 + N_2}, b_2 = b_{\max} \cdot \frac{N_2}{\alpha N_1 + N_2}.$$

Note that when $\alpha = 1$, the vector has no preference for any host and when $\alpha > 1$, the vector prefers host 1, and vice versa.

Substituted b_1, b_2 into Eq. 3, it becomes

$$R_0 = \frac{b_{\max}}{\alpha^2 N_1^* + N_2^*} \sqrt{\frac{(\alpha^2 g_1 N_1^* + g_2 N_2^*) N_v^*}{\Gamma_v}}. \tag{4}$$

By analyzing and numerically simulating Eq. 4, we can figure out how vector preference and host interspecific competition affect disease risk in vector-borne systems.

Another major purpose of this study is to explore the exact conditions under which diversity amplification or dilution occurs. Analytical results of the effect of host species richness on disease risk were obtained *via* a single- and two-host species community comparison. To this end, we calculated the basic reproduction number R_0^1 of a community composed of a single host species (focal host) and compared it to the community composed of focal and alternative host species. The calculation of R_0^1 is similar to the process of calculating R_0 (see Supplementary material), and we obtained

$$R_0^1 = \sqrt{\frac{g_1 b_{\max}^2 N_v^*}{N_1^* \Gamma_v}}.$$

To explore the conditions under which the dilution effect occurs, we need to find the conditions in which disease risk is reduced in a community consisting of a focal and introduced host species compared to a community with only the focal host species, i.e., $R_0 < R_0^1$. If this inequality holds, it is equivalent to

$$\frac{g_1 b_1^2 N_v^*}{N_1^* \Gamma_v} + \frac{g_2 b_2^2 N_v^*}{N_2^* \Gamma_v} < \frac{g_1 b_{\max}^2 N_v^*}{N_1^* \Gamma_v} \tag{5}$$

When Eq. 5 holds, the dilution effect will occur. Otherwise, there will be an amplification effect.

To simplify Eq. 5, a dimensionless parameter $\gamma = g_1/g_2$ is introduced to measure the host competence of species 1 relative to 2, which we define as the transmission ratio. When $\gamma = 1$, the two hosts were comparable in their ability to transmit disease, and when $\gamma > 1$ or $0 < \gamma < 1$, the more competent host is species 1 or 2, respectively.

Next, we will find out the conditions that satisfy Eq. 5 under each of the four combinations with or without vector preference and with or without host interspecific competition. (i) When the vector has no preference for any host ($\alpha = 1$) and there is no interspecific competition between hosts ($c_{12} = c_{21} = 0$), the non-trivial disease-free equilibrium point is $N_1^* = K_1, N_2^* = K_2, N_v^* = K_v,$, and the biting rate $b_i = b_{\max} \cdot \frac{K_i}{K_1+K_2}$, substitute these parameters into Eq. 5, it is equivalent to $g_2 < g_1(2 + \frac{K_2}{K_1})$. Since $\gamma = g_1/g_2$, the expression becomes $\gamma > \frac{K_1}{2K_1+K_2}$. That is, when there is no vector preference and no interspecific competition, as long as $\gamma > \frac{K_1}{2K_1+K_2}$ holds, the dilution effect can occur. (ii) When there is both vector preference and host interspecific competition (i.e., $\alpha \neq 1, c_{12}, c_{21} > 0$), then

$$N_1^* = \frac{K_1 - c_{12}K_2}{1 - c_{12}c_{21}}, N_2^* = \frac{K_2 - c_{21}K_1}{1 - c_{12}c_{21}}, N_v^* = K_v,$$

and $b_1 = b_{\max} \cdot \frac{\alpha N_1}{\alpha N_1+N_2}, b_2 = b_{\max} \cdot \frac{N_2}{\alpha N_1+N_2}$.

In the same way, by substituting these parameters into Eq. 5, it is possible to derive the following criteria for the occurrence of the dilution effect:

$$\gamma > \frac{K_1 - c_{12}K_2}{2\alpha(K_1 - c_{12}K_2) + K_2 - c_{21}K_1}.$$

Note that in this scenario, if interspecific competition is symmetric ($c_{12} = c_{21}$) and both hosts have the same carrying capacity ($K_1 = K_2$), the above inequality is simplified to $\gamma > \frac{1}{2\alpha+1}$, i.e., whether dilution or amplification occurs in this case is only related to vector preference α and transmission ratio γ. The calculation of the conditions for the dilution effect in the other two scenarios (with preference, without competition, or without preference, with competition) is similar to the above. **Table 2** provides a summary of the analytical conditions for the model parameters for which Eq. 5 is valid.

TABLE 2 The analytical conditions for the criterion of $R_0 < R_0^1$ in four different cases.

	Without vector preference	Vector preference
Without host interspecific competition	$\gamma > \frac{K_1}{2K_1+K_2}$	$\gamma > \frac{K_1}{2\alpha K_1+K_2}$
Host interspecific competition	$\gamma > \frac{K_1-c_{12}K_2}{K_1(2-c_{21})+K_2(1-2c_{12})}$	$\gamma > \frac{K_1-c_{12}K_2}{2\alpha(K_1-c_{12}K_2)+K_2-c_{21}K_1}$

Results

The effects of host interspecific competition on R_0

To exclude the impact of the presence of other factors on the outcomes, focusing on how interspecific competition affect R_0, we first investigated the situation where there is no vector preference and both hosts have the same ability to transmit disease. We assumed that the vector bites hosts based on their density, with a daily biting rate $b_{\max} = 0.3$ and the disease transmission ratio $\gamma = 1$. As seen in **Figure 1A** (left panel), the maximum R_0 occurs when both the competition coefficient c_{12} and c_{21} are high (top right), whereas the minimum R_0 occurs when both c_{12} and c_{21} are very low (bottom left). For a fixed value of c_{ij}, an increase in c_{ji} will increase R_0. Moreover, we also found that even when all other parameters are held constant, a change in c_{12} and c_{21} will make R_0 changes from less than 1 to larger than 1 (R_0 ranges from 0.85 to 1.18). That is, by changing the intensity of competition, the disease may change from extinction to endemic. Secondly, we relaxed the restrictions to consider the scenarios where there is vector preference and differences in host competence. To do this, we simulated the following parameter combinations of $\gamma, \alpha \in \{0.5, 1, 2\} \times \{0.5, 1, 2\}$ (**Supplementary Figure 1**). In each subplot of **Supplementary Figure 1**, when the competition coefficients c_{12} and c_{21} are large, R_0 is large, and vice versa. For a fixed value of c_{ij}, R_0 increases with the increase of $c_{ji}(i, j = 1, 2)$, these findings were consistent with the results in **Figure 1**. In addition, we found that for the constant values of $c_{12}$and c_{21}, the larger γ is, the larger R_0 is, especially when the preferred host is the highly competent one (see **Supplementary Figure 1**).

In **Figure 1B** (right panel), we showed how the effect of interspecific competition on R_0 is influenced by the biting rate, which we set $b_{\max} = 0.1, 0.2, 0.3$, respectively. We found that for a fixed interspecific competition coefficient, the larger $b_{\max}$ is, the larger R_0 is. At each value of $b_{\max}$, R_0 increases linearly with $c_{12} = c_{21}$. Since there is no significant difference in the results for any of the three values of $b_{\max}$, we only consider the case of $b_{\max} = 0.3$ in the following study.

Next, we investigated how interspecific competition coefficient c_{12} affects R_0 in the presence of vector preference and differences in host competence (i.e.,$\alpha \neq 1, \gamma \neq 1$) (**Figure 2**). The horizontal axis represents the competition effect of host species 2 on species 1 (i.e., c_{12}), and the vertical axis represents R_0. As can be seen from **Figure 2**, for a fixed c_{12}, the larger the transmission ratio γ, the larger the R_0, especially when the preferred host is a highly competent one. As c_{12}increases, R_0 shows a non-linear trend, increasing or decreasing depending on the combined effect of transmission ratio γ and vector preference α, suggesting that vector feeding preference and differences in host competence may shift the direction of the effect of interspecific competition on R_0 .

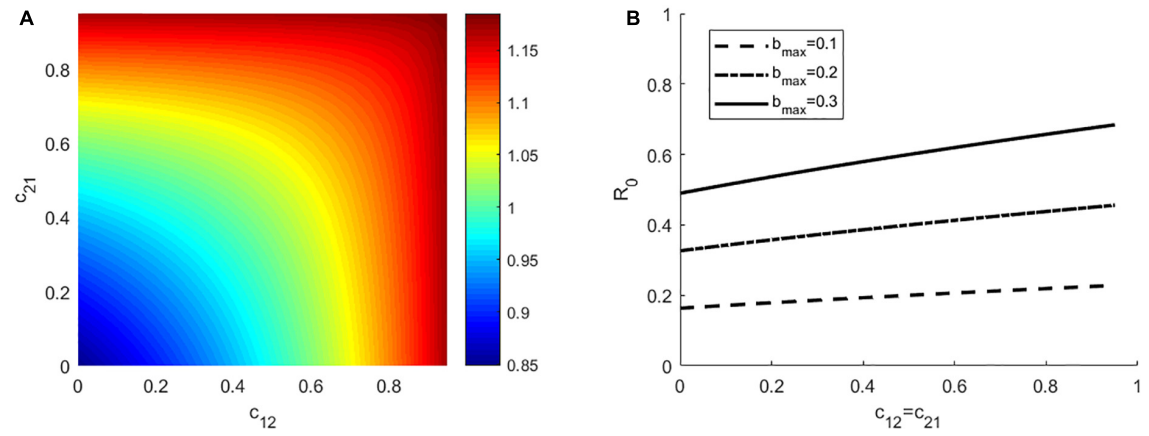

FIGURE 1
(A) The effect of interspecific competition on R_0. **(B)** The effect of interspecific competition (only for $c_{12} = c_{21}$) on R_0at three different values of b_{max} = 0.1, 0.2, 0.3, respectively. In panel **(A)**, b_{max} = 0.3, the other parameters in the two panels have the same values as: $\alpha = 1$, $\gamma = 1$, $K_1 = K_2 = 1000$, $K_v = 4000$, $\Gamma_v = 0.1$, $g_1 = g_2 = 0.4$.

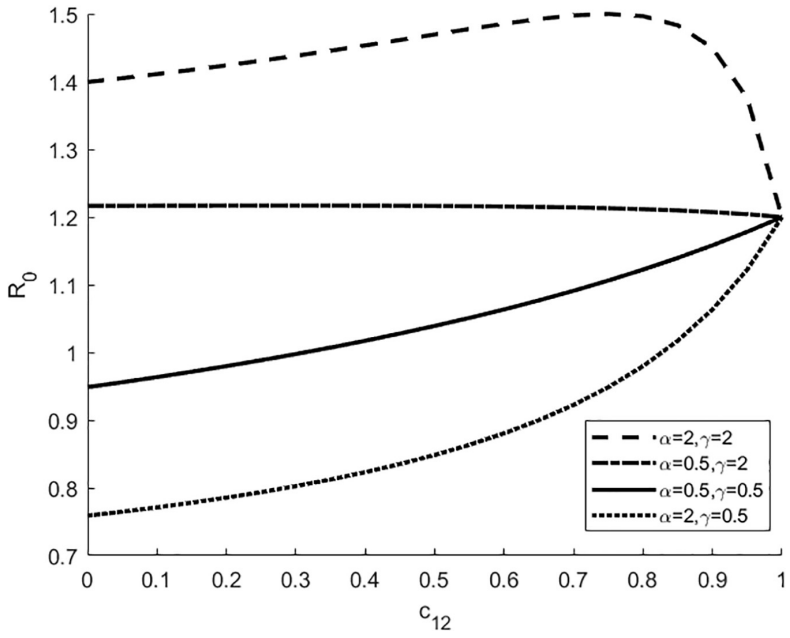

FIGURE 2
R_0 according to interspecific competition coefficient c_{12} in the presence of vector preference and differences in host competence. The four lines represent four different combinations of vector preferences α and transmission ratios γ. Here $c_{21} = 0.5$, b_{max} = 0.3, $K_1 = K_2 = 1000$, $K_v = 4000$, $\Gamma_v = 0.1$, $g_2 = 0.4$.

The effects of vector preference on R_0

Vector feeding preferences can lead to heterogeneity in host-vector contact, which may affect disease dynamics. To understand the effect of vector preference on disease transmission potential, we first assumed that there was no interspecific competition between hosts. In Figure 3, the horizontal axis represents the feeding preference index α, which ranges from 0 to 2, and the vertical axis represents R_0. It can be seen from Figure 1 that as α increases, R_0may increase, decrease, or vary slightly, depending on the host transmission ratio γ. If species 1 is the more competent host at this time ($\gamma > 1$), then R_0increases with the increase of α. On the contrary, if species 1 is the lower competent host, then R_0decreases as αincreases. When the two hosts are comparable in their competence ($\gamma = 1$), R_0varies within a small range as α increases. In fact, in this

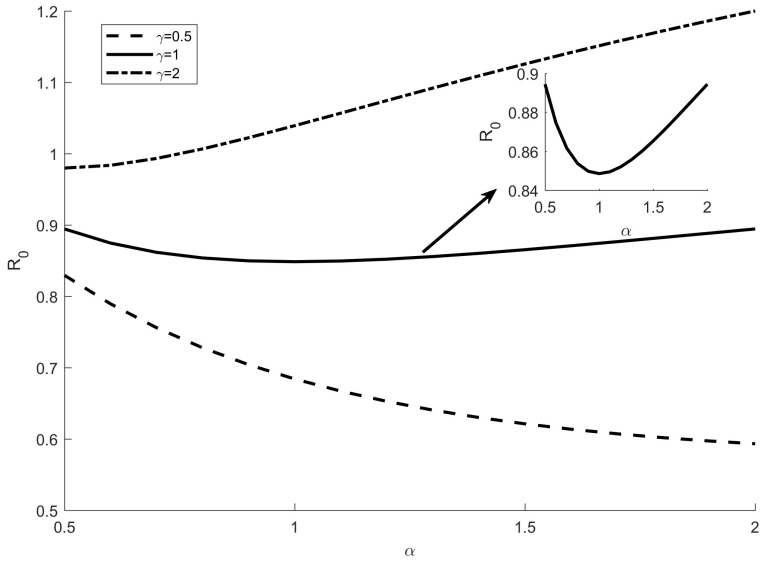

FIGURE 3
The effect of vector preference α on R_0 without host interspecific competition. Different lines represent the results of different values of the transmission ratio γ. The inset of figure shows the case of $\gamma = 1$ when narrowing the vertical axis. The other parameters are: $c_{12} = c_{21} = 0$, $b_{max} = 0.3$, $K_1 = K_2 = 1000$, $K_v = 4000$, $\Gamma_v = 0.1$, $g_2 = 0.4$.

case, when we narrow the range of the vertical axis (the inset graph of Figure 3), we find that R_0 first decreases and then increases as α increases, and when the vector has no preference for any hosts ($\alpha = 1$), R_0 takes the minimum value.

Secondly, we considered the effect of vector preference α on R_0 in the presence of interspecific competition by simulating different competition coefficient combinations (Supplementary Figure 2). Different panels of Figure 2 refer to different values of (c_{12}, c_{21})that assume the values of 0.1, 0.5, 0.9. It was found that there is no qualitative difference with the results in Figure 3, except that when species 1 is a less competent host or the two hosts are comparable in their competence. As α increases, the magnitude of the decrease of R_0 is lower than that in the absence of interspecific competition (Figure 3). All these results indicate that the presence or absence of interspecific competition quantitatively but not qualitatively changes the effect of vector preference on R_0 .

Dilution effect versus amplification effect

Table 2 summarizes the analytical conditions that are satisfied $R_0 < R_0^1$ under each of the four combinations with or without vector preference and with or without host interspecific competition (see section "Materials and methods"). In this section, we focused on how interspecific competition, vector preference, and host competence affect the occurrence of dilution effects. According to Table 2, when both interspecific competition and vector preference exist, a dilution effect can occur when

$$\gamma > \frac{K_1 - c_{12}K_2}{2\alpha(K_1 - c_{12}K_2) + K_2 - c_{21}K_1}.$$

Conditions for $\gamma = \frac{K_1 - c_{12}K_2}{2\alpha(K_1 - c_{12}K_2) + K_2 - c_{21}K_1}$ (i.e., $R_0 = R_0^1$) were represented by a linear configuration of vector preference α and the transmission ratio γ, the line divided α-γ parameter space into disjoint regions for which dilution and amplification effects were exhibited (Figure 4). Different lines represent different competition intensities of c_{12}, which are taken as 0.1, 0.5, and 0.9, respectively. On the upper right side of each line, it shows the parameter area where the dilution effect happens (symbol DE). On the lower left side of each line, it shows the parameter area where the amplification effect happens (symbol AE).

As shown in Figure 4, adding new species to a community can lead to both a dilution effect and an amplification effect, depending on the values of α and γ. When the focal species (species 1) is a highly competent host and the vector prefers the focal species, the addition of the introduced species (species 2) dilutes the proportion of the focal species and reduces the effective contact between the focal species and the vector, resulting in a dilution effect ($R_0 < R_0^1$) (the upper right area of Figure 4). Conversely, when the introduced species is a highly competent host and the vector prefers the introduced species, the addition of the introduced species results in a higher disease risk compared to the community containing only the focal host, and thus an amplification effect occurs ($R_0 > R_0^1$) (the lower left

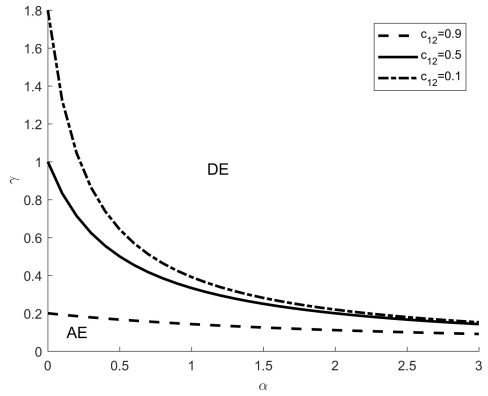

FIGURE 4
Analytical relationships for combinations of interspecific competition, vector preference and transmission ratio. The dotted and solid lines represent parameter sets (α,γ) for which $R_0 = R_0^1$ under different competition intensity c_{12}. These lines divided $\alpha - -\gamma$ parameter space into disjoint regions where dilution and amplification effects were exhibited. The upper right of each line represents parameter pairs for which a dilution effect occurs (symbol DE), whereas the lower left of each line represents parameter pairs for which an amplification effect occurs (symbol AE). The other parameters are: $K_1 = K_2 = 1000$, $c_{21} = 0.5$.

part of **Figure 4**). In addition, for a fixed value of c_{21}, the larger the c_{12}, the larger the parameter area where the dilution effect can occur, and vice versa.

Discussion

Understanding how ecological interactions and significant ecological factors affect vector-borne disease dynamics is crucial given the rapid loss of biodiversity and the rise in newly emerging vector-borne diseases (Rivera et al., 2020). In this study, we constructed a simple compartment model with two competing host species and one vector, in which the vector has different preferences for the hosts, to study the combined impact of vector feeding preferences and host interspecific competition on vector-borne infection ecology. Furthermore, we investigated the relationship between host species richness and disease risk by comparing disease risk R_0 in single- and two-host communities. We demonstrated that disease transmission dynamics in multi-host communities are more complex than anticipated, highlighting the significance of linking vector preference, interspecific competition, and host competence in describing vector-borne infection ecology. More specifically, we found that vector preference and differences in host competence shifted the direction of the effect of competition on R_0, yet interspecific competition quantitatively but not qualitatively changed the effect of vector preference on R_0. Furthermore, this study quantified the conditions of dilution effect and amplification effect, and clarified that incorporating vector preference and interspecific competition into a simple two-host-one-vector model changes the outcomes of how increasing species richness affects disease risk R_0.

For vector-borne diseases, the dynamics of pathogen transmission depend on the ability of host species to maintain and transmit disease and on ecological factors such as interspecific competition and contact rate between hosts and vectors (Simpson et al., 2012). Interspecific competition can either increase R_0 by increasing the vector/host ratio or decrease R_0 by decreasing the density of the host population (Marini et al., 2017), the general pattern of the effect of competition on R_0 is hard to predict, and whether competition has a positive or negative effect on R_0 depends largely on host preferences and host competence. We also found that R_0 is strongly influenced by vector feeding preference. R_0 increases with the increase of vector preference, as long as the preferred host is a highly competent host. The reason for this phenomenon may be that vector preference allows a large number of bites to be concentrated on the preferred host, increasing the effective contact between the vector and highly competent hosts, thereby increasing the efficiency of disease transmission. In fact, these findings have been confirmed in some field experiments and theoretical studies. For example, if all individuals in the community have the same ability to transmit disease, vector-host contact heterogeneity owing to vector preference can increase the risk of disease outbreak (Woolhouse et al., 1997; Miller and Huppert, 2013). These facts tell us that it is important to be scientific and rational in developing disease control strategies, and that if the control measures are not appropriate, they may be counterproductive. For example, for a population with identical individuals, selective use of insect repellent will result in a higher concentration of vectors on the unprotected individuals, which is equivalent to the vector feeding preference, the disease risk R_0 may rise rather than fall (Miller and Huppert, 2013).

Whether increased host species richness results in greater or lower disease risk has been controversial in the literature, leading to calls for theoretical studies on what conditions promote amplification versus dilution (Buhnerkempe et al., 2015; Halsey, 2018). Many previous studies on the biodiversity-diseases risk relationship have demonstrated that when diseases are transmitted in a frequency-dependent mode, an increase in species richness decreases the community R_0 (Dobson, 2004; Rudolf and Antonovics, 2005; Rohr et al., 2019). However, an interesting finding of this study is that, even in frequency-dependent transmission mode, the introduction of new species to a community may increase or decrease disease risk if interspecific competition and contact heterogeneity due to vector preference are taken into account, which is in contrast to the results of previous studies. The reason for this phenomenon can be understood from the mechanism of the dilution effect. Keesing et al. (2006) constructed a general mathematical model framework and proposed five mechanisms by which dilution

effects occur. Among them, encounter reduction and susceptible host regulation have been confirmed in many empirical studies (Allan et al., 2009; Johnson and Thieltges, 2010). In a vector-borne disease system, encounter reduction refers to the presence of additional species that affects host behavior, reduces the probability of contact between vector and host, or influences vector behavior, decreasing the likelihood that susceptible individuals will become infected individuals (Clay et al., 2009). Susceptible host regulation refers to the fact that the addition of new host species to a community regulates susceptible host numbers through interspecific interactions such as competition or predation (Keesing et al., 2006). If the above assumptions are satisfied, an increase in species richness may lead to a dilution effect. Conversely, if the introduced host is a highly competent host or one that the vector prefers to feed on, or if the introduced host has strong interspecific competition ability, which reduces the frequency of low competent hosts through interspecific competition, then an increase in species richness will increase the communityR_0, whereby an amplification effect occurs. This explains, to some extent, why an amplification effect can occur in the frequency-dependent transmission mode. Our study emphasizes the need to focus not only on the transmission mode of disease, but also on interspecific interactions (interspecific competition and vector-host contact rate) and host competence (Cortez and Duffy, 2021; Su et al., 2022).

Although mathematical models have been widely used to study complex ecological phenomena, explaining and validating many empirical studies, there are still several limitations (O'Regan et al., 2015). In fact, the two-host-one-vector Lotka–Volterra competition model used in this study is very simplistic compared to the complexity of real community ecology. For example, we only compared disease risk R_0 when pathogen was transmitted in single- and two-host communities, despite the fact that natural communities can have dozens of host species. We focused only on the effect of interspecific competition on disease risk, ignoring the possible effect of intraspecific competition. Moreover, we used the basic reproduction number R_0 as a measure of community disease risk, which is challenging to estimate in field and empirical studies and does not allow for comparisons between studies (Roberts and Heesterbeek, 2018; Cortez and Duffy, 2021). In addition, we ignored some ecological factors that could affect the potential of outbreaks, including the seasonal variation in vector feeding preference (Burkett-Cadena et al., 2012; Marini et al., 2017) and demographic stochasticity (Dizney and Ruedas, 2009). However, we believe that this study of a simplified scenario provides a theoretical framework for incorporating interspecific competition, vector preference and host competence into vector-borne systems. Our work emphasizes the significance of ecological interactions in determining infection dynamics in a multi-host vector system, and contributes to explaining some of the variation in outcomes in previous empirical and theoretical studies on the dilution effect.

Data availability statement

The original contributions presented in the study are included in the article/**Supplementary material**, further inquiries can be directed to the corresponding author.

Author contributions

LC and SC designed the study and analyzed the model. LC and PK performed the software. LC and LZ drafted the manuscript. All authors have read and approved the manuscript.

Funding

This work was supported by the National Natural Science Foundation of China (31700466 and 82072228), the Foundation of National Key R&D Program of China (2020YFC2008700), the Foundation of Shanghai Municipal Commission of Economy and Informatization (202001007), and the Special Project of Health Shanghai Action (2022–2024).

Acknowledgments

We are grateful to the editor and the reviewers for their constructive comments.

Conflict of interest

The authors declare that the research was conducted in the absence of any commercial or financial relationships that could be construed as a potential conflict of interest.

Publisher's note

Supplementary material

The Supplementary Material for this article can be found online at: https://www.frontiersin.org/articles/10.3389/fevo.2022.993844/full#supplementary-material

References

Allan, B. F., Langerhans, R. B., Ryberg, W. A., Landesman, W. J., Griffin, N. W., Katz, R. S., et al. (2009). Ecological correlates of risk and incidence of West Nile virus in the United States. *Oecologia* 158, 699–708. doi: 10.1007/s00442-008-1169-9

Buhnerkempe, M. G., Roberts, M. G., Dobson, A. P., Heesterbeek, H., Hudson, P. J., and Lloyd-Smith, J. O. (2015). Eight challenges in modelling disease ecology in multi-host, multi-agent systems. *Epidemics* 10, 26–30. doi: 10.1016/j.epidem.2014.10.001

Burkett-Cadena, N. D., Hassan, H. K., Eubanks, M. D., Cupp, E. W., and Unnasch, T. R. (2012). Winter severity predicts the timing of host shifts in the mosquito *Culex erraticus*. *Biol. Lett.* 8, 567–569. doi: 10.1098/rsbl.2012.0075

Clay, C. A., Lehmer, E. M., Jeor, S. S., and Dearing, M. D. (2009). Testing mechanisms of the dilution effect: Deer mice encounter rates, Sin Nombre virus prevalence and species diversity. *EcoHealth* 6, 250–259. doi: 10.1007/s10393-009-0240-2

Cortez, M. H., and Duffy, M. A. (2021). The context-dependent effects of host competence, competition, and pathogen transmission mode on disease prevalence. *Am. Nat.* 198, 179–194. doi: 10.1086/715110

Costa, S. V., Hibberts, S. J., Olive, D. A., Budd, K., Long, A., Meiling, S. S., et al. (2021). Diversity and disease: The effects of coral diversity on prevalence and impacts of stony coral tissue loss disease in Saint Thomas, U.S. Virgin Islands. *Front. Mar. Sci.* 8:682688. doi: 10.3389/fmars.2021.682688

Diekmann, O., Heesterbeek, J. A. P., and Roberts, M. G. (2009). The construction of next-generation matrices for compartmental epidemic models. *J. R. Soc. Interface* 7, 873–885. doi: 10.1098/rsif.2009.0386

Dizney, L. J., and Ruedas, L. A. (2009). Increased host species diversity and decreased prevalence of Sin Nombre virus. *Emerg. Infect. Dis.* 15, 1012–1018. doi: 10.3201/eid1507.081083

Dobson, A. (2004). Population dynamics of pathogens with multiple host species. *Am. Nat.* 164, S64–S78. doi: 10.1086/424681

Gürtler, R. E., Ceballos, L. A., Ordóñez-Krasnowski, P., Lanati, L., Stariolo, R., and Kitron, U. (2009). Strong host-feeding preferences of the vector *Triatoma infestans* modified by vector density: Implications for the epidemiology of chagas disease. *PLoS Negl. Trop. Dis.* 3:e447. doi: 10.1371/journal.pntd.0000447

Halliday, F. W., Heckman, R. W., Wilfahrt, P. A., and Mitchell, C. E. (2017). A multivariate test of disease risk reveals conditions leading to disease amplification. *Proc. R. Soc. B Biol. Sci.* 284:20171340. doi: 10.1098/rspb.2017.1340

Halliday, F. W., Heckman, R. W., Wilfahrt, P. A., and Mitchell, C. E. (2019). Past is prologue: Host community assembly and the risk of infectious disease over time. *Ecol. Lett.* 22, 138–148. doi: 10.1111/ele.13176

Halliday, F. W., Rohr, J. R., and Laine, A. L. (2020). Biodiversity loss underlies the dilution effect of biodiversity. *Ecol. Lett.* 23, 1611–1622. doi: 10.1111/ele.13590

Halsey, S. J. (2018). Defuse the dilution effect debate. *Nat. Ecol. Evol.* 3, 145–146. doi: 10.1038/s41559-018-0764-3

Johnson, P., and Thieltges, D. (2010). Diversity, decoys and the dilution effect: How ecological communities affect disease risk. *J. Exp. Biol.* 213, 961–970. doi: 10.1242/jeb.037721

Johnson, P. T., Preston, D. L., Hoverman, J. T., and Richgels, K. L. (2013). Biodiversity decreases disease through predictable changes in host community competence. *Nature* 494, 230–233. doi: 10.1038/nature11883

Kambatuku, J. R., Cramer, M. D., and Ward, D. (2010). Intraspecific competition between shrubs in a semi-arid Savanna. *Plant Ecol.* 212, 701–713. doi: 10.1007/s11258-010-9856-0

Keesing, F., Belden, L. K., Daszak, P., Dobson, A., Harvell, C. D., Holt, R. D., et al. (2010). Impacts of biodiversity on the emergence and transmission of infectious diseases. *Nature* 468, 647–652. doi: 10.1038/nature09575

Keesing, F., Holt, R. D., and Ostfeld, R. S. (2006). Effects of species diversity on disease risk. *Ecol. Lett.* 9, 485–498. doi: 10.1111/j.1461-0248.2006.00885.x

Kilpatrick, A. M., Daszak, P., Jones, M. J., Marra, P. P., and Kramer, L. D. (2006). Host heterogeneity dominates West Nile virus transmission. *Proc. R. Soc. B Biol. Sci.* 273, 2327–2333. doi: 10.1098/rspb.2006.3575

Liu, X., Lyu, S., Zhou, S., and Bradshaw, C. J. (2016). Warming and fertilization alter the dilution effect of host diversity on disease severity. *Ecology* 97, 1680–1689. doi: 10.1890/15-1784.1

LoGiudice, K., Ostfeld, R. S., Schmidt, K. A., and Keesing, F. (2003). The ecology of infectious disease: Effects of host diversity and community composition on Lyme disease risk. *Proc. Natl. Acad. Sci. U.S.A.* 100, 567–571. doi: 10.1073/pnas.0233733100

Lord, C. C., Woolhouse, M. E. J., Heesterbeek, J. A. P., and Mellor, P. S. (1996). Vector-borne diseases and the basic reproduction number: A case study of African horse sickness. *Med. Vet. Entomol.* 10, 19–28. doi: 10.1111/j.1365-2915.1996.tb00077.x

Luis, A. D., Kuenzi, A. J., and Mills, J. N. (2018). Species diversity concurrently dilutes and amplifies transmission in a zoonotic host–pathogen system through competing mechanisms. *Proc. Natl. Acad. Sci. U.S.A.* 115, 7979–7984. doi: 10.1073/pnas.1807106115

Marini, G., Rosá, R., Pugliese, A., and Heesterbeek, H. (2017). Exploring vector-borne infection ecology in multi-host communities: A case study of West Nile virus. *J. Theor. Biol.* 415, 58–69. doi: 10.1016/j.jtbi.2016.12.009

Miller, E., and Huppert, A. (2013). The effects of host diversity on vector-borne disease: The conditions under which diversity will amplify or dilute the disease risk. *PLoS One* 8:e80279. doi: 10.1371/journal.pone.0080279

Mitchell, C. E., Tilman, D., and Groth, J. V. (2002). Effects of grassland plant species diversity, abundance, and composition on foliar fungal disease. *Ecology* 83, 1713–1726. doi: 10.1890/0012-9658(2002)083[1713:EOGPSD]2.0.CO;2

O'Regan, S. M., Vinson, J. E., and Park, A. W. (2015). Interspecific contact and competition may affect the strength and direction of disease-diversity relationships for directly transmitted microparasites. *Am. Nat.* 186, 480–494. doi: 10.1086/682721

Ostfeld, R. S., and Keesing, F. (2000). Biodiversity series: The function of biodiversity in the ecology of vector-borne zoonotic diseases. *Can. J. Zool.* 78, 2061–2078. doi: 10.1139/z00-172

Ostfeld, R. S., and Keesing, F. (2012). Effects of host diversity on infectious disease. *Annu. Rev. Ecol. Evol. Sci.* 43, 157–182. doi: 10.1146/annurev-ecolsys-102710-145022

Ostfeld, R. S., and LoGiudice, K. (2003). Community disassembly, biodiversity loss, and the erosion of an ecosystem service. *Ecology* 84, 1421–1427. doi: 10.1890/02-3125

Rivera, R. M. C., Bilal, S., and Michael, E. (2020). The relation between host competence and vector-feeding preference in a multi-host model: Chagas and Cutaneous leishmaniasis. *Math. Biosci. Eng.* 17, 5561–5583. doi: 10.3934/mbe.2020299

Roberts, M. G., and Heesterbeek, J. (2013). Characterizing the next-generation matrix and basic reproduction number in ecological epidemiology. *J. Math. Biol.* 66, 1045–1064. doi: 10.1007/s00285-012-0602-1

Roberts, M. G., and Heesterbeek, J. A. P. (2018). Quantifying the dilution effect for models in ecological epidemiology. *J. R. Soc. Interface* 15:20170791. doi: 10.1098/rsif.2017.0791

Rogers, D. J. (1988). The dynamics of vector-transmitted diseases in human communities. *Philos. Trans. R. Soc. B Biol. Sci.* 321, 513–539. doi: 10.1098/rstb.1988.0106

Rohr, J. R., Civitello, D. J., Halliday, F. W., Hudson, P. J., Lafferty, K. D., Wood, C. L., et al. (2019). Towards common ground in the biodiversity–disease debate. *Nat. Ecol. Evol.* 4, 24–33. doi: 10.1038/s41559-019-1060-6

Rudolf, V. H., and Antonovics, J. (2005). Species coexistence and pathogens with frequency-dependent transmission. *Am. Nat.* 166, 112–118. doi: 10.1086/430674

Simpson, J. E., Hurtado, P. J., Medlock, J., Molaei, G., Andreadis, T. G., Galvani, A. P., et al. (2012). Vector host-feeding preferences drive transmission of multi-host pathogens: West Nile virus as a model system. *Proc. R. Soc. B Biol. Sci.* 279, 925–933. doi: 10.1098/rspb.2011.1282

Strauss, A. T., Civitello, D. J., Cáceres, C. E., and Hall, S. R. (2015). Success, failure and ambiguity of the dilution effect among competitors. *Ecol. Lett.* 18, 916–926. doi: 10.1111/ele.12468

Su, M., Jiang, Z., and Hui, C. (2022). How multiple interaction types affect disease spread and dilution in ecological networks. *Front. Ecol. Evol.* 10:862986. doi: 10.3389/fevo.2022.862986

Tirados, I., Costantini, C., Gibson, G., and Torr, S. J. (2006). Blood-feeding behaviour of the malarial mosquito *Anopheles arabiensis*: Implications for vector control. *Med. Vet. Entomol.* 20, 425–437. doi: 10.1111/j.1365-2915.2006.652.x

Vadell, M. V., Gómez Villafañe, I. E., and Carbajo, A. E. (2019). Hantavirus infection and biodiversity in the Americas. *Oecologia* 192, 169–177. doi: 10.1007/s00442-019-04564-0

Wood, C. L., Lafferty, K. D., DeLeo, G., Young, H. S., Hudson, P. J., and Kuris, A. M. (2014). Does biodiversity protect humans against infectious disease? *Ecology* 95, 817–832. doi: 10.1890/13-1041.1

Woolhouse, M. E. J., Dye, C., Etard, J. F., Smith, T. J., Charlwood, J. D., Garnett, G. P., et al. (1997). Heterogeneities in the transmission of infectious agents: Implications for the design of control programs. *Proc. Natl. Acad. Sci. U.S.A.* 94, 338–342. doi: 10.1073/pnas.94.1.338

World Health Organization [WHO] (2004). *Global strategic framework for integrated vector management*. Geneva: WHO.

Zeilinger, A. R., and Daugherty, M. P. (2014). Vector preference and host defense against infection interact to determine disease dynamics. *Oikos* 123, 613–622. doi: 10.1111/j.1600-0706.2013.01074.x

frontiers | Frontiers in Environmental Science

TYPE Original Research
PUBLISHED 15 September 2022
DOI 10.3389/fenvs.2022.1020873

OPEN ACCESS

EDITED BY
Xiang Liu,
Lanzhou University, China

REVIEWED BY
Yao Xiao,
Lanzhou University, China
Mu Liu,
Lanzhou University, China

*CORRESPONDENCE
Jie Cui,
443464199@qq.com
Hui Zhang,
zhanghuitianxia@126.com
Wenfeng Gong,
gwf101@163.com

†These authors have contributed equally to this work

SPECIALTY SECTION
This article was submitted to Conservation and Restoration Ecology, a section of the journal Frontiers in Environmental Science

RECEIVED 16 August 2022
ACCEPTED 25 August 2022
PUBLISHED 15 September 2022

CITATION
Wang L, Li Y, Cui J, Zhang H and Gong W (2022), Food plant diversity determines home range area and formation of a new family group of the world's rarest primate.
Front. Environ. Sci. 10:1020873.
doi: 10.3389/fenvs.2022.1020873

Food plant diversity determines home range area and formation of a new family group of the world's rarest primate

Lu Wang[1†], Yousheng Li[1†], Jie Cui[2*], Hui Zhang[1*] and Wenfeng Gong[1*]

[1]Key Laboratory of Genetics and Germplasm Innovation of Tropical Special Forest Trees and Ornamental Plants, School of Forestry, Hainan University, Haikou, China, [2]Development Research Center of People's Government of Sanya City, Sanya, China

Global primates are endangered, and thus it is important to know the determinants of primate population dynamics. It is widely reported that food plant diversity and nutrients are key determinants of many primate population dynamics. However, it remains unknown whether this can be applied to explain the population dynamics of Hainan gibbon (*Nomascus hainanus*), the world's rarest primate. Recently, two individuals moved out from one family group (group C) and went across more than 9 km to form a new family group (group E), thus providing a perfect chance to quantify whether food plant diversity and nutrients can determine Hainan gibbon's formation of the new family group. Here, we used a plot survey to compare the differences in food plant diversity (species richness and abundance) and nine leaf nutrient traits (leaf water content, total soluble sugar, vitamin C, calorific value, crude fat, crude protein, crude fiber, Zn, and Fe) between group C and group E. We found that plant diversity in group E was indeed higher (1.35–1.41 times) than that in group C. Moreover, in both groups C and E, food plant diversity within the home range was also higher (1.4–1.6 times) than that out of the home range. However, both cases could not be witnessed for all leaf nutrient traits. Results of principal component analysis revealed that food plant species between groups C and E were all significantly separated by food plant diversity but not leaf nutrient traits. Food plant species within and out of the home range of both groups C and E could also be significantly separated by food plant diversity, but not for all leaf nutrient traits. In conclusion, food plant diversity was one key determinant of the formation of a new family group of Hainan gibbons. Choosing high food plant diversity was also one key motivation for Hainan gibbons to select their home range.

KEYWORDS

food plant diversity and nutrients, Hainan gibbon, new formation of the family group, population dynamics, primate conservation, species recovery

Introduction

Globally, approximately 60% of primate species are at threat of extinction (Estrada et al., 2017). Among them, the critically endangered Hainan gibbon (*Nomascus hainanus*), the world's rarest primate, should have a high priority of conservation (Zou et al., 2022). That is because it is restricted to a single population of c.35 individuals within a single protected area, Bawangling National Nature Reserve (BNNR) in Hainan, China (Fellowes et al., 2008; Turvey et al., 2015; Chan and Lo, 2020). Thus, it is essential to perform an effective protection strategy to prevent the early extinction of the Hainan gibbon (Liu et al., 2020). However, without knowing the key determinants of Hainan gibbon population dynamics, it is impossible to make an effective conservation strategy (Turvey et al., 2015; Zhang et al., 2020).

A number of factors (i.e., climate, predation, and stress or disease) can affect Hainan gibbon population dynamics (Turvey et al., 2015), but the effect of food has typically been considered of paramount importance (Hanya and Chapman, 2013; Bach et al., 2017) That is because food is a fundamentally important resource of animals, and the adequacy of food directly affects animal behavior, growth, reproduction, population structure, and population dynamics (Zhao et al., 2013). Quantifying food diversity and nutrients is also a prerequisite for exploring the interaction mechanism between animals and habitats (Clink et al., 2017; Deng and Zhou, 2018). Primates will select a home range with high food tree diversity and high calorie likely as an adaptation for fluctuating food environments (Hladik and Simmen, 1996; Jang et al., 2021). Importantly, this "high-calorie bias" in primates' spatial memory seems to yield consequences for individual eating behavior in food-abundant settings (Arce et al., 2010; de Vries et al., 2022). It has been found that food abundance and distribution can directly determine primate ranging patterns and home range area (Milton and May 1976; Kim et al., 2011; Simmen et al., 2014; Ning et al., 2019). Thus knowledge of habitat and feeding ecology is essential for developing an effective conservation management plan for threatened primates (Fan et al., 2021).

In 2019, two individuals moved out from one family group (group C) and went across more than 9 km to form a new family group (group E) (Zou et al., 2022). As a result, quantifying the differences in food plant diversity and nutrients between group C and group E can provide a perfect chance to reveal 1) whether choosing high food plant diversity or/and nutrients was one key motivation for group C and E to select their home range and 2) whether the formation of a new family gibbon group (group E) is determined by food diversity or/and nutrients. We hypothesized that food plant diversity and nutrients determined both gibbon home range selection and formation of the new family group.

To test this hypothesis, we evaluated differences in food plant diversity and nutrients within and out of home range in groups C and E and between groups C and E by examining the following: 1) food plant diversity (richness and abundance) in 20 plots of 400 m^2 each and 2) nine leaf nutrient traits (leaf water content, total soluble sugar, vitamin C, calorific value, crude fat, crude protein, crude fiber, Zn, and Fe) for all food plant species. Fruit is the favorite for Hainan gibbon, but in the dry season, Hainan gibbons use leaves as fallback food, and when they fed on a higher percentage of leaves, they decreased traveling time (Deng and Zhou, 2018). Based on the phenology of food plant species, it is impossible to provide fruits for all food plant species in 1 or 2 months (Du et al., 2020), which will make measuring fruit nutrients to perform fruit nutrient comparison impossible. Thus, we choose to measure leaf nutrient traits.

The selection of these nine leaf nutrient traits is based on their strong associations with primate population dynamics (growth, abundance, home range, and so on). For example, some gibbons (white-handed gibbons) primarily meet their water requirement by consuming immature leaves as they rarely drink from open water sources (Jildmalm et al., 2008). Maintaining the required calorie value is key for the survival of primates (Grether et al., 1992). Sugar makes food attractive because of its sweet taste and rich sensation (Huang et al., 2021). Since mature leaves have higher crude fiber content but lower crude protein than young leaves (Yeager, 1989), gibbons usually prefer to eat young leaves but not mature leaves. However, some primates, such as the Colobine monkey, prefer leaves with high crude fiber (Borah et al., 2021). Fat serves as an energy reserve of the animal body, and primates usually store surplus energy as fat in preparation for the impending period of food scarcity (Felton et al., 2009). Vitamin C is essential for growth, development, and tissue repair of animals through collagen synthesis (Lee et al., 2022), and primates will suffer from vitamin deficiency or multivitamin deficiency syndrome when they eat leaves with low vitamin C. Zinc determines daily functioning of the animal body, proper growth and regeneration of tissues, structure of some proteins, absorption of vitamins (vitamin A), and functioning of the immune system (Golub et al., 1995; Salachna et al., 2021). Iron is vital for transport of oxygen in the hemoglobin of red blood cells and in the myoglobin of muscles (Chen et al., 2022). Specifically, we aim to use this dataset to quantify 1) whether food plant diversity and nutrient traits within the home range are higher than those out of the home range in both groups C and E and 2) whether group E has higher food plant diversity and nutrient traits than group C.

Method and materials

Study sites

The study was conducted in the location of groups C and E at the northeastern margin of BNNR (109°14′ 47.35″E, 19°5′ 45.17″N; Figure 1). This area is covered by tropical evergreen

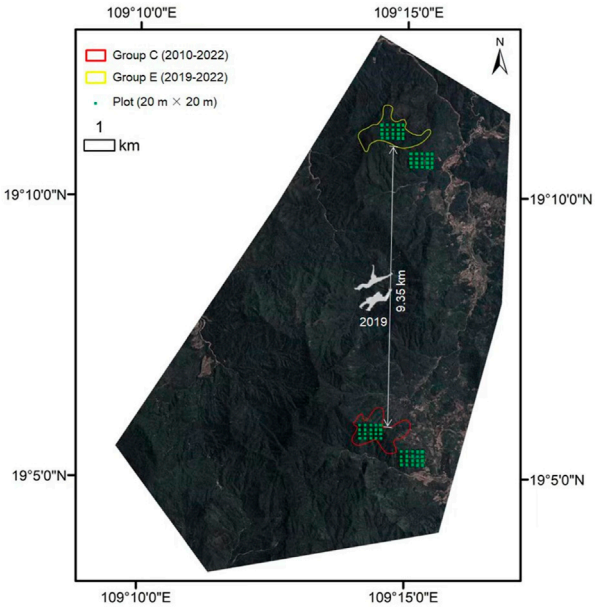

FIGURE 1
Location of our study area, the home range of group C and group E, and spatial location of all 20 m × 20 m plots.

rainforest, and the terrain is relatively rough and mountainous, with a vertical elevation difference of about 500 m. This area is located on the northern edge of the tropics and has a tropical marine monsoon climate with a mean annual rainfall of 1759 mm (Du et al., 2020). There is a distinct wet season from May to October when about 80% of the total rainfall occurs. Its annual temperature is between 22.5 and 26.0°C.

Field sampling

In July 2018 (maximum growing season), within and out of the home range of groups C and E, 20 plots, each of 20 m × 20 m, that are 20 m apart from one another, were arranged along five parallel transects (Figure 1). Then, we recorded and measured all freestanding trees with a diameter of ≥1 cm at breast height (DBH) within each plot and identified them to species. Species were identified as potential food plants based on Zou et al. (2022). We also sampled 20 fully expanded and healthy leaves from five individuals for each food plant species in both groups C and E to measure leaf nutrients [leaf water content (%) and total soluble sugar (mg g^{-1}), vitamin C (mg 100 g^{-1}), calorific value (KJ g^{-1}), crude fat (%), crude protein (%), crude fiber (%), Zn (μg g^{-1}), and Fe (μg g^{-1})]. To minimize intraspecific variation in trait measurements, we selected only individuals with DBH near the species mean value. Importantly, the nine traits for the same species were measured separately if they occurred in both groups C and E. All leaf samples were marked and stored in a sealed bag and immediately transported to the Laboratory of Biodiversity and Ecosystem Functions, School of Forestry, Hainan University. In the laboratory, all samples were weighed fresh, dried to constant weight in an oven at 75°C, and weighed again to determine leaf water content (Fernández et al., 2014). Then, all dried samples were ground to homogenates using a processor grinder for measuring the remaining eight nutrient traits.

Following Arya et al. (2001), total soluble sugar and Vitamin C were measured by using a spectrophotometer. The calorific value was measured by using the oxygen bomb of the automatic calorimeter (ZDHW-5000 type) (Darling, 1976; Gao et al., 2022). Crude fat was measured by using the Soxhlet extraction technique and a fat extractor (JC-ZF-04) (Felton et al., 2009). We first measured the N in all dry leaf samples using a semi-automatic Kjeldahl apparatus (NKB-3100) and then multiplied the N by 6.25 to estimate the crude protein content (Ganzhorn et al., 2017). The crude fiber was quantified by using the fiber analyzer CXC-06 (Honeck et al., 2020). Zn and Fe were measured by using a WA 2081 Atomic Absorption Spectrophotometer (Misra et al., 2020).

Statistic methods

We first calculated food plant diversity (species richness and abundance). Then, for each of the nine leaf nutrient traits (leaf water content, total soluble sugar, vitamin C, calorific value, crude fat, crude protein, crude fiber, Zn, and Fe), we calculated the community-weighted mean (CWM) as follows:

$$CWM = \sum_i p_{ij} t_{ij} \quad (1)$$

where p_{ij} and t_{ij} are the relative abundance and the mean trait value of food plant species i in plot j, respectively. We then utilized non-parametric analysis (Wilcoxon signed-rank test) to quantify whether there were any important differences in food plant diversity (richness and abundance) and leaf nutrient traits between groups C and E and also between within and out of home range in groups C and E. Finally, we used principal component analysis (PCA) to evaluate whether food plant diversity and leaf nutrients can best-discriminate food plant species between groups C and E and food plant species between within and out of home range in groups C and E.

Results

Food plant diversity (richness and abundance) within the home range was significantly much higher (1.35–1.41 times) than that out of the home range in both groups C and E (Figures 2A–D, p of Wilcoxon signed rank test <0.05). Food plant diversity in the home range of group E was also significantly

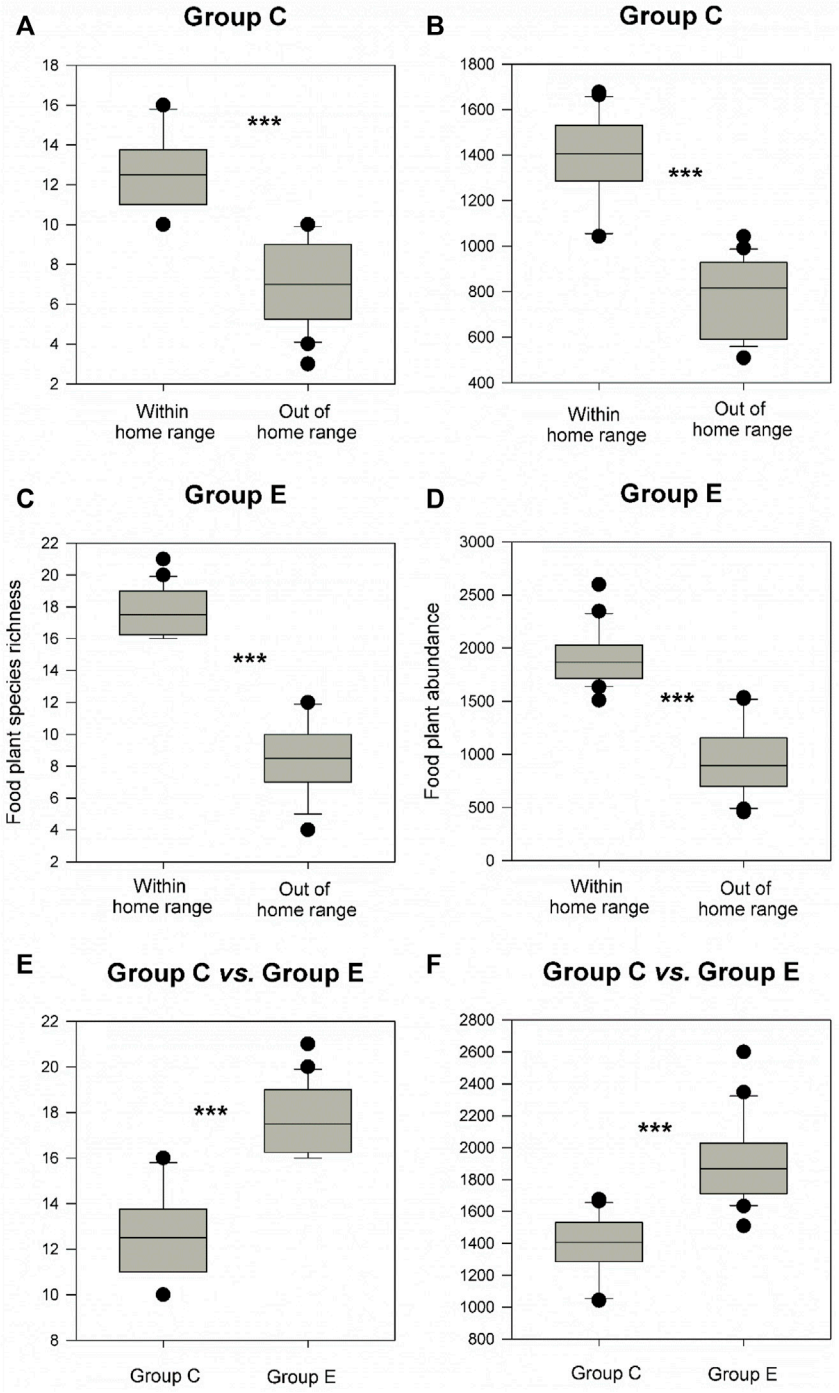

FIGURE 2
Differences in food plant diversity (richness and abundance) between within and out of the home range in groups C and E **(A–D)** and between the home range of groups C and E **(E,F)**. Box plots show the median (line within the box), 25th and 75th percentiles (the boundaries of the box), and 90th and 10th percentiles (error bars). *** indicates $p < 0.05$ and shown are results from Wilcoxon signed rank tests.

much higher (1.4–1.6 times) than that in the home range of group C (Figures 2E,F), p of Wilcoxon signed rank test <0.05). However, there were no significant differences in CWM for all nine leaf nutrient traits within and out of the home range of groups C and E and between the home range of groups C and E (Figures 3–5, p of Wilcoxon signed rank test >0.05).

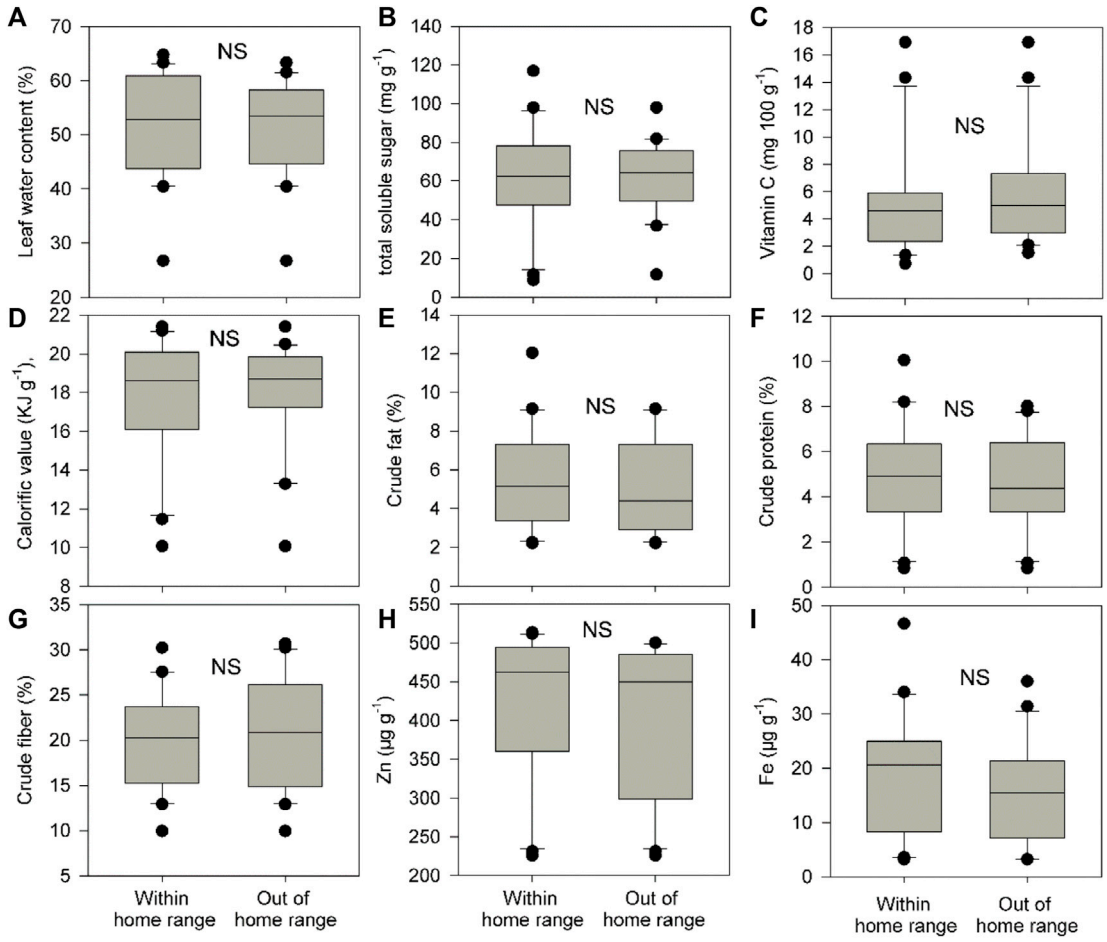

FIGURE 3
Differences in community weighted mean values (CWM) for nine food plant nutrient traits **(A–I)** between within and out of the home range of group C. These nine traits include leaf water content (%), total soluble sugar (mg g^{-1}), vitamin C (mg 100 g^{-1}), calorific value (KJ g^{-1}), crude fat (%), crude protein (%), crude fiber (%), Zn (μg g^{-1}), and Fe (μg g^{-1}). Box plots show the median (line within the box), 25th and 75th percentiles (the boundaries of the box), and 90th and 10th percentiles (error bars) of CWM for food plant leaf nutrient traits. NS indicates $p > 0.05$ and shown are results from Wilcoxon signed rank tests.

Results of PCA revealed that food plant species within and out of the home range of groups C and E and food plant species between the home range of groups C and E all could be significantly separated by food plant diversity (Figure 6). However, CWM for all nine leaf nutrients traits could not significantly separate food plant species within and out of the home range of groups C and E and food plant species between the home range of groups C and E (Figure 6).

Discussion

In this study, we quantified whether food plant diversity and nutrients determined both gibbon home range selection and formation of a new family group as we hypothesized that choosing high food plant diversity was one key motivation for groups C and E to select their home range. Moreover, food plant diversity determined the formation of a new family group of Hainan gibbons.

A number of studies have found that food abundance and distribution can directly determine primate ranging patterns and home range area (Milton and May 1976; Kim et al., 2011; Simmen et al., 2014; Ning et al., 2019). However, until now, it remains unknown whether food plant diversity can directly determine the Hainan gibbon home range area. Primates can use spatial memory of food tree locations (Garber, 1989; Jang et al., 2021). Since group E originates from group C, if food plant diversity can indeed determine the home range area of Hainan gibbon, both groups C and E will select a home range with high food plant diversity. This can be simply revealed by the differences in food plant diversity within and out of the home range of both groups C and E. Our results clearly

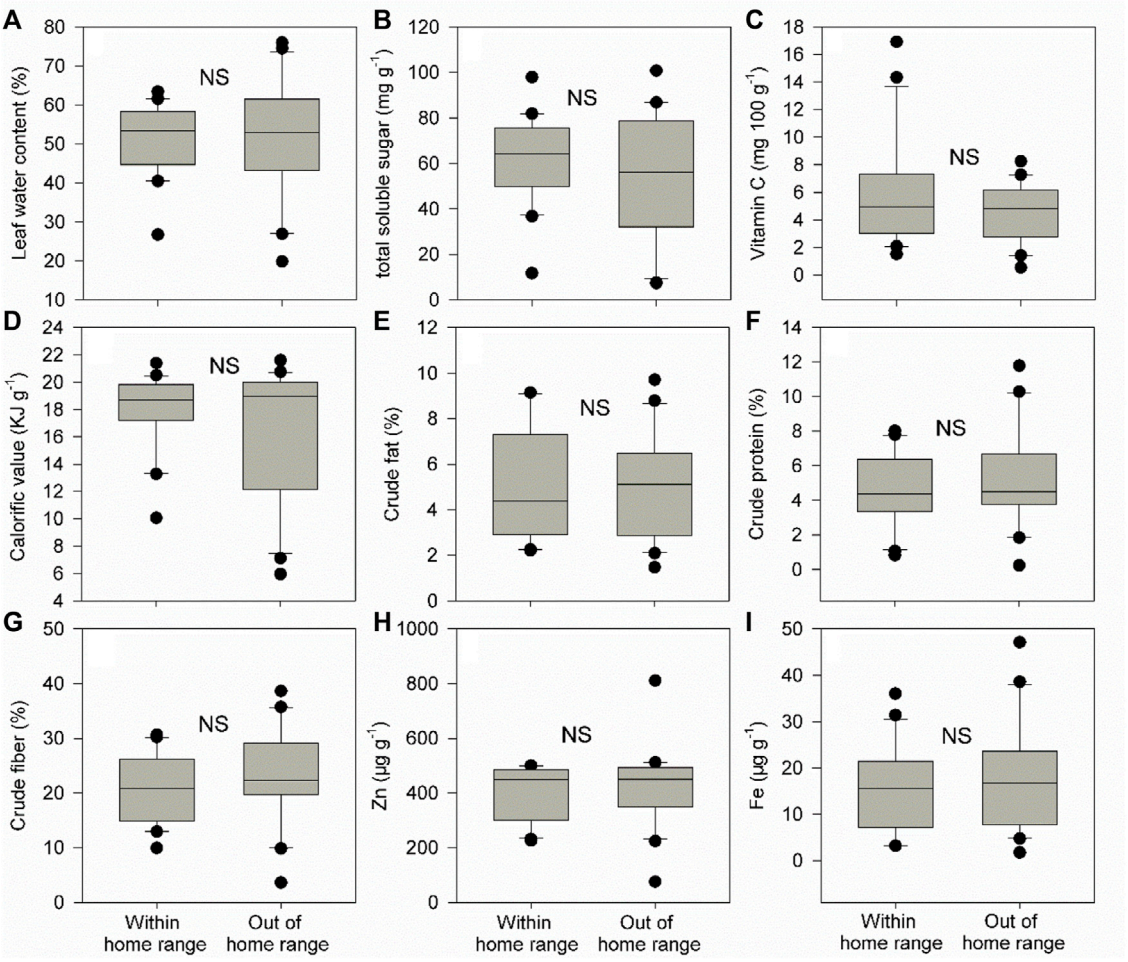

FIGURE 4
Differences in community weighted mean values (CWM) for nine food plant nutrient traits **(A–I)** between within and out of the home range of group E. These nine traits include leaf water content (%), total soluble sugar (mg g^{-1}), vitamin C (mg 100 g^{-1}), calorific value (KJ g^{-1}), crude fat (%), crude protein (%), crude fiber (%), Zn (μg g^{-1}), and Fe (μg g^{-1}). Box plots show the median (line within the box), 25th and 75th percentiles (the boundaries of the box), and 90th and 10th percentiles (error bars) of CWM for food plant leaf nutrient traits. NS indicates $p > 0.05$ and shown are results from Wilcoxon signed rank tests.

demonstrated that in both groups C and E, food plant diversity within the home range was indeed much higher than that out of the home range. Moreover, food plant diversity could also significantly separate food plant species within and out of the home range of groups C and E. These results indeed indicated that choosing high food plant diversity was also one key motivation for groups C and E to select their home range. Thus, our results for the first time revealed that food plant diversity could indeed determine the home range area of Hainan gibbon.

It is also unknown why two individuals move out from group C to go across 9 km to form group E in 2019 (Zou et al., 2022). Here, our results showed that food plant diversity within the home range of group E was indeed much higher than those in the home range of group C. Moreover, food plant diversity could also significantly separate food plant species between the home range of groups C and E. These results also elucidated that food plant diversity was one key determining force to drive Hainan gibbon to form a new family group (group E). It has been found that food plant diversity increased significantly from the oldest group (group A) to the youngest group (group E) (Zou et al., 2022). Thus, food plant diversity may determine the forming of new Hainan gibbon family groups.

Food plant nutrients (leaf water content, total soluble sugar, vitamin C, calorific value, crude fat, crude protein, crude fiber, Zn, and Fe) are also widely reported to affect primate population dynamics (growth, abundance, and home range) (Grether et al., 1992; Laska et al., 2000; Marshall and Leighton, 2006; Hansell et al., 2020). However, it is also unclear whether food plant nutrients can

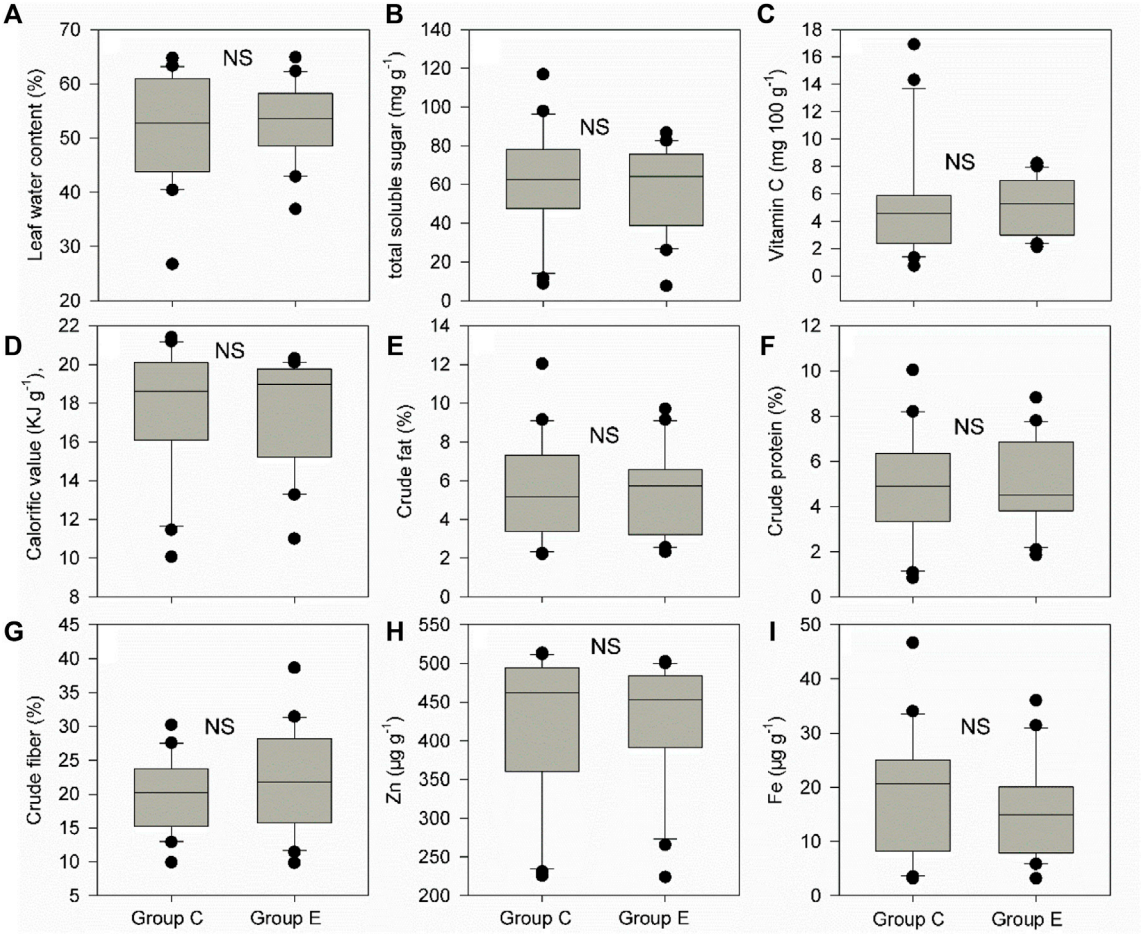

FIGURE 5
Differences in community weighted mean values (CWM) for nine food plant nutrient traits **(A-I)** between the home range of groups C and E. These nine traits include leaf water content (%), total soluble sugar (mg g^{-1}), vitamin C (mg 100 g^{-1}), calorific value (KJ g^{-1}), crude fat (%), crude protein (%), crude fiber (%), Zn (μg g^{-1}), and Fe (μg g^{-1}). Box plots show the median (line within the box), 25th and 75th percentiles (the boundaries of the box), and 90th and 10th percentiles (error bars) of CWM for food plant leaf nutrient traits. NS indicates $p > 0.05$ and shown are results from Wilcoxon signed rank tests.

indeed influence Hainan gibbon population dynamics. If food plant nutrients can indeed determine the Hainan gibbon home range area and the forming of the new family group, plant nutrients within the home range of groups C and E should be much higher than those out of the home range of groups C and E. Similarly, plant nutrients within the home range of group E should also be much higher than those within the home range of group C. Here, our results showed that there are no significant differences in plant nutrients (leaf water content, total soluble sugar, vitamin C, calorific value, crude fat, crude protein, crude fiber, Zn, and Fe) between within and out of the home range of groups C and E and between the home range of group C and E. Furthermore, all food plant nutrients could not significantly separate food plant species within and out of the home range of groups C and E and between the home range of groups C and E. Thus, food plant nutrients can affect neither the home range area nor forming of the new family group of Hainan gibbon. One potential reason is that there is enough food plant diversity within the home range of Hainan gibbon. That is because, usually, when food is scarce, primates will select food in light of nutrients (Marshall et al., 2009).

We noted that although our results indicate that food plant diversity is one potential driver of the formation of the new family group of Hainan gibbon, other factors (i.e., natural enemies, human disturbance, and relatively rough and mountainous terrain) can also be potential determinants. Moreover, we only found the strong influences of food plant diversity on groups C and E, and the effects of food plant diversity on the remaining three family groups (groups A, B, and D) were also necessary to be quantified. As a result, the other drivers of the formation of the new group of Hainan gibbon merit future investigation to explore.

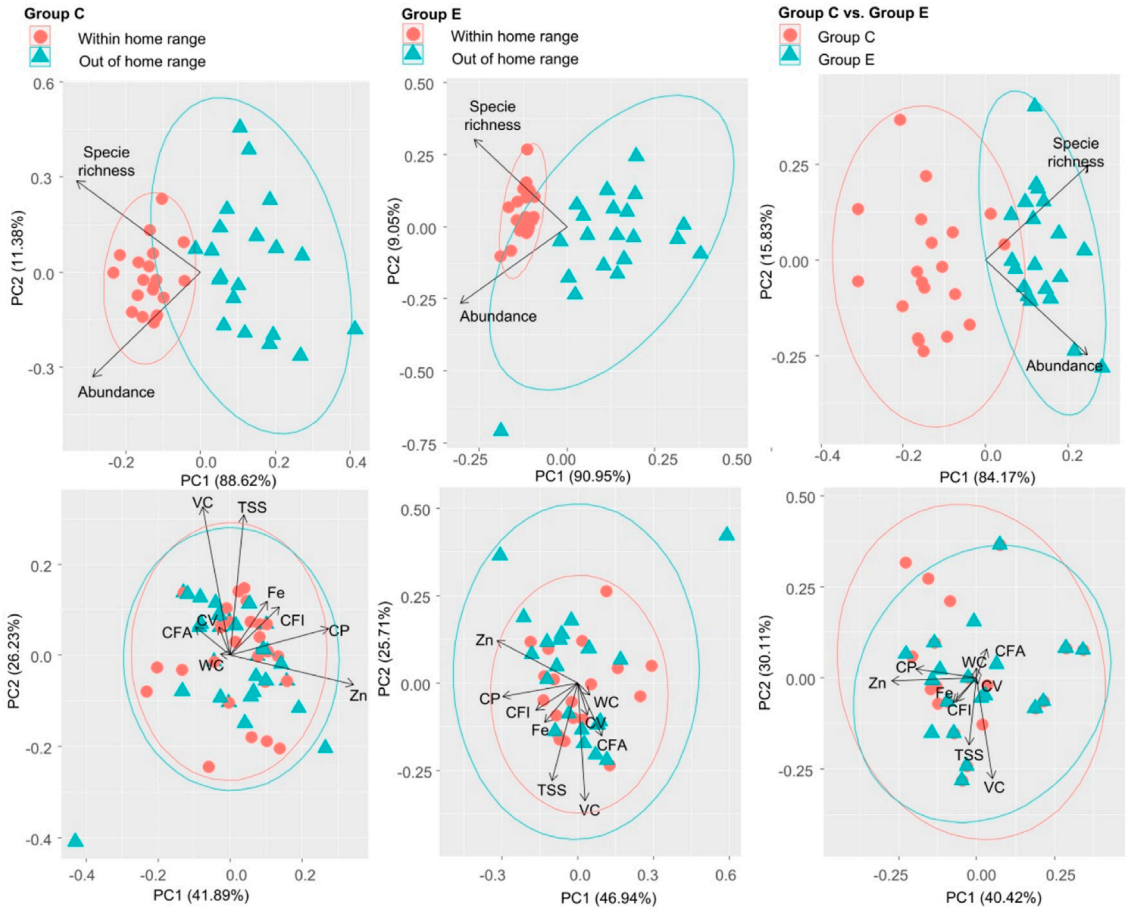

FIGURE 6
Principal component analysis of food plant diversity (richness and abundance) and CWM for nine food plant leaf nutrient traits between within and out of the home range in groups C and E and between the home range of groups C and E. These nine traits include leaf water content (WC, %), total soluble sugar (TSS, mg g^{-1}), vitamin C (VC, mg 100 g^{-1}), calorific value (VC, kJ g^{-1}), crude fat (CFA, %), crude protein (CP, %), crude fiber (CFI, %), Zn (μg g^{-1}), and Fe (μg g^{-1}).

Conclusion

Overall, three important new insights about the influence of food plant diversity and nutrients on Hainan gibbon population dynamics have been revealed by our study. First, choosing high food plant diversity was also one key motivation for Hainan gibbons to select their home range. Second, food plant diversity may be one key determinant of the formation of the new family group of Hainan gibbon. Third, food plant nutrients cannot determine both the home range area and forming of the new family group of Hainan gibbon.

Data availability statement

The original contributions presented in the study are included in the article/Supplementary Material; further inquiries can be directed to the corresponding authors.

Author contributions

JC, HZ, and WG designed the research. LW, YL, JC, HZ, and WG performed the research and wrote the manuscript. LW, JC, and WG analyzed the data. All authors contributed to the article and approved the submitted version.

Funding

This research was supported by the Natural Science Foundation of Hainan province, China (422CXTD508), the Specific Research Fund of the Innovation Platform for Academicians of Hainan Province, Research project of Hainan academician innovation platform (YSPTZX202017), and the Scientific Research Project of

Ecological Restoration of Baopoling Mountain in Sanya, China.

Conflict of interest

The authors declare that the research was conducted in the absence of any commercial or financial relationships that could be construed as a potential conflict of interest.

Publisher's note

References

Arce, M., Michopoulos, V., Shepard, K. N., Ha, Q. C., and Wilson, M. E. (2010). Diet choice, cortisol reactivity, and emotional feeding in socially housed rhesus monkeys. *Physiol. Behav.* 101, 446–455. doi:10.1016/j.physbeh.2010.07.010

Arya, S., Mahajan, M., and Jain, P. (2001). Spectrophotometric determination of vitamin C with iron (II)-4-(2-pyridylazo) resorcinol complex. *Anal. Chim. Acta X.* 427, 245–251. doi:10.1016/s0003-2670(00)01092-8

Bach, T. H., Chen, J., Hoang, M. D., Beng, K. C., and Nguyen, V. T. (2017). Feeding behavior and activity budget of the southern yellow-cheeked crested gibbons (*Nomascus gabriellae*) in a lowland tropical forest. *Am. J. Primatol.* 79, e22667. doi:10.1002/ajp.22667

Borah, D. K., Solanki, G. S., and Bhattacharjee, P. C. (2021). Feeding ecology of capped langur (*Trachypithecus pileatus*) in sri surya pahar, a disturbed habitat in goalpara district, Assam, India. *Trop. Ecol.* 62, 492–498. doi:10.1007/s42965-021-00161-6

Chan, B. P. L., Lo, Y. F. P., and Mo, Y. (2020). New hope for the hainan gibbon: formation of a new group outside its known range. *Oryx* 54, 296. doi:10.1017/s0030605320000083

Chen, W. J., Kung, G. P., and Gnana-Prakasam, J. P. (2022). Role of iron in aging related diseases. *Antioxidants (Basel).* 11, 865–871. doi:10.3390/antiox11050865

Clink, D. J., Dillis, C., Feilen, K. L., Beaudrot, L., and Marshall, A. J. (2017). Dietary diversity, feeding selectivity, and responses to fruit scarcity of two sympatric Bornean primates (Hylobates albibarbis and *Presbytis rubicunda* rubida). *PLoS ONE* 12, e0173369. doi:10.1371/journal.pone.0173369

Darling, M. S. (1976). Interpretation of global differences in plant calorific values: The significance of desert and arid woodland vegetation. *Oecologia* 23, 127–139. doi:10.1007/BF00557851

de Vries, R., Boesveldt, S., and de Vet, E. (2022). Human spatial memory is biased towards high-calorie foods: a cross-cultural online experiment. *Int. J. Behav. Nutr. Phys. Act.* 19, 14. doi:10.1186/s12966-022-01252-w

Deng, H. Q., and Zhou, J. (2018). Thirteen years observation on diet composition of Hainan gibbons (Nomascushainanus). *North-West. J. Zool.* 14, 213–219.

Du, Y. J., Li, D. F., Yang, X. B., Peng, D. X., Tang, X. R., Liu, H., et al. (2020). Reproductive phenology and its drivers in a tropical rainforest national park in China: Implications for Hainan gibbon (Nomascus hainanus) conservation. *Glob. Ecol. Conserv.* 24, e01317. doi:10.1016/j.gecco.2020.e01317

Estrada, A., Garber, P. A., Rylands, A. B., Roos, C., Fernandez-Duque, E., Di Fiore, A., et al. (2017). Impending extinction crisis of the world's primates: Why primates matter. *Sci. Adv.* 3, e1600946. doi:10.1126/sciadv.1600946

Fan, K. X., Xu, Y., Liu, P. C., and Zang, R. G. (2021). Recovery of logged tropical montane rainforests as potential habitats for hainan gibbon. *Forests* 12, 711–716. doi:10.3390/f12060711

Fellowes, J. R., Chan, B., Zhou, J., Chen, S., Yang, S., and Ng, S. C. (2008). Current status of the hainan gibbon (*Nomascus hainanus*): Progress of population monitoring and other priority actions. *Asian. Primates. J.* 1, 2–11.

Felton, A. M., Felton, A., Wood, J. T., Foley, W. J., Raubenheimer, D., Wallis, I. R., et al. (2009). Nutritional ecology of *Ateles chamek* in lowland Bolivia: How macronutrient balancing influences food choices. *Int. J. Primatol.* 30, 675–696. doi:10.1007/s10764-009-9367-9

Ganzhorn, J. U., Arrigo-Nelson, S. J., Carrai, V., Chalise, M. K., Donati, G., Droescher, I., et al. (2017). The importance of protein in leaf selection of folivorous primates. *Am. J. Primatol.* 79, e22550. doi:10.1002/ajp.22550

Gao, T., Zhu, Q., Zhou, Z. D., Wu, Y. B., and Xue, J. H. (2022). Effects of biochar-based fertilizers on energy characteristics and growth of black locust seedlings. *Sustainability* 14, 5045. doi:10.3390/su14095045

Garber, P. A. (1989). Role of spatial memory in primate foraging patterns: *Saguinus mystax* and *Saguinus fuscicollis*. *Am. J. Primatol.* 19, 203–216. doi:10.1002/ajp.1350190403

Golub, M. S., Keen, C. L., Gershwin, M. E., and Hendrickx, A. G. (1995). Developmental zinc deficiency and behavior. *J. Nutr.* 125, 2263S–2271S. doi:10.1093/jn/125.suppl_8.2263s

Grether, G. F., Palombit, R. A., and Rodman, P. S. (1992). Gibbon foraging decisions and the marginal value model. *Int. J. Primatol.* 13, 1–17. doi:10.1007/bf02547724

Hansell, M., Asberg, A., and Laska, M. (2020). Food preferences and nutrient composition in zoo-housed ring-tailed lemurs, *Lemur catta*. *Physiol. Behav.* 226, 113125. doi:10.1016/j.physbeh.2020.113125

Hanya, G., and Chapman, C. A. (2013). Linking feeding ecology and population abundance: a review of food resource limitation on primates. *Ecol. Res.* 28, 183–190. doi:10.1007/s11284-012-1012-y

Hladik, C. M., and Simmen, B. (1996). Taste perception and feeding behavior in nonhuman primates and human populations. *Evol. Anthropol.* 5, 58–71. doi:10.1002/(sici)1520-6505(1996)5:2<58::aid-evan5>3.0.co;2-s

Honeck, A., Ahlhorn, J., Burfeind, O., Gertz, M., Beilage, E. G., Hasler, M., et al. (2020). Influence on tail-biting in weaning pigs of crude fibre content and different crude fibre components in pigs' rations. *J. Agric. Sci.* 158, 233–240. doi:10.1017/S0021859620000404

Huang, F. Y., Sutcliffe, M. P. F., and Grabenhorst, F. (2021). Preferences for nutrients and sensory food qualities identify biological sources of economic values in monkeys. *Proc. Natl. Acad. Sci. U. S. A.* 118, e2101954118. doi:10.1073/pnas.2101954118

Jang, H., Oktaviani, R., Kim, S., Mardiastuti, A., and Choe, J. C. (2021). Do Javan gibbons (*Hylobates moloch*) use fruiting synchrony as a foraging strategy? *Am. J. Primatol.* 83, e23319. doi:10.1002/ajp.23319

Jildmalm, R., Amundin, M., and Laska, M. (2008). Food preferences and nutrient composition in captive white-handed gibbons, *Hylobates lar*. *Int. J. Primatol.* 29, 1535–1547. doi:10.1007/s10764-008-9314-1

Kim, S., Lappan, S., and Choe, J. C. (2011). Diet and ranging behavior of the endangered javan gibbon (*Hylobates moloch*) in a submontane tropical rainforest. *Am. J. Primatol.* 73, 270–280. doi:10.1002/ajp.20893

Laska, M., Hernandez Salazar, L. T., and Rodriguez Luna, E. (2000). Food preferences and nutrient composition in captive spider monkeys, *Ateles geoffroyi*. *Int. J. Primatol.* 21, 671–683. doi:10.1023/a:1005517421510

Lee, S. W., Lee, Y. J., Baek, S. M., Kang, K. K., Kim, T. U., Yim, J. H., et al. (2022). Mega-dose vitamin C ameliorates nonalcoholic fatty liver disease in a mouse fast-food diet model. *Nutrients* 14, 2195–2201. doi:10.3390/nu14112195

Liu, H., Ma, H., Cheyne, S. M., and Turvey, S. T. (2020). Recovery hopes for the world's rarest primate. *Science* 368, 1074. doi:10.1126/science.abc1402

Marshall, A. J., Boyko, C. M., Feilen, K. L., Boyko, R. H., and Leighton, M. (2009). Defining fallback foods and assessing their importance in primate ecology and evolution. *Am. J. Phys. Anthropol.* 140, 603–614. doi:10.1002/ajpa.21082

Marshall, A. J., and Leighton, M. (2006). *How does food availability limit the population density of white-bearded gibbons?* Cambridge: Cambride Studies in Biological and Evolutionary Authropology.

Milton, K., and May, M. L. (1976). Body weight, diet and home range area in primates. *Nature* 259, 459–462. doi:10.1038/259459a0

Misra, G., Joshi-Saha, A., Salaskar, D., Reddy, K. S., Dixit, G. P., Srivastava, A. K., et al. (2020). Baseline status and effect of genotype, environment and genotype × environment interactions on iron and zinc content in Indian chickpeas (*Cicer arietinumL.*). *Euphytica* 216, 137–142. doi:10.1007/s10681-020-02673-z

Ning, W. H., Guan, Z. H., Huang, B., Fan, P. F., and Jiang, X. L. (2019). Influence of food availability and climate on behavior patterns of Western black crested gibbons (*Nomascus concolor*) at Mt. Wuliang, Yunnan, China. *Am. J. Primatol.* 81, e23068. doi:10.1002/ajp.23068

Salachna, P., Mizielinska, M., Ploszaj-Witkowska, B., and Jaszczak, A. (2021). Zinc oxide nanoparticles enhanced biomass and zinc content and induced changes in biological properties of red perilla frutescens. *Materials* 14, 6182–6188. doi:10.3390/ma14206182

Simmen, B., Tarnaud, L., Marez, A., and Hladik, A. (2014). Leaf chemistry as a predictor of primate biomass and the mediating role of food selection: A case study in a folivorous Lemur (*Propithecus verreauxi*). *Am. J. Primatol.* 76, 563–575. doi:10.1002/ajp.22249

Turvey, S. T., Traylor-Holzer, K., Wong, M. H. G., Bryant, J. V., Zeng, X., Hong, X., et al. (2015). *International conservation planning workshop for the hainan gibbon: Final report*. London: Zoological Society of London.

Yeager, C. P. (1989). Feeding ecology of the proboscis monkey (*Nasalis larvatus*). *Int. J. Primatol.* 10, 497–530. doi:10.1007/bf02739363

Zhang, H., Wang, C., Turvey, S. T., Sun, Z. Y., Tan, Z. Y., Yang, Q., et al. (2020). Thermal infrared imaging from drones can detect individuals and nocturnal behavior of the world's rarest primate. *Glob. Ecol. Conserv.* 23, e01101. doi:10.1016/j.gecco.2020.e01101

Zhao, H., Wang, X., Kreigenhofer, B., Qi, X., Guo, S., Wang, C., et al. (2013). Study on the nutritional ecology of wild primates. *Acta Ecol. Sin.* 33, 185–191. doi:10.1016/j.chnaes.2013.05.004

Zou, Y., Turvey, S. T., Cui, J., Zhang, H., and Gong, W. (2022). Recent recovery of the world's rarest primate is not directly linked to increasing habitat quality. *Front. Ecol. Evol.* 10, 953637. doi:10.3389/fevo.2022.953637

frontiers | Frontiers in Environmental Science

TYPE Original Research
PUBLISHED 03 October 2022
DOI 10.3389/fenvs.2022.1038752

OPEN ACCESS

EDITED BY
Xiang Liu,
Lanzhou University, China

REVIEWED BY
Min Zhao,
Northeast Forestry University, China
Daoli Peng,
Beijing Forestry University, China

*CORRESPONDENCE
Xiaodong Rao,
993676@hainanu.edu.cn
Tiedong Liu,
liu@hainanu.edu.cn
Tao Liu,
daliu_1978@126.com

†These authors contributed equally to this work.

SPECIALTY SECTION
This article was submitted to Conservation and Restoration Ecology, a section of the journal Frontiers in Environmental Science

RECEIVED 07 September 2022
ACCEPTED 15 September 2022
PUBLISHED 03 October 2022

CITATION
Gong W, Duan X, Mao M, Hu J, Sun Y, Wu G, Zhang Y, Xie Y, Qiu X, Rao X, Liu T and Liu T (2022), Assessing the impact of land use and changes in land cover related to carbon storage by linking trajectory analysis and InVEST models in the Nandu River Basin on Hainan Island in China.
Front. Environ. Sci. 10:1038752.
doi: 10.3389/fenvs.2022.1038752

Assessing the impact of land use and changes in land cover related to carbon storage by linking trajectory analysis and InVEST models in the Nandu River Basin on Hainan Island in China

Wenfeng Gong[1,2†], Xuanyu Duan[1,2†], Mingjiang Mao[1,2], Jihan Hu[1,2], Yuxin Sun[1,2], Genghong Wu[1,2], Yangyang Zhang[1,2], Yidan Xie[1,2], Xincai Qiu[1,2], Xiaodong Rao[1,2]*, Tiedong Liu[1,2]* and Tao Liu[3]*

[1]Intelligent Forestry Key Laboratory of Haikou City, College of Forestry, Hainan University, Haikou, China, [2]Key Laboratory of Genetics and Germplasm Innovation of Tropical Special Forest Trees and Ornamental Plants, Ministry of Education, College of Forestry, Hainan University, Haikou, China, [3]College of Hydraulic and Electrical Engineering, Heilongjiang University, Harbin, China

This study aims to evaluate the effects of the spatiotemporal patterns of land-use and land-cover (LULC) changes on the dynamics of carbon storage in a tropical region of China by linking the trajectory analysis of LULC changes and the InVEST model. Based on remote sensing (RS), geographic information system (GIS) and change trajectories, the spatiotemporal evolution of LULC changes was explored. This evolution could be coupled with the spatiotemporal LULC change trajectories and the InVEST model for the quantitative study of the spatial distribution and temporal variation in regional carbon stocks. The results showed that during the 2000–2020 period, the built-up land continually increased to 206.05 km^2 through urban expansion, and forestland became the dominant type of land, with an area of 357.39 km^2. In addition to the change in land use, the carbon storage in the study region increased by 4.87 Tg C. The anaphasic trajectory had the largest area ratio at 7.05% in the total area, while the prophasic trajectory contributed to the largest increase in carbon storage, 5.87 Tg C. Moreover, the repetitive trajectories had no impact on carbon sinks and sources, whereas the anaphasic trajectory and the continual trajectory imposed passive impacts on carbon storage. These advances in research underpin scientific efforts to improve the understanding of the relationship between the optimization of land-use structure and patterns and the carbon storage service in the Nandu River Basin.

KEYWORDS

carbon storage, LULC, InVEST model, trajectory analysis, Nandu river basin, Hainan island

1 Introduction

Land-use and land-cover changes (LULCCs) are not only the most crucial link between human activities and the ecological environment but also the main factor affecting regional climate change (Liu et al., 2014). It is estimated that approximately 35% of the carbon emissions in the atmosphere have been the consequence of human activities since the industrial revolution (Houghton et al., 2012). Human activities have altered the original patterns, structures, processes and functions of terrestrial ecosystems through different land-use practices, resulting in serious damage to the land surface of the ecological environment, which directly or indirectly affects carbon storage and carbon-cycle processes in regional ecosystems (Zaehle et al., 2007; Gao and Wang, 2019; Zhang et al., 2021) and the process of regional climate change. Terrestrial ecosystems are an important source and sink of atmospheric greenhouse gases (Cui et al., 2019). Since carbon storage in terrestrial ecosystems is a significant component of global carbon storage, these ecosystems play an important role in mitigating global warming by reducing the concentrations of atmospheric CO_2 and other greenhouse gases (Lal, 2004). The estimation of annual net carbon absorption by global terrestrial ecosystems ranges between 2000 Pg and 2,500 Pg, including 500 Pg to 600 Pg by vegetation and 1,500 Pg to 2,300 Pg by soil (Zhao et al., 2019; Liang X. et al., 2021; Liang Y. et al., 2021). It is widely recognized that terrestrial ecosystems, with a strong carbon absorption capacity, are one of the most economically feasible and ecologically friendly approaches to alleviate the impact of the greenhouse effect on the global climate (Zhu E.et al., 2019). The carbon absorption capacity of terrestrial ecosystems has become the focus of attention for governments and scholars worldwide (Schimel et al., 2001; Ji et al., 2008; Piao et al., 2009; Fang et al., 2015; Dai et al., 2016). Several factors, such as climate change, land-use change, and land management, interact to regulate soil carbon storage (Xia et al., 2010), among which land-use changes and land management measures are key factors influencing greenhouse gases and affecting carbon emissions (Smith and Conen, 2006). The Intergovernmental Panel on Climate Change (IPCC) report states that the contribution of LULCCs to the increase in atmospheric CO_2 is expected to be only second to the combustion of fossil fuels in the future (Houghton, 2003; Foley et al., 2005). It is obvious that LULCCs, as one of the most important factors affecting soil carbon storage in terrestrial ecosystems, also dominate the spatiotemporal evolution of carbon sources and sinks (Houghton et al., 2000). Thus, a deep understanding of the impact of the spatiotemporal evolutionary characteristics of land-use patterns on regional carbon source and sink mechanisms is a prerequisite for reducing and managing carbon dioxide emissions (Hwang et al., 2021).

Estimating the effect of land-use changes on soil carbon storage depends on data sources and techniques (Leifeld, 2013). Assessing and analysing the spatial distribution and mechanisms of soil carbon sources/sinks is a major challenge faced by many researchers (Xu et al., 2011). At present, the methods for assessing regional carbon storage mainly include field surveys (Ren et al., 2011), remote sensing inversion (Lu et al., 2010; Fu et al., 2013) and model simulations (Sohl et al., 2012; Zhao et al., 2013). The field survey method mainly uses regional carbon density profiles of different vegetation and soil types to estimate carbon storage. Although it is relatively simple and accurate, field surveys are only suitable for small regions and have limited effectiveness in reflecting the dynamic changes in carbon storage at large regional scales (Huang et al., 2014). Remote sensing is a cost-effective and useful technique for both qualitative and quantitative analyses of LULC changes in terrestrial ecosystems using satellite imagery (Mayani-Parás et al., 2021). Additionally, time-series analysis of remote sensing data provides an excellent opportunity to understand and map LULCCs from small to large catchments (Abdullah et al., 2016; Yan et al., 2019). Hence, the remote sensing method has been broadly used for LULC change detection from small to large regions/catchments (Kuma et al., 2022). The model simulation method applies different models to simulate and estimate land use, among which the Integrated Valuation of Ecosystem Services and Tradeoffs (InVEST) model is widely used due to the advantages of simplicity, flexible parameters, and relatively accurate results. The approach of combining the GIS, RS and InVEST models has been extensively used by governments, companies and researchers to explore the simulation, prediction and assessment of the carbon storage of ecosystems and has been applied at different scales, such as regional (Chuai et al., 2014), national (Ni, 2013) and global (Nelson et al., 2010) scales. In particular, by combining the InVEST model with the land-use simulation model (CA-Markov, CLUe-S, etc.), some scholars have revealed the temporal and spatial variation characteristics of regional carbon storage at the watershed and urban scales in the past, predicted the trends in the future, and discussed the future scenarios of land-use and land-cover changes and their impact on regional ecosystem carbon storage (Li et al., 2020; Zhu et al., 2020; Liu et al., 2021).

According to the variation in ecosystem carbon storage patterns in different periods, most previous studies have indicated the influence mechanisms of LULCCs on regional carbon storage at different scales. However, it has been difficult to uncover the impact of the spatiotemporal evolution of land-use patterns on the dynamic processes of regional carbon storage patterns under the effect of comprehensive driving forces. In addition, there are still many uncertainties about the impact of land-use change on carbon balance and carbon intensity (Permpool et al., 2016). As a complementary methodology, the LULC change trajectory can dynamically track the spatiotemporal evolution of continuous and long-term land-

use change processes in the same region (Zomlot et al., 2017). For example, Zhou et al. (2008) used multitemporal remotely sensed imagery to derive land-cover change trajectories to understand the spatiotemporal pattern of ecosystem dynamics. Similarly, Wang et al. (2012) proposed trajectory analysis as a new mathematical algorithm to explore the spatiotemporal analysis of land-use/cover change by using GIS and RS. The same approach was carried out by Wang et al. (2013) with high-resolution remote sensing imagery to monitor the spatiotemporal change of land use/cover by using pattern metrics of change trajectories in smaller scale valleys. Zomlot et al. (2017) used trajectory analysis as a preprocessing tool to identify LULC changes to improve spatiotemporal patterns and conduct impact assessments on groundwater recharge. However, there is still a gap in the exploration of the effects of spatial and temporal changes in land use on soil carbon storage at the regional scale, especially in the tropics. The tropics have a greater potential for reducing atmospheric CO_2 (De Sousa-Neto et al., 2018), but no previous study has focused on matching the carbon density of the Nandu River Basin in the tropics over a long span, such as 30 years, to calculate the soil carbon storage caused by LULCCs. Furthermore, the study of trajectory analysis to quantify the impact of land-use change on soil carbon has not been applied in tropical areas at large scales. Therefore, it is necessary to quantify the effect of regional LULCCs on carbon storage by coupling InVEST models with spatiotemporal LULC change trajectories.

The Nandu River, as an important source of drinking water, is the largest river on Hainan Island and is known as the Mother River of Hainan Island, China. With the rapid socioeconomic development and the increasing population of the study region, agricultural water use has increased sharply, and the problem of agricultural nonpoint source pollution has become an urgent issue in the middle and lower reaches of the Nandu River (Liu et al., 2013). In addition, excessive discharge of domestic wastewater has seriously polluted the regional ecological environment, particularly in urban and rural areas. It was reported that the urban domestic sewage treatment rate in some areas was only 2.97% (Province, T.P.s.G.o.H., 2015), whereas rural domestic sewage was rarely treated. Some relevant studies have demonstrated that the water quality of the middle and lower reaches of this river belongs to the fifth type of surface water (Class V) (Liu et al., 2013), which is mainly applicable to agriculture and meets general landscape requirements. Moreover, indiscriminate and illegal mining is very prominent in some sections of the river, which has caused damage to the local ecological environment. Furthermore, the disturbance intensity in the natural ecosystem of the basin caused by human activities has been severe over the last decade. Together with an increased intensity of deforestation, grassland clearance and wetland reclamation for farmland expansion and the built-up land construction encroachment on farmlands and forestlands, this area has incurred significant changes to the LULCC pattern, which has increased the uncertainty of carbon sink functions across the Nandu River Basin. These changes will have a profound impact on the ecological environment of the study area in the future. Nevertheless, less research has been carried out on the relationship between land-use change and carbon storage services in this region. Therefore, we believe that it is necessary to quantify local regional carbon storage and fill in the gap in regional ecological environmental research.

This paper was based on land-use/cover data obtained from remote sensing image interpretation in 1990, 2005 and 2020, coupling the InVEST model with spatiotemporal LULC change trajectories to estimate the distribution of carbon storage, such that this research will provide meaningful resources for land-use managers. The primary objectives of our study include 1) using GIS and RS applications to investigate the spatiotemporal LULC change from 1990 to 2020 by using trajectory analysis; 2) linking the trajectory analysis and the InVEST models to map the carbon storage spatial distribution and exploring its spatiotemporal evolutionary tracking; 3) providing a new way to quantify the response mechanism of land-use dynamic processes on regional carbon source/sink effects; and 4) proposing some suggestions for implementing appropriate land-use policies to wisely control LULCCs to reduce carbon emissions (Zhu W.et al., 2019).

2 Study area

The Nandu River (located between 18° 56′ N and 20°05′ N latitude and 109°12′ E and 110°35′ E longitude) is the largest river on Hainan Island (Figure 1). Its main tributaries include the Longzhou River, Datang River, Yaozi River, etc. It originates from the Nanfeng Mountains in Baisha County and enters the Qiongzhou Strait in Haikou city, where it has a wide channel with many sandbanks, hills and shoals. Both banks of the river are flat platforms, most of which are cropland, covering a total area of 7,033 km^2. The slope of the total terrain of the basin gradually decreases from south to north. The upper reaches of the river are high mountains and hills with large topographic fluctuations, while the slopes in the middle and lower reaches are gentle. The annual average temperature is 23.5°C, and the annual average precipitation is 1935 mm. The main soil types include mountain yellow soil, mountain lateritic soil, lateritic soil, sandy soil, paddy soil, etc. The river basin is rich in forest resources, with more than 1,200 species of coniferous broad-leaved trees and more than 700 species of arbor trees. Moreover, the plant resources in the basin are abundant and diverse. The vegetation type is mainly evergreen broad-leaved forest, with various tropical shrubs, vines, herbs and so on under the forest.

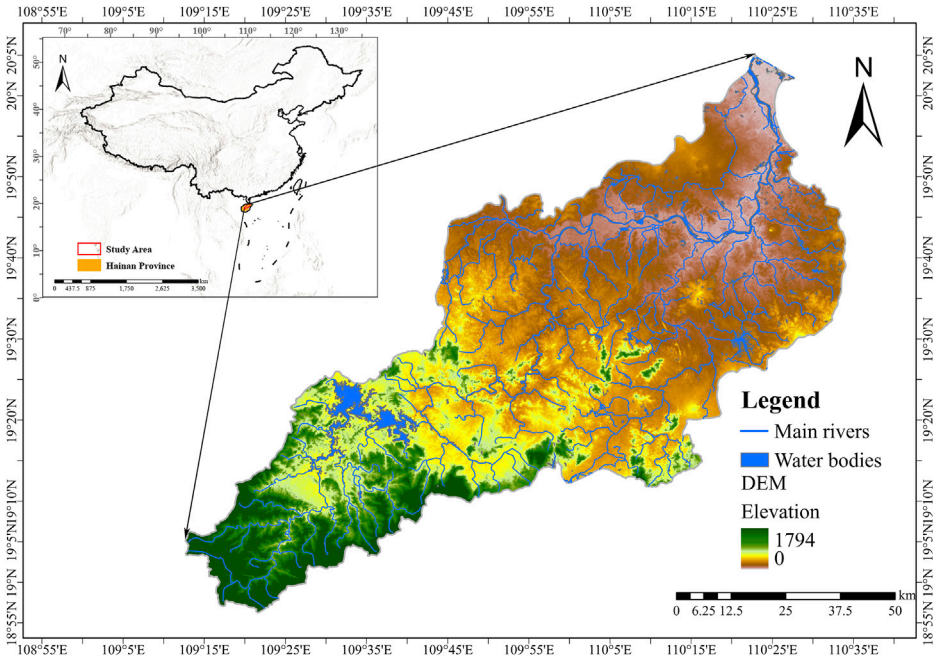

FIGURE 1
Location and elevation of the study area.

3 Methods

3.1 Image collection and processing

Landsat satellite images (5, ETM+, and 8) with Spectral Bands 3 (0.63–0.69 mm), 4 (0.77–0.90 mm) and 5 (1.55–1.75 mm) from Landsat TM5 and ETM+ and Bands 4 (0.64–0.67 mm), 5 (0.85–0.88 mm) and 6 (1.57–1.65 mm) from Landsat Imager OLI were used for 2000, 2010 and 2020 for LULCC mapping. All satellite images were obtained from the USGS (http://glovis.usgs.gov/). At the beginning, ENVI 5. 5 software was employed to process all Landsat scenes, which were reprojected with WGS84/UTM Zone 49 N for geometry and resampled to a 30-m spatial resolution, followed by using the FLAASH (Fast Line-of-sight Atmospheric Analysis of Spectral Hyper cubes) module in ENVI 5.5 software for atmospheric correction. Next, all satellite images were composed using red–green-blue (RGB) colour composition with Band 543 (Landsat TM5 and ETM+) and Band 654 (Landsat OLI). According to the classification criterion issued by the Ministry of Natural Resources of China and the current land-use situation, the land use of the study region was categorized into the following five groups: croplands, forestlands, grasslands, water bodies, and built-up areas. Training of classes was conducted using the data from field surveys, high-resolution Google Earth maps, and previous land-use maps. The support vector machines (SVM) algorithm in ENVI 5.5 was used to classify the images from 2000, 2010 and 2020. The second step was the accuracy assessment of classified images from 2000, 2010 and 2020. Ground truth points were taken from the high-resolution Google Earth maps and from field surveys with a simple GPS instrument for training and testing classified maps and their accuracy assessment. In addition, a confusion matrix was developed to evaluate the accuracy of the classified images from 1990, 2010 and 2020. The overall accuracy and Kappa coefficient are the two most extensively used accuracy assessment methods for classified images. The Kappa indices for all classes exceeded 0.75, with values of 0.813, 0.832 and 0.854, respectively. Finally, five classes for land-use and land-cover maps with a spatial resolution of 30 × 30 m were generated in Grid format with Arc Pro 2.8 (ESRI, United States), which were used to detect the dynamic tracking of the spatiotemporal evolution of broad land-use/land-cover areas in this region.

3.2 Trajectory analysis

A change trajectory of a time series can be expressed by trajectory codes in all forms (e.g., in values or letters) for every pixel in the raster image (Wang et al., 2012). In this paper, the land-use types, croplands, forestlands, grasslands, water bodies, and built-up areas, were assigned the numeric codes 1, 2, 3, 4 and 5, respectively, which were used as trajectory codes for detecting the changes for each pixel at each time node through the three

temporal slices, 2000, 2010 and 2020. The algebraic superposition of the trajectory analysis unit for LUTs was conducted in ArcPro 2.8. Trajectory codes for each land-use/cover object can be achieved by land-use/cover attribute calculation using the formula below (Wang et al., 2012).

$$T_{ij} = (\mathrm{G1})_{ij} \times 10^{n-1} \times (\mathrm{G2})_{ij} \times 10^{n-2} + \ldots + (\mathrm{Gn})_{ij} \quad (1)$$

where T_{ij} has no mathematical sense and represents the trajectory code of the pixel at row i and column j in the trajectory layer, n refers to the number of time codes, and $(G1)_{ij}$, $(G2)_{ij}$ and $(Gn)_{ij}$ represent the LULC map code values in different periods.

In the calculation results, the trajectory analysis of the LULC map in this study was summarized into five types (Gong et al., 2015): 1) A numeric trajectory code in the form of *xxx* was treated as stable, such as 111, 222, 333 and so on, with all the same codes at each time node. This denotes those objects with no land-cover change from 1990 to 2020; 2) *xyy* was identified as prophasic, with 155 representing the change from cropland to built-up land in the second time and kept for in the third period; 3) *xxy* was recognized as anaphasic, with 112 referring to the cropland only converted to forestland in the third period; 4) *xyx* was defined as repetitive, with 121 demonstrating the changes from cropland to forestland only occurred in the second period while the initial and final land types were the same; and 5) *xyz* was seen as continual, with 123 suggesting the transition from cropland to forestland and grassland was continuous during the study period, while the initial and final land types were not the same.

3.3 InVEST model

In this study, the Carbon Storage and Sequestration module of the InVEST model was applied to estimate the amount of carbon stored in this area, which was divided into four basic carbon pools in terrestrial ecosystems, followed by aboveground carbon (AGC), belowground carbon (BGC), soil organic carbon (SOC, 0–20 cm) and dead organic carbon (DOC) in the present study (Zhao et al., 2019). In detail, AGC encompasses the branches, leaves, trunks, bark, and other living plant materials above the soil level, while BGC includes the living roots of AGC, the DOC comprising dead matter as well as litter and the SOC representing the organic components of soil. Additionally, the carbon storage of an ecosystem is calculated by multiplying the average carbon density of AGC, BGC, SOC and DOC of each land-use/cover type by their corresponding areas (Zhao et al., 2019). In this study, the LULC maps generated from the three periods, 2000, 2010 and 2020, were used as input maps, whereas the carbon density for all four carbon pools for each land-use and cover type was derived from the relevant scientific literature with similar conditions to those of the study area in the tropical region (Table 1).

Although the carbon density parameters represent data from a single time point, research has demonstrated that the effects of LUCCs on carbon storage changes can be evaluated well even if the changes in carbon density are ignored (Zhu W.et al., 2019; Li et al., 2021). Using the InVEST model, the calculation formulas for carbon storage estimation are as follows (Li et al., 2021):

$$D = D_{above} + D_{below} + D_{soil} + D_{dead} \quad (2)$$

$$C_{total} = \sum_{i=1}^{k} A_K \times D_K \quad (3)$$

where D denotes the total carbon density of each land-use and land-cover type; D_{above}, D_{below}, D_{soil}, and D_{dead} represent the carbon densities of AGC, BGC, SOC and DOC, respectively; A_K represents the area of each land-use type; and C_{total} denotes total carbon storage.

4 Results

4.1 Land-use/land-cover change detection

To determine the direction of changes in land use and land cover in this study (Table 2), five classes covering a total area of 7,083.63 km^2 were represented in different colours. The results indicated that forestland was the dominant land-use type, accounting for 63.08, 71.08, and 68.13% of the total area, respectively, during each study period and spreading all over the study region. In 2000, the estimated forestland area was 4,468.34 km^2, whereas in 2010 and 2020, it was 5,034.76 km^2 and 4,825.73 km^2, respectively. It represented an upwards trend in the earlier period and a downwards trend in recent times. As the second largest land-use type, cropland played a subsidiary role in the study region, which was mainly distributed in the northeastern region, accounting for 29.97, 24.70 and 23.84% of the total area during the study periods, respectively. Its proportion in the total area presented a downwards trend all the time, possibly due to the implementation of the Grain for Green Program (GGP) by the Chinese government, implemented after 1999, in which a certain proportion of cropland has been abandoned and converted to other land-use types, especially in southwestern mountain areas and northern coastal areas of the study area. As a result, the proportion of cropland decreased to 6.13% from 2000 to 2020. Built-up land was mainly distributed in the northern coastal and northeastern plain areas. It accounted for only 1.36, 1.50 and 4.27% of the total area, respectively, showing a continual upwards trend from 2000 to 2020. The growth of built-up land was mainly observed in the northern coastal areas of Haikou city, the capital of China's largest special economic zone on Hainan Island. The urban areas expanded to 203.7 km^2 in 2020, approximately 6 times the area of 34 km^2 in

TABLE 1 Carbon density of each land-cover type in the study region.

Land-use types	Regional carbon density (kg m^{-2})				Sources
	AGC	BGC	SOC	DOC	
Cropland	1.19	0.36	3.55	0.03	Xi et al. (2013); Wu et al. (2020)
Forestland	4.56	0.64	15.25	0.19	Xi et al. (2013); Wu et al. (2020)
Grassland	0.86	0.39	4.33	0.1	Su (2015); Wu et al. (2020)
Waterbody	0.16	0	3.29	0	Xi et al. (2013); Su (2015)
Built-up land	0.3	0	2.33	0	Song et al. (2016); Wu et al. (2020)

TABLE 2 LULC area coverage and changes between 2000, 2010 and 2020.

Land-use types	Area						Change					
	2000		2010		2020		2000–2010		2010–2020		2000–2020	
	km^2	%	km^2	%	km^2	%	km^2	%	km^2	%	km^2	%
Cropland	2,122.91	29.97	1749.48	24.70	1,688.47	23.84	−373.43	−5.27	−61.01	−0.86	−434.44	−6.13
Forestland	4,468.34	63.08	5,034.76	71.08	4,825.73	68.13	566.42	8.00	−209.03	−2.95	357.39	5.05
Grassland	203.68	2.88	35.62	0.50	36.91	0.52	−168.06	−2.38	1.29	0.02	−166.77	−2.36
Waterbody	192.36	2.72	157.49	2.22	230.13	3.25	−34.87	−0.50	72.64	1.03	37.77	0.53
Built-up land	96.34	1.36	106.28	1.50	302.39	4.27	9.94	0.14	196.11	2.77	206.05	2.91
Total	7,083.63	100	7,083.63	100	7,083.63	100						

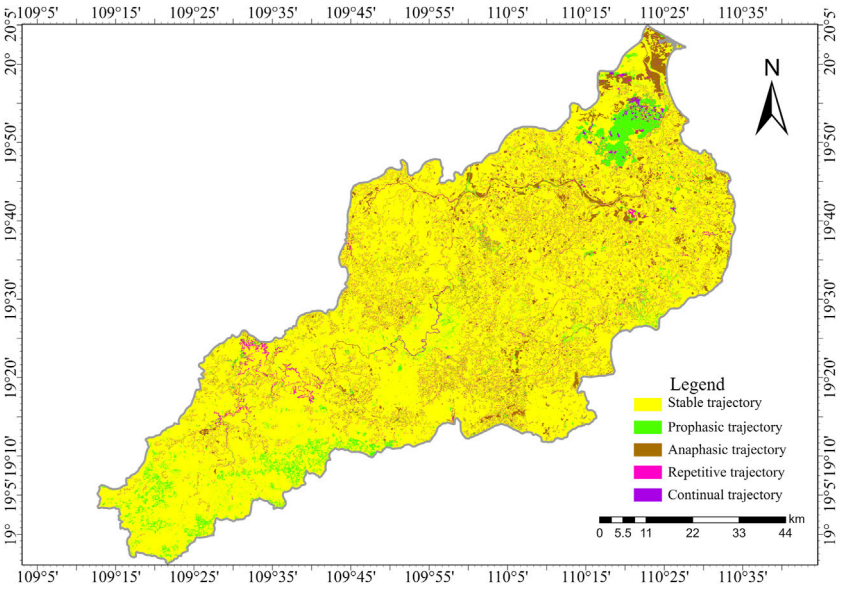

FIGURE 2
Land-use/land-cover change trajectory map of the Nandu River Basin (2000–2020).

TABLE 3 Trajectory analysis of land-use/land-cover change in the study region.

Trajectory type	Area/km^2	Proportion/%	Major trajectory type	Area/km^2
Stable	5,895.66	83.23	Forestland-forestland-forestland (222)	4,194.82
Prophase	465.62	6.57	Cropland-forestland-forestland (122)	222.60
Anaphase	499.62	7.05	Cropland-cropland-forestland (112)	174.01
Respective	183.93	2.60	Cropland-forestland-cropland (121)	126.92
Constant	38.80	0.55	Cropland-forestland-built-up land (125)	21.75
Total	7,083.63	100		

2000. Compared with that in 2000, the spatial distribution of urban areas sharply changed, driven by advancements in modern tropical agriculture, the mass tourism industry and rapid economic development. The proportion of water bodies increased by 0.53% from 2000 to 2020, experiencing a minimal change in spatial distribution, while grassland decreased by 2.36% during the study period, which was mainly observed in the southern mountain region.

4.2 Change trajectory distribution map

Based on the spatiotemporal trajectory calculation, all distribution trajectory maps for the three LULC maps (2000, 2010, and 2020) in the study area are presented in Figure 2. A total of 104 trajectories were identified, among which 99 trajectories varied with time, associated with 16.77% of the total area, whereas the remaining 5 trajectories were trajectories with no land-use changes, accounting for 83.23% of the study area with 59.22% covered forestland (Table 3).

In all change trajectories of the whole area, the anaphasic trajectory occupied the largest area ratio at 7.05% of the total area. The most obvious changes in the anaphasic trajectory were Trajectories 112 and 225, accounting for 34.83 and 22.57% of the total converted land-use types in the anaphasic transition, ranking first and second in the lands with anaphasic trajectories, respectively. While the transformation from cropland to forestland in Trajectory 112 was due to the implementation of GCP, Trajectory 225 mostly occurred in Haikou Jiangdong New Area, which was determined by the Hainan Provincial Government as the main undertaker and the pioneer for the free-trade port policies since 2019. With the construction of the Hainan Free Trade Port, more land was needed for urbanization, and deforestation continued. Moreover, Trajectories 115 and 551 accounted for 12.40 and 0.56% of the total area of the anaphasic transition types, respectively. As they were widely distributed around the suburban area and the urban agglomerations, it implied that a large area of cropland was occupied by built-up land and that only a small proportion of built-up land was compensated by land reclamation.

The area of the prophasic trajectory was 465.62 km^2, the second largest in all land-use change trajectory types, accounting for 6.57% of the total area during this period. In particular, Trajectory Types 122 and 322 were the major prophasic transition types, accounting for 47.81 and 37.12% of the total area of the prophasic trajectory type, respectively. The transition areas of 211 and 233 were only 0.48 and 5.82 km^2, respectively, indicating a large imbalance between forestland, cropland and grassland. Trajectory 122 was closely related to the implementation of forestry ecological policy and readjustment of the local industrial structure, in which a fraction of cropland was converted to forestland. Trajectory 322 indicated that a large area of grassland was occupied by forestland due to economic profits, especially for the extensive planting of fast-growing tree species, such as *Eucalyptus* and *Acacia*.

The area of repetitive transition was 183.93 km^2, accounting for 2.6% of the total area, while the areas of Trajectories 121, 424, and 232 were evidently higher than those of the other repetitive trajectory types, each accounting for 126.92, 30.0, and 7.07 km^2, respectively. Trajectory 121 was the dominant repetitive trajectory type, accounting for 69.01% of the total area in the repetitive trajectory, suggesting that the mutual transition between cropland and forestland was frequent under the context of economic interests and land-protection policies.

The percentage of the continual trajectory type was 0.55%, which was the smallest among all transition types. Among the continual trajectory types, Trajectory 125 was dominant and accounted for 56.04% of the total area, followed by Trajectories 324 and 124 with proportions of 10.34 and 8.36%, respectively. Trajectory 125 occurred in the suburb of Haikou city as an economic development zone, indicating that the transition from cropland to forestland and built-up land was very common in the context of fast-growing urbanization and forestry ecological policy.

4.3 Carbon storage between 2000 and 2020

Over the past 2 decades, the total carbon storage increased from 105.19 Tg C (1 Tg = 10^{12} g) in 2000 to 113.92 Tg C in 2010,

TABLE 4 Total carbon storage of different carbon pools in 2000, 2010 and 2020 in the study region (Tg).

Year	AGC	BGC	SOC	DOC	Total
2000	23.14	3.70	77.42	0.93	105.19
2010	25.13	3.87	83.91	1.01	113.92
2020	24.17	3.71	81.21	0.97	110.06

followed by a decline from 113.92 Tg C in 2010 to 110.06 in 2020 (Table 4). Although it showed an upwards trend followed by a downwards trend, the change was not significant, with only a net increase in carbon storage of 4.87 Tg C and an average annual increasing rate of 0.2316% in the whole study region. Among the four carbon pools during the study period, SOC was dominant and accounted for 73.60, 73.66 and 73.78% of the total carbon storage in 2000, 2010 and 2020, respectively. AGC was the second most significant, accounting for 22.00, 22.06 and 21.96% of the total carbon storage across the whole region in each period, respectively. DOC occupied the lowest proportion of the total area, with an approximate carbon storage of 0.93 Tg C, 1.01 Tg C and 0.97 Tg C during the study period, respectively. Spatially, the carbon density in the southern part of the mountain region was greater than that in the northern part (Figures 3A,B,C). This trend was evident in all three periods because most forestland was widely distributed in the southern mountain region of the study area and had significantly high carbon stocks due to robust photosynthesis. In addition, the southern mountain region is located in the National Park of Hainan Tropical Rainforest, where forestland (tropical rainforest) has been strictly protected and there is almost no human disturbance due to the strict implementation of the Natural Forest Protection Project (NFPP) by the Chinese government.

Figures 4A,B,C shows the spatial changes in carbon density from 2000 to 2020. Generally, the carbon-emission areas for LULC in the study region showed an increase, which was mainly distributed in industrial parks close to the coastal zone and the economic area along the Nan Du River. While the carbon sink areas spread across the whole study region during the study period, they were largely concentrated in the southern mountain region. The total areas of carbon emissions and carbon sinks were approximately 5.25 and 8.93%, respectively, during the whole study period (Table 5), with 85.82% of this area undergoing no change between 2000 and 2020. The change in carbon emissions from land-use conversion between 2000 and 2020 was 4.66 Tg C, whereas the change in carbon sinks from LULC was 9.53 Tg C. To some extent, this indicates that the carbon sequestration

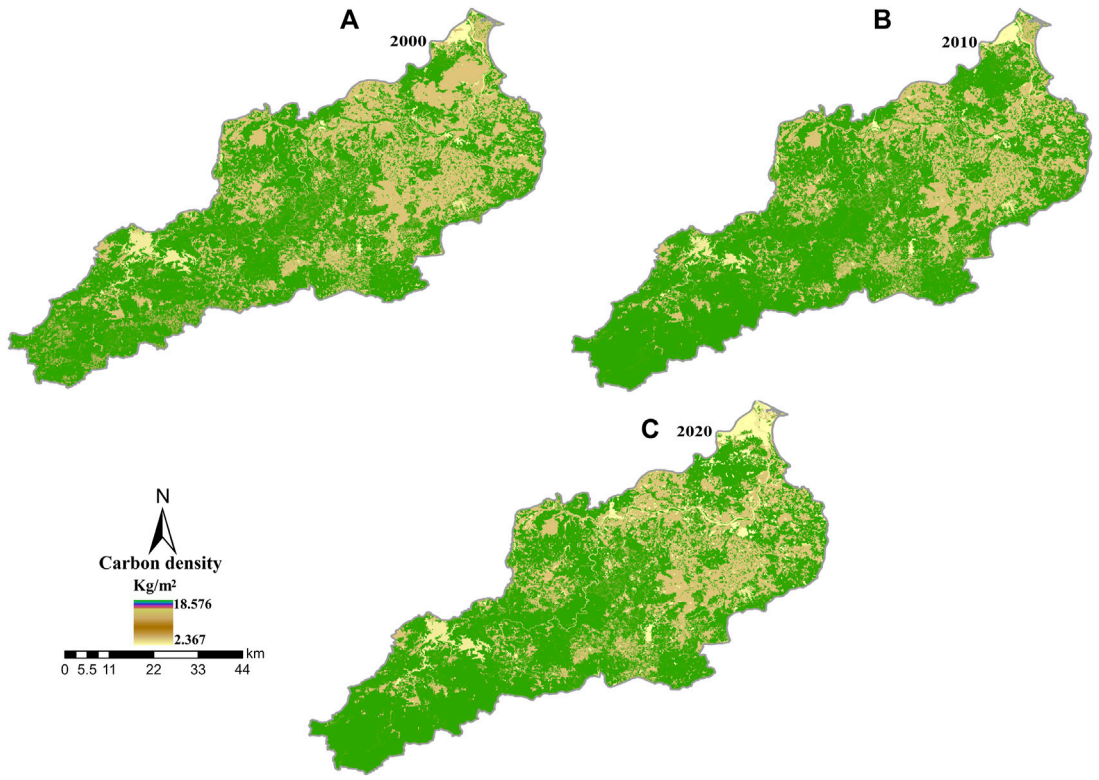

FIGURE 3
The spatial distribution of total carbon density in 2000, 2010 and 2020 **(A–C)**.

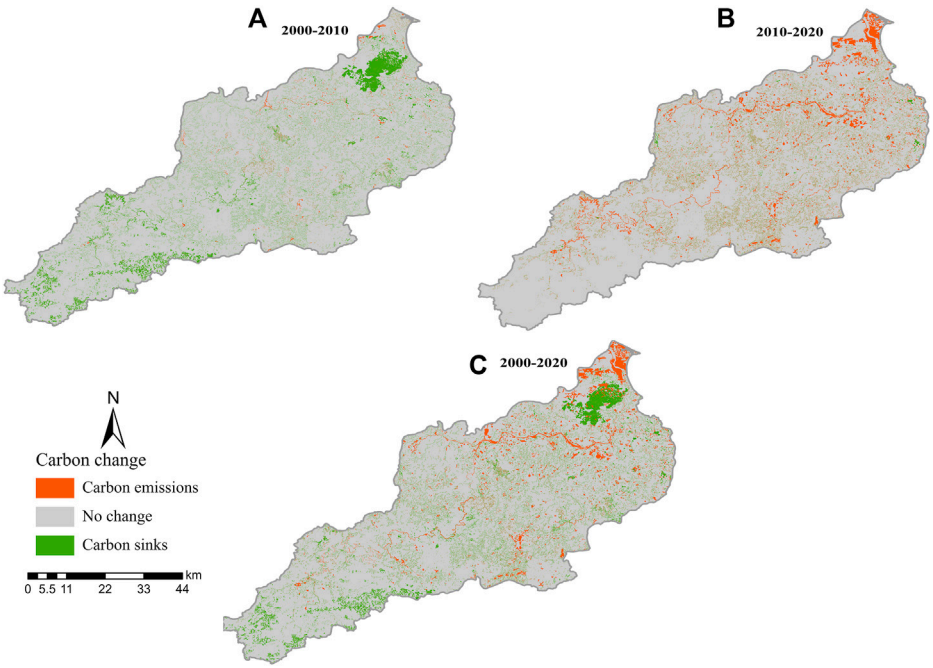

FIGURE 4
Spatiotemporal carbon change between 2000, 2010 and 2020 in the study region **(A–C)**.

TABLE 5 Area percentages of carbon density changes in the study region (%).

Stages	Carbon-emission area	Carbon sink area	Unchanged area	Stages	Carbon-emission area
2000–2010	0.86	8.86	90.28	2000–2010	0.86
2010–2020	7.07	3.13	89.8	2010–2020	7.07
2000–2020	5.25	8.93	85.82	2000–2020	5.25

capacity caused by land-use changes is much more significant than the carbon-emission capacity in this study region. Due to the expansion of forestland and grassland areas for the implementation of the GCP during the study period, the changes in total carbon storage suggest that the land-use and land-cover changes between 2000 and 2020 led to a net increase in carbon by 4.87 Tg C. During 2000–2010, the percentage of carbon emissions was only 0.86% of the total area in this study region, 7.07% between 2010 and 2020, which was 8.22 times higher than that during 2000–2010, showing that the spatial distribution of carbon-emission areas was more dispersive than that in the first stage. While the carbon sink areas accounted for 8.86 and 3.13% in the first and second stages, respectively, they were more spatially scattered in the first stages. The total area of no carbon changes between 2000 and 2010 was approximately 90.28 and 89.80%, respectively, which was dominant in the study area and showed a similar spatial distribution pattern during both stages in the study period.

5 Discussion

5.1 Spatiotemporal trajectory and patterns of carbon storage induced by LULCCs

The results in land-use/cover conversion directly led to the great changes in large carbon sinks and carbon sources. Land use change will change the amount of plant residues entering soil, affect the decomposition and loss of soil organic carbon, break the balance of soil organic carbon, and change the soil carbon density. Land use change will lead to the transfer of vegetation carbon, part of vegetation carbon stays in place in the form of

TABLE 6 Land-use conversion matrix from 2000 to 2010 (in km^2).

2000	2010					2000 total (km^2)
	Cropland	Forestland	Grassland	Waterbody	Built-up land	
Cropland	—	374.98	1.32	4.41	5.04	2,122.92
Forestland	1.26	—	13.47	19.04	14.63	4,468.34
Grassland	0	180.54	—	0.81	1.95	203.68
Waterbody	6.99	51.59	0.46	—	0.19	192.36
Built-up land	4.06	7.71	0	0.1	—	96.34
2010 Total (km^2)	1749.48	5,034.76	35.62	157.49	106.28	

dead branches and leaves, enters the soil and is transformed into soil organic carbon, and the other part of vegetation carbon is used and removed in different ways, and finally enters the atmosphere, which changes the vegetation carbon density. Due to the difference of land transfer area and carbon density, the change of land use types has different effects on carbon storage. In particular, built-up expansion areas affect not only the carbon-emission intensity of human activities but also carbon sinks within terrestrial ecosystems (Hergoualc'h and Verchot, 2013; Tubiello et al., 2015). Therefore, combining the spatiotemporal trajectory of LULC changes with InVEST models, this study aimed to analyse the effects of LULC on carbon storage in the Nandu River watershed in the tropical region of Hainan Island. The following discussion focuses on the effects of land-trajectory analysis on carbon storage.

5.1.1 Impact of land-use patterns for trajectory analysis on carbon storage from 2000 to 2010

The results obtained with the InVEST model revealed that the conversion of LULC classes resulted in an increase in carbon storage in the first stages (2000–2010). The total carbon stock estimated for the land-use pattern in the study area in 2000 amounted to 105.19 Tg C, which increased by 113.92 Tg C in 2010, with a net increase in the total carbon storage of 8.73 Tg C and an annual increase of approximately 0.873 Tg C (Table 3).

From the land-use conversion matrix (Table 6), the area that underwent land-use change in the study region was 688.53 km^2, accounting for 9.72% of the total land. Conversions between cropland and forestland were the major transition during this stage, accounting for 54.64% of the total land change, as 374.98 km^2 of cropland was converted to forestland, and 1.26 km^2 of forestland was transformed into cropland. The benefits of afforestation do not balance out the negative effects of deforestation in this stage. Conversion from cropland to forestland was mostly distributed in the northern part of the study region, which created the largest net carbon storage, 5.82 Tg C, in the study region as a direct result of the GGP, suggesting that afforestation and recovery of forestland had positive effects on carbon sequestration due to its greater carbon density (Krogh et al., 2003; Wang et al., 2020). However, under the impacts of local urbanization and industrialization and industrial restructuring, especially the development of high-efficiency tropical agriculture and the development of international tourism on Hainan Island that expanded rural people's economic prospects beyond farming, an increasing number of farmers are migrating into urban areas for nonfarm employment opportunities. The remaining farmers are primarily elderly people and women with relatively low labour capacity (Li et al., 2014). Our results showed that a certain amount of cropland was converted into forestland for fast-growing timber plantations, rubber plantations, and betel-nut plantations, especially in the plain region, as a direct result of the declining relative profitability of traditional farming businesses (Yan et al., 2016). This transformation in land use will undermine national food security for China in the future. Driven by local economic interests or industrial restructuring, the development from grassland to forestland accounted for 180.54 km^2, which was the second largest transition area with a net carbon storage of 2.70 Tg C. The conversion from water bodies to forestland comprised the third largest area on the trajectory maps, covering an area of 51.59 km^2 and creating 0.89 Tg C.

The shift from forestland to water bodies covered 19.04 km^2, the largest area for the passive impacts on carbon storage, with a total loss of 0.89 Tg C. This indicated that the contribution of water bodies to carbon storage was far less than that of forestland. In addition, interchanges between forestland and built-up land were also observed during the study period. The transformation from forestland to built-up land was another important trajectory for carbon emissions, accounting for 2.13% of the total change area. With rapid economic development and urbanization, the expansion of built-up land occurred in the economic development zone or new urban development zone (Chen et al., 2020). A significant fraction of land was needed for built-up construction, thereby resulting in deforestation and a 0.26 Tg C decrease in regional carbon storage. Moreover, 13.47 km^2 of forestland was estimated to have converted to grassland, causing a 0.20 Tg C decrease in carbon storage.

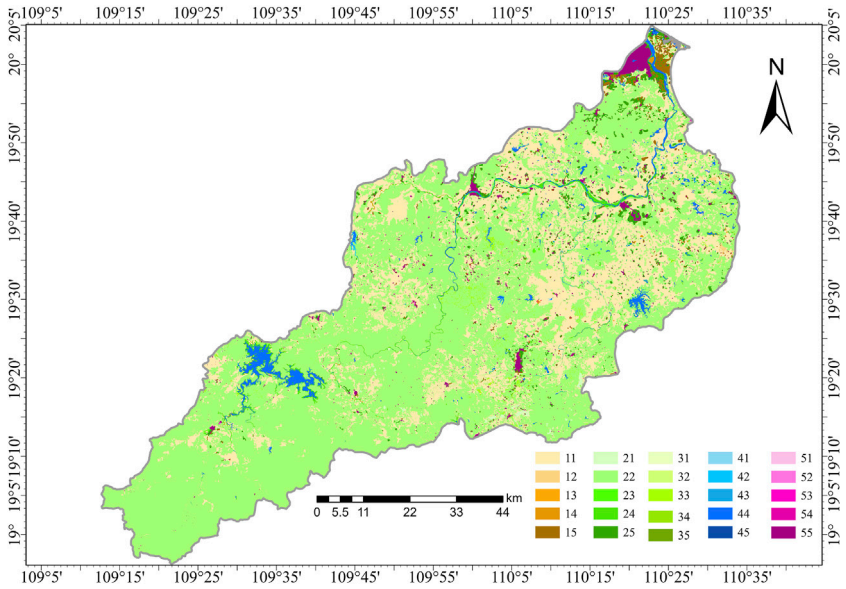

FIGURE 5
Land-use/land-cover change trajectory map of the study region from 2010 to 2020.

5.1.2 Impact of land-use patterns for trajectory analysis on carbon storage from 2010 to 2020

Specifically, during the 2010–2020 period, the spatial distribution of the trajectory in the study region exhibited significant differences (Figure 5).

The most obvious changes in trajectory units were the conversion from forestland to cropland and its reverse, accounting for 25.06 and 24.17% of the total converted land-use types, occupying the largest and the second largest areas of total land changes, respectively. With the implementation of the GCP, 175.25 km^2 of cropland was estimated to be converted to forestland, causing a 2.72 Tg C increase in carbon storage. However, under the influence of local industrial policy, especially with the emphasis on returning *Eucalyptus* to sugarcane or cropland, 181.65 km^2 of forestland was converted to cropland, resulting in a total loss of 2.82 Tg C of carbon storage, while these conversions were estimated to lead to a slight decrease in carbon storage of 0.10 Tg C.

Correspondingly, with the acceleration of urbanization and the expansion of urban areas, carbon storage in the transformation from forestland to built-up land showed a significant decreasing trend, with 140.97 km^2 of forestland estimated to be converted into built-up land. This trajectory was the third largest change area of trajectory types and the main source of decrease in carbon storage by 2.54 Tg C. On the other hand, only 6.49 km^2 of built-up land was estimated to be converted to forestland, resulting in a total increase of 0.12 Tg C. The trajectory change from forestland to built-up land was mostly distributed in Jiangdong New Area, mainly composed of Guilinyang Economic Development Zone and Lingshan Town. Since 2018, the Chinese government announced that Hainan will be built into the largest free-trade port in the world, taking up an area of 3.5 × 104 km^2, especially for international tourism, consumption, and investment centres in the future. Under the guidance of major national policies and strategies and the Free Trade Island policy of Hainan Island, Hainan fully launched the construction of the pilot FTZ (**Free Trade Zone**) and made significant progress in infrastructure development, including key industrial parks, new development zones, and property booms in coastal areas. The planted forest near the coastal region or along the Nandu River was converted into built-up land. Although the local government launched a strict policy of forestland replacement and implemented forest ecological protection measures, a vast amount of land was needed for urbanization, and local deforestation still occurred (Zhu E.et al., 2019).

The trajectory type of cropland transformed to built-up land was also noteworthy, accounting for 8.85% of the total land types that were converted, which was mostly distributed around the major townships on the plains and along the Nandu River. The trajectories resulted in a decrease in carbon storage of 0.16 Tg C, with carbon losses mainly caused by the loss of cropland with high SOC content (Zhu E.et al., 2019). In contrast, only 6.49 km^2 of built-up land was reclaimed as cropland, accounting for 0.90% of the total land-use types that were converted, indicating a severe imbalance in cropland that was created and destroyed. Moreover, the transitions between cropland and built-up land were relatively concentrated (Figure 3). Therefore, how to

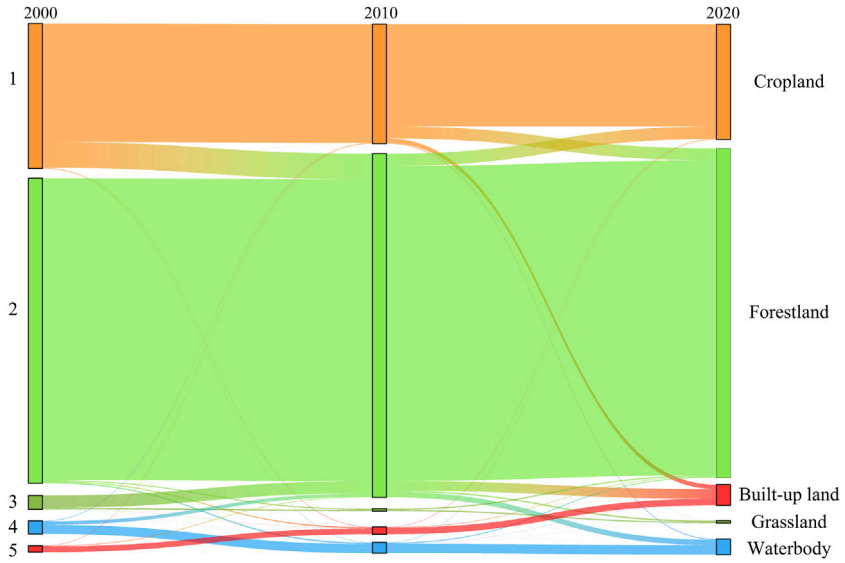

FIGURE 6
Land-use change trajectory of the Nandu River watershed from 2000 to 2020.

coordinate ecological protection and rapid economic development is a major challenge that this basin or even all of Hainan Island will face in the future.

Additionally, "forestland → water body" was another important trajectory type, with an area of 79.92 km^2. This is mainly due to the increase of water body area, and the rising water level leads to part of forestland being covered by water body, mainly concentrated in the reservoir in the study area. While 12.61 km^2 of water bodies was converted to forestland, the conversions between water bodies and forestland were estimated to lead to a net total loss of carbon storage of 1.16 Tg C, partly due to the relatively higher carbon storage capacity of forestland compared with water bodies (Pagiola, 2008). The transition between forestland and grassland exhibited a relative balance, and the trajectory units of "grassland → forestland" and "forestland → grassland" accounted for 16.70 and 18.67 km^2, respectively, resulting in a net decrease in regional carbon storage by only 0.03 Tg C. The decrease is mainly attributed to the diminished forestland, by 1.97 km^2, and grassland has a lower storage capacity than forestland.

5.1.3 Impact of land-use patterns for trajectory analysis on carbon storage from 2000 to 2020

Specifically, during the 2000–2020 period, enormous LULC changes were observed in the trajectory analysis of regional carbon sources and sinks in the Nandu River watershed (Figure 6).

The prophasic trajectory was the major carbon storage sink in the study region, causing a 5.87 Tg C net increase in carbon storage, with a mean accumulation of 0.29 Tg C per year. The most obvious trajectory in the prophasic trajectory was Trajectory 122, which was mainly distributed in the northern region of the suburban area around Haikou city and was the main source of the increase in carbon storage, the contribution rate is 58.77% (3.45 Tg C). As the second significant factor, Trajectory 322 resulted in a total increase of 2.59 Tg C of carbon storage, contributing 44.12% of the increase. Trajectories 122 and 322 led to an increase in carbon storage due to the expansion of forestland and grassland areas with higher carbon storage capabilities. These results were similar to the findings of Zhang et al. (2010) and Lu et al. (2018). On the one hand, local carbon storage was expected to increase under the implementation of the Grain to Green Program (GGP). On the other hand, as a result of the vigorous development of construction driven by urban expansion, tropical ecotourism development and the construction of the international free-trade islands on Hainan Island, especially in Haikou city, the expansion of the urban area has been developing at an am azing speed, with an annual change rate of 16.46% from 1990 to 2020. In addition, the local government implemented a series of policies and measures to develop the economy, such as coastal ecotourism, tropical high-efficiency agriculture, intensive and productive industrial zones, free-trade zones and free-trade port construction, which accelerated the migration flows from rural to urban areas (Yan et al., 2016). The official data showed that the population of Haikou increased from 150.83 × 10^4 in 2000 to 287.33 × 10^4 in 2020, with an increase of 136.50 × 10^4 during the study period (http://stats.hainan.gov.cn/tjj/). With an annual population growth rate of 6.23%, rural–urban labour migration from rural areas was a major cause of the

abandonment of cropland and rural settlement, leading to the "hollow village" phenomenon in rural areas. In addition to population flow, a fraction of cropland was converted to forestland for tropical economic forests or tropical fast-growing timber forests. Zhang et al. (2014) indicated that under the effects of local economic development, China has experienced land abandonment in recent years. The results showed that the changes in regional carbon sink capacity lie in the imbalance between regional economic development and industrial restructuring. Similar situations were reported by Jerath et al. (2016). Therefore, it is very important to coordinate the future processes of urbanization, industrial restructuring and food security in the study region. Trajectory 255 in the prophasic trajectories caused the largest total loss (0.23 Tg C) of carbon storage. In these areas, large tracts of forestland were developed into built-up land and thus caused carbon storage loss from the SOC stock (Zhu E.et al., 2019). The results showed that the change in land use/cover from natural lands to built-up areas led to remarkable carbon emissions. Trajectory 244 was estimated to lead to a second major decrease in carbon storage of 0.22 Tg.

In summary, the net carbon emissions for the anaphasic trajectory in the study region were 0.23 Tg C. Trajectory 112 was the main carbon sink, boosting carbon storage by 2.70 Tg C, followed by Trajectory 332, with an increase in carbon storage of 0.14 Tg C. Trajectory 112 was mainly distributed in the southern mountain region and northern plain region. While the situation of Trajectory 112 in the northern plain region was similar to that of Trajectory 122 in the prophasic trajectory, Trajectory 112 in the southern mountain region mostly occurred in the National Park of Hainan Tropical Rainforest, indicating that the Grain to Green Program has been strictly implemented in the region with an expected increase in regional carbon storage in the form of a local carbon sink. Trajectory 225 caused a considerable amount of carbon losses, 2.03 Tg C, which was mainly distributed in the New Development Area in the coastal region. Due to the special natural tourism resources and the excellent environment, the construction of the Hainan International Island occurred in 2008, and many more people have come to Hainan Island for tourism or to make a living, especially those from the notrtheastern region of China. According to official statistics, the total number of tourists and tourism revenue in Hainan reached 8.07 million and 37.75 billion yuan (RMB) in 2020, 2.4 times and 4.3 times the data in 2000, respectively. Currently, the tourism economy has become an essential engine of economic growth for this area (Cui et al., 2019). The total income of tourism accounts for over 12% of the region's GDP. The booms in the tourism industry have promoted the real estate industry in the region. As a consequence, the construction of seascape housing and the expansion of built-up areas not only occupied the coastal region but also destroyed forestland, especially the coastal protective forest, and expanded onto the beaches and led to corresponding carbon storage losses. Our results showed that human settlements had a great impact on carbon storage losses in the study area. A similar result of increasing carbon emissions in the region was reported by Cai et al. (2018). Although the Chinese government has launched environmental inspections to protect the ecological environment since 2016, illegal land conversion, such as illegal reclamation, deforestation, and wetland destruction, still occurred in some parts of the study region. Therefore, coordinating the complex relationship between LULCCs and carbon sinks and sources is the key point of implementing the optimized local land-use structure. Trajectory 221 experienced the second largest carbon storage loss, 0.81 Tg C, which was due to deforestation for reclamation.

In general, the change of carbon sink capacity is closely related to the change of LULC, and the government needs to regulate carbon storage by macro-regulating LULC change. After 2020, the construction of Hainan Free Trade Port will enter the stage of full implementation and development. In the future, the intensity and direction of land use development should be conducive to the increase of regional carbon storage, explore ways to optimize the land use structure with the goal of carbon balance, and strengthen reasonable control over the expansion of construction land. Decision-makers can take a series of land use control measures such as increasing the proportion of forestland, strengthen the transformation of construction land and unused land into forestland and grassland through reclamation and greening of construction land and restoration of ecological land, and continue to implement ecological transformation projects such as returning farmland to forest and grassland. Meanwhile, the government can strengthen the ecological protection of coastal wetlands and other wetlands, strengthen the protection and restoration of degraded forestland, grassland and wetlands, and realize the land use regulation of regional low-carbon construction and ecological environmental protection.

The repetitive trajectories had no impact on carbon sinks and sources. The contribution to carbon storage for the continual trajectory type was insignificant. The total carbon storage of the repetitive trajectory was estimated to decrease by only 0.075 Tg C. Trajectory 125 in the continual trajectory was the main carbon source, with carbon storage losses of 0.054 Tg C, followed by Trajectory 215, which resulted in a total loss of 0.0133 Tg C of carbon storage, accounting for 72.00% and 17.73% of the total reduction, respectively. The results showed that carbon emissions in the continual trajectory were the primary carbon sources in built-up areas, which was mainly ascribed to human activities. In 2018, the Chinese government announced to the world the establishment of the world's largest free-trade port on Hainan Island. With the implementation of national and local policies, the urbanization process of Hainan International Free Trade Island has accelerated, leading to intensive population expansion, profound regional economic development, unbalanced rapid economic development and regional industrial restructuring. These forces were the root cause of changes in regional LULC patterns, which ultimately affected the capacity of carbon sources and carbon sinks (Cui et al., 2019). The results of the study showed that the carbon sink capacity of economically developed regions with intensive land use declined and became the new significant carbon source area.

Therefore, further exploring the complex relationship between LULCCs and carbon sinks and sources is the key to optimizing land-use structure and patterns. Trajectory 412 in the continual trajectory was the largest carbon sink, with an increase in carbon storage of 0.015 Tg C, followed by Trajectory 512, causing 0.007 Tg C of increased carbon storage.

5.2 Strengths and limitations of the linked model

This study assessed the impact of land-use changes on regional carbon sources and sinks utilizing remote sensing and GIS modelling combined with the InVEST model. Additionally, we improved previous studies by revealing the response mechanisms of land-use dynamic processes on regional carbon sources/sinks by linking trajectory analysis and the InVEST models. Although more effects of spatiotemporal trajectory analysis in LULC change on carbon storage in the Nandu River Basin were examined from 2000 to 2020, this study is still limited in a few aspects. Due to the lack of accurate and long-term ground observation data of carbon density in these land covers during each period, this study could only obtain the approximate carbon storage values during the different periods and suffered the risk of reduced accuracy in the assessment of carbon stocks. However, the overall spatial pattern of carbon storage was not affected. Second, the carbon module of the InVEST model simplified the process of the carbon cycle to a certain extent (Chen et al., 2017) by assuming that the carbon density was homogeneous with constant values and focusing on the difference in carbon density between different land-use types. Additionally, without considering the dynamic changes in carbon density for the same land-use type along with the change in environment and time, the estimated results of carbon stock could be uncertain. Therefore, for future research, to obtain more accurate carbon storage values in these land covers in the study region during each period, it will be increasingly necessary to collect accurate carbon density data through long-term observations and large-scale experiments. There is a need to timely supplement the influence of spatial heterogeneity within land-use types and vegetation age structure on carbon density by using more field data.

6 Conclusion

This study demonstrated a change trajectory methodology to identify the spatiotemporal evolutionary tracking of land-use/land-cover (LULC) changes. The change trajectories and the InVEST models were linked to determine the spatiotemporal dynamics of carbon storage and investigate the impact of land-use change on carbon storage in the Nandu River Basin on Hainan Island in China, the world's largest free-trade island.

Between 2000 and 2020, forestland showed the largest growth, 357.39 km^2, followed by the continuous expansion of built-up land by almost 206.05 km^2, with an annual rate of 24.96%. Urbanization was accompanied by an increase of approximately 4.87 Tg C of carbon storage in the study region. In contrast, the areas of cropland and grassland declined continuously by 434.44 and 166.77 km^2, respectively. The anaphasic trajectory had the largest area fraction, 7.05%, in the total area, whereas the proportion of the continual trajectory was the smallest among all transition types at 0.55%. During the two time spans from 2000–2010 to 2010–2020, the spatiotemporal trajectories for land-use changes significantly contributed to carbon sequestration in the study region through the conversion from cropland to forestland, causing 5.82 Tg C and 2.72 Tg C in carbon storage, respectively. In the trajectory analysis of LULCCs over the whole period, the prophasic trajectories were the major contributor to carbon storage sinks in the study region, resulting in a rise in carbon storage by 5.87 Tg C, while the repetitive trajectories had no impact on carbon sinks and sources.

The findings in this study provide a new way to identify the spatiotemporal patterns of LULC changes by using trajectory analysis as a preprocessing tool. The new methods could be revised for assessing the impact of trajectory analysis for land-use changes on the change in carbon storage by coupling the Invest Model and trajectory analysis in other study areas.

Data availability statement

The original contributions presented in the study are included in the article/Supplementary Material, further inquiries can be directed to the corresponding authors.

Author contributions

XR and TaL designed the research. WG, TiL, XD, and XQ performed the research and wrote the manuscript. GW, MM, JH, YS, YZ, YX, and GW analyzed the data and provided the basics for the optimization of the figure. All authors contributed to the article and approved the submitted version.

Funding

This research was supported by Hainan Provincial Natural Science Foundation of China, grant number 320RC506, 621RC507 and 421MS013; Hainan Ecological Environment Monitoring Project of China Meteorological Administration, grant number ZQC-J20142; the National Natural Science Foundation of China, grant number 32160364; the Hainan Provincial Key Research and Development Plan of China, grant number ZDYF2021SHFZ110; the Science and Technology Project of Haikou City, China, grant number 2020-057; and the Natural Science Foundation of Hainan

University, grant numbers KYQD (ZR) 20058, 1863 and 20057.

Conflict of interest

The authors declare that the research was conducted in the absence of any commercial or financial relationships that could be construed as a potential conflict of interest.

Publisher's note

All claims expressed in this article are solely those of the authors and do not necessarily represent those of their affiliated organizations, or those of the publisher, the editors and the reviewers. Any product that may be evaluated in this article, or claim that may be made by its manufacturer, is not guaranteed or endorsed by the publisher.

References

Abdullah, A. N. M., Stacey, N., Garnett, S. T., and Myers, B. (2016). Economic dependence on mangrove forest resources for livelihoods in the Sundarbans, Bangladesh. *For. Policy Econ.* 64, 15–24. doi:10.1016/j.forpol.2015.12.009

Cai, B., Li, W., Dhakal, S., and Wang, J. (2018). Source data supported high resolution carbon emissions inventory for urban areas of the Beijing-Tianjin-Hebei region: Spatial patterns, decomposition and policy implications. *J. Environ. Manage.* 206, 786–799. doi:10.1016/j.jenvman.2017.11.038

Chen, D., Deng, X., Jin, G., Samie, A., and Li, Z. (2017). Land-use-change induced dynamics of carbon stocks of the terrestrial ecosystem in Pakistan. *Phys. Chem. EarthPhysics Chem. Earth Parts A/B/C* 101, 13–20. doi:10.1016/j.pce.2017.01.018

Chen, W., Zhao, H., Li, J., Zhu, L., Wang, Z., and Zeng, J. (2020). Land use transitions and the associated impacts on ecosystem services in the Middle Reaches of the Yangtze River Economic Belt in China based on the geo-informatic Tupu method. *Sci. Total Environ.* 701, 134690. doi:10.1016/j.scitotenv.2019.134690

Chuai, X., Huang, X., Wang, W., Wu, C., and Zhao, R. (2014). Spatial simulation of land use based on terrestrial ecosystem carbon storage in coastal Jiangsu, China. *Sci. Rep.* 4 (1), 5667. doi:10.1038/srep05667

Cui, X., Wei, X., Liu, W., Zhang, F., and Li, Z. (2019). Spatial and temporal analysis of carbon sources and sinks through land use/cover changes in the Beijing-Tianjin-Hebei urban agglomeration region. *Phys. Chem. Earth, Parts A/B/C* 110, 61–70. doi:10.1016/j.pce.2018.10.001

Dai, E., Huang, Y., Wu, Z., and Zhao, D. (2016). Spatial-temporal features of carbon source-sink and its relationship with climate factors in Inner Mongolia grassland ecosystem. *Acta Geogr. Sin.* 71 (1), 21–34.

De Sousa-Neto, E. R., Gomes, L., Nascimento, N., Pacheco, F., and Ometto, J. P. (2018). "Land use and land cover transition in Brazil and their effects on greenhouse gas emissions," in *Soil management and climate change*. Editors M. A. Munoz and R. Zornoza (Amsterdam, Netherlands: Elsevier), 309–321.

Fang, J., Yu, G., Ren, X., Liu, G., and Zhao, X. (2015). Carbon sequestration in China's terrestrial ecosystems under climate change: Progress on ecosystem carbon sequestration from the CAS Strategic Priority Research Program. *Bull. Chin. Acad. Sci.* 30 (6), 848–857. [(in Chinese)] doi:10.16418/j.issn.1000-3045.2015.06.019

Foley, J. A., Defries, R., Asner, G. P., Barford, C., Bonan, G., Carpenter, S. R., et al. (2005). Global consequences of land use. *Science* 309 (5734), 570–574. doi:10.1126/science.1111772

Fu, Y. C., Lu, X. Y., Zhao, Y. L., Zeng, X. T., and Xia, L. L. (2013). Assessment impacts of weather and land use/land cover (LULC) change on urban vegetation net primary productivity (NPP): A case study in guangzhou, China. *Remote Sens.* 5 (8), 4125–4144. doi:10.3390/rs5084125

Gao, J., and Wang, L. C. (2019). Embedding spatiotemporal changes in carbon storage into urban agglomeration ecosystem management - a case study of the Yangtze River Delta, China. *J. Clean. Prod.* 237, 117764. ARTN 117764. doi:10.1016/j.jclepro.2019.117764

Gong, W., Yuan, L., Fan, W., and Stott, P. (2015). Analysis and simulation of land use spatial pattern in harbin prefecture based on trajectories and cellular automata—markov modelling. *Int. J. Appl. Earth Observation Geoinformation* 34, 207–216. doi:10.1016/j.jag.2014.07.005

Hergoualc'h, K., and Verchot, L. V. (2013). Greenhouse gas emission factors for land use and land-use change in Southeast Asian peatlands. *Mitig. Adapt. Strateg. Glob. Chang.* 19 (6), 789–807. doi:10.1007/s11027-013-9511-x

Houghton, R. A., House, J. I., Pongratz, J., van der Werf, G. R., DeFries, R. S., Hansen, M. C., et al. (2012). Carbon emissions from land use and land-cover change. *Biogeosciences* 9 (12), 5125–5142. doi:10.5194/bg-9-5125-2012

Houghton, R. A. (2003). Revised estimates of the annual net flux of carbon to the atmosphere from changes in land use and land management 1850–2000. *Tellus B Chem. Phys. Meteorology* 55 (2), 378–390. doi:10.3402/tellusb.v55i2.16764

Houghton, R. A., Skole, D. L., Nobre, C. A., Hackler, J. L., Lawrence, K. T., and Chomentowski, W. H. (2000). Annual fluxes of carbon from deforestation and regrowth in the Brazilian Amazon. *Nature* 403 (6767), 301–304. doi:10.1038/35002062

Huang, Q. X., Robinson, D. T., and Parker, D. C. (2014). Quantifying spatial-temporal change in land-cover and carbon storage among exurban residential parcels. *Landsc. Ecol.* 29 (2), 275–291. doi:10.1007/s10980-013-9963-0

Hwang, J., Choi, Y., Kim, Y., Ol, L. N., Yoo, Y.-J., Cho, H. J., et al. (2021). Analysis of the effect of environmental protected areas on land-use and carbon storage in a megalopolis. *Ecol. Indic.* 133, 108352. doi:10.1016/j.ecolind.2021.108352

Jerath, M., Bhat, M., Rivera-Monroy, V. H., Castañeda-Moya, E., Simard, M., and Twilley, R. R. (2016). The role of economic, policy, and ecological factors in estimating the value of carbon stocks in Everglades mangrove forests, South Florida, USA. *Environ. Sci. Policy* 66, 160–169. doi:10.1016/j.envsci.2016.09.005

Ji, J., Huang, M., and Li, K. (2008). Prediction of carbon exchanges between China terrestrial ecosystem and atmosphere in 21st century. *Sci. China Ser. D-Earth. Sci.* 51 (6), 885–898. doi:10.1007/s11430-008-0039-y

Krogh, L., Noergaard, A., Hermansen, M., Greve, M. H., Balstroem, T., and Breuning-Madsen, H. (2003). Preliminary estimates of contemporary soil organic carbon stocks in Denmark using multiple datasets and four scaling-up methods. *Agric. Ecosyst. Environ.* 96 (1-3), 19–28. doi:10.1016/s0167-8809(03)00016-1

Kuma, H. G., Feyessa, F. F., and Demissie, T. A. (2022). Land-use/land-cover changes and implications in southern Ethiopia: Evidence from remote sensing and informants. *Heliyon* 8 (3), e09071. doi:10.1016/j.heliyon.2022.e09071

Lal, R. (2004). Soil carbon sequestration impacts on global climate change and food security. *Science* 304 (5677), 1623–1627. doi:10.1126/science.1097396

Leifeld, J. (2013). Prologue paper: Soil carbon losses from land-use change and the global agricultural greenhouse gas budget. *Sci. Total Environ.* 465, 3–6. doi:10.1016/j.scitotenv.2013.03.050

Li, K., Cao, J., Adamowski, J. F., Biswas, A., Zhou, J., Liu, Y., et al. (2021). Assessing the effects of ecological engineering on spatiotemporal dynamics of carbon storage from 2000 to 2016 in the loess plateau area using the InVEST model: A case study in huining county, China. *Environ. Dev.* 39, 100641. doi:10.1016/j.envdev.2021.100641

Li, L., Song, Y., Wei, X., and Dong, J. (2020). Exploring the impacts of urban growth on carbon storage under integrated spatial regulation: A case study of wuhan, China. *Ecol. Indic.* 111, 106064. doi:10.1016/j.ecolind.2020.106064

Li, Z., Yan, J., Hua, X., Xin, L., and Li, X. (2014). Factors influencing the cultivated land abandonment of households of different types: A case study of 12 typical villages in chongqing municipality. *Geogr. Res.* 33 (4), 721–734. doi:10.11821/dlyj201404012

Liang, X., Guan, Q., Clarke, K. C., Chen, G., Guo, S., and Yao, Y. (2021a). Mixed-cell cellular automata: A new approach for simulating the spatio-temporal dynamics of mixed land use structures. *Landsc. Urban Plan.* 205, 103960. doi:10.1016/j.landurbplan.2020.103960

Liang, Y., Hashimoto, S., and Liu, L. (2021b). Integrated assessment of land-use/land-cover dynamics on carbon storage services in the Loess Plateau of China from 1995 to 2050. *Ecol. Indic.* 120, 106939. doi:10.1016/j.ecolind.2020.106939

Liu, J., Kuang, W., Zhang, Z., Xu, X., Qin, Y., Ning, J., et al. (2014). Spatiotemporal characteristics, patterns, and causes of land-use changes in China since the late 1980s. *J. Geogr. Sci.* 24 (2), 195–210. doi:10.1007/s11442-014-1082-6

Liu, Y., Jia, B., Li, X., Wu, J., Meng, P., Hong, W., et al. (2013). Characteristic of nutrients and evaluation of heavy metal contamination on sediments among Xinpo pond, Nandu River in Hainan province. *Trans. Chin. Soc. Agric. Eng.* 29 (3), 213–224.

Liu, Y., Zhang, J., Zhou, D., Ma, J., Dang, R., Ma, J., et al. (2021). Temporal and spatial variation of carbon storage in the Shule River Basin based on InVEST model. *Acta Ecol. Sin.* 41, 4052–4065. doi:10.5846/stxb201911152452

Lu, D., Xu, X., Tian, H., Moran, E., Zhao, M., and Running, S. (2010). The effects of urbanization on net primary productivity in southeastern China. *Environ. Manage.* 46 (3), 404–410. doi:10.1007/s00267-010-9542-y

Lu, F., Hu, H., Sun, W., Zhu, J., Liu, G., Zhou, W., et al. (2018). Effects of national ecological restoration projects on carbon sequestration in China from 2001 to 2010. *Proc. Natl. Acad. Sci. U. S. A.* 115 (16), 4039–4044. doi:10.1073/pnas.1700294115

Mayani-Parás, F., Botello, F., Castañeda, S., Munguía-Carrara, M., and Sánchez-Cordero, V. (2021). Cumulative habitat loss increases conservation threats on endemic species of terrestrial vertebrates in Mexico. *Biol. Conserv.* 253, 108864. doi:10.1016/j.biocon.2020.108864

Nelson, E., Sander, H., Hawthorne, P., Conte, M., Ennaanay, D., Wolny, S., et al. (2010). Projecting global land-use change and its effect on ecosystem service provision and biodiversity with simple models. *PLoS One* 5 (12), e14327. doi:10.1371/journal.pone.0014327

Ni, J. (2013). Carbon storage in Chinese terrestrial ecosystems: Approaching a more accurate estimate. *Clim. Change* 119 (3-4), 905–917. doi:10.1007/s10584-013-0767-7

Pagiola, S. (2008). Payments for environmental services in Costa Rica. *Ecol. Econ.* 65 (4), 712–724. doi:10.1016/j.ecolecon.2007.07.033

Permpool, N., Bonnet, S., and Gheewala, S. H. (2016). Greenhouse gas emissions from land use change due to oil palm expansion in Thailand for biodiesel production. *J. Clean. Prod.* 134, 532–538. doi:10.1016/j.jclepro.2015.05.048

Piao, S., Fang, J., Ciais, P., Peylin, P., Huang, Y., Sitch, S., et al. (2009). The carbon balance of terrestrial ecosystems in China. *Nature* 458 (7241), 1009–1013. doi:10.1038/nature07944

Province, T.P.s.G.o.H. (2015) Suggestions on strengthening the comprehensive environmental management of Nandu River Basin [Online]. Available at: https://www.hainan.gov.cn/rdjydata-5718.html [Accessed 03-19 2015].

Ren, Y., Wei, X., Wei, X. H., Pan, J. Z., Xie, P. P., Song, X. D., et al. (2011). Relationship between vegetation carbon storage and urbanization: A case study of xiamen, China. *For. Ecol. Manag.* 261 (7), 1214–1223. doi:10.1016/j.foreco.2010.12.038

Schimel, D. S., House, J. I., Hibbard, K. A., Bousquet, P., Ciais, P., Peylin, P., et al. (2001). Recent patterns and mechanisms of carbon exchange by terrestrial ecosystems. *Nature* 414 (6860), 169–172. doi:10.1038/35102500

Smith, K. A., and Conen, F. (2006). Impacts of land management on fluxes of trace greenhouse gases. *Soil Use Manag.* 20 (2), 255–263. doi:10.1111/j.1475-2743.2004.tb00366.x

Sohl, T. L., Sleeter, B. M., Zhu, Z., Sayler, K. L., Bennett, S., Bouchard, M., et al. (2012). A land-use and land-cover modeling strategy to support a national assessment of carbon stocks and fluxes. *Appl. Geogr.* 34, 111–124. doi:10.1016/j.apgeog.2011.10.019

Song, X. D., Brus, D. J., Liu, F., Li, D.-C., Zhao, Y. G., Yang, J. L., et al. (2016). Mapping soil organic carbon content by geographically weighted regression: A case study in the heihe river basin, China. *Geoderma* 261, 11–22. doi:10.1016/j.geoderma.2015.06.024

Su, Y. (2015). *Carbon storage and valuation of grassland ecosystem in the upper reaches of Heihe River*. (Xi'an, China: Master, Shaanxi Normal University). (in Chinese).

Tubiello, F. N., Salvatore, M., Ferrara, A. F., House, J., Federici, S., Rossi, S., et al. (2015). The contribution of agriculture, forestry and other land use activities to global warming, 1990-2012. *Glob. Chang. Biol.* 21 (7), 2655–2660. doi:10.1111/gcb.12865

Wang, D., Gong, J., Chen, L., Zhang, L., Song, Y., and Yue, Y. (2013). Comparative analysis of land use/cover change trajectories and their driving forces in two small watersheds in the Western Loess Plateau of China. *Int. J. Appl. Earth Observation Geoinformation* 21, 241–252. doi:10.1016/j.jag.2012.08.009

Wang, D., Gong, J., Chen, L., Zhang, L., Song, Y., and Yue, Y. (2012). Spatio-temporal pattern analysis of land use/cover change trajectories in Xihe watershed. *Int. J. Appl. Earth Observation Geoinformation* 14 (1), 12–21. doi:10.1016/j.jag.2011.08.007

Wang, H., Yue, C., Mao, Q., Zhao, J., Ciais, P., Li, W., et al. (2020). Vegetation and species impacts on soil organic carbon sequestration following ecological restoration over the Loess Plateau, China. *Geoderma* 371, 114389. doi:10.1016/j.geoderma.2020.114389

Wu, J., Zhang, Y., and Jiang, W. (2020). Spatio-temporal evolution of ecosystem carbon storage in guangdong-Hong Kong-Macao greater bay area. *Landsc. Archit.* 27 (10), 57–63. (in Chinese). doi:10.14085/j.fjyl.2020.10.0057.07

Xi, X., Li, M., Zhang, X., Zhang, Y., Zhang, D., Zhang, J., et al. (2013). Research on soil organic carbon distribution and change trend in middle-east plain and its vicinity in China. *Earth Sci. Front.* 20 (1), 154. (in Chinese).

Xia, X., Yang, Z., Liao, Y., Cui, Y., and Li, Y. (2010). Temporal variation of soil carbon stock and its controlling factors over the last two decades on the southern Song-nen Plain, Heilongjiang Province. *Geosci. Front.* 1 (1), 125–132. doi:10.1016/j.gsf.2010.07.003

Xu, X. W., Pan, G. X., and Hou, P. C. (2011). "Impact of different land use on topsoil organic carbon density in Anhui Province", in *Advanced materials research* Editor: S. Kolisnychenko (Wollerau, Switzerland: Trans Tech Publ), 2687–2692.

Yan, J. N., Wang, L. Z., Song, W. J., Chen, Y. L., Chen, X. D., and Deng, Z. (2019). A time-series classification approach based on change detection for rapid land cover mapping. *Isprs J. Photogrammetry Remote Sens.* 158, 249–262. doi:10.1016/j.isprsjprs.2019.10.003

Yan, J., Yang, Z., Li, Z., Li, X., Xin, L., and Sun, L. (2016). Drivers of cropland abandonment in mountainous areas: A household decision model on farming scale in southwest China. *Land Use Policy* 57, 459–469. doi:10.1016/j.landusepol.2016.06.014

Zaehle, S., Bondeau, A., Carter, T. R., Cramer, W., Erhard, M., Prentice, I. C., et al. (2007). Projected changes in terrestrial carbon storage in europe under climate and land-use change, 1990–2100. *Ecosystems* 10 (3), 380–401. doi:10.1007/s10021-007-9028-9

Zhang, K., Dang, H., Tan, S., Cheng, X., and Zhang, Q. (2010). Change in soil organic carbon following the 'Grain-for-Green' programme in China. *Land Degrad. Dev.* 21 (1), 13–23. doi:10.1002/ldr.954

Zhang, Y., Li, X., and Song, W. (2014). Determinants of cropland abandonment at the parcel, household and village levels in mountain areas of China: A multi-level analysis. *Land Use Policy* 41, 186–192. doi:10.1016/j.landusepol.2014.05.011

Zhang, Z., Peng, J., Xu, Z., Wang, X., and Meersmans, J. (2021). Ecosystem services supply and demand response to urbanization: A case study of the pearl river delta, China. *Ecosyst. Serv.* 49, 101274. doi:10.1016/j.ecoser.2021.101274

Zhao, M., He, Z., Du, J., Chen, L., Lin, P., and Fang, S. (2019). Assessing the effects of ecological engineering on carbon storage by linking the CA-Markov and InVEST models. *Ecol. Indic.* 98, 29–38. doi:10.1016/j.ecolind.2018.10.052

Zhao, S. Q., Liu, S. G., Sohl, T., Young, C., and Werner, J. (2013). Land use and carbon dynamics in the southeastern United States from 1992 to 2050. *Environ. Res. Lett.* 8 (4), 044022. doi:10.1088/1748-9326/8/4/044022

Zhou, Q., Li, B., and Sun, B. (2008). Modelling spatio-temporal pattern of landuse change using multi-temporal remotely sensed imagery. *Int. Archives Photogrammetry, Remote Sens. Spatial Inf. Sci.* 37 (B7), 729–734.

Zhu, E., Deng, J., Zhou, M., Gan, M., Jiang, R., Wang, K., et al. (2019). Carbon emissions induced by land-use and land-cover change from 1970 to 2010 in Zhejiang, China. *Sci. Total Environ.* 646, 930–939. doi:10.1016/j.scitotenv.2018.07.317

Zhu, W., Zhang, J., Cui, Y., Zheng, H., and Zhu, L. (2019). Assessment of territorial ecosystem carbon storage based on land use change scenario: A case study in qihe river basin. *Acta Geogr. Sin.* 74, 446–459. doi:10.11821/dlxb201903004

Zhu, W., Zhang, J., Cui, Y., and Zhu, L. (2020). Ecosystem carbon storage under different scenarios of land use change in Qihe catchment, China. *J. Geogr. Sci.* 30 (9), 1507–1522. doi:10.1007/s11442-020-1796-6

Zomlot, Z., Verbeiren, B., Huysmans, M., and Batelaan, O. (2017). Trajectory analysis of land use and land cover maps to improve spatial-temporal patterns, and impact assessment on groundwater recharge. *J. Hydrology* 554, 558–569. doi:10.1016/j.jhydrol.2017.09.032

frontiers | Frontiers in Ecology and Evolution

TYPE Original Research
PUBLISHED 04 October 2022
DOI 10.3389/fevo.2022.1032931

OPEN ACCESS

EDITED BY
Xiang Liu,
Lanzhou University, China

REVIEWED BY
Li Zhang,
Nanjing Forestry University, China
Mengjiao Huang,
Fudan University, China

*CORRESPONDENCE
Lifan Chen
chenlf@sumhs.edu.cn

SPECIALTY SECTION
This article was submitted to Conservation and Restoration Ecology, a section of the journal Frontiers in Ecology and Evolution

RECEIVED 31 August 2022
ACCEPTED 20 September 2022
PUBLISHED 04 October 2022

CITATION
Chen L, Kong P, Hou L, Zhou Y and Zhou L (2022) Host community composition, community assembly pattern, and disease transmission mode jointly determine the direction and strength of the diversity-disease relationship.
Front. Ecol. Evol. 10:1032931.
doi: 10.3389/fevo.2022.1032931

Host community composition, community assembly pattern, and disease transmission mode jointly determine the direction and strength of the diversity-disease relationship

Lifan Chen[1,2]*, Ping Kong[3], Liying Hou[2], Yanli Zhou[2] and Liang Zhou[3]

[1]Collaborative Innovation Center for Biomedicine, Shanghai University of Medicine and Health Sciences, Shanghai, China, [2]School of Arts and Sciences, Shanghai University of Medicine and Health Sciences, Shanghai, China, [3]Jiading District Central Hospital Affiliated Shanghai University of Medicine and Health Sciences, Shanghai, China

Rapid global biodiversity loss and increasing emerging infectious diseases underscore the significance of identifying the diversity-disease relationship. Although experimental evidence supports the existence of dilution effects in several natural ecosystems, we still know very little about the conditions under which a dilution effect will occur. Using a multi-host Susceptible-Infected-Recovered model, we found when disease transmission was density-dependent, the diversity-disease relationship could exhibit an increasing, decreasing, or non-monotonic trend, which mainly depended on the patterns of community assembly. However, the combined effects of the host competence-abundance relationship and species extinction order may reverse or weaken this trend. In contrast, when disease transmission was frequency-dependent, the diversity-disease relationship only showed a decreasing trend, the host competence-abundance relationship and species extinction order did not alter this decreasing trend, but it could reduce the detectability of the dilution effect and affect disease prevalence. Overall, a combination of disease transmission mode, community assembly pattern, and host community composition determines the direction or strength of the diversity-disease relationship. Our work helps explain why previous studies came to different conclusions about the diversity-disease relationship and provides a deeper understanding of the pathogen transmission dynamics in actual communities.

KEYWORDS

disease risk, dilution effect, amplification effect, community disassembly, host competence, stochastic extinction, deterministic extinction

Introduction

In recent decades, emerging infectious diseases (primarily zoonotic diseases) have been increasing at an unprecedented rate, posing a severe threat to human health and affecting agricultural production and wildlife conservation (Allen et al., 2017; Gibb et al., 2020). At the same time, the increasing disturbance of ecosystems by human activities has accelerated the rate of extinction for species (Estrada-Peña et al., 2014). The biodiversity-disease relationship is one of the fundamental challenges in studying infectious disease ecology (Huang et al., 2016). Accurate prediction of infectious disease risk in the context of declining biodiversity is important both in theory and in practice.

Although the link between host species richness and disease risk has long been identified in entomology, veterinary medicine, and epidemiology (Elton, 1958), this relationship attracted the attention of ecologists only since last two decades. The dilution effect hypothesis, whereby increased host biodiversity reduces disease risk, was formally proposed in studies of Lyme disease transmission dynamics (Keesing et al., 2006). The dilution effect shows a win-win situation in public health and nature conservation, reflecting the service function of ecosystems (Ostfeld and Keesing, 2012). Although many cross-taxa and cross-system empirical studies have confirmed the existence of the dilution effect in nature (Ostfeld and Keesing, 2000; Johnson et al., 2013; Liu et al., 2016), and ecologists have summarized the mechanisms by which the dilution effect occurs (Keesing et al., 2006), there are still some debates about the diversity-disease relationship. Several studies have discovered that the relationship between diversity and disease risk is highly context-dependent (Liu et al., 2020; Cortez and Duffy, 2021), with some studies confirming no effect (Salkeld et al., 2013; Vadell et al., 2020) or even an amplification effect (increased host biodiversity increases disease risk) in some ecosystems (Wood, 2014; Halliday et al., 2017). Clarifying the conditions under which the dilution effect occurs not only helps to gain insight into the dynamics of disease transmission in multi-host communities but also provides a theoretical basis for the prevention and control of infectious diseases in the real world.

Host community composition is essential in determining the relationship between biodiversity and disease risk (Johnson et al., 2015). Due to factors such as life history traits and evolutionary history, host competence (the host's ability to maintain and transmit disease) varies significantly among different species (Downs et al., 2019). The number and proportion of high competent hosts in a community directly determine the disease prevalence of the community, so community composition can affect community disease risk. In fact, changes in community composition are primarily determined by species extinction orders under community disassembly (LoGiudice et al., 2003). Deterministic and stochastic extinctions reflect different host competence-extinction risk relationships. In the case of deterministic extinction, low competent hosts go extinct first. Therefore, it is not difficult to predict that as species richness decreases, the proportion of high competent hosts will increase, leading to an increase in disease risk in the community, i.e., a dilution effect occurs. Both field and theoretical studies have confirmed that deterministic extinction of host species is an important mechanism for the dilution effect (Lacroix et al., 2014; Johnson et al., 2019). However, when host species go extinct at random, it is unclear whether host richness promotes or inhibits disease risk.

Many empirical studies support a negative correlation between host competence and extinction risk, which is considered necessary to cause a dilution effect. Taking Lyme disease as an example, the less competent Virginia opossum and chipmunk are first to go extinct when host species richness decreases, while the most competent white-footed mouse can be abundant in communities with low species richness (Ostfeld and Keesing, 2000; Keesing et al., 2010). Similarly, Johnson et al. (2013) found a non-random nested structure of amphibian community composition in 345 wetlands in California. High competent hosts appeared in almost all wetlands, and low competent hosts usually appeared only in wetlands with higher species richness. This phenomenon also exists in plant communities (Lind et al., 2013; Liu et al., 2017). Although the above examples support a negative correlation between host competence and extinction risk, the generality of this finding remains to be confirmed due to limitations in field observations and experimental conditions (Rohr et al., 2019). For example, in a study of primates, no significant association was found between host competence and extinction risk (Young et al., 2013).

Since species richness and host abundance can influence pathogen transmission (Dobson, 2004), the total community abundance-species richness relationship should influence the diversity-disease relationship (Mihaljevic et al., 2014). The community assembly pattern reflects how community abundance scales with species richness. Compensatory assembly and additive assembly are two extreme assembly patterns often considered in theoretical studies, which yield completely different richness-abundance relationships. The former means that total community abundance does not vary with host richness, and the latter means that total community abundance increases linearly with host richness. It has been demonstrated that when disease transmission is density-dependent, the compensatory assembly will lead to a dilution effect, while the additive assembly will lead to an amplification effect (Rudolf and Antonovics, 2005; Chen and Zhou, 2015). However, some studies found that the saturated relationship between community abundance and species richness is more reasonable than additive and compensatory assemblies, and can better reflect the changes in the total community abundance during biodiversity loss (Lehman and Tilman, 2000; Rohr et al., 2019).

Until now, few studies have considered the effect of saturated community assembly on the diversity-disease relationship [but see Mihaljevic et al. (2014)]. Furthermore, to our knowledge, no studies have explored the combined effects of community composition, community assembly patterns, and disease transmission modes on the diversity-disease relationship.

In this study, using a multi-host Susceptible-Infected-Recovered (SIR) model, we hope to explore how host community composition, community assembly pattern, and disease transmission mode jointly affect community disease risk under community disassembly. We predict that different patterns of community assembly and disease transmission modes will result in different trends in diversity-disease relationships, and that shifts in community composition may alter such trends.

Materials and methods

The SIR model is the most classical and fundamental infectious disease model. It can characterize both density-dependent and frequency-dependent transmission of diseases. Similar to Dobson (2004), we adopt the classical multi-host SIR model to describe the state transition process of disease:

$$\frac{dS_i}{dt} = b_i N_i - \sum_{j=1}^{n} \beta_{ij} S_i I_j - d_i S_i$$

$$\frac{dI_i}{dt} = \sum_{j=1}^{n} \beta_{ij} S_i I_j - (d_i + \gamma_i + \mu_i) I_i$$

$$\frac{dR_i}{dt} = \gamma_i I_i - d_i R_i$$

Here the subscript i represents the host species i (i = 1 … n), S_i, I_i, R_i represent three different states of host i, namely susceptible, infected and recovered. $\sum_{j=1}^{n} \beta_{ij} S_i I_j$ represents the number of newly infected individuals of host i per unit time. d_i, μ_i, and γ_i represent natural death rate, disease-induced death rate, and recovery rate, respectively. Other parameters and their meanings are shown in **Table 1**.

The framework of the simulation was as follows. First, we constructed a global species pool containing 49 host species, the vital parameters of each species followed the parameter setting method established by Roche et al. (2012) and Mihaljevic et al. (2014). Second, we simulated the process of biodiversity loss under deterministic and stochastic extinction respectively, generating local communities with different species richness. Finally, for each local community, we calculated community R_0 as a measure of community disease risk to explore how different combinations of community composition, disease transmission mode, and community assembly pattern affect community disease risk under community disassembly.

TABLE 1 Parameters, definitions, and values for generating the global species pool.

Parameter	Definition	Value
b_i	Per capita birth rate	$0.6M_i^{-0.27}$
d_i	Per capita natural death rate	$0.6M_i^{-0.27}$
m	Constant	1.5
γ_i	Recovery rate	d_i
μ_i	Disease induced mortality	$(m-1)d_i$
β_{ii}	Intraspecific transmission rate	$R_{0i}(d_i+\gamma_i+\mu_i)/K_i$
β_{ij}	Interspecific transmission rate	$\varepsilon\sqrt{\beta_{ii}\beta_{jj}}$
ε	Constant	0.05
s_0	Number of the species in the modal rank	10
z	Constant derived from field study	0.1
P_0	Modal rank	3
P	Rank	1∼8
K_i	The equilibrium abundance of species i	2∼256
M_i	Body weight	$\log(M_i) = a - b\log(P_i)$
a	Constant	2
b	Constant	1
R_{0i}	Intraspecific basic reproduction number	∼Gamma (k,θ)
k	Shape parameter of the gamma distribution	0.5
θ	Scale parameter of the gamma distribution	5

Generating a global species pool

In multi-host communities, different hosts have different epidemiological and ecological traits (Joseph et al., 2013). In order to make the constructed communities closer to the actual communities, we drew heavily on the existing community ecology rules and parameter setting methods to assign reasonable parameter values to each host species (Roche et al., 2012; Joseph et al., 2013). These parameters mainly include species abundance, demographic rate, and epidemiological traits.

Species abundance

Species abundance in the global species pool was assumed to follow Preston's law. This law yields a species-abundance relationship that follows a log-normal distribution, in which a few species are common, and most species are rare (Preston, 1948). This distribution has been proved to describe the abundance distribution patterns in many ecosystems, such as vertebrates, alpine meadows, and fungi (Preston, 1962). It can be expressed as

$$s(P) = s_0 e^{-z(P-P_0)^2}$$

where z is a constant, s_0 is the number of species in the modal rank, and $s(P)$ is the number of species in Pth rank from the

modal rank. We assumed a total of eight ranks, including 49 species (**Table 1**). The abundance at each rank was assigned on a $\log_2$ base, which we considered to be the species' equilibrium abundance K_i (Roche et al., 2012).

Demographic rate

Assuming that the community was in equilibrium, i.e., the birth rate of any host is equal to death rate. Empirical studies have shown that species' birth and death rates tend to be allometrically related to body weight (Charnov, 1993). Similar to Roche et al. (2012), the relationship between birth (death) rate and body weight was expressed as

$$b_i = d_i = 0.6M_i^{-0.27}$$

where M_i represented the average body weight of species i. We assumed the body weight is exponentially related to its abundance (Mihaljevic et al., 2014),

$$\log(M_i) = a - b\log(P_i)$$

It can be seen from the above equation that the species with the smallest body weight is the most abundant.

Epidemiological traits

Field evidence suggests that host species vary significantly in their competence. Taking West Nile Virus as an example, hosts range from birds to horses to humans (Ezenwa et al., 2006). Birds are the most competent hosts, while horses are dead-end hosts, contributing little to the spread of the disease. In order to reflect the variations in host competence, we drew intraspecific values R_{0i} from a truncated gamma distribution. The value of R_{0i} reflects the competence of the host i. If R_{0i} is greater than one, the pathogen can successfully invade the host population, and vice versa.

We considered three possible relationships between host competence R_{0i} and abundance. First, R_{0i} was positively related to abundance, so the most abundant species are the most competent. Then we relaxed this condition by assuming that there was no relationship between R_{0i} and species abundance (neutral). Finally, we considered a negative relationship between R_{0i} and host abundance, where the most abundant species were the least competent (Vinson and Park, 2019).

Similar to Mihaljevic et al. (2014), we calculated intraspecific transmission rate β_{ii} by

$$\beta_{ii} = \frac{R_{0i}(d_i + \gamma_i + \mu_i)}{K_i}$$

The interspecific transmission rate β_{ij} was proportional to the geometric mean of the intraspecific transmission rate β_{ii} and β_{jj}, modified by a constant scaling factor ε, i.e., $\beta_{ij} = \varepsilon\sqrt{\beta_{ii} \cdot \beta_{jj}}$ (Roberts and Heesterbeek, 2018). In this study, we assumed the interspecific transmission rate were symmetrical (i.e., $\beta_{ij} = \beta_{ji}$), and the transmission rates were the same for different individuals of the same species.

Till now, we have constructed a global species pool containing 49 hosts and described in detail how different demographic and epidemiological parameters were assigned to host species (**Table 1**). To get robust results, we repeated the above process 1,000 times to generate different global species pools.

Simulating the process of community disassembly

For each global species pool, we considered deterministic extinction and stochastic extinction of host species to simulate different biodiversity loss processes, generating local communities with species richness ranging from 2 to 49. According to the life history trade-off theory, the higher body weight, the lower number of species, and therefore the higher the risk of extinction (Huang et al., 2013). Thus, under deterministic extinction, we removed the highest body weight (the least abundant) host species from the community at a time until two host species remained in the community. While under stochastic extinction, we randomly selected one host species to remove at a time to simulate the decrease of species richness. Note that these two different species extinction ways correspond to different species extinction orders, thus reflecting different host community compositions.

Next, we separately considered the additive, compensatory, and saturated community assembly under each extinction pattern. In the additive assembly, the addition of new species increases the total community abundance, so the total community abundance was linearly accumulated with species richness. In contrast, in the compensatory assembly, the total community abundance was kept constant, and the abundance of remaining species in the community was compensated in proportion to their abundance when species richness decreased. In the saturated assembly, the community abundance (K_{com}) increased asymptotically with species richness (R) by

$$K_{com} = 800 - \frac{5300}{(R+5)}$$

This asymptotic function is close to the form of the relationship between plant cover and species richness (Tilman et al., 1996). If the total community abundance $K_T < K_{com}$, the abundance of each species was not adjusted, and the increase in community abundance was almost linearly with species richness. In contrast, if $K_T > K_{com}$, the adjusted abundance of each host was obtained by multiplying the abundance of each species by a scaling factor K_{com}/K_T, and then the increase in community abundance was almost a fully compensatory assembly.

In order to get rid of random effects and to get general results, we repeated the process of stochastic extinction

1,000 times for each of the above scenarios [all the nine possible combinations of community assembly patterns (i.e., additive, saturated, and compensatory assembly) and host competence-abundance relationships (i.e., positive, neutral, and negative correlations)].

Community basic reproduction number R_0

As in previous studies, the community basic reproduction number R_0 was used as a proxy for disease risk, which measures the possibility of successful disease invasion in a multi-host community (Roberts and Heesterbeek, 2013; O'Regan et al., 2015). We used the next-generation matrix method to calculate community R_0 (Dobson, 2004). For a local community containing m species, the expression of the next-generation matrix G based on the SIR model is

$$G = \begin{pmatrix} \frac{\beta_{ii}p_{ii}}{(d_i+\gamma_i+\mu_i)} & \cdots & \frac{\beta_{ji}p_{ji}}{(d_i+\gamma_i+\mu_i)} \\ \vdots & \ddots & \vdots \\ \frac{\beta_{ij}p_{ij}}{(d_j+\gamma_j+\mu_j)} & \cdots & \frac{\beta_{jj}p_{jj}}{(d_j+\gamma_j+\mu_j)} \end{pmatrix},$$

where $i, j = 1 \ldots m$. $\frac{1}{d_i+\gamma_i+\mu_i}$ represents the lifespan of the infected host i. p_{ji} depends on whether the disease transmission mode is density-dependent or frequency-dependent. For density-dependent transmission, p_{ji} equals to the equilibrium abundance K_i of infected host species i. For frequency-dependent transmission, p_{ji} equals to the proportion of infected host species i, namely $K_i / \sum_{i=1}^{m} K_i$. By calculating the dominant eigenvalues of the next-generation matrix G, we can obtained the community basic reproduction number R_0.

Results

Results in the case of density-dependent transmission

In the case of density-dependent transmission and stochastic species extinction, the relationship between species richness and community abundance determined how community R_0 varied with species richness (**Figure 1**). Specifically, when community abundance increased linearly with species richness (i.e., the additive assembly), community R_0 increased monotonically with species richness, i.e., the amplification effect. While when community abundance was kept constant with species richness (i.e., the compensatory assembly), the community R_0 initially decreased monotonically with increasing species richness and

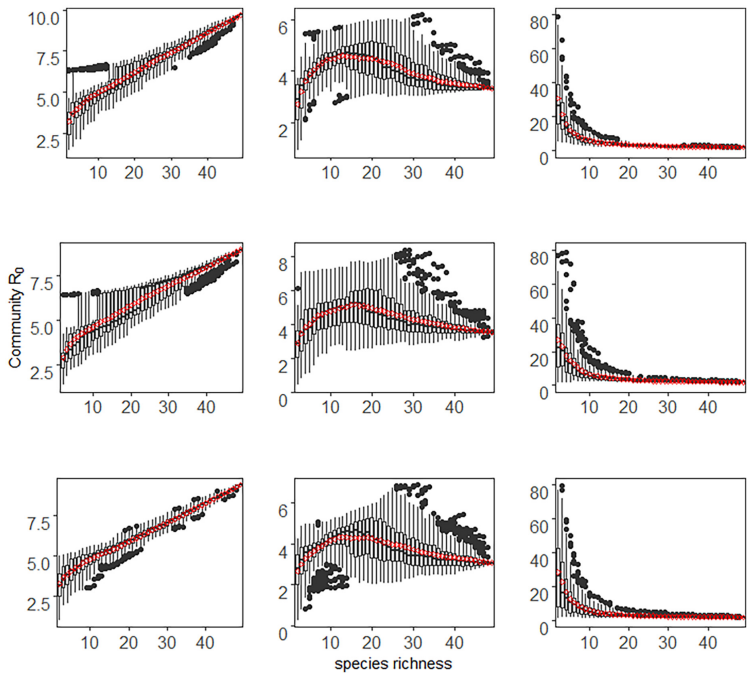

FIGURE 1
The relationship between host species richness and community R_0 under density-dependent transmission and stochastic extinction scenario. Each column represents different community assembly pattern. From the first column to the third column are additive, saturated, and compensatory assembly, respectively. Each row represents the relationship between host competence and abundance. Positive, neutral, and negative correlations are from the first to the third row. The x-axis in each panel represents species richness, and the y-axis represents community R_0. Each boxplot represents the values of 1,000 simulations for each species richness level, and the red dots represent the mean values of community R_0.

then gradually became stable. That is, a dilution effect occurred at low species richness, while when species richness was high, the community R_0 was almost unchanged with species richness. When community abundance was saturated with species richness (the saturated assembly), the diversity-disease relationship showed a non-monotonic hump-shaped trend, with a peak corresponding to species richness of about 15. Along the species richness gradient, the community R_0 first increased (amplification effect) and then decreased (dilution effect).

As shown in **Figure 1**, the above conclusions still hold for positive, neutral, or negative species competence-richness relationships. These findings suggested that in this case, community assembly patterns qualitatively determined whether disease risk increases, decreases, or is non-monotonic under community disassembly. However, the relationship between species competence and extinction risk could only quantitatively but not qualitatively alter the diversity-disease trend.

Conversely, in the case of density-dependent transmission and deterministic species extinction, the community R_0 increased monotonically with species richness when community assembly was additive (**Figure 2**). The host competence-richness relationship only affected the value of community R_0, but did not change this increasing trend. These results were consistent with the stochastic extinction scenario. However, when community abundance was saturated with species richness (saturated), community R_0 increased monotonically with the increase of species richness, which is different from the non-monotonic humped-shaped curve in the stochastic extinction scenario. When community abundance did not change with species richness (compensatory), the direction of the diversity-disease relationship depended on how host competence varied with abundance (The third column in **Figure 2**). If host competence was positively correlated with abundance, then community R_0 decreased as the increase of species richness, i.e., a dilution effect occurred. In contrast, if host competence was negatively correlated with abundance, then community R_0 increased with species richness, i.e., an amplification effect occurred. If host competence was neutral with abundance, community R_0 first slightly decreased and then slightly increased with species richness. An interesting finding is that the results in the latter two cases (negative or neutral relationship between host competence and abundance)

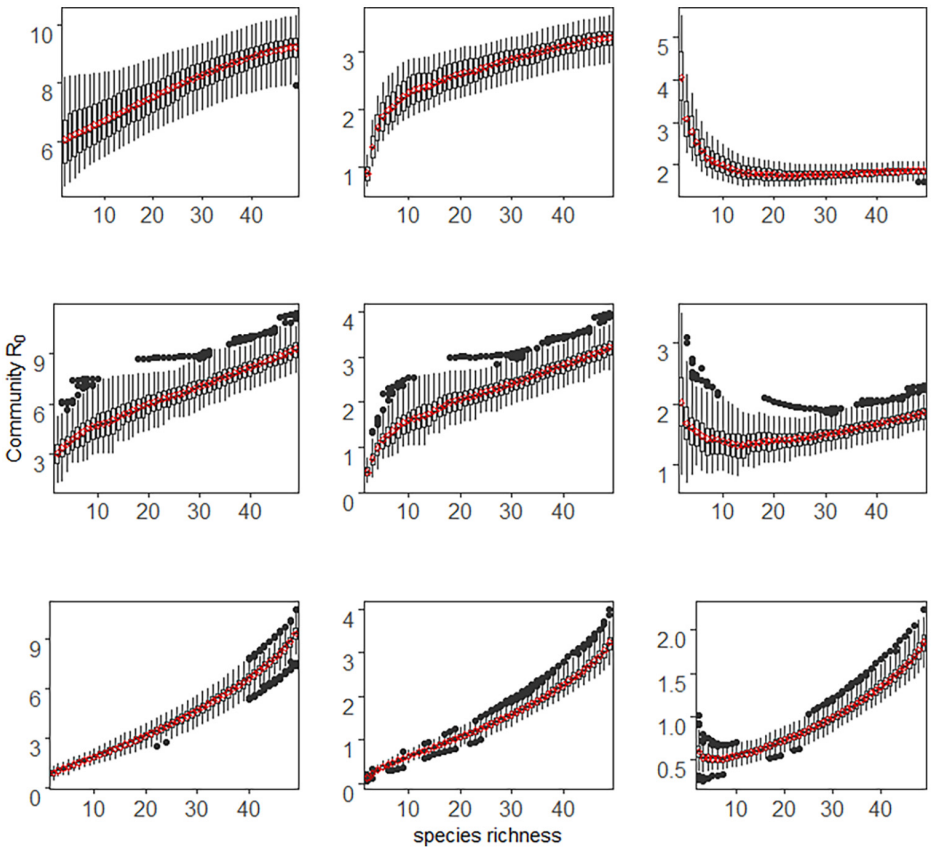

FIGURE 2
The relationship between host species richness and community R_0 under density-dependent transmission and deterministic extinction scenario. Other details are the same as in **Figure 1**.

were quite different from those in stochastic extinction scenario (Figures 1, 2).

In summary, the direction and strength of the relationship between diversity and disease risk under density-dependent transmission were determined by a combination of community assembly pattern, host community composition, and host competence-abundance relationship.

Results in the case of frequency-dependent transmission

In the case of frequency-dependent transmission, disease transmission was determined by the proportion of host species, not by host abundance. Therefore, there was little difference in disease transmission whether the community assembly was additive, compensatory, or saturated. Thus, we used the additive method as an example to show how species extinction pattern and host competence-abundance relationship affect the relationship between diversity and disease risk (Figures 3, 4).

As seen in Figures 3, 4, regardless of whether species extinction was deterministic or stochastic, community R_0 decreased monotonically with the increase of host richness, i.e., only a dilution effect occurred. The host competence-abundance relationship only changed the value of community R_0, but did not alter diversity-disease trends. For a fixed species richness level, the community R_0 was highest when host competence and abundance were positively correlated and lowest when there was a negative correlation between them. In particular, a negative host competence-abundance relationship exhibited a weak dilution effect when the species richness was low, while when species richness was high, community R_0 did not change with species richness, that is species richness had no effect on disease risk (third column in Figures 3, 4).

Discussion

The relationship between host diversity and disease risk is one of the central concerns in disease ecology. In the context of rapid global biodiversity loss and increasing emerging infectious diseases, a deeper understanding of the diversity-disease relationship is important for public health and wildlife conservation. Although extensive experimental evidence supports the existence of dilution effects in natural

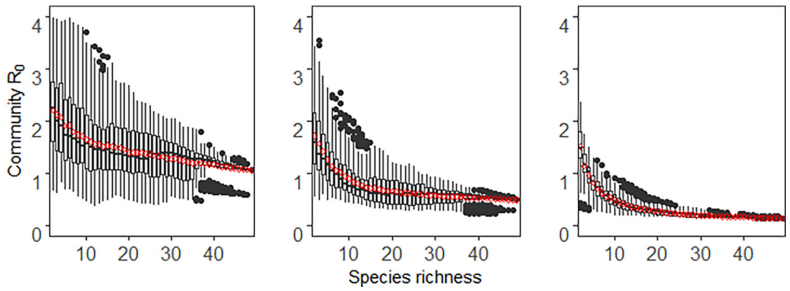

FIGURE 3
The relationship between host species richness and community R_0 under frequency-dependent transmission and stochastic extinction scenario. Each column represents different relationship between host competence and abundance. Positive, neutral, and negative correlations are from the first to the third column. Each boxplot represents the values of 1,000 simulations for each species richness level, and the red dots represent the mean values of community R_0.

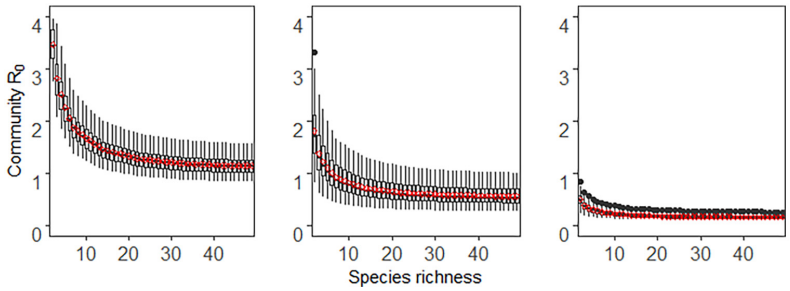

FIGURE 4
The relationship between host species richness and community R_0 under frequency-dependent transmission and deterministic extinction scenario. Other details are the same as in Figure 3.

ecosystems, we still know very little about the conditions under which the dilution effect occurs (Keesing and Ostfeld, 2021). By building a multi-host SIR model, we found when disease transmission was density-dependent, the diversity-disease relationship could exhibit an increasing, decreasing, or non-monotonic trend, which mainly depended on the patterns of community assembly. However, the combined effects of the host competence-abundance relationship and species extinction order may reverse or weaken this trend. In contrast, when disease transmission was frequency-dependent, the diversity-disease relationship only showed a decreasing trend (i.e., only a dilution effect occurred). The host competence-abundance relationship and species extinction order did not alter this decreasing trend in this case, but it could reduce the detectability of the dilution effect and affect the value of the community R_0. Overall, a combination of disease transmission mode, community assembly pattern, and host community composition can alter the direction or strength of the diversity-disease relationship.

Exploring the general consequences of the host competence-abundance relationship on disease risk is one of the main goals of this study. An interesting finding is that under density-dependent and deterministic extinction scenario (**Figure 2**), different host competence-abundance relationships (positive, neutral, or negative) may lead to opposite results in the case of compensatory assembly. The reason may be that a positive relationship between host competence and abundance means that low competent hosts are the first to be extirpated from the community. Therefore, community disease risk increases with decreasing species richness, i.e., a dilution effect occurs (Rosenthal et al., 2021). Conversely, if host competence is negatively related to abundance, then the most competent hosts go extinct first, resulting in community contains a large number of less competent hosts. Hence, disease risk decreases when community disassembly, i.e., an amplification effect occurs. If host competence is neutral with abundance, then host species are randomly removed as species richness decreases, therefore the relationship between diversity and disease risk is weak.

Our results have been confirmed by some empirical studies. For example, a survey of amphibian communities in 147 wetland areas in California found that the relationship between diversity and trematodes disease risk showed a dilution effect when low competent host species went extinct first, but showed no effect when host species went extinct at random (Johnson et al., 2019). Similar results were found for plant communities. For example, for alpine meadow plant communities, the low competent host plants were the first to go extinct after nitrogen addition, and the relationship between plant richness and leaf fungal disease risk showed a dilution effect. However, when plants were randomly removed in controlled experiments, plant richness had almost no effect on fungal disease risk (Liu et al., 2018). It is worth noting that traditional biodiversity-ecosystem function controlled experiments tend to assemble communities by randomly sampling species from the species pool. This may ignore the importance of species loss order and may underestimate disease risk (Wolfi and Zavaleta, 2015).

In the case of deterministic extinction, our results were consistent with previous findings that an amplification effect occurred when community assembly was additive, and a dilution effect occurred when community assembly was compensatory under density-dependent transmission (Rudolf and Antonovics, 2005; Mihaljevic et al., 2014). While under frequency-dependent transmission, the diversity-disease relationship did not change with different patterns of community assembly. However, as mentioned in the Introduction, neither additive nor compensatory community assembly patterns reflect species richness-abundance relationship in actual communities. In a community, both additive and compensatory assembly can occur (Rohr et al., 2019). In general, additive assembly happens in the early stages of a community (Chen and Zhou, 2015). As competition gets tougher and resources are limited, it will switch to compensatory assembly. Therefore, the saturated assembly is more reasonable, and can better reflect the changes in the total community abundance under community disassembly. For example, using three different theoretical models, Lehman and Tilman (2000) found a saturated relationship between total community biomass and species richness due to competition. Similarly, Guo et al. (2006) showed a non-monotonic relationship between grassland biomass and plant richness within a certain range of species richness.

Saturated community assembly resulted in a non-monotonic hump-shaped diversity-disease relationship under density-dependent transmission and stochastic extinction scenario, which emphasized the importance of host richness ranges for identifying diversity-disease relationships in field studies. The occurrence of a dilution or amplification effect depends on whether species richness falls to the left or right side of the peak (Halliday et al., 2019; Rohr et al., 2019). If host species richness falls to the left side of the peak, then an amplification effect can occur when community disassembly. On the contrary, there will be a dilution effect. This finding may explain the divergent results in field studies and the controlled experiments. In most field studies, species richness often falls to the right side of the peak, making it easy to conclude a dilution effect (Johnson et al., 2013; Kilpatrick et al., 2017). However, in controlled experiments, given the difficulty of manipulating species richness, species richness tends to fall to the left side of the peak, so it is easier to conclude an amplification effect (Halliday et al., 2017). In future research, we must focus on evaluating the shape of the diversity-disease relationship and determining where species richness lies on this curve.

Due to the complexity of the multi-host-pathogen system, exploring the general diversity-disease relationship is challenging, for which we made some simplifications. For example, in natural communities, the presence of keystone

species may have a significant impact on diversity-disease relationships (Levi et al., 2016), which we did not take into account. Furthermore, we only considered the saturated community abundance-species richness relationship due to competition. However, in many natural systems where predation has a more substantial effect on disease dynamics than competition (Chen et al., 2022), all of which needs to be addressed in future studies. Despite these limitations, this study demonstrated for the first time that the trends of the diversity-disease relationship did not only depend on community assembly pattern and disease transmission mode. The relationship between host competence and extinction risk could alter the direction and strength of the diversity-disease relationship. This study not only explains the current debate about the dilution effect, but also contributes to a deeper understanding of the pathogen transmission dynamics in actual communities.

Data availability statement

The original contributions presented in this study are included in the article/supplementary material, further inquiries can be directed to the corresponding author.

Author contributions

LC and PK designed the study and analyzed the model. LC, LH, and YZ performed the software. LC, PK, and LZ drafted the original manuscript. LC and LZ reviewed and edited the manuscript. All authors have read and agreed to the published version of the manuscript.

Funding

This work was supported by the National Natural Science Foundation of China (31700466 and 82072228), the Foundation of National Key R&D Program of China (2020YFC2008700), the Foundation of Shanghai Municipal Commission of Economy and Informatization (202001007), and the Special Project of Health Shanghai Action (2022–2024).

Conflict of interest

The authors declare that the research was conducted in the absence of any commercial or financial relationships that could be construed as a potential conflict of interest.

Publisher's note

All claims expressed in this article are solely those of the authors and do not necessarily represent those of their affiliated organizations, or those of the publisher, the editors and the reviewers. Any product that may be evaluated in this article, or claim that may be made by its manufacturer, is not guaranteed or endorsed by the publisher.

References

Allen, T., Murray, K. A., Zambrana-Torrelio, C., Morse, S. S., Rondinini, C., Di Marco, M., et al. (2017). Global hotspots and correlates of emerging zoonotic diseases. *Nat. Commun.* 8:1124. doi: 10.1038/s41467-017-00923-8

Charnov, E. L. (1993). *Life History Invariants: Some Explorations of Symmetry in Evolutionary Ecology*. Oxford: Oxford University Press.

Chen, L., Chen, S., Kong, P., and Zhou, L. (2022). Host competence, interspecific competition and vector preference interact to determine the vector-borne infection ecology. *Front. Ecol. Evol.* 10:993844. doi: 10.3389/fevo.2022.993844

Chen, L., and Zhou, S. (2015). A combination of species evenness and functional diversity is the best predictor of disease risk in multihost communities. *Am. Nat.* 186, 755–765. doi: 10.1086/683774

Cortez, M. H., and Duffy, M. A. (2021). The context-dependent effects of host competence. competition, and pathogen transmission mode on disease prevalence. *Am. Nat.* 198, 179–194. doi: 10.1086/715110

Dobson, A. (2004). Population dynamics of pathogens with multiple host species. *Am. Nat.* 164, S64–S78. doi: 10.1086/424681

Downs, C. J., Schoenle, L. A., Han, B. A., Harrison, J. F., and Martin, L. B. (2019). Scaling of host competence. *Trends Parasitol.* 35, 182–192. doi: 10.1016/j.pt.2018.12.002

Elton, C. S. (1958). *The Ecology of Invasions by Animals and Plants*. London: Methuen & Co. Ltd., 181. doi: 10.1007/978-1-4899-7214-9

Estrada-Peña, A., Ostfeld, R. S., Peterson, A. T., Poulin, R., and de la Fuente, J. (2014). Effects of environmental change on zoonotic disease risk: an ecological primer. *Trends Parasitol.* 30, 205–214. doi: 10.1016/j.pt.2014.02.003

Ezenwa, V. O., Godsey, M. S., King, R. J., and Guptill, S. C. (2006). Avian diversity and West Nile virus: testing associations between biodiversity and infectious disease risk. *Proc. R. Sci.* 273, 109–117. doi: 10.1098/rspb.2005.3284

Gibb, R. J., Redding, D. W., Chin, K. Q., Donnelly, C. A., Blackburn, T. M., Newbold, T., et al. (2020). Zoonotic host diversity increases in human-dominated ecosystems. *Nature* 584, 398–402. doi: 10.1038/s41586-020-2562-8

Guo, Q., Shaffer, T. L., and Buhl, T. K. (2006). Community maturity, species saturation and the variant diversity-productivity relationships in grasslands. *Ecol. Lett.* 9, 1284–1292. doi: 10.1111/j.1461-0248.2006.00980.x

Halliday, F. W., Heckman, R. W., Wilfahrt, P. A., and Mitchell, C. E. (2017). A multivariate test of disease risk reveals conditions leading to disease amplification. *Proc. R. Soc. B Biol. Sci.* 284:20171340. doi: 10.1098/rspb.2017.1340

Halliday, F. W., Heckman, R. W., Wilfahrt, P. A., and Mitchell, C. E. (2019). Past is prologue: host community assembly and the risk of infectious disease over time. *Ecol. Lett.* 22, 138–148. doi: 10.1111/ele.13176

Huang, Z. Y., de Boer, W. F., van Langevelde, F., Olson, V., Blackburn, T. M., and Prins, H. H. (2013). Species' life-history traits explain interspecific variation in reservoir competence: a possible mechanism underlying the dilution effect. *PLoS One* 8:e54341. doi: 10.1371/journal.pone.0054341

Huang, Z. Y. X., van Langevelde, F., Estrada-Peña, A., Suzán, G., and de Boer, W. F. (2016). The diversity–disease relationship: evidence for and criticisms of the dilution effect. *Parasitology* 143, 1075–1086. doi: 10.1017/S0031182016000536

Johnson, P. T., Calhoun, D. M., Riepe, T., McDevitt-Galles, T., and Koprivnikar, J. (2019). Community disassembly and disease: realistic—but not randomized—biodiversity losses enhance parasite transmission. *Proc. R. Sci.* 286:20190260. doi: 10.1098/rspb.2019.0260

Johnson, P. T., Ostfeld, R. S., and Keesing, F. (2015). Frontiers in research on biodiversity and disease. *Ecol. Lett.* 18, 1119–1133. doi: 10.1111/ele.12479

Johnson, P. T., Preston, D. L., Hoverman, J. T., and Richgels, K. L. (2013). Biodiversity decreases disease through predictable changes in host community competence. *Nature* 494, 230–233. doi: 10.1038/nature11883

Joseph, M. B., Mihaljevic, J. R., Orlofske, S. A., and Paull, S. H. (2013). Does life history mediate changing disease risk when communities disassemble? *Ecol. Lett.* 16, 1405–1412. doi: 10.1111/ele.12180

Keesing, F., Belden, L. K., Daszak, P., Dobson, A., Harvell, C. D., Holt, R. D., et al. (2010). Impacts of biodiversity on the emergence and transmission of infectious diseases. *Nature* 468, 647–652. doi: 10.1038/nature09575

Keesing, F., Holt, R. D., and Ostfeld, R. S. (2006). Effects of species diversity on disease risk. *Ecol. Lett.* 9, 485–498. doi: 0.1111/j.1461-0248.2006.00885.x

Keesing, F., and Ostfeld, R. S. (2021). Dilution effects in disease ecology. *Ecol. Lett.* 24, 2490–2505. doi: 10.1111/ele.13875

Kilpatrick, A. M., Salkeld, D. J., Titcomb, G., and Hahn, M. B. (2017). Conservation of biodiversity as a strategy for improving human health and well-being. *Philos. Trans. R. Soc. Lond. B Biol. Sci.* 372:20160131. doi: 10.1098/rstb.2016.0131

Lacroix, C., Jolles, A., Seabloom, E. W., Power, A. G., Mitchell, C. E., and Borer, E. T. (2014). Non-random biodiversity loss underlies predictable increases in viral disease prevalence. *J. R. Soc. Interface* 11:20130947. doi: 10.1098/rsif.2013.0947

Lehman, C. L., and Tilman, D. (2000). Biodiversity, stability, and productivity in competitive communities. *Am. Nat.* 156, 534–552. doi: 10.1086/303402

Levi, T., Keesing, F., Holt, R. D., Barfield, M., and Ostfeld, R. S. (2016). Quantifying dilution and amplification in a community of hosts for tick-borne pathogens. *Ecol. Appl.* 26, 484–498. doi: 10.1890/15-0122

Lind, E. M., Borer, E., Seabloom, E., Adler, P., Bakker, J. D., Blumenthal, D. M., et al. (2013). Life-history constraints in grassland plant species: a growth-defence trade-off is the norm. *Ecol. Lett.* 16, 513–521. doi: 10.1111/ele.12078

Liu, X., Chen, F., Lyu, S., Sun, D., and Zhou, S. (2018). Random species loss underestimates dilution effects of host diversity on foliar fungal diseases under fertilization. *Ecol. Evol.* 8, 1705–1713. doi: 10.1002/ece3.3749

Liu, X., Chen, L., Liu, M., García-Guzmán, G., Gilbert, G. S., and Zhou, S. (2020). Dilution effect of plant diversity on infectious diseases: latitudinal trend and biological context dependence. *Oikos* 129, 457–465. doi: 10.1111/oik.07027

Liu, X., Lyu, S., Sun, D., Bradshaw, C. J., and Zhou, S. (2017). Species decline under nitrogen fertilization increases community-level competence of fungal diseases. *Proc. R. Sci.* 284:20162621. doi: 10.1098/rspb.2016.2621

Liu, X., Lyu, S., Zhou, S., and Bradshaw, C. J. (2016). Warming and fertilization alter the dilution effect of host diversity on disease severity. *Ecology* 97, 1680–1689. doi: 10.1890/15-1784.1

LoGiudice, K., Ostfeld, R. S., Schmidt, K. A., and Keesing, F. (2003). The ecology of infectious disease: effects of host diversity and community composition on Lyme disease risk. *Proc. Natl. Acad. Sci. U.S.A.* 100, 567–571. doi: 10.1073/pnas.0233733100

Mihaljevic, J. R., Joseph, M. B., Orlofske, S. A., and Paull, S. H. (2014). The scaling of host density with richness affects the direction, shape, and detectability of diversity-disease relationships. *PLoS One* 9:e97812. doi: 10.1371/journal.pone.0097812

O'Regan, S. M., Vinson, J. E., and Park, A. W. (2015). Interspecific contact and competition may affect the strength and direction of disease-diversity relationships for directly transmitted microparasites. *Am. Nat.* 186, 480–494. doi: 10.1086/682721

Ostfeld, R. S., and Keesing, F. (2000). Biodiversity series: the function of biodiversity in the ecology of vector-borne zoonotic diseases. *Can. J. Zool.* 78, 2061–2078. doi: 10.1139/z00-172

Ostfeld, R. S., and Keesing, F. (2012). Effects of host diversity on infectious disease. *Annu. Rev. Ecol. Syst.* 43, 157–182. doi: 10.1146/annurev-ecolsys-102710-145022

Preston, F. W. (1948). The commonness, and rarity, of species. *Ecology* 29, 254–283. doi: 10.2307/1930989

Preston, F. W. (1962). The canonical distribution of commonness and rarity: part I. *Ecology* 43, 185–215. doi: 10.2307/1931976

Roberts, M. G., and Heesterbeek, J. (2013). Characterizing the next-generation matrix and basic reproduction number in ecological epidemiology. *J. Math. Biol.* 66, 1045–1064. doi: 10.1007/s00285-012-0602-1

Roberts, M. G., and Heesterbeek, J. A. P. (2018). Quantifying the dilution effect for models in ecological epidemiology. *J. R. Soc. Interface* 15:20170791. doi: 10.1098/rsif.2017.0791

Roche, B., Dobson, A. P., Guégan, J.-F., and Rohani, P. (2012). Linking community and disease ecology: the impact of biodiversity on pathogen transmission. *Philos. Trans. R. Soc. Lond. B Biol. Sci.* 367, 2807–2813. doi: 10.1098/rstb.2011.0364

Rohr, J. R., Civitello, D. J., Halliday, F. W., Hudson, P. J., Lafferty, K. D., Wood, C. L., et al. (2019). Towards common ground in the biodiversity–disease debate. *Nat. Ecol. Evol.* 4, 24–33. doi: 10.1038/s41559-019-1060-6

Rosenthal, L. M., Brooks, W., and Rizzo, D. M. (2021). Species densities, assembly order, and competence jointly determine the diversity-disease relationship. *Ecology* 103:e3622. doi: 10.1002/ecy.3622

Rudolf, V. H., and Antonovics, J. (2005). Species coexistence and pathogens with frequency-dependent transmission. *Am. Nat.* 166, 112–118. doi: 10.1086/430674

Salkeld, D. J., Padgett, K. A., and Jones, J. H. (2013). A meta-analysis suggesting that the relationship between biodiversity and risk of zoonotic pathogen transmission is idiosyncratic. *Ecol. Lett.* 16, 679–686. doi: 10.1111/ele.12101

Tilman, D., Wedin, D. A., and Knops, J. M. H. (1996). Productivity and sustainability influenced by biodiversity in grassland ecosystems. *Nature* 379, 718–720.doi: 10.1038/379718a0

Vadell, M. V., Villafañe, I. E. G., and Carbajo, A. E. (2020). Hantavirus infection and biodiversity in the Americas. *Oecologia* 192, 169–177. doi: 10.1007/s00442-019-04564-0

Vinson, J. E., and Park, A. W. (2019). Vector-borne parasite invasion in communities across space and time. *Proc. R. Soc. B Biol. Sci.* 286:20192614. doi: 10.1098/rspb.2019.2614

Wolfi, A. A., and Zavaleta, E. S. (2015). Species traits outweigh nested structure in driving the effects of realistic biodiversity loss on productivity. *Ecology* 96, 90–98. doi: 10.1890/14-0131.1

Wood, C. L. (2014). Environmental change and the ecology of infectious disease. *Science* 346, 1192–1192. doi: 10.1126/science.aaa1810

Young, H. S., Griffin, R. H., Wood, C. L., and Nunn, C. L. (2013). Does habitat disturbance increase infectious disease risk for primates? *Ecol. Lett.* 16, 656–663. doi: 10.1111/ele.12094

frontiers | Frontiers in Ecology and Evolution

TYPE Original Research
PUBLISHED 04 November 2022
DOI 10.3389/fevo.2022.1056111

OPEN ACCESS

EDITED BY
Hui Zhang,
Hainan University, China

REVIEWED BY
Jiabao Li,
Chengdu Institute of Biology (CAS), China
Qiongfen Qiu,
Ningbo University, China

*CORRESPONDENCE
Shengjing Jiang
jiangshj13@lzu.edu.cn

†These authors have contributed equally to this work

SPECIALTY SECTION
This article was submitted to Conservation and Restoration Ecology, a section of the journal Frontiers in Ecology and Evolution

RECEIVED 28 September 2022
ACCEPTED 24 October 2022
PUBLISHED 04 November 2022

CITATION
Du J, Tan T and Jiang S (2022) Divergent responses of plant and soil microbial community to short-term nutrient addition in alpine grassland on the Qinghai-Tibetan Plateau. *Front. Ecol. Evol.* 10:1056111. doi: 10.3389/fevo.2022.1056111

Divergent responses of plant and soil microbial community to short-term nutrient addition in alpine grassland on the Qinghai-Tibetan Plateau

Juan Du†, Tianyuan Tan† and Shengjing Jiang*

State Key Laboratory of Herbage Improvement and Grassland Agro-ecosystems, College of Pastoral Agriculture Science and Technology, Lanzhou University, Lanzhou, China

Nitrogen (N) and phosphorus (P) are the main restrictive elements in terrestrial ecosystems, which have an important role in determining the community composition of plants and soil microorganisms. However, there is still a lack of understanding about whether plant and soil microbes respond synchronously to external N and P addition deposition, particularly on a short time scale (< 1 year). Here, we conducted a short-term experiment (3 months) involving control, N addition, P addition, and N + P addition in an alpine grassland on the Qinghai-Tibetan Plateau. Responses of plant and soil microbial (bacterial and fungal) communities were analyzed using the quadrat method and high-throughput sequencing, respectively. N addition significantly increased aboveground biomass and changed the plant community composition, but had no significant effect on soil microbes. Thus, microbial and plant processes were asynchronous following the resource availability in this alpine meadow. According to our research, the plant community may react to short-term nutrient deposition more quickly than the soil microbial community.

KEYWORDS

soil microbes, fertilization, alpine meadow, asynchronous response, Qinghai-Tibetan Plateau

Introduction

In terrestrial ecosystems, nitrogen (N) and phosphorus (P) are two crucial nutrients for organisms and have an impact on a variety of biogeochemical processes. Due to several recent worldwide changes (such as climate warming, nitrogen deposition, etc.) caused by human activity, the availability of these nutrients in the environment has dramatically changed (Wang et al., 2020). This change triggered an imbalance between the availability of resources and organisms. On a worldwide scale, numerous studies have been carried out to investigate how plants or bacteria react to simulated N and

P addition (Stiles et al., 2017; Li et al., 2020). These studies considerably contribute to our understanding of biogeochemical cycles in the context of global change (Ling et al., 2022). However, combined field experimental studies about both plant and microbial responses to N and P additions are still comparatively underutilized. In order to comprehend terrestrial ecosystem responses to nutrient deposition more thoroughly, both plant and soil communities should be taken into account at the same time.

Naturally, the aboveground and belowground ecosystems are closely connected (Wardle et al., 2004), and both plant and soil microbial communities could be affected by environmental factors (Dahl et al., 2017; Ma et al., 2018; Adair et al., 2019). The interactions between plants and soil bacteria make it more difficult to distinguish how environmental change affects a single population (Rudgers et al., 2020). On the other hand, little is known about whether these communities respond similarly or synchronously to environment change (Classen et al., 2015). It will be necessary to fill information gaps regarding the sequential or concurrent responses of plant and soil microbial populations to environmental change. In order to achieve this, short-term trials (less than a year) may present the chance to screen out the ephemeral responses brought on by the stepwise change, which are crucial for comprehending and identifying the tipping points (De Boeck et al., 2015).

The Qinghai-Tibetan Plateau is the plateau with the highest altitude and the largest area on earth, known as the "third pole of the world." Affected by global change, the climate in this region has undergone drastic changes, and the annual average temperature, annual precipitation, and total nitrogen deposition rate have increased to varying degrees (Chen et al., 2013; IPCC, 2018). Under such a background, it is necessary to investigate the response mode mechanism of plant and soil microbial organisms to resource availability in this region. Here, we conducted a 3 months experiment with increasing soil fertility (nitrogen and phosphorus addition), the response of species composition of plant and soil microbes under different treatments were measured simultaneously. The following questions were specifically addressed by this study in an effort to provide answers: (1) How do the assemblages of plant and soil microbes respond to temporary external nutrient addition? (2) Do soil microbial and plant communities react simultaneously to resource availability?

Materials and methods

Study site

This experiment was carried out on a flat field located at the Haibei Alpine Grassland Ecosystem Research Station (37°36′N, 101°19′E, c. 3,215 m a.s.l.), located on the northeastern Qinghai-Tibetan Plateau in Qinghai Province, China. The site is a typical continental climate, where the annual average precipitation is 488 mm, and the annual average temperature is −1.1°C. The growing season in this region is from May to September. The vegetation is dominated by *Kobresia humilis*, *Elymus nutans,* and *Stipa aliena*.

Experimental design

Experimental treatments began in June 2021. A two-way factorial design with N and P addition was implemented involving four treatments: (1) control, CK; (2) nitrogen addition, N; (3) phosphorus addition, P; and (4) combined N and P addition, NP. With NH_4NO_3 and $Ca(H_2PO_4)_2$, respectively, 10 g N m^{-2} and 5 g P m^{-2} of N and P addition were added to the meadow's surface. The fertilizer was manually spread in solid form manually on drizzly day. Each treatment was replicated four times, resulting in a total of 16 plots. These plots (2.5 m × 2.5 m) were arranged in a complete randomized block design and each plot was separated by a 2-m buffer zone to minimize nutrient exchange between plots.

Sampling

After 3 months, we collected samples from all plots in the middle of August 2021. The plant species richness was determined for each plot as the total number of species in one 0.5 m × 0.5 m quadrat at the center of each plot. In each plot, three 0.16 m × 0.16 m quadrats were further randomly selected to measure the plant biomass. All individual plants in each quadrat were clipped to the soil surface and used to measure the shoot biomass after drying at 80°C for 48 h. Three soil cores with a depth of 0–10 cm and a diameter of 3.5 cm were randomly collected and mixed as one sample. Fine live roots were carefully separated from each soil sample, washed cleanly, and used for the determination of belowground biomass. The remaining soil samples were transported in sterile plastic bags on dry ice to the laboratory and stored at −20°C until the start of the extraction.

Sequencing and bioinformatics

Total DNA was extracted from soils using a PowerSoil® DNA Isolation Kit (Qiagen, USA), following the manufacturer's instructions. Universal primers were used to amplify the 16S rRNA genes of bacteria (338F and 806R) and ITS genes of fungi (ITS1 and ITS2). Amplicons were purified and sequenced by Magigene (Guangzhou, China) on a NovaSeq6000 platform (Illumina Inc., San Diego, USA). The resulting sequences were first merged using FLASh v1.2.11. Afterward, the primer sequences were removed by the command of "fastq_filter" in VSEARCH 2.14.2. The filtered sequences were assigned to zero-radius operational taxonomic units (zOTUs) using UNOISE3

algorithm. The command of "usearch_global" was then used to map the fastq file into an zOTU table. The representative sequences were annotated for their taxonomic information based on the RDP database version 11.5 for bacteria and UNITE database release version 8.2 for fungi, respectively. All non-bacteria or non-fungi sequences and singletons were removed from the analysis. To correct for sampling effort, the number of sequences per sample was rarefied to the minimum number for the bacterial and fungal community, respectively. Raw sequence data is deposited to the Genome Sequence Archive (GSA) in National Genomics Data Center, China National Center for Bioinformation (CNCB) under the BioProject id PRJCA011844.

Statistical analysis

The data analyses were conducted using various packages in R v4.0.2. Before analysis, the data were tested for normality and $\log_e(x + 1)$-transformed when needed. The effects of treatments on plant and soil microbial richness were analyzed using mixed linear models with block as a random effect. The analysis was performed in R using the "lmer" command in the "lme4" package. The corresponding F and P values were derived from the "anova" function in the "lmerTest" package. Based on the linear mixed-effects models, the differences of each variable between treatments were tested by *post hoc* pairwise comparisons (Tukey method) using "glht" function of multcomp package. The principal coordinates analysis (PCoA) was performed to visualize differences in the plant or microbial community composition using "pcoa" function of the ade4 package in R. Significant differences in the plant or microbial community among treatments were further analyzed by Permutational multivariate ANOVA (PERMANOVA) with constraining permutations within blocks using "adonis2" function of the vegan package.

Results

The N addition significantly increased shoot biomass (F = 21.59, P < 0.001). Compared with unfertilized soils, the shoot biomass was increased by 17.91 and 31.94% under N and NP treatments, respectively (Figure 1A). Besides, the shoot biomass was marginally affected by P addition (F = 3.63,

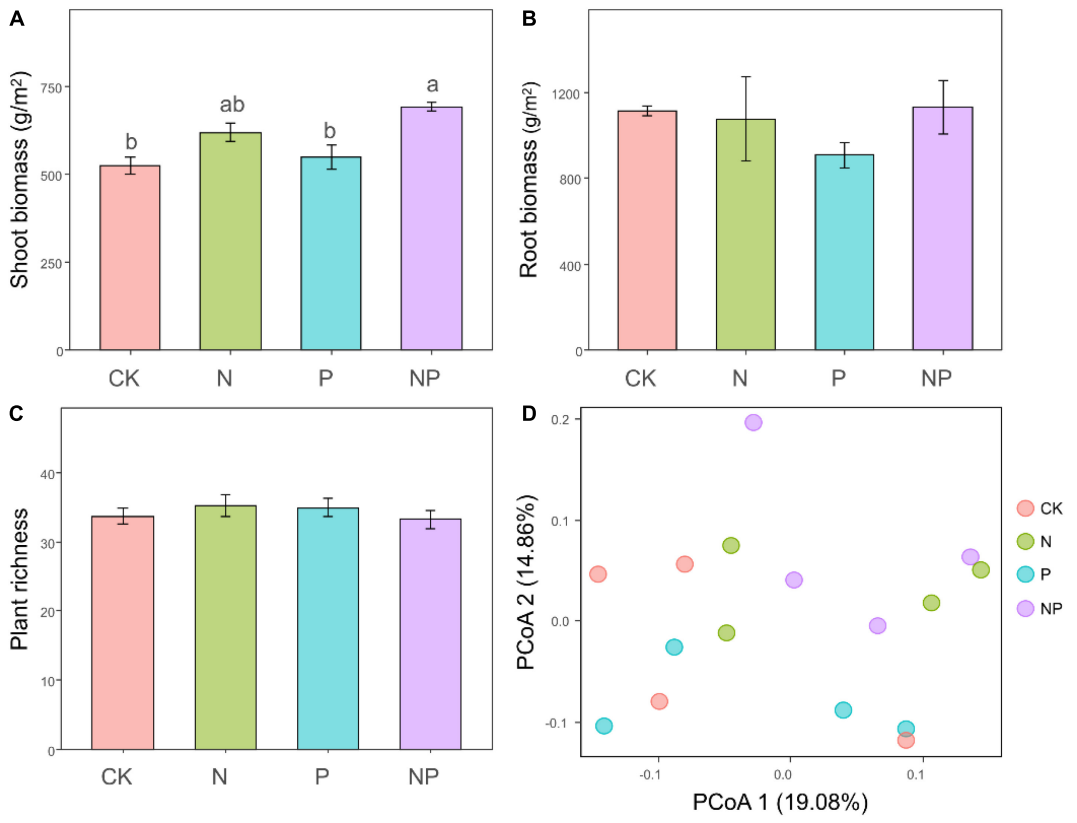

FIGURE 1
Shoot **(A)**, root **(B)** biomass and plant richness **(C)** under different treatments. Bars represent means ± SEs. Significant differences of each variable among treatments are indicated by dissimilar letters above boxes (*post hoc* Tukey's test). Principal coordinate analysis ordination (PCoA) plot based on a Bray–Curtis dissimilarity matrix of plant communities under different treatments **(D)**.

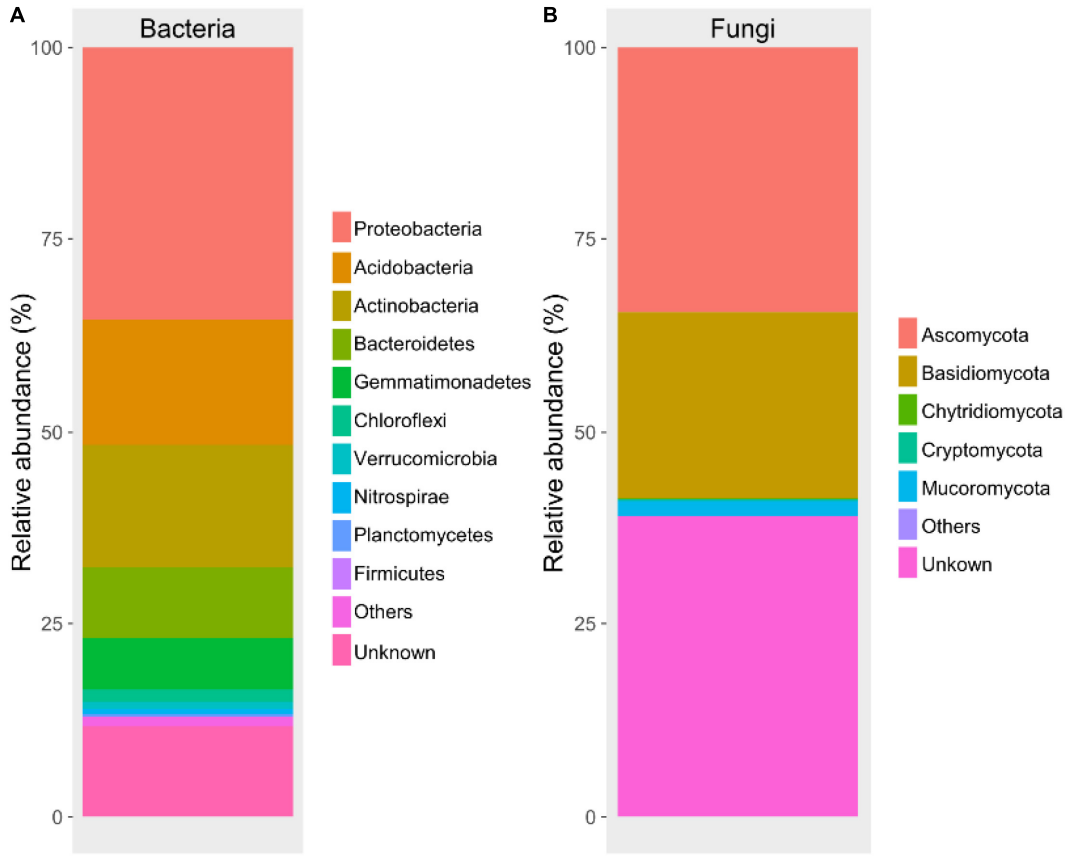

FIGURE 2
Relative abundances (%, proportion of sequencing reads) of bacteria **(A)** and fungi **(B)** at the phylum level in this study.

P = 0.08) and not affected by the interaction between N and P addition (F = 0.95, P = 0.35). On the other hand, we did not observe significant effects of our treatments on the root biomass (all $P > 0.05$, Figure 1B). We recorded 56 plant species belonging to 41 genera and 18 families over the course of the experiment. The richness of plant communities was not significantly affect by N addition (F = 0.01, P = 0.93), P addition (F = 0.07, P = 0.78), or their interaction (F = 1.43, P = 0.25; Figure 1C). PCoA ordinations of plant communities revealed that the species composition was highly changed by nitrogen addition (Figure 1D), which was confirmed by PERMANOVA analysis (F = 1.71, P = 0.01). With an increase in N availability, fast-growing grasses like *E. nutans* are more abundant relatively.

Illumina NovaSeq paired-end sequencing of bacterial V3–V4 and fungal ITS1 region yielded 412,048 and 688,592 clean reads, respectively. These sequences were grouped into 7,016 bacterial zOTUs and 2,142 fungal zOTUs. The bacterial zOTUs were classified into 21 phyla, Proteobacteria (35.89%) and Acidobacteria (16.04%) were the two predominant phyla (Figure 2A), followed by Actinobacteria (15.48%) and Bacteroidetes (9.17%). The fungal communities were mainly dominated by Ascomycota with an average of 34.04% reads, followed by Basidiomycota with 26.94% of reads (Figure 2B). We did not observe any significant effect of our treatment on bacterial or fungal richness (all $P > 0.05$, Figures 3A,B). The PCoA based on Bray–Curtis dissimilarities was conducted to reflect the soil bacterial and fungal beta diversity among different treatments. The results showed that our treatment did not influence the bacterial or fungal community composition (Figures 3C,D), which was confirmed by the PERMANOVA analysis (all $P > 0.05$). Therefore, we speculate that in an alpine meadow on the Qinghai-Tibetan Plateau, the soil microbial community may react to resource availability more slowly than plants.

Discussion

By examining the effect of nutrient addition on the plant and soil microbial community structure, our results provide strong evidence that plant and soil microbes responded asynchronously to short-term nutrient deposition on the Qinghai-Tibetan Plateau.

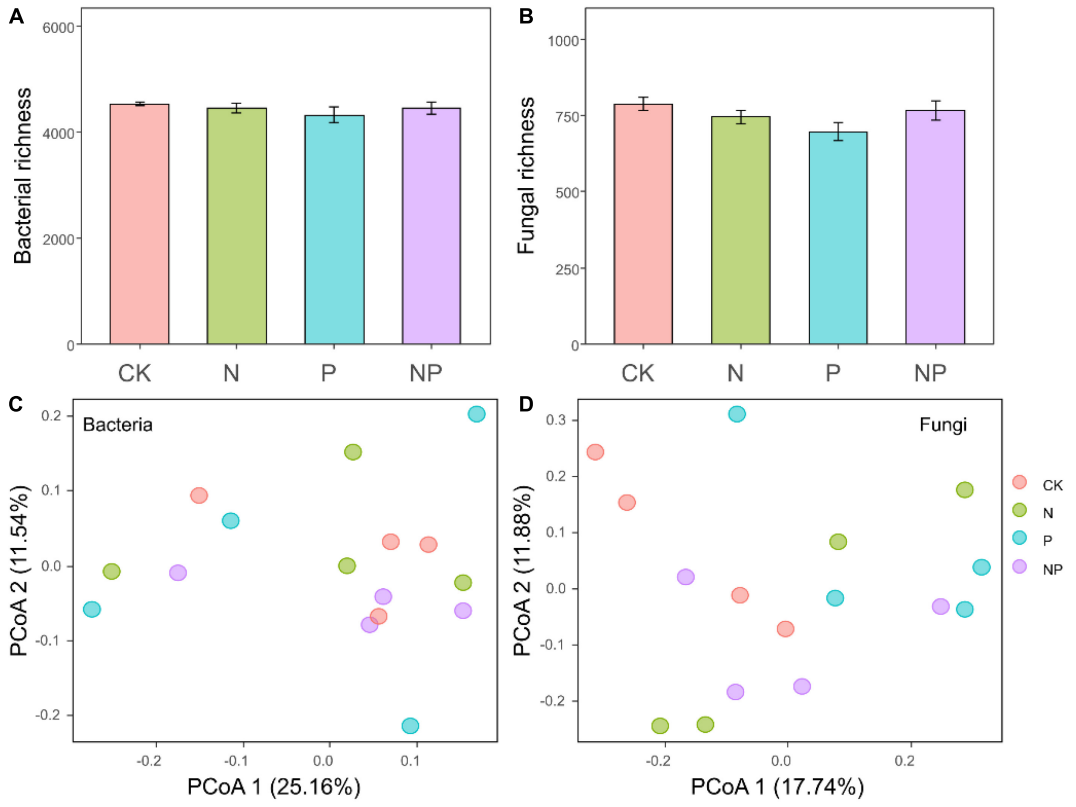

FIGURE 3
Bacterial richness **(A)** and fungal richness **(B)** under different treatments. Bars represent means ± SEs. Principal coordinate analysis ordination (PCoA) plot based on a Bray–Curtis dissimilarity matrix of bacterial communities **(C)** and fungal communities **(D)** under different treatments.

Our results demonstrated that the N addition significantly increased aboveground biomass and altered the composition of plant community. The results are in line with the findings of previous studies, which shown that additional N increases aboveground biomass (Gao et al., 2018) and changed plant community composition (Stiles et al., 2017). However, neither the aboveground biomass nor the plant community composition was substantially influenced by P addition in our study. Therefore, it is possible that N was the predominant limiting nutrient in the alpine grassland on the Qinghai-Tibetan Plateau (Jiang et al., 2018; Li et al., 2021). In contrast to most previous findings, we did not observe any significant effect of nutrient addition on plant richness. In alpine meadows, nutrient addition typically resulted in the loss of some sedges and forbs (Sun et al., 2016). The explanation for the not significant decline of plant richness in response to nutrient enrichment in our study might be the relatively short-term experimental duration (Humbert et al., 2016). So, instead of the loss of species, our data also implied that the response of plants to nitrogen addition is firstly caused by changes in community composition.

Soil microorganisms are commonly thought to respond quickly to short-term events due to their rapid generation rates, high population densities, and diverse communities (Chase et al., 2021). Contrary to what we expected, the addition of fertilizer had no obvious influence on the diversity or composition of the soil microbial community. The following potential reasons might be responsible for the observations. First, soil microbial communities are insensitive to nutrient addition in our ecosystem, because previous study also reported that soil microbial biomass and community structure showed minor responses to 4 years of nitrogen and phosphorus addition (Chen et al., 2019). Since the root biomass was the major determinant of soil microbial community (Rinnan et al., 2005), the insensitivity of soil microbes could be related to the stability of root biomass in this study. The limitation of our study design is that we did not analyze the soil properties from soil. Therefore, we could not conclude whether the stability of soil microbial communities was also related to the soil properties.

Second, soil microbial composition transition may need a longer time than plant community to show up, since many studies reported changes in both plant and soil microbial community composition after long-term scale (Dahl et al., 2017; Ma et al., 2018). An apparent lack of responses in the short term may progress or cascade through the system, leading to long-term changes and adaptations (Knapp et al., 2012). In this case, the changes of soil microbial communities maybe triggered by

plant community or changes in plant resource stoichiometry (Yuan et al., 2016; Liu et al., 2020; Wang et al., 2022). This finding corroborates the previous study which also reported that N deposition has greater effects on the plant community than on the soil microbial community (Wu et al., 2013). However, given that long-term time scale (8 years) used in their study, our current result may relate to different mechanism. Further dynamic monitoring is needed to illustrate the possible effects and mechanisms by which resource availability alter plant and soil microbial development at multiple time points.

In our study, fertilization addition affected plant shoot biomass and community composition while having no effect on the composition of the soil microbial community, demonstrating that, on a short-term time scale, resource availability has a greater impact on the plant community than the soil microbial community. This research contributes to our understanding of how above- and below-ground microbial communities are impacted by short-term environmental change, and the knowledge acquired can be applied to forecast long-term implications in alpine grassland ecosystems.

Data availability statement

The datasets presented in this study can be found in online repositories. The names of the repository/repositories and accession number(s) can be found below: https://ngdc.cncb.ac.cn/structure, PRJCA011844.

Author contributions

SJ designed the research. JD and TT performed the field survey and data analysis. SJ wrote the first draft, with inputs from JD and TT. All authors read and approved the final manuscript.

Funding

This work was supported by the Youth Science and Technology Fund program of Gansu Province (No. 22JR5RA522).

Acknowledgments

We are grateful to the Haibei National Field Research Station in the Alpine Grassland Ecosystem for maintaining the experimental facility.

Conflict of interest

The authors declare that the research was conducted in the absence of any commercial or financial relationships that could be construed as a potential conflict of interest.

Publisher's note

All claims expressed in this article are solely those of the authors and do not necessarily represent those of their affiliated organizations, or those of the publisher, the editors and the reviewers. Any product that may be evaluated in this article, or claim that may be made by its manufacturer, is not guaranteed or endorsed by the publisher.

References

Adair, K. L., Lindgreen, S., Poole, A. M., Young, L. M., Bernard-Verdier, M., Wardle, D. A., et al. (2019). Above and belowground community strategies respond to different global change drivers. *Sci. Rep.* 9:2540. doi: 10.1038/s41598-019-39033-4

Chase, A. B., Weihe, C., and Martiny, J. B. (2021). Adaptive differentiation and rapid evolution of a soil bacterium along a climate gradient. *Proc. Natl. Acad. Sci. U.S.A.* 118:e2101254118. doi: 10.1073/pnas.2101254118

Chen, H., Zhu, Q., Peng, C., Wu, N., Wang, Y., Fang, X., et al. (2013). The impacts of climate change and human activities on biogeochemical cycles on the Qinghai-Tibetan Plateau. *Glob. Change Biol.* 19, 2940–2955. doi: 10.1111/gcb.12277

Chen, X., Hao, B., Jing, X., He, J.-S., Ma, W., and Zhu, B. (2019). Minor responses of soil microbial biomass, community structure and enzyme activities to nitrogen and phosphorus addition in three grassland ecosystems. *Plant Soil* 444, 21–37. doi: 10.1007/s11104-019-04250-3

Classen, A. T., Sundqvist, M. K., Henning, J. A., Newman, G. S., Moore, J. A., Cregger, M. A., et al. (2015). Direct and indirect effects of climate change on soil microbial and soil microbial-plant interactions: what lies ahead? *Ecosphere* 6:130. doi: 10.1890/ES15-00217.1

Dahl, M. B., Priemé, A., Brejnrod, A., Brusvang, P., Lund, M., Nymand, J., et al. (2017). Warming, shading and a moth outbreak reduce tundra carbon sink strength dramatically by changing plant cover and soil microbial activity. *Sci. Rep.* 7:16035. doi: 10.1038/s41598-017-16007-y

De Boeck, H. J., Vicca, S., Roy, J., Nijs, I., Milcu, A., Kreyling, J., et al. (2015). Global change experiments: challenges and opportunities. *BioScience* 65, 922–931. doi: 10.1093/biosci/biv099

Gao, Y., Cooper, D. J., and Zeng, X. (2018). Nitrogen, not phosphorus, enrichment controls biomass production in alpine wetlands on the Tibetan Plateau, China. *Ecol. Eng.* 116, 31–34. doi: 10.1016/j.ecoleng.2018.02.016

Humbert, J. Y., Dwyer, J. M., Andrey, A., and Arlettaz, R. (2016). Impacts of nitrogen addition on plant biodiversity in mountain grasslands depend on dose, application duration and climate: a systematic review. *Glob. Chang. Biol.* 22, 110–120. doi: 10.1111/gcb.12986

IPCC (2018). *Climate change: the physical science basis. Contribution of working group I to the fifth assessment report of the intergovernmental panel on climate change*. Geneva: IPCC.

Jiang, S., Liu, Y., Luo, J., Qin, M., Johnson, N. C., Öpik, M., et al. (2018). Dynamics of arbuscular mycorrhizal fungal community structure and functioning along a nitrogen enrichment gradient in an alpine meadow ecosystem. *New Phytol.* 220, 1222–1235. doi: 10.1111/nph.15112

Knapp, A. K., Smith, M. D., Hobbie, S. E., Collins, S. L., Fahey, T. J., Hansen, G. J., et al. (2012). Past, present, and future roles of long-term experiments in the LTER network. *BioScience* 62, 377–389. doi: 10.1525/bio.2012.62.4.9

Li, C., Li, Y., Li, X., Ma, L., Xiao, Y., and Zhang, C. (2021). Differential responses of plant primary productivity to nutrient addition in natural and restored Alpine Grasslands in the Qinghai Lake Basin. *Front. Plant Sci.* 12:792123. doi: 10.3389/fpls.2021.792123

Li, L., Li, X., Liu, B., Lei, J., Yue, Z., and Li, C. (2020). Imbalanced stoichiometric patterns in foliar nutrient resorption response to N and P addition in grazing alpine grassland. *Acta Oecol.* 102:103505. doi: 10.1016/j.actao.2019.103505

Ling, N., Wang, T., and Kuzyakov, Y. (2022). Rhizosphere bacteriome structure and functions. *Nat. Commun.* 13:836. doi: 10.1038/s41467-022-28448-9

Liu, X., Lamb, E. G., and Zhang, S. (2020). Nitrogen addition impacts on soil microbial stoichiometry are driven by changes in plant resource stoichiometry not by the composition of main microbial groups in an alpine meadow. *Biol. Fertil. Soils.* 56, 261–271. doi: 10.1007/s00374-019-01423-1

Ma, S., Verheyen, K., Props, R., Wasof, S., Vanhellemont, M., Boeckx, P., et al. (2018). Plant and soil microbe responses to light, warming and nitrogen addition in a temperate forest. *Funct. Ecol.* 32, 1293–1303. doi: 10.1111/1365-2435.13061

Rinnan, R., Keinänen, M. M., Kasurinen, A., Asikainen, J., Kekki, T. K., Holopainen, T., et al. (2005). Ambient ultraviolet radiation in the Arctic reduces root biomass and alters microbial community composition but has no effects on microbial biomass. *Glob. Change Biol.* 11, 564–574. doi: 10.1111/j.1365-2486.2005.00933.x

Rudgers, J. A., Afkhami, M. E., Bell-Dereske, L., Chung, Y. A., Crawford, K. M., Kivlin, S. N., et al. (2020). Climate disruption of plant-microbe interactions. *Annu. Rev. Ecol. Evol. Syst*. 51, 561–586. doi: 10.1146/annurev-ecolsys-011720-090819

Stiles, W. A., Rowe, E. C., and Dennis, P. (2017). Long-term nitrogen and phosphorus enrichment alters vegetation species composition and reduces carbon storage in upland soil. *Sci. Total Environ.* 593, 688–694. doi: 10.1016/j.scitotenv.2017.03.136

Sun, X., Yu, K., Shugart, H. H., and Wang, G. (2016). Species richness loss after nutrient addition as affected by N: C ratios and phytohormone GA_3 contents in an alpine meadow community. *J. Plant Ecol.* 9, 201–211. doi: 10.1093/jpe/rtv037

Wang, P., Yang, F., Chen, X., Li, J., Zhou, X., and Guo, H. (2022). Long-term fertilization effects on soil biotic communities are mediated by plant diversity in a Tibetan alpine meadow. *Plant Soil.* 474, 525–540. doi: 10.1007/s11104-022-05356-x

Wang, Y., Ren, Z., Ma, P., Wang, Z., Niu, D., Fu, H., et al. (2020). Effects of grassland degradation on ecological stoichiometry of soil ecosystems on the Qinghai-Tibet Plateau. *Sci. Total Environ.* 722:137910. doi: 10.1016/j.scitotenv.2020.137910

Wardle, D. A., Bardgett, R. D., Klironomos, J. N., Setala, H., Van Der Putten, W. H., and Wall, D. H. (2004). Ecological linkages between aboveground and belowground biota. *Science* 304, 1629–1633. doi: 10.1126/science.109487

Wu, J., Liu, W., Fan, H., Huang, G., Wan, S., Yuan, Y., et al. (2013). Asynchronous responses of soil microbial community and understory plant community to simulated nitrogen deposition in a subtropical forest. *Ecol. Evol.* 3, 3895–3905. doi: 10.1002/ece3.750

Yuan, X., Knelman, J. E., Gasarch, E., Wang, D., Nemergut, D. R., and Seastedt, T. R. (2016). Plant community and soil chemistry responses to long-term nitrogen inputs drive changes in alpine bacterial communities. *Ecology* 97, 1543–1554. doi: 10.1890/15-1160.1

frontiers | Frontiers in Ecology and Evolution

TYPE Original Research
PUBLISHED 07 November 2022
DOI 10.3389/fevo.2022.1034829

OPEN ACCESS

EDITED BY
Xiang Liu,
Lanzhou University, China

REVIEWED BY
Youzheng Zhang,
Second Institute of Oceanography, Ministry of Natural Resources, China
Pei Zhang,
Sichuan University, China

*CORRESPONDENCE
Tiedong Liu
liu@hainanu.edu.cn
Jinhuan Luo
443464199@qq.com

SPECIALTY SECTION
This article was submitted to Conservation and Restoration Ecology, a section of the journal Frontiers in Ecology and Evolution

RECEIVED 02 September 2022
ACCEPTED 22 September 2022
PUBLISHED 07 November 2022

CITATION
Hou W, He M, Qi Y, Liu T and Luo J (2022) Soil nematode community assembly in a primary tropical lowland rainforest.
Front. Ecol. Evol. 10:1034829.
doi: 10.3389/fevo.2022.1034829

Soil nematode community assembly in a primary tropical lowland rainforest

Weichen Hou[1], Mengfei He[1], Yanwen Qi[1], Tiedong Liu[1]* and Jinhuan Luo[2]*

[1]Key Laboratory of Genetics and Germplasm Innovation of Tropical Special Forest Trees and Ornamental Plants, Ministry of Education, School of Forestry, Hainan University, Haikou, China, [2]Sanya Academy of Forestry, Sanya, China

More than half of the world's tropical lowland rainforests have been lost due to conversion to agricultural land (such as rubber plantations). Thus, ecological restoration in degraded tropical lowland rainforests is crucial. The first step to restoration is restoring soil functioning (i.e., soil fertility, carbon, and nitrogen cycling) to levels similar to those in the primary tropical lowland rainforest. This requires understanding soil nematode community assembly in primary tropical lowland rainforest, which has never been explored in this habitat. In this study, we measured species compositions of plant and soil nematode communities and soil characteristics (pH, total and available nitrogen, phosphorus, and soil water content) in a primary tropical lowland rainforest, which is located on Hainan Island, China. We performed two tests (the null-model test and distance-based Moran's eigenvector maps (MEM) and redundancy analysis-based variance partitioning) to quantify the relative contribution of the deterministic (abiotic filtering and biotic interactions) and stochastic processes (random processes and dispersal limitation) to the soil nematode community. We found that a deterministic process (habitat filtering) determined nematode community assembly in our tropical lowland rainforest. Moreover, soil properties, but not plant diversity, were the key determinants of nematode community assembly. We have, for the first time, managed to identify factors that contribute to the nematode community assembly in the tropical lowland rainforest. This quantified community assembly mechanism can guide future soil functioning recovery of the tropical lowland rainforest.

KEYWORDS

biotic interaction, community convergence or divergence, dispersal limitation, habitat filtering, stochastic processes

Introduction

Tropical lowland forests harbor the most biodiversity, but these forests are also easily destroyed due to their suitability for agricultural use (Corlett, 2011). As of now, over half of the tropical lowland rainforest has been lost due to its conversion into agricultural lands (i.e., rubber plantations and palm plantations). (Aleman et al., 2018). Thus, ecological restoration is crucial to restoring the percentage of tropical lowland rainforests worldwide (Brancalion et al., 2019). The first step in reforestation is restoring the soil functioning of degraded soil (Zhang et al., 2019). Soil nematodes are the most abundant soil-dwelling animal group on earth and are vital to soil function (i.e., processing soil

organic nutrients and regulating soil microorganism populations) (Ferris et al., 2001; Ruess, 2003; Pausch et al., 2016; van den Hoogen et al., 2019). Thus, a deep understanding of soil nematode community assembly in the primary tropical lowland rainforest can aid the recovery of soil functioning (Wang et al., 2022). That is because soil nematode community assembly in the primary tropical lowland rainforest can easily establish a restoration standard (Wang et al., 2022). For example, soil nematode community assembly in the restored tropical lowland rainforest should be comparable to that in the primary tropical lowland rainforest.

Identification of different ecological processes that shape the community assembly of different communities is the primary focus of ecological research (Condit et al., 2002; Chave, 2013; Chase, 2014). For more than a century, community ecologists have debated whether the deterministic or stochastic processes play a primary role in structuring ecological communities (Hubbell, 2001; Chase and Myers, 2011; Trisos et al., 2014). This debate has led to conceptual ideas that invoke multiple processes ranging from niche-based habitat filtering and interspecific competition (niche differentiation) to random dispersal and demographic stochasticity (Weiher et al., 2011). The relative contribution of deterministic and stochastic processes to community assembly has been widely investigated for plant communities, soil bacterial, and fungal communities in different ecosystems (Zhang et al., 2015; Moroenyane et al., 2016; Tripathi et al., 2018; Jiao et al., 2021; Ni et al., 2021). However, till now, there has been no study investigating soil nematode community assembly in the tropical lowland rainforest.

A recent global meta-analysis indicated that a deterministic process may dominate soil nematode community assembly globally (Luan et al., 2020). Thus, we hypothesized that deterministic processes (habitat filtering) might also dominate nematode community assembly in the tropical lowland rainforest. To test this hypothesis, in the primary tropical lowland rainforest on Hainan Island, we evaluated the relative contributions of the deterministic and stochastic processes to soil nematode community assembly by examining the following: (i) species compositions of plant and soil nematode communities in 20 plots of 400 m^2 each and (ii) soil characteristics (pH, total and available nitrogen, and phosphorus, and soil water content) in each plot. With this dataset, we first used a null model test to compare the observed beta diversity and the beta diversity of simulated random communities to determine if there is significant community convergence, divergence, or random distribution. Then, we used it to reveal the relative contributions of the deterministic process (soil variables) and stochastic processes (dispersal limitation and random process) to the beta diversity of the nematode community. Finally, by determining the beta diversity of the soil nematode community, we were able to quantify the relative importance of soil variables and plant diversity if a deterministic process dominated the nematode community assembly.

Materials and methods

Study site

The study site is the Xinglong National Forest Park (110.16°E, 18.77°N) in Hainan Province, southern China (Figure 1). It has a unique primary tropical lowland rainforest with high species diversity. Its altitude ranges from 5 to 300 m; the area has a mean annual temperature of 24.5°C, and the lowest and the highest mean monthly temperatures are 18.7°C (January) and 28.5°C (July), respectively (Guo et al., 2018). The mean annual precipitation is ∼2,500 mm, and most of the precipitation is distributed between May and November.

Sampling

On 10 August 2021 (at the peak of the growing season), we randomly sampled 20 plots in the adjacent undisturbed secondary tropical rainforest. Each of these plots was 20 × 20 m^2 and at least 100–300 m apart (Figure 1). The elevation of all 20 plots ranged from 15 to 150 m. Within a plot, all freestanding trees with a DBH (diameter at breast height) of ≥1 cm were measured and identified as species. The spatial locations (x- and y- coordinates) for each plot were also recorded. We randomly collected five soil cores (depth diameter of soil cores, 0–20 cm) from each plot and mixed them into one soil sample. We then used 100 g of soil to measure the soil properties, and soil nematodes were extracted from another 100 g of soil using Baermann's funnel method (Barker et al., 1985). Then, we used a microscope (Leica DM500) to measure nematode abundance in each soil sample by identifying the first 100 nematodes to the genus level based on their morphological traits. All nematode images were identified to genus level for soils with fewer than 100 nematodes. We followed the method used by Yeates et al. (1993) to classify all the identified nematodes into five functional groups: phytophagous nematodes, bacterivores, fungivores, predators, and omnivores (Supplementary Table S1).

As described by Burt (2009), the soil N concentration was determined using the Kjeldahl digestion method and an OIFS 3000 autoanalyzer (OI Analytical, College Station, TX, USA). Both ammonium N and nitrate N were extracted from 2 g of soil using a 2.0 M KCl solution. The ammonium and nitrate N extracts were further analyzed colorimetrically using a KCl extract and an OIFS 3000 autoanalyzer (OI Analytical, College Station, TX, USA). To determine the total P in the soil, we took 2.5 g of fresh soil, added Mehlich III solution, and then evaluated the color change in the soil with a spectrophotometer after the soil was digested with perchloric acid. Elemental analysis of P was performed on the Mehlich III extracts using inductively coupled plasma atomic emission spectroscopy (ICP-AES). Soil pH was measured using a pH meter in a KCl suspension (UB-7, UltraBASIC, Denver, CO, USA). The water content of the soil

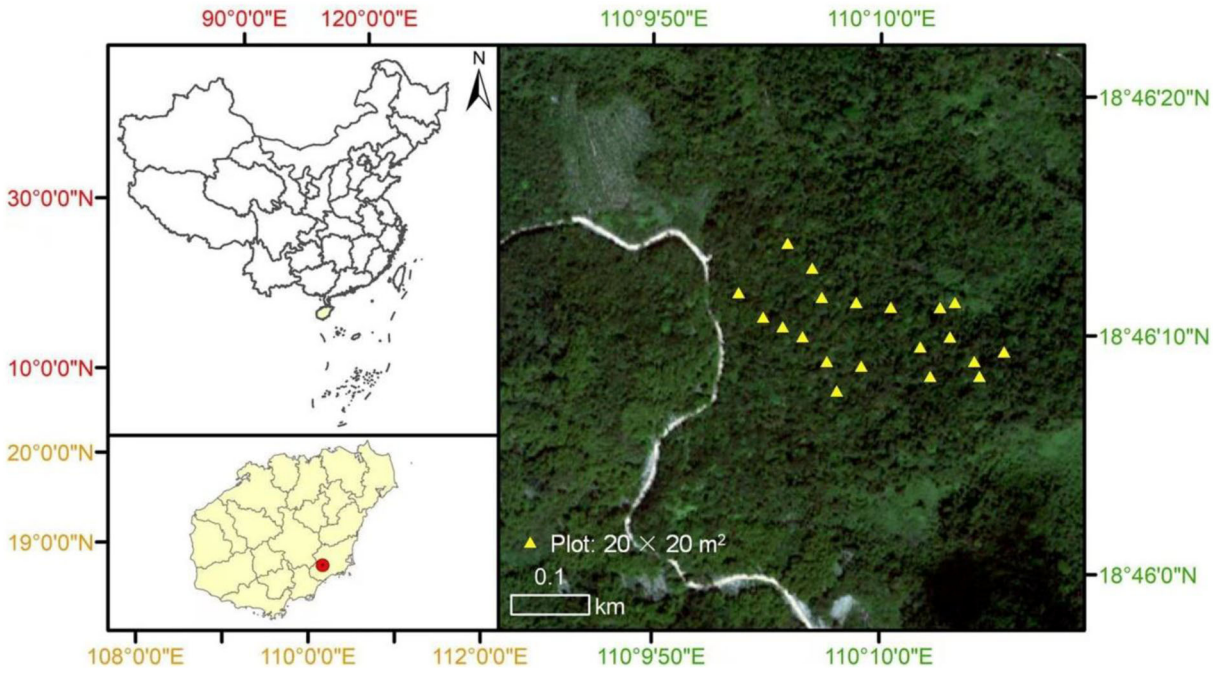

FIGURE 1
The map of our study site and detailed spatial location of our 20 × 20 m^2 plots in the primary tropical lowland rainforest.

was determined by measuring the amount of weight lost upon drying the soil at 100°C for 48 h in an oven.

Statistic methods

We first calculated Bray–Curtis dissimilarities to represent the beta diversity of the nematode community. To test whether any observed beta diversity pattern was a random distribution or showed species convergence or divergence, we first simulated null communities in which species abundance values were randomly assigned. Randomization procedures were applied to calculate "null" distributions for both species composition (i.e., on the species × quadrat matrix) and all species (Götzenberger et al., 2012). We reshuffled the species × quadrat matrices with three constraints simultaneously, following the method of Zhang et al. (2015, 2018); that is, keeping (1) the same number of species (species richness) per plot in the simulated and observed data; (2) the same number of total species occurrences per region (i.e., the number of plots where the species occur in each group of the five spatial scales); and (iii) the total abundance of species in a region constant (i.e., the sum of the number of quadrats occupied in all plots). We implemented this using the function "randomized matrix" in the "Picante" package in R software (Kembel et al., 2010). We then compared the observed beta diversity to the beta diversity simulated in 1,000 randomly assembled communities. Beta diversity was quantified using the standard effect size index (SES) developed by Gotelli and McCabe (2002):

$$\mathrm{SES} = (\text{beta diversity}_{\text{observed}} - \text{beta diversity}_{\text{random}})/\text{beta diversity}_{\text{sd}}$$

where beta diversity $_{\text{observed}}$ and beta diversity $_{\text{random}}$ represent observed beta diversity and mean beta diversity values of the simulated null community, respectively. The beta $\text{diversity}_{\text{sd}}$ represents the standard deviation of beta diversity values generated from the 1,000 simulations. We used the Wilcoxon signed-rank tests to examine whether SES was significantly more than, less than, or ≈0, which indicated the prevalence of significant species divergence, species convergence, and random distribution, respectively.

Partitioning the spatial patterns in the beta diversity of nematodes

We first used the "diversity result" in the "biodiversity" package in r software to calculate plant diversity (richness and abundance). Then, we used Moran's eigenvector maps (MEM) and the spatial location of each plot to quantify spatial autocorrelations in nematode species composition in each plot. The MEM was based on the principal coordinates of neighbor matrix axes (Legendre and Legendre, 2012) and could be

used to describe the spatial autocorrelations in beta diversity (Zhang et al., 2015, 2018). We used the function "cmdscale" in the "SpacemakerR" package in r software (Stephane, 2013) to calculate MEM. We then used the r function"poly" to quantify each variable's polynomial terms, including the linear and nonlinear relationships between soil variables and species composition. While performing redundancy analysis (RDA)-based variance partitioning, we used the method developed by Blanchet et al. (2008) to forward-select significant soil variables and purely spatial variables represented by MEM associated with beta diversity of the soil nematode community. Finally, we used variance partitioning to allocate variations in beta diversity of nematode community to eight complementary components: (a) "purely soil variables" (explained by soil factors only), (b)"purely spatial variables" (spatial autocorrelation in beta diversity independent of soil variables and induced by dispersal limitation and biotic interactions), (c) "purely plant diversity variables (explained by plant diversity (richness and abundance) only)," (d) "spatially structured abiotic variables" (spatial autocorrelation in beta diversity and merely induced by soil variables), (e) "spatially structured plant diversity" (spatial autocorrelation in beta diversity and merely induced by plant diversity), (f) variables explained by both soil variables and plant diversity, (g) variations in beta diversity explained by soil variables, spatial variables, and plant diversity, and "undetermined variables" (Legendre et al., 2009; Zhang et al., 2018). Variation in beta diversity of the soil nematode community explained by soil variables was represented by $a + d + f + g$, whereas $b + d + e + g$ showed the variation in the soil nematode community explained by MEM. In addition, the variation of the soil nematode community explained by plant diversity was reflected by c+e+f+g. Variance partitioning was performed using the function "varpart" in the "vegan" package in R (Oksanen et al., 2016).

Results

There are a total of 29 genera of soil nematodes across all plots in our primary tropical lowland rainforest (Supplementary Table S1). Bacterivores had the most (12) genera, whereas predators had the fewest (2) genera (Supplementary Table S1). Both phytophagous nematodes and omnivores had six genera (Supplementary Table S1). In addition, fungivores had three genera (Supplementary Table S1).

The nematode community converged, as indicated by a significantly smaller SES than zero (Figure 2), indicating that the deterministic processes (habitat filtering or exclusion of weak competitors) dominated the nematode community assembly. The deterministic process (habitat filtering), represented by the soil variables, accounted for 63% of the variation in beta diversity, respectively (Figure 3). By contrast, the stochastic process (dispersal limitation), represented by spatial variables, explained 22% of the variation in beta diversity (Figure 3). In the tests of soil variables on beta diversity of soil nematode communities, the forward selection analysis revealed that the significant abiotic variables that predicted beta diversity of soil nematode communities included pH, soil total and available phosphorus, and soil water content (Supplementary Table S2). When comparing the relative contributions of all soil variables and plant diversity (richness and abundance) to the beta diversity of the soil nematode community, we found that soil variables explained 63% of the variation in beta diversity, whereas plant diversity merely accounted for 25% of the variations in beta diversity (Figure 3).

Discussion

We studied a primary tropical lowland rainforest to estimate the relative importance of the deterministic and stochastic processes in determining soil nematode community assembly in tropical lowland rainforests. As we hypothesized, habitat filtering was the major determinant of the soil nematode community assembly in tropical lowland rainforests. Moreover, soil properties determine soil nematode community assembly.

By comparing observed beta diversity to that simulated from null communities, we found significant convergence (SES < 0), indicating deterministic processes (habitat filtering or exclusion of weak competitors) dominated community assembly of soil nematodes (Kraft et al., 2008; De Bello et al., 2012; Zhang et al., 2015, 2018). We further showed that habitat filtering (indicated by soil variables) explained 63% of the variations in the beta diversity of soil nematodes. We noted that our attribution of the effect of dispersal limitation on the beta diversity of soil nematodes to purely spatial variables might be an overestimate (Legendre et al., 2009), which could be, despite our attempt to include the important soil nutrient variables, because some significant abiotic variables remain unaccounted for (Siefert et al., 2013). However, given the high variations in beta diversity explained by soil variables, we can easily judge habitat-filtering-dominated soil nematode community assembly; this is consistent with a recent meta-analysis, which showed that a deterministic process dominated soil nematode community assembly at the global scale (Luan et al., 2020). However, different results have also been found in other ecosystems. For instance, Zou et al. (2022) found that the stochastic processes are the primary determinants of soil nematode community assembly in three Asian mountains. In contrast, the deterministic process dominated the community assembly of nematodes in a tropical seasonal forest (Wang et al., 2022) and our tropical lowland rainforest. The different soil (i.e., N-limited

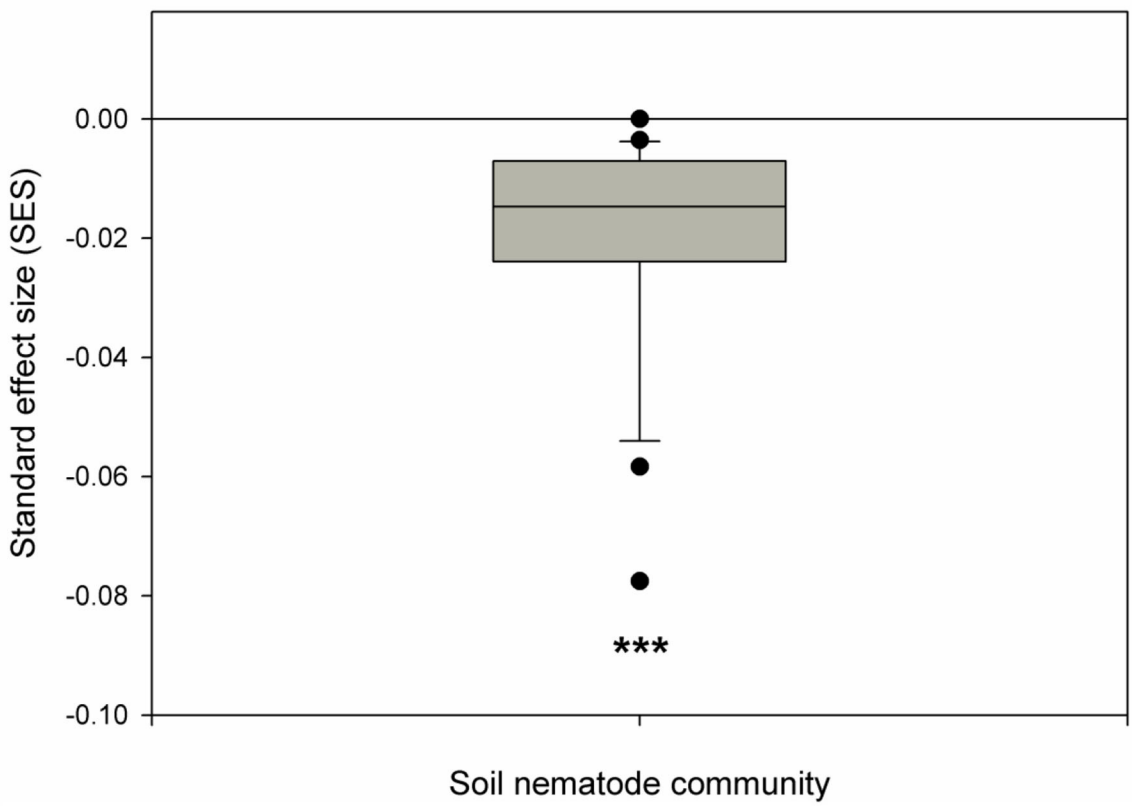

FIGURE 2
Distribution of standard effect size (SES) of beta diversity in our primary tropical lowland rainforest. SES that is significantly greater than, smaller than, or approaching zero indicates significant trait divergence, trait convergence, or random distribution, respectively. The box plot shows the median (line within the box), 25 and 75th percentiles (the boundaries of the box), and 90 and 10th percentiles (error bars) of SES at each spatial scale. ***Indicates a p-value <0.001 based on the Wilcoxon signed-rank tests.

or P-limited) and plant diversity (e.g., high or low) types in different ecosystems may result in inconsistent soil nematode community assembly patterns between our study and other studies. Thus, comparative research on the community assembly mechanisms of soil nematode communities across different ecosystems should be performed in the future to generate a general community assembly mechanism of soil nematodes at the global scale.

A null-model approach developed by Kraft et al. (2008) and distance-based Moran's eigenvector maps (MEM) and redundancy analysis-based variance partitioning have widely proven to be helpful in identifying community assembly mechanisms of plant communities (Kraft and Ackerly, 2010; De Bello et al., 2012; Myers et al., 2013; Zhang et al., 2015, 2018). However, no study used them to identify the relative contributions of deterministic and stochastic processes to community assembly of nematode communities. It remains unclear whether they can also be applied to dissolve soil nematode community assembly. In this study, the results clearly demonstrated that they could successfully determine the key determinants of community assembly of soil nematodes. We recommend that these two methods be used to reveal the community assembly of soil nematodes in future studies.

Soil properties and plant diversity are reported as the key influences on the soil nematode community (Neher, 2010; Viketoft et al., 2011; Liu et al., 2015; Wang et al., 2018). However, the relative contributions of soil characteristics and plant diversity to community assembly of the soil nematode community remain unknown. Our variance partitioning results clearly demonstrated that soil properties explained 63% of the variations in the beta diversity of soil nematodes, whereas plant diversity merely explained 25%. This indicated that soil properties, but not plant diversity, dominated the soil nematode community assembly in the tropical lowland rainforest. However, we only measured plant diversity, and it is highly possible that plant-derived resources (e.g., litter input) may be more important than plant diversity in determining the beta diversity of the soil nematode community. As a result, the plant-derived resources should be measured in the future to identify the relative contributions of soil properties and plant-derived resources in driving the variation in beta diversity of the soil nematode community.

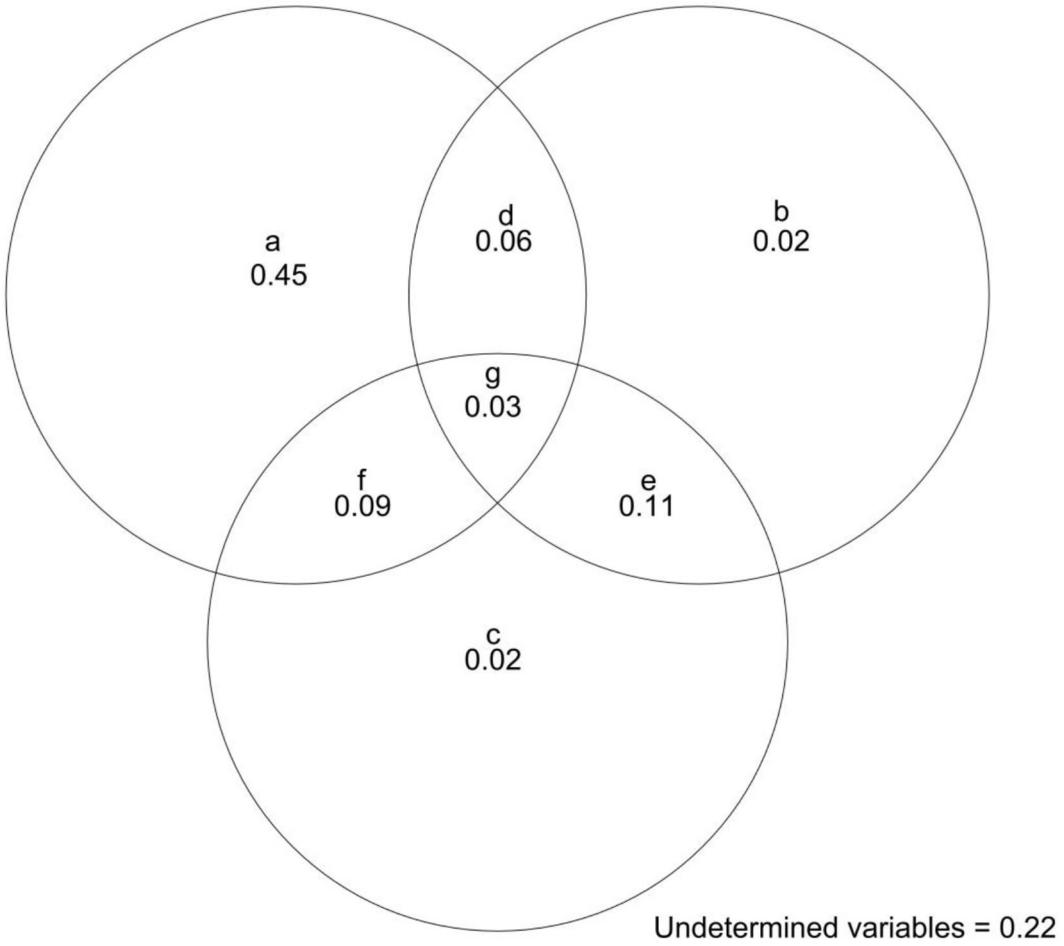

FIGURE 3
The variations of beta diversity are partitioned into eight complementary components if statistically significant ($p < 0.05$). Analysis was performed, including all quadrants. These eight components include (a) "purely soil variables" (explained by soil factors only), (b) "purely spatial variables" (spatial autocorrelation in beta diversity independent of soil variables and induced by dispersal limitation and biotic interactions), (c) "purely plant diversity variables (explained by plant diversity (richness and abundance) only)," (d) "spatially structured abiotic variables" (spatial autocorrelation in beta diversity and merely induced by soil variables), (e) "spatially structured plant diversity" (spatial autocorrelation in beta diversity and merely induced by plant diversity), (f) variables explained by both soil variables and plant diversity, (g) variations of beta diversity explained by soil variables, spatial variables, and plant diversity and "undetermined variables." Variation in beta diversity of the soil nematode community explained by soil variables is represented by $a + d + f + g$, whereas $b + d + e + g$ shows the variation of the soil nematode community explained by MEM. In addition, the variation of soil nematode community explained by plant diversity is reflected by $c + e + f + g$.

Conclusion

Overall, we gained invaluable insights into soil nematode community assembly in tropical lowland forests. The first null-model test, distance-based Moran's eigenvector maps (MEM), and redundancy analysis-based variance partitioning revealed the community assembly of soil nematodes in tropical lowland rainforests. Second, the deterministic process (habitat filtering) dominated the community assembly of soil nematodes. Third, soil properties but not plant diversity were the primary determinants of soil nematode community assembly. This quantified community assembly mechanism can guide future soil functioning recovery of tropical lowland rainforests. For example, since soil properties are the key determinants of soil nematode communities, adding fertilization to improve soil fertility is one key step to recovering the soil nematode community and its induced key soil functioning in degraded tropical lowland rainforest.

Data availability statement

The raw data supporting the conclusions of this article will be made available by the authors, without undue reservation.

Author contributions

WH, TL, and JL designed the research. WH, MH, YQ, TL, and JL performed the research and wrote the manuscript. WH, MH, TL, and JL analyzed the data. All authors contributed to the article and approved the submitted version.

Funding

This research was supported by the Hainan Province Science and Technology Special Fund (ZDYF2022SHFZ320), Hainan Provincial Natural Science Foundation of China (422CXTD508, 421MS013), the Education Department of Hainan Province (Hnjg2021ZD-9), the specific research fund of the Innovation Platform for Academicians of Hainan Province, the research project of the Hainan Academician Innovation Platform (YSPTZX202017), and the scientific research project for the ecological restoration of Baopoling Mountain in Sanya, China.

Conflict of interest

The authors declare that the research was conducted in the absence of any commercial or financial relationships that could be construed as a potential conflict of interest.

Publisher's note

All claims expressed in this article are solely those of the authors and do not necessarily represent those of their affiliated organizations, or those of the publisher, the editors and the reviewers. Any product that may be evaluated in this article, or claim that may be made by its manufacturer, is not guaranteed or endorsed by the publisher.

Supplementary material

The Supplementary Material for this article can be found online at: https://www.frontiersin.org/articles/10.3389/fevo.2022.1034829/full#supplementary-material

References

Aleman, J. C., Jarzyna, M. A., and Staver, A. C. (2018). Forest extent and deforestation in tropical Africa since 1900. *Nat. Ecol. E2*, 26–33. doi: 10.1038/s41559-017-0406-1

Barker, K. R., Carter, C. C., and Sasser, J. N. (1985). *An Advanced Treatise on MELOIDOGYNE (vol.2): |Methodology*. Raleigh: North Carolina State University Press.

Blanchet, F. G., Legendre, P., and Borcard, D. (2008). Forward selection of explanatory variables. *Ecology* 89, 2623–2632. doi: 10.1890/07-0986.1

Brancalion, P. H. S., Niamir, A., Broadbent, E., Crouzeilles, R., Barros, F. S. M., Almeyda Zambrano, A. M., et al. (2019). Global restoration opportunities in tropical rainforest landscapes. *Sci. Adv.* 5, eaav3223. doi: 10.1126/sciadv.aav3223

Burt, R. (2009). *Soil Survey Field and Laboratory Methods Manual*. Lincoln: National Soil Survey Center Press.

Chase, J. M. (2014). Spatial scale resolves the niche versus neutral theory debate. *J. Veg. Sci.* 25, 319–322. doi: 10.1111/jvs.12159

Chase, J. M., and Myers, J. A. (2011). Disentangling the importance of ecological niches from stochastic processes across scales. *Philos. Trans. R. Soc. B Biol. Sci.* 366, 2351–2363. doi: 10.1098/rstb.2011.0063

Chave, J. (2013). The problem of pattern and scale in ecology: what have we learned in 20 years? *Ecol. Lett.* 16, 4–16. doi: 10.1111/ele.12048

Condit, R., Pitman, N., Leigh, E. G., Chave, J., Terborgh, J., Foster, R. B., et al. (2002). Beta-diversity in tropical forest trees. *Science* 295, 666–669. doi: 10.1126/science.1066854

Corlett, R. T. (2011). Impacts of warming on tropical lowland rainforests. *Trends Ecol. E*26, 606–613. doi: 10.1016/j.tree.2011.06.015

De Bello, F., Price, J. N., Münkemüller, T., Liira, J., Zobel, M., Thuiller, W., et al. (2012). Functional species pool framework to test for biotic effects on community assembly. *Ecology* 93, 2263–2273. doi: 10.1890/11-1394.1

Ferris, H., Bongers, T., and de Goede, R. G. M. (2001). A framework for soil food web diagnostics: extension of the nematode faunal analysis concept. *Appl. Soil Ecol.* 18, 13–29. doi: 10.1016/S0929-1393(01)00152-4

Gotelli, N. J., and McCabe, D. J. (2002). Species co-occurrence: a meta-analysis of JM Diamond's assembly rules model. *Ecology* 83, 2091–2096. doi: 10.1890/0012-9658(2002)083[2091:SCOAMA]2.0.CO;2

Götzenberger, L., de Bello, F., Bråthen, K. A., Davison, J., Dubuis, A., Guisan, A., et al. (2012). Ecological assembly rules in plant communities-approaches, patterns, and prospects. *Biol. Rev.* 87, 111–127. doi: 10.1111/j.1469-185X.2011.00187.x

Guo, J., Shang, S., and Zeng, J. (2018). Morphometric study confirms the presence of only Vatica mangachapoi on Hainan Island, China. *J. For. Res.* 29, 639–646. doi: 10.1007/s11676-017-0458-8

Hubbell, S. P. (2001). *The Unified Neutral Theory of Biodiversity and Biogeography*. Princeton: Princeton University Press.

Jiao, S., Zhang, B., Zhang, G., Chen, W., and Wei, G. (2021). Stochastic community assembly decreases soil fungal richness in arid ecosystems. *Mol. Ecol.* 30, 4338–4348. doi: 10.1111/mec.16047

Kembel, S. W., Cowan, P. D., Helmus, M. R., Cornwell, W. K., Morlon, H., Ackerly, D. D., et al. (2010). Picante: R tools for integrating phylogenies and ecology. *Bioinformatics* 26, 1463–1464. doi: 10.1093/bioinformatics/btq166

Kraft, N. J. B., and Ackerly, D. D. (2010). Functional trait and phylogenetic tests of community assembly across spatial scales in an Amazonian forest. *Ecol. Monogr.* 80, 401–422. doi: 10.1890/09-1672.1

Kraft, N. J. B., Valencia, R., and Ackerly, D. D. (2008). Functional traits and niche-based tree community assembly in an amazonian forest. *Science* 322, 580–582. doi: 10.1126/science.1160662

Legendre, P., and Legendre, L. (2012). *Numerical Ecology*. Amsterdam: Elsevier Press.

Legendre, P., Mi, X., Ren, H., Ma, K., Yu, M., Sun, I-. F., et al. (2009). Partitioning beta diversity in a subtropical broad-leaved forest of China. *Ecology* 90, 663–674. doi: 10.1890/07-1880.1

Liu, T., Guo, R., Ran, W., Whalen, J. K., and Li, H. (2015). Body size is a sensitive trait-based indicator of soil nematode community response to fertilization in rice and wheat agroecosystems. *Soil Biol. Biochem.* 88, 275–281. doi: 10.1016/j.soilbio.2015.05.027

Luan, L., Jiang, Y., Cheng, M., Dini-Andreote, F., Sui, Y., Xu, Q., et al. (2020). Organism body size structures the soil microbial and nematode community assembly at a continental and global scale. *Nat. Commun.* 11, 1–11. doi: 10.1038/s41467-020-20271-4

Moroenyane, I., Dong, K., Singh, D., Chimphango, S. B. M., and Adams, J. M. (2016). Deterministic processes dominate nematode community structure in

the Fynbos Mediterranean heathland of South Africa. *Evol. Ecol.* 30, 685–701. doi: 10.1007/s10682-016-9837-4

Myers, J. A., Chase, J. M., Jiménez, I., Jørgensen, P. M., Araujo-Murakami, A., Paniagua-Zambrana, N., et al. (2013). Beta-diversity in temperate and tropical forests reflects dissimilar mechanisms of community assembly. *Ecol. Lett.* 16, 151–157. doi: 10.1111/ele.12021

Neher, D. A. (2010). Ecology of Plant and Free-Living Nematodes in Natural and Agricultural Soil. *Annu. Rev. Phytopathol.* 48, 371–394. doi: 10.1146/annurev-phyto-073009-114439

Ni, Y., Yang, T., Ma, Y., Zhang, K., Soltis, P. S., Soltis, D. E., et al. (2021). Soil pH determines bacterial distribution and assembly processes in natural mountain forests of eastern China. *Glob. Ecol. Biogeogr.* 30, 2164–2177. doi: 10.1111/geb.13373

Oksanen, J., Blanchet, F. G., Kindt, R., Legendre, P., Minchin, P. R., O'Hara, R. B., et al. (2016). *Vegan: Community Ecology Package. R Package Version 2.4-0*. Available online at: https://CRAN.R-project.org/package=vegan (accessed August 15, 2022.).

Pausch, J., Hofmann, S., Scharroba, A., Kuzyakov, Y., and Ruess, L. (2016). Fluxes of root-derived carbon into the nematode micro-food web of an arable soil. *Food Webs* 9, 32–38. doi: 10.1016/j.fooweb.2016.05.001

Ruess, L. (2003). Nematode soil faunal analysis of decomposition pathways in different ecosystems. *Nematology* 5, 179–181. doi: 10.1163/156854103767139662

Siefert, A., Ravenscroft, C., Weiser, M. D., and Swenson, N. G. (2013). Functional beta diversity patterns reveal deterministic community assembly processes in eastern North American trees. *Glob. Ecol. Biogeogr.* 22, 682–691. doi: 10.1111/geb.12030

Stephane, D. (2013). *SpacemakeR: Spatial Modelling. R package version 0.0-5/r113*. Available online at: https://r-forge.r-project.org/projects/sedar/ (accessed August 10, 2022.).

Tripathi, B. M., Stegen, J. C., Kim, M., Dong, K., Adams, J. M., Lee, Y. K., et al. (2018). Soil pH mediates the balance between stochastic and deterministic assembly of bacteria. *ISME J.* 12, 1072–1083. doi: 10.1038/s41396-018-0082-4

Trisos, C. H., Petchey, O. L., and Tobias, J. A. (2014). Unraveling the interplay of community assembly processes acting on multiple niche axes across spatial scales. *Am. Nat.* 184, 593–608. doi: 10.1086/678233

van den Hoogen, J., Geisen, S., Routh, D., Ferris, H., Traunspurger, W., Wardle, D. A., et al. (2019). Soil nematode abundance and functional group composition at a global scale. *Nature* 572, 194–198. doi: 10.1038/s41586-019-1418-6

Viketoft, M., Sohlenius, B., Boström, S., Palmborg, C., Bengtsson, J., Berg, M. P., et al. (2011). Temporal dynamics of soil nematode communities in a grassland plant diversity experiment. *Soil Biol. Biochem.* 43, 1063–1070. doi: 10.1016/j.soilbio.2011.01.027

Wang, W., Sun, Z., Mishra, S., Xia, S., Lin, L., Yang, X., et al. (2022). Body size determines multitrophic soil microbiota community assembly associated with soil and plant attributes in a tropical seasonal rainforest. *Mol. Ecol.* 1, 1–10. doi: 10.1111/mec.16585

Wang, X., Nielsen, U. N., Yang, X., Zhang, L., Zhou, X., Du, G., et al. (2018). Grazing induces direct and indirect shrub effects on soil nematode communities. *Soil Biol. Biochem.* 121, 193–201. doi: 10.1016/j.soilbio.2018.03.007

Weiher, E., Freund, D., Bunton, T., Stefanski, A., Lee, T., Bentivenga, S., et al. (2011). Advances, challenges and a developing synthesis of ecological community assembly theory. *Philos. Trans. R. Soc. B Biol. Sci.* 366, 2403–2413. doi: 10.1098/rstb.2011.0056

Yeates, G. W., Bongers, T., De Goede, R. G., Freckman, D. W., and Georgieva, S. S. (1993). Feeding habits in soil nematode families and genera-an outline for soil ecologists. *J. Nematol.* 25, 315–331.

Zhang, H., Chen, H. Y. H., Lian, J., John, R., Ronghua, L., Liu, H., et al. (2018). Using functional trait diversity patterns to disentangle the scale-dependent ecological processes in a subtropical forest. *Funct. Ecol.* 32, 1379–1389. doi: 10.1111/1365-2435.13079

Zhang, H., Qi, W., John, R., Wang, W., Song, F., Zhou, S., et al. (2015). Using functional trait diversity to evaluate the contribution of multiple ecological processes to community assembly during succession. *Ecography* 38, 1176–1186. doi: 10.1111/ecog.01123

Zhang, W., Zhang, H., Jian, S., and Liu, N. (2019). Tree plantations influence the abundance of ammonia-oxidizing bacteria in the soils of a coral island. *Appl. Soil Ecol.* 138, 220–222. doi: 10.1016/j.apsoil.2019.02.014

Zou, S., Adams, J., Yu, Z., Li, N., Kerfahi, D., Tripathi, B., et al. (2022). Stochasticity dominates assembly processes of soil nematode metacommunities on three Asian mountains. *Pedosphere*, in press. doi: 10.1016/j.pedsph.2022.06.059

frontiers | Frontiers in Ecology and Evolution

TYPE Original Research
PUBLISHED 19 December 2022
DOI 10.3389/fevo.2022.1095946

OPEN ACCESS

EDITED BY
Xiang Liu,
Lanzhou University,
China

REVIEWED BY
Mu Liu,
Lanzhou University,
China
Yunquan Wang,
Zhejiang Normal University,
China
Chen Zhu,
Nanjing Agricultural University,
China

*CORRESPONDENCE
Weihua Li
whli@scnu.edu.cn

†These authors have contributed equally to this work and share first authorship

SPECIALTY SECTION
This article was submitted to Conservation and Restoration Ecology, a section of the journal Frontiers in Ecology and Evolution

RECEIVED 11 November 2022
ACCEPTED 30 November 2022
PUBLISHED 19 December 2022

CITATION
Jia P, Wang J, Liang H, Wu Z-h, Li F and Li W (2022) Replacement control of *Mikania micrantha* in orchards and its eco-physiological mechanism. *Front. Ecol. Evol.* 10:1095946. doi: 10.3389/fevo.2022.1095946

Replacement control of *Mikania micrantha* in orchards and its eco-physiological mechanism

Pu Jia†, Jiayi Wang†, Haolin Liang, Zhuo-hui Wu, Fenglin Li and Weihua Li*

Guangzhou Key Laboratory of Subtropical Biodiversity and Biomonitoring, Guangdong Provincial Key Laboratory of Biotechnology for Plant Development, School of Life Sciences, South China Normal University, Guangzhou, China

Mikania micrantha is one of the most notorious invasive weeds in south China, especially in orchard habitats. Based on the principle of niche competition, screening plants with strong competitiveness and managing vacant niches through natural alternative methods (replacement control) were expected to achieve sustainable ecological management of invasive species. To this end, two legumes, *Desmodium heterocarpon* and *Senna tora*, were selected to conduct field competition experiments with *M. micrantha* to investigate the interspecific competitiveness of these two legumes and *M. micrantha* from the aspects of adaptability to low light and response to drought stress. We found that the relative interaction indexes of *D. heterocarpon* and *S. tora* to *M. micrantha* were both negative and the competitive inhibition of *S. tora* on *M. micrantha* was higher than that of *D. heterocarpon*. Compared with *M. micrantha*, *D. heterocarpon* and *S. tora* have higher photosynthetic efficiency and lower dark respiration efficiency under low-light conditions, thus maintaining positive plant carbon balance capacity in the low-light understory and becoming more shade-tolerant. Besides, the water stress experiment found that *M. micrantha* had the lowest tolerance to drought stress, followed by *S. tora*, and *D. heterocarpon* was the most drought tolerant. These results showed that *D. heterocarpon* and *S. tora* can effectively prevent and control *M. micrantha*, mainly due to their higher competitiveness, shade tolerance, and drought tolerance. The control effect of *D. heterocarpon* is better than that of *S. tora* which is an alien species. Therefore, we believed that the replacement control of the invasive weed *M. micrantha* by *D. heterocarpon* is expected to be a sustainable ecological management strategy for *M. micrantha* biocontrol in the dryland orchard habitat. These findings provide a theoretical basis for the selection of species for alternative control in the future and provide new ideas for solving the problem of repeated regeneration in the existing *M. micrantha* control process.

KEYWORDS

plant invasion, *Mikania micrantha*, *Desmodium heterocarpon*, replacement control, resource competition

1. Introduction

Due to the rapid development of economic globalization and international transportation, more and more species have been introduced, intentionally or unintentionally, into new environments previously isolated by natural barriers (Chen et al., 2016; Courchamp et al., 2017). These alien species are often highly adaptable and able to survive, reproduce, and spread in new environments, resulting in severe alien species invasions (Theoharides and Dukes, 2007). Biological invasions pose an enormous threat to ecosystems and public health by replacing native species, reducing biodiversity, altering community structure, and impairing ecosystem function (Slingenberg et al., 2009), resulting in huge economic losses (Pimentel et al., 2001). Therefore, how to effectively control invasive alien species, especially the control of alien weeds, is a hot spot in the field of invasive ecology research.

Mikania micrantha (mile-a-minute weed) is native to tropical regions of Central and South America and the Caribbean and is a fast-growing perennial vine belonging to the *Asteraceae* family (Choudhury et al., 2016). Due to natural and anthropogenic factors, *M. micrantha* is widely distributed in tropical and subtropical regions of Asia and the Pacific, and is one of the 100 worst invasive alien species announced by the International Union for Conservation of Nature (IUCN; Day et al., 2016). *M. micrantha* germinates early in the growing season, has a fast growth rate (up to 20 cm per day), and can reproduce vegetatively by forming roots and branches at each node, resulting in new individuals (Kaur et al., 2012). Therefore, if not controlled, it may rapidly spread to new habitats, covering the forest or plantation canopy (Day et al., 2012), causing the covered plants to suffocate and die due to lack of sunlight, so *M. micrantha* is also known as "plant killer" (Zhang et al., 2004). The rapid spread of *M. micrantha* not only destabilized the ecosystems in which it invaded, but also caused great economic losses (Day et al., 2016). For example, due to the invasion of *M. micrantha* every year in Neilingding Island in Shenzhen, China, the average annual economic loss amounts to CNY 4.5–10.13 million for the whole island (Zhong et al., 2004). Most notably, *M. micrantha* is responsible for the reduction of the production in many orchards by climbing up the orchard canopy and blocking the sunlight (Macanawai et al., 2012; Shen et al., 2015). It is thus essential to seek an effective method for controlling *M. micrantha* in orchards.

The serious invasion of *M. micrantha* in tropical and subtropical regions has attracted more and more attention around the world. In order to remove *M. micrantha* from the invasion area, different control methods have been developed, mainly divided into physical control, chemical control, and biological control (Li M. et al., 2012, 2015). Physical control, usually harvesting the above-ground part of the *M. micrantha*, can only control the invasion in a short term and does not completely eradicate *M. micrantha*, but may increase the potential threat of further spread (Swamy and Ramakrishnan, 1987). Herbicide is the main method of chemical control to remove *M. micrantha*. However, it can lead to drug resistance and chemical contamination of the local environment (Islam et al., 2018; Mohanty and Jena, 2019). At present, the most successful method for *M. micrantha* is biological control. It has been found that the rust fungus *Puccinia spegazzinii* and the butterfly *Actinote anteas* (natural enemy insect of *M. micrantha*) have good pathogenicity and encroach on *M. micrantha*, and can control *M. micrantha* to a certain extent (Barreto and Evans, 1995; Li et al., 2004; Day et al., 2013). Previous studies found that the parasitic field dodder *Cuscuta campestris* parasitized *M. micrantha*, which could cause *M. micrantha* to die (Li F. L. et al., 2012). However, due to the safety and limitations of biological control, there is no precedent for biological control of *M. micrantha* in orchards. The growth of fruit trees and the formation of orchard habitats have their unique characteristics. With the fruit trees bearing from young age to mature, the stand space appeared obvious differentiation, which was manifested as distinct differences in plant composition, spatial distance, and microclimate between canopy and understory. However, the long-term periodic reclamation and weeding operations of understory make understory vegetation dwarf, sparse, or even lose, and the ecological niche is finally vacant, resulting in ecosystem loopholes, which leads to the invasion of notorious weeds led by *M. micrantha*. If we choose native or valuable species with high competitiveness to cover the orchard ground based on replacement control technology, the growth of *M. micrantha* could be suppressed or its establishment can be prevented.

The current control methods for *M. micrantha* cannot solve the problem of regeneration and proliferation of *M. micrantha*, the main reason is that the management of the vacant ecological niche after the control is neglected. If we can use the principle of niche competition, select plants with strong competitiveness, and fill vacant niches progressively through natural succession, it will be possible to achieve ecological sustainability in the management of invasive species, which can be regarded as replacement control (Piemeisel and Carsner, 1951; Piemeisel, 1954; Li et al., 2015; Shen et al., 2015, 2016). Compared with chemical or mechanical control methods, replacement control is generally considered more economical, safe, eco-friendly, and sustainable. Regarding the replacement control of *M. micrantha*, the reported replacement plants are mainly herbs, shrubs, and fast-growing trees, such as grass species tall fescue *Festuca arundinacea* (Xu et al., 2011), *Mosla chinensis* (Song et al., 2020), perennial Italian ryegrass *Lolium multiflorum* (Xu et al., 2011), annual wormwood *Artemisia annua* (Xu et al., 2011) and sweet potato *Ipomoea batatas* (Shen et al., 2016), leguminous shrub *Stylosanthes guianensis* (Song et al., 2020), southeast Asian pioneer tree *Macaranga tanarius* (Li M. et al., 2012), and kesseru plant *Heteropanax fragrans* (Li M. et al., 2012), etc. Among them, the replacement effect of sweet potato was better, and field experiments have been done. The results showed that when sweet potato was mixed with *M. micrantha*, it can accumulate more biomass and absorb more soil nutrients, so it has a stronger competitive advantage (Shen et al., 2015), and can inhibit the reproductive ability of *M. micrantha* (Shen et al., 2016). However,

the reported replacement plants and *M. micrantha* belong to different life forms and occupy different ecological niches. Although sweet potatoes can disperse by crawling, they cannot climb upward. According to the limiting similarity theory, species with similar niches tend to be more competitive, so whether they have a similar niche to invasive species is an important determinant for replacement plants to resist invasive species (Price and Partel, 2013; Kimball et al., 2014). Different species with the same ecological niche strive to suppress each other in order to compete for limited resources and space, which directly leads to interspecific competition (MacArthur and Levins, 1964). Replacement control research has recently focused on screening valuable or native species for competitiveness, mechanisms of competition, and native ecosystem restoration effects. Therefore, screening native species in similar ecological niches to control invasive species is beneficial to the sustainable ecological management of invasive species.

The principle of replacement control is to use the mutual competition between plant species to control harmful weeds, especially invasive weeds, with one or more plants with competitive advantage. Plant competition plays an important role in shaping individual plant morphology, physiology, and life history and in determining plant community structure and succession (Grace, 2012), thus plant competition is one of the areas that ecologists focus on. The maximum growth rate theory proposed by Grime (1979) and the minimum resource requirement theory by Tilman (1980) are two classic competition theories. Grime's theory is based on the life strategies and traits of plants, and believes that the species with the greatest resource capture potential will be the competition winner (Grime, 1977, 1979). Tilman's theory proposes a numerical model of plant individual populations with resource capture rates as a function of plant traits, which believes that the species with the smallest resource requirements will be the winner of the competition (Tilman, 1988). In recent years, many studies have carried out researches on the competition between indigenous plants and forages and invasive alien plants, and found that some indigenous plants and forages have a strong competitive effect on invasive alien plants, which can better control the growth, development, and spread of alien plants (Scasta et al., 2015). Our preliminary work found that using native legumes can be a better option for the replacement control of invasive weeds (Li et al., 2015). Therefore, in order to elucidate which theory can explain such phenomenon, we selected a variety of plants for trial to screen replacement plants in the orchard, and finally screened out two forage legumes with the potential to control *M. micrantha*, and explored the ecological processes and mechanisms of replacement control of *M. micrantha* under low-light and drought-stressed treatments in two legumes to provide a theoretical basis for the selection of replacement species in the future. The results obtained in this study are of great significance for ensuring ecological security and promoting sustainable prevention and control of invasive species and ecological restoration.

2. Materials and methods

2.1. Screening of replacement plants in the field

We selected an orchard with severe invasion of *M. micrantha* to carry out the replacement control experiment of *M. micrantha*. The orchard was located at Huaguo village in the northeast of Xinxu Town, Huiyang District, Huizhou City, Guangdong Province (22°52′24″N, 114°21′21″E, at the altitude of 93 meters), with a total area of 24 square kilometers and a subtropical monsoon climate. The village has sufficient water resources, and the fruit trees mainly include bananas and wampees. Due to its proximity to Shenzhen, most of the orchards in the village were invaded by *M. micrantha*. In June 2016, clean tillage was carried out in an orchard of Huaguo Village with mowing of natural weed flora in case of weeds emerged. We also applied herbicide with a hand pump sprayer backpack to make the plot weed-free. After the clean tillage was completed, we established 16 plots, including 3 plots of *Desmodium heterocarpon* monoculture, 3 plots of *Senna tora* monoculture, 4 plots of *Spermacoce latifolia* monoculture, 3 plots of *Ageratum conyzoides* monoculture, and 3 plots of *M. micrantha* monoculture. Each plot was 3 m × 3 m. After the experimental plot was constructed, photographs were taken once a month to record the control effects of the four test plants on *M. micrantha*.

2.2. Interspecific competition experiment in the field

The experimental materials were *D. heterocarpon*, *S. tora,* and *M. micrantha*, and the seeds were collected from the replacement control experimental site in Huaguo village, Huizhou city from November to December 2016. The experimental design was as follows: *M. micrantha*, *D. heterocarpon*, and *S. tora* were planted individually; *D. heterocarpon* and *S. tora* were planted with *M. micrantha* together with a ratio of 1:1, respectively. There were five treatments in total, and each plot was 1.5 m × 1.5 m. Three months after transplanting, the coverage and plant height of *D. heterocarpon*, *S. tora* and *M. micrantha* was measured. The number of leaves per plant was counted, and the area of leaves with medium size was measured with a leaf planimeter (LI-3100, LI-COR, USA). At the end of the experiment, the medium-sized plants in each treatment were harvested. The shoots and roots were separated from each plant and dried to constant weight for at least 72 h at 60°C and then weighed to get the total biomass of shoots and roots.

Relative interaction index (RII) was calculated as: RII = (*Bw*-*Bo*)/(*Bw* + *Bo*), where *Bw* was the observed biomass of the target plant when growing with other species and *Bo* was the biomass of the target plant when growing individually. A negative value indicates that other species compete with the target plant and

therefore inhibit the growth of target plants. A positive value indicates that other species promote the growth of the target plant.

2.3. Low-light treatment of *Desmodium heterocarpon*, *Senna tora*, and *Mikania micrantha*

2.3.1. Plant materials and seedling cultivation

The seeds of *M. micrantha*, *D. heterocarpon*, and *S. tora* were collected from the replacement control experimental field and germinated in Petri dishes. After germination, the seedlings were transferred to a float tray with nutrition soil and we watered them to keep the soil moist. After about 30 days of growth, healthy seedlings were selected and transplanted into a pot (plastic flowerpot 13 cm in diameter and 12 cm in height filled with mixed soil up to 2/3 of the height of the pot to ensure that the soil weight of each pot was basically the same) in the greenhouse on the top floor of the School of Life Science, South China Normal University. The mixed soil is composed of garden soil, which was collected from the topsoil of the Botanical Garden of South China Normal University, and nutrition soil in a ratio of 1:1.

2.3.2. Low-light treatment establishment

Three light conditions (light 100%, light 42%, and light 17%) were established. After 2 weeks of adaptive cultivation, the transplanted seedlings were shaded under three light conditions. There were 8 replicates per treatment for *M. micrantha*, *D. heterocarpon*, and *S. tora* (72 pots in total). All pots were positioned randomly and the experiment lasted for 60 days. At the end of the experiment, the plants in each treatment were harvested. The above-ground and below-ground parts were separated from each plant and dried to a constant weight for at least 72 h at 60°C and then weighed. The total biomass was the sum of above-ground and below-ground parts.

2.3.3. Measurements of chlorophyll fluorescence parameters

Chlorophyll fluorescence parameters were determined on a sunny day with a portable PAM-2100 fluorometer (Waltz, Germany) once a week. All fluorescence measurements were started after an additional 20 min dark adaptation. Minimal fluorescence (F_0) and maximal fluorescence (F_m) were recorded and the maximal photochemical efficiency (F_v/F_m) is calculated as: $F_v/F_m = (F_m\text{-}F_0)/F_m$. After the plant leaves were adapted to the light intensity of 200 mol m^{-2} s^{-1}, steady-state fluorescence yield (F_s), maximal fluorescence yield ($F_{m'}$), electron transfer rate (ETR), and quantum yield of photosystem II (Yield) were recorded once per week.

2.3.4. Measurements of the light response curve

The light response curve was determined on a clear sunny day with a Li-6,400 portable photosynthesis analyzer (LiCor Inc., United States). The measurement time was 9:00–11:00 a.m. and 3:00–5:00 p.m. The chamber flow rate was adjusted to 500 μmol s^{-1}. Before measuring the curve, the light intensity of 1,600 μmol m^{-2} s^{-1} was set to induce the leaves to reach a stable state. The light intensity gradient was set to 1,600, 1,400, 1,200, 1,000, 800, 600, 400, 200, 100, 40, 20, and 0 μmol m^{-2} s^{-1}. After reaching the maximum stabilization time, we recorded the parameters of the instrument at each light intensity and measured continuously for 2 days until all data were obtained. Next, we took the light intensity as the x-axis and the net photosynthetic rate as the y-axis to draw a scatter plot of the light response curve. According to the method of Feng et al. (2004), we fitted the light response curve equation to calculate the maximum net photosynthetic rate (P_{max}), light compensation point (LCP), light saturation point (LSP), dark respiration rate (Rd), and apparent quantum yield (AQY). AQY was represented by the initial slope of the light response curve when the light intensity was less than 200 mol m^{-2} s^{-1} and was fitted by the standard form of linear regression.

2.4. Drought-stressed treatment of *Desmodium heterocarpon*, *Senna tora*, and *Mikania micrantha*

After 1 week of adaptive cultivation of the seedlings, drought stress experiment was carried out. All experimental groups were subjected to drought treatment after fully absorbing water. The method of drought stress was carried out by natural drought without water. The control group was normally watered. The experimental group was treated with drought stress for 10 days and rehydrated for 3 days from the 11th day. There were 12 replicates per treatment for *M. micrantha*, *D. heterocarpon*, and *S. tora* (108 pots in total). All pots were placed randomly. At the end of the experiment, the plants in each treatment were harvested. The above-ground and below-ground parts were separated from each plant and dried to a constant weight for at least 72 h at 60°C and then weighed. The total biomass was the sum of above-ground and below-ground parts.

2.4.1. Measurements of gas exchange parameters in the drought stress experiment

Gas exchange parameters were determined using the Li-6,400 portable photosynthesis analyzer (LiCor Inc., United States) at 9:00 a.m. and were completed within 2 h on a sunny day. The photosynthetic photon flux density (PPFD) of the natural light was set to 1,000 μmol m^{-2} s^{-1} under daily ambient temperatures varied from 28 to 30°C. CO_2 concentration inside the leaf chamber was maintained at 380 cm^3 m^{-3} through the CO_2-controlling system of the Li-6,400 attached to a portable CO_2 cylinder. The PPFD of 1,000 μmol m^{-2} s^{-1} on the cuvette surface was provided by an

LED source. Before taking measurements, the leaves were equilibrated under artificial light conditions in the leaf chamber for at least 10 min. Net photosynthetic rate (Pn), intercellular CO_2 concentration (Ci), stomatal conductance (Gs), and transpiration rate (Tr) were recorded.

2.4.2. Measurements of proline content in the drought stress experiment

Proline was extracted by sulfosalicylic acid and the proline content was determined by ninhydrin colorimetry. 0.1 g fresh weight leaves of each plant in the control group (well-watered treatment) and the experiment group on the 10th day of drought treatment and the 3rd day of rehydration were placed in a centrifuge tube, respectively. 2.5 ml 3% sulfosalicylic acid solution was added to each tube and then all tubes were treated in the boiling water bath for 10 min. After filtering and cooling, 1 ml filtrate was absorbed into another centrifuge tube and then 1 ml glacial acetic acid and 1 ml 2.5% acid ninhydrin reagent were added. The mixture was heated in the boiling water bath for 30 min and turned red. After the mixture was cooled, 2 ml toluene was added. After 30 s of oscillation, the supernatant was transferred into a 10 ml centrifuge tube and centrifuged at 3000 rpm for 5 min. The red proline toluene supernatant was absorbed into a colorimetric cup. The toluene solution was used as blank control and the absorbance value was determined at A_{520}. The standard curve of proline was prepared and the content of proline was calculated according to the regression equation of the standard curve.

2.4.3. Measurements of soluble sugar content in the drought stress experiment

The soluble sugar content was determined by thiobarbituric acid method. 0.1 g plant leaves were placed in a pre-cooled mortar and 1 ml pre-cooled 10% acetic acid (TCA) was added. After the leaves were grounded on ice homogeneously, the homogenate was transferred to the centrifuge tube, and then the mortar was washed with 1 ml 10% TCA. The washing liquid was also transferred to the centrifuge tube and centrifuged at the speed of 4,000 rpm for 10 min. 1 ml supernatant (1 ml sterile water in blank control) and 1 ml 0.6% thiobarbituric acid solution (TBA) were added into a new centrifuge tube and thoroughly mixed. The mixture was heated in a boiling water bath for 15 min and centrifuged at the speed of 4,000 rpm for 10 min after cooling down at room temperature. The supernatant of the mixture was taken to determine the absorbance value at A_{450}.

2.5. Statistics analysis

We used one-way ANOVA analysis and Duncan's test ($p < 0.05$) to test for differences between treatments using SPSS 18.0 (SPSS Inc., United States). SigmaPlot 12.0 and Origin 8.5 software were used for data visualization.

3. Results

3.1. The preliminary selection of replacement plants in the field

One month after clean tillage (Figure 1A), the seedlings of *S. tora* successfully established with a survival rate of over 95% (Figure 1B). The seedlings of *D. heterocarpon* successfully established with a survival rate of over 90% (Figure 1C). A large number of *S. latifolia* and a few *M. micrantha* individuals regenerated in the quadrats gap (Figure 1D). A few seedlings of *A. conyzoides* but a large number of *M. micrantha* individuals regenerated in the quadrats (Figure 1E). Four months after clean tillage (Figure 1G), *S. tora* entered into reproductive growth, some of the leaves aged and turned yellow, and lots of pods grew. Few *M. micrantha* was found in the plot, but weeds appeared in the lower layer (Figure 1H). *D. heterocarpon* also entered into reproductive growth, bearing a lot of pods, but the leaves remain green, with a small amount of *M. micrantha* (Figure 1I). When *S. latifolia* entered the aging stage, its stem lodging occurred and leaves withered and turned yellow, and a large amount of *M. micrantha* occupied the quadrats (Figure 1J). *A. conyzoides* entered the aging stage, while *M. micrantha* grew vigorously, occupying most of the quadrats (Figure 1K). Therefore, we did not involve *S. latifolia* and *A. conyzoides* in the following experiments. We observed that compared with the natural growth of *M. micrantha* (Figure 1F, L), *D. heterocarpon* and S. tora had obvious replacement control effect on *M. micrantha*, which can inhibit the growth and regeneration of *M. micrantha* in the orchards. Next, we used these two plants as replacement plants to study the interspecific competition effects between two legumes and *M. micrantha* in the field.

3.2. Interspecific competition between two legumes and *Mikania micrantha* in the field

When *M. micrantha* was planted with *S. tora* or *D. heterocarpon*, its coverage was significantly decreased compared with that of *M. micrantha* monoculture, which was 77% or 73.9%, respectively. Compared to *D. heterocarpon* monoculture, the coverage of *D. heterocarpon* decreased significantly by 17.3% when it was planted with *M. micrantha*, while the coverage of *S. tora* was not significantly different between monoculture and polyculture with *M. micrantha* (Figure 2A). Due to the competition of *S. tora* and *D. heterocarpon*, the leaf area of *M. micrantha* per plant decreased significantly by 30.9 and 36.3%, respectively. On the contrary, the leaf area of *S. tora* and *D. heterocarpon* per plant increased significantly by 7.1 and 25%, respectively, when they were planted with *M. micrantha*, compared to the monoculture (Figure 2B). The total biomass of *M. micrantha* decreased by 23.5 and 58.3%, respectively, when *M. micrantha* was planted with *S. tora* and *D. heterocarpon*, compared to the monoculture. There was no significant difference between the total biomass of *D. heterocarpon* when it was planted with *M. micrantha*

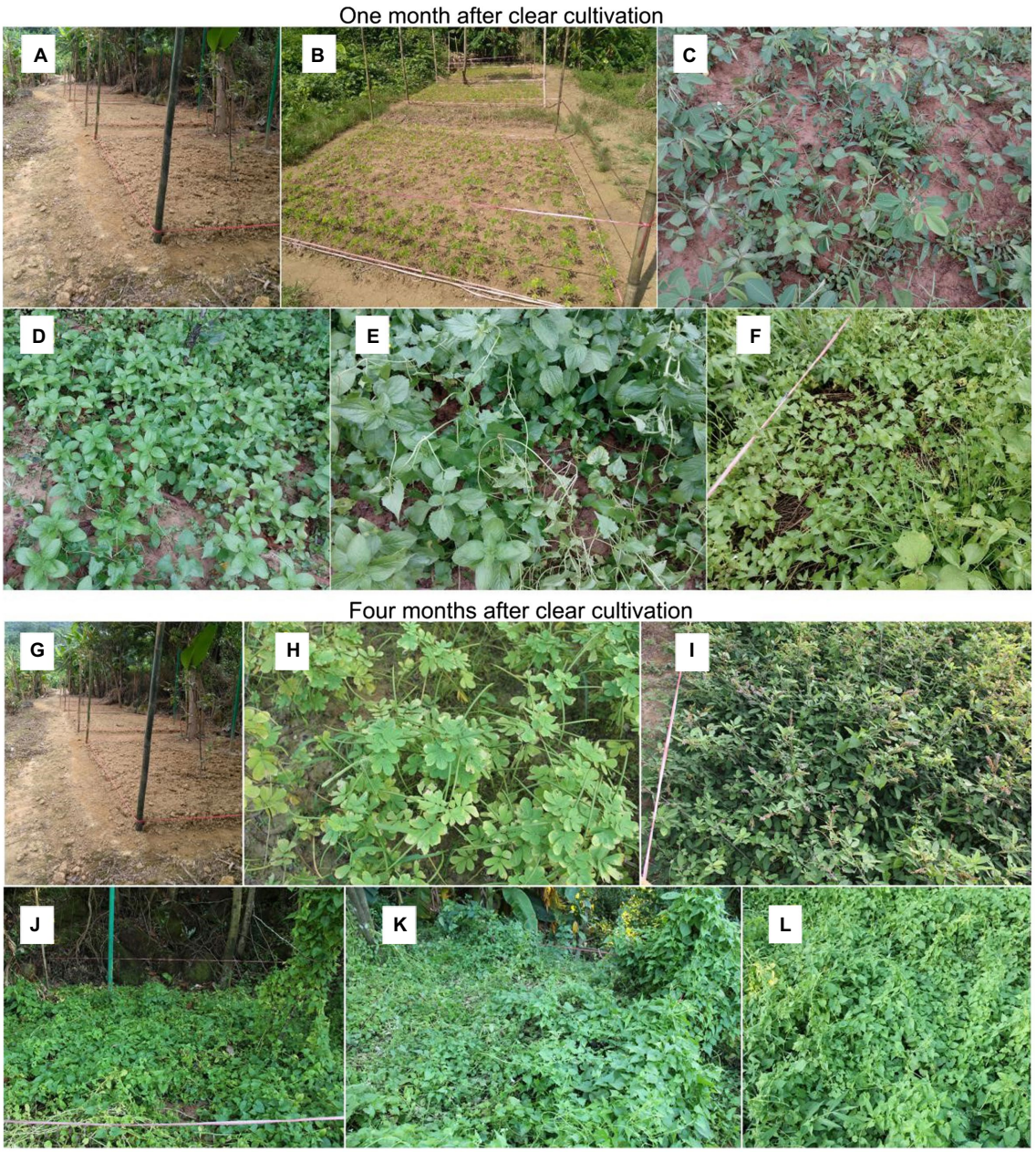

FIGURE 1
Growth status of four replacement plants after one and four months of clean tillage, respectively. **(A, G)** The original status after clean tillage; **(B, H)** *S. tora*; **(C, I)** *D. heterocarpon*; **(D, J)** *S. latifolia*; **(E, K)** *A. conyzoides*; **(F, L)** *M. micrantha* naturally regenerated as the control.

and the monoculture, so as *S. tora* (Figure 2C). The RII can indicate the interaction between plants. A negative value indicates competition and a positive value indicates facilitation. The RII of *M. micrantha* in the presence of *D. heterocarpon* and *S. tora* were both negative ($RII_{Mm(Dh)} = -0.42$, $RII_{Mm(St)} = -0.13$, respectively), indicating that two replacement species competed well with *M. micrantha*, and that the strength of the negative effect of *D. heterocarpon* on *M. micrantha* was larger than that of *S. tora* on *M. micrantha* (Figure 2D). On the other hand, the effect of *M. micrantha* on *D. heterocarpon* was negative [$RII_{Dh(Mm)} = -0.03$], close to zero, while the effect of *M. micrantha* on *S. tora* was positive [$RII_{St(Mm)} = 0.12$, Figure 2D], indicating that *M. micrantha* could promote the growth of *S. tora*.

3.3. The adaptability of two replacement forage legumes and *Mikania micrantha* to low-light stress

Under light 100%, *M. micrantha* had more branches and leaves, but the leaves turned yellow. As the light intensity

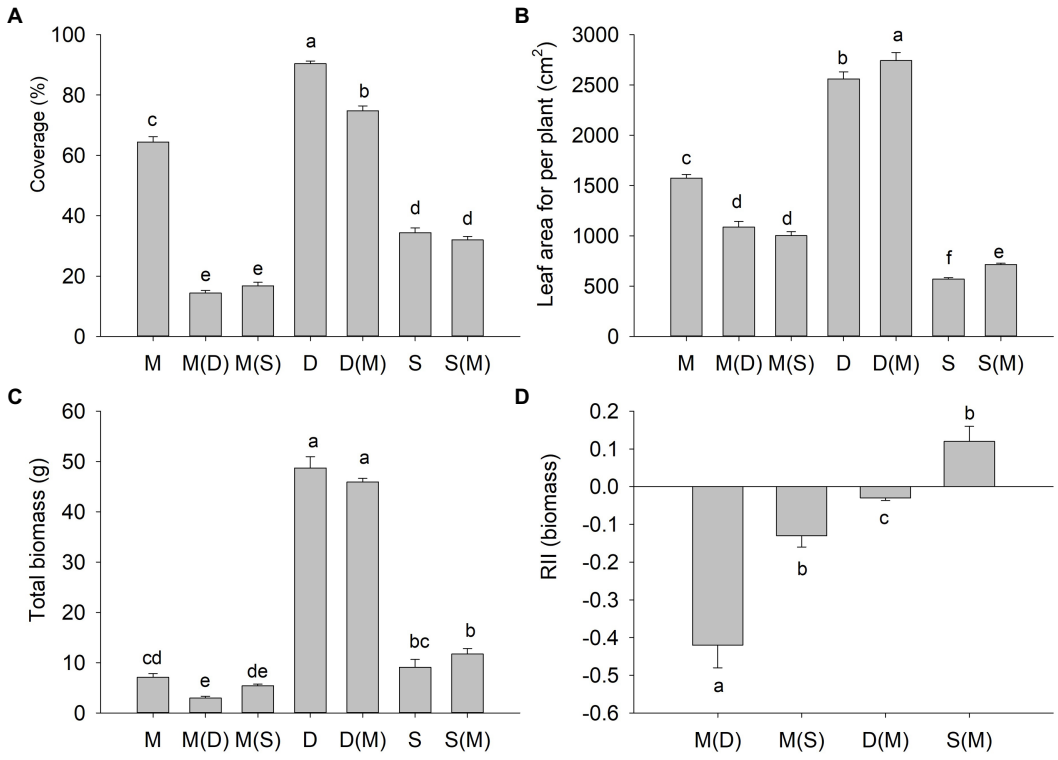

FIGURE 2
Changes of the plant coverage **(A)**, leaf area **(B)**, total biomass **(C)**, and relative interaction index **(D)** *of M. micrantha* and the replacement plants under different interspecific competition experiments (average±SE, n=4). M(D): *M. micrantha* when grown under competition with *D. heterocarpon*; M(S): *M. micrantha* when grown under competition with *S. tora*; D(M): *D. heterocarpon* when grown under competition with *M. micrantha*; S(M): *S. tora* when grown under competition with *M. micrantha*. Different letters above bar plots indicate significant differences (Duncan test, p<0.05).

decreased, the number of branches and leaves of *M. micrantha* decreased significantly and the greenness of the leaves deepened. *M. micrantha* was the smallest and grew the worst under light 17% (Figure 3A). Under light 100% and light 42%, *D. heterocarpon* had more branches and leaves. The number of branches and leaves decreased under light 17%. As the light intensity decreased, the greenness of *D. heterocarpon* leaves deepened (Figure 3B). Under light 100%, *S. tora* grew low and stout with yellowish leaves and branches; with the decrease in light intensity, the plants became thinner and taller, and the greenness of leaves deepened. *S. tora* was the highest under light 42% (Figure 3C).

From the perspective of root phenotype changes, *M. micrantha* had the most developed roots and the largest number of roots under light 100%. With the decrease in light intensity, the number of roots decreased significantly. Under light 17%, the growth of roots was greatly affected and the number of roots was the least (Figure 3D). Under light 100%, the roots of *D. heterocarpon* were the most developed. With the decrease in light intensity, the number of roots gradually decreased, and the number of roots was the least under light 17% (Figure 3E). Under light 100%, the number of *S. tora* roots was the largest, and with the decrease in light intensity, the number of roots decreased dramatically. Under light 17%, the growth of *S. tora* roots was greatly inhibited and the number was the least (Figure 3F).

Compared with light 100%, the above-ground biomass of *M. micrantha* decreased significantly by 32.8 and 78.8% under light 42% and light 17%, respectively (Figure 3G). The above-ground biomass of *D. heterocarpon* and *S. tora* decreased by 55 and 63.6% under light 17% compared with that under light 100%. The root biomass of *M. micrantha* decreased significantly by 63 and 91.3% under light 42% and light 17%, respectively, compared with that under light 100%. The root biomass of *D. heterocarpon* significantly decreased by 81% under light 17% compared with light 100%, while there was no significant difference between the root biomass of *D. heterocarpon* under light 42% and light 100%. The root biomass of *S. tora* was significantly decreased by 31.3 and 79.7% under 42% and light 17% compared with light 100%, respectively. Under light 42% and light 17%, the total biomass of *M. micrantha* decreased significantly by 38.5 and 86.5%, respectively. The total biomass of *D. heterocarpon* decreased significantly by 60.2% under light 17% compared with light 100%and the total biomass of *S. tora* decreased by 66.1% under light 17% compared with light 100%. It can be seen that under the low-light treatment the biomass of *M. micrantha*

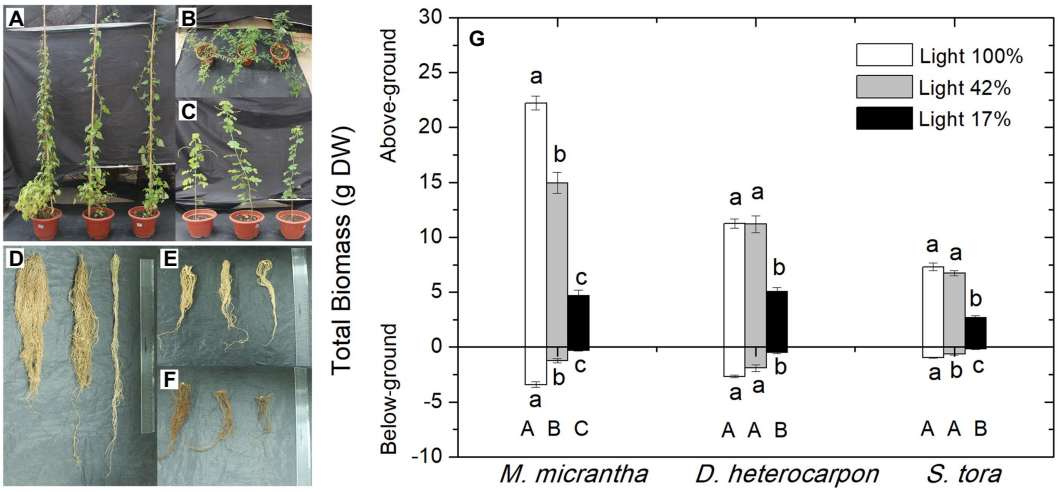

FIGURE 3
Changes of shoot phenotype, root phenotype and biomass of two replacement forage legumes and *M. micrantha* under different light conditions. **(A, D)** Represent *M. micrantha*; **(B, E)** Represent *D. heterocarpon*; **(C, F)** represent *S. tora*. The treatments of each plant from left to right were light 100%, light 42% and light 17%, respectively. **(G)** The average values ± standard errors of five replicates were shown. The lowercase letters above bar plots represent the difference in the above-ground biomass of each plant under different light treatments. The lowercase below bar plots represent the difference in the below-ground biomass of each plant, and the capital letters below bar plots represent the difference in the total biomass (Duncan test, $p<0.05$).

TABLE 1 Changes of photosynthetic parameters under different light conditions (average±SE, $n=4$).

Treatments	P_{max} (μmol CO_2 m^{-2} s^{-1})	LSP (μmol m^{-2} s^{-1})	LCP (μmol m^{-2} s^{-1})	AQY (CO_2 photon^{-1})	Rd (μmol m^{-2} s^{-1})
M. micrantha					
Light 100%	14.77 ± 1.08a	1247.1 ± 126.3a	22.42 ± 1.24a	0.085 ± 0.008a	1.87 ± 0.15a
Light 42%	11.32 ± 0.92b	840.5 ± 69.5b	19.21 ± 1.45ab	0.066 ± 0.002b	1.48 ± 0.12a
Light 17%	9.19 ± 0.31b	724.2 ± 55.4b	16.98 ± 1.29b	0.061 ± 0.011b	1.47 ± 0.28a
D. heterocarpon					
Light 100%	13.61 ± 0.25a	979.2 ± 134.80a	22.24 ± 2.37a	0.065 ± 0.006a	1.47 ± 0.06a
Light 42%	13.63 ± 1.53a	873.8 ± 146.5a	16.79 ± 1.61ab	0.061 ± 0.002a	1.03 ± 0.15b
Light 17%	12.16 ± 0.61a	633.4 ± 102.9a	11.02 ± 0.42b	0.060 ± 0.001a	0.90 ± 0.11b
S. tora					
Light 100%	16.44 ± 0.89a	1498.6 ± 309.5a	22.00 ± 0.90a	0.067 ± 0.002a	1.62 ± 0.19a
Light 42%	16.06 ± 1.25a	991.5 ± 163.4a	21.45 ± 2.19a	0.061 ± 0.002a	1.43 ± 0.3ab
Light 17%	14.70 ± 1.46a	825 ± 115.5a	16.36 ± 1.23b	0.062 ± 0.002a	1.09 ± 0.21b

P_{max}, maximum net photosynthetic rate; LSP, light saturation point; LCP, light compensation point; AQY, apparent quantum yield; Rd, dark respiration rate. Data with different letters for each plant in the column indicate significant differences (Duncan test, $p<0.05$).

decreased the most, followed by *S. tora*, and the biomass of *D. heterocarpon* was the smallest, and it was also the least affected by low light.

From the perspective of photosynthetic parameters, P_{max} of *M. micrantha* significantly decreased by 23.4 and 37.8% respectively, under light 42% and light 17%, compared with light 100% (Table 1). There was no significant difference in P_{max} between *D. heterocarpon* and *S. tora* under three light conditions, indicating that *D. heterocarpon* and *S. tora* have higher photosynthetic efficiency under medium-light and low-light conditions. Under the conditions of light 100% and light 17%, the LSPs of *M. micrantha* and *S. tora* were greater than those of *D. heterocarpon*, indicating that *D. heterocarpon* has stronger photosynthetic utilization ability under low-light conditions. The LCPs of *M. micrantha* and *D. heterocarpon* both decreased with the decrease in light intensity, and the LCP of *D. heterocarpon* was lower than that of *M. micrantha* and *S. tora* under light 42% and light 17%, indicating that *D. heterocarpon* was more tolerant to low-light condition. There was no significant difference in the AQY of *D. heterocarpon* and *S. tora* under different light conditions, while the AQY of *M. micrantha* significantly decreased by 22.4 and 28.2% under light 42% and light 17%, respectively, compared with light 100%, which indicated that the two forage legumes were more efficient for low light. The Rd. of *M. micrantha*

under light 42% and light 17% was not significantly different from that under light 100%. Under light 42% and light 17%, the Rd. of *D. heterocarpon* decreased significantly by 29.9 and 38.8% compared with light 100%, respectively, and that of *S. tora* decreased significantly by 32.7% under light 17% compared with light 100%, which indicated that under low-light conditions, *D. heterocarpon* and *S. tora* can adapt to the low-light environment by reducing their own energy consumption.

With the increase of treatment time, the *Fv*/*Fm* of *M. micrantha* continued to decrease under the three light conditions (Figure 4A), while that of *D. heterocarpon* was not significant under different light conditions and showed an upward trend (Figure 4B). Similar to *M. micrantha*, the *Fv*/*Fm* of *S. tora* also continued to decrease under three light conditions (Figure 4C). Under light 100%, the ETR and Yield of *M. micrantha* remained stable, showed a downward trend under light 42% and light 17%, and decreased dramatically under light 17% (Figures 4D, G). The ETR and Yield of *D. heterocarpon* showed an upward trend under all light conditions (Figures 4E, H), showing good adaptability to the low-light environment. The ETR and Yield of *S. tora* increased gradually with the increase of treatment time, and there was little difference among different treatments (Figures 4F, I). After light 42% and light 17% treatment for 49 days, the photochemical quenching (qp) of *M. micrantha* decreased significantly compared with light 100% (Figure 4J), while that of *D. heterocarpon* and *S. tora* both increased with the increase of treatment time (Figures 4K, L).

3.4. The response of two replacement forage legumes and *Mikania micrantha* to drought stress

After 7 days of drought treatment, the leaves of *M. micrantha* began to wilt and the leaves of *S. tora* wilted on the 10th day, while the leaves of *D. heterocarpon* did not change significantly (Figure 5). After 10 days of drought treatment, the phenotypes of two replacement forage legumes and *M. micrantha* showed obvious differences. The leaves of *D. heterocarpon* were still green without visible changes, while the leaves of *M. micrantha* shrunk due to water loss, and the stem tips were dry and withered. The leaves of *S. tora* also lost water and wilted, and the leaves were closed, but the degree of wilting was significantly lower than that of *M. micrantha*. From the observation of phenotype, the tolerance to drought stress of *D. heterocarpon* was higher than that of *S. tora* and *M. micrantha*, among which *M. micrantha* has the deepest degree of wilting. After rehydration, the leaves of *M. micrantha* were still wilted, the wilting symptoms of *S. tora* leaves disappeared, and the leaves of *D. heterocarpon* did not change significantly and remained green.

Under drought stress, the total biomass of *M. micrantha* and *S. tora* decreased significantly by 65 and 14.9%, respectively, while *D. heterocarpon* was not affected by drought stress (Figure 6A). The root biomass of *M. micrantha* was significantly reduced under drought stress, while neither *D. heterocarpon* nor *S. tora* was affected by drought stress (Figure 6C). Under the drought treatment, the plant height and root length of *M. micrantha* decreased significantly by 38.7 and 32%, respectively, compared with the well-watered group (Figures 6B, D). There were no significant differences in plant height and root length between the well-watered group and drought stress group for *D. heterocarpon* and *S. tora* (Figures 6B, D).

Drought stress had a significant effect on the P_n of *M. micrantha* and *S. tora*. With the increase of drought treatment time, P_n of *M. micrantha* and *S. tora* showed a continuous downward trend, and *M. micrantha* had the largest decrease (96.71%), followed by *S. tora*, with a decrease of 92.4%, while the P_n of *D. heterocarpon* remained at a relatively high level after 10 days of drought treatment, only decreased by 2.4%. After rehydration, the P_n of *M. micrantha* remained at a low level and could not be recovered, and that of *S. tora* recovered to a level comparable to the well-watered group, while that of *D. heterocarpon* increased slightly (Figure 7A). The G_s and T_r of *M. micrantha* and *S. tora* showed similar changing patterns, both of which continued to decline with the increase of drought treatment time. After rehydration, the G_s and T_r of *M. micrantha* could not recover to a level comparable to the well-watered group, while that of *S. tora* could basically recover (Figures 7B, D). During the drought treatment, G_s, C_i, and T_r of *D. heterocarpon* remained at a stable level with little change (Figures 7B–D).

The Fv/Fm of *M. micrantha* and *S. tora* showed a downward trend under drought treatment, which could not be recovered after rehydration, but continued to decline, while that of *D. heterocarpon* did not change and slightly increased after rehydration (Figure 8A). As drought treatment continued, ETR of *M. micrantha* decreased by 16%, and that of *S. tora* decreased by 26.6%, while ETR of *D. heterocarpon* increased by 6.5% (Figure 8B). After rehydration, the ETR of *M. micrantha* was unable to recover, while that of *S. tora* was partially recovered (Figure 8B). On the 10th day of drought treatment, the Yield of *M. micrantha* and *S. tora* decreased by 30.6 and 21.9%, respectively. After rehydration, the Yield of *S. tora* partially recovered, while that of *M. micrantha* could not recover to a level comparable to the well-watered group (Figure 8C). During the drought treatment, the Yield of *D. heterocarpon* was at a high level (Figure 8C). With the increase of drought treatment time, the qP of *M. micrantha* and *S. tora* decreased by 11.6 and 20.7%, respectively, on the 10th day and could be recovered to a level comparable to the untreated group after rehydration, while that of *D. heterocarpon* remained basically unchanged under all conditions (Figure 8D).

Under the drought treatment, the proline content of *M. micrantha*, *D. heterocarpon,* and *S. tora* increased to varying degrees, and were significantly increased by 229.3, 0.96 and 47.7 times, respectively, compared with well-watered treatment (Figure 9A). After rehydration, the proline content of *M. micrantha* remained at a high level and both *D. heterocarpon* and *S. tora* recovered to a level comparable to the well-watered group

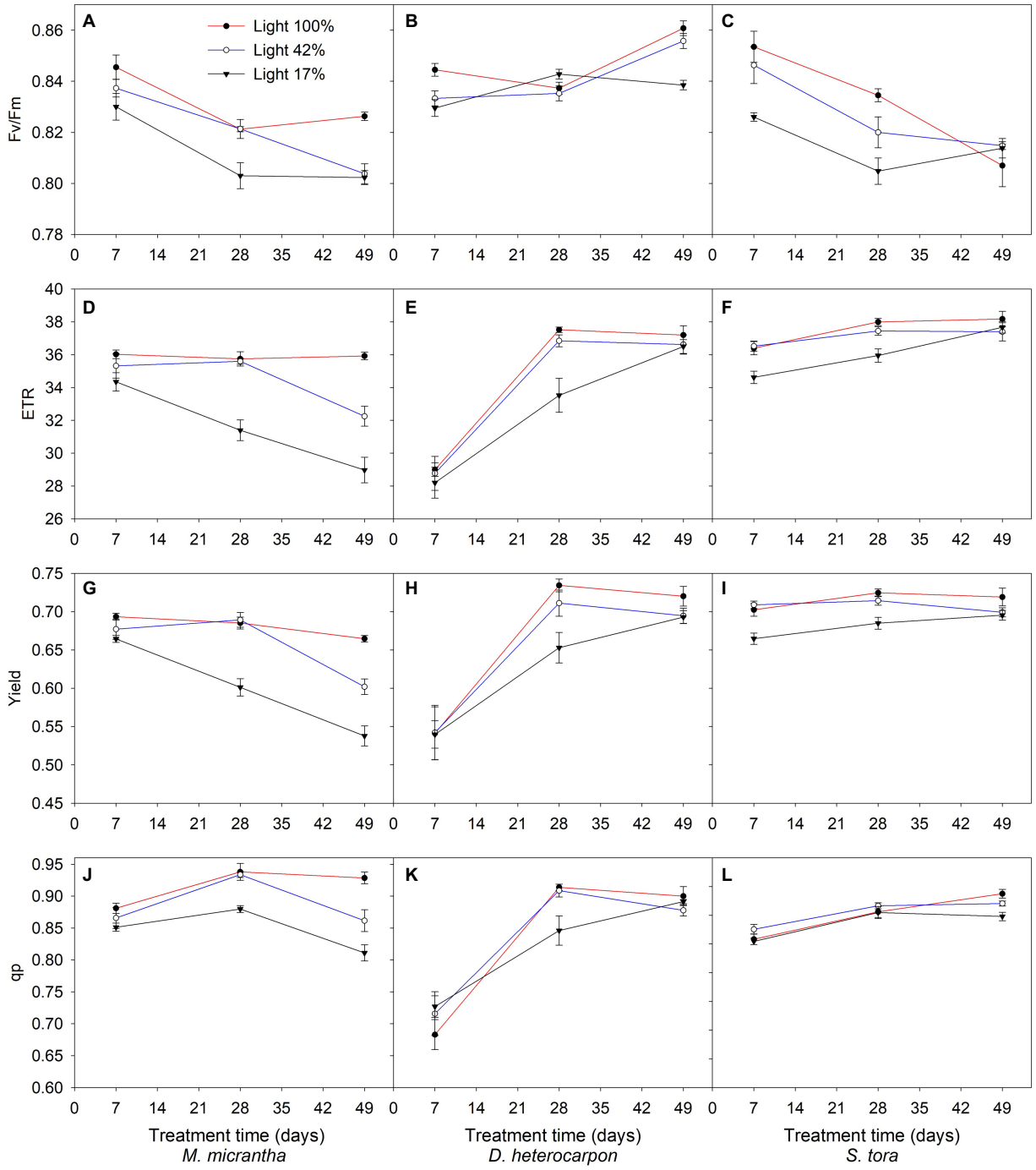

FIGURE 4
Changes of chlorophyll fluorescence parameters of two replacement forage legumes and *M. micrantha* under different light treatments (average±SE, *n*=3). **(A, D, G, J)** *M. micrantha*; **(B, E, H, K)** *D. heterocarpon*; **(C, F, I, L)** *S. tora*.

(Figure 9A). Under drought treatment, the soluble sugar content of *M. micrantha*, *D. heterocarpon,* and *S. tora* increased significantly by 72.4, 28.9, and 31% respectively, compared with the well-watered treatment. The soluble sugar content of all three plants recovered to a level comparable to the well-watered group after rehydration (Figure 9B).

4. Discussion

Much work so far has focused on the ecological mechanism of why biological invasion could be successful (Hengeveld, 1988; van der Putten et al., 2007; Rejmánek, 2014; Olenin et al., 2017). However, rather than understanding the mechanism of the

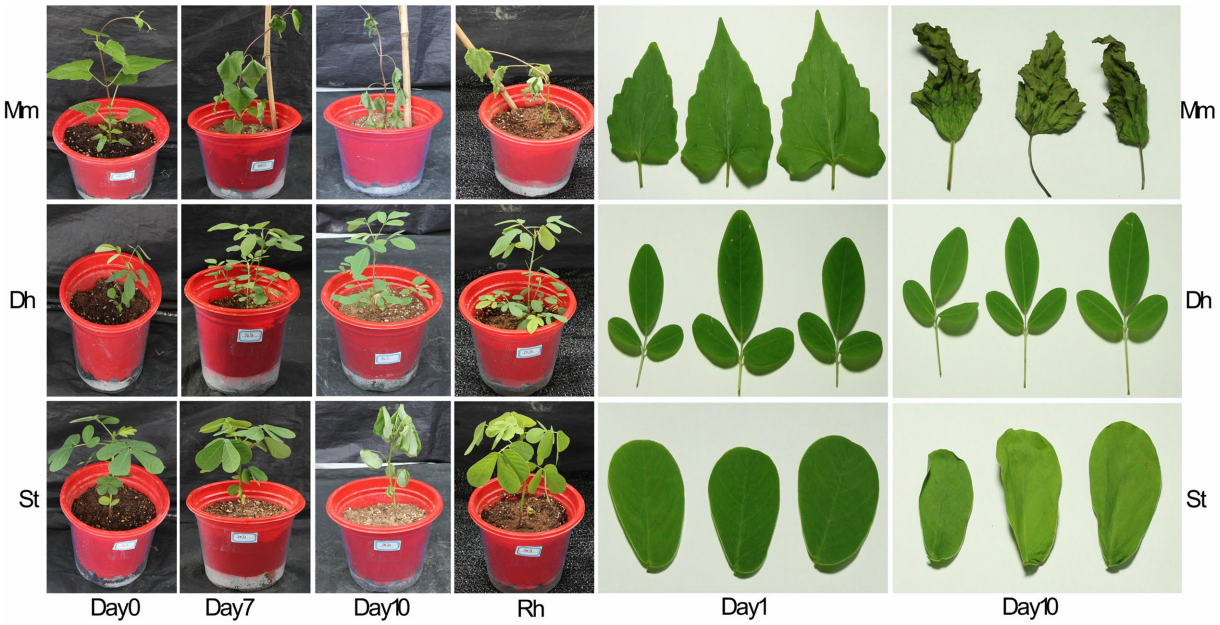

FIGURE 5
Changes of plant phenotype and leaf phenotype of two replacement forage legumes and *M. micrantha* under drought stress. Mm: *M. micrantha*; Dh: *D. heterocarpon*; St: *S. tora*; Rh: rehydration.

invasion, it might be more important to apply the mechanism to the actual restoration and management of invaded sites. We provided experimental evidence that replacement control of invasive plants, through selecting and cultivating suitable native plants, is effective. In the field experiment, we selected 4 replacement plants that commonly appear in orchard habitats (i.e., *D. heterocarpon*, *S. tora*, *S. latifolia,* and *A. conyzoides*) and screened out two potentially effective plants among these four plants, *D. heterocarpon* and *S. tora,* for further experiments to investigate the potential in controlling *M. micrantha*. One of the most important reasons for the successful replacement of invasive plants by replacement plants is the interspecific competitive advantage of replacement plants (Gaudent and Keddy, 1988; Keddy et al., 2002). Species with greater competitiveness can inhibit the growth of invasive plants and replace them, thereby enabling sustainable restoration of damaged soil ecosystems (Chen et al., 2017). We investigated the effect of interspecific competition on the replacement effect of two forage legumes, *D. heterocarpon* and *S. tora* in mixed cultivation with *M. micrantha*. Both *D. heterocarpon* and *S. tora* significantly reduced the coverage of *M. micrantha* and suppress the growth of *M. micrantha*. At the same time, the total leaf area per plant and the total biomass of *M. micrantha* were also significantly reduced when mixed cultivation, indicating that *D. heterocarpon* and *S. tora* had great potential in controlling the expansion of *M. micrantha*. RII is one of the important indicators to measure the competition strength of plants (Ulrich and Perkins, 2014). RII of *M. micrantha* grown in the presence of *D. heterocarpon* [$RII_{Mm(Dh)}$] was −0.42, while that of *M. micrantha* grown in the presence of *S. tora* [$RII_{Mm(St)}$] was −0.13, indicating that these two species have a more competitive advantage compared to the alien species. In addition, we observed that $RII_{Mm(Dh)}$ was significantly smaller than $RII_{Mm(St)}$, indicating that *D. heterocarpon* was more effective in controlling *M. micrantha* than *S. tora*. The question we were trying to answer in this study is why *D. heterocarpon* and *S. tora* are so effective in suppressing the expansion of *M. micrantha* in the field experiment. The field competition experiment was carried out in an orchard habitat with low soil moisture content and some degree of light blocking. Therefore, we simulated low-light and drought-stressed environmental conditions and compared the growth and photosynthetic characteristics of these two plants with *M. micrantha* in order to study the physiological and ecological mechanism of the success replacement controlling effect.

M. micrantha is a tropical heliophytic plant (Han et al., 2017; Sheam et al., 2020), and the biomass of *M. micrantha* decreased significantly with the decrease in light intensity after low-light treatment. On one hand, the AQY of the *M. micrantha* significantly decreased under low-light condition, illustrating that the amount of the light-harvesting pigment–protein complexes which absorbs sunlight and transforms light energy into chemical energy might be reduced, resulting in a decrease of photosynthetic rate and a consequent weakening of the ability to utilize weak light (Richardson and Berlyn, 2002). On the other hand, the dark respiration rate of *M. micrantha* was maintained at a high level, while the photosynthetic rate decreased, leading to a proportional reduction in biomass accumulation. However, under low-light treatment, the dark respiration rate of *D. heterocarpon* and *S. tora*

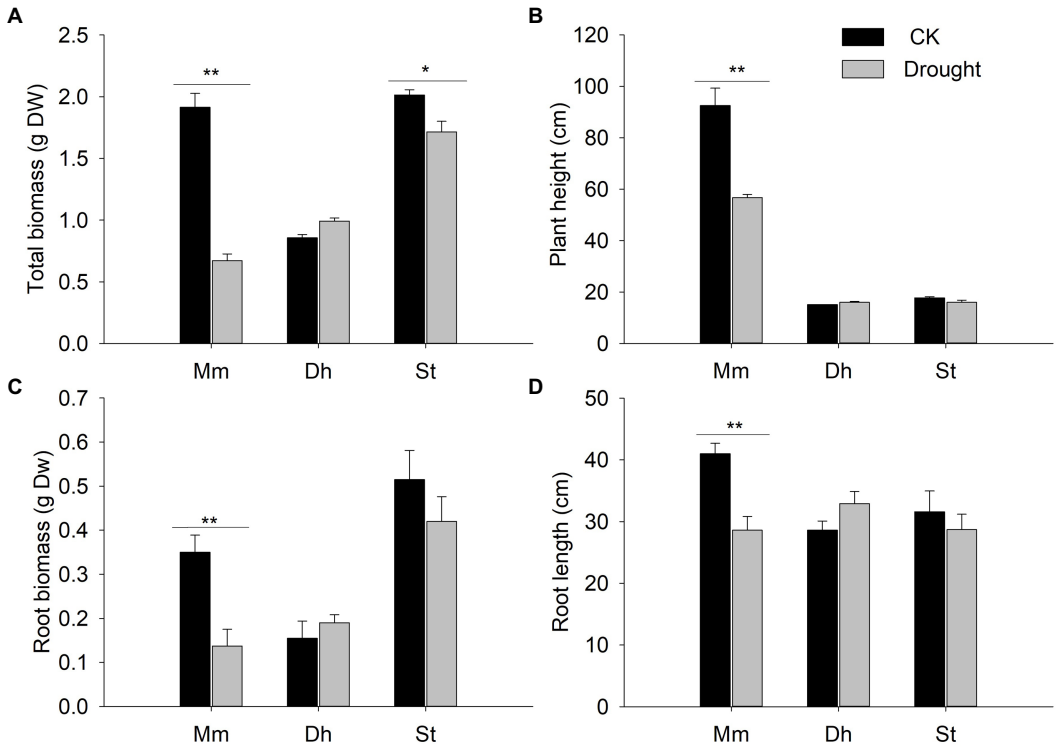

FIGURE 6
Changes of **(A)** total biomass, **(B)** plant height, **(C)** root biomass, and **(D)** root length of two replacement forage legumes and *M. micrantha* under drought stress (average ± SE, $n = 4$). Different letters above bar plots indicate significant differences analyzed using ANOVA followed by Dunnett's test. Significance levels: ** $p<0.01$; * $p<0.05$.

were significantly decreased, indicating that the replacement plants were able to adapt to the low-light environment by reducing energy consumption and maintaining a higher photosynthetic rate (Gyimah and Nakao, 2007; Martínez Pastur et al., 2007). Fv/Fm reflects the maximum light energy conversion efficiency of PSII, which tends to decrease significantly when plants are stressed (Guo and Tan, 2014). ETR reflects the activity of PSII and is directly related to plant photosynthetic rate (Koblížek et al., 2001; Burda, 2007; Yamori et al., 2008), and Yield is also positively correlated with the activity of PSII (Krall and Edwards, 1992). Fv/Fm, ETR, Yield, and qp of the replacement plants under low-light treatment did not change significantly compared with those values under light 100%, while those of *M. micrantha* decreased to different degrees after low-light treatment. Therefore, *D. heterocarpon* and *S. tora* show good adaptability and strong shade tolerance under low-light environment so that they can quickly grow and cover the soil surface to rob most of the light.

Moisture is an important limiting factor during plant growth and development (Davies et al., 1990; Ghaderi and Siosemardeh, 2011). Soil moisture is a key factor in *M. micrantha* seed germination and population expansion, and determines the growth and distribution of *M. micrantha* (Yue et al., 2019). After drought treatment, we found that the biomass of *M. micrantha* decreased by 65% and the plant height and root also decreased by 38.7 and 32%, respectively, compared to the well-watered group, while the replacement plants outperformed *M. micrantha* in all aspects of plant growth parameters. In addition, under drought-stressed condition, phenotype change of *M. micrantha* was the most serious, and the water loss was severe, so that *M. micrantha* needed to absorb more water from the soil for supplementation, resulting in serious soil water loss and soil compaction, which was difficult to restore soil nutrient supply and return to original soil status (Demchik and Sharpe, 2000; Ober and Parry, 2011; Kilpeläinen et al., 2017). A large number of studies have shown that photosynthesis is sensitive to water stress, and the photosynthetic rate decreases with the increase of water stress (Boyer, 1970). We observed that *M. micrantha* was irreversibly damaged after 10 days of drought treatment, and all photosynthetic indexes of *M. micrantha* failed to recover after rehydration. Chlorophyll fluorescence parameters can detect the effects of drought stress on plant photosynthesis (Bi et al., 2008; Su et al., 2015). Chlorophyll fluorescence parameters of *M. micrantha* revealed that drought stress caused irreversible damage to the PSII of *M. micrantha.* However, both the photosynthetic index and chlorophyll fluorescence parameters of *S. tora* recovered after rehydration, indicating that *S. tora* had strong self-repair potential in drought stress and showed resistance to drought stress (Georgieva et al., 2006). The performance of *D. heterocarpon* was better than that of *S. tora*, and its various indicators remained stable during drought stress, reflecting excellent adaptability and

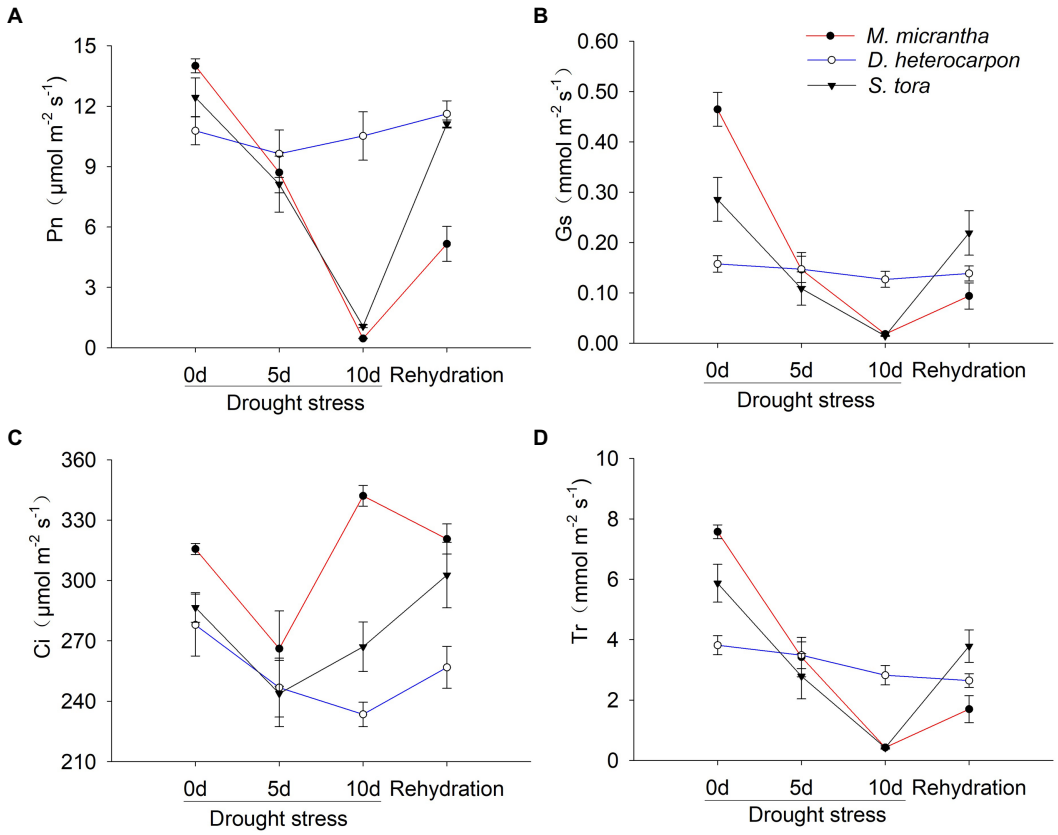

FIGURE 7
Changes of **(A)** net photosynthetic rate, **(B)** intercellular CO^2 concentration, **(C)** stomatal conductance and **(D)** transpiration rate of two replacement forage legumes and *M. micrantha* under drought stress and after rehydration (average±SE, n=4).

tolerance to drought stress. Among two replacement forage legumes and *M. micrantha*, *D. heterocarpon* was the most drought-resistant, while *M. micrantha* was the least drought-resistant and its growth was susceptible to water limitation. In addition, in response to drought stress, *M. micrantha* accumulated a large amount of proline, and after rehydration, the proline concentration remained high, indicating that *M. micrantha* is often difficult to recover after severe damage (Waldren and Teare, 1974; Patel and Vora, 1985; Carvalho et al., 2019). Nevertheless, the proline content of *D. heterocarpon* and *S. tora* recovered to a level comparable to the well-watered group after rehydration. The replacement plants show excellent adaptation to drought stress, suggesting that the use of *D. heterocarpon* and *S. tora* to control the spread of *M. micrantha* in dryland orchards has good application prospects.

Theoretical studies of plant interspecific competition have been the focus of research in the field of ecology, and the long-standing debate on explaining interspecific competition is between Philip Grime and David Tilman (Grime, 1977; Tilman, 1980). A series of previous studies tend to support one side (Jabot and Pottier, 2012; DeMalach et al., 2016). In our study, we found that the replacement plants can obtain sufficient nutrients to sustain themselves and grow rapidly in low-level resource environments, accumulate more above-ground and underground biomass, and more mineral nutrition, water, and sunlight, to eventually win in the competition against invasive plants, eliminate them, and achieve the ecological restoration of the invaded sites. The invasive plants often covered the soil surface quickly through rapid growth and excluded the native plants, which severely disrupted ecological balance and threatening biodiversity (Pyšek and Richardson, 2010; Oduor, 2013). When the resource was sufficient, the plant height and above-ground biomass of *M. micrantha* were significantly higher than those of *D. heterocarpon* and *S. tora*, indicating that these two legumes are not better than *M. micrantha* in terms of growth rate during the same time period. The key to the legume's victory over *M. micrantha* in the field was not its rapid growth, which was not in line with Grime's theory. However, with the reduction of light resources and the lack of water, the difference between the plant heights of *D. heterocarpon, S. tora,* and *M. micrantha* has narrowed, while the above-ground biomass of *D. heterocarpon* has successfully surpassed *M. micrantha* under low light and water shortage. The above-ground biomass of *S. tora* also surpassed that of *M. micrantha* under drought stress. It can be seen that low light and drought were the environmental constraints that can significantly reduce the above-ground biomass of *M. micrantha*. When the light and water resources

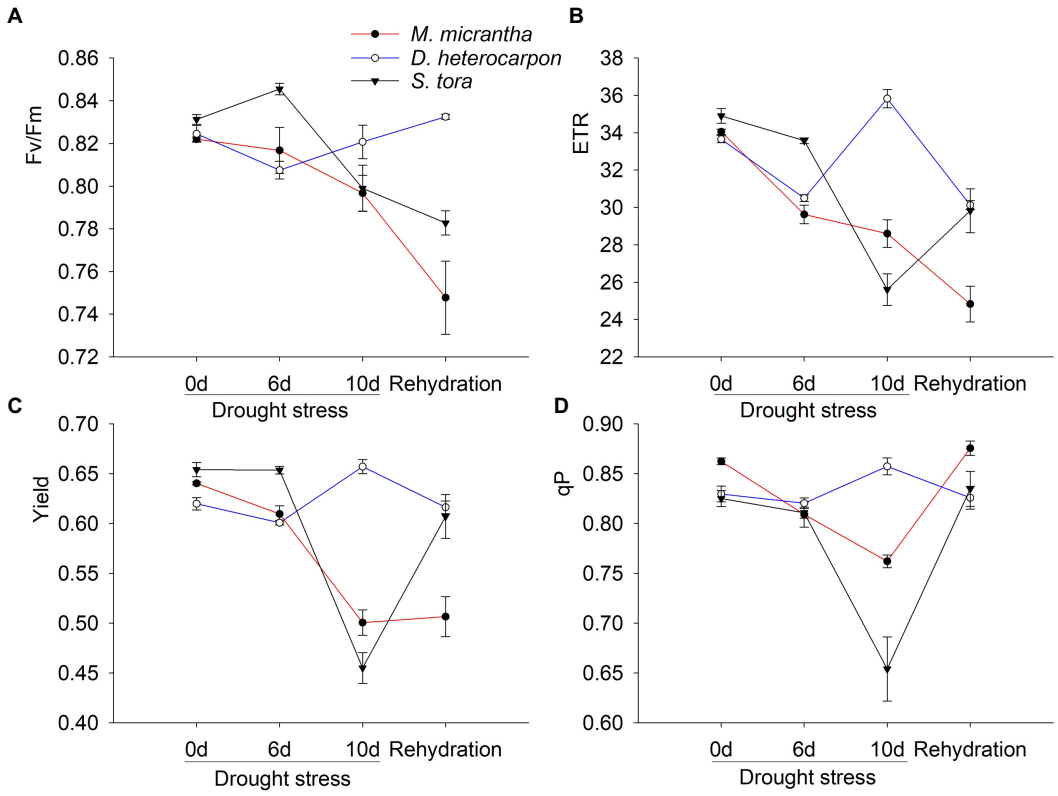

FIGURE 8
Changes of **(A)** maximal photochemical efficiency, **(B)** electron transfer rate, **(C)** quantum yield of photosystem II and **(D)** photochemical quenching of two replacement forage legumes and *M. micrantha* under drought-stressed treatment and after rehydration (average±SE, *n*=4).

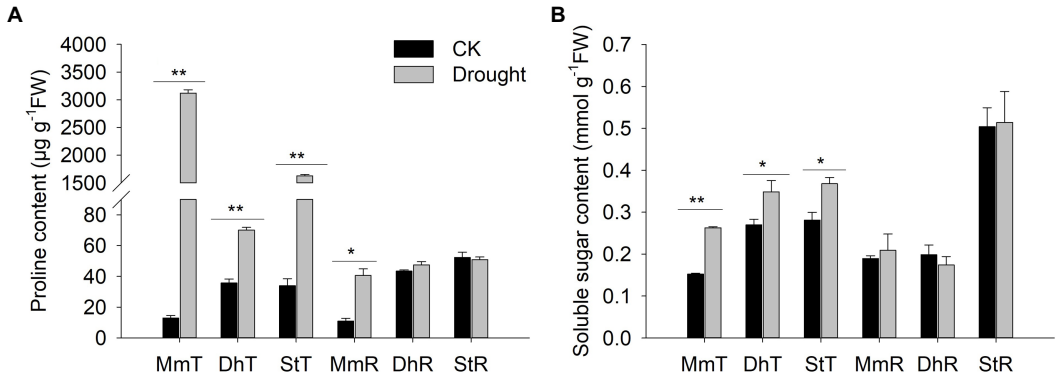

FIGURE 9
Changes of **(A)** proline and **(B)** soluble sugar content of two replacement forage legumes and *M. micrantha* under drought stress and rehydration (average±SE, *n*=3). Different letters above bar plots indicate significant differences analyzed using ANOVA followed by Dunnett's test. Significance levels: ** $p<0.01$; * $p<0.05$.

were limited, the two legumes have higher resource utilization and smaller resource requirements. The limited resources can be fully utilized, thereby accumulating more above-ground biomass and ultimately winning the competition. This is consistent with the idea that "resource availability can affect competition" proposed by Carlyle et al. (2010). Therefore, we propose that the reason why *D. heterocarpon* and *S. tora* are more competitive than *M. micrantha* may be that they have smaller resource requirements and can survive in the absence of light and water resources, which is in line with Tilman's theory of minimum resource requirements.

Because of the rapid growth and expansion of invasive plants, environmental conditions and resources are particularly important to them and also tend to be limiting conditions. The findings of this study mean that in the future, people can control one or more resources that restrict the rapid growth of invasive plants by analyzing the environmental resources of the invaded site, and screening out the native plants that can grow rapidly and cover the soil surface under stressed conditions and eventually the invasive plants can be replaced without leaving other ecological problems. The two-phase resource dynamics hypothesis states that resources appear as pulses rather than continuously, including two stages, one is pulse periods when the available resources are high and most plants can grow and accumulate resources; the other is interpulse periods when the available resources are too low for most plants to absorb, and most plants die due to insufficient resources (Goldberg and Novoplansky, 1997). Our experimental environment is the understory habitat of the orchard, the trees have a canopy effect on light, and soil moisture content is relatively low, which means that light resources and water resources are always in interpulse periods. Therefore, we infer that in the pulse period, the resources can meet the growth of the invasive plant *M. micrantha*, and once transferred to the interpulse period, the replacement plants can survive and grow well, and *M. micrantha* was eventually eliminated because it was at a disadvantage in the competition for resources (Goldberg et al., 2017).

5. Conclusion

In this study, we selected two plants with practical application value for replacement control, which is a potential method to prevent invasive weeds *M. micrantha* from regeneration. *D. heterocarpon* and *S. tora* have strong competitive advantage over *M. micrantha*, mainly due to their strong shade tolerance and drought tolerance. However, considering that *S. tora* is an alien species, it is hoped that the sustainable ecological management of *M. micrantha* in the dryland orchard will be achieved by using *D. heterocarpon*, a native legume, as a competitive substitute for *M. micrantha*. Our study revealed the physiological and ecological mechanism of using replacement plants to control biological invasion, and provide a new method to solve the problem of alien invasive weeds. Based on Tilman's theory of minimum resource requirements, native plants with higher resource utilization and smaller resource requirements (e.g., shade tolerance and drought tolerance) are potential species for controlling *M. micrantha* in dryland orchard habitats.

Data availability statement

The raw data supporting the conclusions of this article will be made available by the authors, without undue reservation.

Author contributions

WL designed the study. PJ, JW, HL, Z-hW, and FL performed the experiments and analyzed the data. PJ and WL wrote the first draft of the manuscript and contributed substantially to revisions. All authors contributed to the article and approved the submitted version.

Funding

This study was financially supported by the National Natural Science Foundation of China (no. 32172430), the Natural Science Foundation of Guangdong Province of China (no. 2022A1515011942), and the Guangdong Basic and Applied Basic Research Foundation (no. 2021B1515120039).

Conflict of interest

The authors declare that the research was conducted in the absence of any commercial or financial relationships that could be construed as a potential conflict of interest.

Publisher's note

References

Barreto, R. W., and Evans, H. C. (1995). The mycobiota of the weed Mikania micrantha in southern Brazil with particular reference to fungal pathogens for biological control. *Mycol. Prog.* 99, 343–352. doi: 10.1016/S0953-7562(09)80911-8

Bi, J. J., Liu, J. D., Ye, B. X., and Xie, L. J. (2008). Effects of drought stress on photosynthesis and chlorophyll fluorescence of the summer maize leaf. *Meteorol. Environ. Sci.* 31, 10–15. doi: 10.16765/j.cnki.1673-7148.2008.01.018

Boyer, J. S. (1970). Differing sensitivity of photosynthesis to low leaf water potentials in corn and soybean. *Plant Physiol.* 46, 236–239. doi: 10.1104/pp.46.2.236

Burda, K. (2007). Dynamics of electron transfer in photosystem II. *Cell Biochem. Biophys.* 47, 271–284. doi: 10.1007/s12013-007-0011-z

Carlyle, C. N., Fraser, L. H., and Turkington, R. (2010). Using three pairs of competitive indices to test for changes in plant competition under different resource and disturbance levels. *J. Veg. Sci.* 21, 1025–1034. doi: 10.1111/j.1654-1103.2010.01207.x

Carvalho, M., Castro, I., Moutinho-Pereira, J., Correia, C., Egea-Cortines, M., Matos, M., et al. (2019). Evaluating stress responses in cowpea under drought stress. *J. Plant Physiol.* 241:153001. doi: 10.1016/j.jplph.2019.153001

Chen, C., Huang, D., Wang, Q., Wu, J., and Wang, K. (2016). Invasions by alien plant species of the agro-pastoral ecotone in northern China: species-specific and environmental determinants. *J. Nat. Conserv.* 34, 133–144. doi: 10.1016/j.jnc.2016.10.004

Chen, B. M., Liao, H. X., Chen, W. B., Wei, H. J., and Peng, S. L. (2017). Role of allelopathy in plant invasion and control of invasive plants. *Allelop. J.* 41, 155–166. doi: 10.26651/2017-41-2-1092

Choudhury, M. R., Deb, P., Singha, H., Chakdar, B., and Medhi, M. (2016). Predicting the probable distribution and threat of invasive Mimosa diplotricha Suavalle and Mikania micrantha Kunth in a protected tropical grassland. *Ecol. Eng.* 97, 23–31. doi: 10.1016/j.ecoleng.2016.07.018

Courchamp, F., Fournier, A., Bellard, C., Bertelsmeier, C., Bonnaud, E., Jeschke, J. M., et al. (2017). Invasion biology: specific problems and possible solutions. *Trends Ecol. Evol.* 32, 13–22. doi: 10.1016/j.tree.2016.11.001

Davies, W. J., Mansfield, T. A., and Hetherington, A. M. (1990). Sensing of soil water status and the regulation of plant growth and development. *Plant Cell Environ.* 13, 709–719. doi: 10.1111/j.1365-3040.1990.tb01085.x

Day, M. D., Clements, D. R., Gile, C., Senaratne, W. K. A. D., Shen, S., Weston, L. A., et al. (2016). Biology and impacts of pacific islands invasive species. 13. Mikania micrantha Kunth (*Asteraceae*). *Pac. Sci.* 70, 257–285. doi: 10.2984/70.3.1

Day, M. D., Kawi, A. P., and Ellison, C. A. (2013). Assessing the potential of the rust fungus Puccinia spegazzinii as a classical biological control agent for the invasive weed *Mikania micrantha* in Papua New Guinea. *Biol. Control* 67, 253–261. doi: 10.1016/j.biocontrol.2013.08.007

Day, M. D., Kawi, A., Kurika, K., Dewhurst, C. F., Waisale, S., Saul-Maora, J., et al. (2012). *Mikania micrantha* Kunth (*Asteraceae*) (mile–a–minute): its distribution and physical and socioeconomic impacts in Papua New Guinea. *Pac. Sci.* 66, 213–223. doi: 10.2984/66.2.8

DeMalach, N., Zaady, E., Weiner, J., and Kadmon, R. (2016). Size asymmetry of resource competition and the structure of plant communities. *J. Ecol.* 104, 899–910. doi: 10.1111/1365-2745.12557

Demchik, M. C., and Sharpe, W. E. (2000). The effect of soil nutrition, soil acidity and drought on northern red oak (Quercus rubra L.) growth and nutrition on Pennsylvania sites with high and low red oak mortality. *For. Ecol. Manag.* 136, 199–207. doi: 10.1016/S0378-1127(99)00307-2

Feng, Y. L., Cao, K. F., and Zhang, J. L. (2004). Photosynthetic characteristics, dark respiration, and leaf mass per unit area in seedlings of four tropical tree species grown under three irradiances. *Photosynthetica* 42, 431–437. doi: 10.1023/B:PHOT.0000046163.83729.e5

Gaudent, C. L., and Keddy, P. A. (1988). Comparative approach to predicting competitive ability from plant traits. *Nature* 334, 242–243. doi: 10.1038/334242a0

Georgieva, K., Szigeti, Z., Sarvari, E., Gaspar, L., Maslenkova, L., Peeva, V., et al. (2006). Photosynthetic activity of homoiochlorophyllous desiccation tolerant plant *Haberlea rhodopensis* during dehydration and rehydration. *Planta* 225, 955–964. doi: 10.1007/s00425-006-0396-8

Ghaderi, N., and Siosemardeh, A. (2011). Response to drought stress of two strawberry cultivars (cv. Kurdistan and Selva). *Hortic. Environ. Biotechnol.* 52, 6–12. doi: 10.1007/s13580-011-0019-6

Goldberg, D. E., Martina, J. P., Elgersma, K. J., and Currie, W. S. (2017). Plant size and competitive dynamics along nutrient gradients. *Am. Nat.* 190, 229–243. doi: 10.1086/692438

Goldberg, D., and Novoplansky, A. (1997). On the relative importance of competition in unproductive environments. *J. Ecol.* 85, 409–418. doi: 10.2307/2960565

Grace, J. B. (2012). *Perspectives on plant competition*. Netherlands: Elsevier.

Grime, J. P. (1977). Evidence for the existence of three primary strategies in plants and its relevance to ecological and evolutionary theory. *Am. Nat.* 111, 1169–1194. doi: 10.1086/283244

Grime, J. P. (1979). *Plant strategies and vegetation processes*. New York: John Wiley & Sons.

Guo, Y., and Tan, J. (2014). Recent advances in the application of chlorophylla fluorescence from photosystem II. *Photochem. Photobiol.* 91, 1–14. doi: 10.1111/php.12362

Gyimah, R., and Nakao, T. (2007). Early growth and photosynthetic responses to light in seedlings of three tropical species differing in successional strategies. *New For (Dordr).* 33, 217–236. doi: 10.1007/s11056-006-9028-1

Han, S., Li, Z., Xu, Q., and Zhang, L. (2017). "Mile-a-minute weed Mikania micrantha Kunth," in *Biological invasions and its Management in China*. *Vol. 2* eds. F. Wan, M. Jiang and A. Zhan (Singapore: Springer), 131–141.

Hengeveld, R. (1988). Mechanisms of biological invasions. *J. Biogeogr.* 15, 819–828. doi: 10.2307/2845342

Islam, F., Wang, J., Farooq, M. A., Khan, M. S. S., Xu, L., Zhu, J., et al. (2018). Potential impact of the herbicide 2,4-dichlorophenoxyacetic acid on human and ecosystems. *Environ. Int.* 111, 332–351. doi: 10.1016/j.envint.2017.10.020

Jabot, F., and Pottier, J. (2012). A general modelling framework for resource-ratio and CSR theories of plant community dynamics. *J. Ecol.* 100, 1296–1302. doi: 10.1111/j.1365-2745.2012.02024.x

Kaur, R., Malhotra, S., and Inderjit. (2012). Effects of invasion of Mikania micrantha on germination of rice seedlings, plant richness, chemical properties and respiration of soil. *Biol. Fertil. Soils* 48, 481–488. doi: 10.1007/s00374-011-0645-2

Keddy, P., Nielsen, K., Weiher, E., and Lawson, R. (2002). Relative competitive performance of 63 species of terrestrial herbaceous plants. *J. Veg. Sci.* 13, 5–16. doi: 10.1111/j.1654-1103.2002.tb02018.x

Kilpeläinen, J., Barbero-López, A., Vestberg, M., Heiskanen, J., and Lehto, T. (2017). Does severe soil drought have after-effects on arbuscular and ectomycorrhizal root colonisation and plant nutrition? *Plant Soil* 418, 377–386. doi: 10.1007/s11104-017-3308-8

Kimball, S., Lulow, M. E., Mooney, K. A., and Sorenson, Q. M. (2014). Establishment and Management of Native Functional Groups in restoration. *Restor. Ecol.* 22, 81–88. doi: 10.1111/rec.12022

Koblížek, M., Kaftan, D., and Nedbal, L. (2001). On the relationship between the non-photochemical quenching of the chlorophyll fluorescence and the photosystem II light harvesting efficiency. A repetitive flash fluorescence induction study. *Photosynth. Res.* 68, 141–152. doi: 10.1023/A:1011830015167

Krall, J. P., and Edwards, G. E. (1992). Relationship between photosystem II activity and CO_2 fixation in leaves. *Physiol. Plant.* 86, 180–187. doi: 10.1111/j.1399-3054.1992.tb01328.x

Li, Z., Han, S., Guo, M., Luo, L. W., Peng, T., et al. (2004). Biology and host specificity of Actinote anteas, a biocontrol agent for controlling Mikania micrantha. *Chin. J. Biol. Control* 20:170. doi: 10.16409/j.cnki.2095-039x.2004.03.006

Li, F. L., Li, M. G., Zan, Q. J., Guo, Q., Zhang, W. Y., Wu, Z., et al. (2012). Effects of the residues of Cuscuta campestris and Mikania micrantha on subsequent plant germination and early growth. *J. Integr. Agric.* 11, 1852–1860. doi: 10.1016/S2095-3119(12)60190-7

Li, M., Lu, E., Guo, Q., Zan, Q., Wei, P., Jiang, L., et al. (2012). Evaluation of the controlling methods and strategies for *Mikania micrantha* H. *B. K. Acta Ecol. Sin.* 32, 3240–3251. doi: 10.5846/STXB201104090460

Li, W., Luo, J., Tian, X., Soon Chow, W., Sun, Z., Zhang, T., et al. (2015). A new strategy for controlling invasive weeds: selecting valuable native plants to defeat them. *Sci. Rep.* 5:11004. doi: 10.1038/srep11004

Macanawai, A., Day, M., Tumaneng-Diete, T., and Adkins, S. (2012). Impact of *Mikania micrantha* on crop production systems in Viti Levu. *Fiji. Pak. J. Weed Sci. Res.* 18, 357–365.

MacArthur, R., and Levins, R. (1964). Competition, habitat selection, and character displacement in a patchy environment. *Proc. Natl. Acad. Sci. U. S. A.* 51, 1207–1210. doi: 10.1073/pnas.51.6.1207

Martínez Pastur, G., Lencinas, M. V., Peri, P. L., and Arena, M. (2007). Photosynthetic plasticity of *Nothofagus pumilio* seedlings to light intensity and soil moisture. *For. Ecol. Manag.* 243, 274–282. doi: 10.1016/j.foreco.2007.03.034

Mohanty, S. S., and Jena, H. M. (2019). A systemic assessment of the environmental impacts and remediation strategies for chloroacetanilide herbicides. *J. Water Process. Eng.* 31:100860. doi: 10.1016/j.jwpe.2019.100860

Ober, E., and Parry, M. A. J. (2011). *The molecular and physiological basis of nutrient use efficiency in crops*. New York: John Wiley & Sons.

Oduor, A. M. O. (2013). Evolutionary responses of native plant species to invasive plants: a review. *New Phytol.* 200, 986–992. doi: 10.1111/nph.12429

Olenin, S., Gollasch, S., Lehtiniemi, M., Sapota, M., and Zaiko, A. (2017). *Biological oceanography of the Baltic Sea*. Dordrecht: Springer.

Patel, J. A., and Vora, A. B. (1985). Free proline accumulation in drought-stressed plants. *Plant Soil* 84, 427–429. doi: 10.1007/BF02275480

Piemeisel, R. L. (1954). Replacement control: changes in vegetation in relation to control of pests and diseases. *Bot. Re.* 20, 1–32. doi: 10.2307/4353509

Piemeisel, R. L., and Carsner, E. (1951). Replacement control and biological control. *Science* 113, 14–15. doi: 10.1126/science.113.2923.14

Pimentel, D., McNair, S., Janecka, J., Wightman, J., Simmonds, C., O'Connell, C., et al. (2001). Economic and environmental threats of alien plant, animal, and microbe invasions. *Agri. Ecosyst. Environ.* 84, 1–20. doi: 10.1016/S0167-8809(00)00178-X

Price, J. N., and Partel, M. (2013). Can limiting similarity increase invasion resistance? A meta-analysis of experimental studies. *Oikos* 122, 649–656. doi: 10.1111/j.1600-0706.2012.00121.x

Pyšek, P., and Richardson, D. M. (2010). Invasive species, environmental change and management, and health. *Annu. Rev. Environ. Resour.* 35, 25–55. doi: 10.1146/annurev-environ-033009-095548

Rejmánek, M. (2014). Biological invasions and ecological hypotheses. *Trends Ecol. Evol.* 29:435. doi: 10.1016/j.tree.2014.06.003

Richardson, A. D., and Berlyn, G. P. (2002). Spectral reflectance and photosynthetic properties of *Betula papyrifera* (*Betulaceae*) leaves along an elevational gradient on Mt. Mansfield, Vermont, United States. *Am. J. Bot.* 89, 88–94. doi: 10.3732/ajb.89.1.88

Scasta, J. D., Engle, D. M., Fuhlendorf, S. D., Redfearn, D. D., and Bidwell, T. G. (2015). Meta-analysis of exotic forages as invasive plants in complex multi-functioning landscapes. *Invas. Plant Sci. Mana.* 8, 292–306. doi: 10.1614/IPSM-D-14-00076.1

Sheam, M., Haque, Z., and Nain, Z. (2020). Towards the antimicrobial, therapeutic and invasive properties of *Mikania micrantha* Knuth: a brief overview. *J. Adv. Biotechnol. Exp. Ther.* 3, 92–101. doi: 10.5455/jabet.2020.d112

Shen, S. C., Xu, G. F., Clements, D. R., Jin, G. M., Chen, A. D., Zhang, F. D., et al. (2015). Suppression of the invasive plant mile-a-minute (*Mikania micrantha*) by local crop sweet potato (*Ipomoea batatas*) by means of higher growth rate and competition for soil nutrients. *BMC Ecol.* 15, 1–10. doi: 10.5061/dryad.vb1qv

Shen, S. C., Xu, G. F., Clements, D. R., Jin, G. M., Chen, A. D., Zhang, F. D., et al. (2016). Suppression of reproductive characteristics of the invasive plant *Mikania micrantha* by sweet potato competition. *BMC Ecol.* 16, 30–39. doi: 10.1186/s12898-016-0085-9

Slingenberg, A., Braat, L., Windt, H. V., Rademaekers, K., Eichler, L., and Turner, K. (2009). Study on understanding the causes of biodiversity loss and the policy assessment framework. Available at: http://ec.europa.eu/environment/enveco/biodiversity/pdf/causes_biodiv_loss.pdf

Song, Z., Wang, Z. H., Fan, Z. W., Zhang, R. H., Zhang, G. L., and Fu, W. D. (2020). Screening and control effects of different alternative plants on *Mikania micrantha*. *Chinese J. Agrometeorol.* 41, 24–33. doi: 10.3969/j.issn.1000-6362.2020.01.003

Su, L. Y., Dai, Z. W., Li, S. H., and Xin, H. P. (2015). A novel system for evaluating drought–cold tolerance of grapevines using chlorophyll fluorescence. *BMC Plant Biol.* 15:82. doi: 10.1186/s12870-015-0459-8

Swamy, P. S., and Ramakrishnan, P. S. (1987). Contribution of *Mikania micrantha* during secondary succession following slash-and-burn agriculture (jhum) in north-East India I. biomass, litterfall and productivity. *For. Ecol. Manag.* 22, 229–237. doi: 10.1016/0378-1127(87)90107-1

Theoharides, K. A., and Dukes, J. S. (2007). Plant invasion across space and time: factors affecting nonindigenous species success during four stages of invasion. *New Phytol.* 176, 256–273. doi: 10.1111/j.1469-8137.2007.02207.x

Tilman, D. (1980). Resources: a graphical-mechanistic approach to competition and predation. *Am. Nat.* 116, 362–393. doi: 10.1086/679066

Tilman, D. (1988). *Plant strategies and the dynamics and the structure of plant communities. Vol. 26*. United States: Princeton University Press.

Ulrich, E., and Perkins, L. (2014). *Bromus inermis* and *Elymus canadensis* but not *Poa pratensis* demonstrate strong competitive effects and all benefit from priority. *Plant Ecol.* 215, 1269–1275. doi: 10.1007/s11258-014-0385-0

van der Putten, W. H., Klironomos, J. N., and Wardle, D. A. (2007). Microbial ecology of biological invasions. *ISME J.* 1, 28–37. doi: 10.1038/ismej.2007.9

Waldren, R. P., and Teare, I. D. (1974). Free proline accumulation in drought-stressed plants under laboratory conditions. *Plant Soil* 40, 689–692. doi: 10.1007/BF00010525

Xu, G. F., Zhang, F. D., Li, T. L., Shen, S. C., and Zhang, Y. H. (2011). Effects of 5 species and planting density on *Mikania micrantha* H. B. K. growth and competitive traits. *Ecol. Environ. Sci.* 20, 798–804. doi: 10.16258/j.cnki.1674-5906(2011)05-0798-07

Yamori, W., Noguchi, K., Kashino, Y., and Terashima, I. (2008). The role of electron transport in determining the temperature dependence of the photosynthetic rate in spinach leaves grown at contrasting temperatures. *Plant Cell Physiol.* 49, 583–591. doi: 10.1093/pcp/pcn030

Yue, M. F., Yu, H. X., Li, W. H., Yin, A. G., Cui, Y., and Tian, X. S. (2019). Flooding with shallow water promotes the invasiveness of *Mikania micrantha*. *Ecol. Evol.* 9, 9177–9184. doi: 10.1002/ece3.5465

Zhang, L. Y., Ye, W. H., Cao, H. L., and Feng, H. L. (2004). Mikania micrantha H. B. K. in China – an overview. *Weed Res.* 44, 42–49. doi: 10.1111/j.1365-3180.2003.00371.x

Zhong, X. Q., Huang, Z., Si, H., and Zan, Q. J. (2004). Analysis of ecological-economic loss caused by weed *Mikania micrantha* on Neilingding Island, Shenzhen. *China. J. Trop. Subtrop. Bot.* 12, 167–170.

frontiers | Frontiers in Ecology and Evolution

TYPE Original Research
PUBLISHED 04 January 2023
DOI 10.3389/fevo.2022.1103937

OPEN ACCESS

EDITED BY
Xiang Liu,
Lanzhou University, China

REVIEWED BY
Zhonghua Zhang,
Nanning Normal University, China
Li Zhang,
Nanjing Forestry University, China

*CORRESPONDENCE
Yunquan Wang
✉ yqwang@vip.126.com

SPECIALTY SECTION
This article was submitted to Conservation and Restoration Ecology, a section of the journal Frontiers in Ecology and Evolution

RECEIVED 21 November 2022
ACCEPTED 13 December 2022
PUBLISHED 04 January 2023

CITATION
Liu L, Xia H, Quan X and Wang Y (2023) Plant trait-based life strategies of overlapping species vary in different succession stages of subtropical forests, Eastern China. *Front. Ecol. Evol.* 10:1103937. doi: 10.3389/fevo.2022.1103937

Plant trait-based life strategies of overlapping species vary in different succession stages of subtropical forests, Eastern China

Libin Liu, Haojun Xia, Xinghua Quan and Yunquan Wang*

College of Chemistry and Life Sciences, Zhejiang Normal University, Jinhua, China

Plants growing in forests at different succession stages in diverse habitats may adopt various life strategies from the perspective of plant functional traits. However, species composition differs with forest succession, and the effects of forest succession on traits have often been explored without considering the effects of species identity. We comprehensively investigated intraspecific variations in 12 traits of six overlapping species (two tree species and four understory shrub species) in three typical subtropical evergreen broad-leaved forests at different succession stages in eastern China. We found that intraspecific variations differed among traits. Fine root specific length presented large intraspecific variation, leaf area, specific leaf area and fine root tissue density showed medium intraspecific variations, and other traits displayed small intraspecific variations. Trees and understory shrubs in the early-stage forest exhibited higher leaf thickness, dry matter contents and tissue densities of leaves, roots, twigs, and stems and lower leaf area and specific leaf area. Those in the medium- and late-stage forests displayed contrasting trait characteristics. From the perspective of plant functional traits, plants in the early-stage forest formed a series of trait combinations for a resource conservative strategy with a low growth rate to adapt to fragile habitats with poor soil nutrients and changeable soil temperature and humidity, and those in the medium- and late-stage forests (especially the former) formed converse trait combinations for a resource acquisitive strategy with a high growth rate to adapt to low light availability and strongly competitive habitats. Our study reveals that plants in forests at different succession stages adopt various life strategies and provides data to the TRY and China plant trait databases.

KEYWORDS

intraspecific trait variation, forest succession, overlapping species, life history strategy, subtropical forests

Introduction

Plant functional traits are measurable characteristics formed from long-term plant-environment interactions and are closely linked to the growth, reproduction, and survival processes of plants (Violle et al., 2007; Garnier et al., 2016; Kattge et al., 2020). A single trait and the combinations of multiple traits not only respond to plant life history strategy, biodiversity, vegetation, environment, and disturbance changes but also affect ecosystem processes and functions (Cornelissen et al., 2003; Vandewalle et al., 2010; Mensens et al., 2017; Wang et al., 2020). Therefore, the study of plant functional traits is at the forefront of modern ecology and global change ecology (Meng et al., 2007; Liu and Ma, 2015; Blondeel et al., 2020).

Forests are the largest vegetated areas in global terrestrial ecosystems and play important roles in global biodiversity maintenance and climate change mitigation (Melillo et al., 1993; Anderson-Teixeira et al., 2015). Plant functional traits, such as morphological traits and C: N: P ecological stoichiometry of leaves, roots, stems, and twigs (especially leaves) in forests worldwide have been intensively investigated at local, regional and global scales (McGroddy et al., 2004; Chave et al., 2009; Díaz et al., 2016; He et al., 2019; Guerin et al., 2021; Liu et al., 2022). Compared to interspecific trait variations (trait differences among species) of woody plants in forests, intraspecific trait variations (trait differences among independent individuals within a species) are yet to be fully investigated. However, intraspecific trait variations are non-negligible, and they may account for an average of 32% of the total trait variations based on a global database (Siefert et al., 2015). Environmental factors, such as climate, topography, and soil nutrition, greatly affect intraspecific trait variations (Hultine and Marshall, 2000; Thuiller et al., 2004; Quested et al., 2007; Wang et al., 2016a).

In addition, most plant functional trait studies conducted in forests have focused on dominant trees, and understory shrubs have rarely been described. As an important component of forest ecosystems, understory shrubs influence the energy and water cycles of forests and participate in forest renewal, development, and succession (Cao et al., 2020). In limited trait studies on understory shrubs, the latitudinal distribution pattern and driving factors of leaf traits (Luo et al., 2019), the correlation between morphological traits and nitrogen and phosphorus nutrients (Wang et al., 2017), relationships between twigs and leaf traits at different succession stages (Ma, 2014), and different phenotypes of understory shrubs (Wang et al., 2016b) have been reported. Light conditions and canopy coverage are the main environmental factors driving intraspecific variations in leaf traits (Burton et al., 2017). However, studies on intraspecific trait variation in understory shrubs in forests at different succession stages in different habitats are scarce (Kumordzi et al., 2019; Vanneste et al., 2019; Cao et al., 2020).

Environments (or habitats), species composition, and the structure of a forest community change with progressive succession. In early-stage forests, illumination is sufficient, but soil nutrients are poor, and soil temperature and humidity fluctuate. Such forests are committed to gap formation, understory initiation, and regeneration (Moridi et al., 2015; Zhang et al., 2016). In medium-stage forests, soil humidity and nutrients are greatly improved, but light availability is the lowest because of the highest canopy coverage and stand density. Such forests are in volume accumulation, lightning, and stem exclusion phases (Zhang et al., 1999; Wang et al., 2004; Yan et al., 2008; Moridi et al., 2015). Light conditions improve in late-stage forests because of slightly lower canopy coverage and stand density (Moridi et al., 2015; Zhang et al., 2016). Some species (turnover species) only appear in forests at one succession stage and disappear in the next stage, whereas, some species (overlapping species) grow in forests at many succession stages (Yang et al., 2014). Overlapping species in the early-stage forest may form a series of trait combinations for a resource conservative strategy to adapt to fragile habitats with poor soil nutrients and changeable soil temperature and humidity, and those in the medium- and late-stage forests may form converse trait combinations for a resource acquisitive strategy to adapt to low light availability and strongly competitive habitats (Li and Ma, 2002).

Originating from the uplift of the Qinghai–Tibet Plateau, a broad subtropical evergreen broad-leaved forest was found in China. This forest is a unique vegetation type on Earth and is essential to the global gene pool and regional environments (Song, 2013). In the present study, dominant overlapping species, including tree and understory shrub species, in three evergreen broad-leaved forests at different succession stages in eastern China were investigated as examples. The leaf, twig, stem, and root traits were comprehensively measured. Here, the life strategies of plants growing in forests at different succession stages in various habitats were determined from the perspective of plant functional traits. Specifically, the following predictions were made. (1) Overlapping species in the forests at three succession stages present significant differences in plant functional traits. (2) Plants (trees and understory shrubs) in the early-stage forest form a series of trait combinations with higher leaf thickness (LT), dry matter contents and tissue densities of leaves, roots, twigs, and stems and lower leaf area (LA) and specific leaf area (SLA) for a resource conservative strategy with a low growth rate. Plants in the medium- and late-stage forests form converse trait combinations for a resource acquisitive strategy with a high growth rate. This study provides basic data to global (Kattge et al., 2020) and China (He et al., 2019) plant trait databases and guides the sustainable management and ecological restoration of evergreen broad-leaved forests in eastern China.

Materials and methods

Study area

Field measurements were conducted in three permanent monitoring plots of the Zhejiang Tiantong Forest Ecosystem National Observation and Research Station (121.783° E, 29.800° N) in the Tiantong National Forest Park, Zhejiang Province, Eastern China. This area is located in mid-subtropical China and controlled by monsoon climates. The mean annual temperature is 16.2°C, with temperatures of 4.2°C and 28.1°C in January and July, respectively. Considerably high and low temperatures are 38.7°C and −8.5°C, respectively. The growing degree days on the base of 10°C is 5,166.2°C. The mean annual

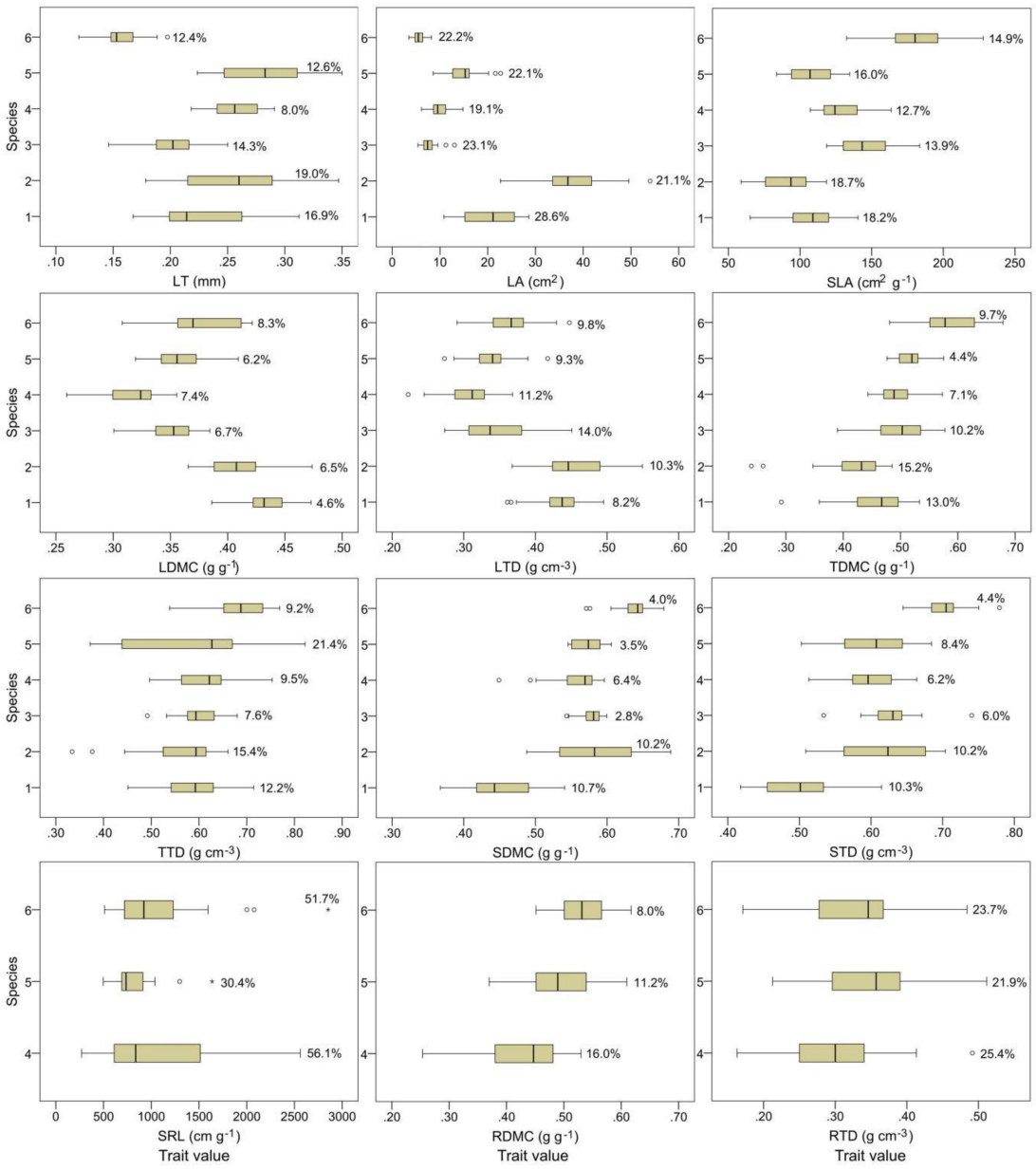

FIGURE 1
Plant functional traits and their intraspecific variations in overlapping species in three evergreen broad-leaved forests. The circles and stars in the box plots indicate the abnormal values. The percentage of data in the box plots are the coefficients of trait intraspecific variation. 1–6 represent species in the ordinate: species number 1, *Castanopsis fargesii*; 2, *Schima superba*; 3, *Camellia fraterna*; 4, *Symplocos sumuntia*; 5, *Eurya rubiginosa* var. *attenuata*; 6, *Loropetalum chinense*. LT, leaf thickness; LA, leaf area; SLA, specific leaf area; LDMC, leaf dry matter content; LTD, leaf tissue density; TDMC, twig dry matter content; TTD, twig tissue density; SDMC, stem dry matter content; STD, stem tissue density; SRL, fine root specific length; RDMC, fine root dry matter content; RTD, fine root tissue density.

precipitation and evaporation are 1,374.7 and 1,320.1 mm, respectively. The native vegetation is subtropical evergreen broad-leaved forest dominated by *Castanopsis fargesii* Franch. and *Schima superba* Gardn. et Champ. Existing forests in the Tiantong National Forest Park are classified as early-, medium-, and late-stage forests along a secondary succession series because of the intensity of human disturbances (Song and Wang, 1995). Three forest plots (each with an area of 2,500 m^2, 50 m × 50 m) at three succession stages (i.e., early, medium and late stages) were established and investigated in 2007.

The early-stage forest (121.786° E, 29.801° N) is 20° south of the east and has a 25° slope. This forest is restored from a shrubland with a stand age of 35 y. The height and coverage of the tree layer are 8 m and 70%, respectively. Its dominant tree species is *S. superba*. Another common species in the tree layer is *C. fargesii*. *Loropetalum chinense* (R. Br.) Oliver and *Symplocos sumuntia* Buch. -Ham. ex D. Don are dominant understory shrub species. The medium-stage forest (121.788° E, 29.786° N) is 70° south of the east and has a 20° slope. The stand age is 90 y, and the height and coverage of the tree layer are 15 m and 95%, respectively. This forest is also dominated by *S. superba*, and *C. fargesii* is distributed in the subtree layer. The main understory shrub species are *Eurya rubiginosa* var. *attenuata* H. T. Chang, *Camellia fraterna* Hance, and *S. sumuntia*. The late-stage forest (121.787° E, 29.808° N) is 45° south of the east and has a 26° slope. This forest is in the climax stage with a stand age of 170 y. The height and coverage of the tree layer are 18 m and 90%, respectively. *C. fargesii* is the dominant tree species, and *S. superba* is widely distributed in the subtree layer. *E. rubiginosa*, *C. fraterna*, and *L. chinense* are common in the understory shrub layer.

Measurement of plant functional traits

Overlapping species, including two tree species (*C. fargesii* and *S. superba*) and four understory shrub species (*C. fraterna*, *S. sumuntia*, *E. rubiginosa*, and *L. chinense*), in the three forests were selected for trait measurements. Ten healthy dominant individuals per species in each plot were chosen. From each individual, a branch was collected from the sunlit tree canopy by using a long reach chain saw (tree species) or collected from the upper canopy by using a lopper (understory shrub species). Twenty mature leaves without visible damage were collected. An approximately 20 cm length current-year twig was sampled using a lopper, and a stem sample was determined using a SY-CO (trees) or a lopper (shrubs). The roots of trees were difficult to recognize, and *C. fraterna* was grown in rocks in the early-stage forest, so only fine roots (root diameter ≤ 2 mm) of three understory shrub species, that is, *S. sumuntia*, *E. rubiginosa*, and *L. chinense*, were sampled using a hoe.

TABLE 1 Plant functional traits and their abbreviations, units, and calculations.

Plant functional trait	Abbreviations	Unit	Calculation
Specific leaf area	SLA	$cm^2\ g^{-1}$	Leaf area/leaf dry mass
Leaf dry matter content	LDMC	$g\ g^{-1}$	Leaf dry mass/fresh mass
Leaf tissue density	LTD	$g\ cm^{-3}$	Leaf dry mass/volume
Twig dry matter content	TDMC	$g\ g^{-1}$	Twig dry mass/fresh mass
Twig tissue density	TTD	$g\ cm^{-3}$	Twig dry mass/volume
Stem dry matter content	SDMC	$g\ g^{-1}$	Stem dry mass/fresh mass
Stem tissue density	STD	$g\ cm^{-3}$	Stem dry mass/volume
Fine root specific length	SRL	$cm\ g^{-1}$	Fine root length/dry mass
Fine root dry matter content	RDMC	$g\ g^{-1}$	Fine root dry mass/fresh mass
Fine root tissue density	RTD	$g\ cm^{-3}$	Fine root dry mass/volume

Fresh masses of leaf, twig, and stem samples were weighed using an electronic balance. Leaf thickness was measured using an electronic Vernier caliper. The length and volume of fine roots and LA were scanned using a WinFOLIA multipurpose leaf area meter (Regent Instruments, Canada). Leaf sample volume was calculated as the product of LA and LT, and twig and stem sample volumes were determined using the drainage method (Cornelissen et al., 2003). All samples were dried in an oven at 80°C for 72 h to determine their dry masses. The values of traits were calculated as shown in **Table 1**.

Data analysis

The coefficient of intraspecific variation (standard deviation divided by mean) was used to characterize the varying degrees of traits among individuals of a certain species. One-way ANOVA was conducted to determine the trait differences among plant growth forms (trees and understory shrubs) and species in the forests at three succession stages. The principal component analysis (PCA) was done to evaluate the effect of plant species on traits, and show the distributions of traits among plant species. Trait data were log-transformed prior to PCA analysis. Fisher's least significant difference (homogeneity of variance) or Tamhane (heterogeneity of variance) methods were used to conduct *post hoc* tests after the homogeneity test of variances.

All statistical analyses were performed using the SPSS version 20 and the CANOCO 5.

Results

Plant functional traits and their intraspecific variations

The 12 plant functional traits varied among plant species (Figure 1). Among the stem, twig, and leaf traits, *C. fargesii* exhibited the highest leaf dry matter content (LDMC) and the lowest stem dry matter content (SDMC) and stem tissue density (STD). *S. superba* showed the highest LA and leaf tissue density (LTD) and the lowest SLA, twig dry matter content (TDMC), and twig tissue density (TTD). *S. sumuntia* presented the lowest LDMC and LTD, *E. rubiginosa* had the highest LT. *L. chinense* displayed the highest SLA, TDMC, TTD, SDMC, and STD and the lowest LT and LA. *C. fraterna* had intermediate trait values. Among the root traits, *S. sumuntia* presented the lowest fine root dry matter content (RDMC) and fine root tissue density (RTD). *E. rubiginosa* had the highest RTD and the lowest fine root specific length (SRL). *L. chinense* displayed the highest SRL and RDMC.

The intraspecific variations differed among plant functional traits (Figure 1). SRL exhibited the largest intraspecific variations. The intraspecific variations in the SRL of *S. sumuntia* and *L. chinense* were highly variable, indicated by large coefficients of intraspecific variation (56.1 and 51.7%, respectively). The coefficients of intraspecific variation of LA, SLA, and RTD generally ranged from 15 to 35%. Other traits displayed small intraspecific variations, indicated by small coefficients of intraspecific variation, especially for LDMC, SDMC, and STD, whose coefficients of intraspecific variation were generally less than 10%.

Plant functional traits of plant growth forms at different succession stages

The LA, SDMC, and STD of trees were close in the forests at three succession stages ($F_{LA} = 2.904$, $F_{SDMC} = 1.694$, $F_{STD} = 2.892$, $P > 0.05$), whereas other traits showed significant differences ($F_{LT} = 20.858$, $F_{SLA} = 20.012$, $F_{LDMC} = 11.176$, $F_{LTD} = 7.204$, $F_{TDMC} = 4.497$, $F_{TTD} = 8.709$, $P < 0.05$; Figure 2). Trees in the early-stage forest presented the highest LT, LDMC, LTD, TTD, SDMC, and STD and the lowest LA and SLA; trees in the medium-stage forest exhibited the highest LA and SLA and the lowest LDMC, TDMC, TTD, SDMC, and STD; and those in the late-stage forest generally displayed intermediate trait values (Figure 2). Understory shrubs in the forests at three succession stages showed small discrepancies in LT, TDMC, and SDMC ($F_{LT} = 1.934$, $F_{TDMC} = 0.169$, $F_{SDMC} = 0.477$, $P > 0.05$), but they exhibited significant differences in other traits ($F_{LA} = 2.082$, $F_{SLA} = 6.294$, $F_{LDMC} = 5.716$, $F_{LTD} = 5.642$, $F_{TTD} = 14.524$, $F_{STD} = 4.676$, $F_{SRL} = 15.995$, $F_{RDMC} = 9.023$, $F_{RTD} = 6.521$, $P < 0.05$; Figure 2). Shrubs in the early-stage forest presented the highest LT, TTD, RDMC, and RTD and the lowest LA, SLA, and SRL; shrubs in the medium-stage forest exhibited the highest SLA and SRL and the lowest LT, LDMC, LTD, TDMC, TTD, SDMC, STD, RDMC, and RTD; and those in the late-stage forest also displayed intermediate trait values (Figure 2).

Plant functional traits of overlapping species at different succession stages

The traits of overlapping species in forests at three succession stages differed to varying degrees (Figures 3, 4 and Supplementary Table 1). In general, plants in the early-stage forest exhibited high LT, LDMC, LTD, TDMC, TTD, SDMC, STD, RDMC, and RTD and low SLA and SRL; plants in the medium-stage forest presented contrary trait characteristics compared with those in the early-stage forest; and those in the late-stage forest displayed intermediate trait values except high LA (Figure 4). Specifically, the LA, TDMC, TTD, SDMC, and STD of *C. fargesii* exhibited small discrepancies in the forests at three succession stages ($F_{LA} = 1.851$, $F_{TDMC} = 2.945$, $F_{TTD} = 0.649$, $F_{SDMC} = 0.183$, $F_{STD} = 0.424$, $P > 0.05$). However, *C. fargesii* in the early-stage forest exhibited significantly higher LT, LDMC, and LTD and significantly lower SLA ($F_{LT} = 7.101$, $F_{LDMC} = 7.469$, $F_{LTD} = 4.041$, $F_{SLA} = 12.254$, $P < 0.05$; Figure 4). All traits of *S. superba* showed significant differences in the forests at three succession stages ($P < 0.05$). *S. superba* in the early-stage forest showed significantly higher LT, LDMC, SDMC, and STD and significantly lower LA and SLA ($F_{LT} = 64.481$, $F_{LDMC} = 10.140$, $F_{SDMC} = 15.454$, $F_{STD} = 19.011$, $F_{LA} = 11.506$, $F_{SLA} = 41.995$, $P < 0.05$); *S. superba* in the medium-stage forest showed significantly lower LTD, TDMC, and TTD ($F_{LTD} = 5.079$, $F_{TDMC} = 16.451$, $F_{TTD} = 17.975$, $P < 0.05$; Figure 4). The LA, SDMC, and STD of *C. fraterna* did not differ in the forests at three succession stages ($F_{LA} = 3.021$, $F_{SDMC} = 0.318$, $F_{STD} = 0.243$, $P > 0.05$). Conversely, *C. fraterna* in the early-stage forest had significantly higher LT and TDMC ($F_{LT} = 11.128$, $F_{TDMC} = 15.314$, $P < 0.05$); *C. fraterna* in the medium-stage forest had significantly higher SLA and significantly lower LDMC ($F_{SLA} = 8.543$, $F_{LDMC} = 13.261$, $P < 0.05$); and *C. fraterna* in the late-stage forest had significantly higher LTD and TTD ($F_{LTD} = 27.678$, $F_{TTD} = 9.051$, $P < 0.05$; Figure 4). The LDMC, LTD, and TDMC of *S. sumuntia* presented small discrepancies in the forests at three succession stages ($F_{LDMC} = 2.181$, $F_{LTD} = 1.721$, $F_{TDMC} = 5.545$, $P > 0.05$). However, *S. sumuntia* in the early-stage forest presented significantly higher LT, TTD, and RTD and significantly lower SLA ($F_{LT} = 2.999$, $F_{TTD} = 3.754$, $F_{RTD} = 6.109$, $F_{SLA} = 6.277$, $P < 0.05$); *S. sumuntia* in the medium-stage forest presented

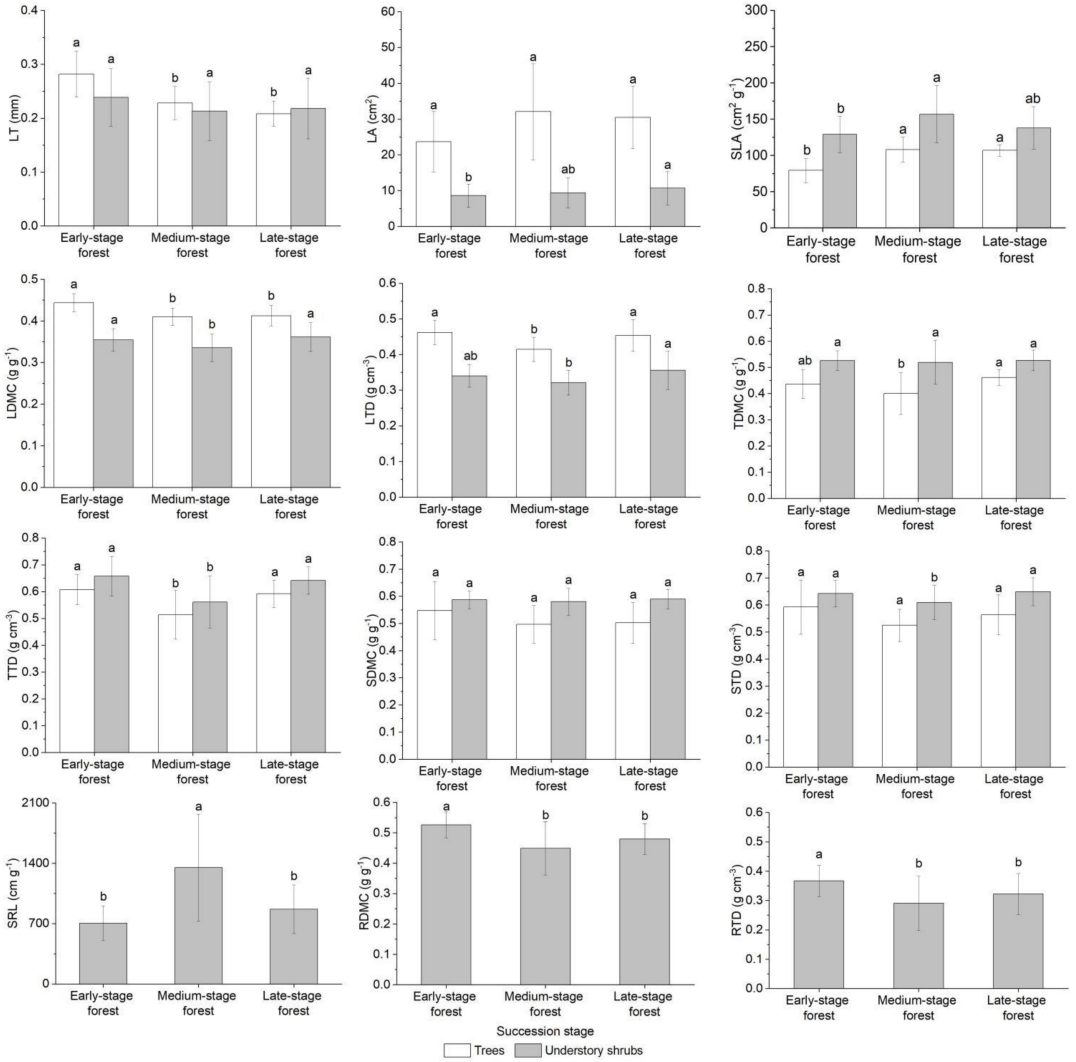

FIGURE 2
Plant functional traits of plant growth forms in forests at different succession stages. Trait values with different letters among succession stages are significantly different (one-way ANOVA, $P < 0.05$). LT, leaf thickness; LA, leaf area; SLA, specific leaf area; LDMC, leaf dry matter content; LTD, leaf tissue density; TDMC, twig dry matter content; TTD, twig tissue density; SDMC, stem dry matter content; STD, stem tissue density; SRL, fine root specific length; RDMC, fine root dry matter content; RTD, fine root tissue density.

significantly higher SRL and significantly lower SDMC, STD, and RDMC (F_{SRL} = 12.966, F_{SDMC} = 10.480, F_{STD} = 5.873, F_{RDMC} = 30.602, $P < 0.05$); and *S. sumuntia* in the late-stage forest presented significantly higher LA (F_{LA} = 4.846, $P < 0.05$; Figure 4). The LT, SLA, LDMC, LTD, SRL, and RTD of *E. rubiginosa* exhibited no differences in the forests at three succession stages (F_{LT} = 0.745, F_{SLA} = 1.043, F_{LDMC} = 0.566, F_{LTD} = 2.468, F_{SRL} = 1.329, F_{RTD} = 0.453, $P > 0.05$). By comparison, *E. rubiginosa* in the medium-stage forest exhibited significantly higher TDMC and SDMC and significantly lower TTD and STD (F_{TDMC} = 3.110, F_{SDMC} = 4.452, F_{TTD} = 49.393, F_{STD} = 22.889, $P < 0.05$). *E. rubiginosa* in the late-stage forest exhibited significantly higher LA and significantly lower RDMC (F_{LA} = 3.057, F_{RDMC} = 4.201, $P < 0.05$; Figure 4). The LA, LTD, TDMC, TTD, SDMC, and STD of *L. chinense* displayed small discrepancies in the forests at three succession stages (F_{LA} = 1.863, F_{LTD} = 1.427, F_{TDMC} = 3.032, F_{TTD} = 3.858, F_{SDMC} = 0.534, F_{STD} = 1.092, $P > 0.05$). Conversely, *L. chinense* in the medium-stage forest exhibited significantly higher SRL and significantly lower LT, SLA, LDMC, RDMC, and RTD (F_{SRL} = 9.020, F_{LT} = 6.386, F_{SLA} = 14.432, F_{LDMC} = 7.311, F_{RDMC} = 2.477, F_{RTD} = 6.157, $P < 0.05$; Figure 4).

Discussion

Few studies on intraspecific trait variations have been conducted compared with studies on interspecific trait variation

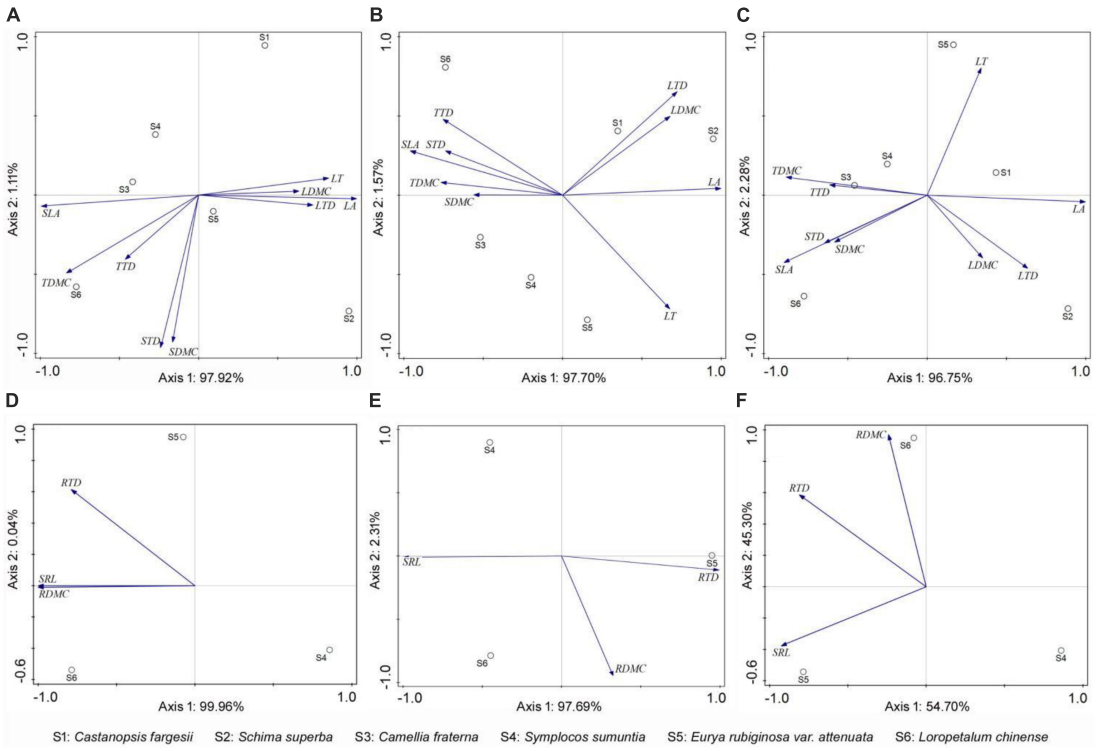

FIGURE 3
PCA showing the distribution of plant functional traits among species in forests at different succession stages. **(A,D)** Early-stage forest; **(B,E)** medium-stage forest; **(C,F)** late-stage forest. LT, leaf thickness; LA, leaf area; SLA, specific leaf area; LDMC, leaf dry matter content; LTD, leaf tissue density; TDMC, twig dry matter content; TTD, twig tissue density; SDMC, stem dry matter content; STD, stem tissue density; SRL, fine root specific length; RDMC, fine root dry matter content; RTD, fine root tissue density.

in the world's forests, and most trait studies have focused on trees and their leaf traits, such as LA, LDMC, and SLA (Rosbakh et al., 2015; Siefert et al., 2015; Zhou, 2016; Heilmeier, 2019; Zhang et al., 2019). The intraspecific trait variation characteristics of understory shrubs and those of the twigs, stems, and roots of trees have rarely been reported (Burton et al., 2017; Zhong et al., 2018; Cao et al., 2020). The present study comprehensively investigated the intraspecific variation characteristics of 12 traits of leaves, twigs, stems, and roots of six common species (two tree species and four understory shrub species) in three typical subtropical evergreen broad-leaved forests in eastern China. This study could fill the gap in plant functional trait studies in subtropical China.

Since the application of succession in plant ecology research, studies on vegetation succession have been widely performed. Biodiversity and carbon storage were often used as indicators to evaluate vegetation succession processes in early studies (Ni et al., 2015; Capellesso et al., 2021). Plant functional traits and trait-based community ecology (a theory using trait-based approaches to determine community composition, structures and functions) offer an alternative approach to reveal the colonization, survival, growth, and death processes of plants and plant communities in different succession vegetation (Song et al., 2018). However, species compositions vary in different succession vegetations, and traits of different species were measured in previous studies. Rather than considering several dominant species in different succession vegetation (Chazdon, 2008; Muscarella et al., 2017), the present study focused on overlapping species and provided another pathway to understand the interaction of plant functional traits and vegetation succession.

Plant functional traits are codetermined by species identity (genetic factors) and environment (Scheiner and Lyman, 1991; Weiher and Keddy, 1995). Environments promote the coexistence of species with similar functional traits in local habitats, but intraspecific trait variations cause differences in the life history strategy of a certain species or different species (Ackerly and Cornwell, 2007; Auger and Shipley, 2013; Siefert et al., 2015; Kumordzi et al., 2019). However, the species composition of a plant community differs with the environment. The effects of environments on traits are often discussed without considering the effects of species identity, or some statistical analysis methods, such as two-way ANOVA, are used in species–environment interactive analysis in other studies (Zhong et al., 2018; Cao et al., 2020). In the present study, overlapping species in three typical subtropical evergreen

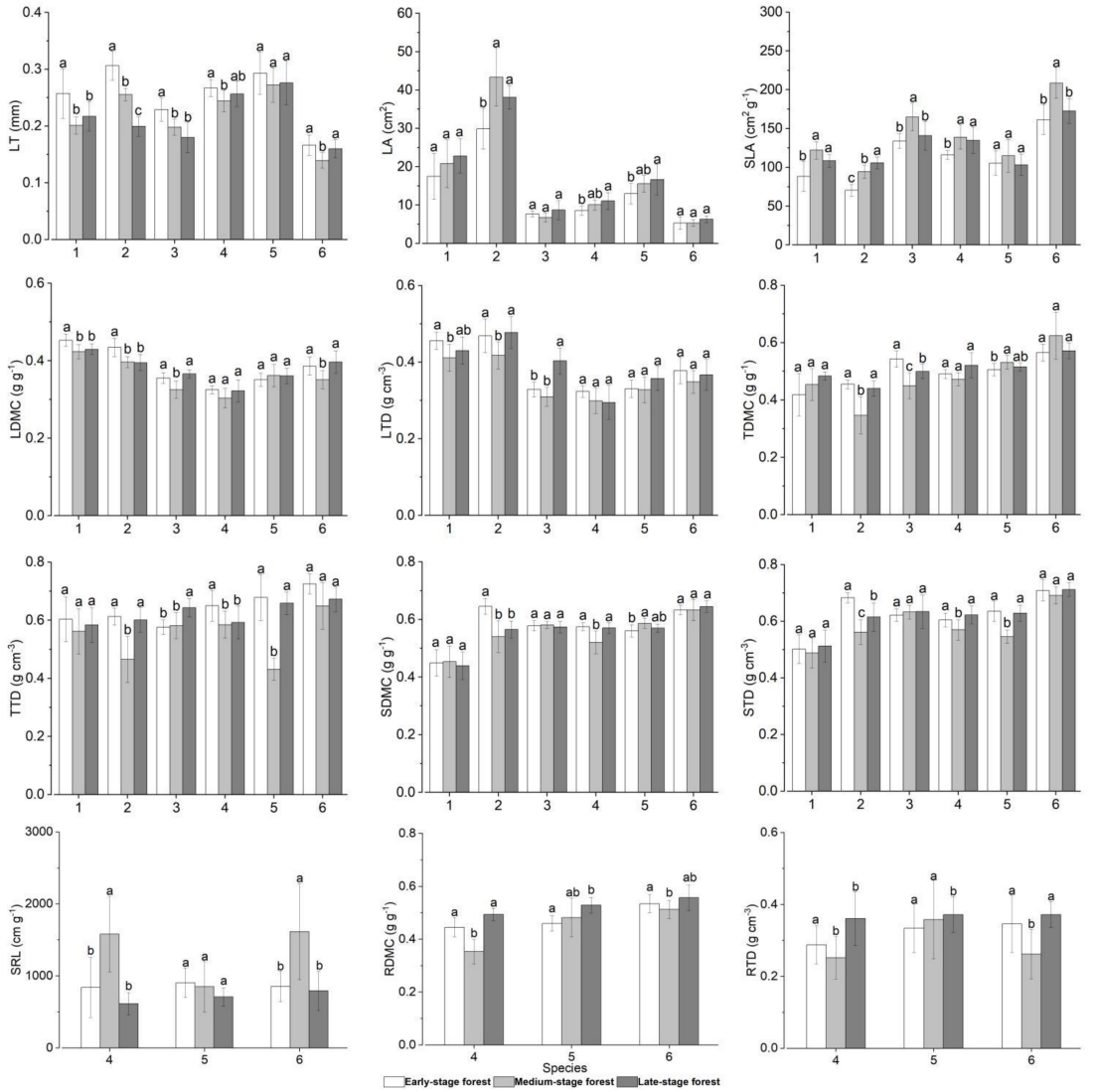

FIGURE 4
Plant functional traits of overlapping species in forests at different succession stages. Trait values with different letters among succession stages are significantly different (one-way ANOVA, $P < 0.05$). 1–6 represent species in the ordinate: species number 1, *Castanopsis fargesii*; 2, *Schima superba*; 3, *Camellia fraterna*; 4, *Symplocos sumuntia*; 5 *Eurya rubiginosa* var. *attenuata*; 6, *Loropetalum chinense*. LT, leaf thickness; LA, leaf area; SLA, specific leaf area; LDMC, leaf dry matter content; LTD, leaf tissue density; TDMC, twig dry matter content; TTD, twig tissue density; SDMC, stem dry matter content; STD, stem tissue density; SRL, fine root specific length; RDMC, fine root dry matter content; RTD, fine root tissue density.

broad-leaved forests with different habitats in eastern China are investigated as an example to explore the effects of the environment on traits. This investigation method is preferred because of the direct exclusion of the effects of species identity.

Root traits often exhibit the largest interspecific and intraspecific variations resulting from complex and diverse below-ground habitats (Comas and Eissenstat, 2004). Leaf traits display larger interspecific and intraspecific variations than twig and stem traits (Ackerly and Reich, 1999; Garnier et al., 2001; Zhong et al., 2018). In the present study, variations in the intraspecific traits of overlapping species in the forests at three succession stages with different habitats ranged from 2.8% to 56.1%, with an average of 13.5%. Some traits of roots and leaves considerably varied. SRL, RTD, LA, and SLA also differed, but RDMC, LT, LTD, and LDMC (especially the last leaf trait) slightly varied. Consistent with early studies (Garnier et al., 2001), our study showed that intraspecific variations in twig and stem traits slightly differed.

A single trait and the combinations of multiple traits can indicate the adaptation and response of plants to certain environments, expose the plant trade-off strategies of resource

acquisition and utilization, and reveal the different life history strategies of plants in different environments (Wright et al., 2004; Díaz et al., 2016). Some species (resource acquisitive strategy adopters) present a high SLA, leaf nitrogen content, photosynthetic and respiratory rates, and short lifespans. Some other species (resource conservative strategy adopters) display low SLA, leaf nitrogen content, photosynthetic and respiratory rates, and long lifespan (Chen and Xu, 2014). Such plant and trait combinations favor niche overlap and competition reduction, rich biodiversity maintenance, and ecosystem stability enhancement (Liu and Ma, 2015). In the present study, the early-stage forest is a relatively fragile ecosystem with poor soil nutrients and fluctuating soil temperature and humidity. Trees and understory shrubs in such forests allocate more nutrients to resist adverse environments. Thus, they adopt a slow investment-return (resource conservation) strategy and form a series of trait combinations with higher LT, LDMC, LTD, TDMC, TTD, SDMC, STD, RDMC, and RTD and lower SLA and SRL for storing more nutrients and growing slower. However, in the medium- and late-stage forests, trees and understory shrubs are exposed to lower light availability and stronger competition. They adopt a quick investment-return (resource acquisitive) strategy and are associated with a series of trait combinations with higher LA, SLA, and SRL and lower LT, LDMC, LTD, TDMC, TTD, SDMC, STD, RDMC, and RTD for faster growth. Plants in medium-stage forests are more resource acquisitive for lower light availability and stronger competition than those in late-stage forests.

The remaining primary evergreen broad-leaved forests only account for 4% of its total distribution area in eastern China because of intensive human disturbances. Degraded secondary forests, shrub and grass communities, and bare land are distributed everywhere. However, excellent hydrothermal conditions promote secondary forest succession once human disturbances stop. Evergreen broad-leaved forests may recover gradually in this area. Therefore, research on the secondary succession mechanism and restoration ecology of evergreen broad-leaved forests should be strengthened (Song, 2013). Understanding the trend of changes in trait characteristics with vegetation succession and the life strategies of plants adapted to different succession vegetation is important not only for providing data to the global and China plant trait databases but also for establishing regional forest management and restoration in eastern China.

Data availability statement

The original contributions presented in this study are included in the article/**Supplementary material**, further inquiries can be directed to the corresponding author.

Author contributions

LL and YW conceived and designed the research. LL and HX analyzed the data. XQ contributed to the field work. LL wrote the first draft with substantial input from YW. All authors contributed to the article and approved the submitted version.

Funding

This study was funded by the Open Research Fund of Zhejiang Tiantong Forest Ecosystem National Observation and Research Station (TTK201902) and the Zhejiang Provincial Natural Science Foundation of China (LQ20C030003 and LQ22C030001).

Acknowledgments

We thank the Zhejiang Tiantong Forest Ecosystem National Observation and Research Station for assistance in all field work. YW acknowledges the support of Zhejiang Qianjiangyuan Forest Biodiversity National Observation and Research Station. We are grateful to Prof. Jian Ni for his suggestions for improving the manuscript.

Conflict of interest

The authors declare that the research was conducted in the absence of any commercial or financial relationships that could be construed as a potential conflict of interest.

Publisher's note

Supplementary material

The Supplementary Material for this article can be found online at: https://www.frontiersin.org/articles/10.3389/fevo.2022.1103937/full#supplementary-material

References

Ackerly, D. D., and Cornwell, W. K. (2007). A trait-based approach to community assembly: Partitioning of species trait values into within- and among-community components. *Ecol. Lett.* 10, 135–145. doi: 10.1111/j.1461-0248.2006.01006.x

Ackerly, D. D., and Reich, P. B. (1999). Convergence and correlations among leaf size and function in seed plants: A comparative test using independent contrasts. *Am. J. Bot.* 86, 1272–1281. doi: 10.2307/2656775

Anderson-Teixeira, K. J., Davies, S. J., Bennett, A. C., Gonzalez-Akre, E. B., Muller-Landau, H. C., Wright, S. J., et al. (2015). CTFS-ForestGEO: A worldwide network monitoring forests in an era of global change. *Glob. Change Biol.* 21, 528–549. doi: 10.1111/gcb.12712

Auger, S., and Shipley, B. (2013). Inter-specific and intra-specific trait variation along short environmental gradients in an old-growth temperate forest. *J. Veg. Sci.* 24, 419–428. doi: 10.1111/j.1654-1103.2012.01473.x

Blondeel, H., Perring, M. P., Depauw, L., Lombaerde, E. D., Landuyt, D., Frenne, P. D., et al. (2020). Light and warming drive forest understorey community development in different environments. *Glob. Change Biol.* 26, 1681–1696. doi: 10.1111/gcb.14955

Burton, J. I., Perakis, S. S., McKenzie, S. C., Lawrence, C. E., and Puettmann, K. J. (2017). Intraspecific variability and reaction norms of forest understorey plant species traits. *Funct. Ecol.* 31, 1881–1893. doi: 10.1111/1365-2435.12898

Cao, J. Y., Liu, J. F., Yuan, Q., Xu, D. Y., Fan, H. D., Chen, H. Y., et al. (2020). Traits of shrubs in forests and bushes reveal different life strategies. *Chin. J. Plant Ecol.* 44, 715–729. doi: 10.17521/cjpe.2020.0024

Capellesso, E. S., Cequinel, A., Marques, R., Sausen, T. L., Bayer, C., and Marques, M. C. M. (2021). Co-benefits in biodiversity conservation and carbon stock during forest regeneration in a preserved tropical landscape. *For. Ecol. Manag.* 492:119222. doi: 10.1016/j.foreco.2021.119222

Chave, J., Coomes, D., Jansen, S., Lewis, S. L., Swenson, N. G., and Zanne, A. E. (2009). Towards a worldwide wood economics spectrum. *Ecol. Lett.* 12, 351–366. doi: 10.1111/j.1461-0248.2009.01285.x

Chazdon, R. L. (2008). "Chance and determinism in tropical forest succession," in *Tropical forest community ecology*, eds W. Carson and S. A. Schnitzer (Hoboken, NJ: Wiley-Blackwell Publishing), 384–408.

Chen, Y. T., and Xu, Z. Z. (2014). Review on research of leaf economics spectrum. *Chin. J. Plant Ecol.* 38, 1135–1153. doi: 10.3724/SP.J.1258.2014.00108

Comas, L. H., and Eissenstat, D. M. (2004). Linking fine root traits to maximum potential growth rate among 11 mature temperate tree species. *Funct. Ecol.* 18, 388–397. doi: 10.1111/j.0269-8463.2004.00835.x

Cornelissen, J. H. C., Lavorel, S., Garnier, E., Díaz, S., Buchmann, N., Gurvich, D. E., et al. (2003). A handbook of protocols for standardised and easy measurement of plant functional traits worldwide. *Aust. J. Bot.* 51, 335–380. doi: 10.1071/BT02124

Díaz, S., Kattge, J., Cornelissen, J. H. C., Wright, I. J., Lavorel, S., Dray, S., et al. (2016). The global spectrum of plant form and function. *Nature* 529, 167–171. doi: 10.1038/nature16489

Garnier, E., Laurent, G., Bellmann, A., Debain, S., Berthelier, P., Ducout, B., et al. (2001). Consistency of species ranking based on functional leaf traits. *New Phytol.* 152, 69–83. doi: 10.1046/j.0028-646x.2001.00239.x

Garnier, E., Navas, M.-L., and Grigulis, K. (2016). *Plant functional diversity: Organism traits, community structure, and Ecosystem properties*. Oxford: Oxford University Press. doi: 10.1093/acprof:oso/9780198757368.001.0001

Guerin, G. R., Gallagher, R. V., Wright, I. J., Andres, S. C., Falster, D. S., Wenk, E., et al. (2021). Environmental associations of abundance-weighted functional traits in Australian plant communities. *Basic Appl. Ecol.* 58, 98–109. doi: 10.1016/j.baae.2021.11.008

He, N. P., Liu, C. C., Piao, S. L., Sack, L., Xu, L., Luo, Y. Q., et al. (2019). Ecosystem traits linking functional traits to macroecology. *Trends Ecol. Evol.* 34, 200–210. doi: 10.1016/j.tree.2018.11.004

Heilmeier, H. (2019). Functional traits explaining plant responses to past and future climate changes. *Flora* 254, 1–11. doi: 10.1016/j.flora.2019.04.004

Hultine, K. R., and Marshall, J. D. (2000). Altitude trends in conifer leaf morphology and stable carbon isotope composition. *Oecologia* 123, 32–40. doi: 10.1007/s004420050986

Kattge, J., Bönisch, G., Díaz, S., Lavorel, S., Prentice, I. C., and Wirth, C. (2020). TRY plant trait database-enhanced coverage and open access. *Glob. Change Biol.* 26, 119–188. doi: 10.1111/gcb.14904

Kumordzi, B. B., Aubin, I., Cardou, F., Shipley, B., Violle, C., and Johnstone, J. (2019). Geographic scale and disturbance influence intraspecific trait variability in leaves and roots of North American understorey plants. *Funct. Ecol.* 33, 1771–1784. doi: 10.1111/1365-2435.13402

Li, Q. K., and Ma, K. P. (2002). Advances in plant succession ecophysiology. *Acta Phytoecol. Sin.* 26, 9–19.

Liu, L. B., Hu, J., Chen, X. Y., Xu, X., Yang, Y., and Ni, J. (2022). Adaptation strategy of karst forests: Evidence from the community-weighted mean of plant functional traits. *Ecol. Evol.* 12:e8680. doi: 10.1002/ece3.8680

Liu, X. J., and Ma, K. P. (2015). Plant functional traits–concepts, applications and future directions. *Sci. Sin. Vitae* 45, 325–339. doi: 10.1360/N052014-00244

Luo, Y. K., Hu, H. F., Zhao, M. Y., Li, H., Liu, S. S., and Fang, J. Y. (2019). Latitudinal pattern and the driving factors of leaf functional traits in 185 shrub species across eastern China. *J. Plant Ecol.* 12, 67–77. doi: 10.1093/jpe/rtx065

Ma, X. L. (2014). *A study on twig and leaf traits of the shrub species in secondary forest succession process.* Ph.D. thesis. Lanzhou: Northwest Normal University.

McGroddy, M. E., Daufresne, T., and Hedin, L. O. (2004). Scaling C, N, P stoichiometry in forests worldwide, implications of terrestrial redfield-type ratios. *Ecology* 85, 2390–2401. doi: 10.1890/03-0351

Melillo, J. M., McGuire, A. D., Kicklighter, D. W., Moore, I. B., Vorosmarty, C. J., and Schloss, A. L. (1993). Global climate change and terrestrial net primary production. *Nature* 363, 234–240. doi: 10.1038/363234a0

Meng, T. T., Ni, J., and Wang, G. H. (2007). Plant functional traits, environments and ecosystem functioning. *Chin. J. Plant Ecol.* 31, 150–165. doi: 10.17521/cjpe.2007.0019

Mensens, C., Laender, F. D., Janssen, C. R., Sabbe, K., and Troch, M. D. (2017). Different response-effect trait relationships underlie contrasting responses to two chemical stressors. *J. Ecol.* 105, 1598–1609. doi: 10.1111/1365-2745.12777

Moridi, M., Sefidi, K., and Etemad, V. (2015). Stand characteristics of mixed oriental beech (*Fagus orientalis* Lipsky) stands in the stem exclusion phase, northern Iran. *Eur. J. For. Res.* 134, 693–703. doi: 10.1007/s10342-015-0883-1

Muscarella, R., Lohbeck, M., Martínez-Ramos, M., Poorter, L., Rodríguez-Velázquez, J. E., van Breugel, M., et al. (2017). Demographic drives of functional composition dynamics. *Ecology* 98, 2743–2750. doi: 10.1002/ecy.1990

Ni, J., Luo, D. H., Xia, J., Zhang, Z. H., and Hu, G. (2015). Vegetation in karst terrain of southwestern China allocates more biomass to roots. *Solid Earth* 6, 799–810. doi: 10.5194/se-6-799-2015

Quested, H., Eriksson, O., Fortunel, C., and Garnier, E. (2007). Plant traits relate to whole-community litter quality and decomposition following land use change. *Funct. Ecol.* 21, 1016–1026. doi: 10.1111/j.1365-2435.2007.01324.x

Rosbakh, S., Romermann, C., and Poschlod, P. (2015). Specific leaf area correlates with temperature: New evidence of trait variation at the population, species and community levels. *Alp. Bot.* 125, 79–86. doi: 10.1007/s00035-015-0150-6

Scheiner, S. M., and Lyman, R. F. (1991). The genetics of phenotypic plasticity. II. Response to selection. *J. Evol. Biol.* 4, 23–50. doi: 10.1046/j.1420-9101.1991.4010023.x

Siefert, A., Violle, C., Chalmandrier, L., Albert, C. H., Taudiere, A., Fajardo, A., et al. (2015). A global meta-analysis of the relative extent of intraspecific trait variation in plant communities. *Ecol. Lett.* 18, 1406–1419. doi: 10.1111/ele.12508

Song, G. M., Han, T. T., Hong, L., Zhang, L. L., Li, X. B., and Ren, H. (2018). Advances in the studies of plant functional traits during succession. *Ecol. Sci.* 37, 207–213.

Song, Y. C. (2013). *China evergreen broad-leaved forest: Classification, ecology, conservation*. Beijing: Science Press.

Song, Y. C., and Wang, X. R. (1995). *Vegetation and flora of Tiantong national forest park Zhejiang province*. Shanghai: Shanghai Science and Technical Literature Press.

Thuiller, W., Lavorel, S., Midgley, G., Lavergne, S., and Rebelo, T. (2004). Relating plant traits and species distributions along bioclimatic gradients for 88 *Leucadendron* taxa. *Ecology* 85, 1688–1699. doi: 10.1890/03-0148

Vandewalle, M., Bello, F., Berg, M. P., Bolger, T., Dolédec, S., Dubs, F., et al. (2010). Functional traits as indicators of biodiversity response to land use changes across ecosystems and organisms. *Biodivers. Conserv.* 19, 2921–2947. doi: 10.1007/s10531-010-9798-9

Vanneste, T., Valdés, A., Verheyen, K., Perring, M. P., Bernhardt-Römermann, M., Andrieu, E., et al. (2019). Functional trait variation of forest understorey plant

communities across Europe. *Basic Appl. Ecol.* 34:02356900. doi: 10.1016/j.baae.2018.09.004

Violle, C., Navas, M. L., Vile, D., Kazakou, E., Fortunel, C., Hummel, I., et al. (2007). Let the concept of trait be functional! *Oikos* 116, 882–892. doi: 10.1111/j.0030-1299.2007.15559.x

Wang, C. Y., Xiao, H. G., Liu, J., and Zhou, J. W. (2016b). Differences in leaf functional traits between red and green leaves of two evergreen shrubs *Photinia* × *fraseri* and *Osmanthus fragrans*. *J. For. Res.* 28, 473–479. doi: 10.1007/s11676-016-0346-7

Wang, M., Wang, P. C., Guo, J. C., Xu, J. S., Chai, Y. F., and Yue, M. (2017). Relationships among leaf, stem and root traits of the dominant shrubs from four vegetation zones in Shanxi province, China. *Isr. J. Ecol. Evol.* 63, 25–32. doi: 10.1163/22244662-06301005

Wang, R. L., Yu, G. R., He, N. P., Wang, Q. F., Zhao, N., and Xu, Z. W. (2016a). Altitudinal variation in the covariation of stomatal traits with leaf functional traits in Changbai Mountain. *Acta Ecol. Sin.* 36, 2175–2184. doi: 10.5846/stxb201411042162

Wang, X. H., Huang, J. J., and Yan, E. R. (2004). Leaf litter decomposition of common trees in Tiantong. *Acta Phytoecol. Sin.* 28, 457–467. doi: 10.17521/cjpe.2004.0063

Wang, Y. Q., Cadotte, M. W., Chen, J. H., Mi, X. C., Ren, H. B., Liu, X. J., et al. (2020). Neighborhood interactions on seedling survival were greatly altered following an extreme winter storm. *For. Ecol. Manag.* 461:117940. doi: 10.1016/j.foreco.2020.117940

Weiher, E., and Keddy, P. A. (1995). Assembly rules, null models, and trait dispersion: New question front old patterns. *Oikos* 74, 159–164. doi: 10.2307/3545686

Wright, I. J., Reich, P. B., Westoby, M., Ackerly, D. D., Baruch, Z., Bongers, F., et al. (2004). The worldwide leaf economics spectrum. *Nature* 428, 821–827. doi: 10.1038/nature02403

Yan, E. R., Wang, X. H., and Zhou, W. (2008). Characteristics of litterfall in relation to soil nutrients in mature and degraded evergreen broad-leaved forests of Tiantong, east China. *Chin. J. Plant Ecol.* 32, 1–12.

Yang, X. D., Yan, E. R., Chang, S. X., Wang, X. H., Zhao, Y. T., and Shi, Q. R. (2014). Twig-leaf size relationship in woody plants vary intraspecifically along a soil moisture gradient. *Acta Oecol.* 60, 17–25. doi: 10.1016/j.actao.2014.07.004

Zhang, Q. F., Song, Y. C., and You, W. H. (1999). Relationship between plant community secondary succession and soil fertility in Tiantong, Zhejiang province. *Acta Ecol. Sin.* 19, 174–178.

Zhang, Q. Q., Zhou, L. L., Zhao, Y. T., Xu, M. S., and Yan, E. R. (2016). Litterfall dynamics of plants in a successional series of evergreen broad-leaved forests in Tiantong region, Zhejiang province. *Chin. J. Ecol.* 35, 290–299.

Zhang, R. Y., Li, Y. P., Ni, Y. L., Gui, X. J., Lian, J. Y., and Ye, W. H. (2019). Intraspecific variation of leaf functional traits along the vertical layer in a subtropical evergreen broad-leaved forest of Dinghushan. *Biodivers. Sci.* 27, 1279–1290. doi: 10.17520/biods.2019267

Zhong, Q. L., Liu, L. B., Xu, X., Yang, Y., Guo, Y. M., Xu, H. Y., et al. (2018). Variations of plant functional traits and adaptive strategy of woody species in a karst forest of central Guizhou province, southwestern China. *Chin. J. Plant Ecol.* 42, 562–572. doi: 10.17521/cjpe.2017.0270

Zhou, L. L. (2016). *Intraspecific trait variability: Extent, sources and spatial structure in an evergreen broad-leaved forest in Tiantong, Zhejiang Province*. Ph.D. thesis. Shanghai: East China Normal University.

frontiers | Frontiers in Ecology and Evolution

TYPE Original Research
PUBLISHED 09 January 2023
DOI 10.3389/fevo.2022.1107421

OPEN ACCESS

EDITED BY
Xiang Liu,
Lanzhou University,
China

REVIEWED BY
Wensheng Bu,
Jiangxi Agricultural University,
China
Yi Ding`,
Chinese Academy of Forestry, China

*CORRESPONDENCE
Qiu Yang
✉ yangqiu0903@163.com

†These authors have contributed equally to this work

SPECIALTY SECTION
This article was submitted to Conservation and Restoration Ecology, a section of the journal Frontiers in Ecology and Evolution

RECEIVED 24 November 2022
ACCEPTED 22 December 2022
PUBLISHED 09 January 2023

CITATION
Yang H, Huang T, Li Y, Liu W, Fu J, Huang B and Yang Q (2023) Spatial heterogeneity and influence mechanisms on soil respiration in an old-growth tropical montane rainforest with complex terrain. *Front. Ecol. Evol.* 10:1107421. doi: 10.3389/fevo.2022.1107421

Spatial heterogeneity and influence mechanisms on soil respiration in an old-growth tropical montane rainforest with complex terrain

Huai Yang[1,2†], Ting Huang[3†], Yide Li[2,4], Wenjie Liu[5], Jialin Fu[6], Biao Huang[6] and Qiu Yang[5*]

[1]Institute of Tropical Bamboo, Rattan and Flower, Sanya Research Base, International Centre for Bamboo and Rattan, Sanya, China, [2]Jianfengling National Key Field Observation and Research Station for Tropical Forest Ecosystem, Hainan Island, Ledong, China, [3]Urban-rural Construction College, Guangxi Vocational University of Agricultural, Guangxi, China, [4]Research Institute of Tropical Forestry, Chinese Academy of Forestry, Guangzhou, China, [5]School of Ecology and Environment, Hainan University, Haikou, China, [6]International Center for Bamboo and Rattan, Beijing, China

Introduction: Although numerous studies have investigated ecosystem-scale soil respiration (SR) at different ecosystem, our understanding of spatial heterogeneity of SR at plot scale is still incomplete, especially in tropical rainforests with complex topography. Further, the ecological factors that drive the variability of SR in tropical rainforests is also poorly understood.

Methods: Here, we investigated the spatial variations and control mechanisms of SR in a 60-ha plot of old-growth tropical rainforest with complex topography. Specifically, we sampled a 60-ha plot in intervals of 20m to measure SR with LI-8100, used semi-variogram of geostatistical tools to examine spatial heterogeneity of SR.

Results: The mean SR rate in this plot was 4.312±0.0410 (SE) μmol m^{-2} s^{-1}. Geostatistical analysis indicated that the SR rate at this plot had a moderate spatial dependence, with a nugget-to-sill ratio of 68.1%. The coefficients variance of SR was 36.2% and the patch size was approximately 112 m. Stepwise linear regression analysis (involving a multiple regression tree) revealed that the independent factors regulated different types of SR's. Liner mix-effect models showed that SR was significantly positively related to soil phosphorus and negatively to the slope in the 60-ha plot. Spatial disturbance of SR along multidimensional habitats that an increase in elevation of the multidimensional habitat, which was accompanied by enhanced SOC and soil phosphorous, also increased its SR in the 60-ha plot.

Discussion: This study would be helpful in designing future field experiments for a better understanding of SR at plot scale.

KEYWORDS

spatial heterogeneity, soil respiration, soil topography, soil properties, geostatistical analysis

1. Introduction

Soil organic carbon (SOC) is the largest pool of carbon (C) in terrestrial ecosystems on a global scale, and soil respiration (SR) is a crucial pathway for the transferring of C to the atmosphere. Even small changes in SR may strongly affect atmospheric CO_2 (Haaf et al., 2021; Watts et al., 2021), and then affect climate change in future. The SR is an important component of the carbon cycle and a sensitive indicator for the overall belowground biogeochemical processes in terrestrial ecosystems (Lei et al., 2021). However, the amount and regulation factors of SR show great uncertainties. Therefore, accurately monitoring and evaluation of SR could meaningfully contribute to predict climate change.

Accurate quantification of SR was extremely difficult largely due to its high variability at different spatial scales (Stell et al., 2021). In fact, spatial heterogeneity of SR was influenced by various soil factors, such as soil nutrient availability (Liang et al., 2021; Xiao et al., 2021), soil C/nitrogen (N)ratio (Cui et al., 2021), soil moisture and temperature (Numa et al., 2021). Moreover, soil topography was regarded as the main factor that was involved the induction of spatial variation of SR (Zhang et al., 2021). Topography, generated a local microclimate, led to variations in soil drainage and SOC distribution, and a change in the soil moisture and temperature, which directly influenced SR (Kang et al., 2003). However, investigation of the influence of complex topography on SR is limited (Chambers et al., 2004).

The magnitude of spatial variation in soil CO_2 could be larger in a tropical forest as compared to other forest ecosystems (Boonriam et al., 2021; Cai et al., 2021). A few studies conducted in undisturbed forest have focused on temporal variation in SR (Hashimoto et al., 2004; Lei et al., 2021). Our knowledge on spatial variations of SR in tropical forests, especially in Asia, is still very poor (Feng and Zhu, 2019).

Environmental perturbations affected abiotic factors could alter SR. For example slope aspect might determine SR rates by modifying the microclimatic conditions (Martínez-García et al., 2017). SR was higher in the upper part of the slope and lower in the lower part (Ohashi and Gyokusen, 2007). However, SR was 6.0% higher in the lower than upper slope over the 2 growing seasons (Xu and Wan, 2008). In the natural forests slope position had a significant effect on SR (Zhao et al., 2018). Most of these studies have indicated that the difference in soil water content between different positions along a slope was the main factor contributing to spatial variation of SR (Takahashi et al., 2011; Hereș et al., 2021). Although the altitude was a variable including various environmental factors, it might be used as a surrogate parameter of SOC (Moriyama et al., 2013). SR was mainly depended on soil temperature (Karhu et al., 2014). Other abiotic factors such as soil texture, SOC, soil nitrogen (SN), C/N ratio and soil phosphorus (SP) could also influence SR (Su et al., 2016; Yazdanpanah et al., 2016). N addition could significantly promote SR (Li et al., 2022). The responses of SR to N addition were also mediated by topography (Duan et al., 2023). Phosphorus (P) addition significantly increased SR by 17.4% in tropical forest, changes of C pools might drive the responses of SR to P addition (Feng and Zhu, 2019). SR was positively related with SOC and P (Tao et al., 2016).

In this study, a series of measurements of SR were conducted in a 60-ha old-growth tropical rainforest with complex topography. Related abiotic factors, such as altitude, convexity, slope, SN, SOC and SP, were also measured to explain the spatial pattern of SR. The specific objectives of this study were to: (i) assess the spatial heterogeneity of SR at the subplot scale (20 m × 20 m) in a tropical rainforest, and (ii) explore the key factors that drive these spatial patterns of SR.

2. Materials and methods

2.1. Study sites

The study was conducted in the Jianfengling National Nature Reserve (JFR), which is located in Ledong county in the southwestern region of Hainan Island, China (latitude and longitude ranges: 18°23′N-18°50′N and 108°36′E-109°05′E, altitude range: 0–1,412 m above sea level). The region comprises mostly of an old-growth tropical montane rainforest (163 km^2) at the northern edge of tropical Asia (Jiang et al., 2002; Wang et al., 2014). It has a tropical monsoon climate that is characterized with distinct wet (May to November) and dry (December to April of the second year) seasons. The mean annual air temperature is 24.5°C, and varies between 19.4°C (January) to 27.3°C (June), whereas there has a yearly mean relative humidity is 88%. The annual rainfall in the region ranges from 1,000 to 3,600 mm, with an average precipitation of 2,449 mm, of which 80–90% occurs from May to October (Zhou et al., 2013; Liu et al., 2021). This region has an irregular topography with granite as the predominant soil parent material. The most common soil type is the montane lateritic red or yellow earth (Xu et al., 2013).

A 60-ha plot was established in the tropical montane rainforest of JFR (Figure 1). It had 1,500 basic plots (20 m × 20 m) with a width of 600 m (East–West) and a length of 1,000 m (South–North; Figure 2). The plot establishment, included topographic mapping (using electronic whole-station theodolites), corner-post setting, and an initial tree census (adapting the techniques developed by the Center for Tropical Forest Science; Condit, 1998), was started in March 2009 and completed in December 2012. The altitude of the plot ranged from 866.3 m to 1016.7 m (Xu et al., 2015).

The primary vegetation of this 60-ha plot is dominated by Lauraceae, Fagaceae, Rubiaceae and Palmaceae families, along with the presence of *Hopea hainanensis* from Dipterocarpaceae, which is a symbol of a typical tropical flora in Southeast Asia. Here, the mean canopy is 23.7 m height, and the mean total basal area per ha is 56 m^2 (Jiang and Lu, 1991).

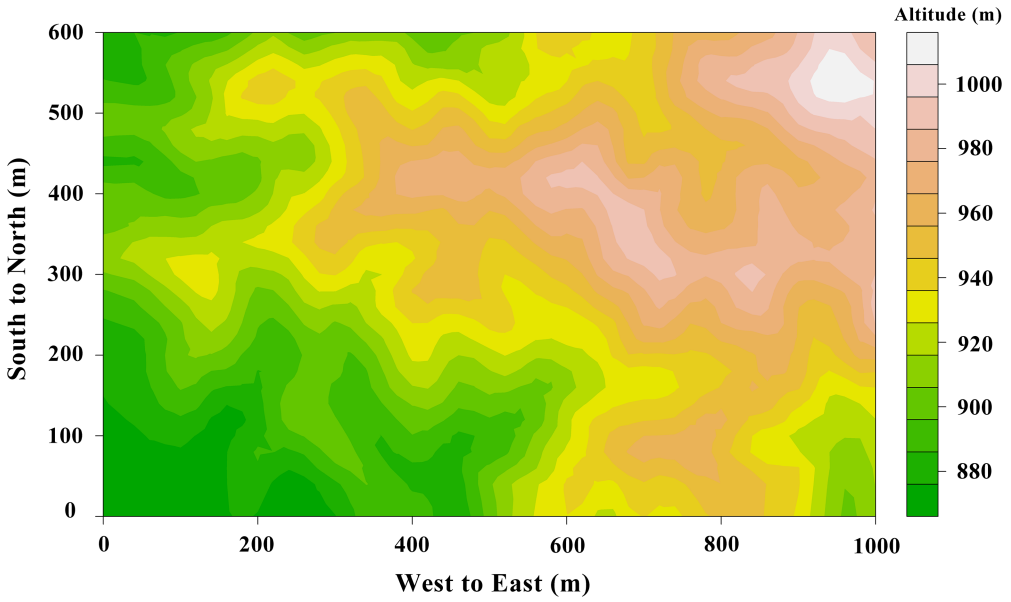

FIGURE 1
The topographic map of 60-ha tropical rainforest plot in Jianfengling, China, color gradient represents the range of altitude (866.3m to 1016.7m).

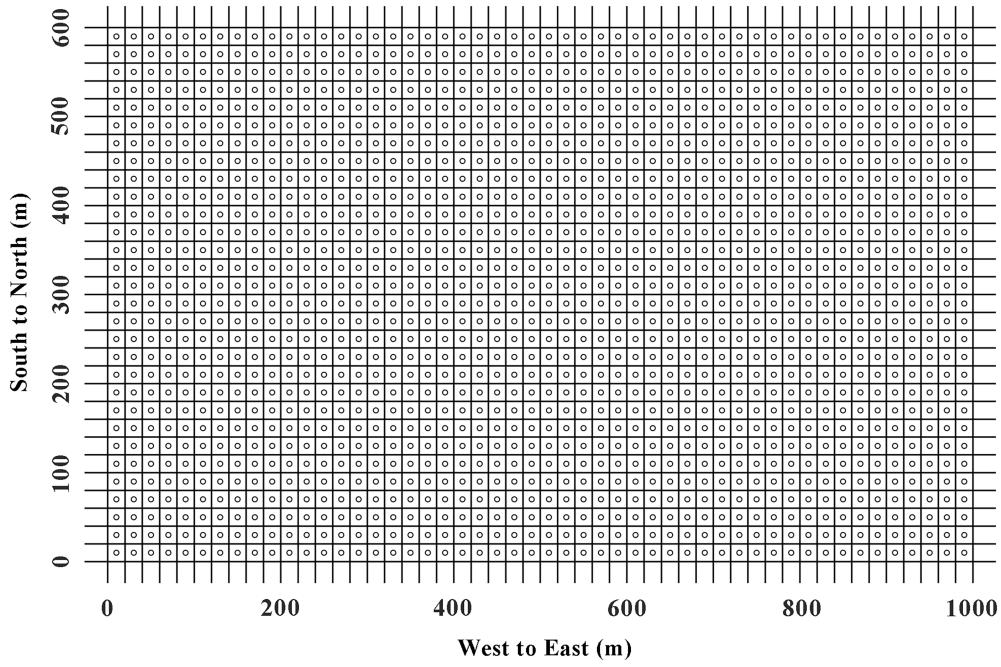

FIGURE 2
The 1,500 measurement points for SR in 60-ha tropical rainforest plot in Jianfengling, China. The blank circles represent the points where SR is tested.

2.2. Sampling design and SR measurements

SR was measured by LI-8100 (LI-COR, Inc., Lincoln, Nebraska United States) from 20th October to 23th November in 2015. In the measurement mode, the LI-8100 system monitors the changes in CO_2 concentration inside the chamber by using an infrared gas analyzer (IRGA). The soil chamber had an internal volume of 4,824 cm^3 with a circular contact area to soil of 317.8 cm^2. Polyvinyl chloride collars were placed in the center of each basic plot

(Figure 2). A collar, 19.6 cm in internal diameter and 5 cm high, was buried in the soil at a depth of 2–3 cm at each point to minimize soil disturbance at least 1 week before the measurement. Plant was not present inside the collars, but small litter and branches were left in the collar. The measurements were replicated three times at each sampling point and the data was collected from 09:00 to 14:00 (Beijing standard time), which represented SR in that day (Sha et al., 2005). This time-frame was regarded as the most suitable period of the day for such types of studies because soil moisture, temperature and SOC were relatively stationary and did not influence the measurements (Yao et al., 2011).

No rainfall occurred during 9-14 h on all days from 20th October to 23th November in 2015 through the experimental plot. At the same time, soil temperature was measured at a depth of 5 cm using a hand-held digital thermometer (SP-E-17 thermometer, Jinzhengmao Instruments China Inc., Beijing), while the chamber temperature at a depth of 5 cm was measured by a conventional thermometer.

The temperature sensitivity of SR was usually described by Q_{10}, which was determined by the following formula:

$$Q_{10} = e^{10b}$$

where b was the soil temperature response coefficient and e was the natural logarithm.

2.3. Soil physical and chemical properties

A 60-ha (600 m × 1,000 m) plot was systematically divided into grids of 40 × 40 m, which generated 416 nodes that were considered as base points. Together with each base point, two additional sampling points were located at random combinations of 2 and 5 m, 2 and 15 m, and 5 and 15 m, along a random compass bearing away from the associated base point. A total of 1,248 topsoil (0–10 cm) samples were collected. Soil samples were air dried, sieved through a 2 mm mesh to remove coarse fragments. SOC was measured with the help of H_2SO_4-$K_2Cr_2O_7$ oxidation method (Schumacher, 2002). SN was measured by the Micro-Kjeldahl method (Bremner, 1960), and the available nitrogen was estimated with the help of a micro-diffusion method (Mulvaney and Khan, 2001). SP were measured by using an inductively coupled plasma atomic-emission spectrometer (Thermo Jarrell Ash Co., Franklin, United States) and HNO_3-$HClO_4$ soil solution (McDowell and Sharpley, 2001). The level of available phosphorus was estimated colorimetrically based on measurements from a 0.03 mol l^{-1} NH_4F and 0.025 mol l^{-1} HCl soil solution (Allen et al., 1974).

2.4. Statistical analyzes

Statistical outliers were eliminated with the help of Grubbs outlier test (the numbers of valid data points were 1,454). Normality of the datasets was assessed with the one-sample Kolmogorov–Smirnov (K-S) test before data analyzes, the datasets would be logarithmically converted if datasets was not a normal distribution. All the analyzes were done in *R* 3.3.0. Principal component analysis (PCA) was used to reduce the number of parameters when several parameters reflected the same underlying process.

2.4.1. Geostatistical methods

Spatial heterogeneity of the SR data was examined with the help of geostatistical tools, which were beneficial for understanding spatially structured phenomena. The theoretical basis of geostatistics used in the current study reflects theories described in several studies (Vieublé Gonod et al., 2006; Liu et al., 2011). Our geostatistics approach consisted of two parts: (i) the calculation of an experimental variogram from the data and model fitting; and (ii) using the knowledge about strength and scale of this variogram to interpolate values of variates at the locations that were not sampled (Burgos et al., 2006).

The calculation of semivariances from the field data and fitting of the models to a semi-variogram was performed using the R 3.3.0 (package gstat; R Foundation for Statistical Computing, Vienna, Austria). Semi-variogram computation was also performed, as following, to ascertain the strength and scale of the spatial dependence of SR.

$$\gamma(h) = \frac{1}{2N(h)} \sum_{i=1}^{N(h)} \left[Z(x_i) - Z(x_i + h) \right]^2$$

where γ(h) was the semivariance for the lag interval h, Z(xi) and Z(xi + h) were the variables at locations xi and xi + h, and N(h) was the number of lag pairs separated by a distance interval h (Stoyan et al., 2000; Mitra et al., 2014). Semivariogram modeling and kriging estimations were performed on the basis of residuals. The final semivariogram model was chosen by minimizing the root mean squared error (RMSE). A spherical model, an exponential model, and a gaussian model were selected to further investigate the spatial structure.

Only isotropic semivariograms were considered for further analysis and the semivariance data was fit to a spherical function. In this analysis, the default active lag distance was set as 60% of the maximum. A typical semivariogram had a nugget variance (C_0), where the nugget represents either a random error or a spatial dependence at a scale smaller than the minimum distance examined (Robertson, 1987). With an increasing lag distance, the variance also increased up to a point of a sill variance ($C_0 + C$), which was spatially independent. The distance at which the sill was reached was called the range. The measurement points estimated within this range were spatially autocorrelated, whereas points outside this range were considered independent (Robertson et al., 1988). The values of the semivariance, and thus C_0 and $C_0 + C$, were scaled to sample variance (Hirobe et al., 2001; Mori and Takeda, 2003). The nugget (C_0) to sill ($C_0 + C$) ratio (NSR) was used to define distinct classes of spatial dependence. If the ratio was ≤25%, the variable was considered as

strongly spatially dependent, a ratio between 25 and 75% indicated the variable to be moderately spatially dependent, and if the ratio was >75%, the variable was considered to be weakly spatially dependent (Liu et al., 2011). The kriging interpolation was hypothesized to be the most accurate when the RMSE was at a minimum and was stable. The accuracy of the kriging method was calculated in the form of RMSE by using the following formula:

$$RMSE = \sqrt{\frac{1}{n}\sum_{i=1}^{n}\left[Y(x_1) - Y^*(x_i)\right]^2}$$

where $Y(x_1)$ was the measured value, $Y^*(x_i)$ was the predicted value, and n was the sampling number.

2.4.2. Linear mixed-effects models

Linear mixed-effects models, computed with the lmer function in the lme4 package of R (Bates et al., 2015), were used to determine the contributions of different factors (e.g., altitude, convexity, slope, and the four soil properties) to the spatial differences in SR. Random effects were groups of topography that could be categorized on the basis of connectivity models (Hierarchical clustering method) and centroid models (partition clustering method, k-means), respectively (Kusiak et al., 1985; Senin et al., 2007). The intercept and slope of altitude, convexity, slope, altitude and convexity, altitude and slope, and convexity and slope were influenced throughout the random effects. Based on the Akaike information criterion (AIC) of these models, the best optimal model was chosen when AIC was the minimum.

2.4.3. Kernel methods for estimating SR along multidimensional habitats

The distribution of SR, soil temperature, altitude, SOC and SP along an environmental gradient were estimated by the methods of Xu et al. (2015). The environmental space was defined as the first and second ordination axes (PC1and PC2) of the PCA of altitude, convexity, slope, and the four soil properties.

3. Results

3.1. Spatial patterns of SR

The spatial mean SR of the entire 60-ha plot was 4.327 ± 0.0411 (standard error) μmol $m^{-2} s^{-1}$, and the coefficient of variation (CV) of SR was 36.2%. These findings were confirmed by semivariogram analysis (Figure 3), and the best-fit semivariogram models and important parameters were provided in Table 1. The range of SR autocorrelation was 112.7 m, and the NSR was 68.1% indicated that there was a moderate spatial dependency of SR (Table 1). The contour maps, obtained by ordinary kriging for SR (Figure 4), showed a patchy distribution pattern.

3.2. Stepwise linear regression analysis of SR

On the basis of a multiple regression tree, 1,454 sampling plots were divided into six types of low altitude (altitude < 914.4, type 1), high altitude(altitude > 991.5, type 2), low convexity and low slope (altitude; 963.5–991.5, convexity < 2.5, slope < 23.6, type 3), low convexity and high slope (altitude; 963.5–991.5, convexity < 2.5, slope ≥ 23.6, type 4), low convexity (altitude; 914.4–963.5, convexity < 2.5, type 5), and high convexity (altitude; 914.4–991.5, convexity ≥ 2.5, type 6; Figure 5). Stepwise linear regression analysis results showed that the SP was a major influencer for types 1, 2, and 5, whereas the SOC and soil available nitrogen were major influencer for types 3 and 4, respectively (Table 2).

3.3. Relationships between covariates and spatial variability of SR

The linear mix-effect model analysis showed that SR was significantly positive correlated to SP, and negatively to the slope in all subplots (Figure 6; Table 3). The low-nitrogen and high-nitrogen plots were distinguished by k-means clustering method; the soil average nitrogen was 1.930 ± 0.00379 g kg^{-1} (n = 831), 2.245 ± 0.00538 g kg^{-1} (n = 623), respectively. In low-nitrogen plots, SR was significantly positive related to SP, and negatively related to the slope (Figure 7; Table 4). In high-nitrogen subplots, SR was significantly positively related to SOC (Figure 8; Table 5). Also, there was a significant index relationship between SR and soil temperature (Q_{10} of 1.92; Figure 9).

3.4. Spatial disturbance of SR, SN, SOC and SP along multidimensional habitats

The cumulative proportion of altitude, convexity, slope, and the four soil properties, explained by PC1 and PC2, was 57.1% of

TABLE 1 The parameters of semivariogram spherical models for SR.

	Nugget(C_0)	Sill ($C+C_0$)	Range (m)	NSR(C_0/($C+C_0$), %)	Fractal	TheoreticalModel	R^2	RMSE	F-value	Significance
SR	0.160	0.235	112.7	68.1	1.96	Exponential	0.905	1.418	5.651	**

Nugget represents the nugget variance, whereas NSR is the nugget-to-sill ratio, represents structural variance. The variable is considered strongly, moderately and weakly spatially dependent when NSR ≤ 25, 25–75% and > 75%, respectively. Range represents the distance over which the structural variance is expressed. Fractal represents the fractal dimension under the isotropic conditions. ** indicate significant differences at $p < 0.01$. F-value is statistical value of F-test.

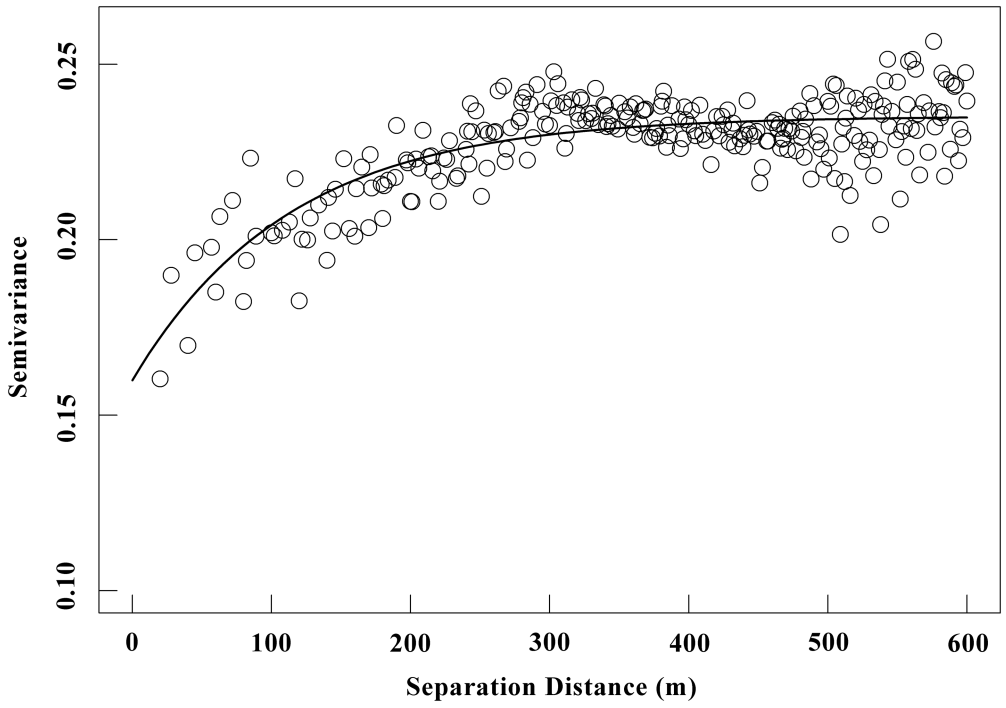

FIGURE 3
Semivariance (γ) of SR versus lag distance within an old-growth tropical rainforest (unit: μmol $m^{-2}s^{-1}$). The solid line represents fitted spherical model (details of the fitted parameters are shown in Table 1), blank circles represent the empirical semivariograms.

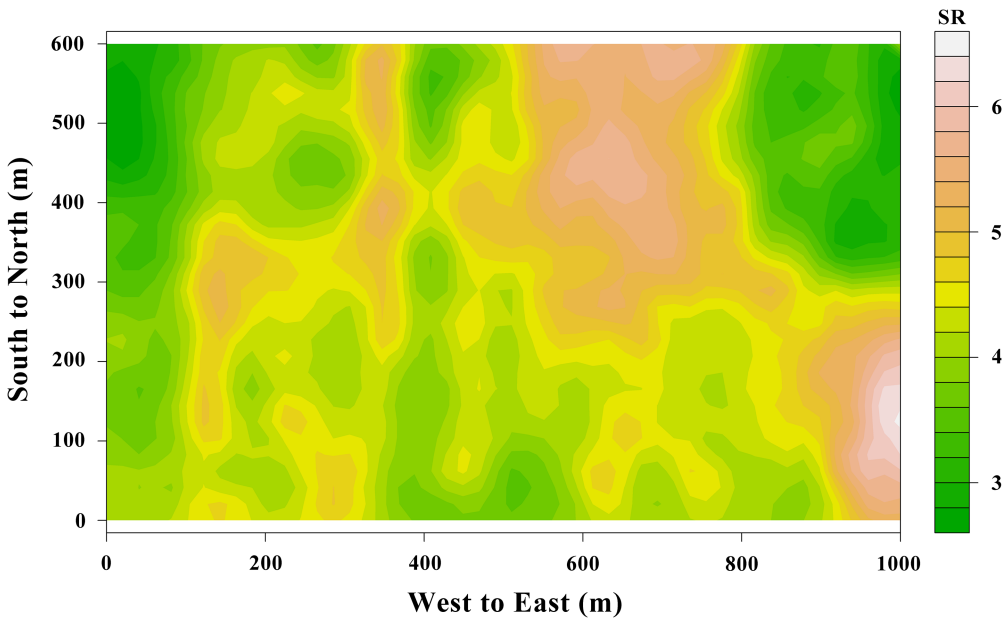

FIGURE 4
The spatial distribution of SR with intervals of 20m from a 60-ha tropical rainforest plot in Jianfengling, China.

the total variance. This showed the distribution of topography and soil properties on the PC1-PC2 axis, indicated a high SR occurs in the habitats of high altitude, high SOC and high SP (Table 6; Figure 10).

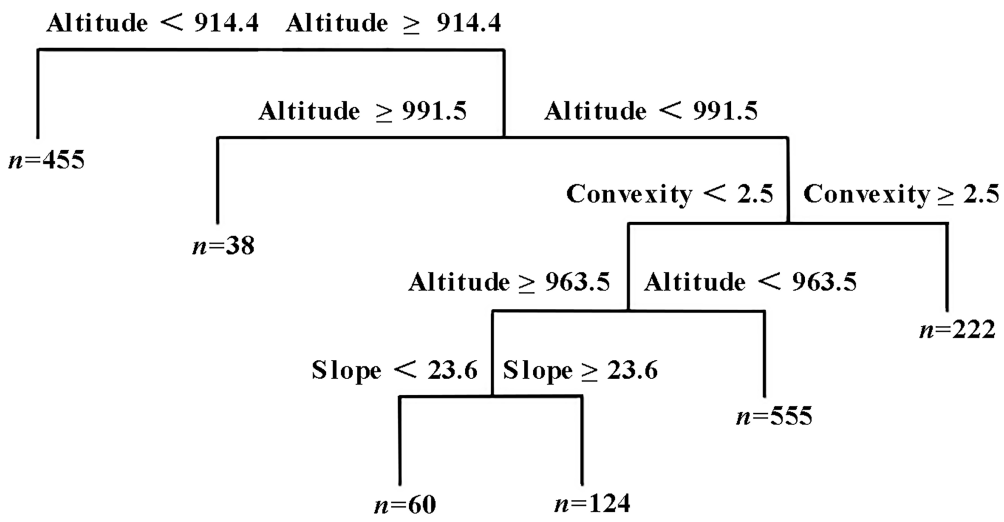

FIGURE 5
A multiple regression tree for SR. SR is the dependent variable, while altitude, convexity and slope are the independent variables. Tree construction is completed by the comprehensive gradient of the elevation, convexity and slope. "*n*" represents the numbers of subplots.

TABLE 2 Stepwise linear regression analysis results between SR and topography, soil properties (*n*=1,454).

Type	Linear equation	Correlation coefficient	*p*-value
1	$Y = 9.138*SP+2.869$	0.094	<0.05
2	$Y = -36.132*SP+8.455$	0.494	<0.01
3	$Y = 0.101*SOC-2.420$	0.307	<0.05
4	$Y = -0.051*$available soil nitrogen $+14.116$	0.300	<0.01
5	$Y = 9.344*SP+3.386$	0.115	<0.01
6	-	-	-

TABLE 3 The estimate of parameters for the optimal liner mixed-effect model in all plots of 60-ha (*n*=1,454).

	Estimate	Std. Error	*t* value	Pr(>|*t*|)
Intercept	−0.2649	0.2275	−1.1647	0.298
Altitude	0.1309	0.0728	1.7971	0.0726
Convexity	0.003	0.0341	0.088	0.9299
Slope	−0.0707	0.027	−2.6143	0.009**
Available nitrogen	−0.0845	0.0565	−1.4963	0.1348
SOC	0.0356	0.0363	0.9801	0.3272
SP	0.0755	0.0306	2.4658	0.0138*
Available phosphorus	0.0034	0.0255	0.1342	0.8933

* and ** indicate significant differences (*$p < 0.05$ and **$p < 0.01$).

4. Discussion

4.1. CV of SR in tropical forests

Quantifying the spatial heterogeneity of SR was a challenging matter, which we accomplished with the help of estimating CV. Here, we found that the CV of tropical montane rainforests in Jianfengling was 36.2%. It was consisted with previous study results of CV for SR of tropical forests in Malaysia (33%) (Katayama et al., 2009) and in Indonesia (36%) (Ishizuka et al., 2005). These were reported over 1,600 m^2 (10 × 10 m) and 567 m^2 (8 × 10 m) grids, respectively. In another Malaysian forest, Kosugi et al. (2007) observed that the CV of SR increased with subplot size, from 29 to 39%, for plot size ranging from 25 to 2,500 m^2, respectively. Further, the CV for SR was 42.7% for 50 lattice positions within a 100 m × 200 m plot (Adachi et al., 2005). Moreover, the spatial variability of SR in perhumid Amazonian and Malaysian rainforests were characterized by CV ranging from 24 to 45% (Schwendenmann et al., 2003; Sotta et al., 2004), and from 26 to 62% (Kosugi et al., 2007; Katayama et al., 2009), respectively. The CV of SR for rainforests in Xishuangbanna was 42% in the rainy seasons and 38% in the dry seasons (Song et al., 2013). Overall, these results showed that the CV of SR in tropical forests generally varied from 20% to 50%.

4.2. Spatial structure of SR

In this study, SR of 60-ha plot had a moderate spatial dependence. Some scholars found SR had a strong spatial

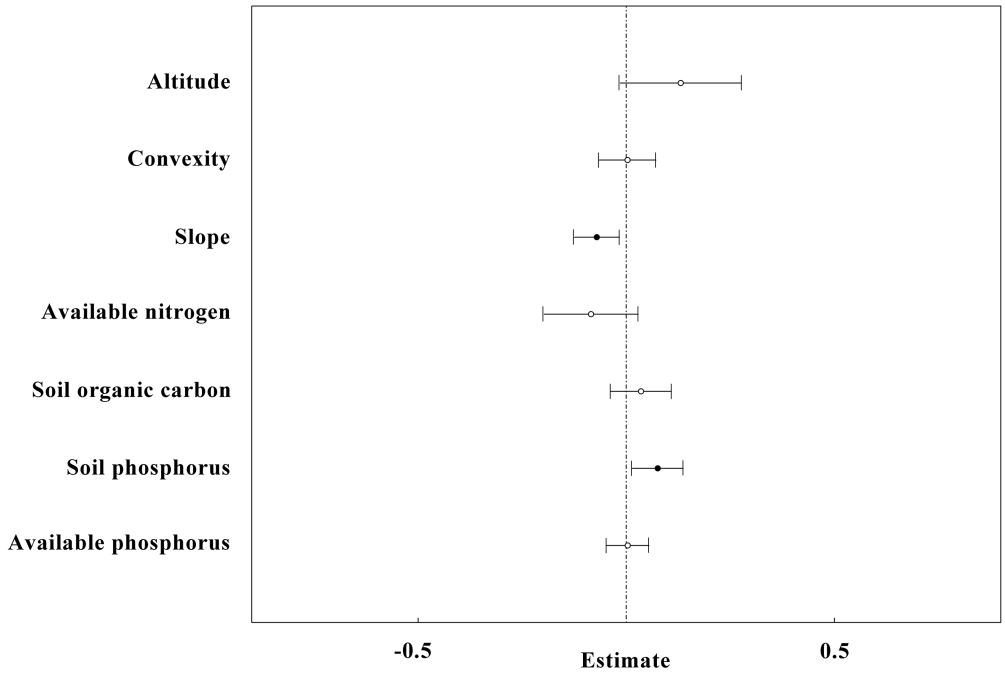

FIGURE 6
The overall result of linear mixed-effects models with all plots (n=1,454) in the study site. SR is the dependent variable, whereas altitude, convexity, slope, SN, available nitrogen, SOC, SP and available phosphorus are independent variables. The black circles and horizontal short lines left to vertical dotted line represent significant level, while the white circles and horizontal short lines intersect to vertical dotted line represent non-significant level.

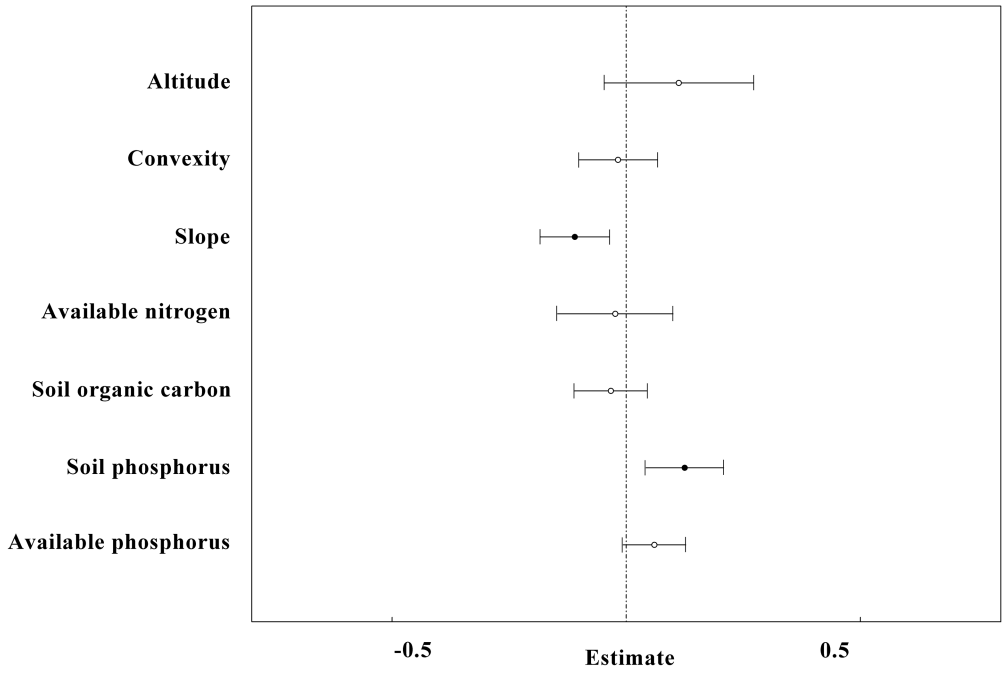

FIGURE 7
The results of linear mixed-effects models for low-nitrogen plots (n=831) in the study site. The black circles and horizontal short lines left to vertical dotted line represent significant levels, while the white circles and horizontal short lines intersect to vertical dotted line represent non-significant levels.

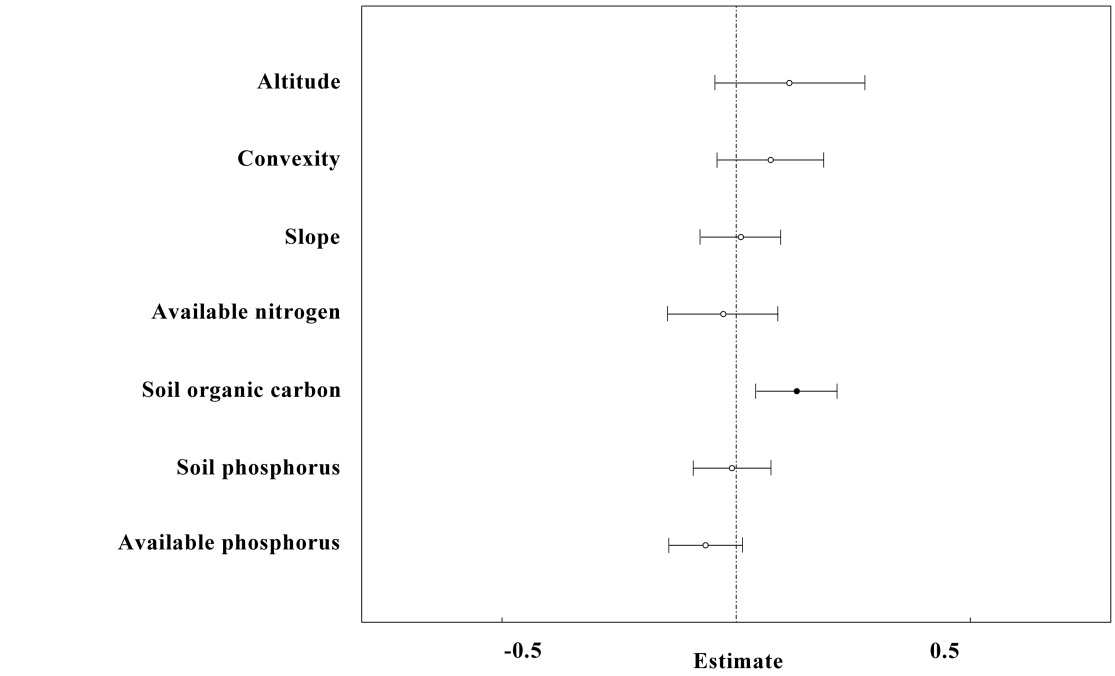

FIGURE 8
The results of linear mixed-effects models for high-nitrogen plots (n=623) in the study site. The black circles and horizontal short lines left to vertical dotted line represent significant levels, while the white circles and horizontal short lines intersect to vertical dotted line represent non-significant level.

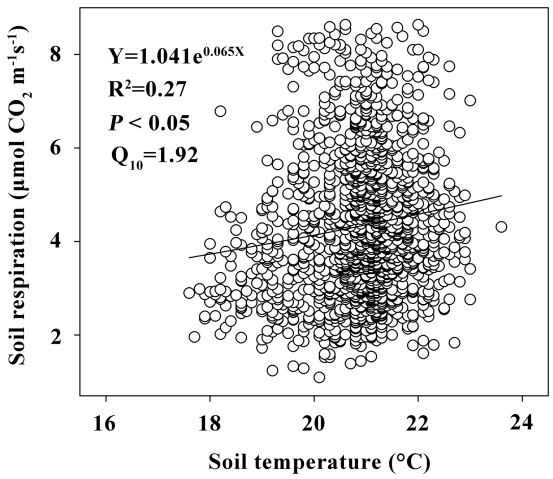

FIGURE 9
The relationships between SR and soil temperature. Y, R^2, P, Q_{10} represents SR, coefficient of determination for this regression equation, probability for rejecting the original assumed, temperature sensitivity of SR, respectively. The circles and line represent SR of each sample point, regression equation, respectively.

TABLE 4 The estimate of parameters for the optimal liner mixed-effect model in low-nitrogen plots of 60-ha (n=831).

	Estimate	Std. Error	t value	Pr(>|t|)
Intercept	−0.0558	0.223	−0.2502	0.8309
Altitude	0.1123	0.0797	1.4089	0.1602
Convexity	−0.0175	0.0422	−0.4146	0.6786
Slope	−0.1099	0.0368	−2.988	0.0029**
Available nitrogen	−0.0236	0.0618	−0.3822	0.7024
SOC	−0.033	0.0388	−0.8507	0.3952
SP	0.1248	0.0415	3.0088	0.0027**
Available phosphorus	0.06	0.0336	1.7889	0.074

* and ** indicate significant differences (*p < 0.05 and **p < 0.01).

dependence in a Southeast Asian tropical rainforest (Kosugi et al., 2007). Investigation of a 20-ha plot, in a seasonal tropical rainforest in Xishuangbanna, also revealed a strong spatial heterogeneity (Song et al., 2013). In this study, the spatial heterogeneity of SR, at small scales (below 20 m) was caused by random factors, accounting for 68.1%, while it was caused by spatially autocorrelated factors at relatively large scales (20 to 112.7 m). There was little information about the spatial structure of SR in tropical forests, and additional studies were needed.

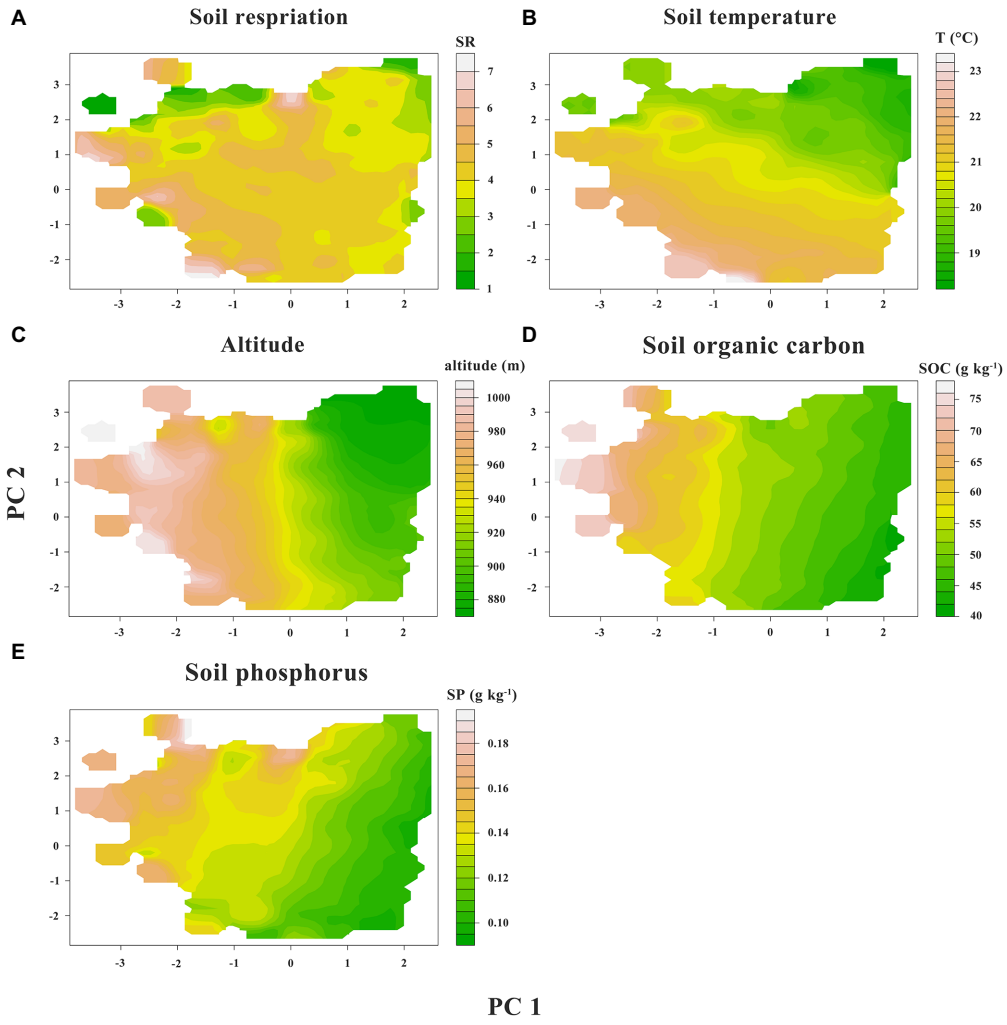

FIGURE 10
Distribution of SR and significantly relevant factors along the first two principal components. Soil temperature, Altitude, Soil organic carbon, Soil phosphorus represent the distribution of Soil temperature, Altitude, Soil organic carbon, Soil phosphorus along the first two principal components, respectively.

4.3. Range of SR

In our study, SR exhibited spatial autocorrelation at the larger scales, across the subplots, with semivariogram ranges of 112.7 m, which have been caused by the influence of large-scale edaphic or topographic gradients, as previously reported by La Scala et al. (2000). They have measured spatial autocorrelation in CO_2 emissions as a result of a heterotrophic activity (bare soil) at scales from 29 to 58 m (La Scala et al., 2000). Kosugi et al. (2007) determined the ranges between 4.4 and 24.7 m on a 50-by 50-m plot for a tropical rainforest. The average range of the spatial autocorrelation for SR was 40 m in rainforests in Xishuangbanna (Song et al., 2013). Furthermore, Pringle and Lark (2006) detected a range of 174 m by using 156 sampling points on a 1,024-m transect, for which incubated bare soil samples were used to measure SR. Since the scales of spatial autocorrelation of SR appear to be ecosystem-and species-specific, nested sampling designs (i.e., two or more sampling intervals) in situations such as ours were recommended (Fox et al., 2015). The scale of measurement of spatial autocorrelation (less than 20 m) from this study might be used as a guide to stratify future sampling schemes in tropical montane rainforests or similar ecosystems. Since the range values were always greater than the chosen grid size, the sampling design was inferred to be adequate for the study site. In addition, column by one column mechanical point sampling was applied in our experiment in order to eliminate the effect of temporal variables. The style was to first do odd columns, followed by even columns. Random factors for mechanical point sampling were not considered; therefore, 1,500 pairs of parameters about distance and angle were randomly generated from 1,500 sub-sample centers as the center; then 1,500 sites were filtered to measure SR for further research.

TABLE 5 The estimate of parameters for the optimal liner mixed-effect model in high-nitrogen plots of 60-ha (n=623).

	Estimate	Std. Error	t value	Pr(>|t|)
Intercept	−0.2432	0.2042	−1.1914	0.2925
Altitude	0.1136	0.0798	1.4225	0.156
Convexity	0.0737	0.0566	1.3009	0.1938
Slope	0.0098	0.0425	0.2301	0.8181
Available nitrogen	−0.0278	0.0586	−0.4737	0.6359
SOC	0.1294	0.043	3.0117	0.0027**
SP	−0.0094	0.0412	−0.2276	0.82
Available phosphorus	−0.0656	0.0389	−1.6878	0.092

** indicate significant differences (**$p < 0.01$).

TABLE 6 Results of the principal components analysis.

Component	PC1	PC2
Eigenvalues	2.87	1.13
Percent	41.0	16.1
Cumulative percent	41.0	57.1
Eigenvectors		
Altitude	0.53*	0.10
Convexity	0.16	0.80*
Slope	0.11	0.12
Available nitrogen	0.54*	−0.13
SOC	0.49*	0.17
SP	0.38*	−0.44*
Available phosphorus	0.13	−0.32*

(*): |Eigenvectors| >0.30|. These percent reflect the fraction of total variance accounted for by each principal component explained by various components of the PCA.

4.4. Influence mechanism of SR

The relationships illustrated in this study advances our understanding of the ecological variables that affected spatial patterns of SR within a forest. This was necessary for enhancing the understanding of mechanistic basis of SR models (Chen et al., 2011; Martin et al., 2012). Spatial relationships were found between SR, soil environment, and topography, but models were not identical across all the plots of 60-ha of sampled area. This suggested that SR might have responded to ecological covariates at varying spatial and temporal scales, created a complex pattern of SR that was not easily modeled. Spatial variations of SR in the forests have been ascribed to differences in soil C (Soe and Buchmann, 2005; Saiz et al., 2006). Many measurements suggested that SOC could be one of the main determinants of SR, particularly at large spatial and temporal scales (Giardina et al., 2003; Davidson and Janssens, 2006). Since it involved the conversion of organic to inorganic C, SR was ultimately controlled by the supply of C (Wan et al., 2007). And significantly positive relationships between SR and SOC had been reported (Chen et al., 2010). Further, SR was reported to be strongly related to SOC in a tropical rain forest in French Guiana (Epron et al., 2006). It was important to know the factors and mechanisms that controlled the spatial pattern of SR for scaling up and predicted patterns of soil C emissions. These results suggested that several soil topography and chemical factors, such as altitude, SOC, and SP, controlled the spatial distribution of SR at this site. Physical and chemical conditions of soil were also related directly and indirectly to SR, increased the complexity of SR. The next step in the process of investigation would be to independently confirm the inferences drawn in our study by generating more datasets.

We observed that the effect of convexity on SR was complex: in the lower N range, the relationship between SR and convexity was negative (Figure 7). However, in the higher N range, the relationship was positive (Figure 8). These effects could offset each other when the data was generalized over the whole of the 60-ha plot, and there was no significant relationship observed initially between convexity and SR (Figure 6). Similarly, the effect of available phosphorus on SR was also two-fold: when N was in the lower range, the relationship between SR and available phosphorus was positive (Figure 7). However, in the higher N range, this relationship became negative (Figure 8). These effects were offset when data of the complete 60 ha-plot was not parsed and no significant relationship between available phosphorus and SR was observed (Figure 6). Tropical ecosystems that were typically developed on old and nutrient-impoverished soils were considered to be rather P limited (Vitousek et al., 2010).

Although soil temperature played a leading role in controlling the temporal patterns of SR, this factor rarely explained the spatial variation of SR (Sotta et al., 2004). Here, we found a weak correlation between the soil temperature and SR ($R^2 < 0.3$; Figure 9). Furthermore, topographically induced microclimates and variations in soil temperature and soil water content could also cause spatial heterogeneity by affecting soil's ability to retain C, water, and nutrients (Kang et al., 2000).

Yang et al. (2018) found that the average emission rate of soil CO_2 during daytime was very close to those for the time from 9:00 to 12:00. Therefore, it was crucial to measure soil CO_2 at this time points as these were the best representatives of the daily flux means. In our study, the measurements of the 1,500 sampling points were carried out during 09:00 to 12:00, and were basically the representatives of the average SR in that day. In our study, the spatial heterogeneity was surveyed only in the dry season. Therefore, more work will be needed to conduct in wet season to fully understand the temporal variation of SR in the tropical rainforest.

5. Conclusion

Investigation involving geostatistical analyzes of a 60-ha permanent plot in an old-growth tropical montane rainforest in

the northwest of Hainan Island (China) revealed a moderate spatial heterogeneity. The variability of 36.2% in SR of this plot was recorded. The patch size of the SR was approximately 112 m. The spatial variation of SR in a tropical rain forest in Jianfengling was closely related to soil's temperature, topography, and other properties. The current study provided some insights in identifing the underlying determinants of spatial variations of SR. This has contributed to develop more mechanistic models of SR. The effect of the community structure of microbes and soil's other properties on SR would be examined in future studies.

Data availability statement

The datasets used or analyzed during the current study are available from the corresponding author on reasonable request.

Author contributions

HY: conceptualization, methodology, software, investigation, formal analysis, and writing–original draft. TH: conceptualization, methodology, software, investigation, formal analysis, and writing–original draft. YL: data curation and writing–original draft. WL: investigation and writing–review and editing. JF: resources. BH: software and validation. QY: conceptualization, funding acquisition, resources, supervision, and writing–review and editing. All authors contributed to the article and approved the submitted version.

Funding

This work was jointly supported by the Fundamental Research Funds of Sanya Research Base, ICBR (1630032022006) and the China Postdoctoral Science Foundation (2018M631414 and 2019T120073).

Conflict of interest

The authors declare that the research was conducted in the absence of any commercial or financial relationships that could be construed as a potential conflict of interest.

The reviewer YD declared a shared parent affiliation with the author YL to the handling editor at the time of review.

Publisher's note

References

Adachi, M., Bekku, Y. S., Konuma, A., Kadir, W. R., Okuda, T., and Koizumi, H. (2005). Required sample size for estimating soil respiration rates in large areas of two tropical forests and of two types of plantation in Malaysia. *For. Ecol. Manag.* 210, 455–459. doi: 10.1016/j.foreco.2005.02.011

Allen, S. E., Grimshaw, H. M., Parkinson, J. A., and Quarmby, C. (1974). *Chemical Analysis of Ecological Materials.* Oxford: Blackwell Scientific Publications.

Bates, D., Mächler, M., Bolker, B., and Walker, S. (2015). Fitting linear mixed-effects models using lme4. *J. Stat. Softw.* 67, 1–48. doi: 10.18637/jss.v067.i01

Boonriam, W., Suwanwaree, P., Hasin, S., Archawakom, T., Chanonmuang, P., and Yamada, A. (2021). Seasonal changes in spatial variation of soil respiration in dry evergreen forest, Sakaerat biosphere reserve, Thailand. *Sci. Asia* 47S:112. doi: 10.2306/scienceasia1513-1874.2021.s009

Bremner, J. M. (1960). Determination of nitrogen in soil by the Kjeldahl method. *J. Agric. Sci.* 55, 11–33. doi: 10.1017/s0021859600021572

Burgos, P., Madejón, E., Pérez-de-Mora, A., and Cabrera, F. (2006). Spatial variability of the chemical characteristics of a trace-element-contaminated soil before and after remediation. *Geoderma* 130, 157–175. doi: 10.1016/j.geoderma.2005.01.016

Cai, Y., Nishimura, T., Ida, H., and Hirota, M. (2021). Spatial variation in soil respiration is determined by forest canopy structure through soil water content in a mature beech forest. *For. Ecol. Manag.* 501:119673. doi: 10.1016/j.foreco.2021.119673

Chambers, J. Q., Tribuzy, E. S., Toledo, L. C., Crispim, B. F., Higuchi, N., Santos, J. D., et al. (2004). Respiration from a tropical forest ecosystem: partitioning of sources and low carbon use efficiency. *Ecol. Appl.* 14, 72–88. doi: 10.1890/01-6012

Chen, X., Post, W. M., Norby, R. J., and Classen, A. T. (2011). Modeling soil respiration and variations in source components using a multi-factor global climate change experiment. *Clim. Chang.* 107, 459–480. doi: 10.1007/s10584-010-9942-2

Chen, Q., Wang, Q., Han, X., Wan, S., and Li, L. (2010). Temporal and spatial variability and controls of soil respiration in a temperate steppe in northern China. *Glob. Biogeochem. Cycles* 24, 1–11. doi: 10.1029/2009gb003538

Condit, R. (1998). *Tropical Forest Census Plots: Methods and results from Barro Colorado Island, Panama and a Comparison with Other Plots*, Berlin: Springer.

Cui, H., Bai, J., Du, S., Wang, J., Keculah, G. N., Wang, W., et al. (2021). Interactive effects of groundwater level and salinity on soil respiration in coastal wetlands of a Chinese delta. *Environ. Pollut.* 286:117400. doi: 10.1016/j.envpol.2021.117400

Davidson, E. A., and Janssens, I. A. (2006). Temperature sensitivity of soil carbon decomposition and feedbacks to climate change. *Nature* 440, 165–173. doi: 10.1038/nature04514

Duan, P., Xiao, K., Wang, K., and Li, D. (2023). Responses of soil respiration to nitrogen addition are mediated by topography in a subtropical karst forest. *Catena* 221:106759. doi: 10.1016/j.catena.2022.106759

Epron, D., Bosc, A., Bonal, D., and Freycon, V. (2006). Spatial variation of soil respiration across a topographic gradient in a tropical rain forest in French Guiana. *J. Trop. Ecol.* 22, 565–574. doi: 10.1017/s0266467406003415

Feng, J., and Zhu, B. (2019). A global meta-analysis of soil respiration and its components in response to phosphorus addition. *Soil Biol. Biochem.* 135, 38–47. doi: 10.1016/j.soilbio.2019.04.008

Fox, G. A., Negrete-Yankelevich, S., and Sosa, V. J. (2015). *Ecological Statistics: Contemporary Theory and Application*, Oxford: Oxford University Press.

Giardina, C. P., Ryan, M. G., Binkley, D., and Fownes, J. H. (2003). Primary production and carbon allocation in relation to nutrient supply in a tropical experimental forest. *Glob. Chang. Biol.* 9, 1438–1450. doi: 10.1046/j.1365-2486.2003.00558.x

Haaf, D., Six, J., and Doetterl, S. (2021). Global patterns of geo-ecological controls on the response of soil respiration to warming. *Nat. Clim. Chang.* 11, 623–627. doi: 10.1038/s41558-021-01068-9

Hashimoto, S., Tanaka, N., Suzuki, M., Inoue, A., Takizawa, H., Kosaka, I., et al. (2004). Soil respiration and soil CO_2concentration in a tropical forest, Thailand. *J. For. Res.* 9, 75–79. doi: 10.1007/s10310-003-0046-y

Hereş, A. M., Bragă, C., Petritan, A. M., Petritan, I. C., and Curiel Yuste, J. (2021). Spatial variability of soil respiration and its controls are subjected to strong seasonality in an even-aged European beech (*Fagus sylvatica* L.) stand. *Eur. J. Soil Sci.* 72, 1988–2005. doi: 10.1111/ejss.13116

Hirobe, M., Ohte, N., Karasawa, N., Zhang, G.-S., Wang, L.-H., and Yoshikawa, K. (2001). Plant species effect on the spatial patterns of soil properties in the mu-us desert ecosystem, Inner Mongolia. *China Plant Soil.* 234, 195–205. doi: 10.1023/a:1017943030924

Ishizuka, S., Iswandi, A., Nakajima, Y., Yonemura, S., Sudo, S., Tsuruta, H., et al. (2005). Spatial patterns of greenhouse gas emission in a tropical rainforest in Indonesia. *Nutr. Cycl. Agroecosyst.* 71, 55–62. doi: 10.1007/s10705-004-5284-7

Jiang, Y. Y., and Lu, J. P. (1991). *Tropical Forest Ecosystems in Jianfengling, Hainan Island*, China: Science Press, Beijing.

Jiang, Y., Wang, B., Zang, R., Jin, J., and Liao, W. (2002). *The Biodiversity and its Formation Mechanism of the Tropical Forests in Hainan Island*, Science Press, Beijing, China.

Kang, S., Doh, S., Lee, D., Lee, D., Jin, V. L., and Kimball, J. S. (2003). Topographic and climatic controls on soil respiration in six temperate mixed-hardwood forest slopes, Korea. *Glob. Chang. Biol.* 9, 1427–1437. doi: 10.1046/j.1365-2486.2003.00668.x

Kang, S., Kim, S., Oh, S., and Lee, D. (2000). Predicting spatial and temporal patterns of soil temperature based on topography, surface cover and air temperature. *For. Ecol. Manag.* 136, 173–184. doi: 10.1016/s0378-1127(99)00290-x

Karhu, K., Auffret, M. D., Dungait, J. A. J., Hopkins, D. W., Prosser, J. I., Singh, B. K., et al. (2014). Temperature sensitivity of soil respiration rates enhanced by microbial community response. *Nature* 513, 81–84. doi: 10.1038/nature13604

Katayama, A., Kume, T., Komatsu, H., Ohashi, M., Nakagawa, M., Yamashita, M., et al. (2009). Effect of forest structure on the spatial variation in soil respiration in a Bornean tropical rainforest. *Agric. For. Meteorol.* 149, 1666–1673. doi: 10.1016/j.agrformet.2009.05.007

Kosugi, Y., Mitani, T., Itoh, M., Noguchi, S., Tani, M., Matsuo, N., et al. (2007). Spatial and temporal variation in soil respiration in a Southeast Asian tropical rainforest. *Agric. For. Meteorol.* 147, 35–47. doi: 10.1016/j.agrformet.2007.06.005

Kusiak, A., Vannelli, A., and Kumar, K. R. (1985). *Clustering Analysis: Models and Algorithms*, Champaign: College of Commerce and Business Administration, University of Illinois at Urbana-Champaign.

La Scala, N., Marques, J., Pereira, G. T., and Cora, J. E. (2000). Short-term temporal changes in the spatial variability model of CO_2 emissions from a Brazilian bare soil. *Soil Biol. Biochem.* 32, 1459–1462. doi: 10.1016/s0038-0717(00)00051-1

Lei, J., Guo, X., Zeng, Y., Zhou, J., Gao, Q., and Yang, Y. (2021). Temporal changes in global soil respiration since 1987. *Nat. Commun.* 12:403. doi: 10.1038/s41467-020-20616-z

Li, Q., Ma, Q., Gao, J., Zhang, J., Li, Y., Shi, M., et al. (2022). Stumps increased soil respiration in a subtropical Moso bamboo (*Phyllostachys edulis*) plantation under nitrogen addition. *Agric. For. Meteorol.* 323:109047. doi: 10.1016/j.agrformet.2022.109047

Liang, G., Wu, X., Cai, A., Dai, H., Zhou, L., Cai, D., et al. (2021). Correlations among soil biochemical parameters, crop yield, and soil respiration vary with growth stage and soil depth under fertilization. *Agron. J.* 113, 2450–2462. doi: 10.1002/agj2.20699

Liu, W., Jiang, Y., Yang, Q., Yang, H., Li, Y., Li, Z., et al. (2021). Spatial distribution and stability mechanisms of soil organic carbon in a tropical montane rainforest. *Ecol. Indic.* 129:107965. doi: 10.1016/j.ecolind.2021.107965

Liu, W., Su, Y., Yang, R., Yang, Q., and Fan, G. (2011). Temporal and spatial variability of soil organic matter and total nitrogen in a typical oasis cropland ecosystem in arid region of Northwest China. *Environ. Earth Sci.* 64, 2247–2257. doi: 10.1007/s12665-011-1053-5

Martin, J. G., Phillips, C. L., Schmidt, A., Irvine, J., and Law, B. E. (2012). High-frequency analysis of the complex linkage between soil CO_2 fluxes, photosynthesis and environmental variables. *Tree Physiol.* 32, 49–64. doi: 10.1093/treephys/tpr134

Martínez-García, E., López-Serrano, F. R., Dadi, T., García-Morote, F. A., Andrés-Abellán, M., Pumpanen, J., et al. (2017). Medium-term dynamics of soil respiration in a Mediterranean mountain ecosystem: the effects of burn severity, post-fire burnt-wood management, and slope-aspect. *Agric. For. Meteorol.* 233, 195–208. doi: 10.1016/j.agrformet.2016.11.192

McDowell, R. W., and Sharpley, A. N. (2001). Soil phosphorus fractions in solution: influence of fertiliser and manure, filtration and method of determination. *Chemosphere* 45, 737–748. doi: 10.1016/s0045-6535(01)00117-5

Mitra, B., Mackay, D. S., Pendall, E., Ewers, B. E., and Cleary, M. B. (2014). Does vegetation structure regulate the spatial structure of soil respiration within a sagebrush steppe ecosystem? *J. Arid Environ.* 103, 1–10. doi: 10.1016/j.jaridenv.2013.12.006

Mori, A., and Takeda, H. (2003). Light-related competitive effects of overstory trees on the understory conifer saplings in a subalpine forest. *J. For. Res.* 8, 163–168. doi: 10.1007/s10310-002-0022-y

Moriyama, A., Yonemura, S., Kawashima, S., Du, M., and Tang, Y. (2013). Environmental indicators for estimating the potential soil respiration rate in alpine zone. *Ecol. Indic.* 32, 245–252. doi: 10.1016/j.ecolind.2013.03.032

Mulvaney, R. L., and Khan, S. A. (2001). Diffusion methods to determine different forms of nitrogen in soil hydrolysates. *Soil Sci. Soc. Am. J.* 65, 1284–1292. doi: 10.2136/sssaj2001.6541284x

Numa, K. B., Robinson, J. M., Arcus, V. L., and Schipper, L. A. (2021). Separating the temperature response of soil respiration derived from soil organic matter and added labile carbon compounds. *Geoderma* 400:115128. doi: 10.1016/j.geoderma.2021.115128

Ohashi, M., and Gyokusen, K. (2007). Temporal change in spatial variability of soil respiration on a slope of Japanese cedar (*Cryptomeria japonica* D. Don) forest. *Soil Biol. Biochem.* 39, 1130–1138. doi: 10.1016/j.soilbio.2006.12.021

Pringle, M. J., and Lark, R. M. (2006). Spatial analysis of model error, illustrated by soil carbon dioxide emissions. *Vadose Zone J.* 5, 168–183. doi: 10.2136/vzj2005.0015

Robertson, G. P. (1987). Geostatistics in ecology: interpolating with known variance. *Ecology* 68, 744–748. doi: 10.2307/1938482

Robertson, G. P., Hutson, M. A., Evans, F. C., and Tiedje, J. M. (1988). Spatial variability in a successional plant community: patterns of nitrogen availability. *Ecology* 69, 1517–1524. doi: 10.2307/1941649

Saiz, G., Green, C., Butterbach-Bahl, K., Kiese, R., Avitabile, V., and Farrell, E. P. (2006). Seasonal and spatial variability of soil respiration in four Sitka spruce stands. *Plant Soil* 287, 161–176. doi: 10.1007/s11104-006-9052-0

Schumacher, B. A. (2002). *Methods for the Determination of Total Organic Carbon (TOC) in Soils and Sediments*. Washington, DC: Ecological Risk Assessment Support Center, 1–23.

Schwendenmann, L., Veldkamp, E., Brenes, T., O'Brien, J. J., and Mackensen, J. (2003). Spatial and temporal variation in soil CO_2 efflux in an old-growth neotropical rain forest, La Selva, Costa Rica. *Biogeochemistry* 64, 111–128. doi: 10.1023/a:1024941614919

Senin, N., Ziliotti, M., and Groppetti, R. (2007). Three-dimensional surface topography segmentation through clustering. *Wear* 262, 395–410. doi: 10.1016/j.wear.2006.06.013

Sha, L., Zheng, Z., Tang, J., Yinghong, W., Yiping, Z., Min, C., et al. (2005). Soil respiration in tropical seasonal rain forest in Xishuangbanna, SW China. *Sci. China Earth Sci.* 48, 189–197. doi: 10.1360/05zd0019

Soe, A. R. B., and Buchmann, N. (2005). Spatial and temporal variations in soil respiration in relation to stand structure and soil parameters in an unmanaged beech forest. *Tree Physiol.* 25, 1427–1436. doi: 10.1093/treephys/25.11.1427

Song, Q. H., Tan, Z. H., Zhang, Y. P., Cao, M., Sha, L. Q., Tang, Y., et al. (2013). Spatial heterogeneity of soil respiration in a seasonal rainforest with complex terrain. *iForest* 6, 65–72. doi: 10.3832/ifor0681-006

Sotta, E. D., Meir, P., Malhi, Y., Nobre, A. D., Hodnett, M., and Grace, J. (2004). Soil CO_2 efflux in a tropical forest in the Central Amazon. *Glob. Chang. Biol.* 10, 601–617. doi: 10.1111/j.1529-8817.2003.00761.x

Stell, E., Warner, D., Jian, J., Bond-Lamberty, B., and Vargas, R. (2021). Spatial biases of information influence global estimates of soil respiration: how can we improve global predictions? *Glob. Chang. Biol.* 27, 3923–3938. doi: 10.1111/gcb.15666

Stoyan, H., De-Polli, H., Böhm, S., Robertson, G. P., and Paul, E. A. (2000). Spatial heterogeneity of soil respiration and related properties at the plant scale. *Plant Soil* 222, 203–214. doi: 10.1023/a:1004757405147

Su, Y. G., Huang, G., Lin, Y. J., and Zhang, Y. M. (2016). No synergistic effects of water and nitrogen addition on soil microbial communities and soil respiration in a temperate desert. *Catena* 142, 126–133. doi: 10.1016/j.catena.2016.03.002

Takahashi, M., Hirai, K., Limtong, P., Leaungvutivirog, C., Panuthai, S., Suksawang, S., et al. (2011). Topographic variation in heterotrophic and autotrophic soil respiration in a tropical seasonal forest in Thailand. *Soil Sci. Plant Nutr.* 57, 452–465. doi: 10.1080/00380768.2011.589363

Tao, X., Cui, J., Dai, Y., Wang, Z., and Xu, X. (2016). Soil respiration responses to soil physiochemical properties in urban different green-lands: a case study in Hefei, China. *Int. Soil Water Conserv. Res.* 4, 224–229. doi: 10.1016/j.iswcr.2016.08.001

Vieublé Gonod, L., Chadoeuf, J., and Chenu, C. (2006). Spatial distribution of microbial 2,4-Dichlorophenoxy acetic acid mineralization from field to microhabitat scales. *Soil Sci. Soc. Am. J.* 70, 64–71. doi: 10.2136/sssaj2004.0034

Vitousek, P. M., Porder, S., Houlton, B. Z., and Chadwick, O. A. (2010). Terrestrial phosphorus limitation: mechanisms, implications, and nitrogen–phosphorus interactions. *Ecol. Appl.* 20, 5–15. doi: 10.1890/08-0127.1

Wan, S., Norby, R. J., Ledford, J., and Weltzin, J. F. (2007). Responses of soil respiration to elevated CO_2, air warming, and changing soil water availability in a model old-field grassland. *Glob. Chang. Biol.* 13, 2411–2424. doi: 10.1111/j.1365-2486.2007.01433.x

Wang, A., Fang, Y. T., Chen, D. X., Koba, K., Makabe, A., Li, Y. D., et al. (2014). Variations in nitrogen-15 natural abundance of plant and soil systems in four remote tropical rainforests, southern China. *Oecologia* 174, 567–580. doi: 10.1007/s00442-013-2778-5

Watts, J. D., Natali, S. M., Minions, C., Risk, D., Arndt, K., Zona, D., et al. (2021). Soil respiration strongly offsets carbon uptake in Alaska and Northwest Canada. *Environ. Res. Lett.* 16:084051. doi: 10.1088/1748-9326/ac1222

Xiao, H. B., Shi, Z. H., Li, Z. W., Chen, J., Huang, B., Yue, Z. J., et al. (2021). The regulatory effects of biotic and abiotic factors on soil respiration under different land-use types. *Ecol. Indic.* 127:107787. doi: 10.1016/j.ecolind.2021.107787

Xu, H., Detto, M., Fang, S., Li, Y., Zang, R., and Liu, S. (2015). Habitat hotspots of common and rare tropical species along climatic and edaphic gradients. *J. Ecol.* 103, 1325–1333. doi: 10.1111/1365-2745.12442

Xu, H., Li, Y. D., Luo, T. S., Chen, D. X., and Lin, M. X. (2013). Environmental factors correlated with species diversity in different tropical rain forest types in Jianfengling, Hainan Island, China. *Chin. J. Plant Ecol.* 37, 26–36. doi: 10.3724/sp.j.1258.2013.00003

Xu, W., and Wan, S. (2008). Water-and plant-mediated responses of soil respiration to topography, fire, and nitrogen fertilization in a semiarid grassland in northern China. *Soil Biol. Biochem.* 40, 679–687. doi: 10.1016/j.soilbio.2007.10.003

Yang, H., Liu, S., Li, Y., and Xu, H. (2018). Diurnal variations and gap effects of soil CO_2, N_2O and CH4 fluxes in a typical tropical montane rainforest in Hainan Island, China. *Ecol. Res.* 33, 379–392. doi: 10.1007/s11284-017-1550-4

Yao, Y., Zhang, Y., Yu, G., Sha, L., Deng, Y., and Tan, Z. (2011). Representative time selection analysis on daily average value of soil respiration in a tropical rain forest. *J. Nanjing For. Univ.* 35, 74–78.

Yazdanpanah, N., Mahmoodabadi, M., and Cerdà, A. (2016). The impact of organic amendments on soil hydrology, structure and microbial respiration in semiarid lands. *Geoderma* 266, 58–65. doi: 10.1016/j.geoderma.2015.11.032

Zhang, Y., Zou, J., Dang, S., Osborne, B., Ren, Y., and Ju, X. (2021). Topography modifies the effect of land-use change on soil respiration: a meta-analysis. *Ecosphere* 12:e03845. doi: 10.1002/ecs2.3845

Zhao, Y. L., Goldberg, S. D., Xu, J. C., and Harrison, R. D. (2018). Spatial and seasonal variation in soil respiration along a slope in a rubber plantation and a natural forest in Xishuangbanna, Southwest China. *J. Mt. Sci.* 15, 695–707. doi: 10.1007/s11629-017-4478-9

Zhou, Z., Jiang, L., Du, E., Hu, H., Li, Y., Chen, D., et al. (2013). Temperature and substrate availability regulate soil respiration in the tropical mountain rainforests, Hainan Island, China. *J. Plant Ecol.* 6, 325–334. doi: 10.1093/jpe/rtt034

frontiers | Frontiers in Ecology and Evolution

TYPE Original Research
PUBLISHED 09 January 2023
DOI 10.3389/fevo.2022.1113742

OPEN ACCESS

EDITED BY
Xiang Liu,
Lanzhou University, China

REVIEWED BY
Shuai Fang,
Institute of Applied Ecology (CAS), China
Fengwei Xu,
Chinese Academy of Forestry, China

*CORRESPONDENCE
Yunquan Wang
✉ yqwang@vip.126.com
Jianhua Chen
✉ sky78@zjnu.cn

†These authors have contributed equally to this work

SPECIALTY SECTION
This article was submitted to Conservation and Restoration Ecology, a section of the journal Frontiers in Ecology and Evolution

RECEIVED 01 December 2022
ACCEPTED 16 December 2022
PUBLISHED 09 January 2023

CITATION
Tian K, Chai P, Wang Y, Chen L, Qian H, Chen S, Mi X, Ren H, Ma K and Chen J (2023) Species diversity pattern and its drivers of the understory herbaceous plants in a Chinese subtropical forest. *Front. Ecol. Evol.* 10:1113742. doi: 10.3389/fevo.2022.1113742

Species diversity pattern and its drivers of the understory herbaceous plants in a Chinese subtropical forest

Kai Tian[1,2†], Pengtao Chai[1†], Yunquan Wang[1*], Lei Chen[3], Haiyuan Qian[4], Shengwen Chen[4], Xiangcheng Mi[3], Haibao Ren[3], Keping Ma[3] and Jianhua Chen[1*]

[1]College of Life Sciences, Zhejiang Normal University, Jinhua, China, [2]College of Life Sciences and Agricultural Engineering, Nanyang Normal University, Nanyang, China, [3]State Key Laboratory of Vegetation and Environmental Change, Zhejiang Qianjiangyuan Forest Biodiversity National Observation and Research Station, Institute of Botany, The Chinese Academy of Sciences, Beijing, China, [4]Center of Ecology and Resources, Qianjiangyuan National Park, Kaihua, China

Understory herbaceous plants are an important component of forest ecosystems, playing important roles in species diversity and forest dynamics in forests. However, the current understanding of the biodiversity of forest communities is mostly from woody plants, and knowledge of community structure and species diversity for understory herbaceous plants remains scarce. In a subtropical forest in China, we investigated understory vascular herbaceous diversity from 300 plots (5 × 5 m) in the main growing season. In this study, we analyzed the community structure and diversity pattern of the understory herbaceous community and linked the species diversity pattern to both abiotic and biotic environments. We found a rich diversity of understory herbaceous communities in this forest (81 species belonging to 55 genera), and floristic elements at the genus level were dominated by tropical elements, followed by temperate elements. The diversity pattern of the understory herbaceous showed a significant habitat preference, with the highest diversity in the lowland valleys and then followed by in middle slopes. In addition, herbaceous diversity was significantly affected by both abiotic factors (such as terrain convexity) and biotic factors (such as the diversity of surrounding woody plants). Our study indicated that species diversity of understory herbaceous showed a remarkable habitat preference, such as lowland valleys, and highlighted the importance of both abiotic and biotic environments in driving herbaceous diversity patterns in the subtropical forest understory.

KEYWORDS

vascular herbaceous plants, community structure, species diversity, Gutianshan, subtropical forest

1. Introduction

Understory herbaceous plants are important components in forest ecosystems worldwide (Murphy et al., 2016), which are the most species-rich plant growth forms, even accounting for 80% of all vascular plant species in temperate forests (Gilliam, 2007). Understory herbaceous communities affect forest regeneration patterns through species interactions with woody plant seedlings (Holeksa, 2003), playing important roles in ecosystem function and biodiversity conservation (Landuyt et al., 2019). In addition, understory herbaceous plants are small in stature and have less-persistent aboveground structures than most woody plants, and their diversity is more sensitive to both spatial and temporal environmental changes (Garg et al., 2022). To date, the majority of our knowledge of forest biodiversity comes from woody plants (Murphy et al., 2016), which only represent a small fraction of biodiversity in the forest community. However, as an important component in forests, knowledge of community structure and species diversity for understory herbaceous communities remains scarce (Wang et al., 2021).

Previous studies showed that the diversity pattern and species coexistence mechanism of herbaceous plants might be quite different from woody plants (Spicer et al., 2021). On the one hand, herbaceous plants and woody plants show quite differences in the root system (Cicuzza et al., 2013), leaves, and stature, which may lead to a significant difference in responding to light resources and available nutrition (Siebert, 2002; Ramadhanil et al., 2008), and ultimately present a different diversity pattern. On the other hand, local environmental factors, such as elevation, slope (Wiharto et al., 2021), soil (Beck and Givnish, 2021; Mao et al., 2021), community edge (De Pauw et al., 2021), thinning intensity (Wang et al., 2021), and climate change (Cacciatori et al., 2022), also have been shown to have significant effects on the diversity of understory herbaceous plants. However, the effect of habitat filtration may be different between woody and herbaceous plants. For example, elevation showed opposite effects on the diversity of woody plants and herbaceous plants (Cicuzza et al., 2013; Xu et al., 2019). Therefore, a more comprehensive analysis of possible mechanisms of understory herbaceous diversity is needed, as are studies on woody plants.

However, these present studies mainly focus on tropical forests and cold temperate forests and usually do not take subtropical understory into consideration (Wang et al., 2021; Garg et al., 2022). Understory herbaceous plants in different climatic zones, such as tropical and temperate forests, may show different species richness and biodiversity (Gilliam, 2007). Moreover, almost no study has been conducted to investigate the effects of both abiotic and biotic environments on understory herbaceous diversity patterns in subtropical forests at the same time. Thus, the assessment of the community structure and diversity pattern of the understory herbaceous community and linked the species diversity pattern to abiotic and biotic environments will further improve our understanding of the ecology of understory herbaceous plant diversity (Lagomarsino et al., 2016).

The subtropical evergreen broad-leaved forest is a typical zonal vegetation type with a vast area in China (Zhu et al., 2008). Its rich vegetation diversity is much higher than that of other evergreen broad-leaved forests, and its species richness is second only to tropical rainforests (Song et al., 2005). However, the research data on herbaceous plant communities in China are limited, especially in the typical subtropical evergreen broad-leaved forest plots (Song et al., 2015).

Thus, in order to understand the community structure and diversity pattern of the understory herbaceous community and the potential contribution of abiotic and biotic environments to the species diversity pattern, we analyzed the community structure and diversity pattern of the understory herbaceous community and linked the species diversity pattern to abiotic and biotic environments in the Gutianshan 24-ha subtropical forest dynamic plot. Specifically, we focused on the following questions:

(1) What is the community structure and diversity pattern of the understory herbaceous community in the subtropical evergreen broad-leaved forest?
(2) To what extent do the species diversity pattern of herbaceous plants in the subtropical understory driven by both abiotic and biotic environments?

2. Materials and methods

2.1. Study area and herbaceous plants survey

The Gutianshan National Nature Reserve (29°10′19.4″–29°17′41.4″N, 118°03′49.7″–118°11′12.2″E) is located in Kaihua County, Zhejiang Province in China, with a total area of 8,107 ha and a typical mid-subtropical evergreen broad-leaved forest (**Supplementary Figure 1A**; Legendre et al., 2009). According to the ForestGEO plot construction standard (Condit, 1998; Davies et al., 2021), the 24-ha (600 m × 400 m) Gutianshan Forest Dynamics Plot (GFDP) was established in 2005 by selecting typical mid-subtropical evergreen broad-leaved forest with dominant species of *Castanopsis eyrei* and *Schima superba* (Legendre et al., 2009). The plot ranges from 446.3 to 714.9 m in elevation, ranges from 12.8 to 62.0° in slope, and ranges from 93.9 to 269.2° in aspect (Ren et al., 2022). The first tree census in the 24-ha forest plot was conducted in 2005 and re-censused at 5-year intervals. All free-standing woody stems ≥1 cm diameter at breast height (d.b.h., 1.3 m) were tagged, measured, mapped, and identified (Legendre et al., 2009;

Wang et al., 2020). According to the first survey, there were 140,700 trees in total, with 159 species belonging to 49 families and 103 genera.

In order to meet the necessary systematic investigation scope and area of systematic investigation and minimize human interference to the plot, on the basis of the original 24-ha plot in Gutianshan, we divided 600 20-m × 20-m unit quadrats (as the basic stations) into two parts evenly in July 2011. Therefore, we conducted a systematic investigation of herbaceous plants in 300 stations with a 5 m × 5 m area. The position of these survey quadrats was relatively fixed in the 20-m × 20-m unit plots; that is, the east of the unit plot was the second 5-m × 5-m quadrat to the north (**Supplementary Figure 1B**). The herbaceous plants in the stations were systematically investigated from August to October in the main growing season in 2011. The species composition of herbaceous vascular plants in each quadrat, the number of individuals of each species (*Poaceae* and *Cyperaceae* record the number of clusters, and ferns that cannot count the number of clusters record the number of members), the average height, the coverage of each species, and the total coverage of all herbaceous vascular plants were all recorded.

2.2. Community structure of understory herbaceous

According to the existing research on the distribution types and floristic division of seed plants (Wu et al., 2003; Li, 2008; Zuo et al., 2017) and ferns (Lu, 2017), the distribution types of herbaceous genera in the plot were divided. We calculated the important value (IV) of each constituent species of the herbaceous plant community in the 24-ha plot by using the survey data of 300 5-m × 5-m quadrats:

$$IV = (\text{relative frequence} + \text{relative coverage} + \text{relative density}) /3 \times 100\% \quad (1)$$

Thus, the relative density refers to the percentage of the number of individuals of one species to the number of individuals of all species in the whole plot.

2.3. Herbaceous diversity and habitat types

We counted the number of herb species (S) in each 5-m × 5-m survey quadrat and calculated the Shannon–Wiener index (H) and Pielou's evenness index (E) (Whittaker, 1972; Whitney and Foster, 1988):

$$H = -\sum_{i=1}^{S} (P_i \ln P_i) \quad (2)$$

$$E = \frac{H}{\ln S} \quad (3)$$

where $P_i = \frac{N_i}{N_0}$, N_0 is the number of individuals of all observed species, N_i is the number of individuals of species i, and S is the species richness.

Based on the multivariate regression tree (MRT) analysis results constructed on the topography, soil, and the first survey data of the plot (Chen et al., 2010), the habitats of the GFDP were divided into the following five types: low valley, low ridge, mid-slope, high slope, and high ridge (**Supplementary Figure 2**). Low ridge and low valley are the two most extensive habitat types among them.

According to the sampling principle of rarefaction (Hurlbert, 1971; Heck et al., 1975), we observed the characteristics of the change curve of community species richness as the sampling number of individual herbaceous plants in the plot increased. We divided herbaceous community individuals based on their habitat types and performed the rarefaction repeated sampling. We compared the abundance of herbaceous plants distributed in different habitats and the differences in the species richness of herbaceous plants in different habitat types under the same sampling amount. We also analyzed the distribution of species diversity index of herbaceous plants in different habitat types by variance analysis and compared the differences in herbaceous plant diversity among different habitat types by the Tukey honestly significant difference (HSD) test.

2.4. Abiotic and biotic drivers of diversity pattern of understory herbaceous

We performed correlation analysis on the total herb coverage, the Shannon–Wiener index (H_{herb}), Pielou's evenness index (E_{herb}), and the main environmental factors of the plot, then calculated the Pearson correlation coefficient matrix among the variables and performed the significance test. Environmental variables that affect the growth of herbaceous plants can reflect environmental factors, such as forest vegetation community coverage, terrain, and light conditions in the quadrat. The variables selected in this study are as follows: terrain concavity and convexity, elevation, slope, and aspect where the plot is located, canopy closure, tree community diversity in the upper and surrounding plots, and the sum of cross-sectional area at breast height (dm^2) during environmental variables that affect the growth of herbaceous plants can reflect environmental factors, such as forest vegetation community coverage, terrain, and light conditions in the quadrat. The four topographic factors are calculated as the same as the 20-m × 20-m plot in which the survey plot is located (Lai et al., 2009); we defined trees on the upper level of the quadrat and surrounding and living

individuals of woody plants with DBH ≥1 cm within a radius of 10 m from the center of the survey plot (including dead, broken and lodging individuals, the data are from the first review of the plot in 2010). The Shannon–Wiener index was used to represent the tree diversity, which is more comprehensive and suitable for tree communities (taking into account both abundance and evenness).

Based on the correlation coefficient test results, we used the distribution patterns of herbaceous plant diversity indices (richness *S*, Shannon–Wiener index *H*, and Pielou's evenness index *E*) in each survey quadrat as fitting variables, performed multiple linear regression fitting with factors that are significantly related to a diversity index as explanatory variables, analyzed the fitting of the model to the variation of the diversity pattern, and compared the effects of each explanatory variable. Then, we further explored the relative importance of each variable to herbaceous plant diversity.

All analyses were performed with R (version 4.1.3): The species diversity index and rarefaction species richness comparison were calculated with the *vegan* package (Jost, 2007). Tukey HSD test was calculated with the *agricolae* package (Hsu, 1996), and the fitted line for scatter graph between variables was performed with *lowess* function (Cleveland, 1979, 1981). The relative importance analysis based on l mg and pmvd methods was implemented by the calc.relimp function in the relaimpo package (Groemping, 2006).

3. Results

3.1. Species composition and flora of understory herbaceous

We recorded a total of 81 species, 31 families, and 55 genera of herbaceous vascular plants in the 24-ha Gutianshan plot (**Supplementary Table 1**). The results of the floristic analysis showed that the world distribution types accounted for the largest proportion of herbaceous community genera, including 15 genera, such as *Dryopteris*, followed by pantropical genera with 12 genera, including local common herbaceous groups, such as *Diplopterygium*, and more genera are widely distributed in Northern hemisphere and East Asia. There are 28 genera of tropical types, accounting for 50.91% of the total, indicating that the herbaceous groups living under the subtropical evergreen broad-leaved forest in Gutianshan are mainly tropical species, while temperate and world distributions account for 49.09% of the total, making it an important constituent group of the herbaceous community (**Table 1**).

The important values of each species are shown in **Supplementary Table 1**; the important value of *Diplopterygium glaucum* is the largest. There are a large number of *D. glaucum* in a total of 162 quadrats, and their rhizomes walk underground with huge leaves, with a wide distribution in the plot. Nearly

TABLE 1 Genus areal types of herbaceous vascular plants in Gutianshan subtropical understory.

Areal-types	Number of genus	Percentage (%)
Cosmopolitan	15	27.27
Pantropic	12	21.82
Old world tropics	3	5.45
Tropical and subtropical	3	5.45
Tropical Asia	3	5.45
Trop. Asia and trop. Australia	3	5.45
Trop. Asia-trop. Afr.	4	7.27
North temperate	5	9.09
East Asia	7	12.73
Total	55	100.00

39,482 clonal component units were counted, accounting for 64.70% of the total number of individuals in the herbaceous plant community. The relative frequency and relative coverage are 11.54 and 81.90%, and the important value is 48.69%, which indicates its extensive distribution and dominant position in the plot. The important values of *Dicranopteris pedata* and *Carex sp.* are also relatively high.

The top 15 important values of herbaceous plants account for 92.19% of the total. These species are the most common in the plot, and their density and coverage are relatively large. In the survey, 24 species of the herbaceous plant appeared in only one quadrat, accounting for 29.63% of the total number of species, and 44 species appeared in no more than five quadrats, accounting for 54.32% of the total species, and the sum of their important values accounted for 2.18%. These reflect the imbalance in the composition pattern of the understory herbaceous plant community in the plots and the differences in the species composition in different areas. When the dominant species status is clear, there are more rare species coexisting in the community, and this structural feature can also be observed in frequency statistics for species (**Figure 1A**).

The coverage of herbaceous plants varies greatly in different plots. In some plots, herbaceous plants cover the entire understory, while there are no herbaceous plants at all in others (**Figure 2A**). There is no particularly obvious regularity in the distribution of the coverage in Gutianshan.

3.2. Herbaceous diversity pattern within habitat types

There are differences in species richness among the 300 survey quadrats, with the number of species ranging from 0 to 25. Only a few quadrats have high species richness

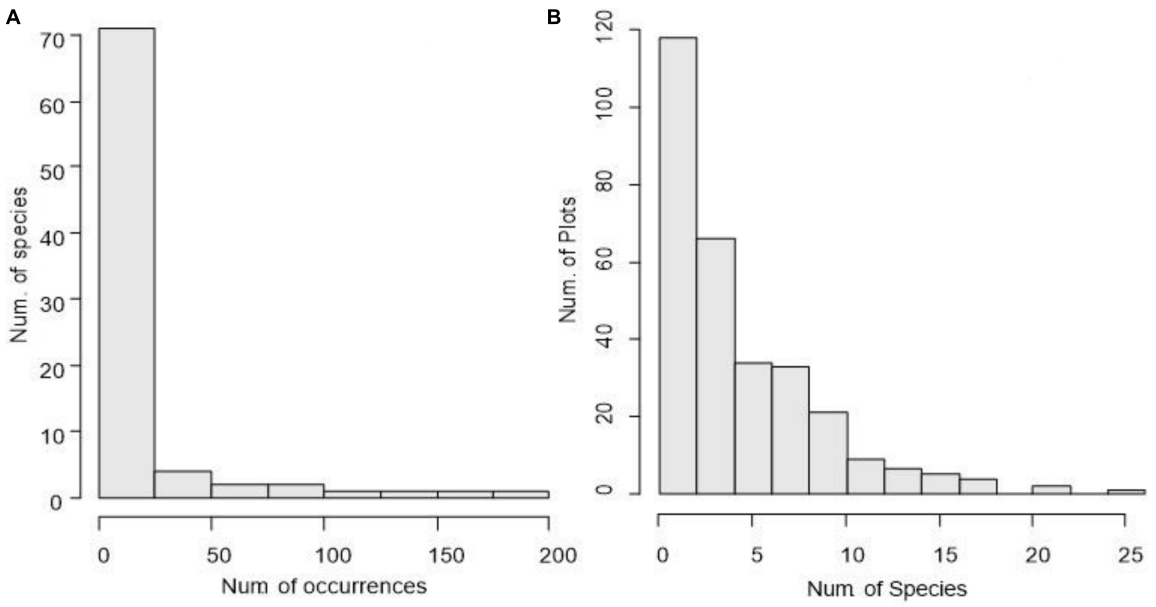

FIGURE 1
Species occurrences **(A)** and species richness distribution of herbaceous plants **(B)** in Gutianshan subtropical understory.

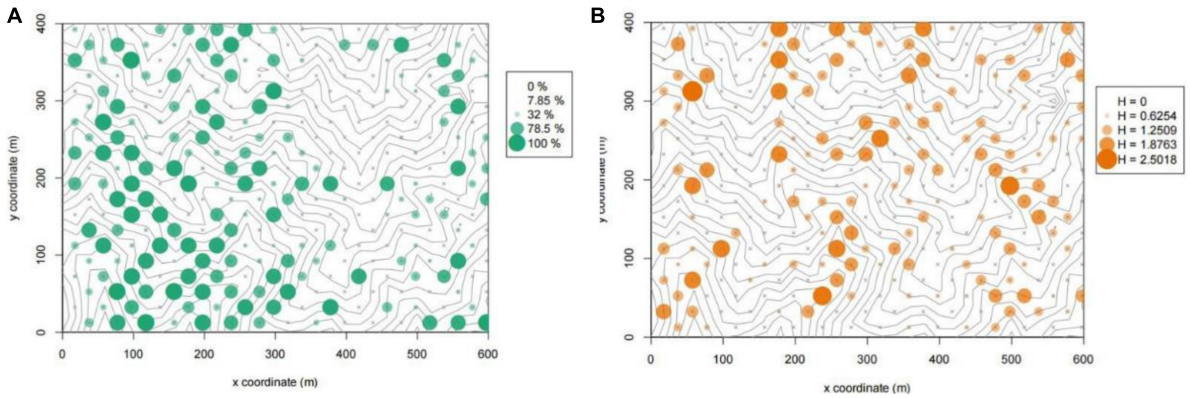

FIGURE 2
Coverage **(A)** and diversity **(B)** distribution of herbaceous plants in Gutianshan subtropical understory. "×" shows the locations of investigation plots, and the size of "●" represents the coverage or diversity index values in each plot.

(Figure 1B), which might be related to the occurrence of specific environmental conditions, and the number of species in most quadrats is less than 10. The range of the Shannon–Wiener index of each quadrat is 0.00–2.50. The diversity of the ridge zone of the quadrats is generally low, while the quadrats with higher diversity index tend to be distributed along the valley (Figure 2B). This shows that the relatively shady and humid environmental conditions in the valley area are conducive to the coexistence of more understory herbaceous plants.

With the increase of rarefaction sampling, the trend of species richness increase in various habitat types is obviously different (Figure 3, five curves representing different habitats are significantly distinguished). The low valley has the fastest increase, followed by the mid-slope, indicating that this habitat type is conducive to maintaining high diversity of herbaceous plants. However, the high ridge rises the slowest, indicating that many herbaceous plants are not suitable for surviving in this habitat. Similarly, although many herbaceous plants are distributed in the low ridge, the species richness is very limited. Even if the number of samples is increased, the potential to find more coexisting species is very low.

The Shannon–Wiener diversity index of herbaceous plants varies greatly among habitat types, with significant differences among different habitats. The highest diversity lies in the low

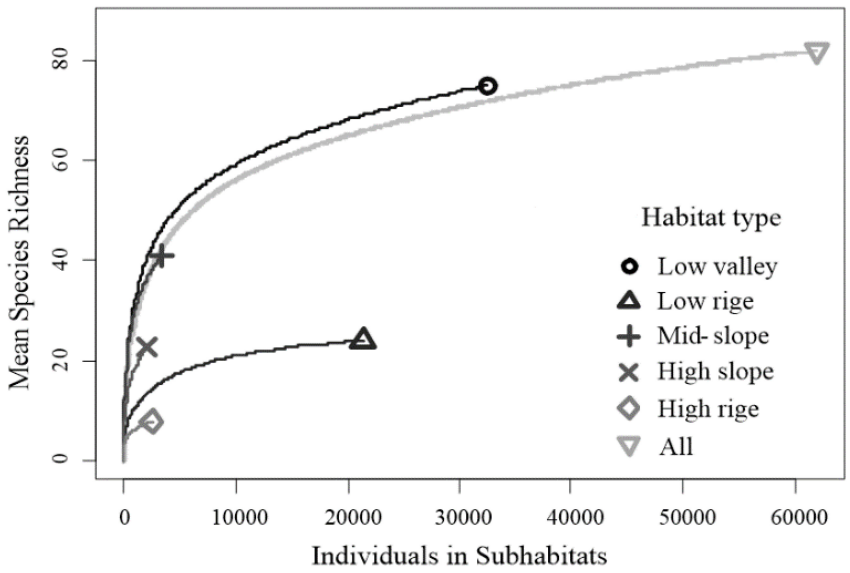

FIGURE 3
Rarefied species richness of herbaceous plants within different habitat types in Gutianshan subtropical understory.

valley and mid-slope, and the lowest in the low ridge and high ridge. The difference between the high slope and other habitat types is not significant (Table 2), and the variation of evenness among different habitats is relatively weak. Compared with different habitats, the low valley was the highest, the low ridge, mid-slope, and high slope were the second, and the high ridge was the lowest.

3.3. Abiotic and biotic drivers of understory herbaceous diversity

According to the results of correlation analysis, H_{herb} is significantly negatively correlated with coverage as a whole, while E_{herb} has a significant positive correlation with coverage (Figure 4). Except for the aspect factor, other abiotic factors were significantly correlated with at least one of the three characteristic variables of the herbaceous plant community, and the diversity of the tree community (H_{trees}) was significantly positively correlated with all three herbal community variables, in particular, the linear fitting degree with the evenness of herbaceous plants is very high, and the linear regression analysis of the two is up to 0.56. The canopy density was significantly negatively correlated with the three herbaceous plant community variables. The tree breast height basal area of the tree and convexity was significantly negatively correlated with H_{herb} and E_{herb}. The elevation was significantly negatively correlated with the E_{herb} and coverage of herbaceous plants. The slope was positively correlated with the coverage of herbaceous plants but was not significantly related to the H_{herb} and E_{herb} (Figure 4).

The multiple linear regression analysis of the herbaceous community diversity index showed that the effect of each influencing factor on community diversity was consistent with the results of correlation coefficient analysis which includes R^2 of species richness (S), Shannon–Wiener index (H), and Pielou's evenness index (E) model is 0.46, 0.47 and 0.61 (Table 3). The results show that the selected explanatory variables can well explain the various characteristics of herbaceous plant community diversity distribution patterns.

The analysis of the relative importance of various factors showed that tree diversity was the main factor affecting the evenness of understory herbaceous plants, and the concavity and basal area of trees made the greatest contribution to the explanation of herbaceous richness and the Shannon–Wiener index variation (Figure 5).

4. Discussion

4.1. Species composition and flora of herbaceous in the subtropical understory

The herbaceous plants in Gutianshan 24-ha plot are dominated by tropical areal types, with both cosmopolitan areal type and temperate characteristics, which is the same as the general trend indicated by the results of the floristic analysis of trees in the plot (Zhu et al., 2008) and the floristic analysis of the middle subtropical evergreen broad-leaved forest in China (Chen, 2006). The species composition of herbaceous plants is

TABLE 2 Tukey honestly significant difference (HSD) test of richness, herbaceous plant diversity, and evenness between different habitat types in Gutianshan subtropical understory.

Habitat types	Number of plots	Richness			Shannon–Wiener index			Pielou's evenness index		
		Mean	Max	Min	Mean	Max	Min	Mean	Max	Min
Low valley	156	6.1667^{a}	26	1	0.8750^{a}	2.5018	0	0.8535^{a}	0.9468	0.7204
Low ridge	97	5.9545^{a}	10	0	0.3311^{b}	1.6288	0	0.8314^{b}	0.9297	0.6927
Mid-slope	22	3.7857^{ab}	21	0	0.9531^{a}	2.1527	0	0.8224^{b}	0.9231	0.7350
High slope	14	2.6186^{b}	17	0	0.4378^{ab}	2.0139	0	0.8078^{b}	0.9042	0.7337
High ridge	11	2.2727^{b}	4	0	0.2602^{b}	0.7441	0	0.7378^{c}	0.8037	0.6596

Different letters (a, b, and c) are used to show the significant differences across habitat types.

rich (81 species, 31 families, and 55 genera). Compared with other plots located in different climatic zones in China, it is found that the species richness of evergreen broad-leaved forest understory herbaceous plants in Gutianshan are less than those in 20-ha *Parashorea chinensis* forest in Xishuangbanna (115 species, 41 families, and 76 genera) (Chen, 2008), which is a tropical forest, and the 25-ha broad-leaved Korean pine forest in Changbai Mountain (102 species, 40 families, and 84 genera) (Li et al., 2008), which is a temporal forest. However, the species richness of Gutianshan is close to that of 90 species in the Longyan forest zone, which is also in the subtropical monsoon climate zone (Su et al., 2022). It shows that there is a different richness of forest herbaceous plants in different climatic zones.

The coverage of herbaceous plant communities varies greatly in different areas, among which ferns are numerous and widely distributed. Ferns are strongly dependent on natural environmental conditions, and their species diversity changes are closely related to environmental conditions (Lwanga et al., 1998). They can respond to changes in environmental conditions with a significant indicative effect (Karst et al., 2005; Gasper et al., 2021). The prosperity of understory ferns may be related to their physiological characteristics. Some studies have suggested that the shade tolerance of ferns is related to their photosynthetic mechanism, so it is suitable for the understory environment (Kawai et al., 2003; Nuccio et al., 2020). *D. glaucum* and *D. pedata* occupy a lot of space in the understory and have high coverage, which is the absolutely dominant species of herbaceous plant community and an important indication of vegetation types in the understory of this area, which may be related to the climatic conditions, light and heat environment, forest succession types, and acidic soil properties of the plots (da Costa et al., 2019; Oseguera-Olalde et al., 2022).

4.2. Herbaceous diversity pattern related to habitat types

Among the five habitat types of the plot, the low valley and mid-slope could maintain higher herbaceous species richness, while the low ridge had the lowest species richness (**Figure 3** and **Table 2**). This is similar to the individual tree distribution pattern and woody seedling regeneration pattern in the plot affected by habitat heterogeneity (Lai et al., 2009). The heterogeneous habitats of the Gutianshan plot also had a significant impact on the diversity distribution pattern of understory herbaceous plant communities. *D. glaucum* is the dominant species with high density in the plot, which mostly occurs in the lowland ridge. It is speculated that the low species richness in the ridge (**Figure 3**) is due to *D. glaucum* being too luxuriant in the herbaceous plant community, and the strong competitive exclusion makes it difficult for other herbaceous species to obtain living space, despite the fact that the light conditions in the valley of the plot are not as good as those in

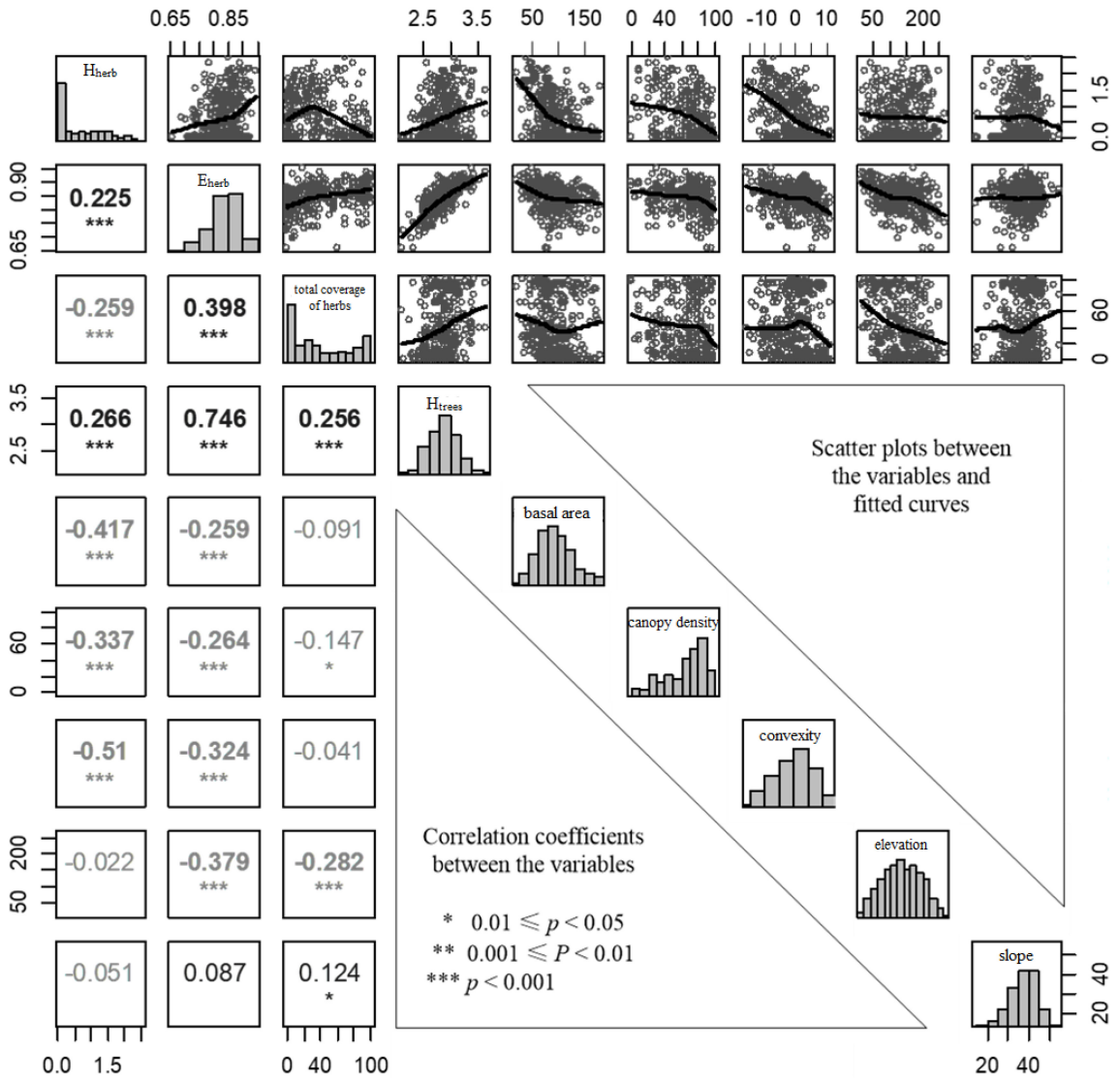

FIGURE 4
Correlation matrix of nine herbaceous plant community and environment variables in Gutianshan subtropical understory. Histograms of variables were shown on the diagonal, scatter plots between the variables were shown on the upper panel, and the lower panel showed Pearson correlation coefficients, where gray represents negative correlation.

the ridge. However, the competitive pressure from the dominant species is less, and the water resources are good, so there may be more species growth (**Figures 2B**, **3**). The proportion of rare species will also be higher. This is also consistent with the negative effect of terrain convexity on herbaceous plant diversity.

4.3. Abiotic and biotic drivers of understory herbaceous diversity

The Shannon–Wiener index and Pielou's evenness index of understory herbaceous plant community are opposite to the coverage of herbaceous plants. Further analysis shows that the Shannon–Wiener index has a better fitting relationship with the quadratic formula of coverage; it shows a unimodal relationship (**Figure 4**). It is speculated that the environmental stress and filtering effect may be stronger in the areas with too low coverage, so the biomass and richness of herbaceous plant communities are limited (Grace, 1999; Fornara and Tilman, 2009; Chase, 2010). In contrast, areas with too large coverage are too dense to compete and repel and do not take advantage of the maintenance of richness. The Pielou's evenness index increases monotonously with the increase of coverage, which may be because the richness of the herbaceous community with low coverage is small and the random variability of species is

TABLE 3 Multivariable linear regression models of three diversity indices of herbaceous plant community to seven environment factors in Gutianshan subtropical understory.

Variables of 3 fixed models	Richness		Shannon–Wiener index		Pielou's eveness index	
	Estimate value	Pr (>| *t*|)	Estimate value	Pr (>| *t*|)	Estimate value	Pr (>| *t*|)
Tree diversity index	2.2040	**0.0090**	0.2705	**0.0415**	0.1254	**<0.001**
Coverage	−0.0083	0.1472	−0.0064	**<0.001**	0.0003	**<0.001**
Canopy density	−0.0469	**<0.001**	−0.0065	**<0.001**	−0.0002	**0.0344**
Basal area of breast-height	−0.0310	**<0.001**	0.0046	**<0.001**	0.000	0.4330
Convexity	−0.2464	**<0.001**	−0.0406	**<0.001**	0.0002	0.4556
Mean elevation	0.0078	**0.0305**	0.0010	0.0900	−0.0001	**0.0049**
Slope	−0.0679	**0.0174**	−0.0082	0.0679	−0.0006	**0.0452**
Adjusted R-squared	0.4567		0.4731		0.6148	

The bold values showed significant correlations between the specific variables and diversity index.

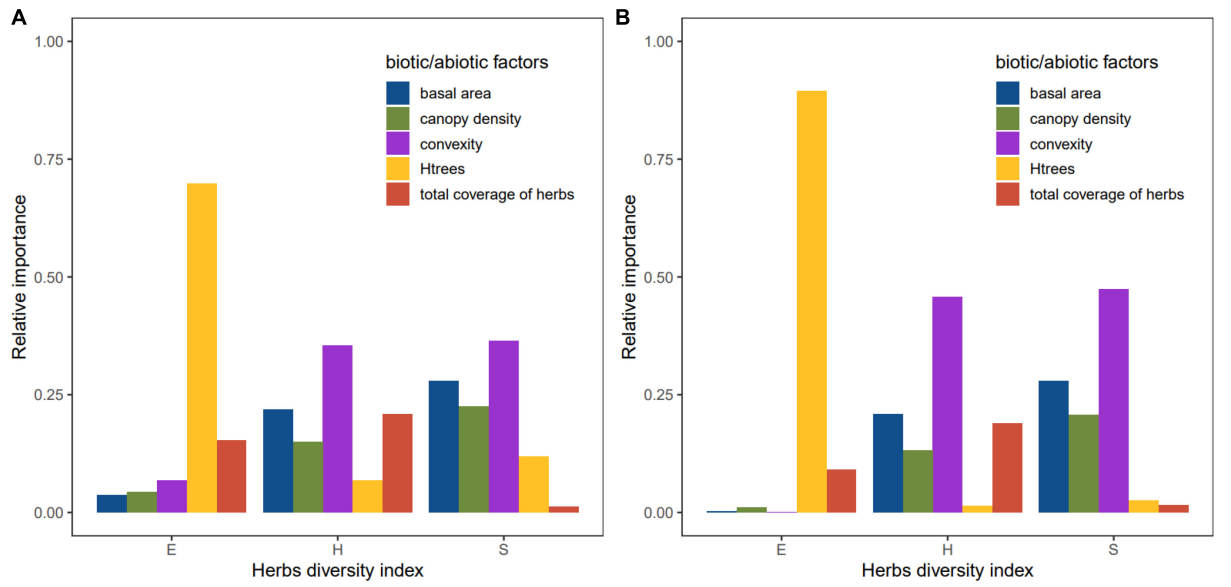

FIGURE 5
Relative importance of biotic/abiotic factors based on lmg **(A)** and pmvd **(B)** to the diversity of understory herbaceous plants.

very large, so the abundance of each species is more inconsistent, that is, the evenness is the lowest. While in the herbaceous plant community with high coverage, because environmental factors are suitable for the growth of more herbaceous species, and the structural composition of the dominant species of the community and even associated species is relatively stable, so the evenness is the highest.

In tropical and temperate forests, the community structure and diversity of herbaceous plants are affected by temperature (Cicuzza et al., 2013), elevation, slope (Wiharto et al., 2021), soil (Mao et al., 2021), canopy (Ford et al., 2000), and other factors. The results of correlation analysis and multiple regression analysis between the diversity of subtropical herbaceous plants and the main biotic/abiotic factors showed that elevation, concavity, basal tree area, tree diversity, and canopy density had certain effects on the diversity pattern of understory herbaceous plants in the subtropical forest. However, this effect showed different significance under different indexes.

Generally speaking, in subtropical forests, the increase of tree diversity is beneficial to maintain the evenness of herbaceous plants, which, in turn, can improve the species diversity of the whole forest vegetation. At the same time, the areas with fewer individuals of big trees will have higher understory herbaceous plant diversity, which may be because the fewer individuals of big trees, the smaller the canopy density of the community, and the more available light quantity will be

obtained by understory herbaceous plants, and ultimately lead to showing higher richness (Facciano et al., 2023). Our results further confirmed the relationship between canopy density and herbaceous diversity under the forest. Therefore, we speculate that the diversity pattern of vegetation in the canopy and herb layer of the subtropical forest community is closely related: In the community with a high degree of coexistence of canopy trees, there will be an under-forest environment suitable for the stable coexistence of more herbaceous species. At the same time, the increase of herbaceous plant diversity can produce a ground cover environment suitable for seedling planting and renewal of multi-tree species, which, in turn, increases the diversity of woody plants (Rawlik et al., 2018; Cheng et al., 2020). Elevation was negatively correlated with Pielou's evenness index and total coverage of herbaceous communities, which was different from the conclusion that there was a unimodal relationship between herbaceous plant diversity and elevation in tropical forests (Gómez-Díaz et al., 2017). In addition, there is no significant relationship between slope and herbaceous community diversity, which may be affected by canopy openness and surface soil (Wiharto et al., 2021).

5. Conclusion

The findings reported here in the community structure and diversity pattern of understory herbaceous, as well as a link between species diversity pattern and abiotic and biotic environments, provide insight into the community structure and biodiversity of herbaceous plants in the subtropical understory. We found that understory herbaceous species diversity is a rich component in the Gutianshan forest, with approximately accounting half of species of woody plant species in this subtropical forest. Understory herbaceous diversity prefers in some specific habitats, which was highest in the lowland valleys, followed by middle slopes. Moreover, we found that herbaceous diversity was driven by both abiotic and biotic environments. Among them, tree diversity and terrain convexity are the main important factors in driving the diversity of understory herbaceous plants. Our results suggest that understory herbaceous communities are a non-negligible and important component of biodiversity in a subtropical forest. Our study also indicates that in order to better protect herbaceous biodiversity in the subtropical understory, more attention should be paid to some special habitats, such as low valleys and mid-slopes.

Data availability statement

The original contributions presented in this study are included in the article/**Supplementary material**, further inquiries can be directed to the corresponding authors.

Author contributions

KT, YW, and JC conceived and designed the study and collected herbaceous data. KT and PC performed statistical analyses and wrote the first draft with substantial input from YW and JC. LC, HQ, SC, XM, HR, and KM provided data and contributed to the development of the final manuscript. All authors have read and agreed to the published version of the manuscript.

Funding

This study was financially supported by the National Natural Science Foundation of China (32001300), the Zhejiang Provincial Natural Science Foundation of China (Y5100361 and LQ22C030001), the State Key Laboratory of Vegetation and Environmental Change (LVEC2010-01), and the key specialized research and development breakthrough program in Henan province (222102320289).

Acknowledgments

We acknowledge the Zhejiang Qianjiangyuan Forest Biodiversity National Observation and Research Station and the Center of Ecology and Resources of Qianjiangyuan National Park for the support provided to this study.

Conflict of interest

The authors declare that the research was conducted in the absence of any commercial or financial relationships that could be construed as a potential conflict of interest.

Publisher's note

Supplementary material

The Supplementary Material for this article can be found online at: https://www.frontiersin.org/articles/10.3389/fevo.2022.1113742/full#supplementary-material

References

Beck, J. J., and Givnish, T. J. (2021). Fine-scale environmental heterogeneity and spatial niche partitioning among spring-flowering forest herbs. *Am. J. Bot.* 108, 63–73. doi: 10.1002/ajb2.1593

Cacciatori, C., Bacaro, G., Chećko, E., Zaremba, J., and Szwagrzyk, J. (2022). Windstorm effects on herbaceous vegetation in temperate forest ecosystems: Changes in plant functional diversity and species trait values along a disturbance severity gradient. *For. Ecol. Manag.* 505:119799. doi: 10.1016/j.foreco.2021.119799

Chase, J. M. (2010). Stochastic community assembly causes higher biodiversity in more productive environments. *Science* 328, 1388–1391. doi: 10.1126/science.1187820

Chen, L., Mi, X., Comita, L. S., Zhang, L., Ren, H., and Ma, K. (2010). Community-level consequences of density dependence and habitat association in a subtropical broad-leaved forest. *Ecol. Lett.* 13, 695–704. doi: 10.1111/j.1461-0248.2010.01468.x

Chen, W. (2006). *Floristic phytogeography of evergreen broad-leaved forest (EBLF) in mid-subtropical China*. Shanghai: MS. East China Normal University.

Chen, Z. (2008). *Study on the diversity and distribution pattern of herbaceous plants under Parashorea forest of Xishuangbanna*. Shanghai: MS. Chinese Academy of Sciences.

Cheng, J., Shi, X., Fan, P., Zhou, X., Sheng, J., and Zhang, Y. (2020). Relationship of species diversity between overstory trees and understory herbs along the environmental gradients in the Tianshan Wild Fruit Forests, Northwest China. *J. Arid Land* 12, 618–629. doi: 10.1007/s40333-020-0055-0

Cicuzza, D., Krömer, T., Poulsen, A. D., Abrahamczyk, S., Delhotal, T., Piedra, H. M., et al. (2013). A transcontinental comparison of the diversity and composition of tropical forest understory herb assemblages. *Biodivers. Conserv.* 22, 755–772. doi: 10.1007/s10531-013-0447-y

Cleveland, W. S. (1979). Robust locally weighted regression and smoothing scatterplots. *J. Am. Stat. Assoc.* 74:829. doi: 10.1080/01621459.1979.10481038

Cleveland, W. S. (1981). Lowess: A program for smoothing scatterplots by robust locally weighted regression. *Am. Stat.* 35:54. doi: 10.1080/00031305.1981.10479306_3

Condit, R. (1998). *Tropical forest census plots*. Berlin: Springer.

da Costa, L. E. N., Arnan, X., de Paiva Farias, R., and Barros, I. C. L. (2019). Community responses to fine-scale environmental conditions: Ferns alpha and beta diversity along Brazilian Atlantic forest remnants. *Acta Oecol.* 101:103475. doi: 10.1016/j.actao.2019.103475

Davies, S. J., Abiem, I., Abu Salim, K., Aguilar, S., Allen, D., Alonso, A., et al. (2021). ForestGEO: Understanding forest diversity and dynamics through a global observatory network. *Biol. Conserv.* 253:108907. doi: 10.1016/j.biocon.2020.108907

De Pauw, K., Meeussen, C., Govaert, S., Sanczuk, P., Vanneste, T., Bernhardt-Römermann, M., et al. (2021). Taxonomic, phylogenetic and functional diversity of understorey plants respond differently to environmental conditions in European forest edges. *J. Ecol.* 109, 2629–2648. doi: 10.1111/1365-2745.13671

Facciano, L., Sasal, Y., and Suarez, M. L. (2023). How do understory trees deal with small canopy openings? The case of release in growth following drought-induced tree mortality. *For. Ecol. Manag.* 529:120692. doi: 10.1016/j.foreco.2022.120692

Ford, W. M., Odom, R. H., Hale, P. E., and Chapman, B. R. (2000). Stand-age, stand characteristics, and landform effects on understory herbaceous communities in southern Appalachian cove-hardwoods. *Biol. Conserv.* 93, 237–246. doi: 10.1016/S0006-3207(99)00126-3

Fornara, D. A., and Tilman, D. (2009). Ecological mechanisms associated with the positive diversity–productivity relationship in an N-limited grassland. *Ecology* 90, 408–418. doi: 10.1890/08-0325.1

Garg, S., Joshi, R. K., and Garkoti, S. C. (2022). Effect of tree canopy on herbaceous vegetation and soil characteristics in semi-arid forests of the Aravalli hills. *Arid Land Res. Manag.* 36, 224–242. doi: 10.1080/15324982.2021.1953634

Gasper, A. L. D., Grittz, G. S., Russi, C. H., Schwartz, C. E., and Rodrigues, A. V. (2021). Expected impacts of climate change on tree ferns distribution and diversity patterns in subtropical Atlantic Forest. *Perspect. Ecol. Conserv.* 19, 369–378. doi: 10.1016/j.pecon.2021.03.007

Gilliam, F. S. (2007). The ecological significance of the herbaceous layer in temperate forest ecosystems. *Bioscience* 57, 845–858. doi: 10.1641/B571007

Gómez-Díaz, J. A., Krömer, T., Kreft, H., Gerold, G., Carvajal-Hernández, C. I., and Heitkamp, F. (2017). Diversity and composition of herbaceous angiosperms along gradients of elevation and forest-use intensity. *PLoS One* 12:e0182893. doi: 10.1371/journal.pone.0182893

Grace, J. B. (1999). The factors controlling species density in herbaceous plant communities: An assessment. *Perspect. Plant Ecol. Evol. Syst.* 2, 1–28. doi: 10.1078/1433-8319-00063

Groemping, U. (2006). Relative importance for linear regression in R: The package relaimpo. *J. Stat. Softw.* 17, 1–27. doi: 10.18637/jss.v017.i01

Heck, K. L. Jr., van Belle, G., and Simberloff, D. (1975). Explicit calculation of the rarefaction diversity measurement and the determination of sufficient sample size. *Ecology* 56, 1459–1461. doi: 10.2307/1934716

Holeksa, J. (2003). Relationship between field-layer vegetation and canopy openings in a Carpathian subalpine spruce forest. *Plant Ecol.* 168, 57–67. doi: 10.1023/A:1024457303815

Hsu, J. (1996). *Multiple comparisons: theory and methods*. Boca Raton, FL: CRC Press.

Hurlbert, S. H. (1971). The nonconcept of species diversity: a critique and alternative parameters. *Ecology* 52, 577–586. doi: 10.2307/1934145

Jost, L. (2007). Partitioning diversity into independent alpha and beta components. *Ecology* 88, 2427–2439. doi: 10.1890/06-1736.1

Karst, J., Gilbert, B., and Lechowicz, M. J. (2005). Fern community assembly : The roles of chance and the environment at local and intermediate scales. *Ecology* 86, 2473–2486. doi: 10.1890/04-1420

Kawai, H., Kanegae, T., Christensen, S., Kiyosue, T., Sato, Y., Imaizumi, T., et al. (2003). Responses of ferns to red light are mediated by an unconventional photoreceptor. *Nature* 421, 287–290. doi: 10.1038/nature01310

Lagomarsino, L. P., Condamine, F. L., Antonelli, A., Mulch, A., and Davis, C. C. (2016). The abiotic and biotic drivers of rapid diversification in A ndean bellflowers (*Campanulaceae*). *New Phytol.* 210, 1430–1442. doi: 10.1111/nph.13920

Lai, J., Mi, X., Ren, H., and Ma, K. (2009). Species-habitat associations change in a subtropical forest of China. *J. Veg. Sci.* 20, 415–423. doi: 10.1111/j.1654-1103.2009.01065.x

Landuyt, D., De Lombaerde, E., Perring, M. P., Hertzog, L. R., Ampoorter, E., Maes, S. L., et al. (2019). The functional role of temperate forest understorey vegetation in a changing world. *Glob. Change Biol.* 25, 3625–3641. doi: 10.1111/gcb.14756

Legendre, P., Mi, X., Ren, H., Ma, K., Yu, M., Sun, I. F., et al. (2009). Partitioning beta diversity in a subtropical broad-leaved forest of China. *Ecology* 90, 663–674. doi: 10.1890/07-1880.1

Li, B., Zhang, J., Yao, X., Ye, J., Wang, X., and Hao, Z. (2008). Seasonal dynamics and spatial distribution patterns of herbs diversity in broadleaved Korean Pine (Pinus koraiensis) mixed forest in Changbai Mountains. *Chin. J. Appl. Ecol.* 19, 467–473.

Li, D. (2008). Floristics and plant biogeography in China. *J. Integr. Plant Biol.* 50, 771–777.

Lu, S. (2017). *An introduction to Pteridology*. Beijing: Science Press.

Lwanga, J. S., Balmford, A., and Badaza, R. (1998). Assessing fern diversity: Relative species richness and its environmental correlates in Uganda. *Biodivers. Conserv.* 7:1387. doi: 10.1023/A:1008865518378

Mao, Q., Chen, H., Gurmesa, G. A., Gundersen, P., Ellsworth, D. S., Gilliam, F. S., et al. (2021). Negative effects of long-term phosphorus additions on understory plants in a primary tropical forest. *Sci. Total Environ.* 798:149306. doi: 10.1016/j.scitotenv.2021.149306

Murphy, S. J., Salpeter, K., and Comita, L. S. (2016). Higher β-diversity observed for herbs over woody plants is driven by stronger habitat filtering in a tropical understory. *Ecology* 97, 2074–2084. doi: 10.1890/15-1801.1

Nuccio, E. E., Starr, E., Karaoz, U., Brodie, E. L., Zhou, J., Tringe, S. G., et al. (2020). Niche differentiation is spatially and temporally regulated in the rhizosphere. *ISME J.* 14, 999–1014. doi: 10.1038/s41396-019-0582-x

Oseguera-Olalde, T. K., Bonilla-Valencia, L., Fonseca, R. M., Martínez-Orea, Y., Lorea-Hernández, F., and Castillo-Argüero, S. (2022). Fern diversity in altitude and anthropogenic gradients in a temperate forest in Mexico City, Mexico. *Trees Forests People* 10:100345. doi: 10.1016/j.tfp.2022.100345

Ramadhanil, R., Tiltrosoedirdjo, S., and Setiadi, D. (2008). Structure and composition of understory plant assemblages of six land use types in the Lore Lindu National Park, Central Sulawesi, Indonesia. *Bangladesh J. Plant Taxon.* 15, 1–12. doi: 10.3329/bjpt.v15i1.911

Rawlik, M., Kasprowicz, M., Jagodziński, A. M., Kaźmierowski, C., Łukowiak, R., and Grzebisz, W. (2018). Canopy tree species determine herb layer biomass and species composition on a reclaimed mine spoil heap. *Sci. Total Environ.* 635, 1205–1214. doi: 10.1016/j.scitotenv.2018.04.133

Ren, H., Svenning, J.-C., Mi, X., Lutz, J. A., Zhou, J., and Ma, K. (2022). Scale-dependent species–area relationship: Niche-based versus stochastic processes in a typical subtropical forest. *J. Ecol.* 110, 1883–1895. doi: 10.1111/1365-2745.13924

Siebert, S. F. (2002). From shade- to sun-grown perennial crops in Sulawesi, Indonesia: Implications for biodiversity conservation and soil fertility. *Biodivers. Conserv.* 11, 1889–1902. doi: 10.1023/A:1020804611740

Song, Y., Chen, X., and Wang, X. (2005). Studies on evergreen broad-leaved forests of China: A retrospect and prospect. *J. East China Norm. Univ. Nat. Sci.* 1, 1–8.

Song, Y., Yan, E., and Song, K. (2015). Synthetic comparison of eight dynamics plots in evergreen broadleaf forests, China. *Biodivers. Sci.* 23:139. doi: 10.17520/biods.2014140

Spicer, M. E., Radhamoni, H. V. N., Duguid, M. C., Queenborough, S. A., and Comita, L. S. (2021). Herbaceous plant diversity in forest ecosystems: Patterns, mechanisms, and threats. *Plant Ecol.* 223, 117–129. doi: 10.1007/s11258-021-01202-9

Su, X., Zheng, G., and Chen, H. Y. H. (2022). Understory diversity are driven by resource availability rather than resource heterogeneity in subtropical forests. *For. Ecol. Manag.* 503:119781. doi: 10.1016/j.foreco.2021.119781

Wang, G., Sun, Y., Zhou, M., Guan, N., Wang, Y., Jiang, R., et al. (2021). Effect of thinning intensity on understory herbaceous diversity and biomass in mixed coniferous and broad-leaved forests of Changbai Mountain. *For. Ecosyst.* 8:53. doi: 10.1186/s40663-021-00331-x

Wang, Y., Cadotte, M. W., Chen, J., Mi, X., Ren, H., Liu, X., et al. (2020). Neighborhood interactions on seedling survival were greatly altered following an extreme winter storm. *For. Ecol. Manag.* 461:117940. doi: 10.1016/j.foreco.2020.117940

Whitney, G. G., and Foster, D. R. (1988). Overstorey composition and age as determinants of the understorey flora of woods of central New England. *J. Ecol.* 76, 867–876. doi: 10.2307/2260578

Whittaker, R. H. (1972). Evolution and measurement of species diversity. *Taxon* 21, 213–251. doi: 10.2307/1218190

Wiharto, M., Wijaya, M., Hamka, L., and Syamsiah. (2021). The understory herbaceous vegetation at tropical mountain forest of mount Bawakaraeng, South Sulawesi. *J. Phys.* 1899:12002. doi: 10.1088/1742-6596/1899/1/012002

Wu, Z., Zhou, Z., Li, D., Peng, H., and Sun, H. (2003). The areal-types of the world families of seed plants. *Plant Divers.* 25, 1–3. doi: 10.1111/j.1744-7909.2008.00711.x

Xu, J., Dang, H., Wang, M., Chai, Y., Guo, Y., Chen, Y., et al. (2019). Is phylogeny more useful than functional traits for assessing diversity patterns under community assembly processes? *Forests* 10:1159. doi: 10.3390/f10121159

Zhu, Y., Zhao, G., Zhang, L., Shen, G., Mi, X., Ren, H., et al. (2008). Community composition and structure of Gutianshan forest dynamic plot in a mid-subtropical evergreen broad-leaved forest, East China. *Chin. J. Plant Ecol.* 32, 262–273.

Zuo, S., Ren, Y., Weng, X., Ding, H., Yun, G., and Chen, Q. (2017). Carbon distribution and its correlation with floristic diversity in subtropical broad-leaved forests during natural succession. *J. Trop. For. Sci.* 29, 493–503. doi: 10.26525/jtfs2017.29.4.493503

frontiers | Frontiers in Ecology and Evolution

TYPE Original Research
PUBLISHED 09 January 2023
DOI 10.3389/fevo.2022.1104369

OPEN ACCESS

EDITED BY
Xiang Liu,
Lanzhou University,
China

REVIEWED BY
Rong Yang,
Northwest Institute of Eco-Environment and Resources (CAS), China
Shengkui Cao,
Qinghai Normal University,
China

*CORRESPONDENCE
Yamin Jiang
✉ jiangyamin2008@163.com
Wenjie Liu
✉ Liuwj@hainanu.edu.cn

SPECIALTY SECTION
This article was submitted to Conservation and Restoration Ecology, a section of the journal Frontiers in Ecology and Evolution

RECEIVED 21 November 2022
ACCEPTED 09 December 2022
PUBLISHED 09 January 2023

CITATION
Xing G, Wang X, Jiang Y, Yang H, Mai S, Xu W, Hou E, Huang X, Yang Q, Liu W and Long W (2023) Variations and influencing factors of soil organic carbon during the tropical forest succession from plantation to secondary and old–growth forest. *Front. Ecol. Evol.* 10:1104369. doi: 10.3389/fevo.2022.1104369

Variations and influencing factors of soil organic carbon during the tropical forest succession from plantation to secondary and old–growth forest

Guitong Xing[1,2], Xiaofang Wang[1,2], Yamin Jiang[1,2,3]*, Huai Yang[4], Siwei Mai[1,2], Wenxian Xu[1,2], Enqing Hou[5], Xingzhao Huang[6], Qiu Yang[1,2], Wenjie Liu[1,2]* and Wenxing Long[7]

[1]Key Laboratory of Agro-Forestry Environmental Processes and Ecological Regulation of Hainan Province, College of Ecology and Environment, Hainan University, Haikou, China, [2]Center for Eco-Environment Restoration Engineering of Hainan Province, College of Ecology and Environment, Hainan University, Haikou, China, [3]College of Tropical Crops, Hainan University, Haikou, China, [4]International Center for Bamboo and Rattan, Beijing, China, [5]Key Laboratory of Vegetation Restoration and Management of Degraded Ecosystems, South China Botanical Garden, Chinese Academy of Sciences, Guangzhou, China, [6]School of Forestry and Landscape Architecture, Anhui Agricultural University, Hefei, Anhui, China, [7]College of Forestry, Hainan University, Haikou, China

Introduction: Soil organic carbon (SOC) accumulation changed with forest succession and hence impacted the SOC storage. However, the variation and underlying mechanisms about SOC during tropical forest succession are not fully understood.

Methods: Soil samples at four depths (0–10 cm, 10–20 cm, 20–40 cm and 40–60 cm), litter, and roots of 0–10 cm and 10–20 cm were collected from three forest succession stages (plantation forest, secondary forest, and old–growth forest) in the Jianfengling (JFL) National Nature Reserve in Hainan Island, China. The SOC, soil enzyme activities, physiochemical properties, the biomass of litter and roots were analyzed.

Results: Results showed that forest succession significantly increased SOC at 0–10 cm and 10–20 cm depth (from 23.00 g/kg to 33.70 g/kg and from 14.46 g/kg to 22.55 g/kg, respectively) but not at a deeper depth (20–60 cm). SOC content of the three forest succession stages decreased with increasing soil depth and bulk density (BD). With forest succession from plantation to secondary and old–growth forest, the soil pH at 0–10 cm and 10–20 cm depth decreased from 5.08 to 4.10 and from 5.52 to 4.64, respectively. Structural equation model (SEM) results showed that the SOC at depths of 0–20 cm increased with total root biomass but decreased with increasing soil pH value. The direct positive effect of soil TP on SOC was greater than the indirect negative effect of decomposition of SOC by soil acid phosphatase (AP).

Discussion: To sum up, the study highlighted there was soil P– limited in tropical forests of JFL, and the increase in TP and total root biomass inputs were main factors favoring SOC sequestration during the tropical forest

succession. In addition, soil acidification is of great importance for SOC accumulation in tropical forests for forest succession in the future. Therefore, forest succession improved SOC accumulation, TP and roots contributed to soil C sequestration.

KEYWORDS

enzyme activity, pH value, root biomass, phosphorus limitation, litter biomass

1. Introduction

Forest soil carbon is the main component of the terrestrial ecosystem carbon pool. Small variations of this component will affect atmospheric carbon concentrations and future global climate changes (Fang et al., 2015). Tropical forests cover only 6% of the world's land area but contain about 40% of the terrestrial ecosystem carbon (Ren et al., 2014), with old–growth forests still accumulating carbon stably in soil (Zhou et al., 2006). However, tropical primary forest areas have been decreasing under the global climate change and human disturbances over the last century (Ma et al., 2022). Studies found a reduction in soil organic carbon (SOC) during the conversion of tropical primary forests to other land–use types (Zhou et al., 2018). Conversely, when forest vegetation is restored, the SOC will increase with positive forest succession (Deng et al., 2013). Meanwhile, long–term observational data show that soil in the northern hemisphere and temperate forests has always acted as a carbon sink, but there are relatively few studies on its dynamic change in tropical forests (Zhu et al., 2020). Therefore, studying the variation characteristics of SOC during tropical forest succession is important to understand the carbon sequestration capacity of forest soil.

SOC accumulation during forest succession is largely influenced by biotic and abiotic factors (Smith, 2008; Hu and Lan, 2020). In terms of abiotic factors, TN and TP are two important factors that influence SOC by regulating SOC input and output, because nitrogen and phosphorus are critical elements for plant growth (Schleuss et al., 2019). The high N/P ratios will increase nitrogen uptake by plants, promote plant growth and increase SOC input (Peng et al., 2019). In terms of biotic factors, the accumulation of SOC depends on the balance of the input of exogenous SOC from litter and roots and the output of SOC through microbial consumption. It is important source of soil nutrients from litter decomposition that replenished by forest ecosystems (Rubino et al., 2010). Huang et al. (2011) reported that the increase of litter decomposition with forward succession help accumulate SOC. The increase of roots and their secretions can also increase SOC in the late afforestation restoration stage (Hu et al., 2016). In addition, soil microbes, one of the main decomposers of organic carbon, act on the decomposition of soil organic matter by regulating enzymatic activity. Soil microbes secreted extracellular enzymes to decompose complex organic matter for obtaining carbon and other nutrients, which also have important impacts on the sequestration of forest SOC (Cui et al., 2019). To reveal the biotic, abiotic factors and their interact effect on SOC accumulation during tropical forest succession is of importance for guiding tropical forest management and SOC sequestration.

The tropical forest in Hainan Island accounts for 31.4% of the total tropical forest area in China, which plays a key role in ecological environment construction and it's largely affected by global climate changes (Li et al., 2019). The Jianfengling (JFL) tropical forest remains one of the few well–preserved tropical primary forests in China (Guo et al., 2015). The slash–and–burn and traditional agricultural methods used over the last century are what have caused severe damage and the subsequent restoration of tropical forests, and form an ideal area to study the variations and influencing factors of SOC during the tropical forest succession. In this study, three forest succession stages, plantation forest, secondary forest, and old–growth forest in JFL, which belong to early, middle and late succession stages were selected. The SOC and other soil physicochemical properties, soil enzyme activities, litter and roots biomass were investigated in different forest succession stages. The objectives were to: (1) explore the variations of SOC and enzyme activities at different succession stages and soil layers; (2) find the effects of soil environmental factors, litter and roots on SOC during tropical forest succession. We proposed two hypotheses: (1) SOC increases with forest succession from plantation forest to secondary forest and old–growth forest; (2) the increase of litter and root biomass is beneficial for SOC accumulation. The study results are expected to provide theoretical reference for soil carbon management in tropical forest.

2. Materials and methods

2.1. Study site

The study site, the JFL National Nature Reserve, is located in the southwestern part of Hainan Island, China (18°23′–18°50″N 108°36′–109°05′E). The area has a typical tropical monsoon climate with a wet season from May to October and a dry season from November to April in the following year (Jiang et al., 2017). The mean annual temperature ranges from 25.2°C in coastal tablelands to 19.7°C in mountainous rainforest areas (Xu et al., 2015). The mean annual precipitation ranges from 1,500 to 2,600 mm, with a maximum of 3,500 mm, 80%–90% of which falls in the wet season. The soil types are mainly montane lateritic red or yellow earth according to the World Reference Base for soil

resources, and granite is the main soil parent material (Yang et al., 2018).

Our study site mainly includes three forest succession types: old–growth forest (OF), secondary forest (SF), and plantation forest (PF). Three 20 m × 20 m plots were established in each forest. In total, there were nine sample plots. We used the space–for–time substitution method, which has been commonly used for similar soil changes over time under consistent climatic conditions (Walker et al., 2010). The OF is natural mature forest without human disturbance for a long time, while SF and PF are the natural regeneration forest which developed on the OF after different degrees of human disturbance. These forests have similar geographical and climatic conditions with uniform temperature and precipitation. *Cryptocarya chinensis, Gironniera subaequalis, Mallotus Hookerianus (Seem.) Muell. Arg,* and *Nephelium topengii (Merr.) H. S. Lo* are the dominant species in OF, which maintains a high biodiversity (Fang et al., 2004). The SF naturally regenerated following selective logging of OF in the 1960s and mainly consists of *Castanopsis fissa, Castanopsis tonkinensis, Sapium discolor, Syzygium tephrodes,* and *Schefflera octophylla* (Xu et al., 2009). *Cunninghami alanceolata (Lamb.) Hook*. is the dominant species in the PF, and it was established after being felled in the 1980s. The basic sample sites information is shown in Table 1.

2.2. Sampling design

In September 2021, we collected litter, root and soil samples along the forest succession stages from PF, SF, to OF. At each forest stage, three sampling plots were selected. At each plot, we divided into four subplots (10 m × 10 m), and litter was collected randomly with three replicates by litter traps (50 cm × 50 cm). A total of 27 above–ground litter samples were obtained. At each sampling plot, root samples at 0–10 cm and 10–20 cm soil depths were collected using an auger (inner diameter, 9.5 cm), and then fully soaked in water for 5 h in the laboratory, and washed with water for 20 mesh to carry out root picking. Roots were divided into two types according to root diameter: they were defined as fine roots and thick roots with root diameter ≤ 2 mm and root diameter > 2 mm, respectively. Root biomass was determined after being oven–dried at 65°C for 24 h.

The soil samples were collected at four depths (0–10 cm, 10–20 cm, 20–40 cm and 40–60 cm) using a stainless soil corer at each plot. A composite sample consisted of five soil cores, and then divided into two subsamples. In total, 72 soil subsamples were collected and transported to the laboratory with ice bags. After removing animal and plant residues, roots and other visible items, soil samples were passed through a 2 mm mesh. Finally, each sample was separated into two parts to measure (1) the basic physical and chemical properties after being air–dried, and (2) the soil enzyme activity within 1 week with soils stored at 4°C. The soil bulk density (BD) sample was collected using a cutting ring (volume of 100 cm^3). We used the method of digging the soil profile, and then collected three soil samples per soil layer using cutting ring, and measured the ratio of the weight of dry soils to the volume of each soil core.

2.3. Laboratory analysis

After drying at 105°C for 12 h, soil water content (SWC) was measured by mass loss. The soil pH was measured by the potentiometric method (the soil: water ratio = 1:2.5). SOC was determined by the $K_2Cr_2O_7$–H_2SO_4 oxidation method (Bao, 2000). Soil total nitrogen (TN) and total phosphorus (TP) were extracted by the semimicro kelvin method and determined by Continuous Flow Analyzer (PROXIMA 1022/1/1, ALLIANCE Instruments, France; Zhang et al., 2019). Soil ammonium nitrogen (NH_4^+–N) and nitrate nitrogen (NO_3^-–N) contents were determined by extracting fresh soil with 2 M KCL and analyzing it using the Continuous Flow Analyzer (SKALAR San++, SKALAR Co., Netherlands). The soil available phosphorus (SAP) was determined by ammonium chloride hydrochloric acid extraction.

TABLE 1 Location and basic characteristics of sampling plots in different succession stages in the Jianfengling National Nature Reserve.

Sampling plots	Longitude (E)	Latitude (N)	Elevation (*m*)	Dominant species	Disturbance history
PF1	108°52′36.83″	18°44′32.45″	853	*Cunninghami alanceolata(Lamb.) Hook*	The PF was established after being felled in 1980s
PF2	108°52′36.29″	18°44′31.57″	863		
PF3	108°52′35.04″	18°44′31.58″	862		
SF1	108°51′57.40″	18°44′43.53″	878	*Castanopsis fissa, Castanopsis tonkinensis, Sapium discolor, Syzygium tephrodes, Schefflera octophylla*	In 1960s, the SF naturally regenerated following selective logging of OF
SF2	108°51′57.36″	18°44′42.89″	891		
SF3	108°51′56.50″	18°44′42.20″	899		
OF1	108°53′4.04″	18°44′15.09″	983	*Cryptocarya chinensis, Gironniera subaequalis, Mallotus Hookerianus (Seem.) Muell.Arg, Nephelium topengii (Merr.) H. S. Lo.*	Undisturbed natural evergreen forest
OF2	108°52′29.17″	18°44′1.04″	1,004		
OF3	108°52′29.14″	18°44′1.02″	1,004		

PF, plantation forest; SF, secondary forest; OF, old-growth forest.

TABLE 2 *F*-values for two–way ANOVAs on the effects of soil depth, forest succession stages, their interaction on the concentrations of soil organic carbon (SOC), total soil nitrogen (TN), total soil phosphorus (TP), C:N, C:P, and N:P ratios.

Independent variable	SOC	TN	TP	C:N	C:P	N:P
Soil depth	148.67**	702.73**	630.27**	1.85	2.69	0.72
Forest succession stages	6.52**	22.32**	95.42**	4.32*	1.57	23.38**
Soil depth × forest succession stages	4.05*	8.68**	14.28**	1.50	0.98	0.14

* and ** indicate significance at $p < 0.05$ and $p < 0.01$, respectively.

The activities of acid phosphatase (AP), β–1,4–glucosidase (BG), β–1,4–N–acetyl–glucosaminidase (NAG) and leucine aminopeptidase (LAP) were determined by 96–well microplates (German et al., 2011; Bach et al., 2013).

Microbial nutrient limitations were determined by calculating the vector length, and angle A with enzyme activity stoichiometry vector analysis using the following formulae (Moorhead et al., 2013):

$$\text{Vector L} = \sqrt{\left(\ln \text{BG} / \ln\left(\text{NAG} + \text{LAP}\right)\right)^2 + \left(\ln \text{BG} / \ln \text{AP}\right)^2} \quad (1)$$

$$\text{Angel A} = \text{DEGREES}\left\{\text{ATAN2}\left[\left(\begin{array}{l}\ln(\text{BG}) / \ln(\text{AP}), \\ \left(\ln \text{BG} / \ln\left(\text{NAG} + \text{LAP}\right)\right)\end{array}\right)\right]\right\} \quad (2)$$

The larger the vector L, the stronger the carbon constraint. Angles A < 45° and >45° indicate that the microbes are limited by nitrogen and phosphorus, respectively.

2.4. Statistical analysis

To identify the differences in SOC, TN, TP, C:N, C:P and N:P ratios, soil enzyme activities and other soil properties in different forest succession stages and different soil layers, one–way ANOVA followed by the Least Significant Difference (LSD) test was applied ($p < 0.05$). On the basis of the homogeneity test of variance, two–way ANOVA followed by the LSD test were used to investigate the effects of soil depth, forest succession stages, and their interactions on SOC, TN, and TP and their stoichiometric ratios. Pearson correlation analysis was used to analyze the correlation between the soils' properties and enzyme activities. The structural equation model (SEM), which combines path analysis and factor analysis, has been applied as causal inference in ecology, mainly using maximum–likelihood (Shipley, 2001). Before starting, to avoid multicollinearity, we used the variance inflation factor (VIF) threshold to eliminate those variables that were strongly correlated (Kock, 2015). Then, we established an a-prior model (Supplementary Figure S4) based on the known effects and relationships among the drivers of SOC. The SEM analyses were performed using R software (4.2.0) lavaan package. SPSS 19.0 (IBM SPSS Predictive Analytics Community, United States) software, Origin 2019b (Origin Lab Corp. United States), and R (R 4.2.0) were used for all statistical analyses and figures in the study.

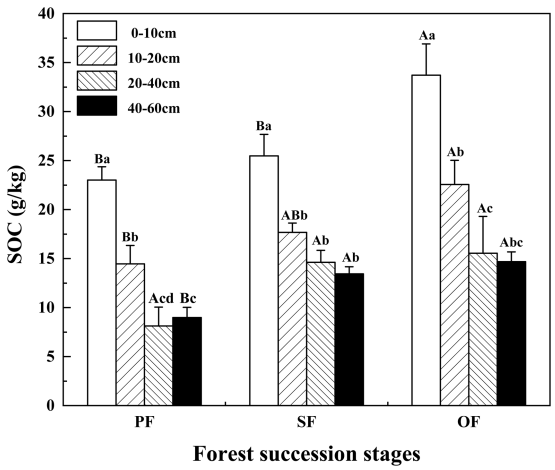

FIGURE 1
Variations of SOC in different forest succession stages in the Jianfengling National Nature Reserve. SOC, soil organic carbon; PF, plantation forest; SF, secondary forest; OF, old-growth forest. Different lowercase letters indicate significant differences between different soil layers at the same stage. Different capital letters indicate significant differences in the same soil layer at different forest succession stages (p<0.05).

3. Results

3.1. Changes of soil organic carbon in different forest succession stages

SOC was significantly affected by soil depth, forest succession stages, and their interactions ($p < 0.05$; Table 2). The SOC in the four soil layers increased with forest succession from PF to SF and OF, with the highest SOC of 33.70 g/kg at the depth of 0–10 cm in OF, which was significantly higher than that of in SF (25.48 g/kg) and PF (23.00 g/kg; $p < 0.05$). The SOC at the depth of 10–20 cm in OF (22.55 g/kg) was significantly higher than that of in PF (14.46 g/kg). In the vertical direction, SOC at the depth of 0–40 cm significantly decreased at each forest stage, but tend to be stable below 40 cm (Figure 1).

TABLE 3 The soil properties at different forest succession stages in the Jianfengling National Nature Reserve (n=6).

Variable	Forest succession stages	Soil depth			
		0–10cm	10–20cm	20–40cm	40–60cm
pH	PF	5.08 ± 0.05^{Ac}	5.52 ± 0.23^{ABbc}	5.70 ± 0.22^{Ab}	6.01 ± 0.06^{Aa}
	SF	5.08 ± 0.05^{Ac}	5.49 ± 0.30^{Abc}	5.60 ± 0.32^{Ab}	5.72 ± 0.18^{ABa}
	OF	4.10 ± 0.13^{Bc}	4.64 ± 0.04^{Bbc}	4.95 ± 0.21^{Ab}	5.22 ± 0.24^{Ba}
SWC	PF	26.82 ± 0.004^{Aa}	25.13 ± 0.01^{Aab}	22.91 ± 0.01^{ABb}	21.69 ± 0.02^{Bb}
(%)	SF	22.10 ± 0.01^{Ba}	19.63 ± 0.01^{Bb}	19.74 ± 0.002^{Bb}	19.64 ± 0.01^{Bb}
	OF	28.78 ± 0.01^{Aa}	27.02 ± 0.02^{Aa}	23.59 ± 0.02^{Aa}	23.69 ± 0.02^{Aa}
BD	PF	1.21 ± 0.01^{Ad}	1.27 ± 0.01^{Ac}	1.35 ± 0.01^{Ab}	1.40 ± 0.01^{Aa}
(g/cm^3)	SF	1.15 ± 0.01^{Bd}	1.24 ± 0.01^{Ac}	1.33 ± 0.01^{Bb}	1.39 ± 0.01^{Aa}
	OF	1.18 ± 0.01^{Ad}	1.23 ± 0.01^{Ac}	$1.31 + 0.01^{Bb}$	1.39 ± 0.01^{Aa}
TN	PF	2.02 ± 0.02^{Ba}	1.47 ± 0.06^{Bb}	1.02 ± 0.05^{Ac}	0.98 ± 0.07^{Acd}
(g/kg)	SF	1.85 ± 0.03^{Ca}	1.44 ± 0.08^{Bb}	1.05 ± 0.06^{Ac}	1.05 ± 0.06^{Acd}
	OF	2.37 ± 0.07^{Aa}	2.06 ± 0.13^{Aa}	1.32 ± 0.14^{Ab}	1.11 ± 0.07^{Ab}
TP	PF	0.073 ± 0.007^{Ba}	0.057 ± 0.004^{Bb}	0.039 ± 0.003^{Bcd}	0.041 ± 0.004^{Bc}
(g/kg)	SF	0.108 ± 0.002^{Aa}	0.098 ± 0.003^{Ab}	0.077 ± 0.005^{Ac}	0.074 ± 0.006^{Acd}
	OF	0.117 ± 0.002^{Aa}	0.098 ± 0.003^{Ab}	0.069 ± 0.005^{Ac}	0.061 ± 0.002^{Acd}
NH_4^+-N	PF	235.66 ± 3.17^{Aa}	41.66 ± 0.75^{Ab}	14.04 ± 0.67^{Ac}	13.25 ± 1.92^{Acd}
(mg/kg)	SF	241.62 ± 0.20^{Aa}	30.68 ± 6.44^{Ab}	15.17 ± 1.37^{Ac}	13.59 ± 2.10^{Acd}
	OF	228.65 ± 5.86^{Aa}	36.26 ± 2.45^{Ab}	15.14 ± 2.72^{Ac}	13.42 ± 1.90^{Acd}
NO_3^--N	PF	1.85 ± 0.16^{B}	1.60 ± 0.08^{Babc}	1.35 ± 0.07^{Bb}	1.34 ± 0.06^{Bc}
(mg/kg)	SF	2.31 ± 0.15^{ABa}	2.07 ± 0.15^{Aa}	1.65 ± 0.06^{Ab}	1.53 ± 0.05^{ABc}
	OF	2.65 ± 0.22^{Aa}	2.50 ± 0.07^{Aa}	1.90 ± 0.08^{Ab}	1.62 ± 0.08^{Ac}
SAP	PF	1.633 ± 0.012^{Ba}	1.546 ± 0.006^{Bb}	1.522 ± 0.005^{Bc}	1.521 ± 0.002^{Acd}
(mg/kg)	SF	1.723 ± 0.020^{Aa}	1.584 ± 0.004^{Ab}	1.535 ± 0.003^{Ac}	1.538 ± 0.001^{Acd}
	OF	1.609 ± 0.023^{Ba}	1.553 ± 0.014^{ABb}	1.53 ± 0.029^{ABb}	1.527 ± 0.012^{Ab}
C/N	PF	11.37 ± 0.77^{Aa}	9.79 ± 0.96^{Aa}	7.86 ± 1.52^{Ba}	9.24 ± 1.08^{Ba}
	SF	13.77 ± 1.23^{Aa}	12.41 ± 0.65^{Aa}	14.16 ± 1.95^{Aa}	12.89 ± 0.63^{Aa}
	OF	14.17 ± 1.01^{Aa}	10.94 ± 0.87^{Aa}	11.54 ± 1.73^{ABa}	13.24 ± 0.65^{Aa}
C/P	PF	325.34 ± 47.85^{Aa}	260.61 ± 48.66^{Aa}	218.29 ± 66.67^{Aa}	227.14 ± 48.19^{Aa}
	SF	216.31 ± 14.94^{Aa}	181.41 ± 14.36^{Aa}	189.67 ± 10.27^{Aa}	184.11 ± 11.61^{Aa}
	OF	286.45 ± 23.61^{Aa}	228.79 ± 21.23^{Aab}	215.61 ± 19.53^{Ab}	239.62 ± 15.55^{Aab}
N/P	PF	28.32 ± 2.39^{Aa}	26.20 ± 2.21^{Aa}	26.83 ± 3.55^{Aa}	24.37 ± 3.54^{Aa}
	SF	15.78 ± 0.44^{Ba}	14.72 ± 0.54^{Ca}	13.77 ± 1.46^{Ba}	14.44 ± 1.66^{Ba}
	OF	20.18 ± 0.33^{Ba}	20.90 ± 0.81^{Ba}	19.05 ± 1.63^{ABa}	18.20 ± 1.60^{ABa}

PF, plantation forest; SF, secondary forest; OF, old-growth forest; SWC, soil water content; BD, bulk density; SOC, soil organic carbon; TN, total nitrogen; TP, total phosphorus; NH_4^+-N, ammonium nitrogen; NO_3^-N, nitrate nitrogen; SAP, soil available phosphorus. Different lowercase letters indicate significant differences between different soil layers at the same stage. Different capital letters indicate significant differences in the same soil layer at different forest succession stages ($p < 0.05$).

3.2. Changes in soil physical and chemical properties in different forest succession stages

As shown in Table 3, the soil pH at each soil layer gradually decreased with forest succession, and the soil pH at a depth of 0–10 cm in OF was significantly lower than that in SF and PF, indicating that surface soil acidification was aggravated at the later stage of forest succession. In the vertical direction, the soil pH increased with soil depth, indicating that the acidification degree decreased with increasing soil depth. The SWC in SF was significantly lower than that in PF and OF in lower soils (0–10 cm and 10–20 cm), and the SWC in SF was significantly lower than that in OF in deeper soils (20–40 cm and 40–60 cm).

The TN, TP and their stoichiometric ratios were significantly affected by soil depth, forest succession stages, and their interactions (Table 2). The TN in OF was significantly higher than that in SF and PF at depths of 0–10 cm and 10–20 cm (Table 3),

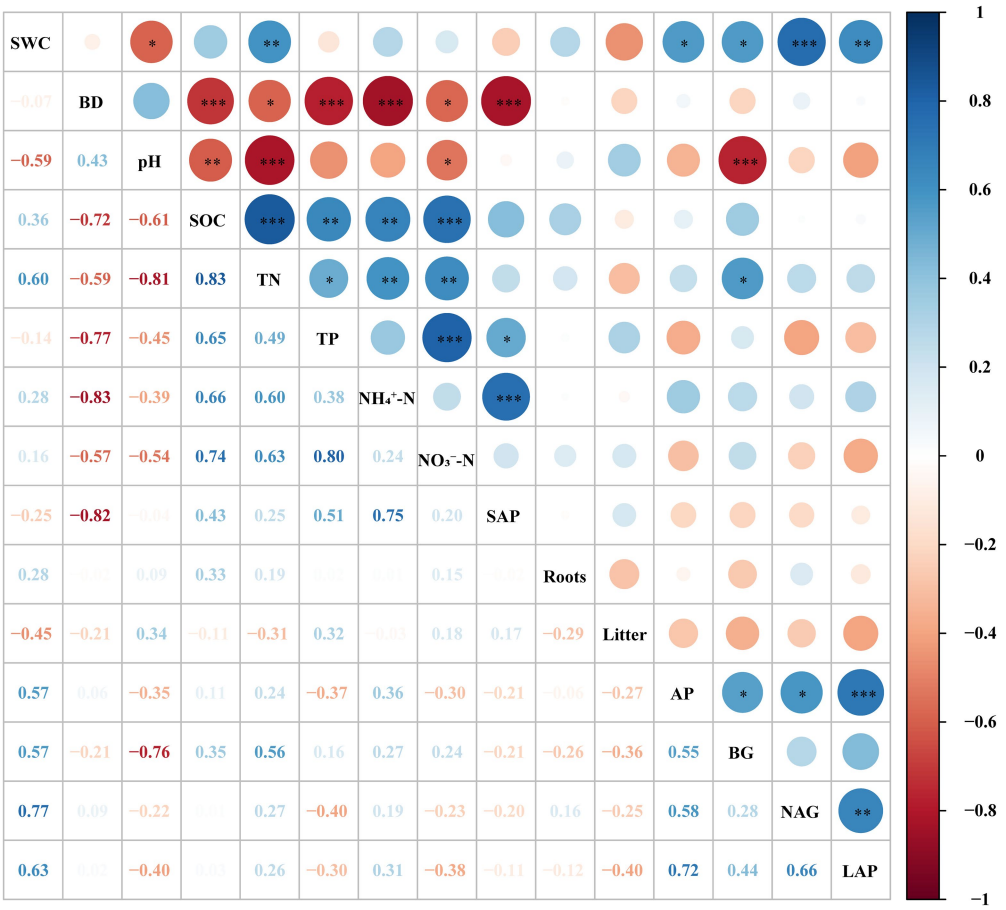

FIGURE 2
The correlation of different soil properties in different forest succession stages in the Jianfengling National Nature Reserve. SWC, soil water content; BD, bulk density; SOC, soil organic carbon; TN, total nitrogen; TP, total phosphorus; NH_4^+–N, ammonium nitrogen; NO_3^-N, nitrate nitrogen; SAP, soil available phosphorus; Roots, total root biomass; Litter, litter biomass; AP, acid phosphatase; BG, β–1,4–glucosidase; NAG, β–1,4–N–acetyl–glucosaminidase; LAP, leucine aminopeptidase. Significance levels: ***p<0.001; **p<0.01; *p<0.05.

indicating that TN increased with forest succession processes. The TN was positively linked with NH_4^+–N and NO_3^-–N ($p < 0.01$), and it was positively correlated with TP and BG ($p < 0.05$; Figure 2).

The TP in the four soil layers increased with forest succession and was obviously lower in PF than in SF and OF. The C:N ratio increased with forest succession but did not change significantly in different soil depths. The ratios of C:P and N:P initially decreased and then increased with forest succession, with the N:P ratio in PF significantly higher than that in the latter two stages (Table 3).

The NH_4^+–N in all four soil layers did not change significantly with forest succession, while the NO_3^-–N increased significantly. The SAP increased first and then decreased with forest succession, where the SAP in SF was obviously higher than that in PF and OF (Table 3).

3.3. Soil enzyme activities in different forest succession stages

The activity of BG first decreased and then increased with forest succession (Figure 3A). The activity of BG decreased with soil depth. The NAG and LAP activities decreased first and then increased (Figures 3B,C). The AP activity showed a general decreasing trend with forest succession and was obviously lower in SF than in PF and OF at a depth of 0–10 cm. In the vertical direction, there was no significant difference for AP in the different soil layer in PF and SF (Figure 3D). BG, NAG, and LAP all had significant correlations with AP activity, while the NAG activity was positively correlated with LAP (Figure 2).

3.4. Changes of litter and total root biomass in different forest succession stages

With the progression of forest succession, the amount of litter per unit area increased first and then decreased, and the litter amount in SF was significantly higher than that of in PF and OF (Figure 4). However, the SOC, TN, and TP contents of litter did not change significantly with forest succession (Supplementary Figure S1).

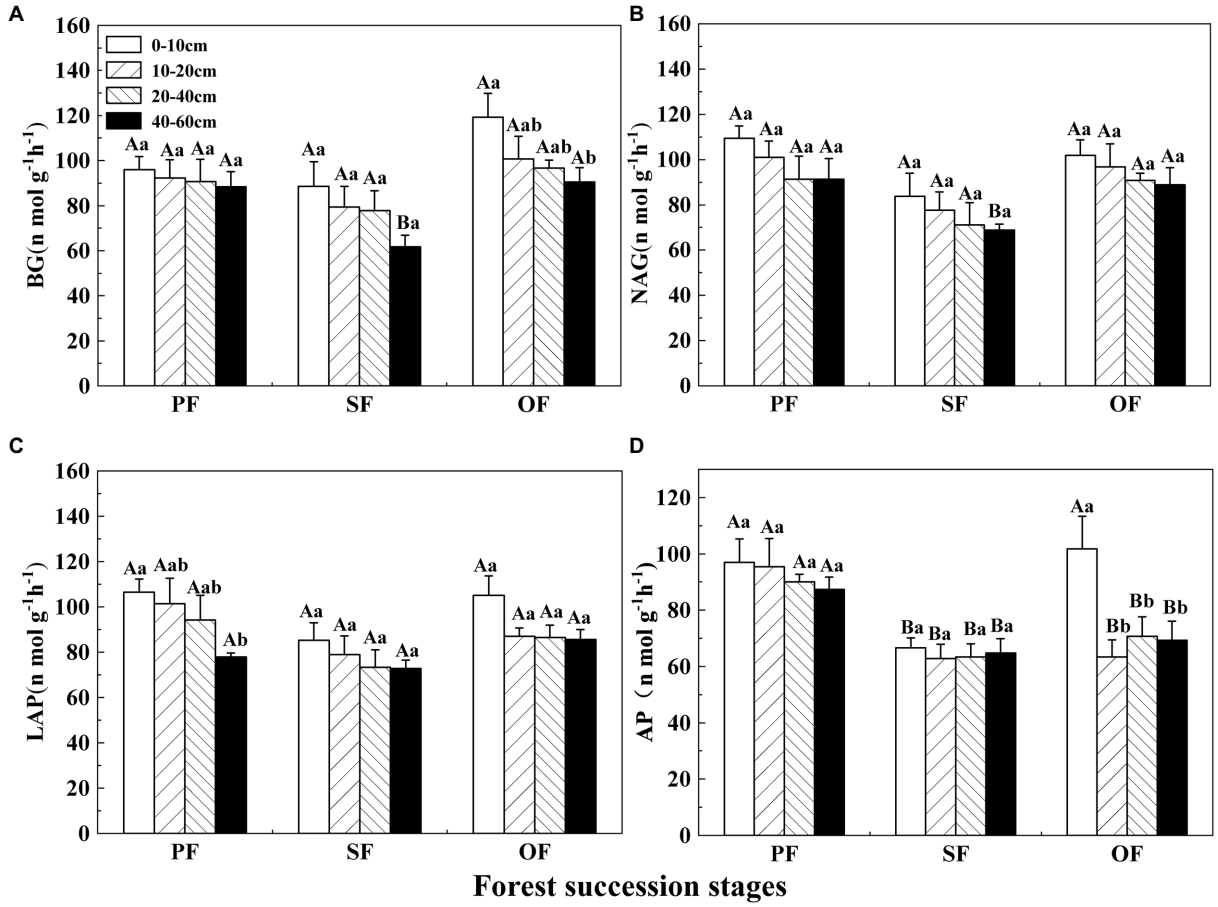

FIGURE 3
Variations of soil enzyme activities in different forest restoration stages in the Jianfengling National Nature Reserve. **(A)** β−1,4−glucosidase (BG), **(B)** β−1,4−N−acetyl−glucosaminidase (NAG), **(C)** leucine aminopeptidase (LAP), and **(D)** acid phosphatase (AP) activities. PF, plantation forest; SF, secondary forest; OF, old-growth forest. Different lowercase letters indicate significant differences between different soil layers at the same stage. Different capital letters indicate significant differences in the same soil layer at different forest succession stages (p<0.05).

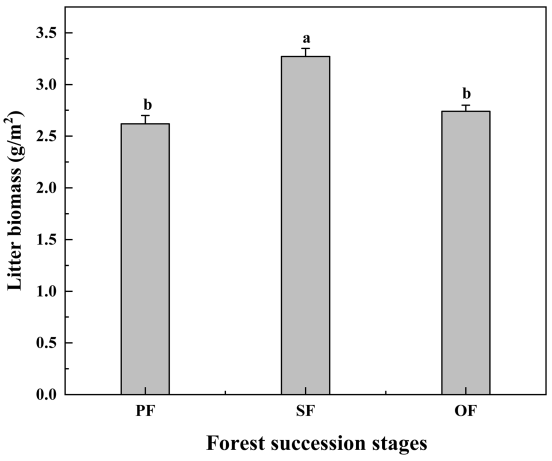

FIGURE 4
Litter biomass in different forest succession stages in the Jianfengling National Nature Reserve. PF, plantation forest; SF, secondary forest; OF, old-growth forest. Different lowercase letters indicate significant differences at different forest succession stages (p<0.05).

From the PF to SF and OF, the total root biomass of different soil layers increased significantly ($p < 0.05$). Especially, the total root biomass of the 10–20 cm soil layer was significantly higher than that of the 0–10 cm soil layer (Figure 5). In different forest succession stages, the SOC, TN, and TP contents of fine and thick roots showed an increasing trend, but not all of them were significant (Supplementary Figure S2).

3.5. The influencing factors of soil organic carbon in different forest succession stages

The SOC substantially negatively correlated with BD and pH, while it obviously positively correlated with TN, TP, NH_4^+–N and NO_3^-–N (Figure 2). The SEM showed that the biological and environmental factors selected in this study explained 79.9% of the variations in SOC (Figure 6A). The AP, total root biomass and pH value were the three main important factors influencing SOC (Figure 6B). The AP and TP had a direct positive effect on SOC

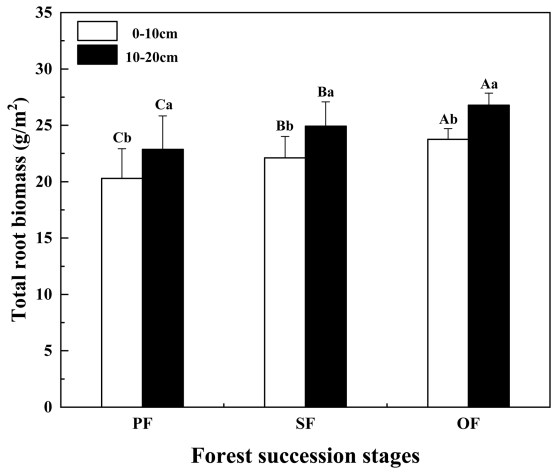

FIGURE 5
Total root biomass in different forest succession stages in the Jianfengling National Nature Reserve. PF, plantation forest; SF, secondary forest; OF, old-growth forest. Different lowercase letters indicate significant differences between different soil layers at the same stage. Different capital letters indicate significant differences in the same soil layer at different forest succession stages (p<0.05).

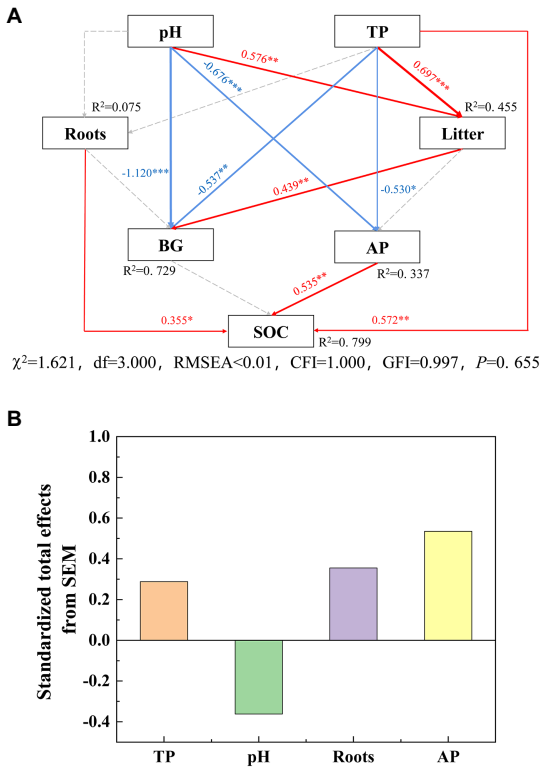

FIGURE 6
Structural equation model (SEM) of the effect of soil properties on SOC (0–20cm) in the Jianfengling National Nature Reserve. The model was fitted by maximum likelihood estimation. In panel **(A)**, red arrows represent significant positive effects and blue arrows represent significant negative effects (p<0.05), and gray dotted line indicates non–significant relationship (p>0.05). The numbers on the line represent normalized path coefficients (*p<0.05, **p<0.01, ***p<0.001). In panel **(B)**, the total effect is the sum of direct and indirect effects. χ^2, global similarity of matrix; df, degree of freedom; GFI, goodness of fit index; CFI, comparative fit index; RMSEA, approximate root mean square error; R^2, variance ratio of priming effect explained by variables; SOC, soil organic carbon; TP, total phosphorus; Roots, total root biomass; Litter, litter biomass; AP, acid phosphatase; BG, β–1,4–glucosidase.

(p < 0.01), while soil TP indirectly affected SOC through its direct effect on AP activity. Total root biomass could affect SOC through its direct effect (p < 0.05). In addition, pH had an indirect effect on SOC by mainly affecting litter biomass and enzyme activities.

4. Discussion

4.1. Effects of forest succession on soil organic carbon

In this study, SOC showed an increasing trend from PF to SF and OF, which supports the first hypothesis. The SOC increased with tropical forest succession, which is similar to the results of previous studies in the subtropical Dinghushan Region (Shao et al., 2017), temperate Loess Plateau (Deng et al., 2013), and subtropical Dashanchong Forest Park (Xu et al., 2018). Litter and roots are the two main resources of carbon input by plants, and the changes in litter and plant roots caused by forest succession affect soil carbon cycling (Guo et al., 2005). Generally, forest succession tends to improve the soil environment, enhance soil microbial activity, improve soil fertility, and increase the input of litter and root biomass (Li et al., 2007; Hu et al., 2016). However, there were no significant differences in litter quantity and quality between different forest stages in the results of this study (Figure 4; Supplementary Figure S1), and further, we found that total root biomass had a direct and significant positive effect on SOC, while litter had no direct effect on SOC (Figure 6A). Those results indicated that the increase in the total root biomass at a later stage of forest succession was more conducive to soil carbon sequestration, which was also consistent with the results in the restoration of tropical forests in India (Lalnunzira et al., 2019). In general, fine roots contribute more to SOC because they have a large surface area and fast turnover rates, and they are the direct way of through which plant photosynthesis transports nutrients to the soil (Zhang et al., 2021). However, Sun et al. (2018) conducted a 6-year experiment on fine root decomposition and found that the decomposition rate of fine roots was slower than that of thick roots, so the contribution of fine roots and thick roots to SOC is still controversial. The results of our study showed that fine root biomass or thick root biomass alone had no significant effect on SOC, while total root biomass had a direct and significant effect on SOC (Figure 6A), which partially supported the second hypothesis. Thus, the role of roots on SOC in tropical forests still needs more attention.

In this study, from PF to OF, the SOC in top soils (0–10 cm and 10–20 cm) increased more significantly than that in

deeper soils (20–40 cm and 40–60 cm; Figure 1), which was consistent with the findings of Yang et al. (2019). The physiochemical properties of top soils and deep soils were significantly different, thus, the regulate factors and mechanism of SOC varied across soil layers (Fontaine et al., 2007; Mobley et al., 2015). Generally, surface SOC accumulation is the result of interactions between environmental factor–regulated abiotic processes and microbe–regulated biotic processes (Hooper et al., 2000). Because the surface soil contains a large amount of vegetation litter, and sufficient water and air in the surface are also conducive to soil microbial activities (Zhang et al., 2021). The SOC changed significantly during forest succession in this study at the depths of 0–10 cm and 10–20 cm (Figure 1). This can be attributed to the increase in organic materials (litter and roots), weathering and microbial decomposition reducing along the forest succession (Smith, 2008). For deep soils (20–40 cm and 40–60 cm), the input of SOC is mainly from the leaching of surface SOC and a few roots. Since the soil clay proportions were higher in the study area (Jiang et al., 2021), there was less leaching of surface SOC to the deep soil. In addition, this study found a significant negative correlation between bulk density (BD) and SOC (Figure 2), which indicates that the high soil BD is also not conducive for the leaching of surface SOC to deep soil layers. A previous study also found that the low SOC in deep soil is related to the high BD in the tropical forests of Hainan Island (Yang et al., 2016).

4.2. Effect of P on soil organic carbon in different forest succession stages

The results of SEM suggest that AP had a direct and positive effect on SOC of the soil layer 0–20 cm (Figure 6A). The AP decreased first and then increased with forest succession, helping in the latter stage of carbon sequestration (Figure 2). Soil extracellular enzymes are associated with soil nutrient utilization, AP can change with the demand phosphorus by soil microbes (Sinsabaugh and Shah, 2012). According to the microbial nutrient allocation theory, microbes will preferentially allocate resources to secrete enzymes that mine the most limited nutrients (Sinsabaugh and Moorhead, 1994; Xiao et al., 2018). In our study, vector analysis of soil extracellular enzymes was used to assess the nutrient limitation of soil microbes (Moorhead et al., 2013). Our results showed that the vector angle of extracellular enzymes was always >45° (Supplementary Figure S3), indicating that soil microbial biomass is limited by soil phosphorus availability (DeForest and Moorhead, 2020). The soil available phosphorus contents and nutrient ecological stoichiometry ratio also show that the tropical forest soil was severely restricted by phosphorus (Table 3), which is consistent with the phosphorus limitation of soil microbe. The soil TP (0.37 g/kg) was lower than the average TP of Chinese soil (0.56 g/kg) and subtropical soil (0.52 g/kg; Han et al., 2005), and the average soil available phosphorus (SAP) was only 1.57 mg/kg. Meanwhile, the soil N:P ratio (as the index of soil to plant nutrient status) is limited by nitrogen when the N:P ratio is <14, and phosphorus when the N:P ratio is >16 (Peng et al., 2019). In our study, this ratio was almost always >16, so it was always limited by phosphorus (Table 3). Previous studies have also shown that tropical forests with high soil acidification tend to exhibit a phosphorus constraint (Waring et al., 2014; Xu et al., 2018). Generally, the change in soil phosphorus limitation will lead to a change in microbial limitation, which affects SOC accumulation (Wang et al., 2022). Hence, soil phosphorus limitation will lead to high AP activity (Wang et al., 2020). A corresponding increase in SOC decomposed by AP. That is, AP and SOC had a positive direct effect relationship, which is consistent with the results of SEM (Figure 6).

In addition, TP had a positive direct effect on SOC (Figure 6A), because soil nutrients and microorganisms were severely restricted by phosphorus in our study area. The increase in soil TP was conducive to the acquisition of phosphorus by plants, which can improve plant productivity and thus increase the input sources of SOC (Schleuss et al., 2019). In conclusion, the negative effect of AP decomposition caused by P restriction was traded off by the direct positive effect of TP on SOC, which was conducive to C sequestration.

4.3. Effect of soil acidification on soil organic carbon in different forest succession stages

Our results suggested that the pH value has no direct effect on SOC, but it has an indirect effect on SOC by inhibiting AP activity (Figure 6A). Previous studies also reported that soil acidification (low pH) has the potential to delay the decomposition of SOM in acid soils by changing the composition of microorganisms, thus favoring SOC accumulation (Lu et al., 2021). In our study, the pH values at a depth of 0–20 cm ranged from 4.01 to 5.52, and the pH values gradually decreased with forest succession from PF to SF and OF (Table 3), indicating that soil acidification was aggregated. Zhu et al. (2021) also found that forest succession can decrease the soil acidity, especially in topsoil. Lower soil pH inhibited the activities of soil microbial activities (Wang et al., 2018a), as the most suitable pH for soil microbe is generally in the neutral range of 6.5–7.5 (San Le et al., 2022). Studies have shown that pH value was negatively correlated with hydrolase activity, which was consistent with the negative correlation between BG, AP and pH in our study (Ghiloufi et al., 2019). Thus, increased soil acidification would be beneficial for SOC accumulation by affecting AP activity under soil nutrient limited by phosphorus (Figure 6). Under the background of future N deposition, soil

acidification accelerates soil carbon sequestration in tropical forests. This has important implications to better understand and predict the effects of P limitation on soil acidification in the global tropical terrestrial ecosystems.

5. Conclusion

Forest succession increased SOC significantly at the depth of 0–20 cm from PF to SF and OF, while there were no significant changes of SOC in deeper soils (20–40 cm and 40–60 cm). Microbial nutrient limitation and N:P ratio reflected that the soil was always limited by phosphorus in the tropical forest of JFL. Except for the microbe–regulated biotic processes, the TP and total root biomass were important factors affecting SOC at depths of 0–20 cm. The increase of total root biomass input rather than litter biomass contributed to SOC sequestration during the tropical forest succession. In addition, the soil acidification caused by forest succession and nitrogen deposition is beneficial to SOC sequestration in tropical forests in the future. This study provides new insights into SOC accumulation during the tropical forest succession.

Data availability statement

The raw data supporting the conclusions of this article will be made available by the authors, without undue reservation.

Author contributions

WLi, QY, and YJ: design the experiments, funding, and reviewing and editing. GX: do the experiments, data analysis, writing–original draft, and writing–reviewing and editing. XW and SM: do the experiments together. WX: put forward relevant improvement suggestions. HY, EH, XH, and WLo: reviewing and editing. All authors contributed to the article and approved the submitted version.

Funding

This research is supported by the National Key Research and Development Program of China (no. 2021YFD2200403-04), the National Natural Science Foundation of China (no. 32160291 and 41663010), and the Natural Science Foundation of Hainan Province (no. 2019RC012). The corresponding authors thank the China Scholarship Council for the financial support.

Acknowledgments

We would like to thank Jianfengling National Key Field Research Station for Tropical Forest Ecosystem.

Conflict of interest

The authors declare that the research was conducted in the absence of any commercial or financial relationships that could be construed as a potential conflict of interest.

Publisher's note

Supplementary material

The Supplementary material for this article can be found online at: https://www.frontiersin.org/articles/10.3389/fevo.2022.1104369/full#supplementary-material

References

Bach, C. E., Warnock, D. D., Van Horn, D. J., Weintraub, M. N., Sinsabaugh, R. L., Allison, S. D., et al. (2013). Measuring phenol oxidase and peroxidase activities with pyrogallol, L–DOPA, and ABTS: effect of assay conditions and soil type. *Soil Biol. Biochem.* 67, 183–191. doi: 10.1016/j.soilbio.2013.08.022

Bao, S. (2000). *Soil Agrochemical Analysis*. Beijing Chinese Agriculture Press.

Cui, Y. X., Fang, L. C., Guo, X. B., Wang, X., Wang, Y. Q., Zhang, Y. J., et al. (2019). Responses of soil bacterial communities, enzyme activities, and nutrients to agricultural-to-natural ecosystem conversion in the loess plateau, China. *J. Soils Sediments* 19, 1427–1440. doi: 10.1007/s11368-018-2110-4

DeForest, J. L., and Moorhead, D. L. (2020). Effects of elevated pH and phosphorus fertilizer on soil C, N and P enzyme stoichiometry in an acidic mixed mesophytic deciduous forest. *Soil Biol. Biochem.* 150:107996. doi: 10.1016/j.soilbio.2020.107996

Deng, L., Wang, K. B., Chen, M. L., Shangguan, Z. P., and Sweeney, S. (2013). Soil organic carbon storage capacity positively related to forest succession on the loess plateau, China. *Catena* 110, 1–7. doi: 10.1016/j.catena.2013.06.016

Fang, J. Y., Li, Y. D., Zhu, B., Liu, G. H., and Zhou, G. Y. (2004). Community structure, species diversity and status of montane rainforest in Jianfengling, Hainan Island. *Biodivers. Sci.* 01, 29–43. doi: 10.17520/biods.2004005

Fang, J. Y., Yu, G. R., Ren, X. B., Liu, G. H., and Zhao, X. Q. (2015). Research progress of ecosystem carbon sequestration task group of the strategic priority science and technology project of Chinese Academy of Sciences "carbon budget certification and related issues in response to climate change". *Bull. Chin. Acad. Sci.* 30:10. doi: 10.16418/j.issn.1000–3045

Fontaine, S., Barot, S., Barre, P., Bdioui, N., Mary, B., and Rumpel, C. (2007). Stability of organic carbon in deep soil layers controlled by fresh carbon supply. *Nature* 450, 277–280. doi: 10.1038/nature06275

German, D. P., Weintraub, M. N., Grandy, A. S., Lauber, C. L., Rinkes, Z. L., and Allison, S. D. (2011). Optimization of hydrolytic and oxidative enzyme methods for ecosystem studies. *Soil Biol. Biochem.* 43, 1387–1397. doi: 10.1016/j.soilbio.2011.03.017

Ghiloufi, W., Seo, J., Kim, J., Chaieb, M., and Kang, H. (2019). Effects of biological soil crusts on enzyme activities and microbial community in soils of an arid ecosystem. *Microb. Eco.* 77, 201–216. doi: 10.1007/s00248–018–1219–8

Guo, L. B., Halliday, M. J., Siakimotu, S. J. M., and Gifford, R. M. (2005). Fine root production and litter input: its effects on soil carbon. *Plant Soil* 272, 1–10. doi: 10.1007/s11104-004-3611-z

Guo, X. W., Luo, T. S., and Li, Y. D. (2015). Soil organic carbon density and influencing factors of primary tropical forests in Hainan Island. *Acta Ecol. Sin.* 35, 56–61. doi: 10.5846/stxb201404180761

Han, W., Fang, J., Guo, D., and Zhang, Y. (2005). Leaf nitrogen and phosphorus stoichiometry across 753 terrestrial plant species in China. *New Phytol.* 168, 377–385. doi: 10.1111/j.1469-8137.2005.01530.x

Hooper, D. U., Bignell, D. E., Brown, V. K., Lijbert, B., Mark, D. J., Wall, D. H., et al. (2000). Interactions between aboveground and belowground biodiversity in terrestrial ecosystems: patterns, mechanisms, and feedbacks. *Bioscience* 12, 1049–1061. doi: 10.1641/0006–3568(2000)050

Hu, N., and Lan, J. C. (2020). Impact of vegetation restoration on soil organic carbon stocks and aggregates in a karst rocky desertification area in Southwest China. *J. Soils Sediments* 20, 1264–1275. doi: 10.1007/s11368-019-02532-y

Hu, Y. L., Zeng, D. H., Ma, X. Q., and Chang, S. X. (2016). Root rather than leaf litter input drives soil carbon sequestration after afforestation on a marginal cropland. *Forest Ecol. Manag.* 362, 38–45. doi: 10.1016/j.foreco.2015.11.048

Huang, Y. H., Li, Y. L., Xiao, Y., Wenigmann, K. O., Zhou, G. Y., Zhang, D. Q., et al. (2011). Controls of litter quality on the carbon sink in soils through partitioning the products of decomposing litter in a forest succession series in South China. *For. Ecol. Manag.* 261, 1170–1177. doi: 10.1016/j.foreco.2010.12.030

Jiang, L., Ma, S. H., Zhou, Z., Zheng, T. L., Jiang, X. X., Cai, Q., et al. (2017). Soil respiration and its partitioning in different components in tropical primary and secondary mountain rain forests in Hainan Island, China. *J. Plant Ecol.* 10, rtw080–rtw799. doi: 10.1093/jpe/rtw080

Jiang, Y. M., Yang, H., Yang, Q., Liu, W. J., Li, Z. L., Mao, W., et al. (2021). The stability of soil organic carbon across topographies in a tropical rainforest. *Peerj* 9:e12057. doi: 10.7717/peerj.12057

Kock, N. (2015). Common method bias in PLS-SEM: a full collinearity assessment approach. *Int. J. e-Collab.* 11, 1–10. doi: 10.4018/ijec.2015100101

Lalnunzira, C., Brearley, F. Q., and Tripathi, S. K. (2019). Root growth dynamics during recovery of tropical mountain forest in north–East India. *J. Mt Sci.–Engl* 16, 2335–2347. doi: 10.1007/s11629-018-5303-9

Li, X. R., Kong, D. S., Tan, H. J., and Wang, X. P. (2007). Changes in soil and vegetation following stabilisation of dunes in the southeastern fringe of the Tengger Desert, China. *Plant Soil* 300, 221–231. doi: 10.1007/s11104-007-9407-1

Li, Q., Wang, B., and Deng, Y. (2019). Relationship between gap spatial pattern and understory plant diversity in tropical rain forest. *Plant Ecol.* 27, 273–285. doi: 10.17520/biods.2018258

Lu, X. K., Vitousek, P. M., Mao, Q. G., Gilliam, F. S., Luo, Y. Q., Turner, B. L., et al. (2021). Nitrogen deposition accelerates soil carbon sequestration in tropical forests. *Proc. Natl. Acad. Sci. U. S. A.* 118:e2020790118. doi: 10.1073/pnas.2020790118

Ma, S. H., Zhu, B., Chen, G. P., Ni, X. F., Zhou, L. H., Su, H. J., et al. (2022). Loss of soil microbial residue carbon by converting a tropical forest to tea plantation. *Sci. Total Environ.* 818:151742. doi: 10.1016/j.scitotenv.2021.151742

Mobley, M. L., Lajtha, K., Kramer, M. G., Bacon, A. R., Heine, P. R., and Richter, D. D. (2015). Surficial gains and subsoil losses of soil carbon and nitrogen during secondary forest development. *Glob. Chang. Biol.* 21, 986–996. doi: 10.1111/gcb.12715

Moorhead, D. L., Rinkes, Z. L., Sinsabaugh, R. L., and Weintraub, M. N. (2013). Dynamic relationships between microbial biomass, respiration, inorganic nutrients and enzyme activities: informing enzyme–based decomposition models. *Front. Microbiol.* 4:223. doi: 10.3389/fmicb.2013.00223

Peng, Y. F., Peng, Z. P., Zeng, X. T., and Houx, J. H. (2019). Effects of nitrogen–phosphorus imbalance on plant biomass production: a global perspective. *Plant Soil* 436, 245–252. doi: 10.1007/s11104–018–03927–5

Ren, H., Li, L., Liu, Q., Wang, X., Li, Y., Hui, D., et al. (2014). Spatial and temporal patterns of carbon storage in Forest ecosystems on Hainan Island, southern China. *PLoS One* 9:e108163. doi: 10.1371/journal.pone.0108163

Rubino, M., Dungait, J. A. J., Evershed, R. P., Bertolini, T., De Angelis, P., D'Onofrio, A., et al. (2010). Carbon input belowground is the major C flux contributing to leaf litter mass loss: evidences from a C–13 labelled–leaf litter experiment. *Soil Biol. Biochem.* 42, 1009–1016. doi: 10.1016/j.soilbio.2010.02.018

San Le, V., Herrmann, L., Hudek, L., Nguyen, T. B., Brau, L., and Lesueur, D. (2022). How application of agricultural waste can enhance soil health in soils acidified by tea cultivation: a review. *Environ. Chem. Lett.* 20, 813–839. doi: 10.1007/s10311–021–01313–9

Schleuss, P. M., Widdig, M., Heintz-Buschart, A., Guhr, A., Martin, S., Kirkman, K., et al. (2019). Stoichiometric controls of soil carbon and nitrogen cycling after long–term nitrogen and phosphorus addition in a Mesic grassland in South Africa. *Soil Biol. Biochem.* 135, 294–303. doi: 10.1016/j.soilbio.2019.05.018

Shao, S., Zhao, Y., Zhang, W., Hu, G. Q., Xie, H. T., Yan, J. H., et al. (2017). Linkage of microbial residue dynamics with soil organic carbon accumulation during subtropical forest succession. *Soil Biol. Biochem.* 114, 114–120. doi: 10.1016/j.soilbio.2017.07.007

Shipley, B. (2001). *Cause and correlation in biology: A User's guide to path analysis structural equations and causal inference*. UK: Cambridge Univ. Press.

Sinsabaugh, R. L., and Moorhead, D. L. (1994). Resource allocation to extracellular enzyme production: a model for nitrogen and phosphorus control of litter decomposition. *Soil Biol. Biochem.* 26(10), 1305–1311. doi:, doi: 10.1016/0038-0717(94)90211-9

Sinsabaugh, R. L., and Shah, J. J. (2012). Ecoenzymatic stoichiometry and ecological theory. *Annu. Rev. Ecol. Evol. Syst.* 43, 313–343. doi: 10.1146/annurev-ecolsys-071112-124414

Smith, P. (2008). Land use change and soil organic carbon dynamics. *Nutr. Cycl. Agroecosys.* 81, 169–178. doi: 10.1007/s10705-007-9138-y

Sun, T., Hobbie, S. E., Berg, B., Zhang, H. G., Wang, Q. K., Wang, Z. W., et al. (2018). Contrasting dynamics and trait controls in first–order root compared with leaf litter decomposition. *Proc. Natl. Acad. Sci. U. S. A.* 115, 10392–10397. doi: 10.1073/pnas.1716595115

Walker, L. R., Wardle, D. A., Bardgett, R. D., and Clarkson, B. D. (2010). The use of chronosequences in studies of ecological succession and soil development. *J. Ecol.* 98, 725–736. doi: 10.1111/j.1365-2745.2010.01664.x

Wang, X. X., Cui, Y. X., Wang, Y. H., Duan, C. J., Niu, Y. A., Sun, R. X., et al. (2022). Ecoenzymatic stoichiometry reveals phosphorus addition alleviates microbial nutrient limitation and promotes soil carbon sequestration in agricultural ecosystems. *J. Soils Sediments* 22, 536–546. doi: 10.1007/s11368-021-03094-8

Wang, C., Lu, X. K., Mori, K., Mao, Q. G., Zhou, J. K., Zhou, G. Y., et al. (2018a). Responses of soil microbial community to continuous experimental nitrogen additions for 13 years in a nitrogen-rich tropical forest. *Soil Biol. Biochem.* 121, 103–112. doi: 10.1016/j.soilbio.2018.03.009

Wang, C., Mori, T., Mao, Q. G., Zhou, K. J., Wang, Z. H., Zhang, Y. Q., et al. (2020). Long-term phosphorus addition downregulates microbial investments on enzyme productions in a mature tropical forest. *J. Soils Sediments* 20, 921–930. doi: 10.1007/s11368-019-02450-z

Waring, B. G., Weintraub, S. R., and Sinsabaugh, R. L. (2014). Ecoenzymatic stoichiometry of microbial nutrient acquisition in tropical soils. *Biogeochemistry* 117, 101–113. doi: 10.1007/s10533-013-9849-x

Xiao, W., Chen, X., Jing, X., and Zhu, B. (2018). A meta-analysis of soil extracellular enzyme activities in response to global change. *Soil Biol. Biochem.* 123, 21–32. doi: 10.1016/j.soilbio.2018.05.001

Xu, H., Li, Y., Lin, M., Wu, J., Luo, T., Zhou, Z., et al. (2015). Community characteristics of a 60 ha dynamics plot in the tropical montane rain forest in Jianfengling, Hainan Island. *Biodivers. Sci.* 23, 192–201. doi: 10.17520/biods.2014157

Xu, H., Li, Y., Luo, T., Lin, M., Chen, D., Mo, J., et al. (2009). Community structure characteristics of tropical montane rain forests with different regeneration types in Jianfengling. *Scientia Silvae Sinicae.* 45, 14–20. doi: 10.1007/978-1-4020-9623-5_5

Xu, C. H., Xiang, W. H., Gou, M. M., Chen, L., Lei, P. F., Fang, X., et al. (2018). Effects of Forest restoration on soil carbon, nitrogen, phosphorus, and their stoichiometry in Hunan, southern China. *Sustainability.* 10:1874. doi: 10.3390/su10061874

Yang, H., Li, Y. D., Ren, H., Luo, T., Chen, R., and Liu, W. (2016). Soil organic carbon density and influencing factors in tropical virgin forests of Hainan Island, China. *Chin. J. Ecol.* 40, 292–303. doi: 10.17521/cjpe.2015.0314

Yang, H., Liu, S. R., Li, Y. D., and Xu, H. (2018). Diurnal variations and gap effects of soil CO_2, N_2O and CH_4 fluxes in a typical tropical montane rainforest in Hainan Island, China. *Ecol. Res.* 33, 379–392. doi: 10.1007/s11284-017-1550-4

Yang, B., Zhang, W. H., Lu, Y. L., Zhang, W. W., and Wang, Y. A. (2019). Carbon storage dynamics of secondary Forest succession in the central loess plateau of China. *Forests* 10:342. doi: 10.3390/f10040342

Zhang, S., Quan, X. U., Yang, Q., Jiang, Y., Wang, X., and Liu, W. (2019). C, N, and P content and C:N ratio in sandy soil in the coastal zone of Hainan Island. *Chin. J. For. Environ.* 39, 398–403. doi: 10.13324/j.cnki.jfcf.2019.04.011

Zhang, C. C., Wang, Y. Q., Jia, X. X., and Shao, M. A. (2021). Estimates and determinants of soil organic carbon and total nitrogen stocks up to 5 m depth across a long transect on the loess plateau of China. *J. Soils Sediments* 21, 748–765. doi: 10.1007/s11368-020-02861-3

Zhang, Y. S., Yu, C. X., Xie, J. J., Du, S. T., Feng, J. X., and Guan, D. S. (2021). Comparison of fine root biomass and soil organic carbon stock between exotic and native mangrove. *Catena* 204:105423. doi: 10.1016/j.catena.2021.105423

Zhou, G., Liu, S., Li, Z., Zhang, D., Tang, X., Zhou, C., et al. (2006). Old–growth forests can accumulate carbon in soils. *Science* 314:1417. doi: 10.1126/science.1130168

Zhou, Z., Wang, C., and Luo, Y. (2018). Effects of forest degradation on microbial communities and soil carbon cycling: a global meta–analysis. *Glob. Ecol. Biogeogr.* 27, 110–124. doi: 10.1111/geb.12663

Zhu, X., Fang, X., Wang, L., Xiang, W., Alharbi, H. A., Lei, P., et al. (2021). Regulation of soil phosphorus availability and composition during forest succession in subtropics. *For. Ecol. Manag.* 502:119706. doi: 10.1016/j.foreco.2021.119706

Zhu, J. X., Wang, C. K., Zhou, Z., Zhou, G. Y., Hu, X. Y., Jiang, L., et al. (2020). Increasing soil carbon stocks in eight permanent forest plots in China. *Biogeosciences* 17, 715–726. doi: 10.5194/bg-17-715-2020

frontiers | Frontiers in Ecology and Evolution

TYPE Perspective
PUBLISHED 20 January 2023
DOI 10.3389/fevo.2022.1099162

OPEN ACCESS

EDITED BY
Robert John,
Indian Institute of Science Education and Research Kolkata, India

REVIEWED BY
Corrado Battisti,
Roma Tre University,
Italy

*CORRESPONDENCE
A. Alonso Aguirre
✉ A.Alonso.Aguirre@colostate.edu

SPECIALTY SECTION
This article was submitted to Conservation and Restoration Ecology, a section of the journal Frontiers in Ecology and Evolution

RECEIVED 15 November 2022
ACCEPTED 29 December 2022
PUBLISHED 20 January 2023

CITATION
Bonacic C, Medellin RA, Ripple W, Sukumar R, Ganswindt A, Padua SM, Padua C, Pearl MC, Aguirre LF, Valdés LM, Buchori D, Innes JL, Ibarra JT, Rozzi R and Aguirre AA (2023) Scientists warning on the ecological effects of radioactive leaks on ecosystems.
Front. Ecol. Evol. 10:1099162.
doi: 10.3389/fevo.2022.1099162

Scientists warning on the ecological effects of radioactive leaks on ecosystems

Cristian Bonacic[1], Rodrigo A. Medellin[2], William Ripple[3], Raman Sukumar[4], Andre Ganswindt[5], Suzana M. Padua[6], Claudio Padua[6], Mary C. Pearl[7], Luis F. Aguirre[8], Lourdes Mugica Valdés[9], Damayanti Buchori[10], John L. Innes[11], J. Tomás Ibarra[1,12,13], R. Rozzi[14,15] and A. Alonso Aguirre[16]*

[1]Department of Ecosystems & The Environment, School of Agriculture and Forestry, Pontifical Catholic University of Chile, Santiago, Chile, [2]Instituto de Ecología, UNAM, Ciudad Universitaria, Mexico City, Coyoacán, Mexico, [3]Department of Forest Ecosystems and Society, Oregon State University, Corvallis, OR, United States, [4]Centre for Ecological Sciences, Indian Institute of Science, Bangalore, Karnataka, India, [5]Mammal Research Institute, Department of Zoology and Entomology, University of Pretoria, Pretoria, Hatfield, South Africa, [6]Instituto de Pesquisas Ecológicas (IPE-Institute for Ecological Research), São Paulo, Nazaré Paulista, Brazil, [7]Distinguished Career Institute, Stanford University, Palo Alto, CA, United States, [8]Centro de Biodiversidad y Genética, Universidad Mayor de San Simón, Campus Universitario, Cochabamba, Bolivia, [9]Faculty of Biology, University of Havana, Havana, Vedado, Cuba, [10]Center for Transdisciplinary and Sustainability Science, IPB University, Bogor, Occidental Java, Indonesia, [11]Faculty of Forestry, University of British Columbia, Vancouver, BC, Canada, [12]ECOS (Ecosystem-Complexity-Society) Co-Laboratory, Center for Local Development (CEDEL), Center for Intercultural and Indigenous Research (CIIR) & Center of Applied Ecology and Sustainability (CAPES), Villarrica Campus, Pontificia Universidad Católica de Chile, Villarrica, Chile, [13]Cape Horn International Center for Global Change Studies and Biocultural Conservation (CHIC), Universidad de Magallanes, Puerto Williams, Chile, [14]Cape Horn International Center (CHIC), Parque Etnobotánico Omora, Universidad de Magallanes, Puerto Williams, Chile, [15]Sub-Antarctic Biocultural Conservation Program, Department of Philosophy and Religion and Department of Biological Sciences, University of North Texas, Denton, TX, United States, [16]Department of Fish, Wildlife and Conservation Biology, Warner College of Natural Resources, Colorado State University, Fort Collins, CO, United States

A nuclear leakage or tactical nuclear weapon use in a limited war could cause immense and long-lasting ecological consequences beyond the direct site of exposure. We call upon all scientists to communicate the importance of the environmental impacts of such an event to all life forms on Earth, including humankind. Changes to ecosystem structure and functioning and species extinctions would alter the biosphere for an unknown time frame. Radiation could trigger cascade effects in marine, atmospheric and terrestrial ecosystems of a magnitude far beyond human capabilities for mitigation or adaptation. Even a "tactical nuclear war" could alter planet Earth's living boundaries, ending the current Anthropocene era.

KEYWORDS

tactical bomb, radiation, pollution, nuclear war, biodiversity loss, ecosystem services, species extinction

One sentence summary

We describe the devastating effects of nuclear radiation and its long-lasting consequences on Earth's ecosystems.

Main text

Recent events related to the armed conflict in Ukraine have been linked to the possibility of radioactive leaks, the risk of using "tactical nuclear bombs," or even full-scale nuclear war. The shelling of the Zaporizhzhia Nuclear Power Plant represents a particular risk. As environmental scientists, ecologists, and conservationists from all corners of the world, we would like to call upon all scientists to communicate the risks associated with radiation to the public and policymakers. We must be proactive and explain to our people the stark implications of an accidental nuclear leak, the use of tactical bombs, or a full-scale nuclear war if any of these were to happen. Our ethical and professional duty is to communicate the multiple potential consequences to life on Earth, including humankind. We propose a key summary of facts to communicate our concerns to leaders, stakeholders, and society effectively.

In any socioecological system, many variables, components, and processes can be affected by human intervention. Radiation leakage and nuclear explosions can severely affect natural (and anthropogenic) systems. Adding a major disturbance to the intrinsic uncertainty and unpredictability of these systems (Battisti et al., 2016). Any nuclear explosion can trigger ecological consequences far beyond the site where it occurs. Nuclear weapons can release massive radiation with total burdens of radionuclides amounting to millions of curies of strontium, cesium, plutonium, and carbon (Leaning, 2000; Pereira et al., 2022). Those consequences are long-lasting, affect ecosystem structure and function, lead to decline and local extinctions, severely hamper life on Earth, and reduce opportunities for humans to sustain our civilization (Leaning, 2000; Burkitbayev et al., 2011).

A nuclear bomb detonation spreading radiation causes direct physical effects to all life forms, including multiple species mortalities, mutations (Schmitz-Feuerhake et al., 2016), and impairment of species' capacity to continue reproducing and playing their ecological roles in nature. Abiotic elements and nutrient cycles will suffer severe radiation contamination and cascading effects on terrestrial and marine life (Paraskevi et al., 2021). Atmospheric dynamics, freshwater resources, underground water, and ocean currents can move particles containing radioactive substances far beyond the point of explosion. Their contamination can last hundreds or even thousands of years (Burkitbayev et al., 2011).

While there has rightly been a focus on the tragic consequences of the ongoing Russian-Ukrainian conflict on the civilian population of Ukraine and its broader implications for geopolitics, the world economy, food security, and human lives, the impacts on ecosystem services have been largely overlooked. We need to recognize urgently the immediate effects of the war on air quality, biodiversity loss due to deforestation, wildfires, habitat loss, and their effects on water resources, soils, and landscape morphology. These impacts would increase significantly in the event of an accidental or deliberate release of radiation (Balonov, 2019; Dombrovski et al., 2022).

Beyond the immediate devastating effects of a nuclear blast, the impact of a nuclear plume, depending on its magnitude, is to obstruct solar radiation, altering climate locally, regionally, and potentially globally. Increased UV radiation, less available atmospheric oxygen, and lower atmospheric temperature will affect plant primary productivity, causing a decline in crop production in the area affected by the plume (Tinus and Roddy, 1990; Nakanishi and Tanoi, 2016). Food security globally could be affected, with more significant plumes, compounding the effects already seen from the restrictions on food exports from Ukraine. Food chains may be contaminated in areas affected by the plume, making any agricultural products unfit for human consumption.

Biodiversity loss can be massive in places where nuclear bombs explode. Large fires can also extend the damage and spread radioactive particles beyond the explosion site, leading to soil erosion and nutrient depletion (Tinus and Roddy, 1990; Gudkov et al., 2011). Nuclear explosions can potentially destroy forests, wetlands, and biodiversity hotspots. Ecosystem services such as pollination would be affected by species extinctions (Møller et al., 2012; Nakanishi and Tanoi, 2016). Multiple nuclear explosions could accelerate the demise of many species already threatened with extinction because of climate change and other anthropogenic causes. Endemic species could be lost as the radioactivity can spread over hundreds of square kilometers, potentially eliminating entire populations of endangered animals and plants. The 1986 explosion of the Chernobyl nuclear reactor and the subsequent open reactor core fire significantly contaminated more than 100,000 km^2. Radioactive dust from the site was identified throughout most of Europe (except for the Iberian Peninsula).

Despite much data about the effects of radiation exposure from bomb detonation sites or nuclear accidents such as Chernobyl, the public and decision-makers are generally unaware of the long-lasting consequences for whole ecosystems. The Chernobyl Forum (Balonov, 2007) summarized the effects of immediate and middle-term radioisotope exposure. The report concluded that long-lasting bioaccumulation pervaded at all trophic levels. The radionuclide fallout could reach regions far beyond the detonation site with a severe nuclear exchange. Earth's carrying capacity to sustain life could be seriously hampered, if not crippled. Contrafactual results suggest that following the Chernobyl accident, biodiversity boomed after a few decades in the surrounding area (Møller and Mousseau, 2011; Deryabina et al., 2015). However, as that accident occurred at a single site, it cannot be used as an argument to suggest that

the impact of multiple nuclear bomb detonations will be minimal. The cumulative effect of nuclear bombs exploding in different locations would have an additive effect with devastating consequences for multi-taxa species abundance and richness, a decline in species recruitment, and artificially changing species composition in communities affected by radiation (Balonov, 2007).

All these cascading effects could directly hamper human survival and living conditions as we know them. The Chernobyl explosion, the Fukushima disaster, and other radiation leaks may have misled decision-makers to underestimate the grave consequences of a nuclear war, even on a limited basis. Global food web disruption, abrupt changes in climate caused by a nuclear winter, and radioactive air, water, and soil pollution could result in the deaths of many people. The direct consequences of a nuclear explosion will be widespread hunger, radiation toxicity, and large areas of uninhabitable ecosystems (Balonov, 2007; Burkitbayev et al., 2011). A "tactical nuclear war" could end the Anthropocene era by moving Earth far from the living boundaries that make the planet habitable for humans and many known species.

In essence, what humanity has failed to recognize, thereby causing extensive damage to the planet, is the value of all life on Earth. All humans must stand together to prevent a catastrophic nuclear event.

Data availability statement

The original contributions presented in the study are included in the article/supplementary material, further inquiries can be directed to the corresponding author.

Author contributions

CB completed the idea, writing, and references compilation. The first drafts were discussed with WR. All other authors commented, added, and proposed ideas and editing changes to the main manuscript. TF helped to format the final manuscript. CA reviewed the grammar. RM also helped handling the first stages of the submission process. All authors contributed to the article and approved the submitted version.

Acknowledgments

The corresponding author is greatful to the National Agency of Research and Development (ANID Fondecyt 1221644).

Conflict of interest

The authors declare that the research was conducted in the absence of any commercial or financial relationships that could be construed as a potential conflict of interest.

Publisher's note

References

Balonov, M. I. (2007). The Chernobyl forum: significant findings and recommendations. *J. Environ. Radioact.* 96, 6–12. doi: 10.1016/j.jenvrad.2007.01.015

Balonov, M. (2019). Health effects of reactor accidents with particular regards to Chornobyl –a review paper. *Jpn. J. Health Phys.* 54, 161–171. doi: 10.5453/jhps.54.161

Battisti, C., Poeta, G., and Fanelli, G. (2016). *An introduction to disturbance ecology: A road map for wildlife management and conservation. Environmental science and engineering*. Springer Int. Publ. Switzerland, 178.

Burkitbayev, M., Priest, N., Mitchell, P., Vintro, L., Pourcelot, L., Kuyanova, Y., et al. (2011). "Ecological impacts of large-scale war preparations: Semipalatinsk test site, Kazakhstan" in *Warfare ecology. NATO science for peace and security series C: Environmental security*. eds. G. Machlis, T. Hanson, Z. Špirić and J. McKendry (Dordrecht: Springer)

Deryabina, T. G., Kuchmel, S. V., Nagorskaya, L. L., Hinton, T. G., Beasley, J. C., Lerebours, A., et al. (2015). Long-term census data reveal abundant wildlife populations at Chernobyl. *Curr. Biol.* 25, R824–R826. doi: 10.1016/j.cub.2015.08.017

Dombrovski, V. C., Zhurauliou, D. V., and Ashton-Butt, A. (2022). Long-term effects of rewilding on species composition: 22 years of raptor monitoring in the Chernobyl exclusion zone. *Restor. Ecol.* 30:633. doi: 10.1111/rec.13633

Gudkov, I. N., Gaychenko, V. A., Pareniuk, O. Y., and Grodzinsky, D. M. (2011). Changes in biocenoses in the Chernobyl NPP accident zone. *Nucl. Phys. At. Energy* 12, 362–374. doi: УДК577.3+504.7:621.039.58

Leaning, J. (2000). Environment and health: 5. Impact of war. *Can. Med. Assoc. J.* 163, 1157–1161. PMID: 11079063

Møller, A. P., Barnier, F., and Mousseau, T. A. (2012). Ecosystems effects 25 years after Chernobyl: pollinators, fruit set, and recruitment. *Oecologia* 170, 1155–1165. doi: 10.1007/s00442-012-2374-0

Møller, A. P., and Mousseau, T. A. (2011). Conservation consequences of Chernobyl and other nuclear accidents. *Biol. Conserv.* 144, 2787–2798. doi: 10.1016/j.biocon.2011.08.009

Nakanishi, T. M., and Tanoi, K. (2016). Agricultural implications of the Fukushima nuclear accident: the first three years. *J. Radiat. Res.* https://link.springer.com/book/10.1007/978-4-431-55828-6#toc

Paraskevi, A. A., Tereshchenko, N. N., Proskurnin, V. Y., and Chuzhikova-Proskurnina, O. D. (2021). Change in plutonium sedimentation fluxes into the bottom sediments of the Sevastopol bay before and after the Chernobyl NPP accident. *Mar. Biol. J.* 6, 69–82. doi: 10.21072/mbj.2021.06.2.05

Pereira, P., Bašić, F., Bogunovic, I., and Barcelo, D. (2022). Russian-Ukrainian war impacts the total environment. *Sci. Total Environ.* 837:155865. doi: 10.1016/j.scitotenv.2022.155865

Schmitz-Feuerhake, I., Busby, C., and Pflugbeil, S. (2016). Genetic radiation risks: a neglected topic in the low dose debate. *Environ. Health Toxicol.* 31:e2016001. doi: 10.5620/eht.e2016001

Tinus, R. W., and Roddy, D. J. (1990). "Effects of global atmospheric perturbations on forest ecosystems in the northern temperate zone; predictions of seasonal depressed temperature kill mechanisms, biomass production, and wildfire soot emissions" in *Global catastrophes in earth history; an interdisciplinary conference on impacts, volcanism, and mass mortality*. eds. V. L. Sharpton and P. D. Ward, vol. *247* (United States: Geological Society of America)

frontiers | Frontiers in Ecology and Evolution

TYPE Original Research
PUBLISHED 10 February 2023
DOI 10.3389/fevo.2023.1127139

OPEN ACCESS

EDITED BY
Xiang Liu,
Lanzhou University,
China

REVIEWED BY
Haitao Wang,
Northeast Normal University,
China
Longwu Wang,
Guizhou Normal University,
China

*CORRESPONDENCE
Xiaodong Rao
✉ 993676@hainanu.edu.cn

SPECIALTY SECTION
This article was submitted to Conservation and Restoration Ecology, a section of the journal Frontiers in Ecology and Evolution

RECEIVED 19 December 2022
ACCEPTED 16 January 2023
PUBLISHED 10 February 2023

CITATION
Rao X, Li J, He B, Wang H, Wu G, Teng T and Ling Q (2023) Nesting success and potential nest predators of the red Junglefowl (*Gallus gallus jabouillei*) based on camera traps and artificial nest experiments.
Front. Ecol. Evol. 11:1127139.
doi: 10.3389/fevo.2023.1127139

Nesting success and potential nest predators of the red Junglefowl (*Gallus gallus jabouillei*) based on camera traps and artificial nest experiments

Xiaodong Rao[1,2]*, Jialing Li[3,4], Binbin He[5], Hesheng Wang[6], Guanmian Wu[1], Tiantian Teng[1] and Qingping Ling[1]

[1]College of Forestry, Hainan University, Haikou, China, [2]Intelligent Forestry Key Laboratory of Haikou City, College of Forestry, Hainan University, Haikou, China, [3]College of Ecology and Environment, Hainan University, Haikou, China, [4]Hainan Tropical Rain Forest National Park Service Wuzhishan Branch, Wuzhishan, China, [5]Hainan Datian National Nature Reserve Administration, Dongfang, China, [6]Hainan Bangxi Provincial Nature Reserve Management Station, Bangxi, China

Breeding success is an important factor determining fecundity with nest predation being the main factor limiting avian breeding success. Understanding of nest predation and its influencing factors are highly significant to explore the dynamics of bird populations and developing appropriate conservation strategies. In two breeding seasons of the year 2020 and 2021, natural nests of the red junglefowl (*Gallus gallus jabouillei*) were systematically searched and monitored using infrared camera, in two nature reserves (Datian and Bangxi) of tropical Hainan island, China. Results showed that breeding season of the red junglefowl is mainly from March to July, with April being the breeding peak. The clutch size was 5.15±1.28 (n=13), and nesting success of natural nests was 31.2%, with nest predation accounting for 45.4% of nest failure. Artificial nest experiments showed that predation rates of artificial nests were 25% (Datian, 2020), 6.67% (Datian, 2021), and 0% (Bangxi, 2020). Rodents, reptiles, and coucals are the main nest predators of red junglefowls, while activities of Hainan Eld's deers (*Panolia siamensis*) may interfere with the reproduction of red junglefowls. We suggest that the conservation management policies should consider the impacts on junglefowls' breeding success when reconstructing the suitable habitat of the Hainan Eld's deer.

KEYWORDS

artificial nest, breeding success, *Gallus gallus jabouillei*, infrared camera, nest predation

Introduction

The study of reproductive biology and the estimation of nest survival rates are critical to understanding avian life history (Martin, 2004; Stutchbury and Morton, 2008, 2023). Life history traits related to reproduction, such as clutch size, parental care, chick development, and survival rate, can provide insights for solving problems related to the assessment of population status and conservation (Martin, 2002, 2008; Martin et al., 2017). Most recent studies on reproductive biology have focused on northern temperate zone birds (Martin, 2004; Lloyd et al., 2014; Xiao et al., 2017), while birds in other regions, especially tropical birds, have been relatively less studied (Xiao et al., 2017). The main reason may be that tropical birds are relatively difficult to monitor (Martin, 1996; Jiang et al., 2017; McCullough and Londoño, 2017). Studies have shown that the reproductive strategies of birds in different regions

are different mainly due to the differences in the breeding habitats of birds and their nest predation rates (Martin, 1996). Compared with temperate birds, tropical birds are characterized by a longer breeding season, smaller clutch size, longer brooding, and hatching periods (Martin, 1996; Lloyd et al., 2014). Therefore, expanding the understanding of the life history of tropical birds can help us better understand the global trend of life history strategies (Ricklefs and Wikelski, 2002; Slevin et al., 2020).

Nest predation is a major factor limiting the success of bird reproduction and affects the life history and population dynamics of birds (Reidy and Thompson, 2012; Thompson and Ribic, 2012; Ibáñez-Álamo et al., 2015; Chen et al., 2020). Especially for ground-nesting birds, nest predation has become one of the most critical factors affecting their reproductive performance and population growth (Sanders and Maloney, 2002; MacDonald and Bolton, 2008; Pedersen et al., 2011; Melville et al., 2014). Based on this, understanding predation on birds and its influencing factors is of great significance for studying bird population dynamics and proposing conservation strategies (Martin, 1993; Chalfoun et al., 2002; Seibold et al., 2013; Chen et al., 2020).

The red junglefowl (*Gallus gallus*) belong to the genus *Gallus* of the pheasant family (Phasianidae) in the order Galliformes and is a ground-active bird (Zheng, 2022). According to the differences in their distribution range and morphological characteristics, the world's red junglefowl can be divided into five subspecies, all of which are distributed in southern Asia (Johnsgard, 1999; del Hoyo et al., 2001). There are two subspecies in China, the southern Yunnan subspecies (*G. g. spadiceus*) and the Hainan subspecies (*Gallus gallus jabouillei*; Zheng, 2022).

In this study, we searched and monitored the natural nests of red junglefowls, the Hainan subspecies, in Datian and Bangxi Nature Reserves, tropical Hainan Island, China, using infrared cameras. Considering that the number of natural nests of Galliformes birds is limited and nest sites are relatively difficult to find (Luo et al., 2017), the use of artificial nests for simulation studies can not only reduce human interference on hatching in the wild but also has the advantage of ease of use, and can provide sufficient samples for research (Martin, 1987; Major and Kendal, 1996; Wilson et al., 1998; Zanette and Jenkins, 2000; McDonald et al., 2009; Melville et al., 2014; Luo et al., 2017), we carried out artificial nest experiments in the study area to compare the survival rates and potential predators of natural nests and artificial nests.

Materials and methods

Study area

This study was conducted in Datian and Bangxi Nature Reserves. The Hainan Datian National Nature Reserve (19°05′-17′ N, 108°47′-49′ E, with 30–80 m in elevation and 1,310 ha in total area) is located in Dongfang city, Hainan Province, with the Hainan Eld's deer and its habitat being the main target for protection. Bangxi Provincial Nature Reserve (19°22′-24′ N, 109°05′-06′ E, with an elevation of 17–80 m and a total area of 361.8 ha) is located in Bangxi town, northwest of Baisha County, Hainan Province, with the Hainan Eld's deer and its habitat also being the main target for protection.

Monitoring of natural nests

In 2020 and 2021, we carried out a search for the natural nests of red junglefowls following Conkling et al. (2012). The search was divided between two groups. The first group consisted of forest rangers in the reserve, who searched for nests during daily routine patrols; the second group consisted of researchers who used the behavioral observation and systematic search technology of adult birds and monitored them at 06:00 ~ 09:00 and 16:00 ~ 19:00 every day. Once the nest was found, we used a GPS device (eTrex 32x, Garmin) to mark its location and recorded the status of the female (brooding or flew away) and of the nest (building, hatched, brooded, or abandoned). To avoid interference, we used a telescope to observe the nest every 3–5 days. If at least one egg in the nest successfully hatched, we considered the reproduction to be successful; if all the eggs were not hatched or were destroyed, we considered the reproduction to be a failure (Visco and Sherry, 2015).

In addition, an infrared camera was also aimed at each breeding nest to accurately identify predators and assess the fate of the nests. To avoid abandonment by parent birds due to human interference, the infrared cameras were installed in the incubation period (DeGregorio et al., 2016). We usually adopted the method of using local materials to fix the camera to the tree trunk at 1–1.5 m away from the nest; for situations in which we were unable to fix the camera to a tree trunk, we used the method of piling objects to set up the camera and disguise it appropriately. The infrared camera was set to record continuously throughout the day, and the shooting mode was set to "photograph + video." Each time the camera was triggered, it shot three photos and 15 s of video, and the trigger sensitivity was set to "medium" (Xiao et al., 2014). After the nest was preyed upon, we reviewed the camera records to identify the type of predator and recorded the time of predation. For predation events in which the predators were not recorded due to camera failure or other reasons, we speculated on the identity of the predators based on the status of the nests after the predation event occurred because some predators will leave evidence behind. For example, rodents usually leave behind eggshell fragments, while some reptiles prey on nests without leaving any traces (Klug et al., 2010).

After breeding, we recorded and measured the following nest site parameters: (1) nest size (long and short diameters); (2) nest depth; (3) nest materials; (4) distance from nest to the nearest water source; and (5) shortest distance from the nest to the road. For the natural nests in which reproduction failed, the following parameters were recorded and measured: (1) clutch size; (2) egg size; and (3) weight of the eggs. We used a tape measure which ranging from 0 to 500 cm to measure the nest size, nest depth, distance from the nest to the nearest water source, and shortest distance from the nest to the road. For indicators that exceeded the measuring range of the tape measure, we used the method of walking estimation. Eggs were measured using a digital Vernier caliper; the egg size measurement was accurate to 0.01 mm. The egg weight measurement was accurate to 0.01 g.

Artificial nest experiments

During the breeding season in 2020, we conducted artificial nest experiments in Datian (6–25 May 2020) and Bangxi (7–25 May 2020). The location for setting up the artificial nests was selected in the same area where natural nests of red junglefowl were found in a previous study (Yuan, 2009) or was determined according to the characteristics of the site of the natural nests (Yuan et al., 2009a). Artificial nests were constructed by imitating the structure of natural nests, which are shallow pits, and using dry leaves, twigs, and feathers as nest materials. Two eggs of domesticated chickens that were similar in size and color to those of wild red junglefowl were placed in each artificial nest. Two

groups of experiments were set up at each study site (the distribution of artificial nests is shown in Figures 1, 2). The first group consisted of 10 nests for the non-covered group (infrared camera), and the second group consisted of 10 nests, with dry leaves used to cover the experimental eggs. The artificial nest incubation period was set as 19 days, which similar to its natural incubation period (Yuan, 2009). The artificial nests were inspected every 6 days for a total of three times, on the 7th day, 13th day, and 19th day after nest set up (Dinsmore et al., 2002). In each inspection, the artificial nest was photographed, and the nest number was recorded. If there were two eggs or one egg in the artificial nest, the nest was inspected again the next time (fully covered nests were covered with leaves again after the inspection); if the two eggs were preyed on or disappeared, the results were recorded immediately after taking pictures, and this signified the end of the experiment. The inspection results were divided into: (1) two eggs intact; (2) one egg intact, one egg preyed on (with eggshell or predation traces); (3) one egg intact, one egg missing (no traces); (4) two eggs preyed on (with eggshell or predation traces); (5) two eggs missing; and (6) experimental eggs were moved by unknown animals.

During the breeding season in 2021, we conducted artificial nest experiments in Datian (11–29 March 2021). Similarly, we set up two sets of experiments, with 15 nests in each group (the distribution of artificial nests is shown in Figure 3). In the non-covered group, every nest was deployed together with an infrared camera, and only some of the nests (three totals) in the fully covered group were deployed together with a camera. The specific operations and methods were the same as described above.

To reduce the influence of researchers on the experiment, human interference should be minimized during artificial nest inspection, for example, to leave as little footprint as possible around the artificial nest and to avoid the behavior that may affect the nest, such as touching the experimental eggs (Driscoll et al., 2005). In the wild, if the nest is disturbed or the eggs in the nest are preyed upon, the female chickens will abandon the nest (Yuan, 2009). Therefore, if the eggs in the artificial nest are damaged, removed or disappeared, we will not replace the new experimental eggs (Nour et al., 1993) and define the nest as a reproductive failure (Noske et al., 2008). Otherwise, the nest is considered a successful breeding nest.

Species identification was performed based on photos or videos taken by the infrared cameras. When identifying species, we mainly referred to the "Chinese Wildlife Manual of Mammals" (Smith and Xie, 2009), "A Checklist on the Classification and Distribution of the Birds of China (third Edition)" (Zheng, 2022) and the "The CNG field guide to the birds of China" (Liu and Chen, 2021). To calculate the number of animals captured by the cameras, when an animal was photographed by the same camera more than 30-min apart, this was considered an independent capture and an individual animal (O'Brien et al., 2003; Rovero et al., 2014).

Results

Natural nests

In the breeding season of 2020 and 2021, we found 16 natural nests of red junglefowl at the two study sites (Table 1; Figure 4). There were 12 nests in Datian and four nests in Bangxi (Figures 5A–D). Among the 16 nests found, infrared cameras were installed in 13 nests for

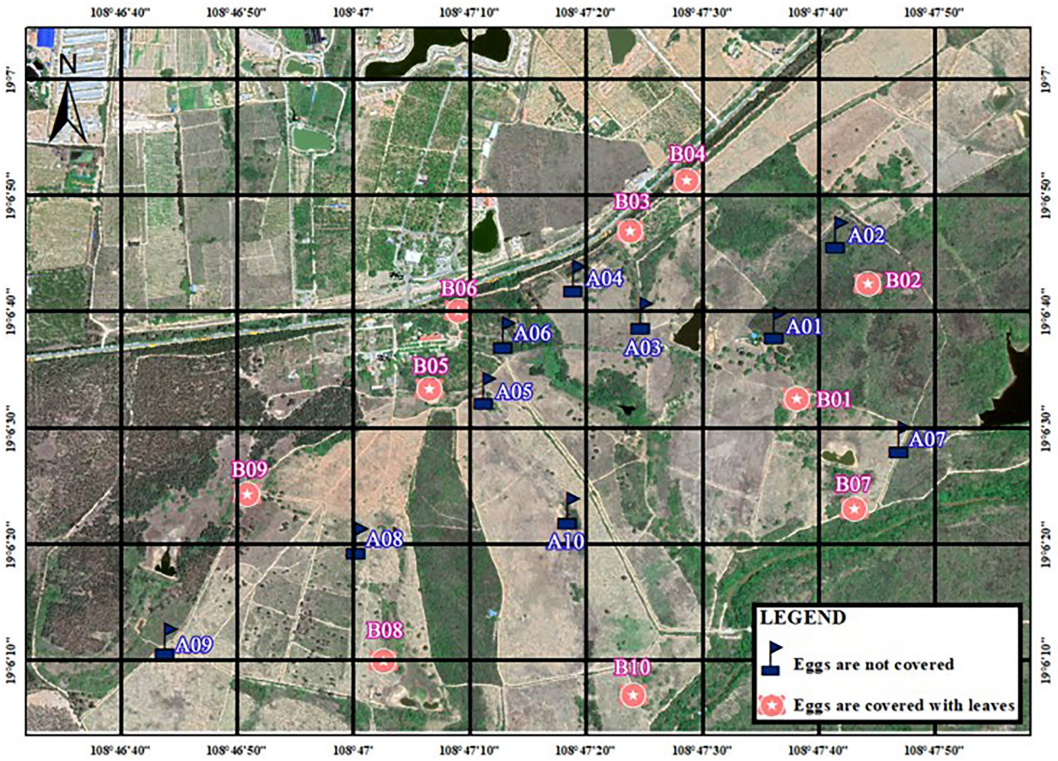

FIGURE 1
Distribution of artificial nests in Datian National Nature Reserve, Hainan, in 2020.

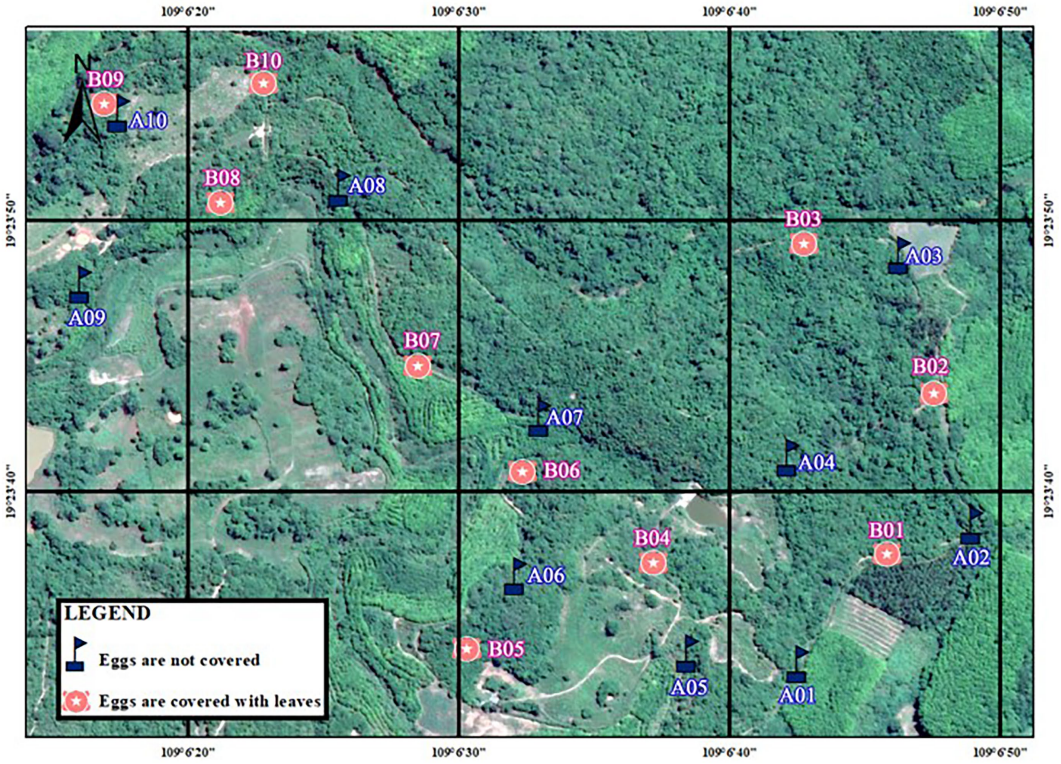

FIGURE 2
Distribution of artificial nests in Bangxi Provincial Nature Reserve, Hainan, in 2020.

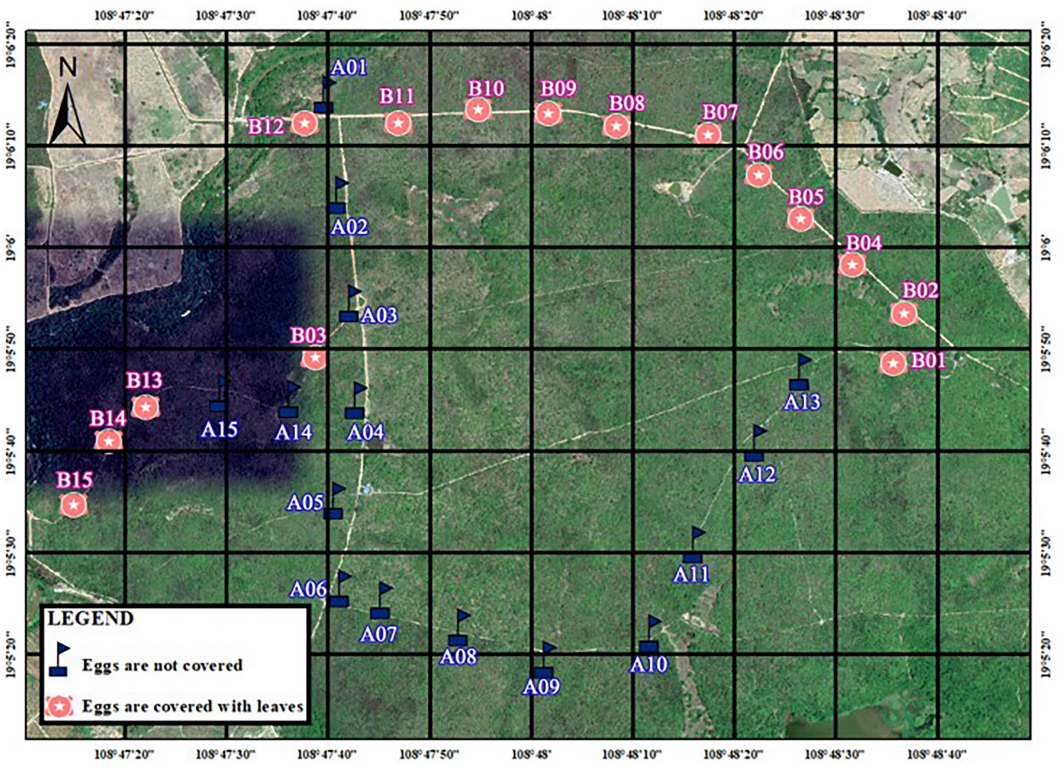

FIGURE 3
Distribution of artificial nests in Datian National Nature Reserve, Hainan, in 2021.

TABLE 1 Active nests of red junglefowls (*Gallus gallus jabouillei*) in Datian and Bangxi Nature Reserves in 2020 and 2021.

Nest	Site	Date found	Content	Observation and nest fate
001	DT	2 April 2020	Two eggs	Adult flew away, Nest abandoned
002*	DT	8 April 2020	Five eggs	Adult flew away, Nest abandoned, Predated
003*	BX	13 April 2020	Four eggs	Adult incubating, Four Nestlings hatched
004*	BX	15 April 2020	Five eggs	Adult flew away, Nest abandoned
005*	DT	16 April 2020	One egg	No adult, Nest abandoned, Predated
006*	DT	21 April 2020	Four eggs	Adult flew away, Nest abandoned
007*	DT	22 April 2020	Two eggs	No adult, Nest abandoned, Predated
008*	DT	26 April 2020	Six eggs	Adult incubating, One Nestling hatched
009**	DT	26 April 2020	Four eggs	No adult, Two Nestlings hatched
010*	BX	7 May 2020	Eight eggs	No adult, Nest abandoned, Predated
011*	BX	18 May 2020	Five eggs	Adult flew away, Nest abandoned
012*	DT	14 June 2020	Six eggs	Adult flew away, Five Nestlings hatched
013*	DT	2 July 2020	Four eggs	Adult flew away, Nest abandoned, Predated
014*	DT	26 March 2021	Seven eggs	Adult flew away, Nest abandoned
015*	DT	10 April 2021	Five eggs	Adult flew away, Nest abandoned
016**	DT	24 April 2021	Four eggs	No adult, Four Nestlings hatched

DT, Datian National Nature Reserve; BX, Bangxi Nature Reserve.
*The nest was monitored by infrared camera; **The nest had finished breeding when discovered.

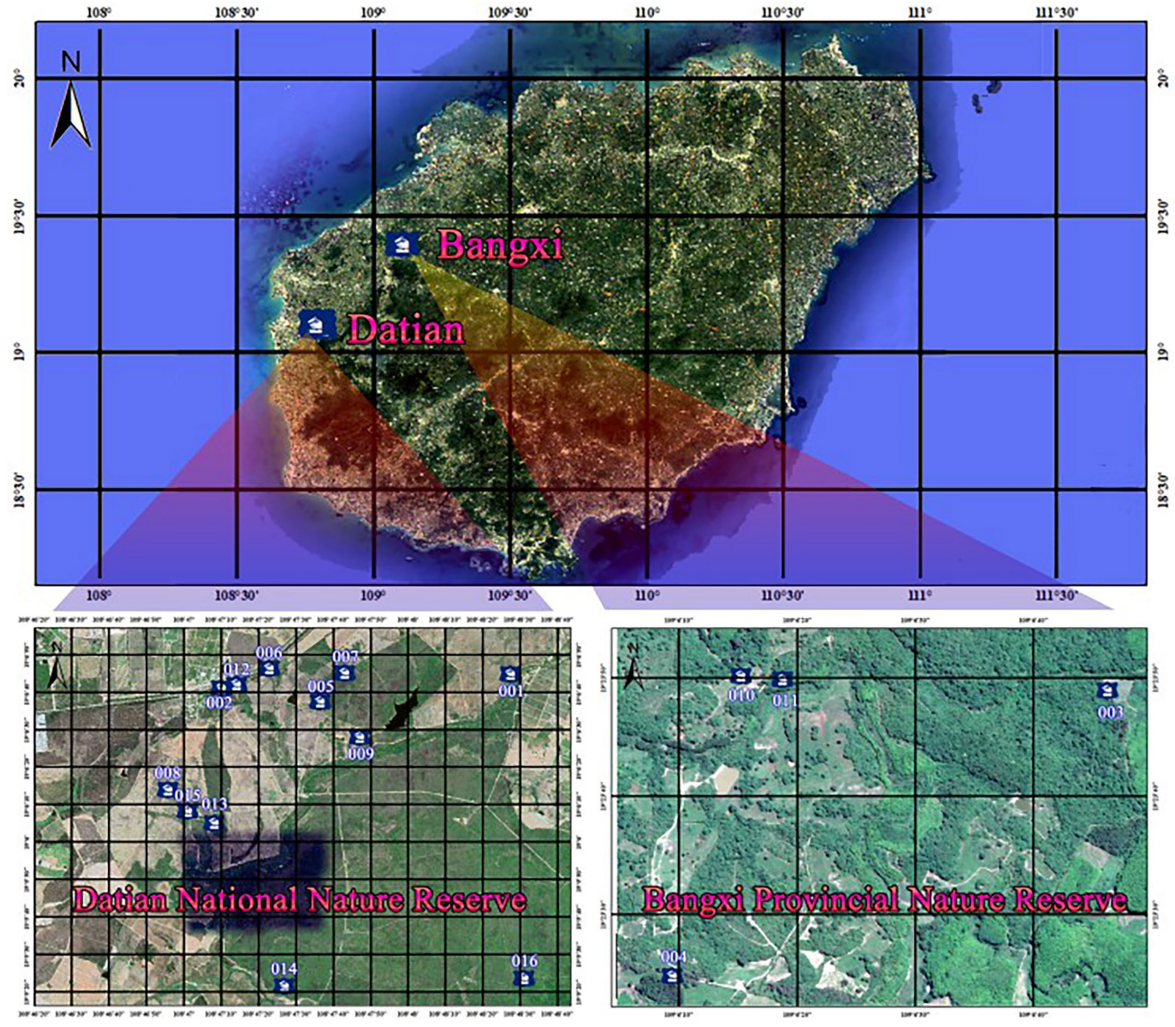

FIGURE 4
Distribution of natural nests of red junglefowls (*Gallus gallus jabouillei*).

monitoring (Figure 6). In total, five out of the 16 nests reproduced successfully (Figures 7A–C), and the reproductive success rate was 31.25%. Among them, five nests were preyed upon and nest predation accounted for 45.45% of nest failures. Nests 008 and 013 were both visited by the Hainan Eld's deer during the hatching period (Supplementary Videos S1, S2; Figure 8); the female bird in nest 008 abandoned it (one chick hatched successfully), and the eggs were preyed upon after the female bird abandoned nest 013.

FIGURE 5
(A,B) Natural nests of red junglefowl (*Gallus gallus jabouillei*) found in the study sites (females brooding), **(C,D)** Natural nests of red junglefowl (*Gallus gallus jabouillei*) found in the study sites (female birds flew away).

FIGURE 6
Infrared camera monitoring of a natural nest of red junglefowl (*Gallus gallus jabouillei*).

The clutch size of red junglefowls was 4.50 ± 1.83 (n = 16). The egg parameters were showed as follows: weight: 24.26 ± 0.60 g, long diameter: 43.88 ± 1.18 mm, and short diameter: 33.45 ± 0.52 mm, n = 9. The nest parameters were showed as follows: long diameter: 15.51 ± 4.21 cm, short diameter: 13.00 ± 4.23 cm, and depth: 3.55 ± 0.80 cm, n = 8. The distance between the natural nest and the nearest water source was 56.18 ± 57.58 m (n = 11), and the closest distance between the natural nest and the road was 12.65 ± 27.40 m (n = 13). The number of nests found was the highest in April, with 11 nests, accounting for 68.75% of the total number of nests, followed by May, with two nests, accounting for 15.38%. Only one nest was found in July.

Artificial nest experiments and potential nest predators

Among the 20 nests in Datian, five nests were preyed upon, and the predation rate was 25%. In one of the nests, the experimental eggs were moved (Figure 9A). However, no predation occurred in the Bangxi. Vertebrates were the main cause of nest predation in the experiments, including two bird incidents (coucals) and two rodent incidents (Figure 9B). There were similarities in the types and numbers of animals that visited the artificial nests at the two study sites. Among them, Hainan Eld's deers (Figure 10A) and several small rodents (*Rattus* spp.; Figure 10B) were photographed at the two experimental sites. Wild boars (*Sus scrofa*; Figure 11A), greater coucals (*Centropus sinensis*; Figure 11B), and lesser coucals (*Centropus bengalensis*; Figure 11C) were only photographed in Datian, while red-bellied squirrels (*Callosciurus erythraeus*; Figure 11D) and domestic chicken (*Gallus gallus domesticus*; Figure 12) were only photographed in Bangxi.

Among 30 artificial nests set up in Datian in March 2021, two nests that were preyed on (Figure 9B), and experimental eggs in two nests were moved by unknown animals. However, they were not preyed upon. The predation event was not captured by the infrared camera, but animals that appeared near the artificial nests were recorded. These animals were the red junglefowl (Figure 13), black-throated laughingthrush (*Garrulax chinensis monachus*), wild boar, Hainan muntjac (*Muntiacus nigripes*; Figure 14), leopard (*Prionailurus bengalensis alleni*; Figure 15), and several small rodents.

Discussion

In the two breeding seasons of 2020 and 2021, we found a total of 16 natural nests and nesting success of the red junglefowl was 31.25%,

FIGURE 7
(A,B) Natural nests with successful reproduction; **(C)** Natural nests that failed to reproduce.

FIGURE 8
A Hainan Eld's deer visited the natural nest (the date was set incorrectly).

FIGURE 9
(A) Experimental eggs were moved by unknown animals; **(B)** Rodent predation of experimental eggs.

FIGURE 10
(A) Hainan Eld's deer near the artificial nest; **(B)** Small rodent near the artificial nest.

FIGURE 11
(A) Wild boar near the artificial nest, **(B)** Greater coucal near the artificial nest, **(C)** Lesser coucal near the artificial nest, and **(D)** Red-bellied squirrel near the artificial nest.

which was higher than the result observed by Yuan (2009) in the same area (18.2%). However, the rate of nest abandonment was as high as 68.75%, higher than the results of previous studies (55.6%; Yuan, 2009).

In a study of the Indian subspecies, it was found that after the first reproductive failure, red junglefowls would choose to reproduce a second time (Collias and Collias, 1967). Similarly, the reproduction record of the southern Yunnan subspecies also mentions that it may reproduce twice a year (Zheng et al., 1978). It is likely that the Hainan subspecies may reproduce multiple times to improve the reproductive success, which needs further confirmation in the wild. The clutch size in our study areas was similar to that of the Indian subspecies (Anwar et al., 2016) but was significantly lower than that of the southern Yunnan subspecies (Zheng et al., 1978). In southern Yunnan, female and male birds brood and hatch eggs together (Zheng et al., 1978). Yuan (2009) observed that in the field, both male and female birds brood nestlings, while we found that only female birds were responsible for brooding in the wild.

We found that the Hainan subspecies was breeding from March to July, and that the number of broods was highest in April. It is thus speculated that the breeding peak in the Hainan subspecies is April. This is consistent with the results of Yuan (2009), but there are differences between the Indian subspecies from different areas and the southern Yunnan subspecies. For example, in India, broiler flocks were found to breed in January–October, and the breeding peak period was March–May (Ali and Ripley, 1987; Anwar et al., 2016); in the Malay Peninsula region, the breeding time is from December to May of the following year, and the breeding peak is from January to February (del Hoyo et al., 2001). In areas with sufficient food, red junglefowl can even breed year-round (Arshad and Zakaria, 1999). In southern Yunnan, the breeding time is from February to October (Zheng et al., 1978). Tropical birds have different life history traits (Stutchbury and Morton, 2023). Anyway, we only carried out the breeding monitoring of the red junglefowl for 2 years, which may be the reason that the breeding season in Hainan subspecies differs from other subspecies. There should be a long-term monitoring to the subspecies in the wild.

Studies have found that red junglefowl tend to choose areas with well-developed herbs and patches for nesting (Collias and Collias, 1967). However, some studies have suggested that deciduous trees and bamboo forests with scattered patches are the favorite nesting habitats of red junglefowls during the breeding season (Johnson, 1963). In this study, it was observed that female birds mostly nested on patrol roads or in open areas near the edge of forests with fewer deciduous leaves. This reflects the geographical differences in the selection of nesting sites among different subspecies. The edge effect hypothesis indicates that because the edge area of the habitat has more abundant vegetation resources and a more complex environment, the predation pressure is usually greater than that of the central area (Ewers and Didham, 2007). However, studies on the Reeves's pheasant (*Syrmaticus reevesii*) do not support this hypothesis, as this species tends to nest in marginal areas with more human interference (Luo et al., 2017). Our results are consistent with that study, as the female birds of the Hainan subspecies chose to nest on patrol roads or at the edge of the forest. It is possible that human activities in these areas are more frequent, and some predators are forced to enter the central area where there are fewer disturbances, thereby

FIGURE 12
Domestic chicken near the artificial nest.

FIGURE 13
Red junglefowl near the artificial nest.

FIGURE 14
Hainan muntjac near the artificial nest.

reducing predation by natural enemies. Nest predation is the main factor in the failure of pheasant reproduction (Lu and Zheng, 2001; Sherry et al., 2015). In the predation events we observed, eggshells were either left in the nest or no trace of the predator was left after the eggs were preyed upon. Therefore, we speculated that rodents and reptiles may be the main nest predators. This is because rodents usually leave eggshells or debris behind after predation, and some reptiles leave no traces when preying on nests (Klug et al., 2010). In addition, in the study area, small carnivorous mammals, such as leopards, falcons, and raptors are the main natural enemies of the subspecies (Zheng et al., 1978; Evans et al., 1993), and snakes are also the main predators of red junglefowls (Anwar et al., 2016).

In our study, although artificial nests were set up in the same study area, their predation rate was lower than that of natural nests, and the types of predators were also different. This result is consistent with the results of a study of the reed parrotbill (*Paradoxornis heudei*) (Chen et al., 2020). This is different from the results of other studies. For example, snakes were found to be the main predators of natural nests, while mammals were found to be the main predators of artificial nests (Thompson and Burhans, 2003; Chen et al., 2020).

The use of infrared camera technology to monitor artificial nests is ideal for the determination of nest predator species (Anthony et al., 2006; Kross et al., 2013). In this study, the infrared cameras captured a number of wild animals, such as greater coucals, lesser coucals, and Hainan Eld's deers. Among them, the greater coucal was the main predator of the experimental eggs, and the feeding activity of Hainan Eld's deers caused female birds to abandon nests. Studies have shown that wild boars can change the terrain by overturn large areas of soil, thereby changing the vegetation structure and composition of their habitats (Singer et al., 1984; Lacki and Lancia, 1986), which is particularly harmful to ground-nesting birds (Barrios-Garcia and Ballari, 2012; Sanders et al., 2020). Therefore, the wild boar may be an opportunistic predator of nests.

FIGURE 15
Leopard near the artificial nest.

A recent study has shown that gray squirrels (*Sciurus carolinensis*) are widely considered to be important predators of bird eggs and chicks (Broughton, 2020). We photographed red-bellied squirrels in the vicinity of artificial nests many times and speculate that the red-bellied squirrel is a potential nest predator. In addition, studies have found that bats are the main nest predators of tropical forest birds (Perrella et al., 2019). In our study, we did not find predation of eggs by bats. In follow-up work, we intend to carry out effective and continuous monitoring of breeding nests and clarify the antipredation strategies of red junglefowl.

In this study, the predation rates of artificial nests varied in Datian. The main reason is that the artificial nest experiments were done at the buffer zone in 2020, while at the core zone in 2021. The habitats in the two regions are significantly different, and so are the predation rates. The predation rate was 0% in Bangxi. There are two possible reasons. Firstly, our sample size is not large enough, secondly, there is a relative lack of potential predators for red junglefowl eggs. Although the survival rates of the artificial nests in the two study sites were higher than those of the natural nests. The possible reason is that the experiment was conducted in May 2020, while in March 2021, the birds had just started breeding, and most of them were in the hatching period in May. Most previous studies used the quadrat survey method (Johnson, 1963; Kalsi, 1992; Arshad and Zakaria, 2009; Yuan et al., 2009a,b) or radio tracking technology (Arshad and Zakaria, 2011) to investigate habitat selection and habitat utilization in red junglefowls. Satellite tracking technology is a tool to effectively track the small-scale movement of highly mobile and inaccessible species (Cagnacci et al., 2010; Coxen et al., 2017). The application of this technology to the study of ground-dwelling pheasants such as red junglefowl is very important for understanding how these birds use their habitat, the motivation for their movements, and the process of space utilization, to ultimately improve pheasant protection.

Conclusion

Red junglefowl are ground-nesting pheasants that are highly alert, which makes field research and tracking difficult (Arshad and Zakaria, 2011; Anwar et al., 2016). Human interference or direct observation of brooding parent birds may lead to abandonment of the nest and reproduction failure (Yuan, 2009). Therefore, there is limited information on the survival rate of red junglefowl nests. Protecting the habitat and reducing human disturbance will play a positive role in the growth of the red junglefowl population in our study areas. Datian and Bangxi are both protected areas with the main goal of protecting Hainan Eld's deer. Burning grassland vegetation, thinning, plowing, and manual removal of waste can alleviate the degradation of Hainan Eld's deer habitat quality (Fu et al., 2016, 2018). We suggest that the conservation area should take into account the impact on the reproduction of ground-dwelling pheasants when rebuilding or reconstructing the suitable habitat of Hainan Eld's deer. In addition, domestic chickens were photographed in the Bangxi Nature Reserve, indicating the possibility of hybridization between wild red junglefowl and domestic chickens. It is recommended that free-range domestic chickens be banned within protected areas to avoid the problem of genetic contamination of wild red junglefowls.

Data availability statement

The original contributions presented in the study are included in the article/Supplementary material, further inquiries can be directed to the corresponding author.

Ethics statement

Ethical review and approval was not required for the animal study because we have obtained the administrative licensing decision of Hainan Forestry Bureau on the study of Red Junglefowl [Hainan Forestry Bureau approval (2019) 083].

Author contributions

XR designed the study. XR, JL, BH, HW, GW, and TT carried out field experiments. XR and QL performed cartography and statistical analyses. XR wrote the draft manuscript. All authors contributed to the article and approved the submitted version.

Funding

This work was supported by the Joint Fund of the Natural Science Foundation of Hainan Province (no. 320RC506 to XR) and the National Natural Science Foundation of China (no. 31800320 to XR). XR was funded by the project supported by the Scientific Research start-up

Fund of Hainan University [no. KYQD (ZR) 20057] and the Teaching Research of Hainan University (no. Hdsz20-9).

Acknowledgments

We are grateful to Datian and Bangxi Nature Reserves for their help and co-operation. We thank Biaoyi Tang for assistance with field work.

Conflict of interest

The authors declare that the research was conducted in the absence of any commercial or financial relationships that could be construed as a potential conflict of interest.

Publisher's note

Supplementary material

The Supplementary material for this article can be found online at: https://www.frontiersin.org/articles/10.3389/fevo.2023.1127139/full#supplementary-material

References

Ali, S., and Ripley, S. D. (1987). *The Compact Handbook of the Birds of India and Pakistan*. Bombay: Oxford University Press

Anthony, R. M., Grand, J. B., Fondell, T. F., and Millar, D. A. (2006). Techniques for identifying predators of goose nests. *Wildl. Biol.* 12, 249–256. doi: 10.2981/0909-6396(2006)12[249:TFIPOG]2.0.CO;2

Anwar, M., Ali, S., Rais, M., and Mahmood, T. (2016). Breeding ecology of red jungle fowl (*Gallus gallus*) in Deva Vatala National Park, Azad Jammu and Kashmir, Pakistan. *J. Appl. Agric. Biotechnol.* 1, 59–65.

Arshad, M. I., and Zakaria, M. (1999). Breeding ecology of red junglefowl (*Gallus gallus spadiceus*) in Malaysia. *J. Malayan Nat.* 53, 355–365.

Arshad, M. I., and Zakaria, M. (2009). Roosting habits of red Junglefowl in orchard area. *Pak. J. Life Soc. Sci.* 7, 86–89.

Arshad, M. I., and Zakaria, M. (2011). Variation in home range size exhibited by red Junglefowl (*Gallus gallus spadiceus*) in oil palm plantation habitat, Malaysia. *Pak. J. Zool.* 43, 33–840.

Barrios-Garcia, M. N., and Ballari, S. A. (2012). Impact of wild boar (*Sus scrofa*) in its introduced and native range: a review. *Biol. Invasions* 14, 2283–2300. doi: 10.1007/s10530-012-0229-6

Broughton, R. K. (2020). Current and future impacts of nest predation and nest-site competition by invasive eastern grey squirrels *Sciurus carolinensis* on European birds. *Mammal Rev.* 50, 38–51. doi: 10.1111/mam.12174

Cagnacci, F., Boitani, L., Powell, R. A., and Boyce, M. S. (2010). Animal ecology meets GPS-based radiotelemetry: a perfect storm of opportunities and challenges. *Philos. Trans. Roy. Soc. B. Biol. Sci.* 365, 2157–2162. doi: 10.1098/rstb.2010.0107

Chalfoun, A. D., Thompson, F., and Ratnaswamy, M. J. (2002). Nest predators and fragmentation: a review and meta-analysis. *Conserv. Biol.* 16, 306–318. doi: 10.1046/j.1523-1739.2002.00308.x

Chen, P., Chen, T., Liu, B., Zhang, M., Lu, C., and Chen, Y. (2020). Snakes are the principal nest predators of the threatened reed parrotbill in a coastal wetland of eastern China. *Glob. Ecol. Conserv.* 23:e01055. doi: 10.1016/j.gecco.2020.e01055

Collias, N. E., and Collias, E. C. (1967). A field study of the red junglefowl in north-Central India. *Condor* 69, 360–386. doi: 10.2307/1366199

Conkling, T. J., Pope, T. L., Smith, K. N., Mathewson, H. A., Morrison, M. L., Wilkins, R. N., et al. (2012). Black-capped vireo nest predator assemblage and predictors for nest predation. *J. Wildl. Manag.* 76, 1401–1411. doi: 10.1002/jwmg.388

Coxen, C. L., Frey, J. K., Carleton, S. A., and Collins, D. P. (2017). Species distribution models for a migratory bird based on citizen science and satellite tracking data. *Glob. Ecol. Conserv.* 11, 298–311. doi: 10.1016/j.gecco.2017.08.001

Degregorio, B. A., Weatherhead, P. J., Ward, M. P., and Sperry, J. H. (2016). Do seasonal patterns of rat snake (*Pantherophis obsoletus*) and black racer (*Coluber constrictor*) activity predict avian nest predation? *Ecol. Evol.* 6, 2034–2043. doi: 10.1002/ece3.1992

del Hoyo, J., Elliott, A., and Sargatal, J. (2001). *Hand Book of Bird of the World. 2: New World vultures to Guinea fowl*. Barecelona: Lynx Editions

Dinsmore, S. J., White, G. C., and Knopf, F. L. (2002). Advanced techniques for modeling avian nest survival. *Ecology* 83, 3476–3488. doi: 10.1890/0012-9658(2002)083[3476:ATFMAN]2.0.CO;2

Driscoll, M. J. L., Donovan, T., Mickey, R., Howard, A., and Fleming, K. K. (2005). Determinants of wood thrush nest success: a multi-scale, model selection approach. *J. Wildl. Manag.* 69, 699–709. doi: 10.2193/0022-541X(2005)069[0699:DOWTNS]2.0.CO;2

Evans, C. S., Macedonia, J. M., and Marter, P. (1993). Effects of apparent size and speed on the response of chickens (*Gallus gallus*) to computer-generator stimulations of aerial predators. *Anim. Behav.* 46, 1–11. doi: 10.1006/anbe.1993.1156

Ewers, R. M., and Didham, R. K. (2007). The effect of fragment shape and species' sensitivity to habitat edges on animal population size. *Conserv. Biol.* 21, 926–936. doi: 10.1111/j.1523-1739.2007.00720.x

Fu, M., Bai, Z., Jia, K., Wen, X., Feng, Y., Zhang, E., et al. (2018). Habitat selection of Hainan Eld's deer after Forest thinning in a deciduous monsoon Forest. *Chin. J. Wildl.* 39, 502–506.

Fu, Y., He, B., Wang, J., Wang, L., and Fu, X. (2016). Discussion and research on habitat reform and reconstruction of Hainan Eld's deer protection area in Datian town. *Trop. For.* 44, 26–30. doi: 10.3969/j.issn.1672-0938.2016.04.008

Ibáñez-Álamo, J. D., Magrath, R. D., Oteyza, J. C., Chalfoun, A. D., Haff, T. M., Schmidt, K. A., et al. (2015). Nest predation research: recent findings and future perspectives. *J. Ornithol.* 156, 247–262. doi: 10.1007/s10336-015-1207-4

Jiang, A., Jiang, D., Zhou, F., and Goodale, E. (2017). Nest site selection and breeding ecology of streaked wren-babbler (*Napothera brevicaudata*) in a tropical limestone forest of southern China. *Avian Res.* 8, 1–8. doi: 10.1186/s40657-017-0086-1

Johnsgard, P. A. (1999). *The Pheasants of the World: Biology and Natural History 2nd Edn.* Washington D.C.: Smithsonian Press

Johnson, R. A. (1963). Habitat preference and behavior of breeding jungle fowl in central western Thailand. *Wilson Bull* 75, 270–272.

Kalsi, R. (1992). Habitat selection of red junglefowl at Kalesar reserve Forest, Haryana, India Pheasants in Asia.

Klug, P. E., Jackrel, S. L., and With, K. A. (2010). Linking snake habitat use to nest predation risk in grassland birds: the dangers of shrub cover. *Oecologia* 162, 803–813. doi: 10.1007/s00442-009-1549-9

Kross, S. M., Mcdonald, P. G., and Nelson, X. J. (2013). New Zealand falcon nests suffer lower predation in agricultural habitat than in natural habitat. *Bird Conserv. Int.* 23, 512–519. doi: 10.1017/S0959270913000130

Lacki, M. J., and Lancia, R. A. (1986). Effects of wild pigs on beech growth in Great Smoky Mountains National Park. *J. Wildl. Manag.* 50, 655–659. doi: 10.2307/3800976

Liu, Y., and Chen, S. (2021). *The CNG Field Guide to the Birds of China*. Changsha: Hunan Science and Technology Press

Lloyd, P., Abadi, F., Altwegg, R., and Martin, T. E. (2014). South temperate birds have higher apparent adult survival than tropical birds in Africa. *J. Avian Biol.* 45, 493–500. doi: 10.1111/jav.00454

Lu, X., and Zheng, G. M. (2001). Habitat selection and use by hybrid White/Tibetan eared-pheasants in eastern Tibet during post-incubation. *Can. J. Zool.* 79, 319–324. doi: 10.1139/z00-203

Luo, X., Zhao, Y., Ma, J., Li, J., and Xu, J. (2017). Nest survival rate of Reeves's pheasant (*Syrmaticus reevesii*) based on artificial nest experiments. *Zool. Res.* 38, 49–54. doi: 10.13918/j.issn.2095-8137.2017.008

MacDonald, M. A., and Bolton, M. (2008). Predation on wader nests in Europe. *Ibis* 150, 54–73. doi: 10.1111/j.1474-919X.2008.00869.x

Major, R. E., and Kendal, C. E. (1996). The contribution of artificial nest experiments to understanding avian reproductive success: a review of methods and conclusions. *Ibis* 138, 298–307. doi: 10.1111/j.1474-919x.1996.tb04342.x

Martin, T. E. (1987). Artificial Nest experiments: effects of nest appearance and type of predator. *Condor* 89, 925–928. doi: 10.2307/1368547

Martin, T. E. (1993). Nest predation among vegetation layers and habitat types: revising the dogmas. *Am. Nat.* 141, 897–913. doi: 10.1086/285515

Martin, T. E. (1996). Life history evolution in tropical and south temperate birds: what do we really know? *J. Avian Biol.* 27, 263–272. doi: 10.2307/3677257

Martin, T. E. (2002). A new view of avian life-history evolution tested on an incubation paradox. *Proc. R. Soc. London, Ser. B* 269, 309–316. doi: 10.1098/rspb.2001.1879

Martin, T. E. (2004). Avian life-history evolution has an eminent past: does it have a bright future? *Auk* 121, 289–301. doi: 10.1642/0004-8038(2004)121[0289:ALEHAE]2.0.CO;2

Martin, T. E. (2008). Egg size variation among tropical and temperate songbirds: an embryonic temperature hypothesis. *PNAS* 105, 9268–9271. doi: 10.1073/pnas.0709366105

Martin, T. E., Riordan, M. M., Repin, R., Mouton, J. C., and Blake, W. M. (2017). Apparent annual survival estimates of tropical songbirds better reflect life history variation when based on intensive field methods. *Glob. Ecol. Biogeogr.* 26, 1386–1397. doi: 10.1111/geb.12661

McCullough, J. M., and Londoño, G. A. (2017). Nesting biology of the black-throated Tody-tyrant (*Hemitriccus granadensis*) with notes on mating displays. *Wilson J. Ornithol.* 129, 820–826. doi: 10.1676/16-122.1

McDonald, P. G., Wilson, D. R., and Evans, C. S. (2009). Nestling begging increases predation risk, regardless of spectral characteristics or avian mobbing. *Behav. Ecol.* 20, 821–829. doi: 10.1093/beheco/arp066

Melville, H. I. A. S., Conway, W. C., Morrison, M. L., Comer, C. E., and Hardin, J. B. (2014). Artificial nests identify possible nest predators of eastern wild turkeys. *Southeast. Nat.* 13, 80–91. doi: 10.1656/058.013.0106

Noske, R. A., Fischer, S., and Brook, B. W. (2008). Artificial nest predation rates vary among habitats in the Australian monsoon tropics. *Ecol. Res.* 23, 519–527. doi: 10.1007/s11284-007-0403-y

Nour, N., Matthysen, E., and Dhondt, A. A. (1993). Artificial nest predation and habitat fragmentation: different trends in bird and mammal predators. *Ecography* 16, 111–116. doi: 10.1111/j.1600-0587.1993.tb00063.x

O'Brien, T. G., Kinnaird, M. F., and Wibisono, H. T. (2003). Crouching tigers, hidden prey: Sumatran tiger and prey populations in a tropical frost landscape. *Anim. Conserv.* 6, 131–139. doi: 10.1017/S1367943003003172

Pedersen, Å. Ø., Asmyhr, L., Pedersen, H. C., and Eide, N. E. (2011). Nest-predator prevalence along a mountain birch-alpine tundra ecotone. *Wildl. Res.* 38, 525–536. doi: 10.1071/WR11031

Perrella, D. F., Zima, P. V. Q., Ribeiro-Silva, L., Biagolini, C. H., Carmignotto, A. P., Galetti, P. M., et al. (2019). Bats as predators at the nests of tropical forest birds. *J. Avian Biol.* 51:e02277. doi: 10.1111/jav.02277

Reidy, J. L., and Thompson, F. (2012). Predatory identity can explain nest predation patterns. *Stud. Avian Biol.* 43, 135–148. doi: 10.1525/california/9780520273139.003.0011

Ricklefs, R. E., and Wikelski, M. (2002). The physiology/life-history nexus. *Trends Ecol. Evol.* 17, 462–468. doi: 10.1016/S0169-5347(02)02578-8

Rovero, F., Martin, E., Rosa, M., Ahumada, J. A., and Spitale, D. (2014). Estimating species richness and modeling habitat preferences of tropical forest mammals from camera trap data. *PLoS One* 9:e103300. doi: 10.1371/journal.pone.0103300

Sanders, H. N., Hewitt, D. J., Vercauteren, K. C., and Snow, N. P. (2020). Opportunistic predation of wild Turkey nests by wild pigs. *J. Wildl. Manag.* 84, 293–300. doi: 10.1002/jwmg.21797

Sanders, M. D., and Maloney, R. F. (2002). Causes of mortality at nests of ground-nesting birds in the upper Waitaki Basin, South Island, New Zealand: a 5-year video study. *Biol. Conserv.* 106, 225–236. doi: 10.1016/s0006-3207(01)00248-8

Seibold, S., Hempel, A., Piehl, S., Bässler, C., Brandl, R., Rösner, S., et al. (2013). Forest vegetation structure has more influence on predation rate of artificial ground nests than human activities. *Basic Appl. Ecol.* 14, 687–693. doi: 10.1016/j.baae.2013.09.003

Sherry, T. W., Wilson, S., Hunter, S., and Holmes, R. T. (2015). Impacts of nest predators and weather on reproductive success and population limitation in a long-distance migratory songbird. *J. Avian Biol.* 46, 559–569. doi: 10.1111/jav.00536

Singer, F. J., Swank, W. T., and Clebsch, E. E. (1984). Effects of wild pig rooting in a deciduous forest. *J. Wildl. Manag.* 48, 464–473. doi: 10.2307/3801179

Slevin, M. C., Bin Soudi, E. E., and Martin, T. E. (2020). Breeding biology of the mountain wren-babbler (*Gypsophila crassus*). *Wilson J. Ornithol.* 132, 124–133. doi: 10.1676/1559-4491-132.1.124

Smith, A. T, and Xie, Y. (2009). *A Guide to the Mammals of China*. Changsha: Hunan Education Publishing House

Stutchbury, B. J. M., and Morton, E. S. (2008). Recent advances in the behavioural ecology of tropical birds. *Wilson J. Ornithol.* 120, 26–37. doi: 10.1676/07-018.1

Stutchbury, B. J. M., and Morton, E. S. (2023). *Behavioral Ecology of Tropical Birds*. San Diego (CA): Academic Press

Thompson, F., and Burhans, D. E. (2003). Predation of songbird nests differs by predator and between field and forest habitats. *J. Wildl. Manag.* 67, 408–416. doi: 10.2307/3802781

Thompson, F., and Ribic, C. A. (2012). "Conservation implications when the nest predators are known" in *Video Surveillance of Nesting Birds. Studies in Avian Biology (no.43)*. eds. C. A. Ribic, F. R. Thompson and P. J. Pietz (Berkeley, CA: University of California Press), 23–34.

Visco, D. M., and Sherry, T. W. (2015). Increased abundance, but reduced nest predation in the chestnut-backed antbird in costa rican rainforest fragments: surprising impacts of a pervasive snake species. *Biol. Conserv.* 188, 22–31. doi: 10.1016/j.biocon.2015.01.015

Wilson, G. R., Brittingham, M. C., and Goodrich, L. J. (1998). How well do artificial nests estimate success of real nests? *Condor* 100, 357–364. doi: 10.2307/1370277

Xiao, H., Hu, Y., Lang, Z., Fang, B., Guo, W., Zhang, Q., et al. (2017). How much do we know about the breeding biology of bird species in the world? *J. Avian Biol.* 48, 513–518. doi: 10.1111/jav.00934

Xiao, Z., Li, X., and Jiang, G. (2014). Applications of camera trapping to wildlife surveys in China. *Biodivers. Sci.* 22, 683–684. doi: 10.3724/SP.J.1003.2014.14244

Yuan, L. (2009). *Field Studies on Red Junglefowl (Gallus gallus jabouillei) in Hainan, China*. Beijing: University of the Chinese Academy of Sciences

Yuan, L., Zhang, C., Zhang, H., Fu, H., Lin, X., Fu, Y., et al. (2009a). Nest-site characteristics of red jungle fowl, *Gallus gallus jabouillei*. *Zool. Res.* 30, 457–462. doi: 10.3724/SP.J.1141.2009.04457

Yuan, L., Zhang, C., Zhang, H., Zhang, C., Fu, Y., Lin, X., et al. (2009b). Roosting site selection of red jungle fowl during the breeding season in Hainan. *Sichuan J. Zool.* 28, 652–657.

Zanette, L., and Jenkins, B. (2000). Nesting success and nest predators in forest fragments: a study using real and artificial nests. *Auk* 117, 445–454. doi: 10.1093/auk/117.2.445

Zheng, G. (2022). *Checklist on the Classification and Distribution of the Birds of China*. Beijing: Science Press

Zheng, Z., Tan, Y, and Lu, T. (1978). *Fauna Sinica, Aves (Volume IV): Galliformes*. Beijing: Science Press, 148–154

frontiers | Frontiers in Ecology and Evolution

TYPE Original Research
PUBLISHED 23 February 2023
DOI 10.3389/fevo.2023.1125749

OPEN ACCESS

EDITED BY
Xiang Liu,
Lanzhou University, China

REVIEWED BY
Xinwei Guo,
Chinese Academy of Tropical Agricultural Sciences, China
Yi Ding,
Chinese Academy of Forestry, China

*CORRESPONDENCE
Bin Zhang
✉ al332501575@163.com
Biao Huang
✉ huangbiao@icbr.ac.cn

†These authors have contributed equally to this work and share first authorship

SPECIALTY SECTION
This article was submitted to Conservation and Restoration Ecology, a section of the journal Frontiers in Ecology and Evolution

RECEIVED 16 December 2022
ACCEPTED 26 January 2023
PUBLISHED 23 February 2023

CITATION
Yang H, Mai S, Liu W, Fu J, Yang Q, Zhang B and Huang B (2023) Variations of arbuscular mycorrhizal fungi following succession stages in a tropical lowland rainforest ecosystem of South China. *Front. Ecol. Evol.* 11:1125749. doi: 10.3389/fevo.2023.1125749

Variations of arbuscular mycorrhizal fungi following succession stages in a tropical lowland rainforest ecosystem of South China

Huai Yang[1†], Siwei Mai[2†], Wenjie Liu[2], Jialin Fu[3], Qiu Yang[2], Bin Zhang[4*] and Biao Huang[3*]

[1]Institute of Tropical Bamboo, Rattan and Flower, Sanya Research Base, International Centre for Bamboo and Rattan, Sanya, China, [2]School of Ecology and Environment, Hainan University, Haikou, China, [3]International Centre for Bamboo and Rattan, Beijing, China, [4]Agricultural Technology Extension Service Center of Sanya, Sanya, China

Introduction: The grasslands in the Nature Reserve of Ganshenling, in the south of Hainan Island, were first formed after deforestation disturbance before a natural restoration of shrubs and secondary forests. However, the stages of grassland and shrubs in some parts of Ganshenling regions could not be naturally restored to secondary forests. In addition, the forest form of the secondary forest after 40 years (40a) of succession was similar to that of the secondary forest of 60 years (60a). However, it was not known whether the microorganisms recovered to the level of the secondary forest of 60a. Arbuscular mycorrhizal fungi (AMF) are plant root symbionts that can improve the nitrogen and phosphorus absorption of plants and play a key role in secondary forest succession. An understanding of the essential role of soil AMF in secondary forest succession of tropical rainforest in Ganshenling regions is still limited.

Methods: Therefore, the soil of 0–10 cm was collected with the help of a 5-point sampling method in grassland, shrubs, and second tropical lowland rainforest of 40a and 60a. We studied community changes in AMF with the succession and explored the impacts of soil physicochemical properties on soil AMF.

Results: Our findings were as follows: (1) Different successional stages showed divergent effects on soil AMF communities. (2) After 40a recovery, the alpha-diversity indices of AMF recovered to the level of secondary forest of 60a, but the similarity of soil AMF communities only recovered to 25.3%. (3) Species richness of common species, rare species, and all the species of AMF showed a significantly positive correlation with soil nitrogen. (4) OTU10; OTU6, OTU9, and OTU141; OTU3 and OTU38; and OTU2, OTU15, OTU23, and OTU197 were significantly unique AMF for grasslands, shrubs, and secondary forests of 40a and 60a, respectively. (5) The phylogenetic tree and the heatmap of AMF showed that the OTUs in grasslands and shrubs were in contrast to the OTUs in secondary forests of 40a and 60a.

Discussion: We concluded that the succession of a secondary forest after deforestation disturbance was probably limited by its AMF community.

KEYWORDS

arbuscular mycorrhizal fungi, succession stages, soil physicochemical properties, tropical lowland rainforest, Nature Reserve of Ganshenling

1. Introduction

Grasslands (G) and shrubs (S) are formed after deforestation, and are restored to the tropical rainforest by nature (Szefer et al., 2020; Liu et al., 2021). However, the G and S in the Natural Reserve of Ganshenling in the south of Hainan Island do not lead to succession for a long time. This leads to a decline in biomass and degradation in soil fertility, the reason remains unknown.

An estimated 90% of terrestrial plants are associated with mycorrhizal fungi, 80% of these being arbuscular mycorrhizal fungi (AMF), including in tropical lowland rainforests (Haug et al., 2021). AMF play critical roles in facilitating the supply of immobile nutrients (especially nitrogen and phosphorus) and water to the host plants in exchange for photosynthates (Delavaux et al., 2017; Nie et al., 2022). They are sensitive to vegetation as the nature of vegetation along the successional stages of an ecosystem can shape the associated AMF community and vice versa (Asmelash et al., 2016).

A comprehensive understanding of the physicochemical properties of the interactions of soil AMF with different vegetation types helps in understanding the stability and resilience of the tropical rainforest ecosystem. Numerous studies were conducted to investigate the effect of the composition and diversity of vegetation on soil AMF (Šmilauer et al., 2021; Zhang et al., 2021). Some previous studies showed that soil AMF significantly increased along the successional stages in a tropical rainforest ecosystem (Cowan et al., 2022). In contrast to early successional species, late-successional plant species were highly dependent on AMF (Koziol and Bever, 2015). In addition, the changes in AMF could mediate plant species turnover among successional stages (Koziol and Bever, 2016). However, other studies showed that the soil AMF had no response to the diversity and productivity of vegetation (Bauer et al., 2015). In pasture and secondary natural succession, the biomass and catabolic diversity of soil microbial communities were regulated by soil organic carbon (SOC) and soil nitrogen (SN) (Iyyemperumal et al., 2007; Zhang et al., 2022).

Recently, various studies focused on the changes in soil AMF across various successional stages in temperate and subtropical forest ecosystems. However, less information is available on tropical lowland forest ecosystems. While the importance of AMF for a tropical secondary forest successional stage is well understood (Vasconcellos et al., 2013; Reyes et al., 2019), less is known about the potential impacts of AMF on G and S. Furthermore, the possibility that a limited presence of AMF species could influence secondary forest regrowth dynamics is also less explored (Heilmann-Clausen et al., 2015).

The National Nature Reserve of Ganshenling offers a typical ecosystem that comprises G, S, and secondary forests. Its succession follows a vegetation transect sequence of G, S, the secondary forest of 40a (SF40), and the secondary forest of 60a (SF60). Our geographical study sites differ from those of most other studies on AMF communities in tropical vegetation with their coverage of G and S (Zangaro et al., 2012; Leal et al., 2013). Long-term non-succession of G and S has reduced vegetation diversity and biomass recovery (Šmilauer et al., 2020). This is representative of the future of many more recent G and S regions throughout the tropical lowland rainforests. In this study, soil AMF composition in different successional stages was investigated. We analyzed the influence of topsoil fertility (acidity and nutrient availability) on soil AMF.

The specific objectives of this study were as follows: (1) to explore the characteristics of soil AMF community along the successional stages and (2) to identify the factors that drive the changes in soil AMF community along these successional stages.

2. Materials and methods

2.1. Study area

This study was carried out at the Natural Reserve of Ganshenling (109°37'−109°41'E, 18°19'−18°24'N), which has a typical tropical lowland rainforest with a tropical marine monsoon climate. The annual average precipitation and temperature are 1,800 mm and 25.4°C, respectively. The dominant plant species in this area include *Hopea reticulata*, *Vatica mangachapoi*, *Koilodepas hainanense*, *Rhodomyrtus tomentosa*, *Melastoma sanguineum*, *Scleria elata*, and *Blechnum orientale* (Qi et al., 2014; Mao et al., 2021).

2.2. Sampling collection and environmental variables

Four successional stages in the Natural Reserve of Ganshenling were selected: (1) G (109°39'−109°41'E, 18°21'−18°23'N); (2) S (109°39'−109°41'E, 18°22'−18°23'N); (3) SF40 (109°39'−109°40'E, 18°21'−18°23'N); and (4) SF60 (109°39'−109°40'E, 18°22'−18°23'N).

From each successional stage, five soil samples of 0–10 cm depth were collected by following the 5-point sampling method from five plots of 900 m^2 (30 m × 30 m) in August 2019 (Wang et al., 2020). These samples were divided into two groups: one was stored at −80°C until the measurement of soil AMF communities; the other group was used to measure soil physicochemical properties. These soil samples were subsequently air-dried. A 2-mm screen sieve was used to sieve air-dried soil samples for analyzing soil pH, SOC, SN, and soil phosphorus (SP). The SOC was measured with the help of the H_2SO_4-$K_2Cr_2O_7$ oxidation method (Bisutti et al., 2004). SN was measured using the Micro-Kjeldahl method (Bremner, 1960), and the available nitrogen was estimated with the help of a micro-diffusion method (Mulvaney and Khan, 2001). SP was measured using an inductively coupled plasma atomic-emission spectrometer (Thermo Jarrell Ash Corporation, Franklin, USA) and HNO_3-$HClO_4$ soil solution (McDowell and Sharpley, 2001).

2.3. DNA extraction and amplicon sequencing

Soil DNA was extracted from 250 mg soil samples with the help of a MO-BIO PowerSoil DNA Isolation Kit (MO BIO Laboratories, Carlsbad, CA, USA). DNA was analyzed and quantified with the help of a NanoDrop ND-2000 Spectrophotometer (Thermo Fisher Scientific, Waltham, MA, USA). A standard concentration of AMF was used for PCR amplification.

For PCR amplification, AMV4.5NF (5′-AAGCTCGTAGTTGAATTTCG-3′) and AMDGR (5′-CCCAACTATCCCTATTAATCAT-3′) were used as primers. An AMF library was constructed using two-step PCR amplification. Target fragments were amplified using these primers. Then, an Illumina adapter sequence, a primer pad, and a barcode were added to both the forward and reverse target fragments. A 50-μL reaction volume was used for PCR of each sample, comprising 10 μL of 5x buffer, 1 μL of dNTP (10 m/M), 1 U of Phusion High-Fidelity DNA Polymerase (New England Biolabs, Ipswich, MA, USA), 1 μL of forward and reverse phasing primers, and 3–10 ng of target sequencing. The reaction volume was supplemented with 50 μL of RNase-free ultrapure water. An ABI9700 PCR amplifier (Applied Biosystems, Waltham, MA, USA) was used to amplify DNA. The holding temperature was set at 10°C. PCR products were run on an agarose gel and PCR products were purified from the gel with the help of an AxyPrep DNA Gel Recovery Kit (Axygen Biosciences, Corning, NY, USA) and pooled. FTC-3000TM real-time PCR instrument (Richmond Biotechnology Inc., Richmond Hill, Ontario, Canada) was used to quantify purified DNA and mixed it to an equal molar ratio to perform the second PCR amplification, for which the reaction volume changed to 40 μl: 5x buffer (8 μl), dNTP (1μL, 10 m/M), Phusion High-Fidelity DNA Polymerase (0,8 U, New England Biolabs, Ipswich, MA, USA), both forward and reverse primers (1 μl, 5 μmol/L), respectively, and DNA template (5 μl, 100 μg/ml) and RNase-free ultrapure water (5 μl).

Barcodes were used to identify sequences of different samples in a parallel sequencing test. The sequence with a complete barcode was regarded as valid and extracted to a dataset stored in the FASTQ format. Quality assurance and splicing were performed on such valid sequences and included the following steps: (1) Poorly overlapped and low-quality sequences (quality score < 20 and window size < 5) were removed with the help of the Trimmomatic program (Bolger et al., 2014); (2) paired reads were merged into a sequence, where the overlap of PEreads (>10 bp) was evaluated with the help of the FLASH program (Magoc and Salzberg, 2011); and (3) merged sequences were screened according to an error ratio (<0.2). Mothur V.1.39.5 was used for quality control of merged reads by removing sequences that were ambiguous, homologous, or chimeras generated during PCR amplification (Schloss et al., 2009). Further analysis of information on species and clustering of operational taxonomic units (OTUs) was based on the clean tags. OTUs were selected with the help of UPARSE with a cutoff of 97% similarity (Edgar, 2013). The dataset was screened for chimeric reads using UCHIME in a reference database mode (Edgar et al., 2011). Through USEARCH global, all sequences were compared to OTU representative sequences to obtain the OTU abundance table. The identity of OTU taxonomy was determined with BLAST (Ye et al., 2006) by comparing them to representative sequences in the MaarjAM database (Zhang et al., 2000; Opik et al., 2010). The taxonomy of an OTU was obtained for the species that had the highest similarity or identity with OTU representative sequences in the MaarjAM database. Some OTUs didnot contain any species information and were therefore marked as "Nomatch". The library preparation and sequencing were performed by TinyGene Bio-Tech (Shanghai, China). Raw sequence data were submitted to NCBI's Sequence Read Archives (SRP399604).

2.4. Bioinformatics and environmental correlation analyses

We analyzed the overall AMF species richness and diversity (Shannon H' and Simpson indices) and equitability (Pielou J'). Following the classification proposed by Logares et al. (2014), we classified species' relative abundances within each successional stage as "dominant" (>1%), "common" (1–0.01%), and "rare" (<0.01%) (Galand et al., 2009).

OTUs that included an unknown genus and contained <5 sequences were not used for bioinformatics analysis. The species diversity was calculated in R package "vegan." The principal coordinate analysis (PCoA) was performed using Bray–Curtis distances with 999 permutations with the help of R 4.2.2. The linear discriminant analysis effect size (LEfSe) and linear discriminant analysis (LDA) were performed with R 4.2.2 (Sirova et al., 2018; Nauta et al., 2020). The phylogenetic tree and heatmap of AMF were analyzed with the help of R 4.2.2.

3. Results

3.1. AMF community and Bray–Curtis similarity

Bray–Curtis-based PCoA showed that successional stages had different effects on AMF communities (Figure 1). The AMF communities clustered according to different successional stages, demonstrating that there were large differences between G and S, as well as between SF40 and SF60 (Figure 1).

The PERMANOVAs of Bray–Curtis distances also revealed significant differences among the AMF communities at different successional stages ($P = 0.001$). Additionally, our beta-diversity results were not significant ($P = 0.149$), indicating that our groups had the same dispersions. This fact also confirmed that our PERMANOVA results were reliable. Successional stages had a significant effect on the overall AMF community, which contributed to 33.7% of the total variation (Figure 1).

To further elucidate the trend in recovery of the AMF communities during successional stages, the similarity of community composition at the OTU level between different successional stages and SF60 was calculated. There was an average Bray–Curtis similarity of 35.6% between all AMF communities and SF60. The average Bray–Curtis similarity of AMF community between the different successional stages and SF60 was 21.0% for G, 16.0% for S, and 25.3% for SF40, respectively (Figure 2). This

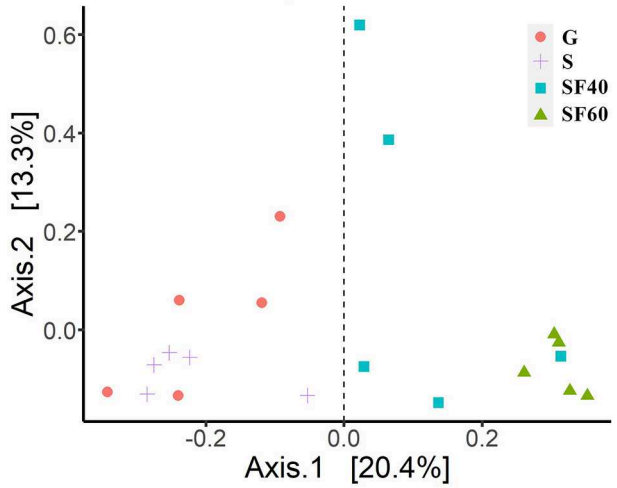

FIGURE 1
Principal coordinate analyses of Bray–Curtis distances of AMF. G: grasslands; S: shrubs; SF40: secondary forest of 40a; and SF60: secondary forest of 60a.

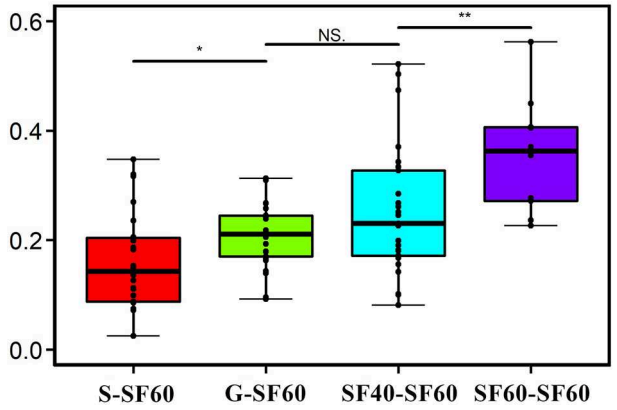

FIGURE 2
Bray–Curtis similarity of AMF on the basis of OTUs between other successional stages and secondary forest of 60a. G: grasslands; S: shrubs; SF40: secondary forest of 40a; and SF60: secondary forest of 60a.

suggested that there was a trend of increasing similarity of soil AMF communities from S and G to SF40 compared to SF60.

3.2. Phylogenetic diversity and composition of soil AMF community

The alpha-diversity indices that were based on phylogenetic species richness and phylogenetic diversity of soil AMF communities exhibited different trends (Supplementary Figure S1). AMF phylogenetic species richness and phylogenetic diversity of G were significantly lower than those of SF60 ($P < 0.01$). However, these parameters showed no significant differences between SF40 and SF60 (Supplementary Figure S1).

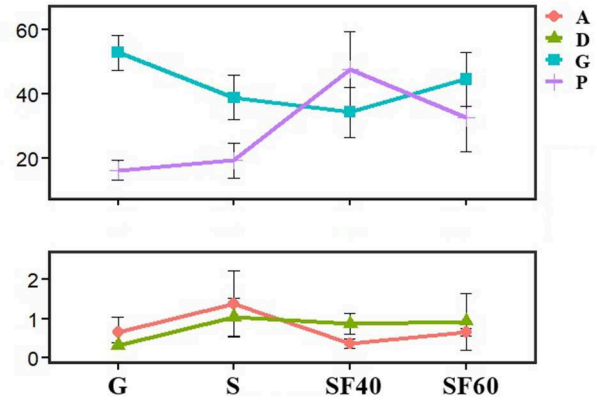

FIGURE 3
The relative abundance of dominant AMF orders along successional stages. Error bars denote the standard deviation. A: Archaeosporales; D: Diversisporales; G: Glomerales; P: Paraglomerales; G: grassland; S: shrubs; SF40: secondary forest of 40a; and SF60: secondary forest of 60a. Different lowercase letters represent signicant differences along successional stages. Glomerales:a,a,a,a; Paraglomerales:b,b,a,ab; Archaeosporales:a,a,a,a; and Diversisporales:a,a,a,a.

The dominant orders of AMF communities among all samples were Glomerales (42.8 ± 3.8%; means ± SD), followed by Paraglomerales (29.1 ± 5.1%), Archaeosporales (0.8 ± 0.3%), and Diversisporales (0.8 ± 0.2%). Together, these accounted for more than 73.5% of the total AMF sequences in all the samples (Supplementary Table S1). The relative abundance of Paraglomerales was significantly increased along the successional stages (Figure 3). Interestingly, the lowest relative abundances of Glomerales and Archaeosporales were found in SF40. However, these relative abundances had no significant differences among the successional stages (Figure 3; Supplementary Table S1). These findings indicated a partial recovery of AMF communities at the order levels (Paraglomerales increasing, while Glomerales and Archaeosporales were decreasing) through the 40a recovery after deforestation disturbance.

The AMF were mainly distributed in the orders Glomerales (42.8% of the total AMF reads) and Paraglomerales (29.1% of the total AMF reads). The relative abundances of Glomerales were no significant differences among the successional stages (Figure 3). In addition, no significant changes were observed at the family or lower levels, except for OTU13, OTU15, OTU23, and OTU28 (Supplementary Table S1).

3.3. Relationship between AMF community composition and soil factors

SOC, SN, carbon/nitrogen ratio (C/N), and pH had significant differences among the successional stages (Supplementary Table S2). The species richness of common species, rare species, and all species of AMF exhibited a significantly positive relationship with SN (Figure 4). However, species richness of all species of AMF, species richness, Shannon H', Simpson, and Pielou J' indices of rare species of AMF showed a significantly negative relationship with C/N (Figure 4).

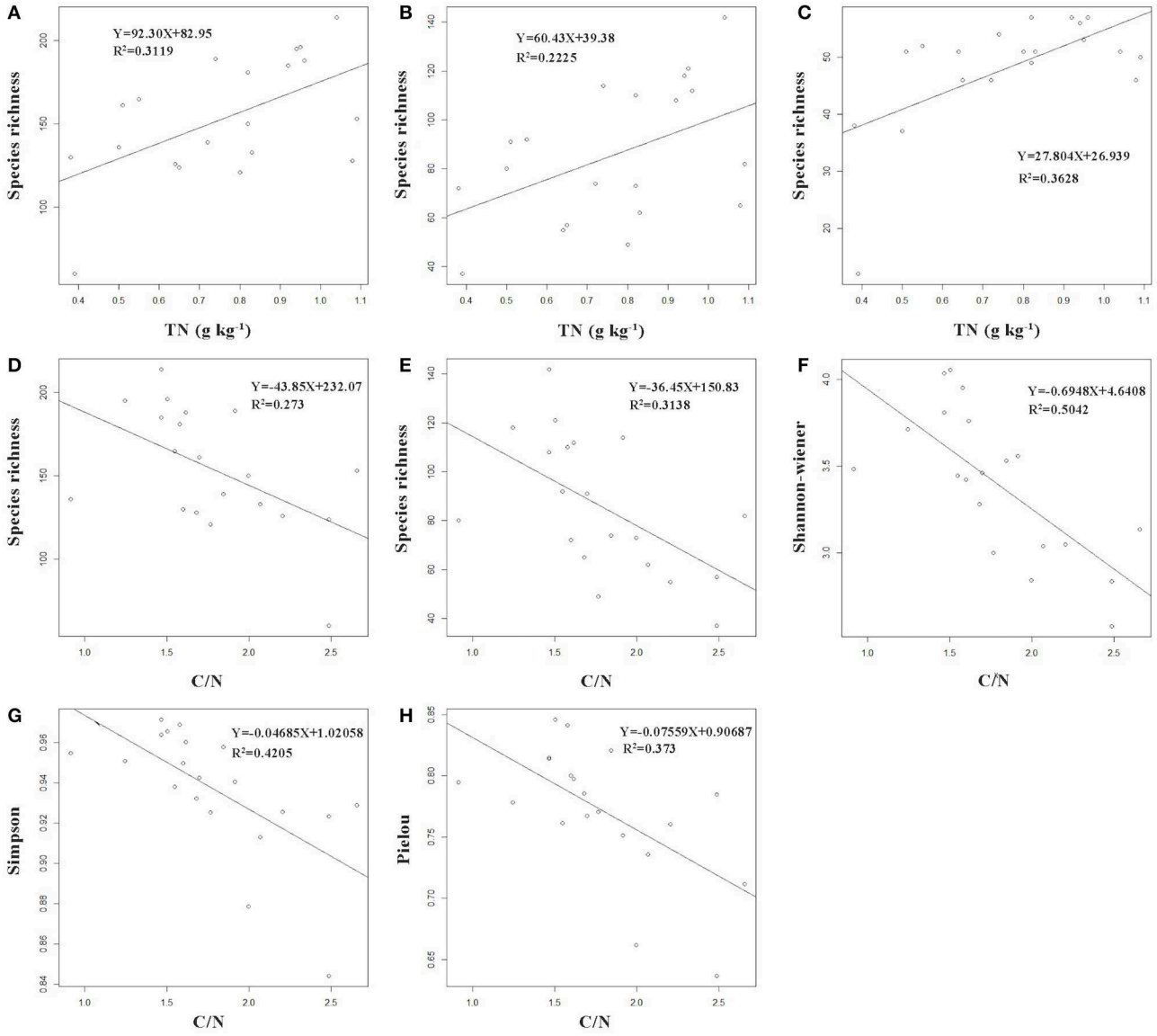

FIGURE 4
The relationship between diversity indices of AMF and soil physicochemical properties. Y and R^2 represent the diversity indices of AMF and the coefficient of determination for this regression equation, respectively. Diagrams of all species of AMF: **(A, D)**; Diagrams of rare species of AMF: **(B, E–H)**; Diagrams of common species of AMF: **(C)**; TN, soil nitrogen; C/N, carbon/nitrogen ratio.

3.4. The LEfSe of AMF

The LEfSe of AMF at successional stages were OTU10 for G; OTU6, OTU9, and OTU141 for S; OTU3 and OTU38 for SF40; and OTU2, OTU15, OTU23, and OTU197 for SF60, respectively (Figure 5).

3.5. The phylogenetic tree and heatmap of AMF

The most dominant orders of AMF communities among successional stages were Glomerales and Paraglomerales. The distribution of OTUs of G was similar to that of S, whereas this was in contrast to those of SF40 and SF60 (Figure 6).

4. Discussion

4.1. The differences in AMF composition across successional stages

Significant differences were observed in AMF communities between G and S, as well as between SF40 and SF60. Previous studies demonstrated that changes in fungal composition occurred during field successions, where late-successional plant species were highly dependent on AMF as compared to the early-successional plant species, which were not observed in the study of Koziol and Bever (2015). As many the mid- and late-successional plant species were shown to have a high overall beneficial response to AMF, these species were also likely to be more sensitive to the presence of particular beneficial AMF in their environment (Maitra et al., 2021). The changes in AMF composition could mediate

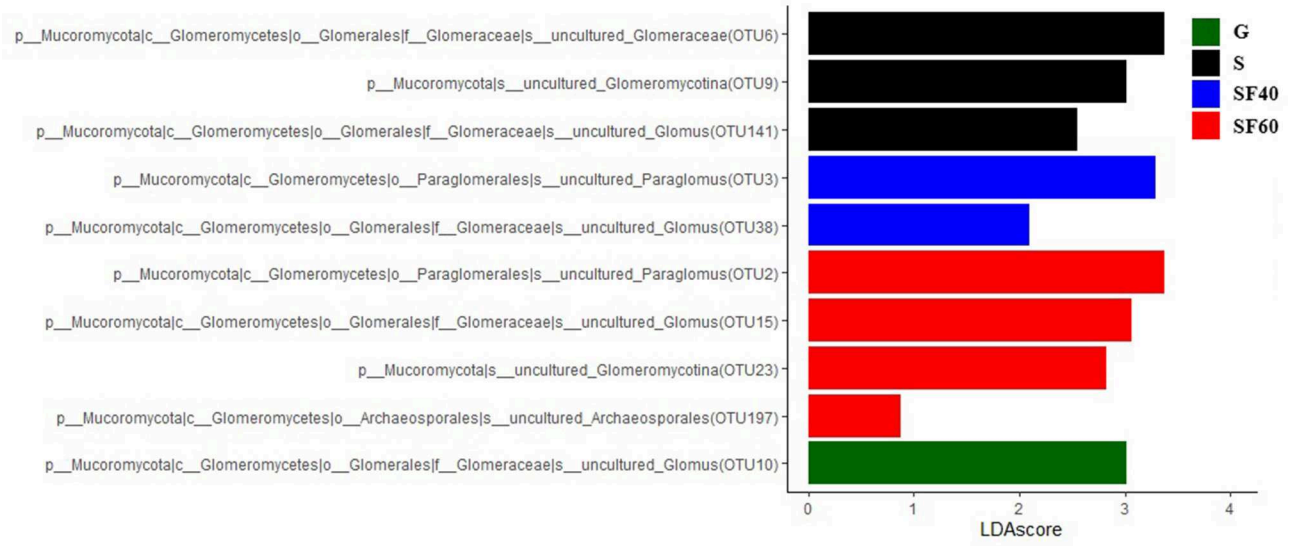

FIGURE 5
The LEfSe of soil AMF communities along successional stages. G: grasslands; S: shrubs; SF40: secondary forest of 40a; and SF60: secondary forest of 60a.

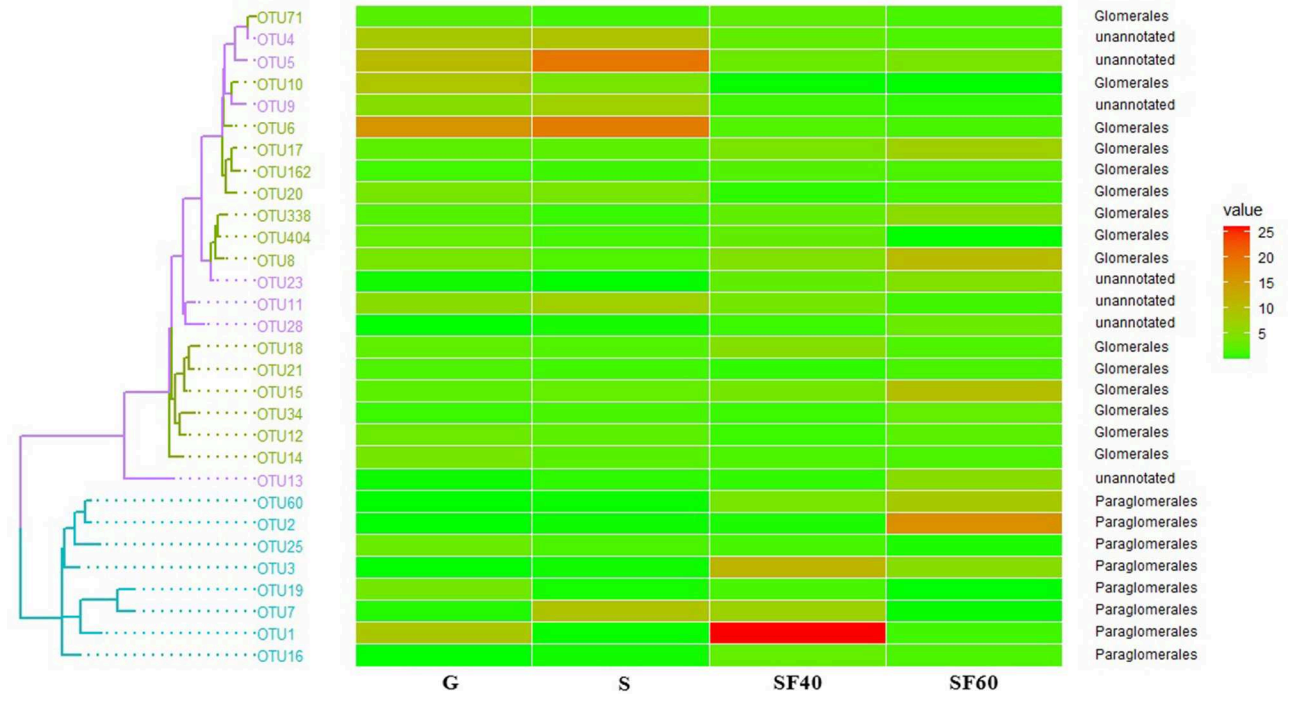

FIGURE 6
The phylogenetic tree and heatmap of soil AMF along successional stages, drawn on the basis of the top 30 OUTs. G: grasslands; S: shrubs; SF40: secondary forest of 40a; and SF60: secondary forest of 60a.

plant species turnover during successional periods, which could be particularly important for the establishment and subsequent dynamics of late-successional plants (Koziol and Bever, 2016). AMF have played an important role in secondary forest successions (Heilmann-Clausen et al., 2015). Differences in AMF species composition along the successional stages were also found in the eastern periphery of Amazonia (Reyes et al., 2019), which confirmed the results of Pereira et al. (2014) in Atlantic rainforest areas of Northeast Brazil and those of Leal et al. (2013) in western Amazonia.

4.2. The relationship between AMF and soil physicochemical properties

In this study, the SOC, SN, C/N, and pH showed significant differences with succession, and the species richness of common species, rare species, and all species of AMF indicated a significantly positive relationship with SN. Whereas, the species richness of all species of AMF showed a significantly negative relationship with C/N. Some previous studies reported that SOC and SN were increased along with proceeding successions (Allison et al., 2007; Eisenhauer et al., 2010). In addition, C/N in S was significantly lower than those of other successional stages (Xue et al., 2017). Both SOC and SN were increased along with the succession from G to other stages, which stimulated microbial metabolisms and changed bacterial and fungal community structure by increasing soil amino sugars (Shao et al., 2017). The C/N could significantly affect the structure of the soil microbial community and the nitrogen supply of plants (Waring et al., 2013).

The soil nutrient availability had been proven to be the key determinant that regulated the assembly of AMF communities (Johnson et al., 2015; Jiang et al., 2018) and vice versa (Rillig et al., 2015). The SN could directly drive the change in the AMF community in mixed roots (Shi et al., 2022). The change in SN indirectly regulated the species composition of the AMF community by driving plant species richness at both the whole-community scale and the individual plant species scale (Shi et al., 2022).

5. Conclusion

The changes in AMF along the successional stages were examined in this study. We found that successional stages had different effects on AMF communities. After 40a recovery, the alpha-diversity indices of AMF had recovered to the level of SF60, but the species of AMF had not recovered. The species richness of common species, rare species, and all species of AMF was found to be significantly positively associated with SN. The vegetation succession after deforestation was likely limited by the AMF community. Further research will need to be focused on exploring the effects of soil physicochemical properties on the AMF function diversity along the successional stages in tropical lowland rainforest ecosystems.

Data availability statement

The datasets presented in this study can be found in online repositories. The names of the repository/repositories and accession number(s) can be found below: https://www.ncbi.nlm.nih.gov/sra/PRJNA927263.

Author contributions

The study was conceived and designed by HY and SM. The lab work and the analysis were done by SM and JF. HY wrote the main text of the manuscript. Insightful discussions were contributed by WL, BH, BZ, and QY. All authors reviewed and approved the manuscript.

Funding

This study was jointly supported by the Fundamental Research Funds of ICBR (1632020022), the Fundamental Research Funds of Sanya Research Base, ICBR (1630032022006), and the China Postdoctoral Science Foundation (2018M631414; 2019T120073).

Acknowledgments

We thank all the colleagues and the staff who were involved in maintaining the field maps and collecting samples. We also greatly thank the staff of the Sanya Research Base, International Center for Bamboo and Rattan who provided help in this research work.

Conflict of interest

The authors declare that the research was conducted in the absence of any commercial or financial relationships that could be construed as a potential conflict of interest.

Publisher's note

Supplementary material

The Supplementary Material for this article can be found online at: https://www.frontiersin.org/articles/10.3389/fevo.2023.1125749/full#supplementary-material

References

Allison, V. J., Condron, L. M., Peltzer, D. A., Richardson, S. J., and Turner, B. L. (2007). Changes in enzyme activities and soil microbial community composition along carbon and nutrient gradients at the Franz Josef chronosequence, New Zealand. *Soil Biol. Biochem.* 39, 1770–1781. doi: 10.1016/j.soilbio.2007.02.006

Asmelash, F., Bekele, T., and Birhane, E. (2016). The potential role of arbuscular mycorrhizal fungi in the restoration of degraded lands. *Front. Microbiol.* 7, 1095. doi: 10.3389/fmicb.2016.01095

Bauer, J. T., Mack, K. M. L., and Bever, J. D. (2015). Plant-soil feedbacks as drivers of succession: evidence from remnant and restored tallgrass prairies. *Ecosphere.* 6, 1–12. doi: 10.1890/ES14-00480.1

Bisutti, I., Hilke, I., and Raessler, M. (2004). Determination of total organic carbon–an overview of current methods. *Trends Analyt. Chem.* 23, 716–726. doi: 10.1016/j.trac.2004.09.003

Bolger, A. M., Lohse, M., and Usadel, B. (2014). Trimmomatic: a ?exible trimmer for Illumina sequence data. *Bioinformatics.* 30, 2114–2120. doi: 10.1093/bioinformatics/btu170

Bremner, J. M. (1960). Determination of nitrogen in soil by the Kjeldahl method. *J. Agric. Sci.* 55, 11–33. doi: 10.1017/S0021859600021572

Cowan, J. A., Gehring, C. A., Ilstedt, U., and Grady, K. C. (2022). Host identity and neighborhood trees affect belowground microbial communities in a tropical rainforest. *Trop. Ecol.* 63, 216–228. doi: 10.1007/s42965-021-00203-z

Delavaux, C. S., Smith-Ramesh, L. M., and Kuebbing, S. E. (2017). Beyond nutrients: a meta-analysis of the diverse effects of arbuscular mycorrhizal fungi on plants and soils. *Ecology.* 98, 2111–2119. doi: 10.1002/ecy.1892

Edgar, R. C. (2013). Uparse: Highly accurate OTU sequences from microbial amplicon reads. *Nat. Methods.* 10, 996–998. doi: 10.1038/nmeth.2604

Edgar, R. C., Haas, B. J., Clemente, J. C., Quince, C., and Knight, R. (2011). UCHIME improves sensitivity and speed of chimera detection. *Bioinformatics.* 27, 2194–2200. doi: 10.1093/bioinformatics/btr381

Eisenhauer, N., Beßler, H., Engels, C., Gleixner, G., Habekost, M., Milcu, A., et al. (2010). Plant diversity effects on soil microorganisms support the singular hypothesis. *Ecology.* 91, 485–496. doi: 10.1890/08-2338.1

Galand, P. E., Casamayor, E. O., Kirchman, D. L., and Lovejoy, C. (2009). Ecology of the rare microbial biosphere of the Arctic Ocean. *Proc. Natl. Acad. Sci.* 106, 22427–22432. doi: 10.1073/pnas.0908284106

Haug, I., Setaro, S. S., and Suárez, J. P. (2021). Global AM fungi are dominating mycorrhizal communities in a tropical premontane dry forest in Laipuna, South Ecuador. *Mycol. Prog.* 20, 837–845. doi: 10.1007/s11557-021-01699-4

Heilmann-Clausen, J., Barron, E. S., Boddy, L., Dahlberg, A., Griffith, G. W., Nordén, J., et al. (2015). A fungal perspective on conservation biology. *Conserv. Biol.* 29, 61–68. doi: 10.1111/cobi.12388

Iyyemperumal, K., Israel, D. W., and Shi, W. (2007). Soil microbial biomass, activity and potential nitrogen mineralization in a pasture: Impact of stock camping activity. *Soil Biol. Biochem.* 39, 149–157. doi: 10.1016/j.soilbio.2006.07.002

Jiang, S., Liu, Y., Luo, J., Qin, M., Johnson, N. C., Öpik, M., et al. (2018). Dynamics of arbuscular mycorrhizal fungal community structure and functioning along a nitrogen enrichment gradient in an alpine meadow ecosystem. *New Phytol.* 220, 1222–1235. doi: 10.1111/nph.15112

Johnson, N. C., Wilson, G. W. T., Wilson, J. A., Miller, R. M., and Bowker, M. A. (2015). Mycorrhizal phenotypes and the l aw of the minimum. *New Phytol.* 205, 1473–1484. doi: 10.1111/nph.13172

Koziol, L., and Bever, J. D. (2015). Mycorrhizal response trades off with plant growth rate and increases with plant successional status. *Ecology.* 96, 1768–1774. doi: 10.1890/14-2208.1

Koziol, L., and Bever, J. D. (2016). AMF, phylogeny, and succession: specificity of response to mycorrhizal fungi increases for late-successional plants. *Ecosphere.* 7, e01555. doi: 10.1002/ecs2.1555

Leal, P. L., Siqueira, J. O., and Stuermer, S. L. (2013). Switch of tropical Amazon forest to pasture affects taxonomic composition but not species abundance and diversity of arbuscular mycorrhizal fungal community. *Appl. Soil Ecol.* 71, 72–80. doi: 10.1016/j.apsoil.2013.05.010

Liu, Y., Zhang, G., Luo, X., Hou, E., Zheng, M., Zhang, L., et al. (2021). Mycorrhizal fungi and phosphatase involvement in rhizosphere phosphorus transformations improves plant nutrition during subtropical forest succession. *Soil Biol. Biochem.* 153, 108099. doi: 10.1016/j.soilbio.2020.108099

Logares, R., Audic, S., Bass, D., Bittner, L., Boutte, C., Christen, R., et al. (2014). Patterns of rare and abundant marine microbial eukaryotes. *Curr. Biol.* 24, 813–821. doi: 10.1016/j.cub.2014.02.050

Magoc, T., and Salzberg, S. L. (2011). Flash: Fast length adjustment of short reads to improve genome assemblies. *Bioinformatics.* 27, 2957–2963. doi: 10.1093/bioinformatics/btr507

Maitra, P., Zheng, Y., Wang, Y., Mandal, D., Lü, P., Gao, C., et al. (2021). Phosphorus fertilization rather than nitrogen fertilization, growing season and plant successional stage structures arbuscular mycorrhizal fungal community in a subtropical forest. *Biol. Fertil. Soils.* 57, 685–697. doi: 10.1007/s00374-021-01554-4

Mao, H., Liu, W., Yang, Q., Yao, H., Liu, G., Yang, H., et al. (2021). Characteristics of root biomass in the tropical lowland rain forest at different succession stages in ganshiling natural reserve, hainan Island. *J. Trop. Biol.* 12, 176–184. doi: 10.15886/j.cnki.rdswxb.2021.02.006

McDowell, R. W., and Sharpley, A. N. (2001). Soil phosphorus fractions in solution: influence of fertiliser and manure, fltration and method of determination. *Chemosphere.* 45, 737–748. doi: 10.1016/S0045-6535(01)00117-5

Mulvaney, R. L., and Khan, S. A. (2001). Diffusion methods to determine different forms of nitrogen in soil hydrolysates. *Soil Sci. Soc. Am. J.* 65, 1284–1292. doi: 10.2136/sssaj2001.6541284x

Nauta, J. F., Hummel, Y. M., Tromp, J., Ouwerkerk, W., van der Meer, P., Jin, X., et al. (2020). Concentric vs. eccentric remodelling in heart failure with reduced ejection fraction:Clinical characteristics, pathophysiology and response to treatment. *Eur. J. Heart Fail.* 22, 1147–1155. doi: 10.1002/ejhf.1632

Nie, X., Wang, D., Chen, Y., Yang, L., and Zhou, G. (2022). Storage, distribution, and associated controlling factors of soil total phosphorus across the Northeastern Tibetan Plateau Shrublands. *J. Soil Sci. Plant Nutr.* 22, 2933–2942. doi: 10.1007/s42729-022-00857-1

Opik, M., Vanatoa, A., Vanatoa, E., Moora, M., Davison, J., Kalwij, J. M., et al. (2010). The online database MaarjAM reveals global and ecosystemic distribution patterns in arbuscular mycorrhizal fungi (Glomeromycota). *New Phytol.* 188, 223–241. doi: 10.1111/j.1469-8137.2010.03334.x

Pereira, C. M. R., da Silva, D. K. A., de Almeida Ferreira, A. C., Goto, B. T., and Maia, L. C. (2014). Diversity of arbuscular mycorrhizal fungi in Atlantic forest areas under different land uses. *Agric. Ecosyst. Environ.* 185, 245–252. doi: 10.1016/j.agee.2014.01.005

Qi, L., Liang, C., Mao, C., Qin, X., Fan, S., Du, W., et al. (2014). Species composition and geographic elements of the tropical lowland secondary rain forest of Ganshenling, Hainan Island, China. *Chin. J. Ecol.* 33, 922–929.

Reyes, H. A., Ferreira, P. F. A., Silva, L. C., Costa, M. G., Nobre, C. P., Gehring, C., et al. (2019). Arbuscular mycorrhizal fungi along secondary forest succession at the eastern periphery of Amazonia: Seasonal variability and impacts of soil fertility. *Appl. Soil Ecol.* 136, 1–10. doi: 10.1016/j.apsoil.2018.12.013

Rillig, M. C., Aguilar-Trigueros, C. A., Bergmann, J., Verbruggen, E., Veresoglou, S. D., Lehmann, A., et al. (2015). Plant root and mycorrhizal fungal traits for understanding soil aggregation. *New Phytol.* 205, 1385–1388. doi: 10.1111/nph.13045

Schloss, P. D., Westcott, S. L., Ryabin, T., Hall, J. R., Hartmann, M., Hollister, E. B., et al. (2009). Introducing mothur: Open-source, platform-independent, community-supported software for describing and comparing microbial communities. *Appl. Environ. Microbiol.*75, 7537–7541. doi: 10.1128/AEM.01541-09

Shao, S., Zhao, Y., Zhang, W., Hu, G., Xie, H., Yan, J., et al. (2017). Linkage of microbial residue dynamics with soil organic carbon accumulation during subtropical forest succession. *Soil Biol. Biochem.* 114, 114–120. doi: 10.1016/j.soilbio.2017.07.007

Shi, G., Yang, Y., Liu, Y., Uwamungu, J. Y., Liu, Y., Wang, Y., et al. (2022). Effect of Elymus nutans on the assemblage of arbuscular mycorrhizal fungal communities enhanced by soil available nitrogen in the restoration succession of revegetated grassland on the Qinghai-Tibetan Plateau. *Land Degrad. Dev.* 33, 931–944. doi: 10.1002/ldr.4201

Sirova, D., Barta, J., Simek, K., Posch, T., Pech, J., Stone, J., et al. (2018). Hunters or farmers? Microbiome characteristics help elucidate the diet composition in an aquatic carnivorous plant. *Microbiome.* 6, 225. doi: 10.1186/s40168-018-0600-7

Šmilauer, P., Košnar, J., Kotilínek, M., and Šmilauerová, M. (2020). Contrasting effects of host identity, plant community, and local species pool on the composition and colonization levels of arbuscular mycorrhizal fungal community in a temperate grassland. *New Phytol.* 225, 461–473. doi: 10.1111/nph.16112

Šmilauer, P., Košnar, J. K., Kotilínek, M., Pecháčková, S., and Šmilauerová, M. (2021). Host age and surrounding vegetation affect the community and colonization rates of arbuscular mycorrhizal fungi in a temperate grassland. *New Phytol.* 232, 290–302. doi: 10.1111/nph.17550

Szefer, P., Molem, K., Sau, A., and Novotny, V. (2020). Impact of pathogenic fungi, herbivores and predators on secondary succession of tropical rainforest vegetation. *J. Ecol.* 108, 1978–1988. doi: 10.1111/1365-2745.13374

Vasconcellos, R. L. F., Segat, J. C., Bonfim, J. A., Bonfim, J. A., Baretta, D., Cardoso, E. J. B. N., et al. (2013). Soil macrofauna as an indicator of soil quality in an undisturbed riparian forest and recovering sites of different ages. *Eur. J. Soil. Biol.* 58, 105–112. doi: 10.1016/j.ejsobi.2013.07.001

Wang, Y., Liu, K., Wu, Z., and Jiao, L. (2020). Comparison and analysis of three estimation methods for soil carbon sequestration potential in the Ebinur Lake Wetland, China. *Front. Earth Sci.* 14, 13–24. doi: 10.1007/s11707-019-0763-y

Waring, B. G., Averill, C., and Hawkes, C. V. (2013). Differences in fungal and bacterial physiology alter soil carbon and nitrogen cycling: insights from meta-analysis and theoretical models. *Ecol. Lett.* 16, 887–894. doi: 10.1111/ele.12125

Xue, L., Ren, H., Li, S., Leng, X., and Yao, X. (2017). Soil bacterial community structure and co-occurrence pattern during vegetation restoration in karst rocky desertification area. *Front. Microbiol.* 8, 2377. doi: 10.3389/fmicb.2017.02377

Ye, J., McGinnis, S., and Madden, T. L. (2006). BLAST: improvements for better sequence analysis. *Nucleic Acids Res.* 34, W6–W9. doi: 10.1093/nar/gkl164

Zangaro, W., Alves, R. A., Lescano, L. E., Ansanelo, A. P., and Nogueira, M. A. (2012). Investment in fine roots and arbuscular mycorrhizal fungi decrease during succession in three Brazilian ecosystems. *Biotropica*. 44, 141–150. doi: 10.1111/j.1744-7429.2011.00781.x

Zhang, J., Quan, C., Ma, L., Chu, G., Liu, Z., Tang, X., et al. (2021). Plant community and soil properties drive arbuscular mycorrhizal fungal diversity: A case study in tropical forests. *Soil Ecol. Lett*. 3, 52–62. doi: 10.1007/s42832-020-0049-z

Zhang, M., Shi, Z., Xu, X., Xu, X., and Wang, X. (2022). Arbuscular Mycorrhizal Fungi Associated with Roots Reveal High Diversity Levels at Different Elevations in Tropical Montane Rainforests. *Diversity*. 14, 587. doi: 10.3390/d14080587

Zhang, Z., Schwartz, S., Wagner, L., and Miller, W. (2000). A greedy algorithm for aligning DNA sequences. *J. Comput. Biol.* 7, 203–214. doi: 10.1089/10665270050081478

frontiers | Frontiers in Ecology and Evolution

TYPE Original Research
PUBLISHED 23 February 2023
DOI 10.3389/fevo.2023.1118175

OPEN ACCESS

EDITED BY
Hui Zhang,
Hainan University,
China

REVIEWED BY
Han Xu,
Chinese Academy of Forestry,
China
Shidan Zhu,
Guangxi University,
China

*CORRESPONDENCE
Yuelin Li
yuelin@scbg.ac.cn

†These authors have contributed equally to this work

SPECIALTY SECTION
This article was submitted to Conservation and Restoration Ecology, a section of the journal Frontiers in Ecology and Evolution

RECEIVED 07 December 2022
ACCEPTED 25 January 2023
PUBLISHED 23 February 2023

CITATION
Li Y, Nyongesah MJ, Deng L, Haider FU, Liu S, Mwangi BN, Zhang Q, Chu G, Zhang D, Liu J and Meng Z (2023) Clustered tree size analysis of bio-productivity of Dinghushan National Nature Reserve in China. *Front. Ecol. Evol.* 11:1118175. doi: 10.3389/fevo.2023.1118175

Clustered tree size analysis of bio-productivity of Dinghushan National Nature Reserve in China

Yuelin Li[1,2,3*†], Maina John Nyongesah[4†], Libin Deng[5†], Fasih Ullah Haider[1,3], Shizhong Liu[1,3], Brian Njoroge Mwangi[1,2,3], Qianmei Zhang[1,3], Guowei Chu[1,3], Deqiang Zhang[1,3], Juxiu Liu[1,3] and Ze Meng[1,3]

[1]Key Laboratory of Vegetation Restoration and Management of Degraded Ecosystems, South China Botanical Garden, Chinese Academy of Sciences, Guangzhou, China, [2]South China National Botanical Garden, University of Chinese Academy of Sciences, Beijing, China, [3]South China National Botanical Garden, Guangzhou, China, [4]Department of Biological Sciences, Jaramogi Oginga Odinga University of Science and Technology, Bondo, Kenya, [5]Academy of Forestry Inventory and Planning, State Forestry Administration, Beijing, China

Over various terrain types, natural forests exhibit tree size and biomass variation. We started long- term research that consists of forest vegetation surveys in the Dinghushan National Nature Reserve to comprehensively investigate productivity based on the structure and species composition of China's forest communities. We grouped the trees into three categories, i.e., as large or mature (DBH>30cm), medium-sized or growing (DBH 10–30cm), and small-sized or regenerating seedlings (DBH<10cm). Forest data observations, i.e., species DBH, height, and biomass components (trunk, leaves, branches, above-ground dry weight, and below-ground dry weight) were recorded by use of standard protocols. All recorded observations were statistically analyzed by use of SPSS version 25. To comprehend the connections between the many elements of forest bio-productivity, linear regression analysis was utilized. Total above-ground biomass was 34.19±5.75Kg/tree, but varied results were obtained when the forest was clustered based on DBH. Large-sized trees contributed an average of 2400.54±510.4kg/tree (93.24%), while medium-sized trees contributed 171.61±25.06kg/tree, and the least was regenerating seedlings which contributed 3.013±0.07kg/tree. There were positive linear relationships for all life forms between biomass and DHB, as well as DBH and height. The evergreen broadleaved shrubs were shorter in height (3.06±0.99m) than palm-leaved life forms (19.29±5.39m). Height influenced biomass accumulation and hence C gain, where life forms with tall stands had higher biomass. Generalized biomass estimation without clustering based on life forms or size class underestimates biomass components and hence lower C stocks for most forests worldwide. It's also crucial to remember that trees with big DBH have tall, broad, well-lit crowns, which raise the primary productivity of forests and increase carbon storage. Besides natural disturbance (Typhoon) and climate change, it could be interesting to understand the relationship between soil resources such as nutrient and soil moisture content. These are factors that have direct impact on growth and biomass accumulation.

KEYWORDS

bio-productivity, forest biomass, life forms, diameter at breast height, broadleaved

1. Introduction

Comparative productivity and large-scale patterns of plant species richness have been described in parts of Asia (Guo, 1999; Shen et al., 2013; Wu et al., 2015), but more attempts have yet to be made to identify the mechanisms of such patterns. Forests are constantly in flux as they grow and vary in size, composition, structure, and health, as well as in response to climate shifts and oscillations (Shen et al., 2013; Maina and Li, 2021). Within natural forests and plantations, tree size and stock diversity can be noticed at any moment, especially over varied terrain (Weiner and Thomas, 1986; Maina and Li, 2021). Because of this temporal and spatial heterogeneity, it can be challenging to derive accurate estimates of forest carbon stocks and biomass accumulation (Skovsgaard and Vanclay, 2013). Climate change driven increase in CO_2 has been predicted to affect forest productivity by affecting biomass accumulation in different plant functional groups (Shaver et al., 2000) as well as their carbon storage (carbon stock) ability (Shaver et al., 2000; Gielen and Ceulemans, 2001). Therefore, understanding the factors that influence changes in forest carbon stocks and biomass accumulation is essential for sound management decisions and scientific researches.

Site index, or average height at a given age, is a popular indicator for forest site quality used by forest growth modelers to consider productivity differences between stands. The application of site index is not appropriate for trees that have experienced height suppression since it frequently relies on time- consuming increment core ring-count data to estimate stand age and needs to completely account for changes in volume growth (Skovsgaard and Vanclay, 2013). The ability to stratify sampling among more homogeneous subsets of the population of interest and to identify relatively homogeneous areas to serve as "blocks" in replicated field experiment installations are made possible by changes in forest growth (Husch et al., 2002). When links between forest production and its environment are taken into account or known and integrated into decision support systems, we can research or forecast changes in forest structure and productivity brought on by climate shifts, management actions, or other disturbances in ecosystems such as Dinhushan nature reserve. Aboveground biomass in the forest reflects the status of forest in terms of environmental conditions and health of the entire ecosystem (KoÈh et al., 2017; Lutz et al., 2018). Although this biomass is a key component in forest contribution to gas and water fux, available studies have focused on remotely sensed data (Skovsgaard and Vanclay, 2013), with scanty data available for in situ measurements especially for Dinghushan nature reserve. Available measurements have considered the entire ecosystem without clustering in trunk diameter classes. Field-based data from Dinghushan forest will provide relevant information on the forest characteristics and unveil determinants of forest carbon stocks, the structure and composition as well the history of disturbance.

For modelers of forest carbon stocks or biomass accumulation, different growth forms or habits lead to further problems, particularly in multi-aged stands (Murali et al., 2005). This study intends to overcome this challenge by estimating biomass, tree height, and DBH based on life forms and grouped DBH.

Several researchers have reported allometric connections between standing biomass and diameter at breast height (DBH) (Comley and McGuinness, 2005; Kirui et al., 2006) and linear equations between DBH and height for biomass estimation (Murali et al., 2005). These correlations have been calculated between DBH and above-ground biomass or its component elements (Kirui et al., 2006). However, limited information is available for allometric relationships or linear equations between above-ground biomass and DBH or height and DBH for different life forms of group datasets in a heterogenous forest like the Dinghushan forest. We explored different growth facets in the Dinghushan forest to examine relationships between biophysical gradients and productivity. Our goal was to determine which biophysical factors account for regional variations in forest productivity. We hypothesized the strongest correlations between DBH and height for various biophysical parameters for distinct life forms.

2. Materials and methods

2.1. Study site description

This study was carried out in Dinghushan National Nature Reserve (23°09′21″–23°11′ 30″N, 112°30′39″–112°33′41″E), which is located in Dinghu District, Zhaoqing City, Guangdong Province, covering a total area of 1,155 ha. The region experiences a south subtropical monsoon climate, with 1714 mm of annual rainfall and 76% annual humidity. The dry season lasts from October to March, and the wet season is from April to September. About 80% of the annual precipitation falls during the wet season. The coldest month is January, which has a mean temperature of 13.8°C, while the hottest month is July, which has a mean temperature of 28.8°C. The predominant topography comprises low mountains and hills ranging from 100 to 700 meters. Southern subtropical lateritic red soil comprises the zonal soil, which comprises Devonian sandstone, shale, sandstone, and quartz sandstone (Zou et al., 2018). Dinghushan's plant community has a 95% canopy density and is year-round evergreen. The plant community in Dinghushan can be separated into three stages based on the succession of the forest ecosystem: Masson pine coniferous forest in the early stage, coniferous and broad-leaved mixed forest in the middle stage, and monsoon evergreen broad-leaved forest in the later stage. *Aidia canthioides*, *Macarashell cnga sampsonii*, *Gironniera subaequalis*, *Cryptocarya chinensis*, *Cryptocarya concinna*, *Schima superba*, *Castanopsis chinensis*, etc., are the dominant species in the tree layer of monsoon evergreen broad-leaved forests (Zou et al., 2018).

A long-term monitoring experiment on the dynamics of the monsoon evergreen broadleaved forest was started in 1978 to examine the longer-term effects of climate change and human activity on ecological resilience, biodiversity, and ecosystem services. A 1-ha permanent monitoring site was also created in the monsoon evergreen broad-leaved forest. The core section of the reserve is made up of monsoon evergreen broadleaved forest that has not been altered and is located adjacent to a Buddhist monastery (Zhou et al., 2013). The landscape of the location before (A) and after (B) the typhoon is depicted in Figure 1 as the well-preserved monsoon evergreen broad-leaved forest suffered greatly from typhoon Mangkhut in 2018. Although previous studies have indicated Dinghushan nature reserve has not been heavily disturbed for more than 400 years (Zhou et al., 2006, 2013), the 2018 typhoon affected the number of tree stands as indicated in our previous study

FIGURE 1
Figure showing landscape of the study site location before **(A)** and after **(B)** the typhoon.

(Li et al., 2021). This study also illustrated that trees with <10 cm DBH and < 10 m heaigh were completelu destroyed by the storm as shown in Figure 1B while those with > 20 cm DBH were moderately destroyed. Table 1 provides a quick summary of the permanent site based on historical monitoring data (Zhang, 2011; Zhou et al., 2013, 2014).

TABLE 1 Description of the permanent site.

No.	Site name	Monsoon evergreen broad-leaved forest site
1	Succession stage	Top-stage
2	Location	23°10′24.41″N, 112°32′50.85″E
3	Altitude/*m*	230–350
4	Aspect	NE
5	Slope/(°)	25–35
6	Area/m^2	1
7	Stand age/a	>400
8	Crown density/%	>95
9	Leaf area index	6.2
10	Stand density/plant·ha	4,538
11	Biomass/*t*·ha	290.0
12	Soil type	Red soil

3. Methods

3.1. Tree selection

Within the 100 m by 100 m 1-ha permanent plot, 10 sites were established and sub-divided into 10 m by 10 m, 100 subplots (quadrats) where inventories of trees was carried out. In the clearly defined plots and with the appearance of being in good health, trees of the four life types were marked for measurements. Following that, DBH measurements were taken for each tree, with each multi-stemmed tree's stems being treated separately, as reported by Clough et al. (1997). Each stem's DBH was measured at a height of around 1.3 meters above the substrate or above the highest buttress root. The life/growth forms includes: Broadleaf evergreen trees that had large leaves, that stay green all year long; Broadleaf evergreen shrub that are small tree-like multi-stemmed trunk plants with year round green leaves; deciduous evergreen broadleaved tree that shed their leaves during cold and dry seasons and palm leaved trees that were tall, slender with smooth trunks and occasionally with no branches but have large spreading leaves at the top.

3.2. Biomass

Based on the harvesting quadrats described by Luo et al. (2009), biomass for all the components was estimated in all 100 plots. All trees had a diameter at breast height larger than 3 cm; their height (H, m) and diameter (D, cm) were measured. We removed six to eight trees in each sub-plot, each with a different diameter, and measured the amounts of stem, branch, leaf, and root biomass. Linear equation as described by Murali et al. (2005) was adopted where height and basal area relations facilitated calculation of biomass. Additionally, the "clear-cutting approach" (all trees in a plot were chopped down) and the "mean tree method" (a number of "mean trees" in a plot were fallen) were used in a few plots to estimate the tree biomass.

Data analysis.

SPSS 25 was used for all statistical analysis (IBM, Armonk, NY, United States). To comprehend the correlations between the biomass of various components and predictor variables, linear regression analysis was utilized. All values were reported as mean and standard error for each parameter.

4. Results

4.1. Stand characteristics

In the study, 6,883 trees and shrubs stands were recorded in the 100 sub-plots from which four life forms were identified within which several species were investigated for their diameter at breast height (DBH), stand height and biomass of trunk, leaves, branches, total above ground and below ground dry weights. The plots were dominated by evergreen broadleaved trees (5,723) followed by evergreen broadleaved shrubs (1,145), palm type life form (7), and the least dominant being deciduous broadleaved trees (8). Total number of trees per hectare varied before and after the typhoon as described in our study site section and presented in Figure 1. A study carried out by Li et al. (2021) indicated a total of 5,682 trees in 2015 and 5,022 trees per hectare in 2018. This is indicated that the typhoon caused a decline in the number of tree stands. Our study indicated an increase in trees and shrubs by 1,861 stands accounting for 37% recovery in 2020.

4.2. Tree height (m)

The average tree height for the entire forest was 4.7 ± 3.22 m. This height varied depending on the life form where the tallest trees were from the palm leaved trees (19.29 ± 5.39 m) followed by deciduous broadleaved trees (8.05 ± 4.55 m), evergreen broadleaved trees (5.11 ± 3.35 m) and shortest being evergreen broadleaved shrubs (3.06 ± 0.99 m; Figure 2A). Tall trees from evergreen broadleaved trees and palm leaved life forms with over 30 cm DBH had heights above 22 m (Figure 3D).

Similar to stand height, the mean forest DBH was 3.76 ± 6.26 cm but this was contributed differently by different life forms. Palm-leaved trees had large trunks with DBH of 25.8 ± 8 cm followed by

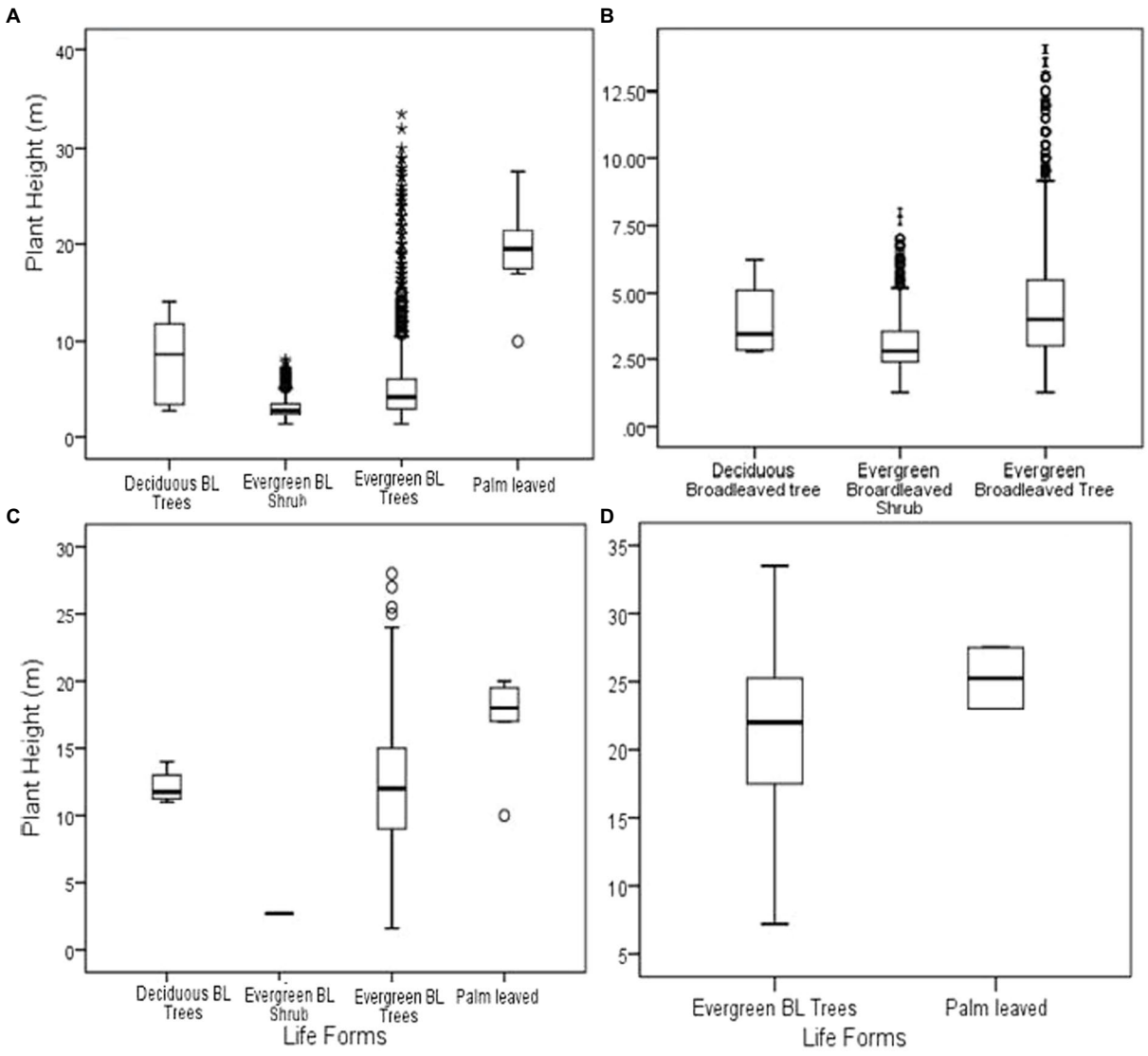

FIGURE 2
Tree height for the entire forest **(A)**; less than 10cm DBH **(B)**, 10–30cm DBH **(C)**, and above 30cm DBH **(D)**. *BL (Broad leaved).

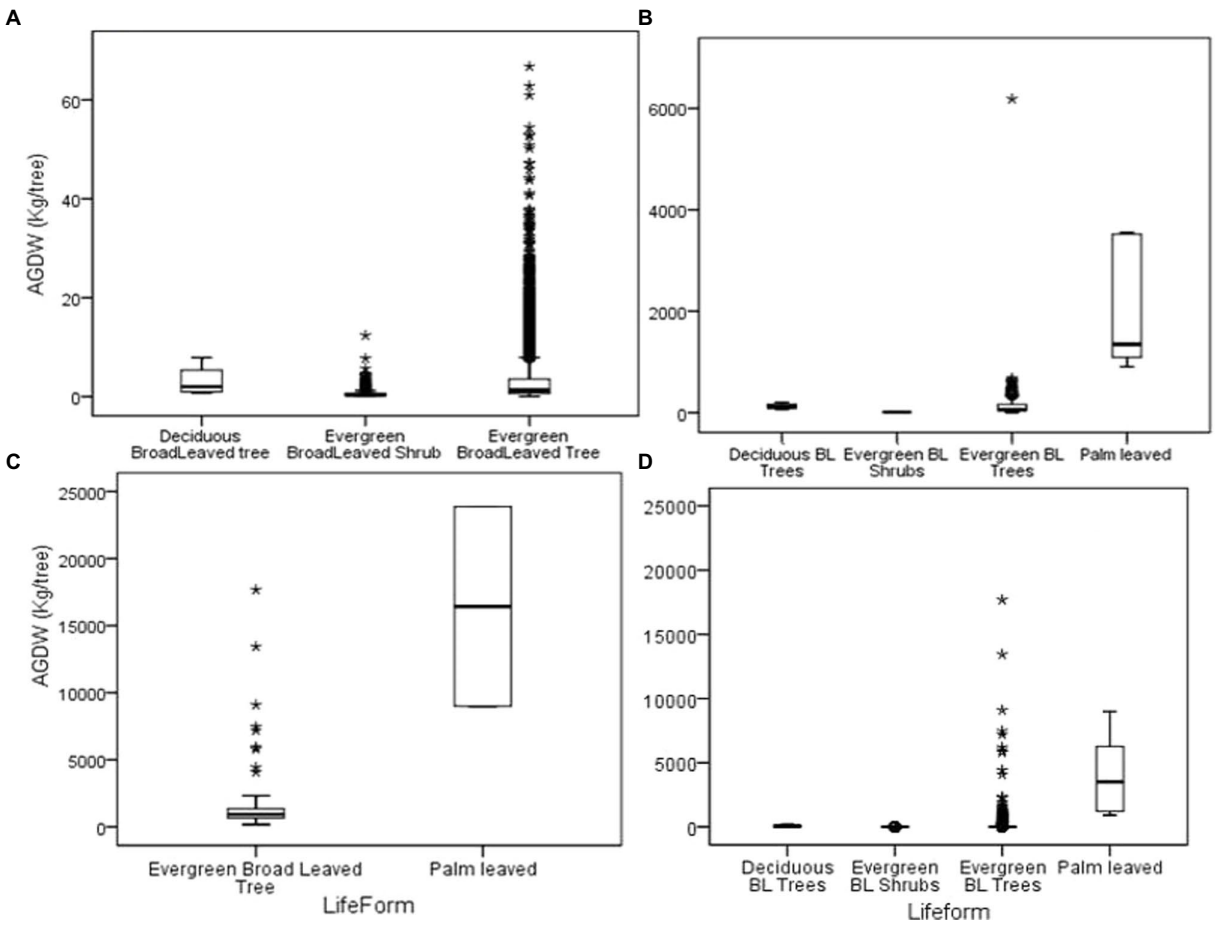

FIGURE 3
Above-ground dry weight (ABDW) for Dinghushan forest: **(A)** below 10cm DBH; **(B)** 10– 30cm DBH; **(C)** above 30cm DBH and **(D)** the entire forest data.

deciduous broadleaved trees (8.97 ± 6.88 cm), evergreen broadleaved trees (4.13 ± 6.73 cm), and the smallest trees being evergreen broadleaved shrubs (1.75 ± 0.73 cm) Figure 4A.

4.3. Forest biomass

Biomass varied depending on the life form whereas the highest biomass was recorded in broad- leaved evergreen forest and the least in deciduous broad-leaved evergreen trees. Looking at the entire above-ground dry weight for the forest, 63.91 kg/tree was recorded. However, forest life forms contributed differently to this biomass where palm-leaved trees recorded the highest above ground (6180.46 kg/tree) followed by deciduous broadleaved trees (63.91 ± 26.43 kg/tree), evergreen broadleaved trees (33.36 kg/tree) and evergreen broadleaved shrub had the least above ground biomass (0.56 kg/tree; Figure 3).

Below-ground dry weight for the Dinghushan forest was lower than the above-ground biomass. The palm-leaved type had the highest biomass of 1827.02 ± 24.82 kg/tree. Deciduous broad-leaved trees recoded 8.89 ± 3.52 kg/tree while evergreen broad-leaved shrubs had the lowest below- ground biomass of 0.11 ± 2.2 kg /tree. Grouping datasets based on DBH size class revealed that only broad- leaved evergreen and palm tree type had below-ground biomass of >30 cm DBH (Figure 5).

Based on Table 2, generalizing biomass for the entire forest underestimates the contribution of each life form in the Dinghushan forest. Total above-ground biomass was 34.19 ± 5.75Kg/tree but varied results are obtained when the forest is stratified based on DBH. Trees with DBH above 30 cm contributed an average of 2400.54 ± 510.4 kg/tree while trees with DBH 20–30 contributed 171.61 ± 25.06 kg/tree and the least was below 10 cm DBH which contributed 3.013 ± 0.07 kg/tree. More than 50% of the total above-ground mass was mainly contributed by trunk dry weight regardless of the size of the tree. The leaves contributed less than 10.3% to the total above- ground biomass whereas large-diameter trees had only a 7.3% contribution from leaves. Similarly, below-ground biomass was highest in trees with more than 30 cm DBH (632.23 ± 148.68 kg/tree). The overall forest below-ground biomass was 8.66 ± 1.64 kg/tree which was higher than trees with less than 10 cm DBH (0.77 ± 0.016 kg/tree).

4.4. Relationships between biophysical characteristics and biomass

This study found variability in the relationship between DBH and tree height depending on class size clustering (Figure 6). Regardless of tree size (DBH), DBH was positively correlated with tree heights whereas below 10 cm DBH was highly correlated ($R^2 = 0.63$) compared

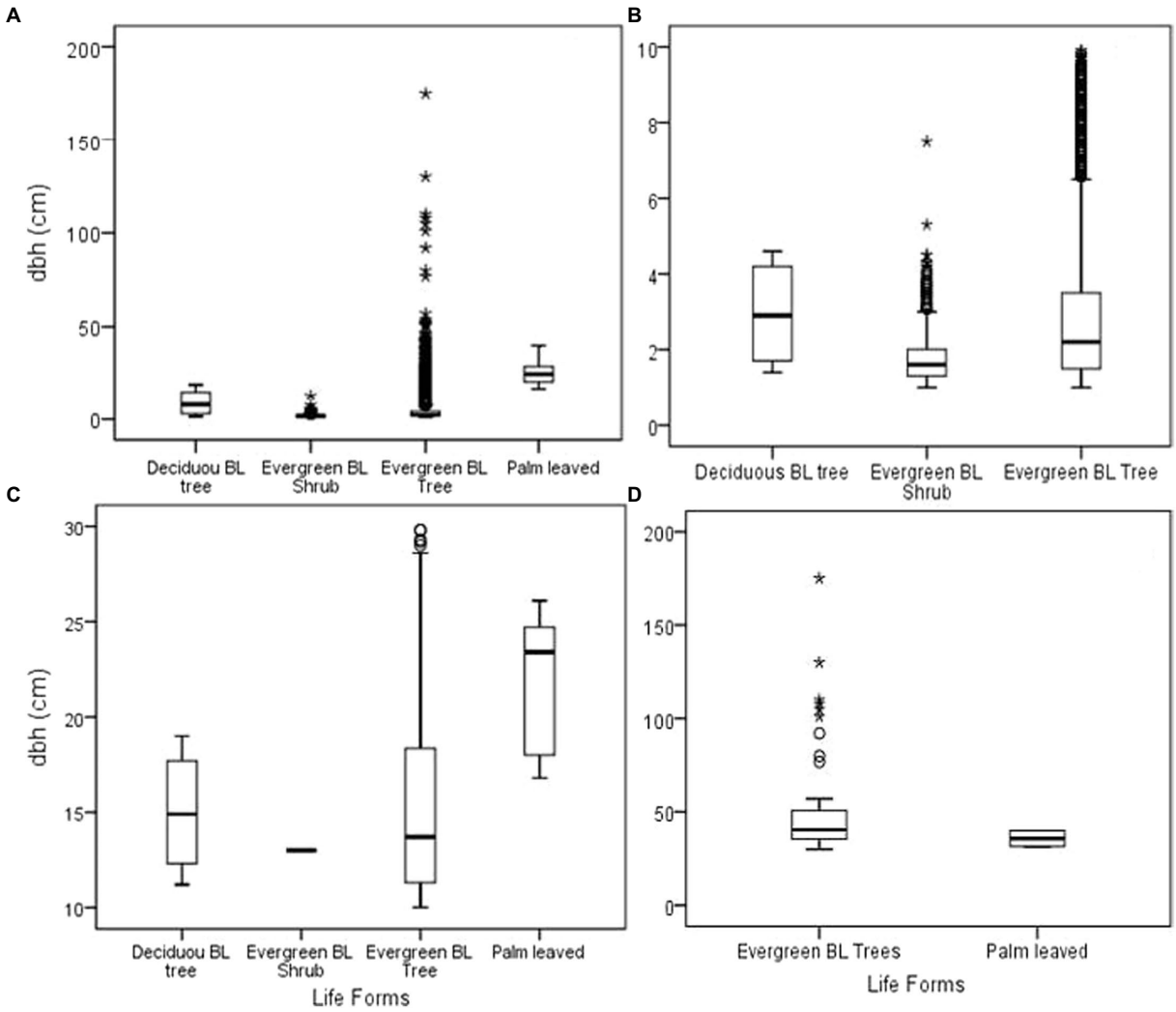

FIGURE 4
Diameter at breast height (cm) for the entire forest **(A)**; less than 10cm DBH **(B)**, 10–30cm DBH **(C)**, and above 30cm DBH **(D)**. *BL (Broad leaved).

to large tree size which had an R^2 of 0.102. Pooled data without clustering showed a highly positive relationship ($R^2 = 0.68$).

Diameter at breast height (DBH) showed a significant relationship with above-ground biomass ($R^2 = 0.7$) for small-sized trees which reduced with the increase in tree size (Figure 7). 10–30 cm tree sizes exhibited the weakest relationship ($R^2 = 0.18$) between DBH and biomass. Considering the overall relationship without size class clustering could overestimate the relationship for the 10–30 cm diameter trees by 45% and underestimate for the small-sized trees (less than 10 cm DBH) by 57%.

5. Discussion

Forests are always changing as they adapt to variations in climatic fluctuations by changing their structure and composition (Weiner and Thomas, 1986; Skovsgaard and Vanclay, 2013). In the current study, large trees (with DBH >30 cm) stored large amounts of biomass as observed from below-ground and above-ground biomass. They may have significant controls over the Dinghushan forest carbon store due to the dynamics and sensitivity of biomass to environmental change. Previous studies have shown that large-diameter trees constitute roughly half of the mature forest biomass worldwide (Lutz et al., 2018). According to previous research, big trees may be more susceptible to climate change, ultimately diminishing forest biomass storage (KoÈh et al., 2017; Lutz et al., 2018). In natural forests, tree size and stocking variation could be seen at any time, especially over varied terrain (Weiner and Thomas, 1986), similar to our study. This was true for the Dinghushan forest, where variability in tree height and diameter at breast height (DBH) produced varied biomass for different life forms. This study also showed that due to this temporal and spatial variability, when various life forms occur in a forest and individual species are of different size classes, it might be challenging to acquire reliable estimations of forest carbon stocks and biomass accumulation (Skovsgaard and Vanclay, 2013).

Previous studies have indicated that large-diameter forest trees (≥ 60 cm DBH) can account for up to 41% of above-ground biomass (AGB) globally (Lutz et al., 2018). In the current study site, big- sized trees (≥30 cm DBH) contributed 93.24% of the total AGB if we considered contribution based on DBH size class. Large-sized

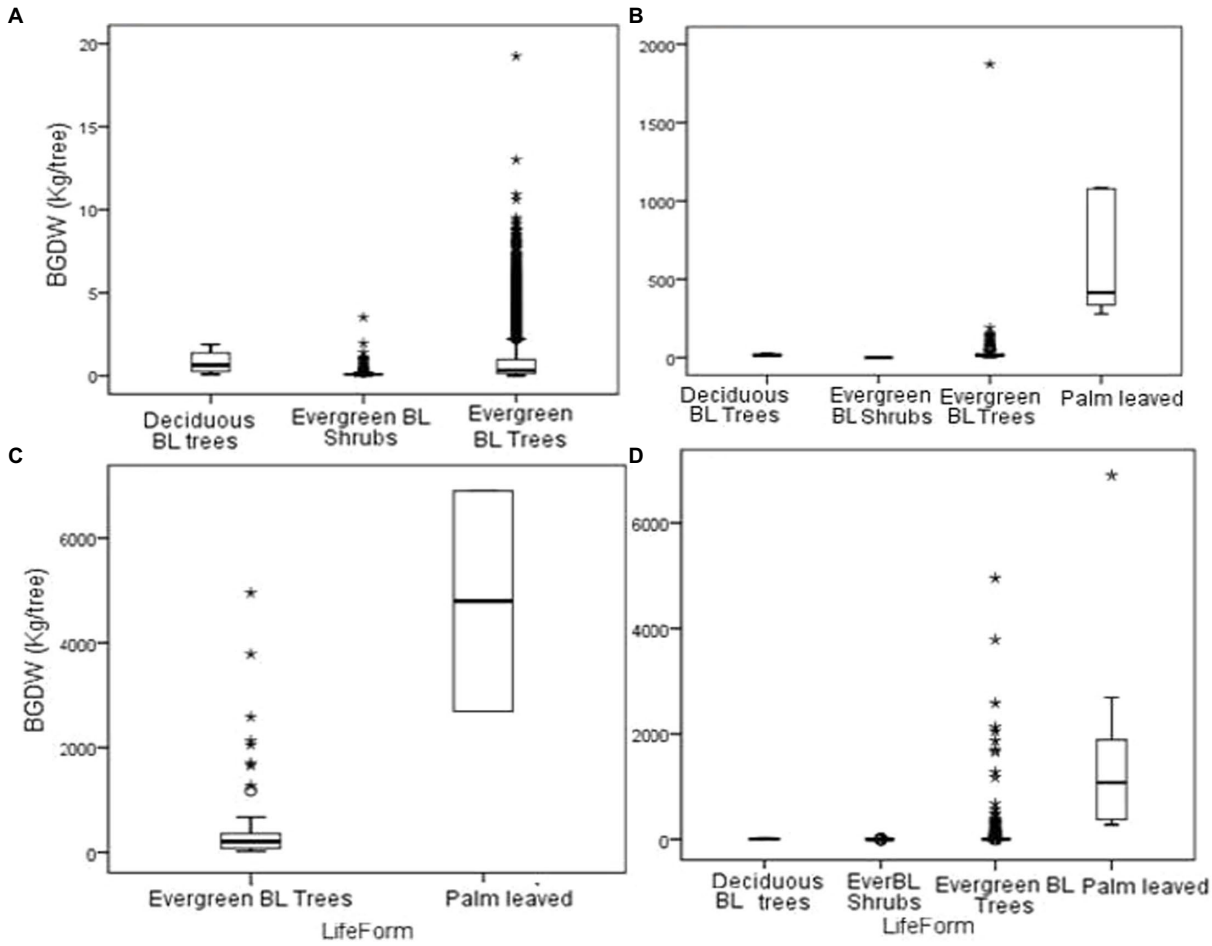

FIGURE 5
Below ground dry weight (ABDW) for Dinghushan forest: **(A)** below 10cm DBH; **(B)** 10– 30cm DBH; **(C)** above 30cm DBH and **(D)** the entire forest data. *BL (Broad leaved).

TABLE 2 Forest attributes for the entire data stratified based on DBH.

Below 10cm DBH			10–30cm DBH		Above 30cm DBH		All the data	
Attributes	*n*	$\mu \pm$SE	*N*	$\mu \pm$SE	*N*	$\mu \pm$SE	*N*	$\mu \pm$SE
DBH (cm)	6,486	2.68 ± 0.023	330	15.75 ± 0.3	66	49.28 ± 3.28	6,883	3.76 ± 0.08
Plant Height(m)	6,486	4.25 ± 0.024	330	12.15 ± 0.25	66	21.06 ± 0.781	6,883	4.79 ± 0.04
Trunk DW (kg)	6,486	1.98 ± 0.044	330	97.05 ± 9.58	66	1297.31 ± 222.8	6,883	19.01 ± 2.66
Branch D W(kg)	6,486	0.72 ± 0.019	330	57.52 ± 9.89	66	945.91 ± 233.9	6,883	12.56 ± 2.54
Leave DW (kg)	6,486	0.31 ± 0.006	330	17.03 ± 6.12	66	157.31 ± 96.2	6,883	2.62 ± 0.98
AG DW (kg)	6,486	3.013 ± 0.07	330	171.61 ± 25.06	66	2400.54 ± 510.4	6,883	34.19 ± 5.75
BG DW(kg)	6,486	0.77 ± 0.016	330	38.92 ± 7.52	66	632.23 ± 148.68	6,883	8.66 ± 1.64

DBH trees had tall, broad, well-lit crowns that increased the primary productivity of forests and allowed them to store more carbon. This was different when we compared the contribution of evergreen broadleaved shrubs. The evergreen broadleaved shrubs were shorter in height (3.06 ± 0.99 m) than palm-leaved life forms (19.29 ± 5.39 m). Studies have demonstrated that the growth and biomass accumulation of trees are subject to year-to-year and long-term fluctuations (KoÈh et al., 2017), with the majority of the carbon being accumulated at older ages, even though we did not take the age of the trees into account. Therefore, it is assumed that the large-sized trees in our study accumulated more carbon and recorded higher biomass.

This study revealed that the Dinghushan forest is constantly changing in size and composition over time as the trees develop and react to climatic fluctuations. When growing in a dense forest, small-diameter trees have been found to take advantage of canopy gaps and concentrate biomass production through height growth rather than

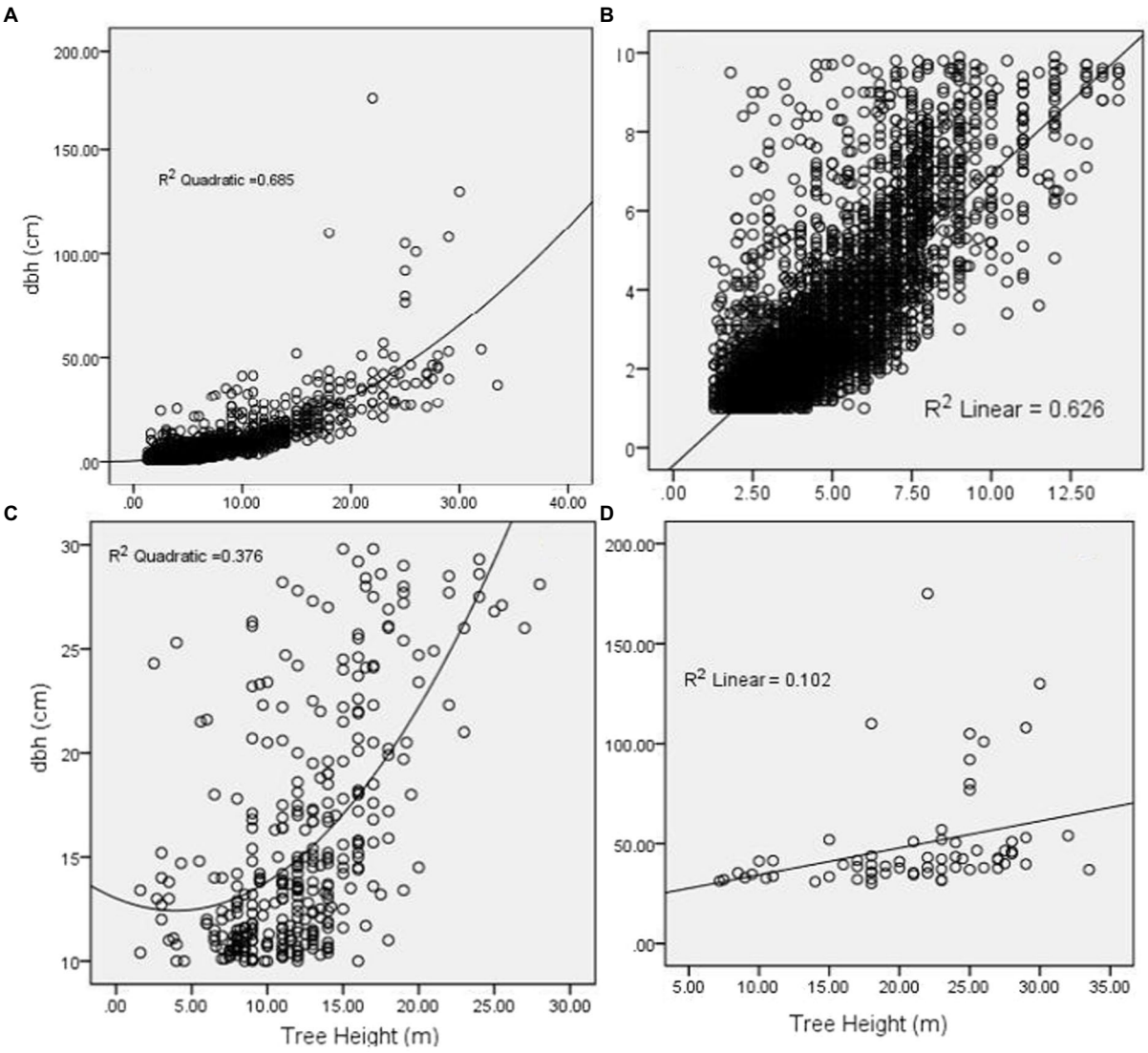

FIGURE 6
A quadratic and linear relationship between DBH and height for pooled data **(A)**, DBH below 10cm **(B)**, DBH between 10 and 30cm **(C)**, and DBH above 30cm **(D)**.

diameter expansion until they reach the high crown layers (McGregor et al., 2021). Tree DBH and height relationship are important elements describing attributes of forest stands. Although stand height has been applied as a variable in volume and biomass models (Comley and McGuinness, 2005) and DBH with height relationships used to determine volume and biomass estimates (Gobakken et al., 2008), such relationships may not provide accurate information regarding the entire forest if datasets are not grouped based on life forms or size class for the heterogeneous forest like Dinghushan forest. Furthermore, generalizing the entire dataset without grouping based on DBH, as observed in our study, may underestimate the forest biomass for less than 30 cm DBH trees and overestimate for trees with more than 30 cm DBH. It is worth noting that large-diameter trees represented fewer species in the entire forest (low stem density). However, they exhibited tall trees with more biomass in the trunk, leaves, branches, and below and above-ground dry weights. The dry weight of the Dinghushan forest is a complex trait that combines a variety of functional processes and structural characteristics. These attributes are linked to individual tree height, forest bio-productivity, and stem density (Shen et al., 2013). Since long-term forest biomass is driven by a balance between the rates at which wood growth and mortality rates, the observed differences in biomass between different life forms in this study emphasize the importance of understanding forest carbon budgets separately based on growth forms. Furthermore, biomass estimates should be based on carbon allocation ratios to foliage, branches, roots, and woody tissues, as described in (Sitch et al. (2008).

The results were more life-form specific than the others, and as a result, the weights recorded underestimated the true below-ground biomass of the larger trees. This resulted in a poor relationship between DBH and below-ground biomass. Trees with larger DBH had the most expansive root system for the life forms studied. The observed linear relationship between above- ground and DBH, and height and DBH indicated a close linkage between stand-level productivity and biomass across this forest complex. The differences

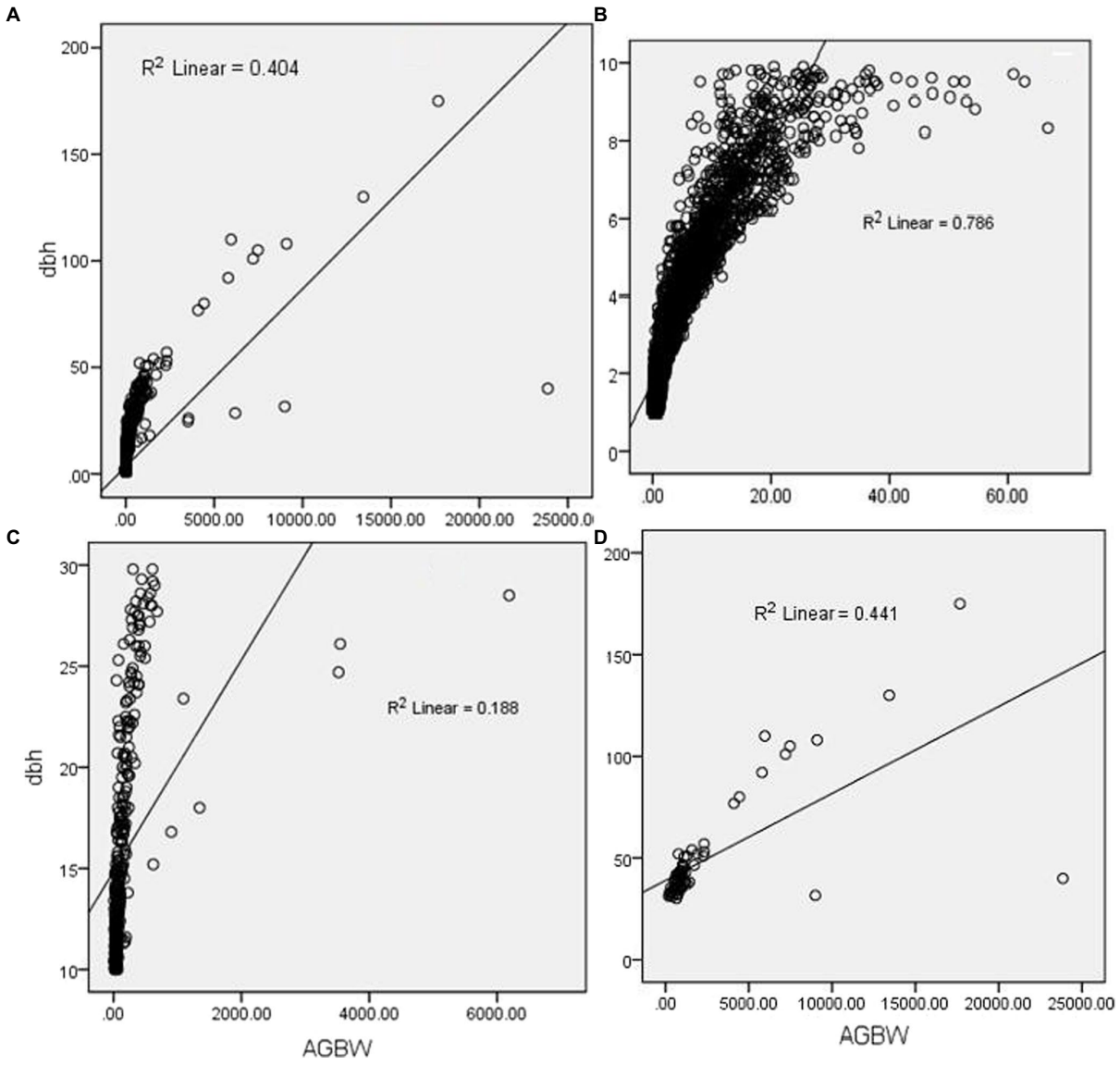

FIGURE 7
Relationship between DBH and above-ground dry weight; **(A)** (overall dataset); **(B)** (less than 10cm DBH dataset); **(C)** (10–30cm DBH dataset) and **(D)** (above 30cm DBH dataset).

in biomass between different DBH classes for different life forms reflect the differences in species composition, tree density, and basal area. Although the tree density was higher in species with DBH less than 10 cm, the biomass was lower than in species with larger DBH >10 cm. This is due to lower height and hence less accumulation of biomass. This was evident where large-sized trees recorded higher biomass accumulation and hence C gain.

It's possible that environmental and biological heterogeneity within the forest will make it difficult to generalize findings from one location to another. The results of this study occasionally differed significantly from those of Ong et al. (2004), where high tree density (10 cm DBH) contributed the least to below-ground and above-ground biomass. As a result of the lifetime of the main tree species, which provides outstanding contributions to their spectacular heights and vast biomass, studies have demonstrated that a few temperate rainforest locations have excessive above-ground biomass compared to their yearly net productivity (KoÈh et al., 2017). Dinghushan forest complex is a subtropical monsoon forest; trees have a more open canopy than rain forests, creating a dense, closed forest floor or a sub-tropical forest. Therefore, the high biomass accumulation in large-sized trees may be driven by their higher carbon use efficiency; hence large fractions of their photosynthetic products are used for accumulating biomass. Though tropical forests are often more productive, this may conflict with the fact that they utilize less carbon (DeLucia et al., 2007). The typical biomass turnover and mortality rates in tropical forests can be rather high, which prevents the buildup of living biomass (Maina and Li, 2021). Previous studies have indicated an above-ground biomass in the inland and coastal tropical dry evergreen forests of peninsular India to be estimated at 39.69 to 170.02 Mg/ha (Mani and Parthasarathy, 2017). This values were way too low if we compared our data where aboveground biomass ranged between 3.013 ± 0.07 kg/Tree and 2400.54 ± 510.4 kg/Tree depending

on DBH class. We must emphasize that the natural disturbance in this forest such as the 2018 typhoon destroyed the forest and affected its structure and functioning based on comparative data by Li et al. (2021). Although other studies have revealed the commercial role of biomass (Mani and Parthasarathy, 2017), the obtained biomass estimates from Dinghushan nature reserve is scientifically relevant for understanding the entire of ecosystem health and productivity, nutrient flow and energy balance. Our findings are important for assessing the contribution of each life form to the entire forest role in global carbon cycle. With combined effects of climate change, different life forms may respond differently to disturbances and this is an area that should be researched across succession stages in the nature reserve.

Furthermore, generalized forest biomass underestimates the contribution of each life form to the total forest carbon stock. Nevertheless, apart from the life forms with less than 30 cm DBH, our study site still has on average the greatest biomass stocks. Most earlier research (Comley and McGuinness, 2005) concentrated only on the above-ground biomass C stocks in tree species, neglecting to take into account the contributions made by C stocks of other life forms like shrubs, herbs, or even roots (below ground), as well as small diameter < 10 cm DBH tree individuals in tropical forest ecosystems. Our focus on assessing the C stocks and their allocation in different structural components between life forms provides a new front in understanding the general components and their contribution to the overall biomass accumulation for the entire ecosystem.

6. Conclusion

This is the first study to cluster the Dinghushan forest based on tree size class. Biomass (C stocks) is influenced by structural attributes (DBH, height) and diversity attributes (life forms). The dynamics of individual tree collectives can be used to explain why the observed forest bio- productivity dynamics occur over such vast areas. High biomass carbon stocks cause size distributions to shift in favor of trees with bigger DBH. The Dinghushan forest complex's C storage will be improved by maintaining big-sized trees and stand structures and continuing to preserve biodiversity. Although this study found a positive relationship between DBH and stand height (h), physical measurements of these parameters are time-consuming. Due to optical interference from nearby trees or rounded crown forms, it might be challenging to acquire a clear view of the treetop. Thus, measurement costs can be decreased while maintaining an acceptable degree of H accuracy by creating predictive models of H from DBH. The results help to highlight the regions in action plans that require additional attention for conservation and C stock improvement. We suggest managing forests to preserve existing big-diameter trees or those that may soon achieve large diameters as a straightforward method to preserve and possibly improve ecosystem services. Our study on biomass in four life forms in a forest plot ws based on data obtained after the typhoon destruction. These possess a limitation on wider application of our findings. Additionally, we did not consider biomass accumulation in relation to environmental variables within the nature reserve. Therefore, future studies could consider spatio-temporal variation in biomass in relation to environmental conditions.

Data availability statement

The original contributions presented in the study are included in the article/Supplementary material, further inquiries can be directed to the corresponding author.

Author contributions

YL and MN analyzed data and writing. LD and FH data process and writing. SL data collection and vegetation investigation. BM data process and writing. QZ data process. GC data collection. DZ experimental design. JL data process and writing support. ZM site maintenance. All authors contributed to the article and approved the submitted version.

Funding

This research was supported by the National Natural Science Foundation of China (Grant No. 31961143023); the National Key Research and Development Program of China (Grant No. 2021YFF0703905); the Strategic Priority Research Program of the Chinese Academy of Sciences (Grant No. XDA23080302); the National Science and Technology Basic Work Project (Grant No. 2015FY1103002); the Dinghushan Forest Ecosystem Positioning Research Station of the National Science and Technology Infrastructure Platform, the Chinese Ecosystem Research Network (CERN); and the Operation Service Project of the National Scientific Observation and Research Field Station of the Dinghushan Forest Ecosystem of Guangdong, the Ministry of Science and Technology of the People's Republic of China.

Conflict of interest

The authors declare that the research was conducted in the absence of any commercial or financial relationships that could be construed as a potential conflict of interest.

Publisher's note

Supplementary material

The Supplementary material for this article can be found online at: https://www.frontiersin.org/articles/10.3389/fevo.2023.1118175/full#supplementary-material

References

Comley, B. W. T., and McGuinness, K. A. (2005). Above- and below-ground biomass, and allometry, of four common northern Australian mangroves. *Aust. J. Bot.* 53, 431–436. doi: 10.1071/BT04162

Clough, B. F., Dixon, P., and Dalhaus, O. (1997). Allometric relationships for estimating biomass in multi-stemmed mangrove trees. *Australian Journal of Botany* 45, 1023–1031. doi: 10.1071/BT96075

DeLucia, E. H., Drake, J., Thomas, R. B., and Gonzalez-Meler, M. A. (2007). Forest carbon use efficiency: is respiration a constant fraction of gross primary production?. *Global Change Biology* 13, 1157–1167.

Gielen, B., and Ceulemans, R. (2001). The likely impact of rising atmospheric CO_2 on natural and managed Populus: a literature review. *Environ. Pollut.* 115, 335–358. doi: 10.1016/S0269-7491(01)00226-3

Gobakken, T., Lexerød, N. L., and Eid, T. (2008). A forest simulator for bioeconomic analyses based on models for individual trees. *Scand. J. For. Res.* 23, 250–265.

Guo, Q. (1999). Ecological comparisons between eastern Asia and North America: historical and geographical perspectives. *J. Biogeogr.* 26, 199–206. doi: 10.1046/j.1365-2699.1999.00290.x

Husch, B., Beers, T. W., and Kershaw Jr., J. A. (2002). *Forest Mensuration*. 4th edn. USA: John Wiley & Sons.

Kirui, B., Kairo, J. G., and Karachi, M. (2006). Allometric equations for estimating above ground biomassof *Rhizophora mucronata* Lamk. (Rhizophoraceae) mangroves at Gazi Bay, Kenya. Western Indian Ocean. *J. Mar. Sci.* 5, 27–34. doi: 10.4314/wiojms.v5i1.28496

KoÈh, M., Neupane, P. R., and Lotfiomran, N. (2017). The impact of tree age on biomass growth and carbon accumulation capacity: a retrospective analysis using tree ring data of three tropical tree species grown in natural forests of Suriname. *PLoS One* 12:e0181187. doi: 10.1371/journal.pone.0181187

Li, Y., Mwangi, B., Zhou, S., Liu, S., Zhang, Q., Liu, J., et al. (2021). Effects of typhoon Mangkhut on a monsoon Evergreen broad-leaved Forest Community in Dinghushan nature reserve, lower subtropical China. *Front. Ecol. Evol.* 9:692155. doi: 10.3389/fevo.2021.692155

Luo, T., Zhang, L., Zhu, H., Daly, C., Li, M., and Luo, J. (2009). Correlations between net primary productivity and foliar carbon isotope ratio across a Tibetan ecosystem transect. *Ecography* 32, 526–538. doi: 10.1111/j.1600-0587.2008.05735.x

Lutz, J. A., Furniss, T. J., Johnson, D. J., Davies, S. J., Allen, D., Alonso, A., et al. (2018). Global importance of large-diameter trees. *Glob. Ecol. Biogeogr.* 27, 849–864. doi: 10.1111/geb.12747

Maina, J. N., and Li, Y. (2021). Spatio-temporal variation in species diversity between plantation and secondary Forest of Kakamega tropical rain Forest in Kenya. *Ecol. Eng. Environ. Technol.* 5, 1–11. doi: 10.12912/27197050/139410

Mani, S., and Parthasarathy, N. (2017). Above-ground biomass estimation in ten tropical dry evergreen forest sites of peninsular India. *Biomass Bioenergy* 31, 284–290. doi: 10.1016/j.biombioe.2006.08.006

McGregor, I. R., Helcoski, R., Kunert, N., Tepley, A. J., Gonzalez-Akre, E. B., Herrmann, V., et al. (2021). Tree height and leaf drought tolerance traits shape growth responses across droughts in a temperate broadleaf forest. *New Phytol.* 231, 601–616. doi: 10.1111/nph.16996

Murali, K. S., Bhat, D. M., and Ravindranath, N. H. (2005). Biomass estimation equation for tropical deciduous and evergreen forests. *Int. J. Agric. Resour. Gov. Ecol.* 4, 81–92. doi: 10.1504/IJARGE.2005.006440

Ong, J. E., Gong, W. K., and Wong, C. H. (2004). Allometry and partitioning of mangrove, *Rhizophora apiculata*. *For. Ecol. Manag.* 188, 395–408. doi: 10.1016/j.foreco.2003.08.002

Shaver, G. R., Canadell, J., Chapin, F. S. III, Gurevitch, J., Harte, J., Henry, G., et al. (2000). Global warming and terrestrial ecosystems: a conceptual framework for analysis. *Bioscience* 50, 871–882. doi: 10.1641/0006-3568(2000)050[0871:GWATEA]2.0.CO;2

Shen, Y., Santiago, L. S., Ma, L., Guo-Jun, L., Ju-Yu, L., Hong-Lin, C., et al. (2013). Forest dynamics of a subtropical monsoon forest in Dinghushan, China: recruitment, mortality and the pace of community change. *J. Trop. Ecol.* 29, 131–145. doi: 10.1017/S0266467413000059

Sitch, S., Huntingford, C., Gedney, N., Levy, P. E., Lomas, M., Piao, S. L., et al. (2008). Evaluation of the terrestrial carbon cycle, future plant geography and climate-carbon cycle feedbacks using five Dynamic Global Vegetation Models (DGVMs). *Global change biology*. 14, 2015–2039. doi: 10.1111/j.1365-2486.2008.01626.x

Skovsgaard, J. P., and Vanclay, J. K. (2013). Forest site productivity: a review of spatial and temporal variability in natural site conditions. *Forestry* 86, 305–315. doi: 10.1093/forestry/cpt010

Weiner, J., and Thomas, S. C. (1986). Size variability and competition in plant monocultures. *Oikos* 47, 211–222. doi: 10.2307/3566048

Wu, X., Wang, X., Tang, Z., Shen, Z., Zheng, C., Xia, X., et al. (2015). The relationship between species richness and biomass changes from boreal to subtropical forests in China. *Ecography* 38:2015. doi: 10.1111/ecog.00940

Zhang, Q. (2011). *China Ecosystem Positioning Observation and Research Data set Forest Ecosystem Volume Guangdong Dinghushan Station: 1998–2008*. Beijing: China Agricultural Publishing House.

Zhou, G., Houlton, B. Z., Wang, W., Huang, W., Xiao, Y., Zhang, Q., et al. (2014). Substantial reorganization of China's tropical and subtropical forests: based on the permanent plots. *Glob. Chang. Biol.* 20, 240–250. doi: 10.1111/gcb.12385

Zhou, G. Y., Liu, S. G., Li, Z., Zhang, D. Q., Tang, X. L., Zhou, C. Y., et al. (2006). Old-growth forests can accumulate carbon in soils. *Science* 314:1417. doi: 10.1126/science.1130168

Zhou, G., Peng, C., Li, Y., Liu, S., Zhang, Q., Tang, X., et al. (2013). A climate change-induced threat to the ecological resilience of a subtropical monsoon evergreen broad-leaved forest in southern China. *Glob. Chang. Biol.* 19, 1197–1210. doi: 10.1111/gcb.12128

Zou, S., Zhou, G. Y., Zhang, Q. M., Shan, X. U., Xiong, X., Xia, Y. J., et al. (2018). Dynamics of community structure of monsoon evergreen broad-leaved forest in Dinghushan from 1992 to 2015. *J. Plant Ecol.* 42, 442–452.

frontiers | Frontiers in Ecology and Evolution

TYPE Original Research
PUBLISHED 16 March 2023
DOI 10.3389/fevo.2023.1122505

OPEN ACCESS

EDITED BY
Xiang Liu,
Lanzhou University,
China

REVIEWED BY
Yawen Lu,
Fudan University,
China
Fei Chen,
Nanjing University,
China

*CORRESPONDENCE
Xiaodan Tan
✉ tanxiaodan114143@163.com
Shurong Zhou
✉ zhshrong@hainanu.edu.cn

SPECIALTY SECTION
This article was submitted to Conservation and Restoration Ecology, a section of the journal Frontiers in Ecology and Evolution

RECEIVED 13 December 2022
ACCEPTED 28 February 2023
PUBLISHED 16 March 2023

CITATION
Qi Y, Sun X, Peng S, Tan X and Zhou S (2023) Effects of fertilization on soil nematode communities in an alpine meadow of Qinghai-Tibet plateau.
Front. Ecol. Evol. 11:1122505.
doi: 10.3389/fevo.2023.1122505

Effects of fertilization on soil nematode communities in an alpine meadow of Qinghai-Tibet plateau

Yanwen Qi, Xinhang Sun, Sichen Peng, Xiaodan Tan* and Shurong Zhou*

Key Laboratory of Genetics and Germplasm Innovation of Tropical Special Forest Trees and Ornamental Plants, Ministry of Education, College of Forestry, Hainan University, Haikou, China

Nitrogen and phosphorus are important nutrient elements for plants and underground organisms. The nematode is an important part of the soil food web. Although many studies have explored the effects of fertilization on soil nematode community structure, little is known about the response mechanism of the nematode community to fertilization. In this study, we investigated the diversity and functional diversity of soil nematode communities, as well as soil physicochemical properties, root functional traits, and plant richness. We explored the response mechanism of soil nematode communities to nitrogen and phosphorus fertilizer. Nitrogen fertilizer increased the abundance and richness of bacterivorous nematodes, while phosphorus fertilizer decreased the total abundance of bacterivorous nematodes. Meanwhile, the diversity of the nematode community was significantly affected by soil physicochemical properties and plant root functional traits. Therefore, our study revealed the effects of nitrogen and phosphorus fertilizer on soil nematode community diversity and functional diversity. Exploring the response mechanism of soil nematode communities to fertilization interference provides further evidence for the role of nematodes in maintaining the function of subsurface ecosystems.

KEYWORDS

alpine meadow, soil nematode, fertilization, functional diversity, species diversity, root traits

Introduction

Nematodes are *pseudocoelomata* belonging to the phylum Nematoda, the most abundant phylum in the kingdom Animalia (Lorenzen, 1994; van den Hoogen et al., 2019). Nematodes are widespread in terrestrial ecosystems, where they are noted for their diversity and hardiness (Yeates et al., 1993; Wu, 1999). These organisms are the most important component of the soil food web, and monitoring changes to nematode community composition is a useful tool for assessing soil quality (Liu et al., 2018). Soil nematodes are classified according to their feeding habits as bacterivores, fungivores, plant-feeders, or omnivore-predators (Wu, 1999). In recent years, atmospheric nitrogen deposition has emerged as an important global change factor (Vitousek et al., 1997; Reay et al., 2008). In many natural or semi-natural plant communities, nitrogen is often the

main factor limiting plant growth and development, and phosphorus is an essential nutrient for plant growth (Bardgett et al., 1998). Nitrogen addition can mitigate this limitation, inducing changes in the productivity of above-ground vegetation communities and preferentially promoting the growth of particular species, resulting in a loss of diversity (Bobbink et al., 2010). Moreover, nitrogen addition can also change plant community structure (Reich et al., 2006; Yang H. et al., 2012) and productivity, and affect plant root exudates and soil physicochemical properties (DeForest et al., 2004; Niu et al., 2010; Contosta et al., 2011). Human agricultural management has greatly altered the amount of nitrogen and phosphorus found in the soil (Villenave et al., 2010; Liu et al., 2012; Yang Y. et al., 2012).

Recently, the focus has shifted to the effects of fertilization on soil faunal communities (Qi et al., 2010; Zhang et al., 2022), especially on soil nematode communities. Fertilizer application is not only known to affect the structure and composition of vegetation but also belowground organisms and the soil environment has potential effects (Bardgett et al., 1998) and may alter nematode community structure. In grassland ecosystems, the long-term addition of nitrogen fertilizer reduces the number of plant-feeders (Ruan et al., 2012); the application of nitrogenous fertilizers is associated with a decline in the size of fungivore, plant-feeder, and omnivore-predator populations and an increase in the size of bacterivore populations (Murray et al., 2006; Zhang et al., 2022). Nitrogen fertilization is also associated with soil acidification, which may directly contribute to nematode population declines (Wei et al., 2012). Scientists have observed a negative correlation between plant-feeder and fungivore population sizes and levels of ammonium and nitrate after fertilization (Sarathchandra et al., 2001; Pey et al., 2014), suggesting that nitrogen fertilization has a direct effect on soil nematodes. The addition of phosphorus fertilizer increases the number of bacterivores (Qi et al., 2010) and overall soil nematode population, while at the same time altering organic matter decomposition pathways and reducing the number of rare species (Chen et al., 2014). In tropical rainforest, phosphorus supplementation significantly inhibited the total density of soil nematodes and the density of omnivore-predators nematodes (Zhao et al., 2014). In contrast, Rovira and Simon (1985) found that the addition of phosphorus fertilizer significantly increased the number of nematodes. There are few studies on the effects of mixed application of N and P fertilizer on soil nematode community. It has been found that in a long-term fertilization experiment for agricultural ecosystems in Heilongjiang Province, China, mixed application of N and P fertilizer increased the abundance of bacterivores nematodes (Pan et al., 2015).

The health of soil nematode populations is coupled to interactions with other animals, fungi, and bacteria, as well as to soil physicochemical properties and inter-root resource inputs from plants (Bongers and Ferris, 1999). Plants promote soil nematode diversity (Liu et al., 2012) by increasing the diversity of nematode food sources (Hooper et al., 2000; De Deyn et al., 2004). Changes in the soil environment or vegetation composition can directly or indirectly affect soil nematode communities (Wang et al., 2019; Chen et al., 2021). An increase in soil water content is associated with an increase in the number of plant-feeders (Ruan et al., 2012) and a decrease in the number of bacterivores and omnivore-predators (Chen et al., 2021); changes in the biomass of dominant plants in an ecosystem indirectly affects soil nematode abundance (Yeates, 1999; Wang et al., 2019).

With increasing scientific interest in soil nematodes and the development of functional ecology (Violle et al., 2007), researchers have begun to quantify the functional attributes of soil nematodes using traits such as individual size. The objective of these efforts is to understand how nematode functional diversity changes in response to environmental changes and their associated effects on ecosystem function (Tita et al., 1999; Pey et al., 2014). One metric for assessing functional attributes is community-weight mean (CWM), which is calculated as the weighted average of individual size and relative abundance of each genus. Wang et al. (2002) found that soil organic carbon, microbial biomass, and plant tissues provided food resources for soil nematodes, contributing to nematode growth and overall size. Recent work found that increasing soil nutrient concentrations by applying fertilizers increased the length of individual nematodes (Liu et al., 2015). When soil organic matter and total nitrogen content are higher, food resources for larger nematodes increase, thereby increasing CWM (Liu et al., 2015; Andriuzzi and Wall, 2018). In contrast, phosphorus limitation favors the survival of smaller soil animals and, as such, phosphorus content is positively correlated with community level size (Mulder and Elser, 2009). Consistent with this finding, researchers found that small individual nematodes have a better survival rate in gully bottoms with lower phosphorus levels in alpine meadow ecosystems (Wang and Niu, 2020).

The Qinghai-Tibet Plateau alpine meadow is an important grassland ecosystem in China (Du et al., 2003), and numerous studies have investigated the effects of fertilization on plant communities and soil factors in this ecosystem (Yang Z. et al., 2012). A recent experiment in alpine meadows on the Tibetan plateau did not find significant changes to nematode communities resulting from long-term nitrogen and phosphorus fertilization (Andriuzzi and Wall, 2018). However, little research has been conducted on the effects of fertilizer application on the functional diversity of soil nematode communities in this ecosystem. It is unclear whether the effect of fertilization on the nematode community is due to changes in the soil microenvironment or plant community composition, and there are few studies on the interaction between plants and nematodes. In this study, we conducted an experiment in alpine meadows on the Tibetan Plateau were continuously fertilized for 4 years to investigate the effects of nitrogen and phosphorus addition on soil nematode diversity. CWM was used as an indicator of soil nematode response to fertilization. We also investigated the effects of aboveground vegetation, soil physicochemical properties, and plant root characteristics on soil nematode communities and the mechanisms of fertilization on nematode communities. We hypothesized that (1) fertilization reduces soil nematode abundance and the species richness of aboveground vegetation; (2) fertilization increases CWM values of the individual size of soil nematode communities; and (3) fertilization affects soil nematode communities by changing plant community structure.

Materials and methods

Study site and experimental design

The study was conducted at the Haibei Alpine Meadow Ecosystem Open Experimental Station of the Chinese Academy of Sciences in Menyuan County, Qinghai Province, in the northeastern part of the Tibetan Plateau (101°12′–101°23′, 37°29′–37°45′). The area has a plateau continental climate with damp and rainy summers and cold and dry winters, with an average altitude of 3,215 m, an average annual temperature of −1.2°C, and annual precipitation of 489 mm. Precipitation occurs mainly between May and September (Wang et al., 2012). The plant community in this typical alpine meadow is dominated mainly by Poaceae, Asteraceae, and members of the buttercup family, such as silver lotus (*Anemone obtusiloba*), sheep grass (*Elymus nutans*), big leaf gentian (*Gentiana macrophylla*), yellow flower Poaannua, fern (*Potentilla bifurca*), and black snowdrop (*Saussurea nigrescens*) (Liu et al., 2020). The soils are thin with high organic matter content but low effective phosphorus and nitrogen content; thus, plant communities in this area are limited by both nitrogen and phosphorus (Niu et al., 2016).

Fertilization experiments began in 2018 in sample plots in the study area. Four fertilization treatments were randomly distributed among six blocks arranged across the sample plots, with six replicates of each treatment and a 3 m buffer interval between each block. Each sample square was 3 × 3 m in size, with a 2 m distance separating each square. A 0.5 m × 0.5 m fixed sample square in the middle of each 3x3m square was used to assess plant cover and abundance. There were four treatments in this study: blank control (CK), phosphorus fertilizer (P, added amount: 10 g m^{-2} $year^{-1}$), nitrogen fertilizer (N, added amount: 10 g m^{-2} $year^{-1}$), and nitrogen and phosphorus fertilizer applied together (NP, N: 10 g m^{-2} $year^{-1}$, P: 10 g m^{-2} $year^{-1}$) (Liu et al., 2020). Fertilization treatments were applied every June.

Sample collection

Sampling was conducted at the end of August 2021 after 4 years of fertilization treatments. Plants were at the time of sampling. A 0.5 m × 0.5 m area was randomly selected within the lower left 1/4 of the sample plot for plant species identification and counting. Above-ground plant parts were cut, sorted, and taken to the laboratory, where they were dried at 65°C before weighing.

Soil and root samples were collected and analyzed in early September 2021. Soil samples were taken from each 3 m × 3 m treatment sample square with a 4-cm diameter soil auger, using the five-point method to bore five holes 15 cm deep. Each set of five samples was mixed into a single sample and placed into a self-sealing bag, after which it was labeled and stored at 4°C during transit to the laboratory. In the laboratory, a 2 mm soil sieve was used to remove debris and sort out plant roots in the soil. Samples were divided into 2 parts: one portion was stored at 4°C for 1 day until soil nematodes could be extracted, and the other one was used to characterize soil physicochemical properties.

Measurement of plant root functional traits

Sorted roots were gently washed with deionized water to remove attached soil and other residues, wrapped in plastic wrap and tin foil and refrigerated at 1°C. Root samples were scanned and imaged (Winrhizo, Regent Instruments, Inc. Nepean, Ontario, Canada) to determine total root length (Length), total root volume (Root Volume), and total root surface area (Surf Area). Specific root area (SRA: root length per unit weight), root tissue density (RTD), total root biomass (Root biomass), specific root length (SRL), and root length density (RLD) were calculated from root dry weights (Freschet et al., 2021).

Physical and chemical soil properties

10 g of soil was placed in an aluminum box and dried at 105°C for 72 h to determine soil moisture content (SM). Soil pH was determined using a pH analyzer (meter-s210 Seven Compact™, Switzerland) with a 1:2 ratio of soil to water. Soil total nitrogen (TN) was determined by the semi-Kaeschner method (Sparks et al., 1996), soil total phosphorus (TP) by the sulfuric acid-perchloric acid digestion-molybdenum antimony anti-colorimetric method, soil available phosphorus (P) by the sodium bicarbonate leaching-molybdenum antimony anti-colorimetric method, and soil organic carbon (SOC) by the walker-black method (Nelson and Sommers, 1982). Soil ammonium (NH_4^+) and soil nitrate (NO_3^-) were determined by the indophenol blue colorimetric method (Dorich and Nelson, 1983) and salicylate colorimetric method (Yang et al., 1998), respectively.

Isolation, identification, and measurement of soil nematodes

Soil nematodes were isolated using a modified Bellman funnel method (Liu et al., 2015). The soil was stored in a refrigerator at 4°C, after which a 50 g sample was taken and isolated for 48 h before being fixed and filmed with glycerol. Head and tail morphology were used to sort nematodes into genera, after which nematodes were counted and photographed under a compound microscope (Olympus BX53 microscope at 10–1,000×). Nematodes were identified using the Soil Fauna of China Retrieval Atlas (Yin, 1998) and the Study of Freshwater and Soil Nematodes in China (Wu, 1999).

The number of individual nematodes was converted to bars/100 g of dry soil. When the number of isolated nematodes was less than 100, all nematodes were identified; if the number was greater than 100, 100 individuals were randomly selected. The nematodes were classified into four groups according to their feeding characteristics: bacterivores, fungivores, plant-feeders, and omnivore-predators (Bongers and Bongers, 1998).

For each sample, the overall size was calculated by summing the sizes of all identified nematodes. The relative abundance of a genus was calculated as the ratio of the abundance of a genus to the total abundance of nematodes in a sample. Community-weighted mean (CWM) was calculated by weighting the average body size to relative diversity. The calculation of the cluster

individual size weighted mean is based on the equation presented by Liu et al. (2015):

$$\mathrm{CWM} = \sum_{i=1}^{N} P_i X_i$$

where N represents the number of nematode genera, X_i represents the mean body size value for genus i; P_i represents the relative abundance of genus i.

The body type characteristics of soil nematodes were determined by Digimizer software. The nematode body size (V) was calculated using the following equation:

$$\mathrm{V} = \left(\mathrm{L} \times \mathrm{D}^2\right) / 1.7$$

where V represents the volume of each nematode; L represents the body length of each nematode; D represents the maximum body width of each nematode, and 1.7 is a constant.

Statistical analysis

Here, we assess how soil nematode diversity is influenced by changes in soil physicochemical properties and plant communities occurring in response to nitrogen and phosphorus fertilization. Species richness was calculated from plant community data; Soil physicochemical properties (e.g., soil pH, soil organic carbon, total nitrogen, total phosphorus, ammonium nitrogen, nitrate nitrogen, and available phosphorus) were measured from soil samples; Plant root traits were determined from subsurface sections.

At the community level, nematode abundance, functional group abundance, genus richness, and Shannon diversity were calculated. CWM was calculated using individual body length and body width data. This index was used to better explain the response of nematode communities to nitrogen and phosphorus additions. Through the analysis of different functional groups of nematodes, the changes in the structure and function of the soil food web were studied, to evaluate the response of the soil food web to environmental disturbance.

A linear mixed-effects model and two-factor ANOVA were used to analyze changes to soil physicochemical factors, root functional traits, plant species richness, soil nematode diversity, and each nematode functional group. Principal component analysis (PCA) was used to standardize the soil physicochemically and root functional trait variables, and the respective first axis principal component data were extracted and recorded as "SoilPC1" and "RootPC1." SoilPC1 and RootPC1 were then used to analyze the effects of soil physicochemical properties and root functional traits on soil nematode diversity (i.e., total abundance, abundance, Shannon diversity, Simpson diversity, and evenness) and functional diversity (i.e., CWM values dispersion based on body size). Simple linear regression analysis was used to investigate the correlation between soil nematode diversity and functional diversity and "SoilPC1," "RootPC1," and plant species richness using the "lm" function in R. Finally, structural equation modeling (SEM) was used to explore the pathways by which fertilizer application influences soil nematode communities, with "SoilPC1," "RootPC1," and plant species richness as potential variables.

All data were analyzed using R software version 4.1.2. The "FD" package was used to calculate CWM and FDis based on nematode size (Laliberté et al., 2014). The "vegan" package was used to calculate Shannon diversity, Simpson diversity, and evenness metrics for nematodes. PCA was also conducted using the "vegan" package (Oksanen, 2016). The "lme" function in the "lme4" package was used to calculate linear mixed effects (Bates et al., 2015). Finally, the "ggplot2" package was used for plotting, and the "piecewiseSEM" package was used for SEM (Lefcheck, 2016).

Results

The influence of fertilizer application on nematode and plant diversity

Fertilizer application had different effects on soil nematode diversity and functional diversity. Shannon diversity, Simpson diversity, and evenness increased significantly when only nitrogen (N) fertilizer was applied. When only phosphorus (P) fertilizer was added, the individual abundance of soil nematodes was reduced significantly and the functional richness index (FRic) of nematode communities increased significantly. Nematode abundance, Shannon diversity, Simpson diversity, community functional dispersion (FDis), and Rao's quadratic entropy index (RaoQ) decreased significantly with the co-application of nitrogen and phosphorus (NP) fertilizers. Moreover, the co-application of NP fertilizer significantly reduced above-ground plant species richness (Table 1). This indicates that the addition of different chemical fertilizers has different effects on the soil nematode community. Soil nematode diversity was greater in all cases of N-only fertilization compared to P-only fertilization, suggesting that phosphorus deposition may be a key factor affecting nematode communities.

The influence of fertilizer application on soil physicochemical properties and root functional traits

Fertilization treatments were observed to affect the subsurface soil environment and plant roots. Under N addition, soil pH decreased significantly and nitrate (NO_3^-) content increased significantly, but the effect of N addition on root traits was not significant (Table 2). Under P addition, soil effective phosphorus content and total soil phosphorus (TP) content increased significantly; fine root dry weight (FM) and root length density (RLD) values of the underground root fraction decreased significantly (Table 2). However, the effect of fertilization on soil physicochemical factors and root traits was not significant under the NP treatment (Table 2). These changes indicate that soil physicochemical factors were more sensitive to the addition of either N or P fertilizers compared to NP treatment. Changes to root system functional properties were stronger for P treatment than for N or NP.

10.3389/fevo.2023.1122505

TABLE 1 Effect of fertilizer application on soil nematode and plant diversity.

	Differences between treatments with blanks as reference		
	N	P	N:P
Nematode diversity			
Nematode richness	4.83	−2.33	**−10.50***
Nematode abundance	−38.74	**−568.44***	−55.98
Shannon Wiener	**0.35[a]**	0.04	**−0.60***
Simpson	**0.04***	0.01	**−0.06***
Community evenness (E)	**0.04[a]**	0.02	−0.01
Functional diversity of soil nematode communities			
CWM for body-size	0.13	1.25	−1.45
FRic	0.03	**1.38[a]**	−1.80
FEve	−0.002	−0.07	0.13
FDiv	0.04	−0.02	−0.04
FDis	0.06	0.07	**−0.24***
RaoQ	0.06	0.37	**−0.73[a]**
Plant richness	−3.00	−0.83	**−9.33****

A linear mixed-effects model was used to test the effect of fertilization treatments on soil nematode and plant diversity (numbers are the slope values of the linear mixed-effects model. Blank was used as a control, positive and negative values indicate whether the fertilization conditions increased or decreased relative to other fertilization conditions in control, ***: $p < 0.001$; **: $p < 0.01$; *: $p < 0.05$; a: $p < 0.1$). FRic, functional richness index; FEve, functional evenness index; FDiv, functional divergence index; FDis, functional dispersion index; RaoQ, Rao's quadratic entropy index. The bold numbers are indicate significant effects.

TABLE 2 Effect of N and P fertilizer addition and their interaction on subsurface soil environmental factors and functional attributes of the root system.

	Differences between study sites with gaps as reference		
	N	P	N:P
Soil physicochemical index			
Soil available P (AP)	−0.18	**41.17*****	−13.82
Soil pH (pH)	**−0.17***	−0.10	0.17
Soil ammonium (NH_4^+)	0.09	−0.91	0.29
Soil nitrate (NO_3^-)	**10.80***	2.68	−9.14
Soil organic matter (SOC)	0.21	−0.17	−0.18
Soil total N (TN)	0.02	−0.02	−0.02
Soil total C (TC)	0.25	−0.25	−0.14
Soil total P (TP)	0.03	**0.15*****	−0.01
Soil moisture content (SM)	0.02	−0.03	−0.03
Root system functional properties			
The dry weight of fine roots (FM)	0.002	**−0.008[a]**	−0.004
Root biomass	−0.99	−1.06	2.45
Total root length (Length)	−4,456	−1931	13,779
Total root volume (RootVolume)	−1.83	−0.51	6.38
Total root surface area (SurfArea)	−330.7	−116.5	1062.4
Specific root length (SRL)	93.65	498.43	240.21
Specific root area (SRA)	8.63	50.26	13.44
Root tissue density (RTD)	−17.74	−7.69	54.85
Root length density (RLD)	−0.01	**−0.06[a]**	−0.01

A linear mixed-effects model was used to test the effects of fertilization treatments on the subsurface soil environment and functional attributes of the root system (numbers are slope values of the linear mixed-effects model. Positive and negative values indicate whether the fertilization conditions increased or decreased relative to other fertilization conditions in control, ***: $p < 0.001$; **: $p < 0.01$; *: $p < 0.05$; a: $p < 0.1$). The bold numbers are indicate significant effects.

Effect of fertilizer application on nematode functional groups

Fertilizer application also affected soil nematodes of different functional groups. Bacterivore richness and abundance increased significantly under the N application and decreased significantly under the NP application (Table 3). In the P treatment, only the abundance of plant-feeder nematodes was reduced significantly (Table 3). The abundance and richness of omnivore-predator nematodes decreased significantly in the NP treatment (Table 3). We found that fertilization did not significantly affect soil nematode volume in any group. This indicates that N fertilization favored the growth of bacterivore nematode communities, P fertilization inhibited the survival of plant-feeder nematodes, and NP fertilization was determinantal to the development of soil nematode communities (Table 3).

Effects of soil physicochemical properties and root traits on soil nematode diversity

Principal component analysis (PCA) was performed on soil physicochemical properties and root characteristics. Results showed a significant positive correlation between soil physicochemical properties, nematode species richness, Shannon diversity, Simpson diversity, and FDis (Figure 1A; Supplementary Figure S1). CWM and nematode community evenness (E) were not correlated to soil physicochemical properties (Figure 1A). There was a significant negative correlation between root characteristics, Shannon diversity, and Simpson diversity (Figure 1B; Supplementary Figure S2). Plant species richness was negatively correlated to E and root characteristics (Supplementary Figure S3).

Structural equation modeling (SEM) analysis was performed to illuminate the relative importance of relationships between measured variables. The model included plant community richness, root functional attributes, and soil nematode community variables. NP fertilization significantly reduced plant community richness, and soil

10.3389/fevo.2023.1122505

TABLE 3 Effect of fertilization treatments on soil nematode communities of each functional group.

	Differences between study sites with gaps as reference		
	N	P	N:P
Different functional groups of nematodes			
Abundance of bacterivores	**88.35****	−30.20	**−78.81**[a]
Abundance of fungivores	3.12	−24.17	−28.31
Abundance of plant-feeders	−18.33	**−104.26***	−39.54
Abundance of omnivores-predators	9.87	−7.80	**−22.78**[a]
Richness of bacterivores	**4.17****	0.33	**−4.17***
Richness of fungivores	−0.83	−0.83	−0.33
Richness of plant-feeders	0.83	−1.67	−3.00
Richness of omnivores-predators	1.17	0.50	**−3.00***
Bacterivores volume	1513.00	2205.00	−3,284
Fungivores volume	899.72	3184.58	−2789.00
Plant-feeders volume	243.90	1727.70	−1078.30
Omnivores-predators volume	−13327.82	3363.50	−2164.10

A linear mixed-effects model was used to test the effect of fertilization treatments on soil nematodes for each functional taxon (numbers are slope values of the linear mixed-effects model. Using blank as a control, positive and negative values indicate whether the fertilization conditions increased or decreased relative to other fertilization conditions of control, ***: $p < 0.001$; **: $p < 0.01$; *: $p < 0.05$; a: $p < 0.1$). The bold numbers are indicate significant effects.

physicochemical properties; N and P treatments had a direct effect on soil physicochemical properties (Figures 2A,B). P fertilization directly resulted in lower nematode abundance (Figure 2A). NP treatment indirectly affected nematode species richness by altering soil physicochemical properties (Figure 2B). Therefore, we concluded that P fertilization exerts a direct effect on soil nematode communities. N and P fertilization had no significant effect on CWM (Table 1). In summary, we found that P fertilization had a direct effect on soil nematode abundance and that NP fertilization had an indirect effect on nematode species richness.

Discussion

The influence of fertilization on soil nematode diversity

Fertilization significantly altered the soil nitrogen and phosphorus levels. This experiment found that the addition of N significantly altered soil nitrate N content and pH; P treatment significantly altered soil effective P and total soil P, while the mixed addition of N and P fertilizer had no effect on soil physical and chemical properties. The effects of the treatment type on soil nematodes were different from their effects on physicochemical properties. N fertilization significantly increased Shannon diversity, Simpson diversity, and E, which is consistent with previous work conducted in Inner Mongolia (Wang et al., 2019).

These results corroborated our first hypothesis and found that P fertilization greatly reduced soil nematode abundance and that the interaction of N and P fertilizers significantly reduced soil nematode

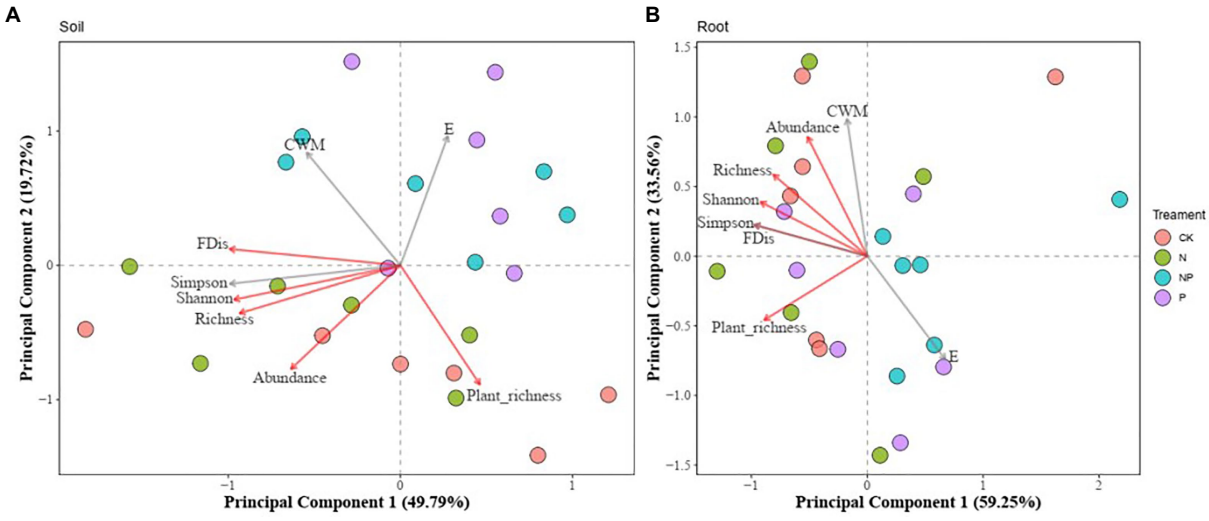

FIGURE 1
Principal component analysis (PCA). Relationship between soil nematode diversity and soil physicochemical properties **(A)** and plant root functional traits **(B)** under fertilization treatments. CWM, community means based on nematode body size; FDis, Functional dispersion index; Abundance, Abundance of soil nematodes in 100g of dry soil; Richness, Soil nematode richness; E, Community evenness; Plant_ richness, Plant species richness. Soil physical and chemical properties and root functional traits were extracted separately from the first principal component (PC1) after dimensionality reduction by principal component analysis. The indicators measured for root functional traits were RTD, Root tissue density; RLD, Root length density; FM, Fine root dry weight; Length, Total root length; RootVolume, Total root volume; SRL, Specific root length; SRA, Specific root area; SurfArea, Total root surface area. Soil physical and chemical properties were measured as follows: SOC, Soil organic carbon; TN, Total soil nitrogen; TC, Total soil carbon; TP, Total soil phosphorus; P, Soil available phosphorus; pH, Soil pH; NH_4^+, Soil ammonium; NO_3^-, Soil nitrate. Variables corresponding to the red arrows indicate that the effect on soil or root traits is significant. Gray arrows indicate that the effects are not significant.

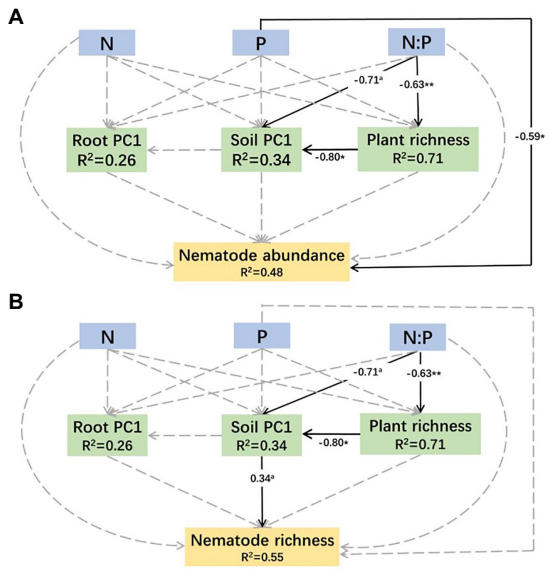

FIGURE 2
SEM analysis showed the interaction between plant and soil and its effects on **(A)** soil nematode abundance (AIC=60, Fisher's C=0, p=1) and **(B)** richness (AIC=60, Fisher's C=0, p=1). Roots and soils are represented by principal component analysis (PCA) of the reduced dimensional first principal component, respectively. Root functional property variables include all indices measured, and soil physicochemical property variables include so-measured soil physicochemical indicators. Boxes in the model represent individual variables; solid arrows represent significant effects (p<0.1); dashed arrows represent non-significant effects (p>0.1); numbers on the arrows represent path coefficients. R^2 values represent the variance of response variables explained by other variables. ***: p<0.001; **: p<0.01; *: p<0.05; a: p<0.1.

richness. The addition of P fertilizer significantly decreased overall nematode abundance, consistent with work done in a low-lying paddy field located on the Ivory Coast of Africa and a tropical forest (Zhao et al., 2014; Čerevková et al., 2017). However, other studies have shown that fertilization can have a positive effect on nematodes and improve overall species richness (Sarathchandra et al., 2001). One of the reasons for this inconsistency is likely due to the amount of fertilizer applied. In the study by Sarathchandra et al., the amount of fertilizer applied was 20 g per m ^{2} N and 20 g per m ^{2} P, and our application amount of N and P fertilizer was only 10 g per m ^{2}. Most of the fertilizer was probably taken up by the plants, and the remaining amount was insufficient to change the soil nematode community. Moreover, the effects of N and P fertilization on soil physicochemical properties are also important. N application lowers soil pH and increases soil nitrate N content, and P application increases the content of effective and total phosphorus; the decrease in soil pH leads to soil acidification, which contributes to the decreasing nematode populations because soil acidification destroys optimal growth conditions, and some soil nematodes are sensitive to changes in the soil environment (Li et al., 2013), especially large nematodes (Liang et al., 2009). Furthermore, it has been shown that P fertilization is toxic to nematodes and can restrict their reproductive ability (Hu et al., 2017). Here, we found that N fertilization increased the abundance and richness of bacterivores, similar to findings by other researchers (Hu et al., 2017). Hu et al. found that soil microbial biomass, C and N increased significantly, increasing the amount of food available for bacterivore nematodes. Consistent with these findings, PCA revealed that soil N and organic matter content increased, positively impacting bacterivores (Figure 1A).

In contrast, a study conducted in a New Zealand pasture found that P additions significantly increased fungivore abundance (Chen et al., 2014), while other work found that P fertilization resulted in slight increases in bacterivore and omnivore-predator populations as well as soil nematode species richness (Sarathchandra et al., 2001). Bottom-up control mechanisms are widely present in subsurface ecosystems (Neher, 2010), and P input changes the composition and functional characteristics of the soil microbial community by promoting the rapid growth of vegetation (Leff et al., 2015). In this study, structural equation modeling revealed that P fertilization had a direct negative effect on soil nematode abundance (Figure 2A), which was inconsistent with hypothesis 3. Other nematode studies found that the addition of P fertilizer under N-enriched conditions significantly increased the functional variables in soil nematode communities, which attenuated the positive effect of P (Zhao et al., 2014). In contrast, our experiments found that NP application significantly reduced nematode richness and functional diversity, and P attenuated the positive effect of N on soil nematode communities.

At the same time, fertilization reduces plant species richness. Numerous studies have shown that fertilizer application increases above-ground plant biomass, increasing canopy cover. This results in decreased light for non-grass vegetation and legumes, ultimately leading to the loss of these species (Qi, 2013). Previous studies have found that fertilization alters soil nematode community structure by decreasing plant species diversity. However, our results differ in that fertilization did not affect the functional traits of plant roots (Figure 2). The reduction in nematode abundance under P fertilization was mostly due to a decrease in the number of plant-feeders (Table 3); this is probably because plant-feeders subsist on root secretions, and P fertilization reduced fine root dry weight and root tissue density and had an indirect negative effect on root functional attributes by reducing plant species diversity. Thus, changes in root functional attributes may affect root exudation, thereby affecting the population of plant-feeders. An additional explanation may be that the loss of plant species that results from fertilization causes changes in root biomass (Cortois et al., 2017), which in turn reduces plant-feeder nematode populations.

Roots play a vital role in ecosystems and provide habitats for many underground organisms (Bardgett and van der Putten, 2014). Thin roots provide more space for herbivores and predators to survive in the soil (Legay et al., 2020). The greater the root length, the more beneficial it is to microbial life, and thus to the microfauna living there (Picot et al., 2019). Second, there is a strong selectivity of root secretions to rhizosphere microorganisms, and the addition of nitrogen has a significant effect on the rhizosphere bacterial community (Wang et al., 2022). Although we did not find any significant effect of fertilization on the root functional traits, research based on root characteristics can help us to better understand the soil nematode community.

The influence of fertilization on plant functional diversity

To improve investigation into the relationship between soil nematode communities and environmental changes and ecosystem functions, nematode body size indicators are increasingly used as a

measure of functional diversity in soil systems (Mulder et al., 2009). Indicators such as CWM, which are based on body size, are more reliable than those based on abundance to explain the response of soil nematode communities to fertilization (Liu et al., 2015). Of the large variation in body size among different genera of nematodes, CWM was introduced to facilitate the description of soil nematode communities (Niu et al., 2014). Work in rice fields found that CWM values of soil nematode communities were positively correlated with soil nutrients, and could serve as a sensitive indicator of nematode community response to fertilizer application (Liu et al., 2015). Research by Christian et al. found that low P soils were more favorable for the survival of small-bodied soil animals, and high P soils supported larger-bodied soil animals at higher trophic levels; this was because increased P content improved the quality of food for small soil animals, who were previously limited by their food's stoichiometric ratio and also improved the quality of organic matter in the soil, Together, these factors increased the nutrient transfer rate among soil animals (Mulder and Elser, 2009). However, some work suggests that in areas with high P content, small nematodes such as bacterivores, fungivores, and plant-feeders can survive better due to higher microbial diversity (Zhao et al., 2020). Other studies have also found that functional diversity improves as soil N and soil organic matter increases (van den Hoogen et al., 2019) and results in increasing size of individual nematodes, indicating that nitrogen fertilization favors the survival of large-bodied nematodes (Liu et al., 2015; Andriuzzi and Wall, 2018).

Here, we found that the CWM of soil nematode communities did not respond significantly to fertilization, which was not consistent with hypothesis 2. Changes in nematode communities take place over long periods, and 4 years of fertilization may not be long enough to induce substantial changes in nematode community structure. As such, we need longer-term fertilization experiments to understand soil nematode community dynamics under such conditions. Additionally, further investigation is needed to determine how fertilization affects soil nematodes at different trophic levels.

Conclusion

In alpine meadow ecosystems of the Tibetan Plateau, although N fertilization increased the abundance and richness of bacterivore nematodes, the abundance and richness of both bacterivore and omnivore-predator nematodes decreased under NP application, suggesting that P fertilization has a greater impact on soil nematode communities than N fertilization does. Here, we use soil physicochemical properties and root functional traits to understand how fertilization alters nematode communities; however, we did not investigate how changes in plant root secretions and soil microorganisms resulting from fertilization influence nematode communities. Longer-term studies examining how fertilization alters subsurface biological communities and abiotic factors are needed. Moreover, the effects of fertilization, the soil environment, and plant root systems are intertwined. We must further investigate how interactions between these factors alter soil nematode communities in fertilized soils to provide a scientific basis for the management of alpine meadows in the Tibetan Plateau.

Data availability statement

The raw data supporting the conclusions of this article will be made available by the authors, without undue reservation.

Author contributions

SZ designed the experiment. SZ and YQ conceived the research. YQ, XS, XT, and SP collected the data. YQ and XT analyzed the data. YQ wrote the manuscript and all authors contributed to revisions. All authors approved the final manuscript.

Funding

This study was supported by the National Natural Science Foundation of China (grant no. 31830009) and the Fundamental Research Funds in Hainan University (KYQD (ZR)-20081).

Conflict of interest

The authors declare that the research was conducted in the absence of any commercial or financial relationships that could be construed as a potential conflict of interest.

Publisher's note

Supplementary material

The Supplementary material for this article can be found online at: https://www.frontiersin.org/articles/10.3389/fevo.2023.1122505/full#supplementary-material

References

Andriuzzi, W. S., and Wall, D. H. (2018). Grazing and resource availability control soil nematode body size and abundance-mass relationship in semi-arid grassland. *J. Anim. Ecol.* 87, 1407–1417. doi: 10.1111/1365-2656.12858

Bardgett, R. D., and Van Der Putten, W. H. (2014). Belowground biodiversity and ecosystem functioning. *Nature* 515, 505–511. doi: 10.1038/nature13855

Bardgett, R. D., Wardle, D. A., and Yeates, G. W. (1998). Linking above-ground and below-ground interactions: how plant responses to foliar herbivory influence soil organisms. *Soil Biol. Biochem.* 30, 1867–1878. doi: 10.1016/S0038-0717(98)00069-8

Bates, D., Mächler, M., Bolker, B., and Walker, S. (2015). Fitting linear mixed-effects models using lme4. *J. Stat. Softw.* 67, 1–48. doi: 10.18637/jss.v067.i01

Bobbink, R., Hicks, K., Galloway, J., Spranger, T., Alkemade, R., Ashmore, M., et al. (2010). Global assessment of nitrogen deposition effects on terrestrial plant diversity: a synthesis. *Ecol. Appl.* 20, 30–59. doi: 10.1890/08-1140.1

Bongers, T., and Bongers, M. (1998). Functional diversity of nematodes. *Appl. Soil Ecol.* 10, 239–251. doi: 10.1016/S0929-1393(98)00123-1

Bongers, T., and Ferris, H. (1999). Nematode community structure as a bioindicator in environmental monitoring. *Trends Ecol. Evol.* 14, 224–228. doi: 10.1016/S0169-5347(98)01583-3

Čerevková, A., Miklisová, D., and Cagáň, Ľ. (2017). Effects of experimental insecticide applications and season on soil nematode communities in a maize field. *Crop Prot.* 92, 1–15. doi: 10.1016/j.cropro.2016.10.007

Chen, X., Daniell, T. J., Neilson, R., O'Flaherty, V., and Griffiths, B. S. (2014). Microbial and microfaunal communities in phosphorus limited, grazed grassland change composition but maintain homeostatic nutrient stoichiometry. *Soil Biol. Biochem.* 75, 94–101. doi: 10.1016/j.soilbio.2014.03.024

Chen, H., Luo, S., Li, G., Jiang, W., Qi, W., Hu, J., et al. (2021). Large-scale patterns of soil nematodes across grasslands on the Tibetan plateau: relationships with climate, soil and plants. *Diversity* 13:369. doi: 10.3390/d13080369

Contosta, A. R., Frey, S. D., and Cooper, A. B. (2011). Seasonal dynamics of soil respiration and N mineralization in chronically warmed and fertilized soils. *Ecosphere* 2:art36. doi: 10.1890/ES10-00133.1

Cortois, R., Veen, G. F. C., Duyts, H., Abbas, M., Strecker, T., Kostenko, O., et al. (2017). Possible mechanisms underlying abundance and diversity responses of nematode communities to plant diversity. *Ecosphere* 8:e01719. doi: 10.1002/ecs2.1719

De Deyn, G. B., Raaijmakers, C. E., Van Ruijven, J., Berendse, F., and Van Der Putten, W. H. (2004). Plant species identity and diversity effects on different trophic levels of nematodes in the soil food web. *Oikos* 106, 576–586. doi: 10.1111/j.0030-1299.2004.13265.x

DeForest, J. L., Zak, D. R., Pregitzer, K. S., and Burton, A. J. (2004). Atmospheric nitrate deposition, microbial community composition, and enzyme activity in northern hardwood forests. *Soil Sci. Soc. Am. J.* 68, 132–138. doi: 10.2136/sssaj2004.1320

Dorich, R. A., and Nelson, D. W. (1983). Direct colorimetric measurement of ammonium in potassium chloride extracts of soils. *Soil Sci. Soc. Am. J.* 47, 833–836. doi: 10.2136/sssaj1983.03615995004700040042x

Du, G.-Z., Qin, G.-L., Li, Z.-Z., Liu, Z.-H., and Dong, G.-S. (2003). Relationship between species richness and productivity in an alpine Meadow Plant community. *Chin. J. Plant Ecol.* 27, 125–132. doi: 10.17521/cjpe.2003.0019

Freschet, G. T., Pagès, L., Iversen, C. M., Comas, L. H., Rewald, B., Roumet, C., et al. (2021). A starting guide to root ecology: strengthening ecological concepts and standardising root classification, sampling, processing and trait measurements. *New Phytol.* 232, 973–1122. doi: 10.1111/nph.17572

Hooper, D. U., Bignell, D. E., Brown, V. K., Brussard, L., Mark Dangerfield, J., Wall, D. H., et al. (2000). Interactions between aboveground and belowground biodiversity in terrestrial ecosystems: patterns, mechanisms, and feedbacks. *Bioscience* 50:1049. doi: 10.1641/00063568(2000)050[1049:IBAABB]2.0.CO;2

Hu, J., Chen, G., Hassan, W. M., Chen, H., Li, J., and Du, G. (2017). Fertilization influences the nematode community through changing the plant community in the Tibetan plateau. *Eur. J. Soil Biol.* 78, 7–16. doi: 10.1016/j.ejsobi.2016.11.001

Laliberté, E., Legendre, P., and Shipley, B. (2014). *FD: Measuring functional diversity (FD) from multiple traits, and other tools for functional ecology*. R package version 1.0-12.1, 1-12.

Lefcheck, J. S. (2016). piecewiseSEM: piecewise structural equation modelling in r for ecology, evolution, and systematics. *Methods Ecol. Evol.* 7, 573–579. doi: 10.1111/2041-210X.12512

Leff, J. W., Jones, S. E., Prober, S. M., Barberán, A., Borer, E. T., Firn, J. L., et al. (2015). Consistent responses of soil microbial communities to elevated nutrient inputs in grasslands across the globe. *Proc. Natl. Acad. Sci.* 112, 10967–10972. doi: 10.1073/pnas.1508382112

Legay, N., Clément, J. C., Grassein, F., Lavorel, S., Lemauviel-Lavenant, S., Personeni, E., et al. (2020). Plant growth drives soil nitrogen cycling and N-related microbial activity through changing root traits. *Fungal Ecol.* 44:100910. doi: 10.1016/j.funeco.2019.100910

Li, Q., Bai, H., Liang, W., Xia, J., Wan, S., and van der Putten, W. H. (2013). Nitrogen addition and warming independently influence the belowground micro-food web in a temperate steppe. *PLoS One* 8:e60441. doi: 10.1371/journal.pone.0060441

Liang, W., Lou, Y., Li, Q., Zhong, S., Zhang, X., and Wang, J. (2009). Nematode faunal response to long-term application of nitrogen fertilizer and organic manure in Northeast China. *Soil Biol. Biochem.* 41, 883–890. doi: 10.1016/j.soilbio.2008.06.018

Liu, T., Guo, R., Ran, W., Whalen, J. K., and Li, H. (2015). Body size is a sensitive trait-based indicator of soil nematode community response to fertilization in rice and wheat agroecosystems. *Soil Biol. Biochem.* 88, 275–281. doi: 10.1016/j.soilbio.2015.05.027

Liu, X., Lu, Y., Zhang, Z., and Zhou, S. (2020). Foliar fungal diseases respond differently to nitrogen and phosphorus additions in Tibetan alpine meadows. *Ecol. Res.* 35, 162–169. doi: 10.1111/1440-1703.12064

Liu, Y., Shi, G., Mao, L., Cheng, G., Jiang, S., Ma, X., et al. (2012). Direct and indirect influences of 8 yr of nitrogen and phosphorus fertilization on Glomeromycota in an alpine meadow ecosystem. *New Phytol.* 194, 523–535. doi: 10.1111/j.1469-8137.2012.04050.x

Liu, A., Yang, T., Xu, W., Shangguan, Z., Wang, J., Liu, H., et al. (2018). Status, issues and prospects of belowground biodiversity on the Tibetan alpine grassland. *Biodivers. Sci.* 26, 972–987. doi: 10.17520/biods.2018119

Lorenzen, S. (1994). *The phylogenetic systematics of free-living nematodes[M]*. London: Ray Society, 1–383.

Mulder, C., den Hollander, H. A., Vonk, J. A., Rossberg, A. G., Jagers op Akkerhuis, G. A. J. M., and Yeates, G. W. (2009). Soil resource supply influences faunal size–specific distributions in natural food webs. *Naturwissenschaften* 96, 813–826. doi: 10.1007/s00114-009-0539-4

Mulder, C., and Elser, J. J. (2009). Soil acidity, ecological stoichiometry and allometric scaling in grassland food webs: Soil pH, Stoichiometry And Allometric Scaling. *Glob. Chang. Biol.* 15, 2730–2738. doi: 10.1111/j.1365-2486.2009.01899.x

Murray, P. J., Cook, R., Currie, A. F., Dawson, L. A., Gange, A. C., Grayston, S. J., et al. (2006). Interactions between fertilizer addition, plants and the soil environment: implications for soil faunal structure and diversity. *Appl. Soil Ecol.* 33, 199–207. doi: 10.1016/j.apsoil.2005.11.004

Neher, D. A. (2010). Ecology of plant and free-living nematodes in natural and agricultural soil. *Annu. Rev. Phytopathol.* 48, 371–394. doi: 10.1146/annurev-phyto-073009-114439

Nelson, D. W., and Sommers, L. E. (1982). "Total carbon, organic carbon and organic matter" in *Methods of soil analysis, part 2*. eds. A. L. Page, R. H. Miller and D. R. Keenay (Madison: ASA), 539–580.

Niu, K., Choler, P., de Bello, F., Mirotchnick, N., Du, G., and Sun, S. (2014). Fertilization decreases species diversity but increases functional diversity: a three-year experiment in a Tibetan alpine meadow. *Agric. Ecosyst. Environ.* 182, 106–112. doi: 10.1016/j.agee.2013.07.015

Niu, K., He, J.-S., and Lechowicz, M. J. (2016). Foliar phosphorus content predicts species relative abundance in P-limited Tibetan alpine meadows. *Perspect. Plant Ecol. Evol. Syst.* 22, 47–54. doi: 10.1016/j.ppees.2016.08.002

Niu, S., Wu, M., Han, Y., Xia, J., Zhang, Z., Yang, H., et al. (2010). Nitrogen effects on net ecosystem carbon exchange in a temperate steppe: Carbon Flux Responses To Nitrogen Enrichment. *Glob. Chang. Biol.* 16, 144–155. doi: 10.1111/j.1365-2486.2009.01894.x

Oksanen, J. (2016). *Design decisions and implementation details in vegan. The vignette of the package is vegan. R package version*, 2–4.

Pan, F., Han, X., Mclaughlin, N. B., Li, C., and Xu, Y. (2015). Effect of long-term fertilization on free-living nematode community structure in Mollisols. *J. Soil Sci. Plant Nutr.* 15, 129–141. doi: 10.4067/S0718-95162015005000011

Pey, B., Nahmani, J., Auclerc, A., Capowiez, Y., Cluzeau, D., Cortet, J., et al. (2014). Current use of and future needs for soil invertebrate functional traits in community ecology. *Basic Appl. Ecol.* 15, 194–206. doi: 10.1016/j.baae.2014.03.007

Picot, A., Monnin, T., and Loeuille, N. (2019). From apparent competition to facilitation: impacts of consumer niche construction on the coexistence and stability of consumer-resource communities. *Funct. Ecol.* 33, 1746–1757. doi: 10.1111/1365-2435.13378

Qi, R. *Response of plant community to nitrogen and phosphorous additions in sub-alpine meadows of the Qinghai Tibetan plateau[D]*. Diss. Lanzhou University, Lanzhou, (2013).

Qi, S., Zhao, X., Zheng, H. X., and Lin, Q. (2010). Changes of soil biodiversity in Inner Mongolia steppe after 5 years of N and P fertilizer applications. *Acta Ecol. Sin.* 30, 5518–5526.

Reay, D. S., Dentener, F., Smith, P., Grace, J., and Feely, R. A. (2008). Global nitrogen deposition and carbon sinks. *Nat. Geosci.* 1, 430–437. doi: 10.1038/ngeo230

Reich, P. B., Hobbie, S. E., Lee, T., Ellsworth, D. S., West, J. B., Tilman, D., et al. (2006). Nitrogen limitation constrains sustainability of ecosystem response to CO2. *Nature* 440, 922–925. doi: 10.1038/nature04486

Rovira, A. D., and Simon, A. (1985). Growth, nutrition and yield of wheat in calcareous sandy loams of South Australia: effects of soil fumigation, fungicide, nematicide and nitrogen fertilizers. *Soil Biol. Biochem.* 17, 279–284. doi: 10.1016/0038-0717(85)90061-6

Ruan, W., Sang, Y., Chen, Q., Zhu, X., Lin, S., and Gao, Y. (2012). The response of soil nematode community to nitrogen, water, and grazing history in the inner Mongolian steppe, China. *Ecosystems* 15, 1121–1133. doi: 10.1007/s10021-012-9570-y

Sarathchandra, S. U., Ghani, A., Yeates, G. W., Burch, G., and Cox, N. R. (2001). Effect of nitrogen and phosphate fertilisers on microbial and nematode diversity in pasture soils. *Soil Biol. Biochem.* 33, 953–964. doi: 10.1016/S0038-0717(00)00245-5

Sparks, D. L., Page, A., Helmke, P., Loeppert, R., Soltanpour, P., Tabatabai, M., et al. (1996). *Methods of soil analysis, part 3, Chemical Methods*. Madison, WI: Soil Science Society of America, Madison.

Tita, G., Vincx, M., and Desrosiers, G. (1999). Size spectra, body width and morphotypes of intertidal nematodes: An ecological interpretation. *J. Mar. Biol. Assoc.* 79, 1007–1015. doi: 10.1017/S0025315499001241

van den Hoogen, J., Geisen, S., Routh, D., Ferris, H., Traunspurger, W., Wardle, D. A., et al. (2019). Soil nematode abundance and functional group composition at a global scale. *Nature* 572, 194–198. doi: 10.1038/s41586-019-1418-6

Villenave, C., Saj, S., Pablo, A.-L., Sall, S., Djigal, D., Chotte, J.-L., et al. (2010). Influence of long-term organic and mineral fertilization on soil nematofauna when growing Sorghum bicolor in Burkina Faso. *Biol. Fertil. Soils* 46, 659–670. doi: 10.1007/s00374-010-0471-y

Violle, C., Navas, M.-L., Vile, D., Kazakou, E., Fortunel, C., Hummel, I., et al. (2007). Let the concept of trait be functional! *Oikos* 116, 882–892. doi: 10.1111/j.0030-1299.2007.15559.x

Vitousek, P. M., Aber, J. D., Howarth, R. W., Likens, G. E., Matson, P. A., Schindler, D. W., et al. (1997). Human alteration of the global nitrogen cycle: sources and consequences. *Ecol. Appl.* 7, 737–750. doi: 10.1890/1051-0761(1997)007[0737:HAOTGN]2.0.CO;2

Wang, J., Liao, L., Ye, Z., Liu, H., Zhang, C., Zhang, L., et al. (2022). Different bacterial co-occurrence patterns and community assembly between rhizosphere and bulk soils under N addition in the plant–soil system. *Plant and Soil* 471, 697–713. doi: 10.1007/s11104-021-05214-2

Wang, W., Ma, Y., Xu, J., Wang, H., Zhu, J., and Zhou, H. (2012). The uptake diversity of soil nitrogen nutrients by main plant species in Kobresia humilis alpine meadow on the Qinghai-Tibet plateau. *Sci. China Earth Sci.* 55, 1688–1695. doi: 10.1007/s11430-012-4461-9

Wang, Y., and Niu, K. (2020). Effect of soil environment on the functional diversity of soil nematodes in Tibetan alpine meadows. *Biodivers. Sci.* 28, 707–717. doi: 10.17520/biods.2020042

Wang, K., Sipes, B. S., and Schmitt, D. P. (2002). Crotalaria as a cover CROP for nematode management: a review. *Nematropica* 32, 35–57. doi: 10.1046/j.1365-2907.2002.00105.x

Wang, X., Xiao, S., Yang, X., Liu, Z., Zhou, X., Du, G., et al. (2019). Dominant plant species influence nematode richness by moderating understory diversity and microbial assemblages. *Soil Biol. Biochem.* 137:107566. doi: 10.1016/j.soilbio.2019.107566

Wei, C., Zheng, H., Li, Q., Lü, X., Yu, Q., Zhang, H., et al. (2012). Nitrogen addition regulates soil nematode community composition through ammonium suppression. *PLoS One* 7:e43384. doi: 10.1371/journal.pone.0043384

Wu, J. H. (1999). *Studies on freshwater and soil nematodes in China*. Institute of Hydrobiology, Chinese Academy of Science.

Yang, Y., Ji, C., Ma, W., Wang, S., Wang, S., Han, W., et al. (2012). Significant soil acidification across northern China's grasslands during 1980s-2000s. *Glob. Chang. Biol.* 18, 2292–2300. doi: 10.1111/j.1365-2486.2012.02694.x

Yang, H., Jiang, L., Li, L., Li, A., Wu, M., and Wan, S. (2012). Diversity-dependent stability under mowing and nutrient addition: evidence from a 7-year grassland experiment: diversity-dependent stability in steppe. *Ecol. Lett.* 15, 619–626. doi: 10.1111/j.1461-0248.2012.01778.x

Yang, J. E., Kim, J. J., Skogley, E. O., and Schaff, B. E. (1998). A simple spectrophotometric determination of nitrate in water, resin, and soil extracts. *Soil Sci. Soc. Am. J.* 62, 1108–1115. doi: 10.2136/sssaj1998.03615995006200040036x

Yang, Z., Powell, J. R., Zhang, C., and Du, G. (2012). The effect of environmental and phylogenetic drivers on community assembly in an alpine meadow community. *Ecology* 93, 2321–2328. doi: 10.1890/11-2212.1

Yeates, G. (1999). Effects Of Plants On Nematode Community Structure. *Annu. Rev. Phytopathol.* 37, 127–149. doi: 10.1146/annurev.phyto.37.1.127

Yeates, G. W., Bongers, T., De Goede, R. G., Freckman, D. W., and Georgieva, S. S. (1993). Feeding habits in soil nematode families and genera-an outline for soil ecologists. *J. Nematol.* 25, 315–331.

Yin, W. Y. (1998). *Soil animal search guide of China*. Beijing: Science Press.

Zhang, Z.-W., Li, Q., Hu, Y.-Y., Wei, H.-W., Hou, S.-L., Yin, J.-X., et al. (2022). Nitrogen and phosphorus additions interactively affected composition and carbon budget of soil nematode community in a temperate steppe. *Plant and Soil* 473, 109–121. doi: 10.1007/s11104-021-05145-y

Zhao, J., Wang, F., Li, J., Zou, B., Wang, X., Li, Z., et al. (2014). Effects of experimental nitrogen and/or phosphorus additions on soil nematode communities in a secondary tropical forest. *Soil Biol. Biochem.* 75, 1–10. doi: 10.1016/j.soilbio.2014.03.019

Zhao, X., Zhang, S., and Niu, K. (2020). Association of soil bacterial diversity with plant community functional attributes in alpine meadows. *Scientia Sinica Vitae* 50, 70–80. doi: 10.1360/SSV-2019-0072

frontiers | Frontiers in Ecology and Evolution

TYPE Original Research
PUBLISHED 22 March 2023
DOI 10.3389/fevo.2023.1151182

OPEN ACCESS

EDITED BY
Hui Zhang,
Hainan University,
China

REVIEWED BY
Xiao Xu,
Yunnan University,
China
Pu Jia,
South China Normal University,
China

*CORRESPONDENCE
Shengyun Chen
✉ sychen@lzb.ac.cn
Jihua Wu
✉ wjh@lzu.edu.cn

SPECIALTY SECTION
This article was submitted to Conservation and Restoration Ecology, a section of the journal Frontiers in Ecology and Evolution

RECEIVED 25 January 2023
ACCEPTED 28 February 2023
PUBLISHED 22 March 2023

CITATION
Zhang Y, Tian Z, Liu B, Chen S and Wu J (2023) Effects of photovoltaic power station construction on terrestrial ecosystems: A meta-analysis.
Front. Ecol. Evol. 11:1151182.
doi: 10.3389/fevo.2023.1151182

Effects of photovoltaic power station construction on terrestrial ecosystems: A meta-analysis

Yong Zhang[1], Zhengqing Tian[1], Benli Liu[2], Shengyun Chen[1,3]* and Jihua Wu[1]*

[1]State Key Laboratory of Herbage Improvement and Grassland Agro-ecosystems/College of Ecology, Lanzhou University, Lanzhou, China, [2]Key Laboratory of Desert and Desertification/Dunhuang Gobi and Desert Ecology and Environment Research Station, Northwest Institute of Eco-Environment and Resources, Chinese Academy of Sciences, Lanzhou, China, [3]State Key Laboratory of Cryospheric Science, Northwest Institute of Eco-Environment and Resources, Chinese Academy of Sciences, Lanzhou, China

The rapid increase in construction of solar photovoltaic power stations (SPPs) has motivated ecologists to understand how these stations affect terrestrial ecosystems. Comparing study sites, effects are often not consistent, and a more systematic assessment of this topic remains lacking. Here, we evaluated the effects of SPP construction on carbon emissions, edaphic variables, microclimatic factors and vegetation characteristics in a meta-analysis. We employed log response ratios (as effect sizes) to assess how control plots differed from those beneath solar photovoltaic panels. We found that SPP construction decreased the local air temperature and photosynthetically active radiation, while increasing air humidity, especially in grasslands. Furthermore, plant aboveground biomass and vegetation cover were also enhanced by SPP construction in grassland ecosystems. In farmland ecosystems, photovoltaic panel installation increased plant aboveground biomass, soil available phosphorus and soil pH, while reducing CO_2 flux, plant species richness and vegetation cover in woodlands. Thus, while SPP construction had profound ecological impacts in terrestrial ecosystems, the direction and strength of these effects were largely dependent on ecosystem type. Most studies of SPP construction to date have focused on local microclimatic and plant diversity effects, but few studies have examined effects on ecosystem functions and services. Future assessments are needed of both the benefits and disbenefits of SPP construction across different ecosystems, to improve SPP site selection and adaptive management.

KEYWORDS

comprehensive assessment, ecosystem types, microclimatic factors, vegetation characteristics, soil environment

1. Introduction

Replacing fossil fuels with clean energy sources to reduce carbon emissions is an important step toward achieving carbon neutrality (Armstrong et al., 2014). In recent years, great progress has been made in exploiting renewable resources to optimize existing energy infrastructure (Li, 2021). Photovoltaic (PV) power generation using solar energy is one of the most promising technologies for sustainable energy generation (Wilberforce et al., 2019; Bogdanov et al., 2021). In 2018, global solar PV capacity accounted for 55% of all new renewable energy capacity (Dunnett et al., 2020). The installed capacity of solar PV systems is expected to reach 4,600 GW

by 2050 and avert up to 4 Gt of CO_2 emissions annually (Wang and Cong, 2021). Currently, the world's PV power capacity accounts for about 1% of total power capacity, by 2030, it is expected to provide 15% of the global electricity supply (Helveston et al., 2022), crucially helping achieve global carbon neutrality (Liu et al., 2012).

The construction of SPPs has profound effects on terrestrial ecosystems, because ground-mounted PV panels are considered a new form of land use change, shading large areas of previously open land (Turney and Fthenakis, 2011; Armstrong et al., 2016; Chang et al., 2016). Previous studies have found that SPP construction can affect the local climate and soil environment (Hong and Kim, 2008; De Marcoa et al., 2014; Choi et al., 2020) by perturbing the surface energy balance (Mercado et al., 2009; Nemet, 2009; Broadbent et al., 2019; Yu et al., 2020; Lambert et al., 2021). Photovoltaic panels can affect air humidity and soil water content by moderating the photosynthetically active radiation (PAR) received (Weinstock and Appelbaum, 2009; Lu, 2013), as well as by significantly reducing wind speed and turbulence (Armstrong et al., 2016; Zhao, 2016; Yin et al., 2017). These effects in turn affect plant communities, altering plant biomass, species richness and vegetation cover (Liu et al., 2019; Zhai et al., 2020; Lambert et al., 2022). Local impacts of SPPs on the microclimate and vegetation may further influence broader ecosystem processes, such as carbon flux balance and soil water retention capacity, leading to changes in ecosystem services across spatial scales (Armstrong et al., 2014; Liu et al., 2020).

However, the ecological impacts of SPPs reported to date vary substantially among studies. In the Mu Us Desert, China (Liu et al., 2019), PAR was reduced by 67.4% beneath PV panels as compared to an unaltered area. However, the installation of PV panels did not affect PAR in the desert ecosystems of Inner Mongolia, China (Zhao, 2016) or in the farmland ecosystems of Italy (Vervloesem et al., 2022). A 83.9% increase in vegetation cover and 68.7% increase in plant biomass were associated with PV panels in the Gonghe Basin, Qinghai Province, China (Li et al., 2016). Similarly, Wang et al. (2016) reported a 128% increase in the fresh weight of plant biomass under PV panels. In contrast, in a woodland ecosystem in the south of France (Lambert et al., 2022), aboveground biomass, soil temperature and vegetation cover were significantly reduced beneath PV panels, with soil temperature a full 10% lower (Lambert et al., 2021). Similarly, in a farmland ecosystem in central Italy (Moscatelli et al., 2022), soil temperature was reduced by PV panels. However, in the Mu Us Desert (Liu et al., 2019), soil temperature was 3°C higher under PV panels as compared to controls. For soil pH, contrasting results have also been reported. Under PV panels, soil pH increased by 14.04% in central Italy (Moscatelli et al., 2022) but decreased by 13.93% in Datong, China (Liu, 2020).

To understand the overall ecological impacts of SPPs on terrestrial ecosystems. We conducted a meta-analysis of SPP effects on carbon processes, edaphic factors, microclimatic factors and vegetation characteristics. We hypothesized that the mixed effects observed to date were caused by variations among study ecosystems; we therefore examined how ecosystem type (i.e., desert, farmland, grassland, or woodland) affected the SPP ecological impacts. Our study is hoped to provide a comprehensive evaluation of SPP impacts on terrestrial ecosystems and to improve the rational management and ecological restoration of SPP localities.

2. Materials and methods

2.1. Data collection

To test how PV panels affected terrestrial ecosystem ecology, we conducted a systematic literature search using the ISI Web of Science and CNKI for the terms [photovoltaic AND (ecology system OR vegetation OR biodiversity OR soil nutrient OR soil moisture OR soil temperature)]. The investigations spanned published records from 1st January 2010 to 31st December 2022. This search led to an initial set of 1,491 publications. These were checked for relevance by examining the title, abstract and main text in succession (Supplementary Figure S1).

We collected data from publications that met the following three criteria: (1) a focus on the ecological and environmental impact of SPPs, including at least one indicator of carbon flux, microclimatic factors, the soil environment and/or vegetation characteristics; (2) the experimental design included both control and experimental groups, and each group contained at least three replicates; (3) the mean and standard deviation (or variance, standard error and 95% confidence interval) of relevant indexes were provided. After screening, a total of 16 papers were selected for data extraction and further analysis (Supplementary Table S1).

Data were extracted from the main text and tables, or indirectly from figures using "GetData." The indices we extracted included microclimatic factors (air humidity, air temperature and PAR), soil characteristics (available phosphorus, CO_2 flux, pH, soil temperature, soil water content, total carbon and total nitrogen) and vegetation characteristics (plant aboveground biomass, Shannon-Wiener diversity index, Simpson's diversity index, species richness and vegetation cover). For each indicator, we recorded the mean, standard deviation (or variance, standard error and 95% confidence interval) and sample size.

2.2. Statistical analysis

We calculated effect sizes based on the mean (Y), standard deviation (SD) and sample size (n) of each indicator and derived the variance associated with each study. In cases where only a standard error (SE) was provided, it was converted to a SD using (1):

$$SD = SE \times \sqrt{n} \tag{1}$$

The log response ratio (RR) was used as a measure of the effect size to quantify differences between control and experimental groups (Hedges et al., 1999) and was calculated as follows:

$$y_i = lnRR = LN\frac{Y_e}{Y_c} \tag{2}$$

where Ye is the mean value of the experimental group, and Yc is the mean value of the control group. The corresponding variance (Vi) for RR was calculated as follows:

$$Vi = \frac{S_e^2}{N_e \times Y_e^2} + \frac{S_e^2}{N_c \times Y_c^2} \quad (3)$$

where Ne is the sample size of the experimental group and Nc the control group.

We built a series of random effects models by employing the rma.mv function from the "metafor" package in R (4.2.1) (Wallace et al., 2017). "Study case" was nested in "literature" as a random effect. The cumulative effect value ($\bar{y}$), weights of individual studies (w_i^*), population variance (V_M), and the total standard error (SE_M) and its 95% confidence interval were calculated according to the following formulas:

$$\bar{y} = \frac{\sum_{i=1}^{k} w_i^* \times y_i}{\sum_{i=1}^{k} w_i^*} \quad (4)$$

$$w_i^* = 1/(v_i + \tau^2) \quad (5)$$

$$V_M = \sqrt{\frac{1}{\sum_{i=1}^{k} w_i^*}} \quad (6)$$

$$SE_M = \sqrt{V_M} \quad (7)$$

$$95\%CI = \bar{y} \pm 1.96 \times SE_M \quad (8)$$

If the 95% confidence interval encompassed zero, the indicator in question did not differ significantly between the control and experimental groups ($p > 0.05$). Lastly, we used "Origin 2022" to draw a "forest map" showing the meta-analysis results.

3. Results

3.1. Effects of solar photovoltaic panel construction on microclimate factors

Overall, air temperature (mean ln RR = −0.073, 95% CI = [−0.125, −0.021], $p = 0.006$) and PAR (ln RR = −1.563, [−2.537, −0.590], $p = 0.002$) were significantly lower within PV panel plots than within control plots, while air humidity (ln RR = 0.144, [0.013, 0.274], $p = 0.031$) showed the opposite pattern (Figure 1). Due to shading by PV panels, the PAR received by farmland (ln RR = −2.830, [−3.664, −1.996], $p < 0.001$) and grassland (ln RR = −2.100, [−2.558, −1.642], $p < 0.001$) ecosystems was lower, respectively, as compared to control plots. Meanwhile, air humidity (ln RR = 0.223, [0.088, 0.357], $p = 0.001$) increased and air temperature (ln RR = −0.099, [−0.144, −0.054], $p < 0.001$) decreased by in grassland ecosystems in experimental versus control plots (Figure 1).

3.2. Effects of solar photovoltaic panel construction on soil conditions

The construction of SPPs had no significant effect on total carbon, soil total nitrogen, soil temperature, or soil water content in terrestrial ecosystems (Figure 2). In farmland ecosystems, the soil available phosphorus (ln RR = 2.363, [0.279, 4.448], $p = 0.026$) and soil pH (ln RR = 0.154, [0.003, 0.304], $p = 0.045$) were higher within PV panel plots versus controls, whereas the soil pH (ln RR = −0.108, [−0.136, −0.081], $p < 0.001$) decreased with PV panel construction in grassland ecosystems. SPP construction did not affect the overall CO_2 flux, but reduced CO_2 fluxes (ln RR = −1.053, [−1.404, −0.702], $p < 0.001$) in woodland ecosystems (Figure 2).

3.3. Effects of solar photovoltaic panel construction on vegetation characteristics

The use of SPPs enhanced vegetation cover in grassland (ln RR = 1.000, [0.290, 1.709], $p = 0.006$) and desert (ln RR = 1.960, [1.742, 2.178], $p < 0.001$) ecosystems while decreasing the vegetation cover in woodland ecosystems (ln RR = −0.806, [−1.230, −0.398], $p < 0.001$; Figure 3). Compared with control plots, the aboveground biomass was higher in PV panel plots, with the aboveground biomass greater in grasslands (ln RR = 0.751, [0.571, 0.931], $p < 0.001$) and farmlands (ln RR = 0.823, [0.750, 0.896], $p < 0.001$), respectively (Figure 3). In general, PV panel construction did not affect plant species diversity indices, with the exception that plant species richness (ln RR = −0.555, [−0.720, −0.390], $p < 0.001$) was significantly reduced in woodland ecosystems.

4. Discussion

Overall, SPP construction had a significant effect on microclimatic factors such as air humidity, air temperature and PAR, which are major climate moderators influencing vegetation growth and terrestrial ecosystem functioning. In PV panel plots, PAR was much lower than in control plots, especially in grassland and farmland ecosystems. Photovoltaic panels convert solar radiation into electricity and therefore block sunlight from reaching the ground (Lewis and Nocera, 2006), the land surface beneath PV panels receives less radiation than uncovered land (Zhou et al., 2012). Here, we found that SPP had no significant effect on PAR in deserts, while another study (Liu et al., 2019) found a 67.3% decrease. In the desert system studied by Liu et al. (2019), vegetation cover was enhanced under the PV panels, resulting in less solar radiation reaching the surface. Changes in PAR induced by SPPs may lead to further alterations of other environmental factors. For example, in the Sahara, the PV panels of large-scale solar farms directly reduce surface albedo, creating a positive albedo-precipitation-vegetation feedback loop that triggers increases in temperature and precipitation (Li et al., 2018).

Compared to control plots, PV panel plots had significantly lower air temperature, with an average air temperature decrease in grassland ecosystems. The cooling of the land surface associated with SPP construction is related to the physical shading caused by PV panels (Marrou et al., 2013) and the interception of shortwave radiation by the PV arrays (Weinstock and Appelbaum, 2009). In grassland

10.3389/fevo.2023.1151182

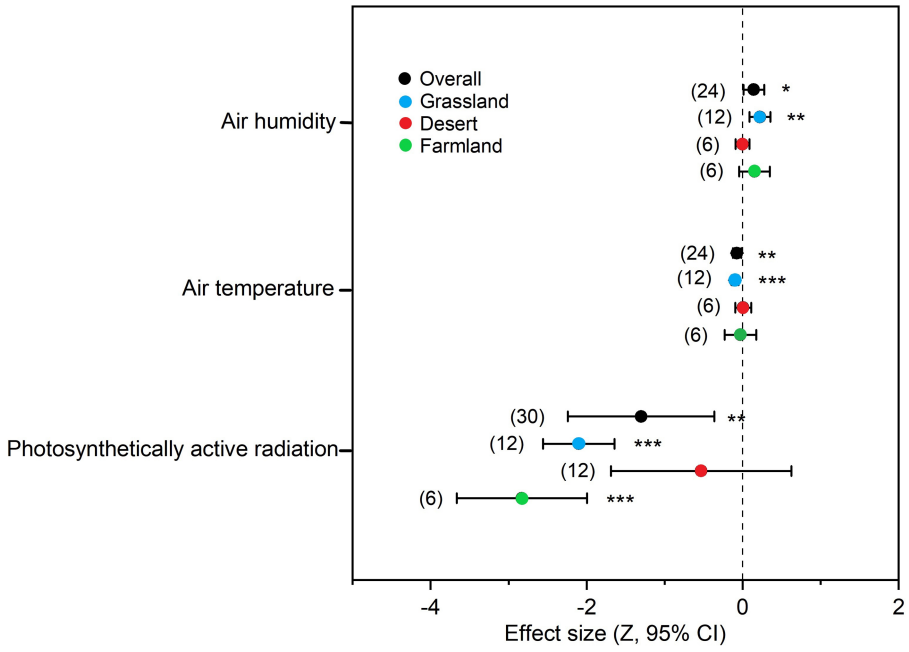

FIGURE 1
Effects of solar photovoltaic panels on microclimatic conditions in terrestrial ecosystems. Error bars indicate 95% confidence intervals (CIs). If the CI did not overlap zero, the response was considered significant: *p<0.05, **p<0.01, and ***p<0.001. The numbers in parentheses represent the sample size of each observation.

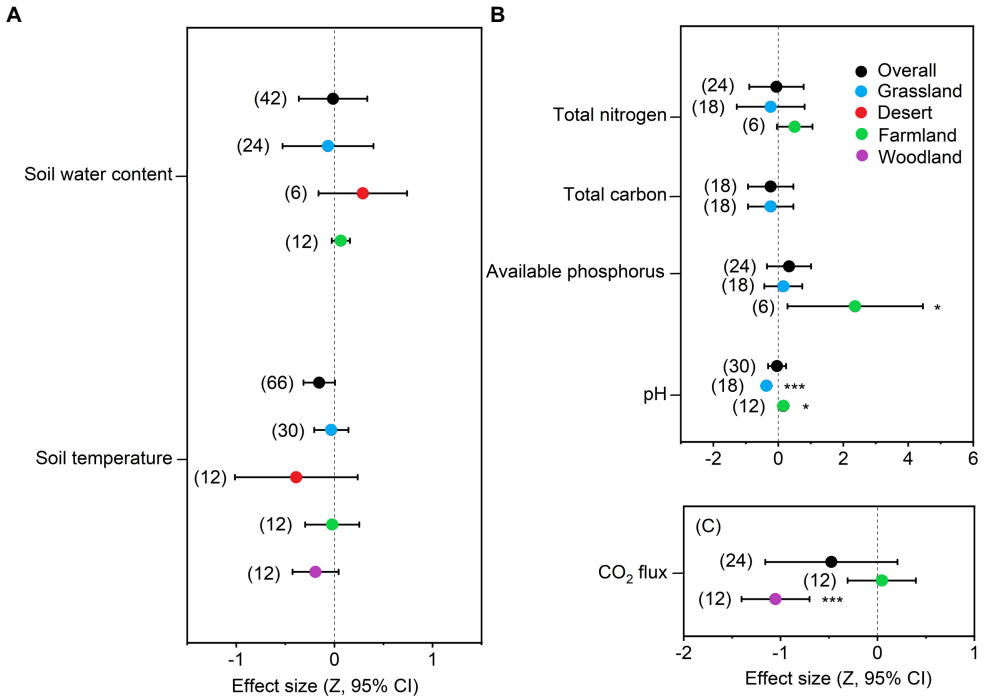

FIGURE 2
Effects of solar photovoltaic panels on the soil environment in terrestrial ecosystems. **(A)** Soil physical properties, **(B)** soil chemical properties, and **(C)** soil functions. Error bars indicate 95% confidence intervals (CIs). If the CI did not overlap zero, the response was considered significant: *p<0.05, **p<0.01, and ***p<0.001. The numbers in parentheses represent the sample size of each observation.

ecosystems, hot PV panel surfaces can heat the ambient air, driving a PV heat-island effect (Chang et al., 2018).

Air humidity is another important factor affecting vegetation. Overall, SPP construction led to a significant increase in air humidity,

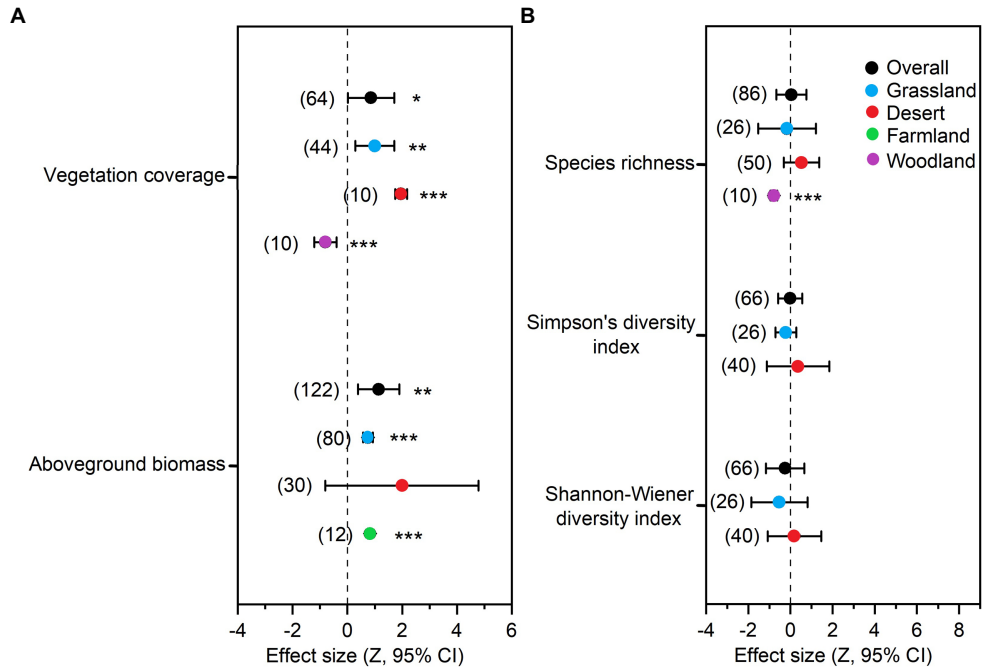

FIGURE 3
Effects of solar photovoltaic panels on vegetation characteristics in terrestrial ecosystems. **(A)** Aboveground biomass and cover and **(B)** plant diversity. Error bars indicate 95% confidence intervals (CIs). If the CI did not overlap zero, the response was considered significant: *p<0.05, **p<0.01, and ***p<0.001. The numbers in parentheses represent the sample size of each observation.

especially in grassland ecosystems, where air humidity increased. This increase in air humidity may be caused by a reduction in net radiation and air temperature under the PV panels (Chang et al., 2018), or by changes in wind speed and turbulent mixing at the land surface (Armstrong et al., 2014). How SPPs affect air humidity can also be closely linked to the vegetation status of an area. For example, Zhu et al. (2021) found that SPPs tended to indirectly affect humidity by regulating plant distribution and growth within the area.

Changes in microclimatic factors can produce corresponding changes in soil temperature and soil water content. However, SPP construction did not impact the overall physical properties of the soil. In a recent study (Zhou and Wang, 2019), soil organic matter, pH and total N and P varied little between PV panel rows and undisturbed areas outside the panel rows. We also did not detect an effect of SPP construction on soil total C or N content. However, SPP construction had contrasting effects on soil pH in farmlands versus grasslands. This may be due to variation among ecosystems in a number of important influential factors, including: Na salt leaching from PV panels, precipitation, soil erosion, surface runoff, vegetation characteristics and wind speed (Golubiewski, 2006; Cook, 2011; Barron-Gafford et al., 2019; Moscatelli et al., 2022). In farmland ecosystems, elevation of soil pH (from moderately acidic to slightly acidic) can increase the availability of soil P (Moscatelli et al., 2022). This reduction in soil C and N content is likely caused by the removal of topsoil during PV array construction (Choi et al., 2022). However, soil texture may also be an important determinant of how PV panels affect soil nutrient cycling (Mazaheri and Mahmoodabadi, 2012).

Our study found no net effect of SPP construction on CO_2 flux, but a decrease in CO_2 flux in woodland ecosystems. This decline in soil respiration may be due to reductions in plant growth and surface clearance under the PV panels (Lambert et al., 2021). To date, there remain few case studies of CO_2 fluxes under SPP construction, with only a small amount of data from agricultural and forest ecosystems and no data from other ecosystems. Therefore, our assessment of SPP impacts on CO_2 fluxes and other greenhouse gas emissions in terrestrial ecosystems is preliminary, and considerable future research will be required to fully elucidate these effects.

The construction of SPPs leads to changes in local shading and a redistribution of precipitation, as well as the evaporation of soil water (Cui et al., 2017). Together, the combined effect of these changes, as well as shifts in PAR and other soil variables, can greatly affect plant growth and community succession (Yan, 2017; Liu et al., 2022). Overall, in this study, both the vegetation cover and plant productivity (as aboveground biomass) were much increased under PV panels as compared to controls. In farmland and grassland ecosystems, aboveground biomass and vegetation cover increased significantly. For comparison, Wang et al. (2016) found increases in both the fresh (128%) and dry (127%) weight of aboveground plant materials under PV panels, while in the Gonghe Basin of China, PV panels resulted in increases in vegetation cover (83.9%) and aboveground biomass (68.7%) (Li et al., 2016). Despite variation in plant productivity and cover changes, SPP construction appears to be beneficial to plant growth in most cases.

Improved plant growth can lead to the absorption of more carbon from the atmosphere, while also regulating the terrestrial carbon cycle through plant–soil processes and thereby affecting soil carbon storage, greenhouse gas emissions and ecosystem stability (Bardgett et al., 2008). The enhanced plant productivity seen at SPP sites allows more litter to enter the soil, providing a greater influx of nutrients, improving soil structure and increasing soil water

holding capacity (Jia et al., 2018). More vegetation cover, especially in arid, sandy areas where vegetation cover is typically low, can provide protection from wind erosion (Wang, 2015). Taken together, the establishment of SPPs can not only provide electricity (*via* a new energy source), but also precipitate ecological benefits by enhancing vegetation cover.

We found no significant impact of SPP construction on plant species diversity. However, Wang et al. (2016) found that the Shannon-Wiener and Simpson's diversity indices increased by 60% and 32%, respectively, under PV panels as compared to control areas. The same trend was found by Zhang et al. (2020) in a desert ecosystem, where species richness, the Shannon-Wiener diversity index and Simpson's diversity indices were higher below PV panels than outside the SPP. In Gonghe Basin, plant species richness increased by 119.2% under PV panels (Li et al., 2016). However, fewer plant species and lower species diversity occurred under PV panels in a typical grassland area (Du and Sun, 2017; Zhai et al., 2018). This indicates that the effects of PV panels on plant diversity are varied and may even be in opposite directions. Furthermore, SPP construction may cause changes in plant community structure, which may not necessarily be reflected in plant diversity shifts (Zhai et al., 2018). Understanding the specifics of how SPP construction affects plant community structure requires further study.

Woodland ecosystems showed different responses to SPP construction than other ecosystem types. In woodlands, we found reductions in plant species richness and vegetation cover beneath PV panels. This is probably because, in woodland ecosystems, woody plants are removed and the land surface cleared prior to PV array construction (Lambert et al., 2022).

5. Conclusion

In our meta-analysis, SPP construction was found to significantly alter the local climate, increasing air temperature and PAR, while decreasing air humidity, these impacts were more prominent in grasslands versus other terrestrial ecosystems. However, SPP effects on soil parameters were generally not significant, perhaps due to the substantial spatial and temporal variation observed in these effects. Nevertheless, changes in vegetation caused by shifting environmental factors were evident. In most studies, SPP construction has been found to increase plant productivity (as aboveground biomass) and vegetation cover, except for in woodlands, where woody plants are removed during SPP construction. SPP projects not only generate clean energy, but also provide additional benefits by greening land surfaces in arid areas and increasing carbon sequestration. However, given the variation in these effects among ecosystem types, caution needs to be taken when considering future SPP development and management across regions.

Data availability statement

The original contributions presented in the study are included in the article/Supplementary material, further inquiries can be directed to the corresponding authors.

Author contributions

JW and SC conceived the work. YZ and ZT collected the data. YZ analyzed the data and wrote the first draft. All authors contributed to the article and approved the submitted version.

Funding

This work was supported by the Gansu Provincial Key Program of Science Fund (22JR5RA396), Fundamental Research Funds for the Central Universities (lzujbky-2021-sp51) and National Key Research and Development Program of China (2022YFB4202102).

Conflict of interest

The authors declare that the research was conducted in the absence of any commercial or financial relationships that could be construed as a potential conflict of interest.

Publisher's note

Supplementary material

The Supplementary material for this article can be found online at: https://www.frontiersin.org/articles/10.3389/fevo.2023.1151182/full#supplementary-material

References

Armstrong, A., Ostle, N. J., and Whitaker, J. (2016). Solar park microclimate and vegetation management effects on grassland carbon cycling. *Environ. Res. Lett.* 11:074016. doi: 10.1088/1748-9326/11/7/074016

Armstrong, A., Waldron, S., Whitaker, J., and Ostle, N. J. (2014). Wind farm and solar park effects on plant-soil carbon cycling: uncertain impacts of changes in ground-level microclimate. *Glob. Chang. Biol.* 20, 1699–1706. doi: 10.1111/gcb.12437

Bardgett, R. D., Freeman, C., and Ostle, N. J. (2008). Microbial contributions to climate change through carbon cycle feedbacks. *ISME J.* 2, 805–814. doi: 10.1038/ismej.2008.58

Barron-Gafford, G. A., Pavao-Zuckerman, M. A., Minor, R. L., Sutter, L. F., Barnett-Moreno, I., Blackett, D. T., et al. (2019). Agrivoltaics provide mutual benefits across the food-energy-water nexus in drylands. *Nat. Sust.* 2, 848–855. doi: 10.1038/s41893-019-0364-5

Bogdanov, D., Gulagi, A., Fasihi, M., and Breyer, C. (2021). Full energy sector transition towards 100% renewable energy supply: integrating power, heat, transport and industry sectors including desalination. *Appl. Energy* 283:116273. doi: 10.1016/j.apenergy.2020.116273

Broadbent, A. M., Krayenhoff, E. S., Georgescu, M., and Sailor, D. J. (2019). The observed effects of utility-scale photovoltaics on near-surface air temperature and energy balance. *J. Appl. Meteorol. Climatol.* 58, 989–1006. doi: 10.1175/JAMC-D-18-0271.1

Chang, Z. F., Liu, S. Z., Zhu, S. J., Han, F. G., Zhong, S. N., and Duan, X. F. (2016). Ecological functions of PV power plants in the desert and Gobi. *J. Resour. Ecol.* 7, 130–136. doi: 10.5814/j.issn.1674-764x.2016.02.008

Chang, R., Shen, Y. B., Luo, Y., Wang, B., Yang, Z. B., and Guo, P. (2018). Observed surface radiation and temperature impacts from the large-scale deployment of photovoltaics in the barren area of Gonghe. *Chin. Renew. Energ.* 118, 131–137. doi: 10.1016/j.renene.2017.11.007

Choi, C. S., Cagle, A. E., Macknick, J., Macknick, J., Bloom, D. E., and Caplan, J. S. (2020). Effects of revegetation on soil physical and chemical properties in solar photovoltaic infrastructure. *Front. Environ. Sci.* 8:140. doi: 10.3389/fenvs.2020.00140

Choi, C. S., Cagle, A. E., Macknick, J., Bloom, D. E., Caplan, J. S., and Ravi, S. (2022). Effects of revegetation on soil physical and chemical properties in solar photovoltaic infrastructure. *Front. Environ. Sci.* 8:140. doi: 10.3389/fenvs.2020.00140

Cook, P. (2011). Infrastructure, rural electrification and development. *Energy Sust. Dev.* 15, 304–313. doi: 10.1016/j.esd.2011.07.008

Cui, Y. Q., Feng, Q., Sun, J. H., and Xiao, J. H. (2017). A review of revegetation pattern of photovoltaic in Northwest China. *B. Soil Water Conserv.* 37, 200–203. doi: 10.13961/j.cnki.stbctb.2017.03.033

De Marcoa, A., Petrosillo, I., Semeraro, T., Pasimeni, M. R., Aretano, R., and Zurlini, G. (2014). The contribution of utility-scale solar energy to the global climate regulation and its effects on local ecosystem services. *Glob. Ecol. Conserv.* 2, 324–337. doi: 10.1016/j.gecco.2014.10.010

Du, H., and Sun, F. (2017). Preliminary study on the impact of photovoltaic power plant operation on vegetation. *Environ. Dev.* 29, 30–31. doi: 10.16647/j.cnki.cn15–1369/x.2017.08.015

Dunnett, S., Sorichetta, A., Taylor, G., and Eigenbrod, F. (2020). Harmonised global datasets of wind and solar farm locations and power. *Sci. Data.* 7:130. doi: 10.1038/s41597-020-0469-8

Golubiewski, N. E. (2006). Urbanization increases grassland carbon pools: effects of landscaping in Colorado's front range. *Ecol. Appl.* 16, 555–571. doi: 10.1890/1051-0761(2006)016[0555:UIGCPE]2.0.CO;2

Hedges, L. V., Gurevitch, J., and Curtis, P. S. (1999). The meta-analysis of response ratios in experimental ecology. *Ecol.* 80, 1150–1156. doi: 10.1890/0012-9658(1999)080[1150:TMAORR]2.0.CO;2

Helveston, J. P., He, G., and Davidson, M. R. (2022). Quantifying the cost savings of global solar photovoltaic supply chains. *Nature* 612, 83–87. doi: 10.1038/s41586-022-05316-6

Hong, J., and Kim, J. (2008). Simulation of surface radiation balance on the Tibetan plateau. *Geophys. Res. Lett.* 35:L08814. doi: 10.1029/2008GL033613

Jia, C., Huang, Z., Miao, H. T., Lu, R., Li, J., and Liu, Y. (2018). Litter crusts promote herb species formation by improving surface microhabitats in a desert ecosystem. *Catena* 171, 245–250. doi: 10.1016/j.catena.2018.07.024

Lambert, Q., Bischoff, A., Cueff, S., Cluchier, A., and Gros, R. (2021). Effects of solar park construction and solar panels on soil quality, microclimate, CO_2 fluxes, and vegetation under a Mediterranean climate. *Land Degrad. Dev.* 32, 5190–5202. doi: 10.1002/ldr.4101

Lambert, Q., Gros, R., and Bischoff, A. (2022). Ecological restoration of solar park plant communities and the effect of solar panels. *Ecol. Eng.* 182:106722. doi: 10.1016/j.ecoleng.2022.106722

Lewis, N. S., and Nocera, D. G. (2006). Powering the planet: chemical challenges in solar energy utilization. *Proc. Natl. Acad. Sci. U. S. A.* 104, 15729–15735. doi: 10.1073/pnas.06 03395103

Li, Q. S. (2021). Discussion on the path of China's energy transformation under the goal of carbon neutrality. *Chin. Coal.* 47, 1–7. doi: 10.19880/j.cnki.ccm.2021.08.001

Li, S. H., Gao, Q., Wang, X. Q., Lan, L., and Yang, Z. W. (2016). Characteristics of vegetation and soil property changes by photovoltaic plant interference in alpine desert steppe. *J. Soil Water Conserv.* 30, 325–329. doi: 10.13870/j.cnki.stbcxb.2016.06.054

Li, Y., Kalnay, E., Motesharrei, S., Rivas, J., Kucharski, F., and Kirk-Davidoff, D. (2018). Climate model shows large-scale wind and solar farms in the Sahara increase rain and vegetation. *Science* 361, 1019–1022. doi: 10.1126/science.aar5629

Liu, Y. (2020). Effects of photovoltaic power station on two typical degraded ecosystems in northern Shanxi Province. *Shanxi Univ. Fin. Econ.* 1–80. doi: 10.27283/d.cnki.gsxcc.2020.000066

Liu, J., Cao, L., Ma, J., and Zhang, J. (2012). Economic analysis of user's grid-connected PV system based on energy storage system. *Acta. Energ. Sol. Sin.* 33, 1887–1892. doi: 10.3969/j.issn.0254–0096.2012.11.009

Liu, Y., Zhang, R. Q., Huang, Z., Cheng, Z., Lopez-Vicente, M., Ma, X. R., et al. (2019). Solar photovoltaic panels significantly promote vegetation recovery by modifying the soil surface microhabitats in arid sandy ecosystem. *Land Degrad. Dev.* 30, 2177–2186. doi: 10.1002/ldr.3408

Liu, X., Zhang, P., and Liu, J. Q. (2022). Inorganic fertilizers are limiting factors of vegetation restoration of Qinghai Tala shoal photovoltaic power station. *Biodivers. Sci.* 30, 22100–22136. doi: 10.17520/biods.2022100

Liu, Y., Zhang, R. Q., Ma, X. R., and Wu, G. L. (2020). Combined ecological and economic benefits of the solar photovoltaic industry in arid sandy ecosystems. *J. Clean. Prod.* 262:121376. doi: 10.1016/j.jclepro.2020.121376

Lu, X. (2013). *The environment effect analysis of PV power plant construction in desert Gobi* Lanzhou University Available at: https://kns.cnki.net/KCMS/detail/detail.aspx?dbname=CMFD201302&filename=1013237744.nh.

Marrou, H., Dufour, L., and Wery, J. (2013). How does a shelter of solar panels influence water flows in a soil-crop system? *Eur. J. Agron.* 50, 38–51. doi: 10.1016/j.eja.2013.05.004

Mazaheri, M. R., and Mahmoodabadi, M. (2012). Study on infiltration rate based on primary particle size distribution data in arid and semiarid region soils. *Arab. J. Geosci.* 5, 1039–1046. doi: 10.1007/s12517-011-0497-y

Mercado, L. M., Bellouin, N., Sitch, S., Boucher, O., Huntingford, C., Wild, M., et al. (2009). Impact of changes in diffuse radiation on the global land carbon sink. *Nature* 458, 1014–1017. doi: 10.1038/nature07949

Moscatelli, M. C., Marabottini, R., Massaccesi, L., and Marinari, S. (2022). Soil properties changes after seven years of ground mounted photovoltaic panels in Central Italy coastal area. *Geoderma Reg.* 29:e00500. doi: 10.1016/j.geodrs.2022.e00500

Nemet, G. F. (2009). Net radiative forcing from widespread deployment of photovoltaics. *Environ. Sci. Technol.* 43, 2173–2178. doi: 10.1021/es801747c

Turney, D., and Fthenakis, V. (2011). Environmental impacts from the installation and operation of large-scale solar power plants. *Renew. Sust. Energ. Rev.* 15, 3261–3270. doi: 10.1016/j.rser.2011.04.023

Vervloesem, J., Marcheggiani, E., Choudhury, M. A. M., and Muys, B. (2022). Effects of photovoltaic solar farms on microclimate and vegetation diversity. *Sustain.* 14:7493. doi: 10.3390/su14127493

Wallace, B. C., Lajeunesse, M. J., Dietz, G., Dahabreh, I. J., Trikalinos, T. A., Schmid, C. H., et al. (2017). OpenMEE: intuitive, open-source software for meta-analysis in ecology and evolutionary biology. *Methods Ecol. Evol.* 8, 941–947. doi: 10.1111/2041-210X.12708

Wang, T. (2015). *The impact of photovoltaic power construction on soil and vegetation in Jingbian County* Northwest A&F University Available at: https://kns.cnki.net/kcms/detail/detail.aspx?FileName=1015329905.nh&DbName=CMFD2016.

Wang, W. H., and Cong, W. (2021). Analysis of IEAs net zero by 2050:a roadmap for the global energy sector. *Int. Petroleum. Econ.* 29, 1–7. Available at: https://kns.cnki.net/kcms/detail/detail.aspx?FileName=GJJJ202106002&DbName=CJFQ2021

Wang, T., Wang, D. X., Guo, T. D., Zhang, G. G., Zhao, S. X., Niu, H. C., et al. (2016). The impact of photovoltaic power construction on soil and vegetation. *Res. Soil Water Conserv.* 23, 90–94. doi: 10.13869/j.cnki.rswc.2016.03.016

Weinstock, D., and Appelbaum, J. (2009). Optimization of solar photovoltaic fields. *J. Sol. Energy. Eng.* 131:031003. doi: 10.1115/1.3142705

Wilberforce, T., Baroutaji, A., El Hassan, Z., Thompson, J., Soudan, B., and Olabi, A. G. (2019). Prospects and challenges of concentrated solar photovoltaics and enhanced geothermal energy technologies. *Sci. Total Environ.* 659, 851–861. doi: 10.1016/j.scitotenv.2018.12.257

Yan, W. M. (2017). *Synergic relation between plantgrowth and soil water and evaluation of soil water availability on the loess plateau* Northwest A&F University Available at: https://kns.cnki.net/KCMS/detail/detail.aspx?dbname=CDFDLAST2017&filename=1017100365.nh.

Yin, D. Y., Ma, L., Ju, J. J., Zhao, S. P., Yu, Y., Tan, L. H., et al. (2017). Effect of large photovoltaic power station on microclimate of desert region in Gonghe basin. *Bull. Soil Water Conserv.* 37, 15–21. doi: 10.13961/j.cnki.stbctb.2017.03.003

Yu, G. R., Xu, X. L., and Wang, Q. F. (2020). Progress of the effects of global changes on the resource and environment carrying capacity of the ecological fragile areas. *Chin. Basic Sci.* 22, 16–20. doi: 10.3969/j.issn.1009–2412.2020.05.003

Zhai, B., Dang, X. H., Chen, X., Liu, X. J., and Yang, S. R. (2020). Difference regularity of precipitation redistribution and soil water evapotranspiration in photovoltaic panels in typical steppe areas of Inner Mongolia. *J. Chin. Agric. Univ.* 25, 144–155. doi: 10.11841/j.issn.1007-4333.2020.09.15

Zhai, B., Gao, Y., Dang, X. H., Chen, X., Cheng, B., Liu, X. J., et al. (2018). Effects of photovoltaic panels on the characteristics and diversity of *Leymus chinensis* community. *Chin. J. Ecol.* 37, 2237–2243. doi: 10.13292/j.1000–4890.201808.029

Zhang, Z. P., Shang, W., Wang, Q., Fu, G. Q., Zhang, W. X., and Wang, X. (2020). Biodiversity of herbaceous species under large photovoltaic power stations in desert region of Hexi corridor. *J. Northwest. For. Univ.* 35, 190–196. doi: 10.3969/j.issn.1001–7461.2020.02.28

Zhao, P. Y. (2016). *Effects of photovoltaic panels on surface soil particles and microclimate* Inner Mongolia Agricultural University Available at: https://kns.cnki.net/KCMS/detail/detail.aspx?dbname=CMFD201701&filename=1016249431.nh.

Zhou, L., Tian, Y., Roy, S. B., Thorncroft, C., and Hu, Y. (2012). Impacts of wind farms on land surface temperature. *Nat. Clim. Chang.* 2, 539–543. doi: 10.1038/nclimate1505

Zhou, M. R., and Wang, X. J. (2019). Influence of photovoltaic power station engineering on soil and vegetation: taking the Gobi Desert area in the Hexi corridor of Gansu as an example. *J. Soil Water Conserv.* 17, 132–138. doi: 10.16843/j.sswc.2019.02.016

Zhu, S. K., Wang, S., Zhang, J. T., Gao, D. D., and Shen, H. Y. (2021). Microclimate characteristics of photovoltaic arrays and their effects on plant growth in a solar power station area. *Chinese. J. Ecol.* 40, 3078–3087. doi: 10.13292/j.1000–4890.202110.016

frontiers | Frontiers in Ecology and Evolution

TYPE Original Research
PUBLISHED 11 April 2023
DOI 10.3389/fevo.2023.1170197

OPEN ACCESS

EDITED BY
Xiang Liu,
Lanzhou University, China

REVIEWED BY
Jing Yang,
East China Normal University, China
Jinliang Liu,
Wenzhou University, China

*CORRESPONDENCE
Yunquan Wang
yqwang@vip.126.com
Jianhua Chen
sky78@zjnu.cn

SPECIALTY SECTION
This article was submitted to Conservation and Restoration Ecology, a section of the journal Frontiers in Ecology and Evolution

RECEIVED 20 February 2023
ACCEPTED 14 March 2023
PUBLISHED 11 April 2023

CITATION
Chai P, Xie J, Yang L, Zheng R, Bian Y, Fu J, Wang Y and Chen J (2023) Community vertical stratification drives temporal taxonomic and phylogenetic beta diversity in a mixed broadleaf-conifer forest. *Front. Ecol. Evol.* 11:1170197. doi: 10.3389/fevo.2023.1170197

Community vertical stratification drives temporal taxonomic and phylogenetic beta diversity in a mixed broadleaf-conifer forest

Pengtao Chai[1], Jiajie Xie[1], Lisheng Yang[2], Rong Zheng[1], Yuxuan Bian[1], Jiaqin Fu[1], Yunquan Wang [1,3]* and Jianhua Chen[1]*

[1]College of Life Sciences, Zhejiang Normal University, Jinhua, China, [2]Zhuji Natural Resources and Planning Bureau, Zhuji, China, [3]College of Life Sciences, Zhejiang University, Hangzhou, China

Temporal change of beta diversity provides a better understanding of the extent and consequences of species composition in forest communities with the ongoing global climate change. However, relatively little is known about temporal beta diversity changes across vertical stratification in the forest. In this study, we divided more than 5,000 tree individuals from a mixed broadleaf-conifer forest into four vertical strata (i.e., shrub, subcanopy, lower canopy, and upper canopy) to quantify how vertical stratification drives the temporal change of taxonomic and phylogenetic beta diversity. We found that taxonomic beta diversity significantly decreased while phylogenetic beta diversity showed an insignificant increase after 5 years. When considering vertical stratification, taxonomic beta diversity in the subcanopy, lower canopy, and upper canopy significantly changed with inconsistent directions, but phylogenetic beta diversity in the shrub significantly increased. Moreover, the significant decrease in taxonomic beta diversity is mainly driven by changes in species composition in shrub and subcanopy stratification (with 85.89% contributions). The changes in phylogenetic beta diversity are driven by shifts in the shrub and upper canopy (with 96.02% contributions). Our study suggests that taking community vertical stratification into consideration contributes to a better understanding of temporal beta diversity in forest communities.

KEYWORDS

vertical structure, phylogenetic, taxonomic, temporal beta diversity, mixed broadleaf-conifer forest, Dongbaishan forest plot

1. Introduction

Beta diversity is defined as the spatial variation in species composition among sites, providing insights into the ecological processes and driving patterns of biodiversity in the context of the ongoing global climate change (Whittaker, 1960; Anderson et al., 2011; Magurran et al., 2018, 2019; Reu et al., 2022). Growing concerns about the state of biodiversity change with climate change highlight the need for a better understanding of the extent and consequences of species composition in forest communities. Forest communities are dynamic (Hilmers et al., 2018; Legendre, 2019; Wang et al., 2020a), and the shifts within

the community may drive temporal patterns of beta diversity (Magurran et al., 2018; Tatsumi et al., 2021). However, relatively little is known about how temporal beta diversity changes across vertical stratification in forest communities. The understanding of temporal beta diversity within forests can help us to understand forest community succession and highlight principal driving factors (Magurran et al., 2019).

In the process of forest community succession, the change in landscape of beta diversity may be affected by multiple factors. A study on the Loess Plateau of China (Chai et al., 2016) showed that taxonomic beta diversity did not change significantly with succession; however, other studies have found that taxonomic beta diversity decreased with succession (Kavgacı et al., 2010; Purschke et al., 2013). This difference may be related to forest age (Dalmaso et al., 2020), local climate (Keil et al., 2012), topography (Ahmad et al., 2020), research scales (Zhang et al., 2015), and other factors. Most studies of phylogenetic beta diversity showed a downward trend with succession (Purschke et al., 2013; Chai et al., 2016), indicating that deterministic processes gradually dominated the shift of phylogenetic structure in the community. The changes in temporal taxonomic and phylogenetic beta diversity can be explained at the species level (Tatsumi et al., 2021), and exploring the variation in diversity of different community structures containing different species composition can help provide greater insight into community successional mechanisms.

The vertical structure is an important structural feature of forests (Hao et al., 2007). Each vertical stratification has different levels of light absorption and transpiration (Tian et al., 2023), resulting in a pattern of vertical stratification of species composition (Onaindia et al., 2004; Wang et al., 2020b). Species occupying different vertical strata may show different responses to disturbance (Peterson and Reich, 2008; Decocq et al., 2014) such as climate change (Nakamura et al., 2017), among others. Therefore, as natural community succession progresses, the biodiversity represented across vertical stratification may also show alternative temporal changes with consequential impacts on the community as a whole. However, the contribution of diversity changes of each vertical stratum to overall diversity shifts during succession is unknown. Exploring this part of the research gap may help us to better understand the different outcomes of temporal beta diversity. In addition, previous studies have adopted a fixed standard method for measuring vertical stratification (Onaindia et al., 2004). However, this method does not account for the difference in local forest structure or the temporal change in structure that may occur during succession (Marziliano et al., 2013). Thus, in this study, we utilize a quantitative stratification method that accounts for the local variation of forest structure (Latham et al., 1998; Maeda et al., 2022). It is practical and meaningful to explore the temporal diversity of vertical stratification based on quantitative methods.

In this study, we explored the changes in taxonomic and phylogenetic beta diversity of vertical forest stratification during succession. We utilized tree census data from the Dongbaishan 1 ha mixed broadleaf-conifer forest in the Zhejiang Province in China (Wang et al., 2015), which was surveyed in 2013 and 2018. Individuals with DBH $\geq$ 1 cm were divided into different vertical stratification according to their height by using the TSTRAT algorithm and k-means cluster analysis. We focused on the following questions:

(1) How does taxonomic and phylogenetic beta diversity change within vertical stratification in this forest?
(2) How does the beta diversity in different vertical stratification contribute to the total temporal taxonomic and phylogenetic beta diversity?

2. Materials and methods

2.1. Study area and tree survey

The study was carried out in the Dongbaishan Provincial Nature Reserve (120°22′45″–120°30′48″E, 290°30′4″–290°30′48″N) in the Zhejiang Province in China with a total area of 5,071.5 ha and the main peak at an altitude of 1,194.6 m. Dongbaishan Nature Reserve has a mid-north subtropical monsoon climate with an average annual temperature of 11.7°C and an average annual precipitation of 1,541.4 mm. The area is rich in species with a total of 179 families, 749 genera, and 1,530 species of vascular plants (Wang et al., 2015).

In 2013, a 1 ha (100 m × 100 m) fixed dynamic monitoring plot (120°23′35.69″–120°23′40.63″ E, 290°23′40.63″–290°23′40.63″ N) was established in the Dongbaishan Nature Reserve following the construction standard of CForBio (Feng et al., 2016). The plot ranges from 135 to 157 m in elevation, ranges from 8° to 62° in slope, and consists of 25 20 m × 20 m quadrats. In 2013, all woody plants with DBH (diameter at breast height) $\geq$ 1 cm in the plot were investigated; the investigation content includes species name, DBH, height (vertical height from root to crown), crown base height, etc. Since then, the first re-census was conducted in 2018 (**Supplementary Table 1**).

2.2. Division of vertical stratification

The heights of all individuals were analyzed by the k-means clustering algorithm (Hartigan and Wong, 1979) to obtain the height of definitive vertical stratification. Before that, the range of optimal clustering number k is determined based on the number of strata under different competition coefficients obtained by the TSTRAT algorithm (Latham et al., 1998). The TSTRAT algorithm defines strata based on competing cut-off points with the tree canopy in a given area:

$$CCH = a * CL + HBLC \quad (1)$$

where CCH is the competition cut-off height, CL is the crown length, HBLC is the height-to-base of the live crown, and a is the competition coefficient. The range of a in this study is 0.3–0.5.

Then, the ideal clustering number k is found when the total sum of squares plateaus and when the gap statistic is at its maximum.

2.3. Analysis of taxonomic and phylogenetic beta diversity

The abundance-based Bray-Curtis index (β_{bc}) (Baselga and Chao, 2016) was chosen to measure the taxonomic beta diversity

of the total community and each vertical stratification:

$$\beta_{bc} = \frac{B + C}{2A + B + C} \quad (2)$$

where A is the abundance of individuals of each species that exist in both sites j and k; B and C are the abundances of individuals that are unique to sites j and k, respectively.

The MPD_beta (interassemblage mean pairwise distance) was chosen to measure the phylogenetic beta diversity of the total community and each vertical stratification because MPD_beta was the most robust beta diversity metric to the source of the phylogeny (Li et al., 2019). In order to test whether the phylogenetic structure was different from the random expectation, a further comparison of MPD_beta with the null model was required (Miller et al., 2017). Specifically, the null model was constructed by fixing the species richness and occurrence frequency of each quadrat, and the identities of those species were randomly drawn from the whole species pool (Li et al., 2015). After constructing the null model 9,999 times, the standardized effect sizes of MPD_beta (SES.MPD_beta) were calculated as:

$$SES.MPD\_beta = \frac{(\chi_{obs} - \overline{\chi_{null}})}{SD_{null}} \quad (3)$$

where χ_{obs} is the observed value, $\overline{\chi_{null}}$ is the mean of the simulated values, and SD_{null} is the standard deviation of the simulated values. Positive SES.MPD_beta values indicate phylogenetic overdispersion, whereas negative values indicate clustering. If SES.MPD_beta $= 0$, it indicates that the species between the quadrats are random in the phylogenetic structure.

2.4. Statistical analysis

To examine the dynamic changes in the beta diversity of vertical stratification from 2013 to 2018, we used mixed effects models to fit β_{bc} and SES.MPD_beta as a function of years. The year was treated as a single continuous fixed factor, and the pairwise groups between the quadrats were considered random effects. In addition, to measure the contribution of different vertical stratification to the beta diversity of the whole community, we used the "lmg" method which is a measure of the relative importance of the independent variables (Grömping, 2009).

All analyses were performed in R (version 4.2.2). The Bray-Curtis index and SES.MPD_beta were calculated using the "betapart" package (Baselga and Orme, 2012) and the "pincate" package (Kembel et al., 2010). Construction of the phylogenetic tree (**Supplementary Figure 1**) was completed through the

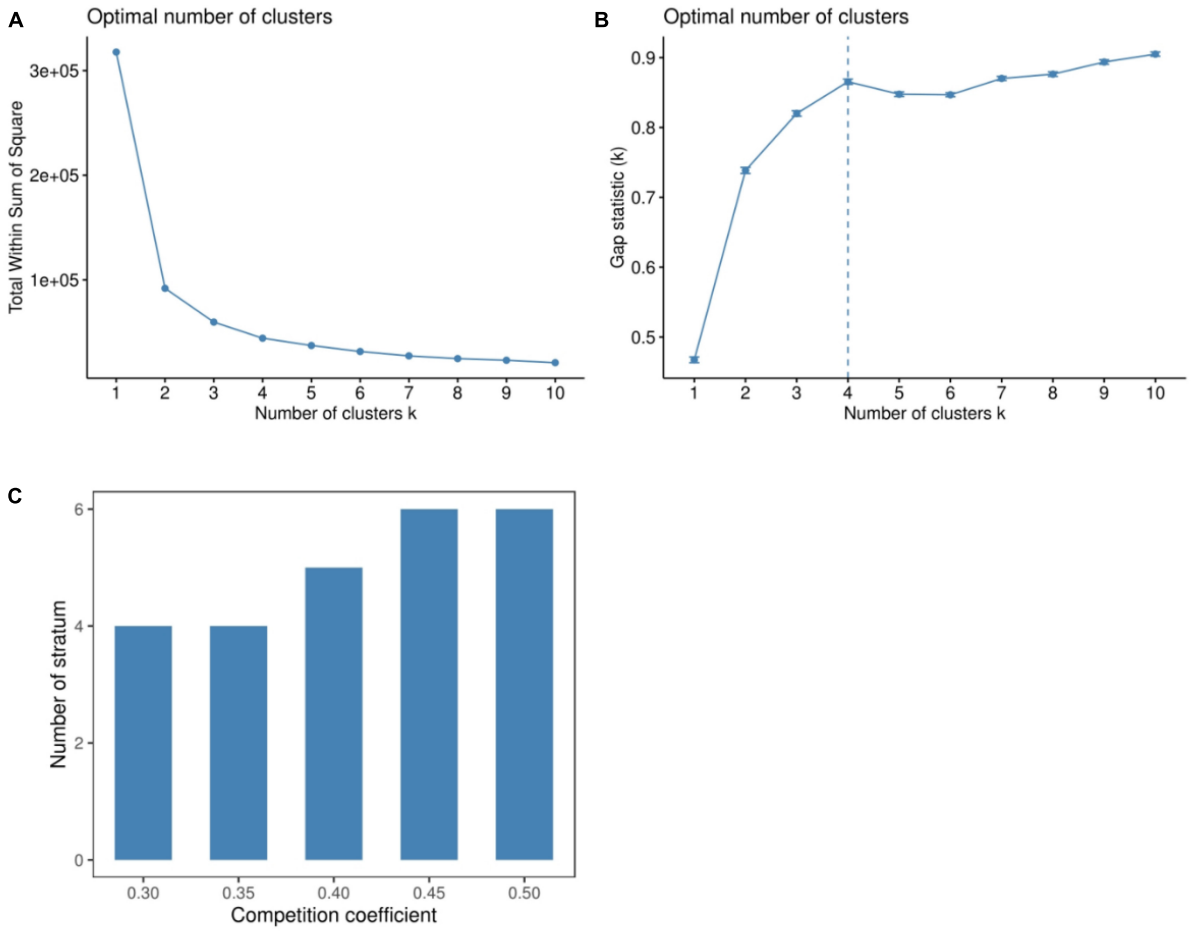

FIGURE 1
Results of the sum of squares **(A)**, gap statistics **(B)**, and TSTRAT algorithm **(C)**.

TABLE 1 Basic information on each vertical stratum in the Dongbaishan forest between 2013 and 2018.

Year	Layer	Minimum height	Maximum height	Average DBH	Abundance	Richness
2013	Shrub	0.0	4.6	2.135	1,770	37
	Subcanopy	4.7	8.2	5.704	1,103	32
	Lower canopy	8.3	11.2	11.079	1,504	14
	Upper canopy	11.3	17.0	14.908	1,118	13
2018	Shrub	0.4	5.8	2.042	963	25
	Subcanopy	6.0	11.2	6.379	864	20
	Lower canopy	11.5	16.5	12.253	1,110	13
	Upper canopy	16.8	23.0	16.451	1,116	12

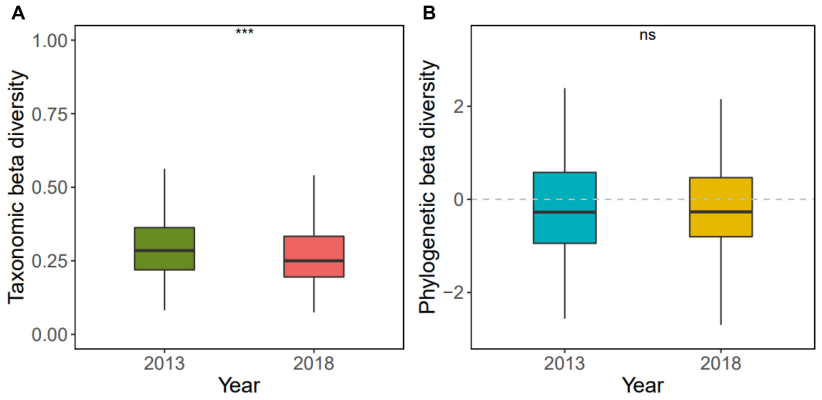

FIGURE 2
Changes in taxonomic beta diversity **(A)** and phylogenetic beta diversity **(B)** in the Dongbaishan forest between 2013 and 2018. $^{ns}p > 0.05$, $^{*}p \leq 0.05$, $^{**}p \leq 0.01$, $^{***}p \leq 0.001$, $^{****}p \leq 0.0001$.

"V.PhyloMaker" package (Jin and Qian, 2019, 2022). The mixed effects model was built by "lme4" packages (Bates et al., 2014). The "lmg" method was completed through the "relaimpo" package (Groemping, 2006).

3. Results

3.1. Division of vertical stratification

According to the k-means clustering algorithm and TSTRAT algorithm, when the number of classified groups reached four groups, the change of the sum of squares within the group tended to be flat (Figure 1A). The line chart of gap statistics showed that when k was four, it was the optimal number of clusters (Figure 1B). At the same time, the number of classification groups could be divided into four to six strata according to the competition coefficient (Figure 1C). Therefore, the vertical structure of the plot was divided into four strata. Combined with height data of each vertical stratum obtained according to the clustering algorithm, these four strata can be defined as shrub, subcanopy, lower canopy, and upper canopy.

Comparing the community characteristics of the four vertical strata in 2013 and 2018 (Table 1), we found that the height of each vertical stratum increased, especially in the lower canopy and upper canopy. Additionally, except for the shrub layer, the average DBH increased for each layer. Lastly, the abundance of the shrub, subcanopy, and lower canopy decreased, and the richness of the shrub and subcanopy decreased.

3.2. Temporal beta diversity change across vertical stratification

The taxonomic beta diversity of the secondary Dongbaishan mixed broadleaf-conifer forest decreased significantly ($p < 0.001$) during succession from 2013 to 2018 (Figure 2A and Supplementary Table 2), indicating that the species composition among the quadrats homogenized over time. On the other hand, phylogenetic beta diversity showed no significant trend (Figure 2B and Supplementary Table 2).

The taxonomic beta diversity of each vertical stratum varied from 2013 to 2018 (Figure 3 and Supplementary Table 2). The taxonomic beta diversity of the subcanopy decreased significantly ($p < 0.001$), which indicates that the species composition among the quadrats homogenized. The taxonomic beta diversity of the upper canopy and lower canopy increased significantly ($p < 0.0001$), which means that the species composition among the quadrats heterogenized.

The phylogenetic beta diversity of each vertical stratum also varied from 2013 to 2018 (Figure 4 and Supplementary Table 2). In 2013, the phylogenetic distance of the lower canopy was more distant than that of other vertical strata, but by 2018, the

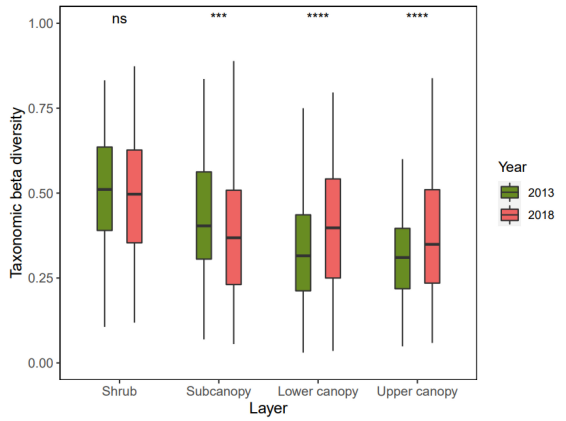

FIGURE 3
Changes of taxonomic beta diversity in four vertical stratification in the Dongbaishan forest between 2013 and 2018. $^{ns}p > 0.05$, $^{*}p \leq 0.05$, $^{**}p \leq 0.01$, $^{***}p \leq 0.001$, $^{****}p \leq 0.0001$.

vertical stratification with the most distant phylogenetic distance between the quadrats were the upper canopy. Across time periods, the phylogenetic distance of the shrub significantly increased ($p < 0.0001$) and the upper canopy slightly significantly increased ($p = 0.0687$), whereas the lower canopy decreased.

3.3. Relative contribution of different vertical stratification to temporal taxonomic and phylogenetic beta diversity

The changes in beta diversity of each vertical stratum had different implications for the changes of beta diversity for the whole community (**Figure 5**). The changes in beta diversity in the shrub and subcanopy were the main explanatory variables of community beta diversity. Shrub and subcanopy together were responsible for 85.89% of the changes in taxonomic beta diversity. Shrub and upper canopy jointly were responsible for 96.02% of the changes in phylogenetic beta diversity, although, overall, there was no significant increase or decrease with succession.

4. Discussion

4.1. Temporal taxonomic and phylogenetic beta diversity change across vertical stratification

With succession at our site, the height of each vertical stratum gradually increased, highlighting the different growth conditions and environmental adaptability of the species in each stratum. The abundance and frequency of the shrub decreased, especially the dominant species such as *Schima superba* and other rare species such as *Litsea cubeba* (**Supplementary Tables 3, 4**). Nevertheless, the results of partitioning beta diversity showed that there were no significant changes in abundance gradients and abundance balances (**Supplementary Figures 2, 3** and **Supplementary Table 5**) likely because of the decrease of common abundance (concatenation of abundance among quadrats) in dominant species and the decrease of unique abundance (complementary of abundance among quadrats) caused by rare species counteracting each other on the difference of species composition of the whole community. Finally, the results also showed that the taxonomic beta diversity did not change significantly. It is worth noting that the difference in species composition between shrub stratification is determined more by the turnover of species abundance (i.e., the decrease of common abundance), which indicates that shrub species may be more vulnerable to dispersal limitation and environmental filtering (Shi et al., 2021; Hu et al., 2022).

The decrease in abundance of some rare species in the subcanopy and the frequency of some dominant species such as *Pinus massoniana* and *Lithocar pusglaber* reduced the change of abundance balances (that is, the turnover of species abundance decreased), which was characterized by a significant decrease in taxonomic beta diversity. The canopy showed an increase in taxonomic beta diversity, indicating that the difference between canopies within the community gradually increased. This result may be related to the increase of the abundance gradients, thereby indicating an influence of selective local extinction/colonization of some species in the canopy (Wang et al., 2010). Unlike the shrub, the difference in species composition among the subcanopy, lower canopy, and upper canopy was determined primarily by abundance gradients, indicating that there may be strong selective local extinction/colonization in these vertical strata. In addition, there were some species in the three higher vertical strata that do not exist in the shrub stratification (**Supplementary Table 1**), which might inhibit the growth of other species because of the priority effect (Gui et al., 2019; Solarik et al., 2020), thus making the components of the abundance turnover of beta diversity smaller.

Importantly, there were two extreme droughts in Dongbaishan from 2013 to 2018, which significantly inhibited the plant growth of herbs and shrubs (Copeland et al., 2016; Jacobsen and Pratt, 2018). In addition, rare species have rarer numbers of individuals and seed sources, making them more vulnerable to local extinction from strong disturbances such as drought (Tilman and El Haddi, 1992), which may have impacted the shift in community composition in Dongbaishan.

The phylogenetic beta diversity of the shrub and the upper canopy showed a downward trend and were not greater than 0, suggesting that the phylogenetic beta diversity change in the two vertical strata was driven by an increase in relatedness in the community. The phylogenetic beta diversity of the subcanopy did not change significantly, but the values were all less than 0, indicating that the phylogenetic turnover between the subcanopies was also driven by closely related individuals (Chai et al., 2016). On the other hand, the phylogenetic turnover of the lower canopy changed from being driven by randomized individuals to closely related individuals. This may be due to different responses from different vertical stratification to biotic/abiotic factors such as extreme drought and negative density dependence (Fibich et al., 2021; Yan et al., 2022).

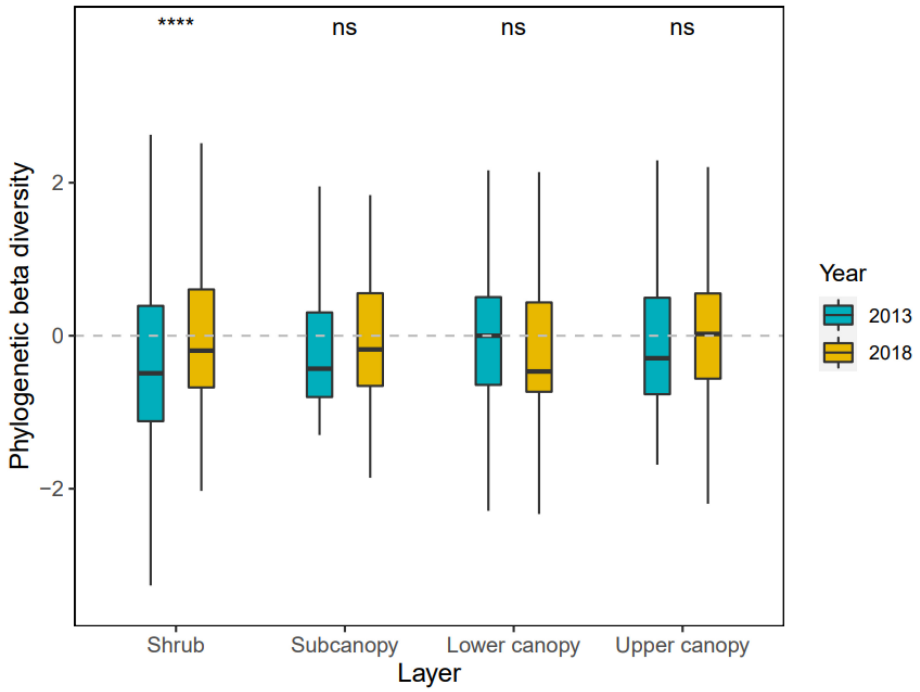

FIGURE 4
Changes of phylogenetic beta diversity in four vertical stratification in the Dongbaishan forest between 2013 and 2018. $^{ns}p > 0.05$, $^{*}p \leq 0.05$, $^{**}p \leq 0.01$, $^{***}p \leq 0.001$, $^{****}p \leq 0.0001$.

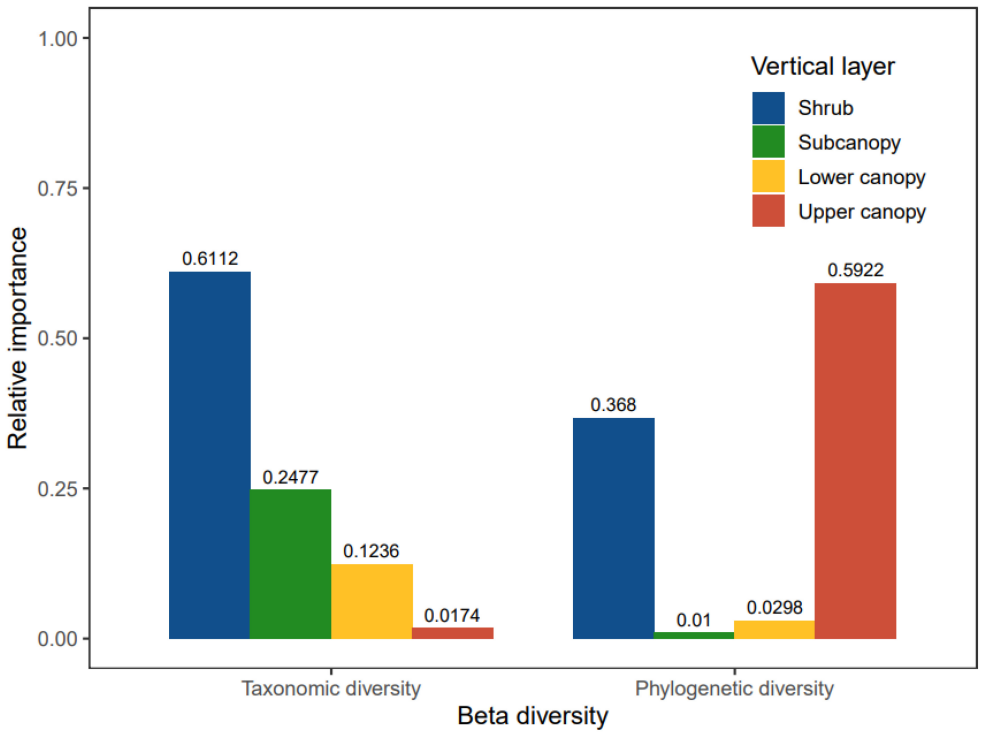

FIGURE 5
The relative contribution of different vertical stratification to temporal taxonomic and phylogenetic beta diversity in the Dongbaishan forest.

4.2. Contribution of each vertical stratification to temporal taxonomic and phylogenetic beta diversity

In this study, we found that the taxonomic beta diversity of the community decreased with succession, indicating that the species composition among the quadrats is becoming homogenized. This can be seen in the decrease in community abundance balances and the decline of the abundance gradients (**Supplementary Table 5**). Combined with the changes in abundance and frequency (**Supplementary Table 1**), the decrease in unique abundance is essential for the changes in the taxonomic beta diversity, especially the unique abundance of rare species. From the perspective of vertical structure, this difference is mainly affected by changes in the shrub and subcanopy stratification (although the interannual taxonomic beta diversity of the shrub is only weakly significant). This may be due to the high richness of the shrub and subcanopy stratification, and there are more rare species in a few quadrats than the canopy, but because the trees are relatively small and weakly resistant to disturbance, they are easily affected by external factors (such as fire, drought, and pests) and local extinction (Lang and Knight, 1983; Klesse et al., 2021; Masaki et al., 2021; Yang et al., 2022). At the same time, the dominant species of these two strata are more likely to be affected by negative density dependence restriction and upper stratification (Sercu et al., 2017).

The phylogenetic beta diversity of the community increased, indicating that the phylogenetic turnover in the community is driven by closely related individuals to randomized individuals. This is different from the result of other studies (Purschke et al., 2013; Chai et al., 2016), possibly because the time span of this study was small and involved extreme weather events. The randomization of community phylogenetic turnover was mainly affected by changes in the shrub and the upper canopy stratification, especially the upper canopy. We found that this is because the dominant species in the upper canopy may have a greater relative influence on the species composition and phylogenetic structure of the vertical stratification below the upper canopy (Yuan et al., 2012; Nakamura et al., 2017). For example, the upper canopy may influence competition in the lower stratification, especially in the shrub (Oberle et al., 2009).

5. Conclusion

Analysis of taxonomic and phylogenetic beta diversity in each vertical stratification of the community during succession provides insight into the influence of dynamic vertical distribution patterns on the forest plant community as a whole (Chai et al., 2016; Gui et al., 2019; Magurran et al., 2019). During succession, taxonomic and phylogenetic beta diversity varied across vertical stratification, suggesting that the assessment of community diversity requires data collected across the vertical space. In this subtropical secondary mixed coniferous forest, species composition differences across a successional period were mainly influenced by a decrease in unique abundance in the shrub and subcanopy stratification, while the phylogenetic turnover of the community tended to randomize, mainly driven by stochastic processes in the shrub and upper canopy stratification. We found that temporal beta diversity in this community was driven by the uppermost and lowermost stratification of the vertical structure.

Data availability statement

The original contributions presented in this study are included in the article/**Supplementary material**, further inquiries can be directed to the corresponding authors.

Author contributions

PC, YW, and JC conceived and designed the study and collected the data. PC performed the statistical analyses and wrote the first draft with substantial input from YW and JC. JX, LY, RZ, YB, and JF contributed to the development of the final manuscript. All authors read and agreed to the published version of the manuscript.

Funding

This study was financially supported by the "Pioneer" and "Leading Goose" R&D Program of Zhejiang (2023C03137) and Zhejiang Provincial Natural Science Foundation of China (LQ22C030001).

Acknowledgments

We acknowledge the Zhuji Natural Resources and Planning Bureau for the support provided for this study. We are grateful to Yu Mingjian from Zhejiang University for the helpful feedback in improving this manuscript and Joseph Elliot at the University of Kansas for his assistance with the English language and grammatical editing of the manuscript.

Conflict of interest

The authors declare that the research was conducted in the absence of any commercial or financial relationships that could be construed as a potential conflict of interest.

Publisher's note

Supplementary material

The Supplementary Material for this article can be found online at: https://www.frontiersin.org/articles/10.3389/fevo.2023.1170197/full#supplementary-material

References

Ahmad, M., Uniyal, S. K., Batish, D. R., Singh, H. P., Jaryan, V., Rathee, S., et al. (2020). Patterns of plant communities along vertical gradient in dhauladhar mountains in lesser himalayas in North-Western India. *Sci. Total Environ.* 716:136919. doi: 10.1016/j.scitotenv.2020.136919

Anderson, M. J., Crist, T. O., Chase, J. M., Vellend, M., Inouye, B. D., Freestone, A. L., et al. (2011). Navigating the multiple meanings of β diversity: a roadmap for the practicing ecologist. *Ecol. Lett.* 14, 19–28. doi: 10.1111/j.1461-0248.2010.01552.x

Baselga, A., and Chao, A. (2016). Partitioning abundance-based multiple-site dissimilarity into components: balanced variation in abundance and abundance gradients. *Methods Ecol. Evol.* 8, 799–808. doi: 10.1111/2041-210X.12693

Baselga, A., and Orme, C. D. L. (2012). betapart: an R package for the study of beta diversity. *Methods Ecol. Evol.* 3, 808–812. doi: 10.1111/j.2041-210X.2012.00224.x

Bates, D. M., Machler, M., Bolker, B. M., and Walker, S. C. (2014). Fitting linear mixed-effects models using lme4. *J. Stat. Softw.* 67, 1–48. doi: 10.18637/jss.v067.i01

Chai, Y., Yue, M., Liu, X., Guo, Y., Wang, M., Xu, J., et al. (2016). Patterns of taxonomic, phylogenetic diversity during a long-term succession of forest on the Loess Plateau, China: insights into assembly process. *Sci. Rep.* 6:27087. doi: 10.1038/srep27087

Copeland, S. M., Harrison, S. P., Latimer, A. M., Damschen, E. I., Eskelinen, A. M., Fernandez-Going, B., et al. (2016). Ecological effects of extreme drought on Californian herbaceous plant communities. *Ecol. Monogr.* 86, 295–311. doi: 10.1002/ecm.1218

Dalmaso, C. A., Marques, M. C. M., Higuchi, P., Zwiener, V. P., and Marques, R. (2020). Spatial and temporal structure of diversity and demographic dynamics along a successional gradient of tropical forests in southern Brazil. *Ecol. Evol.* 10, 3164–3177. doi: 10.1002/ece3.5816

Decocq, G., Beina, D., Jamoneau, A., Gourlet-Fleury, S., and Closset-Kopp, D. (2014). Don't miss the forest for the trees! evidence for vertical differences in the response of plant diversity to disturbance in a tropical rain forest. *Perspect. Plant Ecol. Evol. Syst.* 16, 279–287. doi: 10.1016/j.ppees.2014.09.001

Feng, G., Mi, X., Yan, H., Li, F. Y., Svenning, J.-C., and Ma, K. (2016). CForBio: a network monitoring Chinese forest biodiversity. *Sci. Bull.* 61, 1163–1170. doi: 10.13287/j.1001-9332.202108.001

Fibich, P., Ishihara, M. I., Suzuki, S. N., Doležal, J., and Altman, J. (2021). Contribution of conspecific negative density dependence to species diversity is increasing towards low environmental limitation in Japanese forests. *Sci. Rep.* 11:18712. doi: 10.1038/s41598-021-98025-5

Groemping, U. (2006). Relative importance for linear regression in R: the package relaimpo. *J. Stat. Softw.* 17, 1–27. doi: 10.18637/jss.v017.i01

Grömping, U. (2009). Variable importance assessment in regression: linear regression versus random forest. *Am. Statistician* 63, 308–319. doi: 10.3389/fpls.2022.722442

Gui, X., Lian, J., Zhang, R., Li, Y., Shen, H., Ni, Y., et al. (2019). Vertical structure and its biodiversity in a subtropical evergreen broad-leaved forest at dinghushan in Guangdong province, China. *Biodiversity Sci.* 27:619. doi: 10.17520/biods.2019107

Hao, Z., Zhang, J., Song, B., Ye, J., and Li, B. (2007). Vertical structure and spatial associations of dominant tree species in an old-growth temperate forest. *For. Ecol. Manag.* 252, 1–11. doi: 10.1016/j.foreco.2007.06.026

Hartigan, J. A., and Wong, M. A. (1979). Algorithm as 136: a k-means clustering algorithm. *J. R. Stat. Soc. Ser. C* 28, 100–108. doi: 10.2307/2346830

Hilmers, T., Friess, N., Bässler, C., Heurich, M., Brandl, R., Pretzsch, H., et al. (2018). Biodiversity along temperate forest succession. *J. Appl. Ecol.* 55, 2756–2766. doi: 10.1111/1365-2664.13238

Hu, D., Jiang, L., Hou, Z., Zhang, J., Wang, H., and Lv, G. (2022). Environmental filtration and dispersal limitation explain different aspects of beta diversity in desert plant communities. *Glob. Ecol. Conserv.* 33:e01956. doi: 10.1016/j.gecco.2021.e01956

Jacobsen, A. L., and Pratt, R. B. (2018). Extensive drought-associated plant mortality as an agent of type-conversion in chaparral shrublands. *New Phytol.* 219, 498–504. doi: 10.1111/nph.15186

Jin, Y., and Qian, H. (2019). V.PhyloMaker: an R package that can generate very large phylogenies for vascular plants. *Ecography* 42, 1353–1359. doi: 10.1111/ecog.04434

Jin, Y., and Qian, H. (2022). V.PhyloMaker2: an updated and enlarged R package that can generate very large phylogenies for vascular plants. *Plant Divers.* 44, 335–339. doi: 10.1016/j.pld.2022.05.005

Kavgacı, A., Čarni, A., Başaran, S., Başaran, M. A., Košir, P., Marinšek, A., et al. (2010). Long-term post-fire succession of *Pinus brutia* forest in the east mediterranean. *Int. J. Wildland Fire* 19, 599–605. doi: 10.1071/WF08044

Keil, P., Schweiger, O., Kühn, I., Kunin, W. E., Kuussaari, M., Settele, J., et al. (2012). Patterns of beta diversity in Europe: the role of climate, land cover and distance across scales. *J. Biogeogr.* 39, 1473–1486. doi: 10.1111/j.1365-2699.2012.02701.x

Kembel, S. W., Cowan, P. D., Helmus, M. R., Cornwell, W. K., Morlon, H., Ackerly, D. D., et al. (2010). Picante: R tools for integrating phylogenies and ecology. *Bioinformatics* 26, 1463–1464. doi: 10.1093/bioinformatics/btq166

Klesse, S., Abegg, M., Hopf, S. E., Gossner, M. M., Rigling, A., and Queloz, V. (2021). Spread and severity of ash dieback in Switzerland - tree characteristics and landscape features explain varying mortality probability. *Front. For. Glob. Change* 4:645920. doi: 10.3389/ffgc.2021.645920

Lang, G. E., and Knight, D. H. (1983). Tree growth, mortality, recruitment, and canopy gap formation during a 10-year period in a tropical moist forest. *Ecology* 64, 1075–1080. doi: 10.2307/1937816

Latham, P. A., Zuuring, H. R., and Coble, D. W. (1998). A method for quantifying vertical forest structure. *For. Ecol. Manag.* 104, 157–170. doi: 10.1016/S0378-1127(97)00254-5

Legendre, P. (2019). A temporal beta-diversity index to identify sites that have changed in exceptional ways in space–time surveys. *Ecol. Evol.* 9, 3500–3514. doi: 10.1002/ece3.4984

Li, D., Trotta, L., Marx, H. E., Allen, J. M., Sun, M., Soltis, D. E., et al. (2019). For common community phylogenetic analyses, go ahead and use synthesis phylogenies. *Ecology* 100:e02788. doi: 10.1002/ecy.2788

Li, S. P., Cadotte, M. W., Meiners, S. J., Hua, Z. S., Jiang, L., and Shu, W. S. (2015). Species colonisation, not competitive exclusion, drives community overdispersion over long-term succession. *Ecol. Lett.* 18, 964–973. doi: 10.1111/ele.12476

Maeda, E. E., Nunes, M. H., Calders, K., Moura, Y. M. D., Raumonen, P., Tuomisto, H., et al. (2022). Shifts in structural diversity of Amazonian forest edges detected using terrestrial laser scanning. *Remote Sens. Environ.* 271:112895. doi: 10.1016/j.rse.2022.112895

Magurran, A. E., Deacon, A. E., Moyes, F., Shimadzu, H., Dornelas, M., Phillip, D. A. T., et al. (2018). Divergent biodiversity change within ecosystems. *Proc. Natl. Acad. Sci. U S A.* 115, 1843–1847. doi: 10.1073/pnas.1712594115

Magurran, A. E., Dornelas, M., Moyes, F., and Henderson, P. A. (2019). Temporal β diversity—a macroecological perspective. *Glob. Ecol. Biogeogr.* 28, 1949–1960. doi: 10.1111/geb.13026

Marziliano, P. A., Lafortezza, R., Colangelo, G., Davies, C., and Sanesi, G. (2013). Structural diversity and height growth models in urban forest plantations: a case-study in northern Italy. *Urban For. Urban Greening* 12, 246–254. doi: 10.1016/j.ufug.2013.01.006

Masaki, T., Kitagawa, R., Nakashizuka, T., Shibata, M., and Tanaka, H. (2021). Interspecific variation in mortality and growth and changes in their relationship with size class in an old-growth temperate forest. *Ecol. Evol.* 11, 8869–8881. doi: 10.1002/ece3.7720

Miller, E. T., Farine, D. R., and Trisos, C. H. (2017). Phylogenetic community structure metrics and null models: a review with new methods and software. *Ecography* 40, 461–477. doi: 10.1111/ecog.02070

Nakamura, A., Kitching, R. L., Cao, M., Creedy, T. J., Fayle, T. M., Freiberg, M., et al. (2017). Forests and their canopies: achievements and horizons in canopy science. *Trends Ecol. Evol.* 32, 438–451. doi: 10.1016/j.tree.2017.02.020

Oberle, B., Grace, J. B., and Chase, J. M. (2009). Beneath the veil: plant growth form influences the strength of species richness–productivity relationships in forests. *Glob. Ecol. Biogeogr.* 18, 416–425. doi: 10.1111/j.1466-8238.2009.00457.x

Onaindia, M., Dominguez, I., Albizu, I., Garbisu, C., and Amezaga, I. (2004). Vegetation diversity and vertical structure as indicators of forest disturbance. *For. Ecol. Manag.* 195, 341–354. doi: 10.1371/journal.pone.0164917

Peterson, D. W., and Reich, P. B. (2008). Fire frequency and tree canopy structure influence plant species diversity in a forest-grassland ecotone. *Plant Ecol.* 194, 5–16. doi: 10.1007/s11258-007-9270-4

Purschke, O., Schmid, B. C., Sykes, M. T., Poschlod, P., Michalski, S. G., Durka, W., et al. (2013). Contrasting changes in taxonomic, phylogenetic and functional diversity during a long-term succession: insights into assembly processes. *J. Ecol.* 101, 857–866. doi: 10.1111/1365-2745.12098

Reu, J. C., Catano, C. P., Spasojevic, M. J., and Myers, J. A. (2022). Beta diversity as a driver of forest biomass across spatial scales. *Ecology* 103:e3774. doi: 10.1002/ecy.3774

Sercu, B. K., Baeten, L., van Coillie, F., Martel, A., Lens, L., Verheyen, K., et al. (2017). How tree species identity and diversity affect light transmittance to the understory in mature temperate forests. *Ecol. Evol.* 7, 10861–10870. doi: 10.1002/ece3.3528

Shi, W., Wang, Y. Q., Xiang, W. S., Li, X. K., and Cao, K. F. (2021). Environmental filtering and dispersal limitation jointly shaped the taxonomic and phylogenetic beta diversity of natural forests in southern China. *Ecol. Evol.* 11, 8783–8794. doi: 10.1002/ece3.7711

Solarik, K. A., Cazelles, K., Messier, C., Bergeron, Y., and Gravel, D. (2020). Priority effects will impede range shifts of temperate tree species into the boreal forest. *J. Ecol.* 108, 1155–1173. doi: 10.1111/1365-2745.13311

Tatsumi, S., Iritani, R., and Cadotte, M. W. (2021). Temporal changes in spatial variation: partitioning the extinction and colonisation components of beta diversity. *Ecol. Lett.* 24, 1063–1072. doi: 10.1111/ele.13720

Tian, K., Chai, P., Wang, Y., Chen, L., Qian, H., Chen, S., et al. (2023). Species diversity pattern and its drivers of the understory herbaceous plants in a Chinese subtropical forest. *Front. Ecol. Evol.* 10:1113742. doi: 10.3389/fevo.2022.1113742

Tilman, D., and El Haddi, A. (1992). Drought and biodiversity in grasslands. *Oecologia* 89, 257–264. doi: 10.1007/BF00317226

Wang, Y., Bao, Y., Yu, M., Xu, G., and Ding, P. (2010). Biodiversity research: Nestedness for different reasons: the distributions of birds, lizards and small mammals on islands of an inundated lake. *Divers. Distrib.* 16, 862–873. doi: 10.1111/j.1472-4642.2010.00682.x

Wang, Y., Cadotte, M. W., Chen, J., Mi, X., Ren, H., Liu, X., et al. (2020a). Neighborhood interactions on seedling survival were greatly altered following an extreme winter storm. *For. Ecol. Manag.* 461:117940. doi: 10.1016/j.foreco.2020.117940

Wang, Y., Yu, J., Xiao, L., Zhong, Z., Wang, Q., and Wang, W. (2020b). Dominant species abundance, vertical structure and plant diversity response to nature forest protection in Northeastern China: conservation effects and implications. *Forests* 11:295. doi: 10.3390/f11030295

Wang, Y., Tian, L., Zhong, L., Yang, H., Jin, H., Liu, C., et al. (2015). Community structure and species diversity of schima superba-Pinus massoniana communities in dongbaishan nature reserve. *J. Zhejiang Univer.* 42, 38–46.

Whittaker, R. H. (1960). Vegetation of the siskiyou mountains, oregon and California. *Ecol. Monogr.* 30, 279–338. doi: 10.1002/ecy.3764

Yan, M., Liu, Z., Subei, M., Liang, L., and Xi, W. (2022). The complex impacts of unprecedented drought on forest tree mortality: a case study of dead trees in east Texas, USA. *Acta Ecologica Sinica* 42, 1034–1046. doi: 10.5846/stxb202101150152

Yang, Y., Ji, Y., Wang, Y., Xie, J., Jin, Y., Mi, X., et al. (2022). Extreme winter storms have variable effects on the population dynamics of canopy dominant species in an old-growth subtropical forest. *Forests.* 13:1634. doi: 10.3390/f13101634

Yuan, Z., Gazol, A., Wang, X., Xing, D., Lin, F., Bai, X., et al. (2012). What happens below the canopy? direct and indirect influences of the dominant species on forest vertical layers. *Oikos* 121, 1145–1153. doi: 10.1111/j.1600-0706.2011.19757.x

Zhang, Y., Ma, K., Anand, M., Ye, W., and Fu, B. (2015). Scale dependence of the beta diversity-scale relationship. *Community Ecol.* 16, 39–47. doi: 10.1556/168.2015.16.1.5

frontiers | Frontiers in Ecology and Evolution

TYPE Original Research
PUBLISHED 28 April 2023
DOI 10.3389/fevo.2023.1187996

OPEN ACCESS

EDITED BY
Xiang Liu,
Lanzhou University, China

REVIEWED BY
Mu Liu,
Lanzhou University, China
Fei Chen,
Nanjing University, China

*CORRESPONDENCE
Xiaohua Chen
✉ 965819833@qq.com

RECEIVED 16 March 2023
ACCEPTED 11 April 2023
PUBLISHED 28 April 2023

CITATION
Yang Q and Chen X (2023) Plant phylogenetic relatedness and herbivore specialization interact to determine pest biocontrol efficiency in mixed plantations.
Front. Ecol. Evol. 11:1187996.
doi: 10.3389/fevo.2023.1187996

Plant phylogenetic relatedness and herbivore specialization interact to determine pest biocontrol efficiency in mixed plantations

Qingqing Yang and Xiaohua Chen*

Hainan Academy of Forestry (Hainan Academy of Mangrove), Haikou, China

Pest herbivory regulation is one of the key functions provided by diverse ecosystems, especially when compared to species depauperate agro-ecosystems and in the context of increased pest outbreaks due to global change. The dilution effect of host diversity on insect herbivory suggests that mixed plantations are feasible for regulating pest herbivory in agroecosystems. Dilution effect of increased plant diversity on insect herbivory has been widely observed, yet little is known about how it may change with plant phylogenetic relatedness and herbivore specialization, especially at the community level. Here, we compared herbivore richness, abundance, and degree of herbivory (i.e., the ratio of trees damaged by pest and total trees in a given area) among the two monocultures and the four mixed plantations in Wenchang city, Hainan Province, China. We also respectively assessed the effects of phylogenetically close or distant species on generalist and specialist herbivores in monocultures and mixture. We found that increasing the number of phylogenetically closely-related tree species could dilute generalist herbivore richness, abundance, and degree of herbivory but amplify specialist herbivore richness, abundance, and degree of herbivory. In contrast, increasing the number of phylogenetically distant tree species increased generalist herbivore richness, abundance, and degree of herbivory, while reducing specialist herbivore richness, abundance, and degree of herbivory. Our results suggest that plant phylogenetic relatedness and herbivore specialization can indeed interact to influence pest control efficiency when using mixed plantations to manage pest herbivory in agroecosystems. Thus, both herbivore specialization and plant phylogenetic relatedness should be taken into account in the management of agro-ecosystems and biodiversity conservation with respect to herbivory.

KEYWORDS

phylogenetic relatedness, herbivore specialization, plant-insect herbivore interaction amplification effect, dilution effect, generalist, herbivory, specialist

1. Introduction

The anthropogenic acceleration of biodiversity loss (Pimm et al., 2014) and its detrimental effects on ecosystem functions remain one of the major concerns in ecology (Tilman et al., 2014). Pest herbivory regulation is one of the key functions provided by diverse ecosystems, which is especially important for agro-ecosystems in the context of increased pest outbreaks due to global change (Jactel et al., 2012; Klapwijk et al., 2012; Castagneyrol et al., 2014; Andrew and Hill, 2017). Given the widely acknowledged phenomenon that increasing plant diversity can have a dilution effect (i.e., increasing plant diversity results in decreased pest herbivory)

on insect herbivory, mixed plantations can potentially provide a key ecosystem service for the regulation of pest herbivory in mono-plantation in agroecosystems (Castagneyrol et al., 2014). However, the magnitude of the dilution effect of plant diversity on pest herbivory is known to vary according to the composition of plant and herbivore communities (Jactel and Brockerhoff, 2007; Vehvilainen et al., 2007; Barbosa et al., 2009). Moreover, evidence refuting this effect (i.e., that increasing plant diversity leads to increased pest herbivory) has also been found in other studies (Schuldt et al., 2015; Zhang et al., 2017; Grossman et al., 2018). As a result, it remains unclear whether increasing plant diversity through mixed plantations can be used to help manage pest herbivory in agroecosystems.

Recent synthesis studies highlight two primary factors that may be responsible for the lack of consensus regarding plant diversity-herbivory relationships (Jactel and Brockerhoff, 2007; Castagneyrol et al., 2014). First, host specificity of herbivores, particularly herbivory by specialist species (feeding on a specific plant genus), is usually reduced in diverse communities compared to monocultures (but see Plath et al., 2012). In contrast, the response of generalist species (feeding on different plant genus) is asynchronous in terms of its direction and magnitude (Schuldt et al., 2015). The second possibility regards the plant diversity being examined. Previous studies have shown that plant functional and phylogenetic diversity of the host community, and the relative abundance of the focal plant species, is more important than plant species richness in regulating the magnitude of herbivory (Mouquet et al., 2012). Moreover, herbivore specificity and plant phylogenetic relatedness interact to regulate the intensity of herbivory (Castagneyrol et al., 2014).

Till now, the associational resistance hypothesis has been recognized as the primary mechanism driving the dilution effect of increased plant diversity on specialist herbivory (Root, 1973; Agrawal et al., 2006; Lewinsohn and Roslin, 2008). This hypothesis claims that specialist herbivores prefer homogeneous neighbors to the same host plants for increase their herbivore loads (Lewinsohn and Roslin, 2008). As such, mixing closely related plant species with a mono-plantation may amplify herbivory caused by specialist herbivores. In contrast, mixing phylogenetically distant plant species with mono-plantations may dilute the effects from specialist herbivores (Figure 1). Likewise, the associational susceptibility hypothesis has been considered key to explaining the dilution effect of increased plant diversity on generalist herbivory (Unsicker et al., 2008; Plath et al., 2012). The hypothesis assumes that generalist herbivores require heterospecific neighbors to a focal plant to increase their herbivore load (Plath et al., 2012). As a result, mixing phylogenetically distant plant species with mono-plantation consumed by generalist herbivores may amplify herbivory due to generalist herbivores. In contrast, mixing closely related plant species with mono-plantations can dilute generalist herbivory (Figure 1). To the best of our knowledge, however, little is known about whether and how herbivore specificity and plant phylogenetic relatedness interact to alter the efficiency of mixed plantation on controlling herbivore in monoculture agroecosystem.

Current knowledge regarding the effect of plant phylogenetic diversity on generalist vs. specialist herbivores is largely based on comparisons of generalist and specialist herbivore intensity between monoculture and mixed plantations (Castagneyrol et al., 2014). By doing so, however, herbivore-herbivore interactions are largely overlooked. In fact, more complexity and even inverse patterns may emerge when multiple hosts and herbivores are taken into account as in the realty. For instance, phylogenetic relatedness of a host community may have different effect on the mean intensity of herbivory for multiple generalist herbivores and a specific herbivore respectively. An assemblage of phylogenetically distant plants may harbor more generalist herbivore species, and may also suffer from a higher level of herbivory through the sampling effect (i.e., higher possibility of attracting herbivores with high herbivory) (Schuldt et al., 2014). Similarly, phylogenetically similar species can also trigger many new specialist species, which may also lead to higher specialist herbivory via the sampling effect. As a result, pest species diversity (species richness and abundance) and the herbivore intensity by the targeted generalist or specialist herbivores should be compared simultaneously among monocultures and mixed plantations. However, experimental studies addressing the specificity of multiple herbivores and their community composition at the community level remain scarce.

Here, we sampled two monocultures in Wenchang City, Hainan Province, China. One was one subspecies of *Cocos nucifera* (we called "green *Cocos nucifera*") stand and the other is a pure stand of *Pinus elliottii.* Based on 20 years' pest herbivore survey in this area, "green *Cocos nucifera*" is attacked by generalist herbivores (e.g., *Brontispa longissima*, *Rhynchophorus ferrugineus*, *Oryctes rhinoceros*, *Diocalandra frument*, *Aspidiotus destucto*, and *Aleurocanthus spiniferus*) (Lin et al., 2010). In contrast, *Pinus elliottii* is attacked merely by a specialist herbivore (*Dendrolimus puntatus*) (Xu et al., 2014). We mixed ten tree species which are phylogenetically distant with the two monocultures (Supplementary Figure S1) to simulate the influence of mixture of phylogenetically distant species on generalist and specialist pest herbivory respectively. These ten tree species are *Litsea glutinosa*, *Calophyllum inophyllum*, *Casuarina equisetifolia*, *Rapsnea linearis*, *Rhodomyrtus tomentosa*, *Psychotria rubra*, *Clerodendrum cyrtophyllum*, *Zanthoxylum piperitum*, *Wikstroemia indica,* and *Atalantia buxifoli* (Supplementary Figure S1). We also mixed another subspecies of *Cocos nucifera* (we called "red *Cocos nucifera*") with the pure "green *Cocos nucifera*" stand "red *Cocos nucifera*" is phylogenetically close to "green *Cocos nucifera*" stand (Supplementary Figure S1), so we use this design to assess the effect of mixing phylogenetically close species on generalist pest herbivory. Similarly, since *Pinus caribaea* is phylogenetically close to *Pinus elliottii* (Supplementary Figure S1), we mixed *Pinus caribaea* with the pure *Pinus elliottii* stand to assess the impacts of mixing phylogenetically similar species on specialist pest herbivory too. Specifically, we compared herbivore richness, abundance, and degree of herbivory (i.e., the ratio of trees damaged by pest and total trees in a given area) among the two monocultures and the four mixed plantations. This experimental design aims to test: (1) if the addition of distantly related plant species can amplify herbivory by generalist herbivores, but dilute herbivory caused by specialist herbivores in a diverse host community; and (2) if adding closely related species to a host community can dilute herbivory caused by generalist herbivores, but amplify herbivory caused by specialist herbivores.

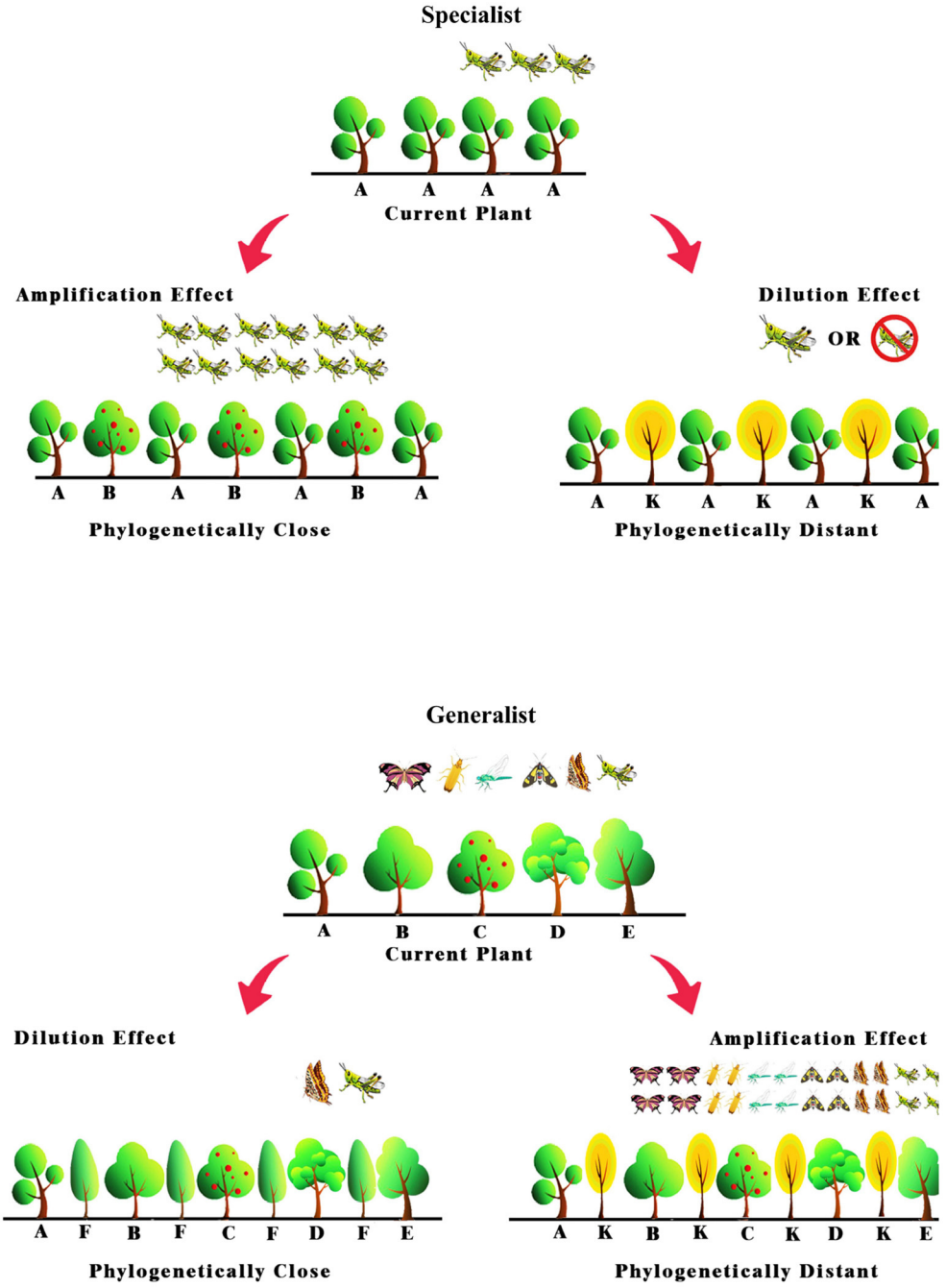

FIGURE 1
Hypothesized dilute and amplified effects of mixing closely and distantly related tree species on specialist and generalist pest herbivory respectively.

2. Materials and methods

2.1. Study sites

Our study site included four mixed stands (mixed stand 1, 110°57′34″E, 19°43′58″N; mixed stand 2, 110°56′39″E, 19°44′4″N; mixed stand 3, 110°58′34″E, 19°44′23″N and mixed stand 4: 110°49′24″E, 19°32′29″N), one monoculture pure "green *Cocos nucifera*" stand (110°51′15″E, 19°34′58″N), and one monoculture pure *Pinus elliottii* stand (110°43′19″E, 19°34′01″N) in Wenchang City, Hainan Province, China (Supplementary Figure S2). These sites have a mean annual temperature (1978–2010) of 23.9 °C, with a low monthly mean temperature of 16.2°C in January and high of 33°C in August. Average annual precipitation is 1,729 mm, most of which occurs from April to October.

One hundred stems from each of ten species (i.e., *Litsea glutinosa*, *Calophyllum inophyllum*, *Casuarina equisetifolia*, *Rapsnea linearis*, *Rhodomyrtus tomentosa*, *Psychotria rubra*, *Clerodendrum cyrtophyllum*, *Zanthoxylum piperitum*, *Wikstroemia indica,* and *Atalantia buxifoli*) were randomly mixed with 1,000

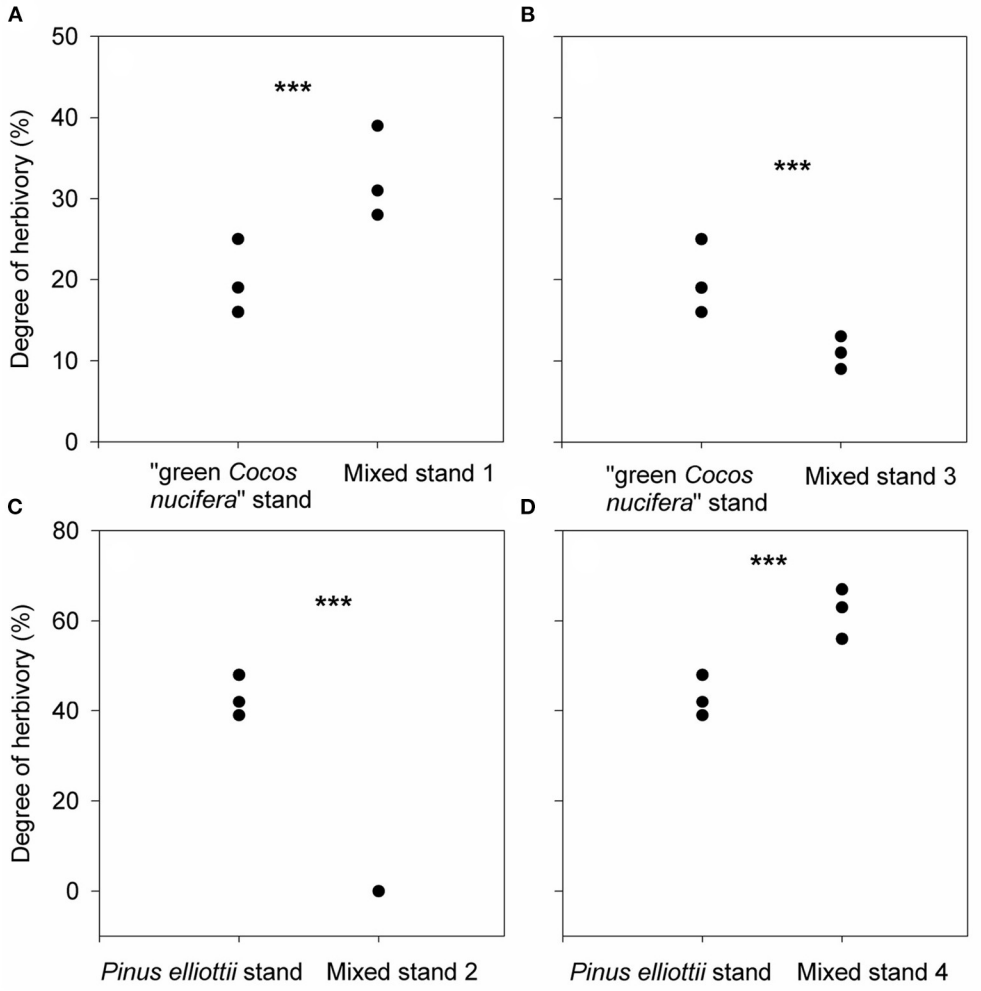

FIGURE 2
Differences in degree of herbivory [the percentage of trees damaged by a pest (%)] of "green *Cocos nucifera*" and *Pinus elliottii* between mixed stand 1 and the pure "green *Cocos nucifera*" stand **(A)**, mixed stand 2 and the pure *Pinus elliottii* stand **(C)**, mixed stand 3 and the pure "green *Cocos nucifera*" stand **(B)**, and mixed stand 4 and the pure *Pinus elliottii* stand **(D)**, respectively. ***indicates $p < 0.05$, results from our generalized linear mixed effect model with Poisson error.

individuals of "green *Cocos nucifera*" in mixed stand 1 and 1,000 individuals of *Pinus elliottii* in mixed stand 2. Thus, this planting was used to test the influence of mixing phylogenetically distant plant species on generalist and specialist pest herbivory individually. In mixed stand 3, 1,000 individuals of "green *Cocos nucifera*" and 1,000 individuals of "red *Cocos nucifera*" were planted to determine the influence of mixing phylogenetically similar plant species on generalist pest herbivory. In mixed stand 4, 1,000 individuals of *Pinus elliottii* and 1000 individuals of *Pinus caribaea* were therefore randomly mixed to assess the impact of mixing phylogenetically similar plant species on specialist pest herbivory. Pure "green *Cocos nucifera*" and *Pinus elliottii* stands of at least 1000 ha were established in Wenchang for nearly 30 years. Pure "green *Cocos nucifera*" and *Pinus elliottii* stands, mixed stand 1, 2, 3, and 4 have been planted for at least 20 years, and their planting densities were all kept at 500 stems per hectare. Since all six stands were very near the ocean, the local government forbids any human management (e.g., pesticide spraying and fertilization), thereby to avoid any potential ocean pollution.

2.1.1. Measurements of degree of herbivory for "green *Cocos nucifera*" and *Pinus elliottii*

We randomly selected three 20 × 20 m^2 subplots from each of the six stands described above. The subplots within each stand were at least 500 m apart from one another and from the edges of the stands. We then checked all "green *Cocos nucifera*" and *Pinus elliottii* trees in the three 20 × 20 m^2 subplots from each of the six stands to see how many "green *Cocos nucifera*" and *Pinus elliottii* trees were damaged by pests. Examples of different types of pest herbivory in "green *Cocos nucifera*" and *Pinus elliottii* stands are shown in Supplementary Figure S3. Then we calculated the degree of herbivory as the ratio of trees damaged by a pest by the total number of trees found in each of the three 20 × 20 m^2 subplots within each of the six plantation stands.

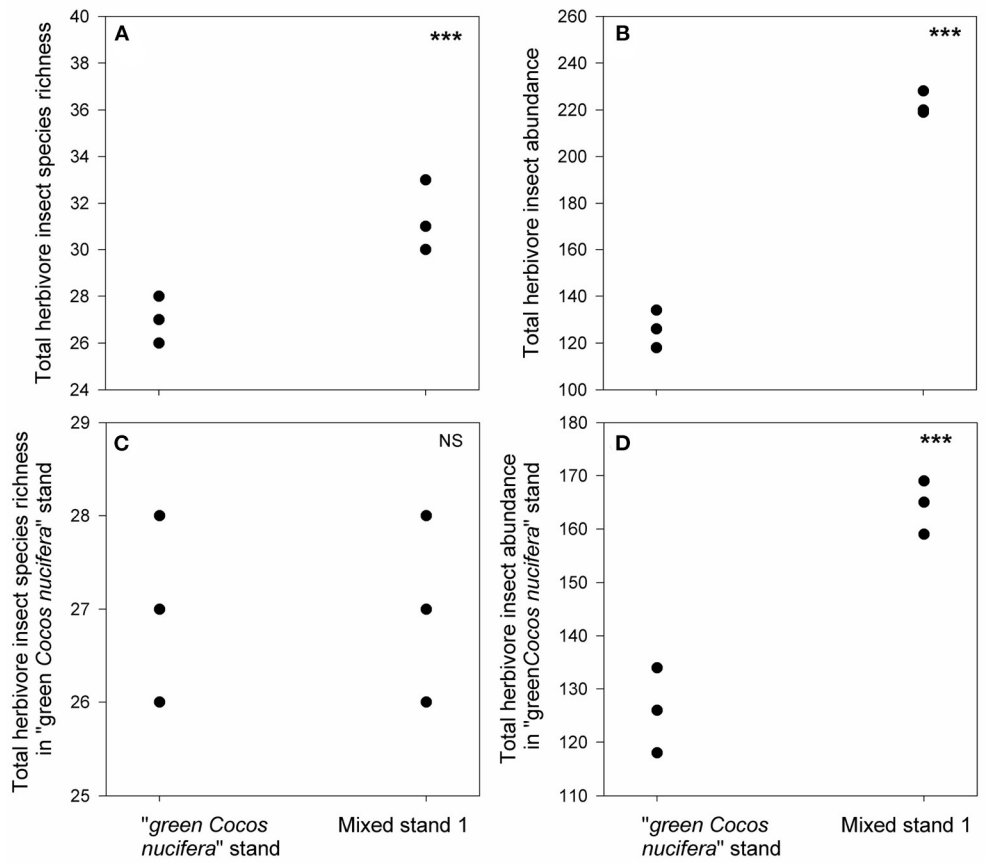

FIGURE 3
Differences in total herbivore insect species richness **(A)**, total herbivore insect abundance **(B)**, total herbivore insect species richness in "green *Cocos nucifera*" stand **(C)** and their abundance **(D)** between mixed stand 1 and "green *Cocos nucifera*" stand. *** indicates $p < 0.05$, results from our generalized linear mixed effect model with Poisson error.

2.1.2. Insect species richness and abundance trapping

Following Xue et al. (2021), we used 18 insect nets trap that were 50 cm in diameter and 160 cm in length to collect all flying insects during the day from July 26–28, 2019 in the three 20 × 20 m^2 subplots from each of the six stands. We also used 18 mercury lamps (450W) and 18 white cloths (2 × 3 m) (Supplementary Figure S4) to trap nocturnal insects from 8:00 pm to 10:00 pm during the same period. All non-larval herbivore insects were sorted and identified to species, and the abundance of each species was also recorded within each subplot.

2.1.3. Constructing phylogenetic tree of the 12 tree species and two subspecies of *Cocos nucifera*

The chloroplast genome of the 12 tree species and two subspecies of *Cocos nucifera* ("green *Cocos nucifera*" and "red *Cocos nucifera*") were measured to quantify the phylogenetic relationships of the 12 tree species and two subspecies of *Cocos nucifera*. The chloroplast genome for *Pinus elliottii, Casuarina equisetifolia, Clerodendrum cyrtophyllum, Litsea glutinosa, Rhodomyrtus tomentosa, Zanthoxylum piperitum,* and *Wikstroemia indica* can be directly found in NCBI. Thus, we only sequenced chloroplast genome for "green *Cocos nucifera*" and "red *Cocos nucifera*", *Pinus caribaea, Calophyllum inophyllum, Rapsnea linearis, Psychotria rubra,* and *Atalantia buxifolia.* Detail descriptions of the chloroplast genome for these seven tree species or subspecies were described in detail in Supplementary Table S1. A maximum likelihood tree (Supplementary Figure S1) was then constructed using RAxML (Stamatakis, 2014).

2.2. Statistical methods

Since species richness and abundance are discrete random variables (count data here), we used the generalized linear mixed effect model (GLMM) with Poisson error to test whether phylogenetic relatedness, herbivore specialization and their interactive effects can significantly influence degree of herbivory, total insect species richness and abundance, and total herbivore insect species richness and abundance. Specifically, we used a GLMM model [Degree of herbivory or Richness or Abundance ~ herbivore specialization × phylogenetic relatedness + (1|plantation type)]. Here *richness* and *abundance* indicate total insect or herbivore species richness and insect or herbivore

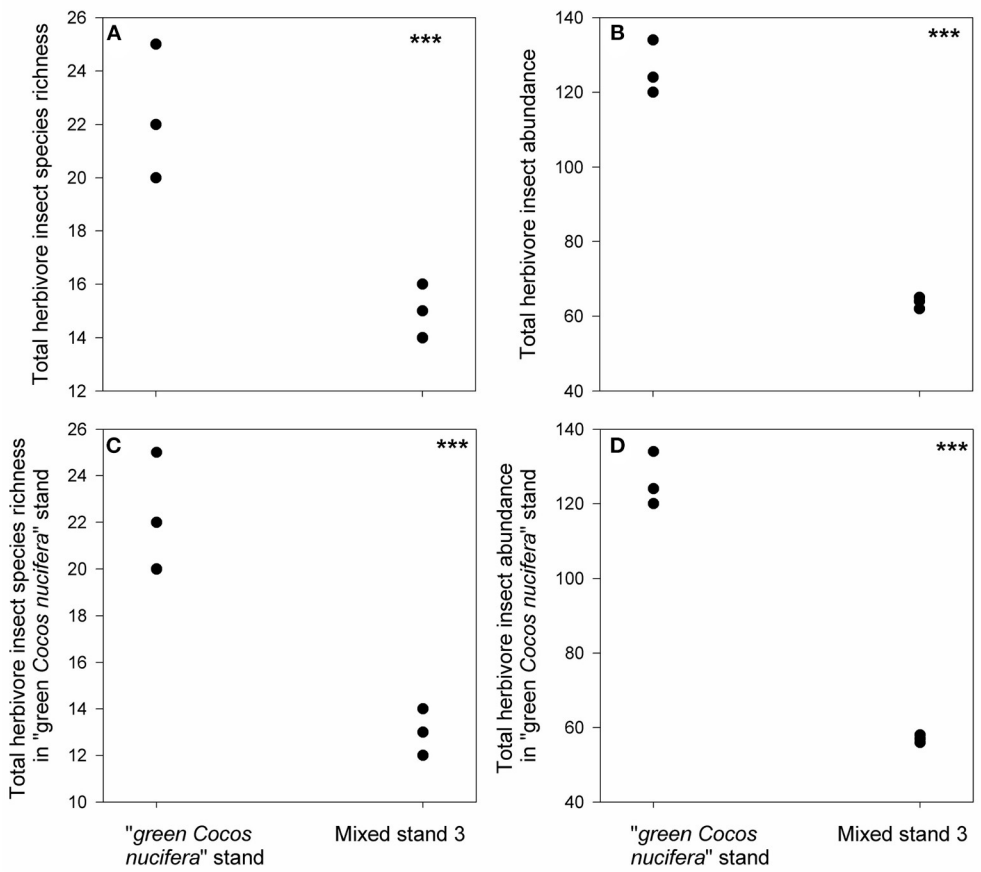

FIGURE 4
Differences in total herbivore insect species richness **(A)**, total herbivore insect abundance **(B)**, total herbivore insect species richness in "green *Cocos nucifera*" stand **(C)** and their abundance **(D)** between mixed stand 3 and "green *Cocos nucifera*" stand. ***indicates $p < 0.05$, results from our generalized linear mixed effect model with Poisson error.

insect abundance respectively. Herbivore specialization was either generalist or specialist. Phylogenetic relatedness coded phylogenetically close and distant individually. Plantation type indicated the six stands (green *Cocos nucifera* stand, mixed stand 1, mixed stand 3, *Pinus elliottii* stand, mixed stand 2, and mixed stand 4).

3. Results

The GLMM model results demonstrated that herbivore specialization, phylogenetic relatedness and their interactive effects all significantly influenced degree of herbivory, total insect species richness and abundance and total herbivore insect species richness and abundance (p of GLMM <0.05, Supplementary Table S2). Our GLMM model results showed that degree of herbivory of "green *Cocos nucifera*" in mixed stand 1 was 1.63 times higher than that in the pure "green *Cocos nucifera*" stand (Figure 2A). The degree of herbivory of *Pinus elliottii* decreased from 43% in the pure *Pinus elliottii* stand to 0% in mixed stand 2 (Figure 2C). Degree of herbivory of "green *Cocos nucifera*" in mixed stand 3 was 1.82 times lower than that in the pure "green *Cocos nucifera*" stand, while the degree of herbivory of *Pinus elliottii* in mixed stand 4 was 1.44 times higher than that in the pure *Pinus elliottii* stand (Figures 2B, D).

We found 25 herbivore species in the pure "green *Cocos nucifera*" stand, all of which were generalist feeders (Figure 3A, Supplementary Figure S2, Supplementary Table S3). They also emerged in mixed stand 1 (Figure 3C, Supplementary Table S3), but their total abundance in mixed stand 1 increased to 1.4 times higher than that in the pure "green *Cocos nucifera*" stand (Figures 3B, D). Moreover, 10 generalist herbivore species that were absent from the pure *Cocos nucifera* stand appeared in mixed stand 1 (Figure 3A, Supplementary Table S3). In contrast, although one new generalist species emerged (Figure 4A, Supplementary Table S3), only 14 out of the 25 generalist herbivore species observed in the pure "green *Cocos nucifera*" stand were found in mixed stand 3 (Figure 4C, Supplementary Table S3). Moreover, herbivore abundances in mixed stand 3 decreased 2-fold compared with the pure "green *Cocos nucifera*" stand (Figures 4B, D, Supplementary Table S3).

In the *Pinus elliottii* stand we only found one specialist herbivore species (*Dendrolimus puntatus*), which was absent from mixed stand 2 (Figure 5C, Supplementary Figure S2, Supplementary Table S3). However, another 24 generalist herbivore species were found in mixed stand 2, leading to both

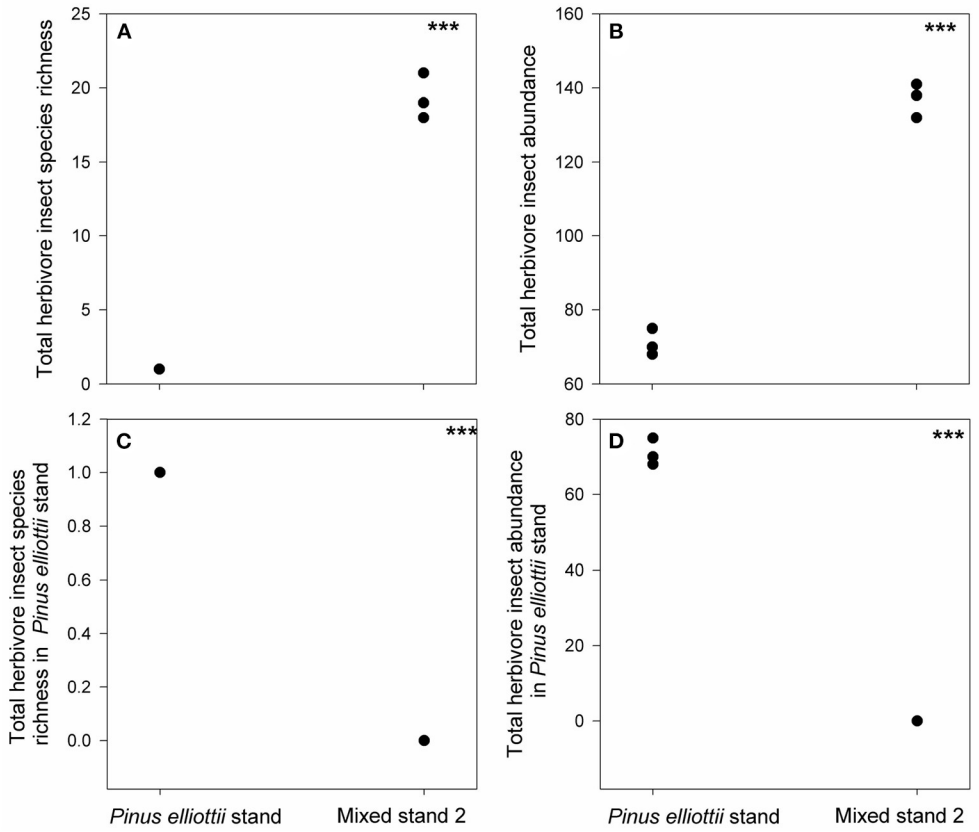

FIGURE 5
Differences in total herbivore insect species richness **(A)**, total herbivore insect abundance **(B)**, total species richness of herbivore insects found in *Pinus elliottii* stand **(C)** and their abundance **(D)** between mixed stand 2 and *Pinus elliottii* stand. ***indicates $p < 0.05$, results from our generalized linear mixed effect model with Poisson error.

higher total herbivore species richness and total abundance than those found in the *Pinus elliottii* stand (Figures 5A, B, D, Supplementary Table S3). In contrast, in mixed stand 4, *one* more new specialist herbivore (*Dioryctria splendidella*) emerged, except for *Dendrolimus puntatus* (Figures 6A, C, Supplementary Table S3). Moreover, the abundance of *Dendrolimus puntatus* increased 2-fold compared to that in the mono-*Pinus elliottii* stand (Figures 6B, D, Supplementary Table S3).

4. Discussion

Herbivores play key functions in ecosystems across the world, and multiple herbivore species can interact to regulate ecosystem processes and functions (Schemske et al., 2009). Hence, studies focusing on herbivory of a single focal plant species and by a single herbivore species may provide misleading information regarding biodiversity conservation and agroecosystem management. By investigating herbivory from multiple herbivores and across six different plant communities, we found that the addition of phylogenetically distant plants and the mixture of phylogenetically close plants can have opposite effects on herbivory. Specifically, mixing closely related tree species diluted herbivory of generalist pest herbivores, but amplified the impact from specialist pest. In contrast, mixing phylogenetically distant tree species enhanced the herbivory of generalist pest while diluting the herbivory effects from specialist pest. As mixed plantations are widely acknowledged as a useful management strategy, our results highlight the need to carefully consider the combined effects of multiple herbivore types on overall herbivore load and damage. Our results also emphasized the importance of which plants being added into monoculture forests.

By comparing mixed stands 1 and 3 with the pure "green *Cocos nucifera*" stand, we found that increasing the number of distantly related tree species can increase herbivory from generalist pest (i.e., increasing "green *Cocos nucifera*" generalist pest degree of herbivory). This is consistent with some previous studies (Schuldt et al., 2010, 2012, 2014) which find that increasing plant diversity can dilute pest herbivore. This finding can be explained, in part, by the widely acknowledged "associational susceptibility hypothesis," which claims that generalist herbivores need many distantly related plants to increase their herbivore load, thereby increasing herbivore intensity (i.e., increased damage percentage) (Brown and Ewel, 1987; Jactel and Brockerhoff, 2007; Unsicker et al., 2008; Plath et al., 2012). For instance, more distantly related plants in a community may benefit the growth of generalist herbivores via dietary mixing (Bernays et al., 1994). Likewise, high diversity stands may increase damage from non-preferred host species due to spillover effects from preferred hosts (Power and Mitchell, 2004). However, we propose an alternative explanation, which is that phylogenetically

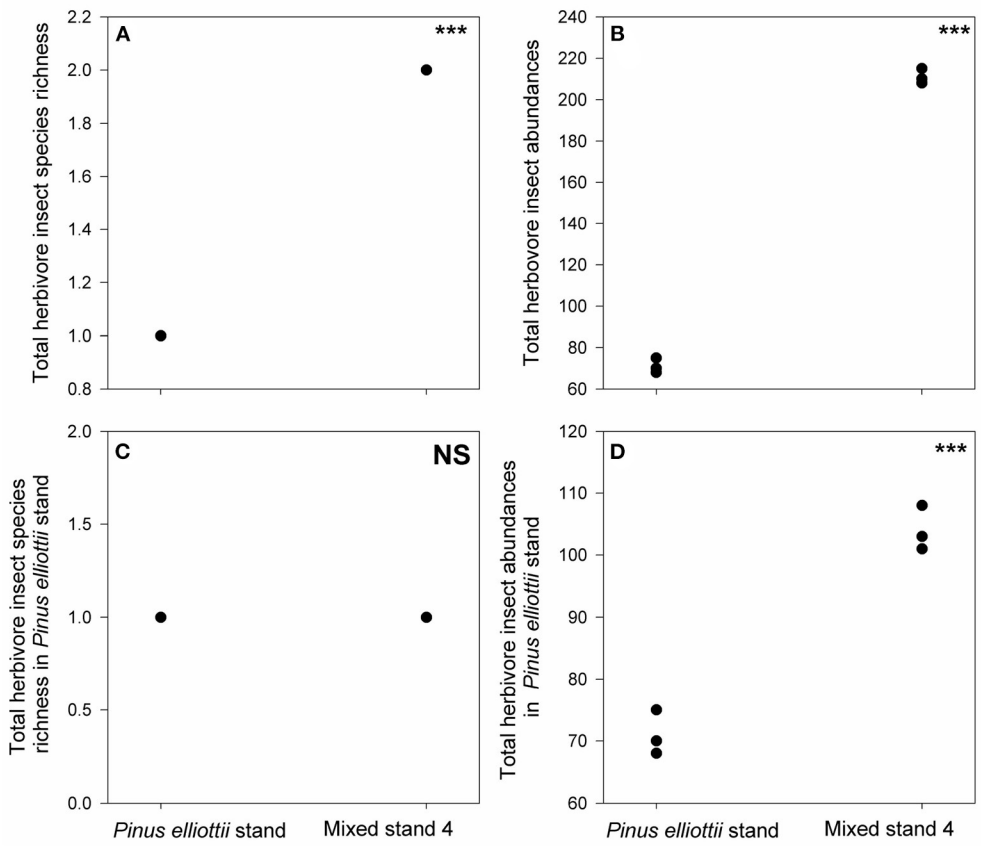

FIGURE 6
Differences in total herbivore insect species richness **(A)**, total herbivore insect abundance **(B)**, total species richness of herbivore insects in *Pinus elliottii* stand **(C)** and their abundance **(D)** between mixed stand 4 and *Pinus elliottii* stand. *** indicates $p < 0.05$ and NS (non-significant) indicates $p > 0.05$, results from our generalized linear mixed effect model with Poisson error.

distant plant species may support many new generalist herbivore species and increase total abundance of generalists found in monocultures, which may in turn lead to a higher possibility of obtaining high generalist herbivory intensity (i.e., sampling effect). Indeed, in mixed stand 1, the number of generalist herbivores was 1.4 times greater than the pure "green *Cocos nucifera*" stand. Moreover, 10 new generalist herbivore species were found in mixed stand 1.

We found that increasing the number of closely related tree species can reduce the generalist degree of herbivory in stand of pure "green *Cocos nucifera*". This can also be explained by the associational susceptibility hypothesis. Nevertheless, another potential reason is that phylogenetically similar plant species may result in new generalist species for "green *Cocos nucifera*", which may in turn compete with or directly prey upon the generalist pest of "green *Cocos nucifera*". Indeed, although one new generalist species emerged, 11 generalist pest herbivore species in the pure "green *Cocos nucifera*" stand disappeared in mixed stand 3. Moreover, herbivore abundance in mixed stand 3 decreased 2-folds compared with the pure "green *Cocos nucifera*" stand.

By comparing mixed stands 2 and 4 with the pure *Pinus elliottii* stand, we found the effects of phylogenetic relatedness on herbivory differed for specialist pest herbivores compared with generalist pest herbivores. For *Pinus elliottii*, the degree of herbivory of the specialist pest, *Dendrolimus puntatus*, was reduced to zero when it was mixed with ten phylogenetically distant tree species (i.e., mixed stand 2). This result suggests that mixed plantation of phylogenetically distant plant species can have a clear dilution effect on herbivory intensity from specialist pest. This pattern can be explained by the associational resistance hypothesis, which claims that specialist herbivores prefer more homogeneous neighbors to their preferred host plants to increase their loads (Root, 1973; Agrawal et al., 2006; Lewinsohn and Roslin, 2008). Thus, increasing the numbers of phylogenetically distant tree species will dilute specialist herbivores, thereby decreasing the abundance of specialist herbivores (Tahvanainen and Root, 1972; Barbosa et al., 2009). However, another possibility is that phylogenetically distant tree species are favored by generalist herbivores that may compete with or directly prey upon the specialist herbivores (Brown and Ewel, 1987). Indeed, we observed 24 generalist herbivore species in mixed stand 2, but we cannot observe original specialist pest (*Dendrolimus puntatus*) anymore.

The degree of herbivory of *Pinus elliottii* by the specialist pest herbivore was 1.44 times greater when it was mixed with phylogenetically close tree species (mixed

stand 4), thus providing support for the associational resistance hypothesis. However, it is also highly possible that phylogenetically close tree species (*Pinus caribaea*) can trigger new specialists, which in turn results in higher specialist degree of herbivory via sampling effects. Indeed, we ended up sampling a new specialist (*Dioryctria splendidella*) in mixed stand 4.

5. Conclusions

Our study provides clear evidence that herbivore specialization and plant phylogenetic relatedness interact to influence the efficiency of mixed plantations on the regulation of pest herbivory in agroecosystems. Mixing phylogenetically distant tree species with monocultures enhanced herbivory by generalist herbivores, while simultaneously diluting herbivory by specialist herbivores. In contrast, mixing phylogenetically close tree species with monocultures can give rise to totally opposite influences on generalist and specialist herbivory. Our results may differ with those observed on a single focal plant species attacked by a single herbivore species. Although investigations in other agroecosystems are needed to test the generality of the conclusion, our results suggest that both herbivore specialization and plant phylogenetic relatedness should be taken into account when using mixed plantations to manage pest herbivory in agroecosystems.

Data availability statement

The original contributions presented in the study are included in the article/Supplementary material, further inquiries can be directed to the corresponding author.

Author contributions

QY and XC: conceptualization, methodology, writing—original draft preparation, and writing—reviewing and editing. Both authors contributed to the article and approved the submitted version.

Funding

This work was funded by the Special Technical Innovation Project of Provincial Scientific Research Institutes (jscx202023).

Conflict of interest

The authors declare that the research was conducted in the absence of any commercial or financial relationships that could be construed as a potential conflict of interest.

Publisher's note

All claims expressed in this article are solely those of the authors and do not necessarily represent those of their affiliated organizations, or those of the publisher, the editors and the reviewers. Any product that may be evaluated in this article, or claim that may be made by its manufacturer, is not guaranteed or endorsed by the publisher.

Supplementary material

The Supplementary Material for this article can be found online at: https://www.frontiersin.org/articles/10.3389/fevo.2023.1187996/full#supplementary-material

References

Agrawal, A. A., Lau, J. A., and Hambäck, P. A. (2006). Community heterogeneity and the evolution of interactions between plants and insect herbivores. *Quart. Rev. Biol.* 81, 349–376. doi: 10.1086/511529

Andrew, N. R., and Hill, S. J. (2017). Effect of climate change on insect pest management. *Environ. Pest Manage.* 2017, 195–223. doi: 10.1002/9781119255574.ch9

Barbosa, P., Hines, J., Kaplan, I., Martinson, H., Szczepaniec, A., Szendrei, Z., et al. (2009). Associational resistance and associational susceptibility: having right or wrong neighbors. *Ann. Rev. Ecol. Evolut. System.* 40, 1–20. doi: 10.1146/annurev.ecolsys.110308.120242

Bernays, E. A., Bright, K. L., and Gonzalez, N. (1994). Dietary mixing in a generalist herbivore: tests of two hypotheses. *Ecology* 75, 1997–2006. doi: 10.2307/1941604

Brown, B. J., and Ewel, J. J. (1987). Herbivory in complex and simple tropical successional ecosystems. *Ecology* 68, 108–116. doi: 10.2307/1938810

Castagneyrol, B., Jactel, H., Vacher, C., Brockerhoff, E. G., and Koricheva, J. (2014). Effects of plant phylogenetic diversity on herbivory depend on herbivore specialization. *J. Appl. Ecol.* 51, 134–141. doi: 10.1111/1365-2664.12175

Grossman, J. J., Cavender-Bares, J., Reich, P. B., Montgomery, R. A., and Hobbie, S. E. (2018). Neighborhood diversity simultaneously increased and decreased susceptibility to contrasting herbivores in an early stage forest diversity experiment. *J. Ecol.* 107, 1492–1505. doi: 10.1111/1365-2745.13097

Jactel, H., and Brockerhoff, E. G. (2007). Tree diversity reduces herbivory by forest insects. *Ecol. Lett.* 10, 835–848. doi: 10.1111/j.1461-0248.2007.01073.x

Jactel, H., Petit, J., Desprez-Loustau, M. L., Delzon, S., Piou, D., Battisti, A., et al. (2012). Drought effects on damage by forest insects and pathogens: a meta-analysis. *Global Change Biol.* 18, 267–276. doi: 10.1111/j.1365-2486.2011.02512.x

Klapwijk, M. J., Myres, A. M. P., Battisti, A., and Larsson, S. (2012). "Assessing the impact of climate change on outbreak potential," in *Insect Outbreaks Revisited*, eds P. Barbosa, D. K. Letourneau and A. A. Agrawal 429–450. doi: 10.1002/9781118295205.ch20

Lewinsohn, T. M., and Roslin, T. (2008). Four ways towards tropical herbivore megadiversity. *Ecol. Lett.* 11, 398–416. doi: 10.1111/j.1461-0248.2008.01155.x

Lin, M., Han, Y., Li, W., Liu, F., Xu, W., Ao, S., et al. (2010). Monitoring and survey on pest insects and diseases of coconut trees in Hainan. *Plant Quarant.* 24, 21–24.

Mouquet, N., Devictor, V., Meynard, C. N., Munoz, F., Bersier, L. F., Chave, J., et al. (2012). Ecophylogenetics: advances and perspectives. *Biol. Rev.* 87, 769–785. doi: 10.1111/j.1469-185X.2012.00224.x

Pimm, S. L., Jenkins, C. N., Abell, R., Brooks, T. M., Gittleman, J. L., Joppa, L. N., et al. (2014). The biodiversity of species and their rates of extinction, distribution, and protection. *Science* 344, 1246752–1246752. doi: 10.1126/science.1246752

Plath, M., Dorn, S., Riedel, J., Barrios, H., and Mody, K. (2012). Associational resistance and associational susceptibility: specialist herbivores show contrasting responses to tree stand diversification. *Oecologia* 169, 477–487. doi: 10.1007/s00442-011-2215-6

Power, A. G., and Mitchell, C. E. (2004). Pathogen spillover in disease epidemics. *Am. Natural.* 164, S79–S89. doi: 10.1086/424610

Root, R. B. (1973). Organization of a plant-arthropod association in simple and diverse habitats: the fauna of collards (Brassica oleracea). *Ecol. Monog.* 43, 95–124. doi: 10.2307/1942161

Schemske, D. W., Mittelbach, G. G., Cornell, H. V., Sobel, J. M., and Roy, K. (2009). Is there a latitudinal gradient in the importance of biotic interactions? *Ann. Rev. Ecol. Evol. System.* 40, 245–269. doi: 10.1146/annurev.ecolsys.39.110707.173430

Schuldt, A., Assmann, T., Bruelheide, H., Durka, W., Eichenberg, D., Härdtle, W., et al. (2014). Functional and phylogenetic diversity of woody plants drive herbivory in a highly diverse forest. *New Phytol.* 202, 864–873. doi: 10.1111/nph.12695

Schuldt, A., Baruffol, M., Böhnke, M., Bruelheide, H., Härdtle, W., Lang, A. C., et al. (2010). Tree diversity promotes insect herbivory in subtropical forests of south-east China. *J. Ecol.* 98, 917–926. doi: 10.1111/j.1365-2745.2010.01659.x

Schuldt, A., Bruelheide, H., Durka, W., Eichenberg, D., Fischer, M., Kröber, W., et al. (2012). Plant traits affecting herbivory on tree recruits in highly diverse subtropical forests. *Ecol. Lett.* 15, 732–739. doi: 10.1111/j.1461-0248.2012.01792.x

Schuldt, A., Bruelheide, H., Härdtle, W., Assmann, T., Li, Y., Ma, K., et al. (2015). Early positive effects of tree species richness on herbivory in a large-scale forest biodiversity experiment influence tree growth. *J. Ecol.* 103, 563–571. doi: 10.1111/1365-2745.12396

Stamatakis, A. (2014). RAxML version 8: a tool for phylogenetic analysis and post-analysis of large phylogenies. *Bioinformatic* 30, 1312–1313. doi: 10.1093/bioinformatics/btu033

Tahvanainen, J. O., and Root, R. B. (1972). The influence of vegetational diversity on the population ecology of a specialized herbivore, Phyllotreta cruciferae (Coleoptera: Chrysomelidae). *Oecologia* 10, 321–346. doi: 10.1007/BF00345736

Tilman, D., Isbell, F., and Cowles, J. M. (2014). Biodiversity and ecosystem functioning. *Ann. Rev. Ecol. Evol. System.* 45, 471–490. doi: 10.1146/annurev-ecolsys-120213-091917

Unsicker, S. B., Oswald, A., Kohler, G., and Weisser, W. W. (2008). Complementarity effects through dietary mixing enhance the performance of a generalist insect herbivore. *Oecologia* 156, 313–324. doi: 10.1007/s00442-008-0973-6

Vehvilainen, H., Koricheva, J., and Ruohomaki, K. (2007). Tree species diversity influences herbivore abundance and damage: meta-analysis of long-term forest experiments. *Oecologia* 152, 287–298. doi: 10.1007/s00442-007-0673-7

Xu, L. N., Xue, Y., Wang, X. Y., Su, X. F., and Lin, Z. P. (2014). The survey and control strategy of Pinus elliottii×Pinus oaribaea. *Trop. Forestry* 2, 21–23. doi: 10.3969/j.issn.1672-0938.2014.02.006

Xue, Y., Robert, J., Liu, X., Wang, X. Y., Su, S. F., Tan, Z. Y., et al. (2021). Rocket launching activities are associated with reduced insect species richness and abundance in two types of tropical plantations around the Wenchang Satellite Launch Center, southern China. *Ecol. Indic.* 127, 17751. doi: 10.1016/j.ecolind.2021.107751

Zhang, J., Bruelheide, H., Chen, X., Eichenberg, D., Kröber, W., Xu, X., et al. (2017). Tree diversity promotes generalist herbivore community patterns in a young subtropical forest experiment. *Oecologia* 183, 455–467. doi: 10.1007/s00442-016-3769-0

frontiers | Frontiers in Ecology and Evolution

TYPE Original Research
PUBLISHED 09 May 2023
DOI 10.3389/fevo.2023.1175031

OPEN ACCESS

EDITED BY
Xiang Liu,
Lanzhou University, China

REVIEWED BY
Mu Liu,
Lanzhou University, China
Mengjiao Huang,
Fudan University, China

*CORRESPONDENCE
Libin Liu
✉ liulibin@zjnu.cn

RECEIVED 27 February 2023
ACCEPTED 19 April 2023
PUBLISHED 09 May 2023

CITATION
Wang C, Lu X, Yang T, Zheng Y, Chen L, Liu L and Ni J (2023) Should more individuals be sampled when measuring functional traits of tree species in habitat-heterogeneous karst forests?
Front. Ecol. Evol. 11:1175031.
doi: 10.3389/fevo.2023.1175031

Should more individuals be sampled when measuring functional traits of tree species in habitat-heterogeneous karst forests?

Chenling Wang[1], Xiaoling Lu[1], Tingting Yang[2], Yawen Zheng[1], Linhao Chen[1], Libin Liu[1]*and Jian Ni[1]

[1]College of Life Sciences, Zhejiang Normal University, Jinhua, China, [2]Management Department of Maolan National Nature Reserve, Libo, China

When measuring plant functional traits across geomorphologies, 5–10 healthy individuals of a plant species are commonly sampled. However, whether more individuals should be sampled in habitat-heterogeneous karst vegetation remains unknown. In this study, two dominant tree species (*Clausena dunniana* and *Platycarya strobilacea*) in karst evergreen and broadleaved mixed forests in Southwestern China were selected. On the basis of a large quantity of individuals of the two species grown in different peak clumps and slope positions, variations of 10 morphological traits in the two species were statistically analyzed. The suggested sampling number of individuals, which could mostly represent the common trait characteristics, was further explored. All traits showed significant differences between the two species ($p<0.05$). The traits of *P. strobilacea* displayed larger intraspecific variations than those of *C. dunniana*, except for twig dry matter content. The bark thickness (BT), leaf area (LA), and specific leaf area (SLA) of *C. dunniana* and the BT, SLA, LA, leaf tissue density, and bark tissue density of *P. strobilacea* presented large intraspecific variations. Most traits exhibited significant differences between peak clumps and/or among slope positions ($p<0.05$). Random sampling analysis indicated that the suggested sampling numbers of individuals for the 10 traits are 6–23 in *C. dunniana* and 9–29 in *P. strobilacea*. The common accepted sample size in normal geomorphologies is not sufficiently large in most cases. Larger sample sizes are recommended for traits, such as SLA, BT, and LA, with larger intraspecific variations. Therefore, under sufficient labor, material, and time, more individuals should be sampled when measuring plant functional traits in habitat-heterogeneous karst vegetation.

KEYWORDS

morphological traits, interspecific and intraspecific variations, sampling number, habitat heterogeneity, evergreen and deciduous broadleaved mixed forest, karst geomorphology

1. Introduction

Plant functional traits (PFTs) are the morphological and physiological characters highly connected with the survival, growth, reproduction, and death dynamics of plants (Violle et al., 2007). PFTs, especially the morphological traits such as leaf area (LA), bark thickness (BT), and wood density, are easy to measure and could reveal the relationships between plants and

environments; For example, plants grow in harsh environments display small leaves, thick barks, and hard woods (Wright et al., 2004; Liu et al., 2022; Kambach et al., 2023). The study of PFTs offers an alternative approach to comprehend community species coexistence and predict the effects of global environmental changes on plant distribution (Thuiller et al., 2004; Kraft et al., 2008; Cui et al., 2020). Currently, the morphological traits of leaves, barks, and twigs (especially leaves) of various vegetation types in diverse geomorphologies worldwide have been considerably explored (Wright et al., 2010; Auger and Shipley, 2013; Myers-Smith et al., 2019; Jin et al., 2023; Liu et al., 2023).

When measuring PFTs in the field across geomorphologies, 5–10 healthy individuals of a species are commonly selected, and leaf, bark, twig, and root samples are further collected from the selected individuals (Cornelissen et al., 2003; Pérez-Harguindeguy et al., 2013). However, PFTs vary among species (interspecific variation) and individuals within a species (intraspecific variation). Interspecific trait variations are determined by species identity (genetic factors), and intraspecific trait variations are more influenced by environmental factors (Weiher and Keddy, 1995; Westoby et al., 2002; Bolnick et al., 2011). Plant scientists generally agree that PFTs show large interspecific variations among species (Cornelissen et al., 2003; Wright et al., 2004). In the last decade, a growing body of studies suggested that intraspecific trait variations could not be ignored (Albert et al., 2010; Auger and Shipley, 2013; Niu et al., 2020). Climate, soil, altitude, aspect, illumination, and many other environmental factors all cause intraspecific trait variations (Hultine and Marshall, 2000; McDonald et al., 2003; Peppe et al., 2011). Plants of a certain species growing in diverse environments may present large intraspecific trait variations (Liu et al., 2023). A global meta-analysis indicated that intraspecific trait variations occupy an average of 32% of the total trait variations (Siefert et al., 2015). Intraspecific trait variations may even be larger than interspecific trait variations in some studies (Lecerf and Chauvet, 2008; Messier et al., 2010). Thus, the traits of different species and those of individuals within a species growing in different environments vary inevitably. The trait characteristics (especially for traits with large interspecific and intraspecific variations) may be accompanied by much uncertainty on the basis of a unified sample individual number without regard to species identity and environmental conditions.

Karst is a fantastically particular geomorphology formed from the solution of carbonate rocks (such as limestone and dolomite) by underground and surface water. This geomorphology is sporadically distributed over the world, with an area of 22 million km^2, occupying approximately 14.8% of the global land area (Jiang et al., 2014). Southwestern China, Southern America, and the Mediterranean coast of Europe are the three major areas with widespread distribution of karst geomorphology (Sweeting, 1972). Due to long-range geologic functions of weathering, denudation, and leaching, the karst geomorphology in Southwestern China is well known for its high habitat heterogeneity. Karst mountain areas have various landforms, such as dissolved gully, stone bud, peak clump, peak forest, isolated peak, doline funnel, and solution depression (Song, 2000). Rock exposure, soil depth and nutrients, light intensity, and water conditions relatively differ among mountains and slope positions within a mountain (Pan, 2003; Peng et al., 2019; Liu et al., 2021). Researchers have studied the PFT characteristics and PFT-based adaptation strategies of karst plants and plant communities in this region and found that PFTs, such as morphological traits and ecological stoichiometry, in karst plants presented large interspecific and intraspecific variations due to highly heterogeneous environments/habitats (Jiang et al., 2016; Geekiyanage et al., 2018; Yang et al., 2020; Liu et al., 2022).

However, most PFT studies conducted in karst geomorphology in Southwestern China sampled a similar small individual number of plants (for example, five plant individuals were sampled) in normal geomorphologies (Pang et al., 2019; Yu et al., 2021; Shui et al., 2022). The results from such sampling method may not indicate the entire trait characteristics in plants, and plant communities grow in considerably heterogeneous environments/habitats. For example, plants grow in stone gullies, on stone surfaces and soil surfaces in a karst forest presented significantly different leaf trait values (Zhou et al., 2022). Thus, researchers may raise a question of whether more individuals should be sampled when measuring PFTs in habitat-heterogeneous karst regions.

In this study, two dominant tree species (an evergreen species and a deciduous species) in habitat-heterogeneous primary forests in peak clump depression karst geomorphology in Southwestern China were used as samples. The morphological traits of leaf, bark, and twig in a large quantity of individuals of the two tree species were measured. Trait differences between peak clumps and among slope positions within a mountain were analyzed. This study aimed to answer whether more individuals should be sampled when measuring PFTs of tree species in habitat-heterogeneous karst forests. It could provide theoretical support for the sampling quantity of PFT measurements in karst regions in future studies.

2. Materials and methods

2.1. Study area

Peak clump depression karst geomorphology is one of the eight karst geomorphological types in Southern China and mainly distributed in Southern Guizhou Province and Northern Guangxi Autonomous Region. Libo County, located in Southern Guizhou, is one of the representative areas of the region, especially its Maolan National Nature Reserve (107°52′–108°05′ E, 25°09′–25°21′ N) with an area of 21,285 km^2 (Figure 1). This terrain is located in mid-subtropical China and has a humid monsoon climate. According to records from the Libo meteorological station (107°53′ E, 25°25′ N, 429 m), the mean annual temperature is 18.3°C, with temperatures of 8.5°C and 26.5°C in January and July, respectively. The mean annual precipitation is 1,269 mm, of which 86% falls between April and October. The mean annual sunshine duration is 1,273 h, with a low sunshine percentage of 26%. The altitude of the reserve is between 430 and 1,078 m above sea level, with a relative height of most hills at 100–200 m. Limestone and dolomite (especially the former) are distributed everywhere in the reserve. Black limestone soil is shallow and discontinuous. The continuous evergreen and deciduous broadleaved mixed forests in this reserve are the most widely distributed, best protected, and most original karst forest in the world. The forests here are known as the gene bank of biological resources with the best preserved biodiversity in the subtropical karst geomorphology. Primary evergreen and deciduous broadleaved mixed forests are distributed in the peak clumps, and rice fields are the key land use in the depressions.

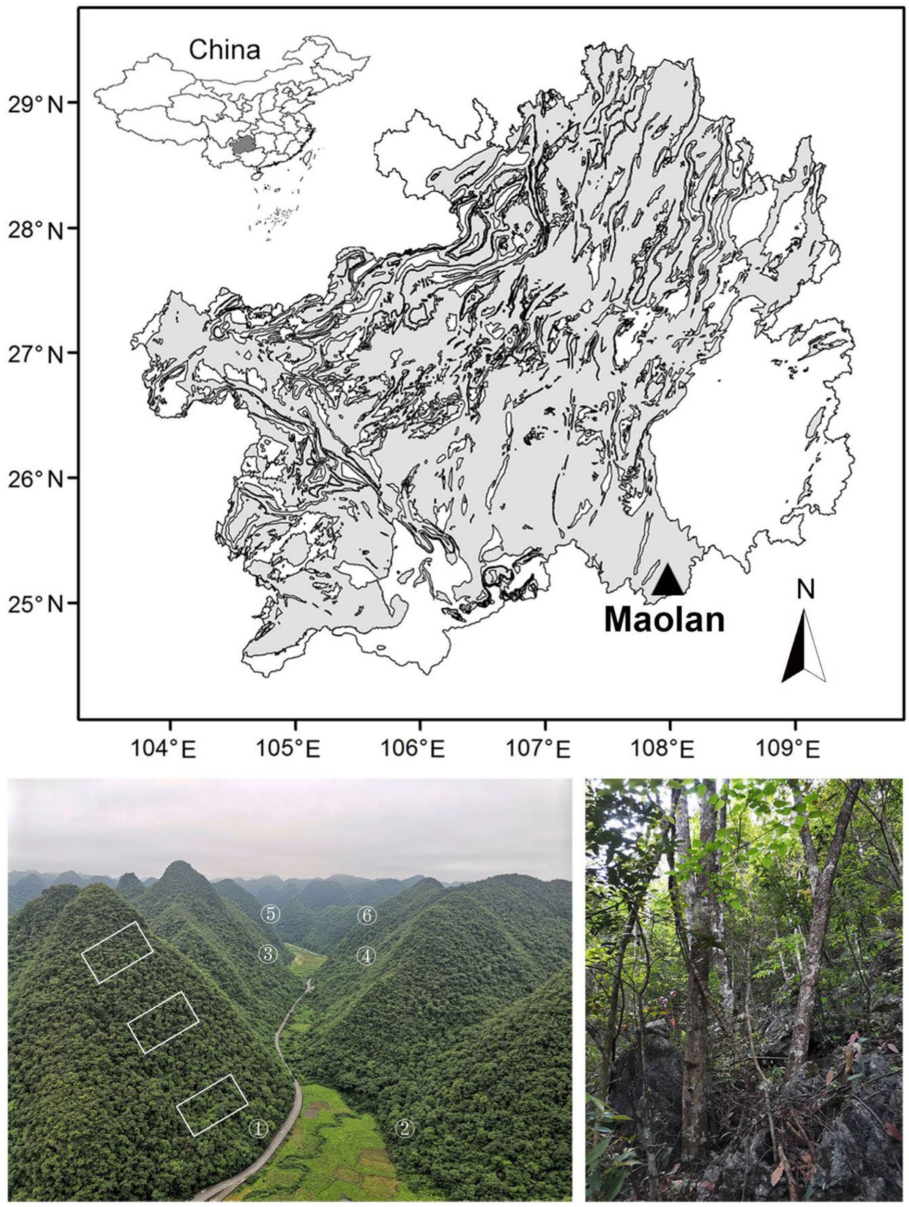

FIGURE 1
Location of Maolan National Nature Reserve, physiognomy of peak clump depression karst geomorphology and plot setting (left bottom), and interior view of karst forests (right bottom) in the distribution map of karst geomorphology (grey) in Guizhou Province, Southwestern China.

2.2. Vegetation survey and plant functional trait measurements

After a vegetation survey in the reserve was completed, six mountains in two opposite peak clumps (three mountains on each side peak clumps separated by a depression) at Poling site (107°56′ E, 25°17′ N) representing the karst peak clump depression geomorphology, vegetation, and soil of the whole reserve were selected. In each mountain, three plots (each with an area of 20 m × 30 m) at the upper, middle, and lower slopes (18 plots in total) were established (Figure 1). The species identity, diameter at breast height (DBH), and height of each woody plant with DBH ≥ 1 cm were recorded. *Clausena dunniana*, *Platycarya strobilacea*, *Cyclobalanopsis glauca*, *Lindera communis*, and *Swida parviflora* are the dominant tree species of the primary forests.

Habitats, such as slope, aspect, rock exposure rate, and soil depth and nutrient, are highly heterogeneous between peak clumps and among slope positions (Pan, 2003; Peng et al., 2019; Liu et al., 2021). Two typical dominant karst tree species, *C. dunniana* and *P. strobilacea*, distributed in all plots were selected as samples to explore the effects of highly heterogeneous habitats on PFTs and whether more individuals should be sampled when measuring PFTs of tree species in karst forests. Ten healthy individuals per species in each plot were randomly sampled (180 individuals of each tree species were sampled). Four branches in different positions of the sunlit side of the tree canopy in each sampled individual were cut using a long reach chain

saw. Twenty healthy mature leaves and three approximately 20 cm-length terminal twigs were collected from the four branches by using a scissor. Three bark samples at the DBH position of each individual were collected by using a sickle.

Fresh and dry (dried at 85°C for 72 h in an oven) masses of leaf, bark, and twig (peeled) samples were weighed using an electronic balance. Leaf thicknesses (LTs) and BT were measured using an electronic Vernier caliper. LA was scanned using the WinFOLIA multipurpose leaf area meter (Regent Instruments, Canada). The volumes of bark and twig samples were determined using the drainage method, and those of leaf samples were calculated as the product of LA and LT. The values of specific leaf area (SLA), leaf dry matter content (LDMC), leaf tissue density (LTD), bark dry matter content (BDMC), bark tissue density (BTD), twig dry matter content (TDMC), and twig tissue density (TTD) were calculated using their corresponding equations (Cornelissen et al., 2003).

2.3. Data analysis

All statistical analyses were performed using SPSS version 20 and the R software version 3.5.1 (Xue, 2017; R Core Team, 2018). The coefficients of intraspecific variation (standard deviation divided by mean times 100%) were used to characterize the varying degrees of PFTs within a species. Independent sample t-test was conducted to determine trait differences between the two species and between peak clumps. One-way ANOVA was used to analyze trait differences among slope positions. Sampling without replacement (2,000 times of duplicate sampling under each sample size from two to the suggested sample individual number) was conducted for each trait (each trait of each species had 180 values from 180 individuals, Supplementary Table S1) by using the "Sample" package in the R software to determine the suggested individual numbers when measuring the PFTs of tree species in karst forests. Then, independent sample *t*-test was conducted to determine trait differences between object samples and total samples, and the corresponding *p* values were obtained (2,000 *p* values were obtained for each trait). When the number of $p > 0.05$ exceeded 1,900 of 2,000 times *p* values (95%), this sample size is the suggested sample individual number for the trait of this tree species (Gao et al., 2018).

3. Results

All traits showed significant differences between the two species ($p < 0.05$). *C. dunniana* presented significantly higher LT, LA, BDMC, BTD, TDMC, and TTD values and significantly lower SLA, LDMC, LTD, and BT values than *P. strobilacea* ($p < 0.05$). The coefficients of intraspecific trait variation of *C. dunniana* ranged from 6.32% to 35.95%. The BT, LA, and SLA of *C. dunniana* showed large intraspecific variations, indicated by large coefficients of intraspecific variation (Figure 2). The coefficients of intraspecific trait variation of *P. strobilacea* ranged from 8.13% to 45.62%. The BT, SLA, LA, LTD, and BTD of *P. strobilacea* displayed large intraspecific variations, indicated by large coefficients of intraspecific variation (Figure 2). In general, the traits of *P. strobilacea* displayed larger intraspecific variations than those of *C. dunniana*, except for TDMC (Figure 2).

The LA and LTD of *C. dunniana* showed no differences between peak clumps and among slope positions ($p > 0.05$). The SLA, BT, and BTD of *P. strobilacea* also displayed no differences between peak clumps ($p > 0.05$). Other traits presented significant differences between peak clumps and/or among slope positions ($p < 0.05$) (Figure 3). The LTD, BT, BDMC, and TDMC of *C. dunniana* and the LDMC, LTD, BT, BDMC, and BTD of *P. strobilacea* increased with increasing slope position. The SLA of the two tree species decreased with increasing slope position (Figure 3).

Based on the results of sampling without replacement and independent sample *t*-test, the average LT values of object samples and

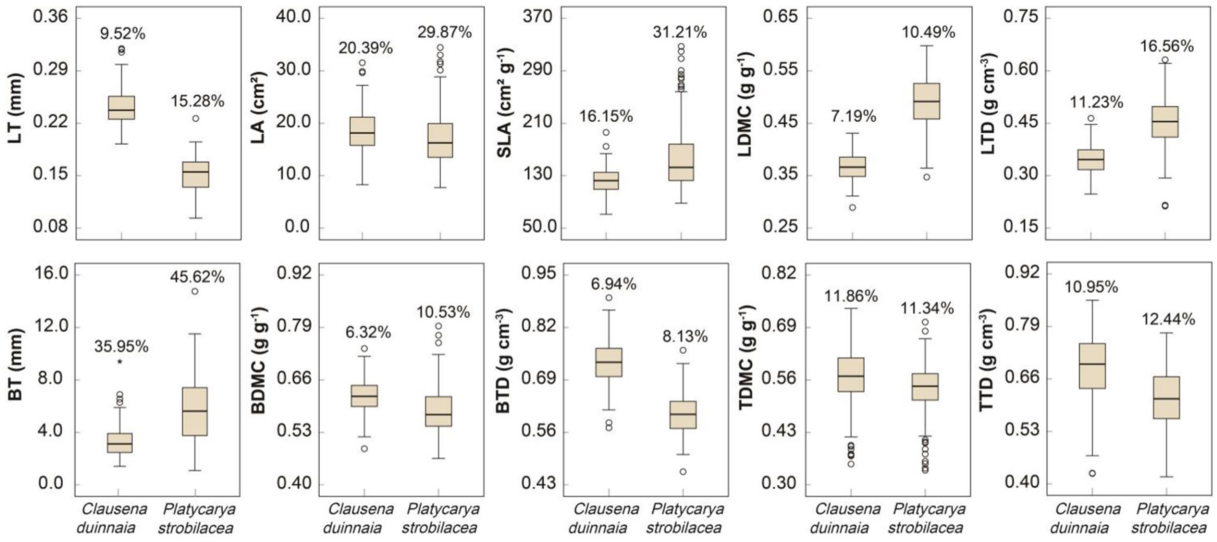

FIGURE 2
Plant functional traits and their intraspecific variations in two tree species in karst forests in Guizhou Province, Southwestern China. The circles in the box plots indicate abnormal values. The percentages of data in the box plots are the coefficients of intraspecific trait variation. LT, leaf thickness; LA, leaf area; SLA, specific leaf area; LDMC, leaf dry matter content; LTD, leaf tissue density; BT, bark thickness, BDMC, bark dry matter content; BTD, bark tissue density; TDMC, twig dry matter content; TTD, twig tissue density.

total samples showed no significant differences when the sample sizes for the LT of *C. dunniana* and *P. strobilacea* exceeded 18 and 14, respectively. That is, the suggested sample individual numbers for the LT of *C. dunniana* and *P. strobilacea* are 18 and 14, respectively (Figure 4). The corresponding suggested sample individual numbers for the LA, SLA, LDMC, LTD, BT, BDMC, BTD, TDMC, and TTD of *C. dunniana* were 12, 8, 10, 13, 23, 9, 6, 12, and 15, respectively (Figure 4), and those for *P. strobilacea* were 20, 29, 12, 13, 22, 23, 11, 15, and 9, respectively. In general, more individuals of *P. strobilacea* should be sampled than *C. dunniana*, and more individuals should be sampled when measuring traits with larger intraspecific variations.

4. Discussion

The PFTs of various vegetation types worldwide across geomorphologies have been considerably measured with reference to the handbooks for standardized measurements of PFTs

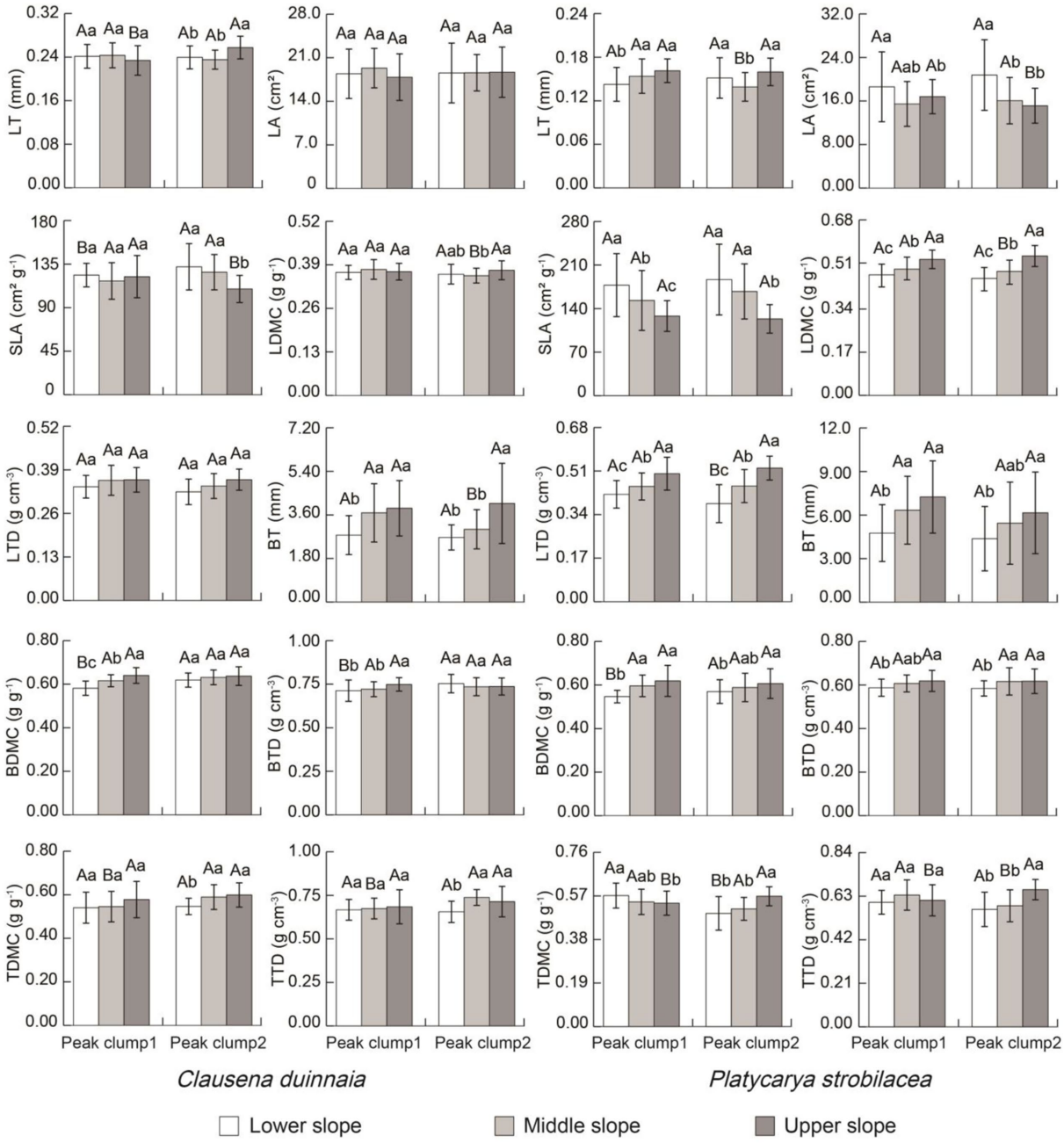

FIGURE 3
Plant functional trait differences between peak clumps and among slope positions in two tree species in karst forests in Guizhou Province, Southwestern China. Trait values with different capital letters between peak clumps in the same slope position are significantly different (independent sample *t*-test, $p<0.05$). Trait values with different small letters among slope positions in a peak clump are significantly different (one-way ANOVA, $p<0.05$). LT, leaf thickness; LA, leaf area; SLA, specific leaf area; LDMC, leaf dry matter content; LTD, leaf tissue density; BT, bark thickness, BDMC, bark dry matter content; BTD, bark tissue density; TDMC, twig dry matter content; TTD, twig tissue density.

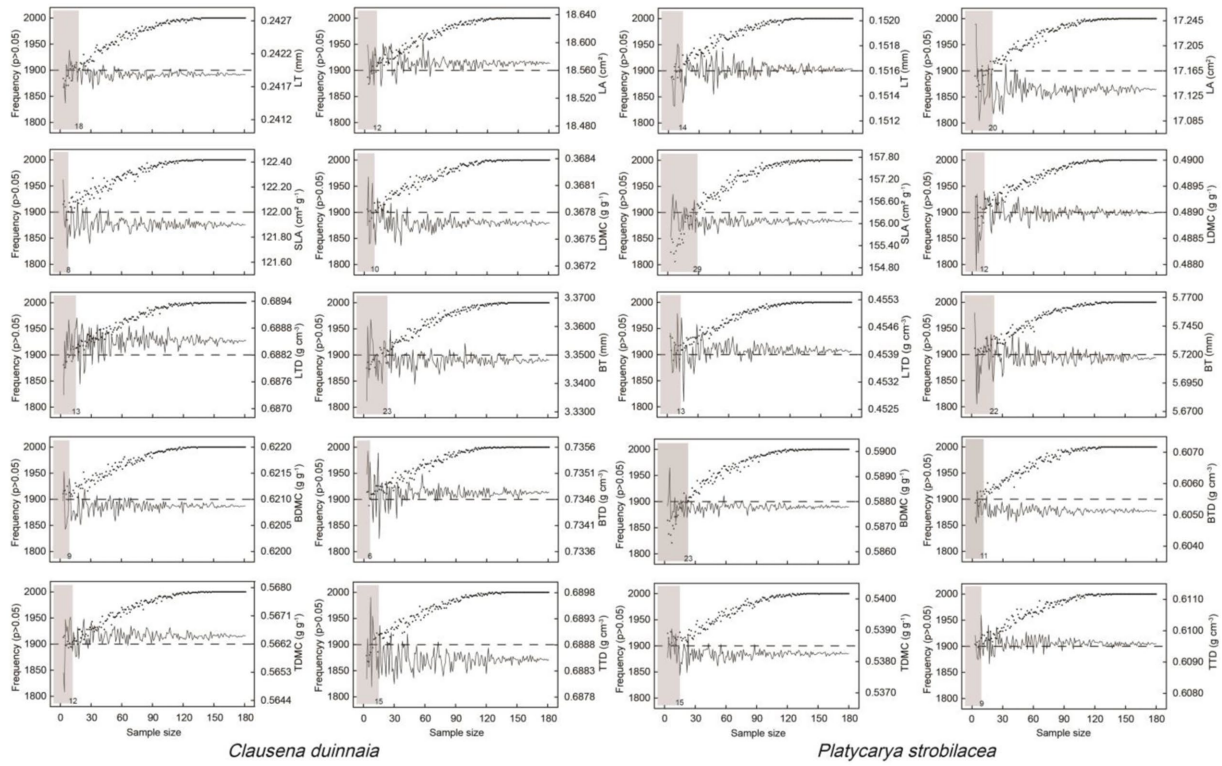

FIGURE 4
Mean of random sampling, frequency, and significant test of plant functional traits in two tree species in karst forests in Guizhou Province, Southwestern China. The solid line indicates the mean trait value of random sampling. The dots indicate frequencies of $p>0.05$. The grey blocks are the areas of significant differences between object samples and total samples, indicating that the sample size of the right position of the block is the suggested sampling number of individuals. LT, leaf thickness; LA, leaf area; SLA, specific leaf area; LDMC, leaf dry matter content; LTD, leaf tissue density; BT, bark thickness, BDMC, bark dry matter content; BTD, bark tissue density; TDMC, twig dry matter content; TTD, twig tissue density.

(Cornelissen et al., 2003; Pérez-Harguindeguy et al., 2013). However, the PFT characteristics of some vegetation in remote or certain topographical areas have not been fully determined yet, such as those of the karst vegetation in Southwestern China. Most of the existing studies adopted the same sampling method as conducted in normal geomorphology (Geekiyanage et al., 2018; Pang et al., 2019; Yu et al., 2021; Shui et al., 2022). With regard to the effects of highly heterogeneous habitats on PFTs in karst geomorphology, in the present study, whether more individual numbers should be sampled when measuring PFTs in karst vegetation was explored for the first time. This study could provide not only basic data to the TRY and the China plant trait databases but also methodology for future detailed PFT measurements (especially for intraspecific trait variation measurements) in vegetation types grow in highly heterogeneous environments/habitats worldwide other than in karst vegetation in Southwestern China (He et al., 2019; Kattge et al., 2020).

Taxonomic status (genetic factors) and environmental conditions codetermine PFT characteristics (Weiher and Keddy, 1995; Westoby et al., 2002; Bolnick et al., 2011). In the present study, considerably different trait values between two karst tree species, and among individuals within a species but under different habitats were observed. Thus, the sampling quantities are supposed to be different when measuring PFTs in different species and within a species, but individuals grow in different environments/habitats. Besides, traits in different organs vary to some degree (Liu et al., 2022). The sampling quantities should also differ when measuring PFTs in different organs.

The common accepted practice considers that the number of individuals is often 5–10 when measuring PFTs across geomorphologies. In the present study, the suggested sampling quantities for 10 morphological traits in two tree species (*C. dunniana* and *P. strobilacea*) in karst forests in Southwestern China are 6–23 and 9–29, respectively. The common accepted sample size across geomorphologies is not sufficiently large in most cases. Therefore, more individuals should be sampled when measuring PFTs in habitat-heterogeneous karst vegetation, and the traits in different organs and species should be treated differently. *C. dunniana* is an evergreen species with long leaf life. It increases resource investments for survival. Large intraspecific variations in PFTs are not conducive for evergreen species to adapt to environments. *P. strobilacea* is a deciduous species with short leaf life. It increases resource investments for growth (Aerts, 1995; Givnish, 2002). Thus, more individuals should be sampled when measuring PFTs in deciduous species than evergreen ones. Larger sample sizes are also recommended for traits with larger intraspecific variations (such as LA, SLA, and BT) than smaller intraspecific variations (such as LDMC, LTD, and BTD).

Other PFTs, such as root specific length, C:N:P stoichiometry, leaf net photosynthetic rate, and water use efficiency, of tree species, shrubs, and herbs in karst vegetation also displayed large interspecific and intraspecific variations (Zhong et al., 2018; Zhang et al., 2020,

2021; Jing et al., 2021; Liu et al., 2022; Dong et al., 2023). The same method is also recommended to explore the sample sizes of those PFTs. In conclusion, when measuring PFTs in habitat-heterogeneous karst vegetation, the sample size should not be limited to 5–10. More plant individuals should be sampled under sufficient labor, material, and time.

Data availability statement

The original contributions presented in the study are included in the article/Supplementary material, further inquiries can be directed to the corresponding author.

Author contributions

LL and JN conceived and designed the research. CW, XL, LL, TY, YZ, and LC contributed to the field work. CW and LL analyzed the data and wrote the first draft with substantial input from JN. All authors contributed to the article and approved the submitted version.

Funding

This study was funded by the Zhejiang Provincial Natural Science Foundation of China (LQ20C030003).

Acknowledgments

The authors thank the Management Department of Maolan National Nature Reserve for assistance in all field work.

Conflict of interest

The authors declare that the research was conducted in the absence of any commercial or financial relationships that could be construed as a potential conflict of interest.

Publisher's note

Supplementary material

The Supplementary material for this article can be found online at: https://www.frontiersin.org/articles/10.3389/fevo.2023.1175031/full#supplementary-material

References

Aerts, R. (1995). The advantages of being evergreen. *Trends Ecol. Evol.* 10, 402–407. doi: 10.1016/S0169-5347(00)89156-9

Albert, C. H., Thuiller, W., and Yoccoz, N. G. (2010). Intraspecific functional variability: extent, structure and sources of variation. *J. Ecol.* 98, 604–613. doi: 10.1111/j.1365-2745.2010.01651.x

Auger, S., and Shipley, B. (2013). Inter-specific and intra-specific trait variation along short environmental gradients in old-growth temperate forest. *J. Veg. Sci.* 24, 419–428. doi: 10.1111/j.1654-1103.2012.01473.x

Bolnick, D. I., Amarasekare, P., Araojo, M. S., Burger, R., Levine, J. M., Novak, M., et al. (2011). Why intraspecific trait variation matters in community ecology. *Trends Ecol. Evol.* 26, 183–192. doi: 10.1016/j.tree.2011.01.009

Cornelissen, J. H. C., Lavorel, S., Garnier, E., Díaz, S., Buchmann, N., Gurvich, D. E., et al. (2003). A handbook of protocols for standardised and easy measurement of plant functional traits worldwide. *Aust. J. Bot.* 51, 335–380. doi: 10.1071/BT02124

Cui, E. Q., Weng, E. S., Yan, E. R., and Xia, J. Y. (2020). Robust leaf trait relationships across species under global environmental changes. *Nat. Commun.* 11:2999. doi: 10.1038/s41467-020-16839-9

Dong, Y. P., Wang, B., Wei, Y. L., He, F., Lu, F., Li, D. X., et al. (2023). Leaf micromorphological, photosynthetic characteristics and their ecological adaptability of dominant tree species in a karst seasonal rain forest in Guangxi, China. *Guihaia* 42, 415–428. doi: 10.11931/guihaia.gxzw202203031

Gao, S. H., Ge, Y. X., Zhou, L. Y., Zhu, B. L., Ge, X. Y., Li, K., et al. (2018). What is the optimal number of leaves when measuring leaf area of tree species in a forest community? *Chin. J. Plant Ecol.* 42, 917–925. doi: 10.17521/cjpe.2018.0087

Geekiyanage, N., Goodale, U. M., Cao, K. F., and Kitajima, K. (2018). Leaf trait variations associated with habitat affinity of tropical karst tree species. *Ecol. Evol.* 8, 286–295. doi: 10.1002/ece3.3611

Givnish, T. J. (2002). Adaptive significance of evergreen vs. deciduous leaves: solving the triple paradox. *Silva Fenn.* 36, 703–743. doi: 10.14214/sf.535

He, N. P., Liu, C. C., Piao, S. L., Sack, L., Xu, L., Luo, Y. Q., et al. (2019). Ecosystem traits linking functional traits to macroecology. *Trends Ecol. Evol.* 34, 200–210. doi: 10.1016/j.tree.2018.11.004

Hultine, K. R., and Marshall, J. D. (2000). Altitude trends in conifer leaf morphology and stable carbon isotope composition. *Oecologia* 123, 32–40. doi: 10.1007/s004420050986

Jiang, Y., Chen, X. B., Ma, J. M., Liang, S. C., Huang, J., Liu, R. H., et al. (2016). Interspecific and intraspecific variation in functional traits of subtropical evergreen and deciduous broadleaved mixed forests in karst topography, Guilin, Southwest China. *Trop. Conserv. Sci.* 9, 194008291668021–194008291668029. doi: 10.1177/1940082916680211

Jiang, Z. C., Lian, Y. Q., and Qin, X. Q. (2014). Rocky desertification in Southwest China: impacts, causes, and restoration. *Earth-Sci. Rev.* 132, 1–12. doi: 10.1016/j.earscirev.2014.01.005

Jin, Y. L., Wang, H. Y., Xia, J., Ni, J., Li, K., Hou, Y., et al. (2023). TiP-leaf: a dataset of leaf traits across vegetation types on the Tibetan plateau. *Earth Syst. Sci. Data* 15, 25–39. doi: 10.5194/essd-15-25-2023

Jing, H. X., Sun, N. X., Umair, M., Liu, C. J., and Du, H. M. (2021). Leaf stoichiometric response of two typical herbaceous plants to water additions in degraded karst areas in southern Yunnan, China. *J. Yunnan Univ. Nat. Sci. Ed.* 43, 1254–1263. doi: 10.7540/j.ynu.20200450

Kambach, S., Sabatini, F. M., Attorre, F., Biurrun, I., Boenisch, G., Čarni, A., et al. (2023). Climate-trait relationships exhibit strong habitat specificity in plant communities across Europe. *Nat. Commun.* 14:712. doi: 10.1038/s41467-023-36240-6

Kattge, J., Bönisch, G., Díaz, S., Lavorel, S., Prentice, I. C., and Wirth, C. (2020). TRY plant trait database-enhanced coverage and open access. *Glob. Chang. Biol.* 26, 119–188. doi: 10.1111/gcb.14904

Kraft, N. J. B., Valencia, R., and Ackerly, D. D. (2008). Functional traits and niche-based tree community assembly in an Amazonian forest. *Science* 322, 580–582. doi: 10.1126/science.1160662

Lecerf, A., and Chauvet, E. (2008). Intraspecific variability in leaf traits strongly affects alder leaf decomposition in a stream. *Basic Appl. Ecol.* 9, 598–605. doi: 10.1016/j.baae.2007.11.003

Liu, L. B., Hu, J., Chen, X. Y., Xu, X., Yang, Y., and Ni, J. (2022). Adaptation strategy of karst forests: evidence from the community-weighted mean of plant functional traits. *Ecol. Evol.* 12:e8680. doi: 10.1002/ece3.8680

Liu, L. B., Wu, Y. N., Zhong, Q. L., Guo, Y. M., Xu, X., Yang, Y., et al. (2021). Tree species influences soil microbial community diversity but not biomass in a karst forest in southwestern China. *J. Plant Ecol.* 14, 280–290. doi: 10.1093/jpe/rtaa096

Liu, L. B., Xia, H. J., Quan, X. H., and Wang, Y. Q. (2023). Plant trait-based life strategies of overlapping species vary in different succession stages of subtropical forests. *Eastern China. Front. Ecol. Evol.* 10:1103937. doi: 10.3389/fevo.2022.1103937

McDonald, P. G., Fonseca, C. R., Overton, J., and Westoby, M. (2003). Leaf-size divergence along rainfall and soil-nutrient gradients: is the method of size reduction common among clades? *Funct. Ecol.* 17, 50–57. doi: 10.1046/j.1365-2435.2003.00698.x

Messier, J., McGill, B. J., and Lechowica, M. J. (2010). How do traits vary across ecological scales? A case for trait-based ecology. *Ecol. Lett.* 13, 838–848. doi: 10.1111/j.1461-0248.2010.01476.x

Myers-Smith, I. H., Thomas, H. J. D., and Bjorkman, A. D. (2019). Plant traits inform predictions of tundra responses to global change. *New Phytol.* 221, 1742–1748. doi: 10.1111/nph.15592

Niu, K. C., Zhang, S., and Lechowicz, M. (2020). Harsh environmental regimes increase the functional significance of intraspecific variation in plant communities. *Funct. Ecol.* 34, 1666–1677. doi: 10.1111/1365-2435.13582

Pan, Z. (2003). *Habitat Heterogeneity of Karst Ecological System and Plant Adaptability*. Ph.D. thesis. Guilin: Guangxi Normal University.

Pang, Z. Q., Lu, W. L., Jiang, L. S., Jin, K., and Qi, Z. (2019). Leaf traits of different growing plants in karst area of Shilin, China. *Guihaia* 39, 1126–1138. doi: 10.11931/guihaia.gxzw201810009

Peng, X., Dai, Q., Ding, G., and Li, C. (2019). Role of underground leakage in soil, water and nutrient loss from a rock-mantled slope in the karst rocky desertification area. *J. Hydrol.* 578:124086. doi: 10.1016/j.jhydrol.2019.124086

Peppe, D. J., Royer, D. L., Cariglino, B., Oliver, S. Y., Newman, S., Leight, E., et al. (2011). Sensitivity of leaf size and shape to climate: global patterns and paleoclimatic applications. *New Phytol.* 190, 724–739. doi: 10.1111/j.1469-8137.2010.03615.x

Pérez-Harguindeguy, N., Díaz, S., Garnier, E., Lavorel, S., Poorter, H., Jaureguiberry, P., et al. (2013). New handbook for standardised measurement of plant functional traits worldwide. *Aust. J. Bot.* 61, 167–234. doi: 10.1071/BT12225

R Core Team. (2018). *R: A Language and Environment for Statistical Computing*. R Foundation for Statistical Computing. Vienna.

Shui, W., Guo, P. P., Zhu, S. F., Feng, J., Sun, X., and Li, H. (2022). Variation of plant functional traits and adaptive strategy of woody species in degraded karst tiankeng of Yunnan Province. *Sci. Geogr. Sin.* 42, 1295–1306. doi: 10.13249/j.cnki.sgs.2022.07.016

Siefert, A., Violle, C., Chalmandrier, L., Albert, C. H., Taudiere, A., Fajardo, A., et al. (2015). A global meta-analysis of the relative extent of intraspecific trait variation in plant communities. *Ecol. Lett.* 18, 1406–1419. doi: 10.1111/ele.12508

Song, L. H. (2000). Progress and trend of karst geomorphology study. *Prog. Geogr.* 19, 193–202. doi: 10.11820/dlkxjz.2000.03.001

Sweeting, M. M. (1972). *Karst Landforms*. Macmillan: London.

Thuiller, W., Lavorel, S., Midgley, G., Lavergne, S., and Rebelo, T. (2004). Relating plant traits and species distributions along bioclimatic gradients for 88 Leucadendron taxa. *Ecology* 85, 1688–1699. doi: 10.1890/03-0148

Violle, C., Navas, M. L., Vile, D., Kazakou, E., Fortunel, C., Hummel, I., et al. (2007). Let the concept of trait be functional! *Oikos* 116, 882–892. doi: 10.1111/j.0030-1299.2007.15559.x

Weiher, E., and Keddy, P. A. (1995). Assembly rules, null models, and trait dispersion: new question front old patterns. *Oikos* 74, 159–164. doi: 10.2307/3545686

Westoby, M., Falster, D. S., Moles, A. T., Vesk, P. A., and Wright, I. J. (2002). Plant ecological strategies: some leading dimensions of variation between species. *Annu. Rev. Ecol. Syst.* 33, 125–159. doi: 10.1146/annurev.ecolsys.33.010802.150452

Wright, S. J., Kitajima, K., Kraft, N. J. B., Reich, P. B., Wright, I. J., Bunker, D. E., et al. (2010). Functional traits and the growth-mortality trade-off in tropical trees. *Ecology* 91, 3664–3674. doi: 10.1890/09-2335.1

Wright, I. J., Reich, P. B., Westoby, M., Ackerly, D. D., Baruch, Z., Bongers, F., et al. (2004). The worldwide leaf economics spectrum. *Nature* 428, 821–827. doi: 10.1038/nature02403

Xue, W. (2017). *Statistical Analysis and SPSS Application*. Beijing: China Renmin University Press.

Yang, Y., Xu, X., Xu, Y., and Ni, J. (2020). Adaptation strategies of three dominant plants in the trough-valley karst region of northern Guizhou Province, southwestern China, evidence from associated plant functional traits and ecostoichiometry. *Earth Environ.* 48, 413–423. doi: 10.14050/j.cnki.1672-9250.2020.48.061

Yu, Y. H., Zhong, X. P., Zheng, W., Chen, Z. X., and Wang, J. X. (2021). Species diversity, functional traits, stoichiometry and correlation of plant community in different succession stages of karst forest. *Acta Ecol. Sin.* 41, 2408–2417. doi: 10.5846/stxb202005031089

Zhang, S. H., Zhang, Y., Xiong, K. N., Yu, Y. H., and Min, X. Y. (2020). Changes of leaf functional traits in karst rocky desertification ecological environment and the driving factors. *Glob. Ecol. Conserv.* 24:e01381. doi: 10.1016/j.gecco.2020.e01381

Zhang, Q. W., Zhu, S. D., Jansen, S., and Cao, K. F. (2021). Topography strongly affects drought stress and xylem embolism resistance in woody plants from a karst forest in Southwest China. *Funct. Ecol.* 35, 566–577. doi: 10.1111/1365-2435.13731

Zhong, Q. L., Liu, L. B., Xu, X., Yang, Y., Guo, Y. M., Xu, H. Y., et al. (2018). Variations of plant functional traits and adaptive strategy of woody species in a karst forest of Central Guizhou Province, southwestern China. *Chin. J. Plant Ecol.* 42, 562–572. doi: 10.17521/cjpe.2017.0270

Zhou, T., Cui, Y. C., Ye, Y. Y., Zhao, W. J., Hou, Y. J., Wu, P., et al. (2022). Leaf functional traits of typical karst forest plants under different niches. *J. Cent. South Univ. Forestry Technol.* 42, 129–140. doi: 10.14067/j.cnki.1673-923x.2022.10.015

frontiers | Frontiers in Ecology and Evolution

TYPE Original Research
PUBLISHED 18 August 2023
DOI 10.3389/fevo.2023.1198085

OPEN ACCESS

EDITED BY
Xiang Liu,
Lanzhou University, China

REVIEWED BY
Yunquan Wang,
Zhejiang Normal University, China
David Gorchov,
Miami University, United States

*CORRESPONDENCE
Arundhati A. Das
arundhatid74@gmail.com

RECEIVED 31 March 2023
ACCEPTED 01 August 2023
PUBLISHED 18 August 2023

CITATION
Das AA, Ratnam J and Jathanna D (2023) Patterns and consequences of invasion of tropical montane forests by *Cestrum aurantiacum* Lindl. in the Western Ghats. *Front. Ecol. Evol.* 11:1198085. doi: 10.3389/fevo.2023.1198085

Patterns and consequences of invasion of tropical montane forests by *Cestrum aurantiacum* Lindl. in the Western Ghats

Arundhati A. Das[1]*, Jayashree Ratnam[1] and Devcharan Jathanna[2]

[1]Wildlife Biology and Conservation Program, National Centre for Biological Sciences, Tata Institute of Fundamental Research, Bangalore, Karnataka, India, [2]Carnivore & Herbivore Ecology & Conservation Programme, Wildlife Conservation Society-India, Kodigehalli, Bangalore, Karnataka, India

In the montane forest-grassland mosaics of the Western Ghats, land cover conversion to silviculture and agriculture over the last five decades has resulted in both loss of natural habitats and widespread invasion of remnant habitat patches. While invasion of the grassland habitats of the mosaic has been relatively well studied, there have been few attempts to understand the extent to which forest habitats (locally known as *sholas*) have been affected by the spread of exotic species. Here we examine the patterns and impacts of invasion of *shola* forest understoreys by *Cestrum aurantiacum* Lindl., an exotic shrub species. At the landscape scale, we demonstrate that the presence and abundance of this invasive in *shola* understories is negatively related to distance from tea plantations. Further, the intensity of invasion is higher in areas with greater seasonality of temperature and lower mean annual precipitation. At the patch scale, invasion is greatest at *shola* edges and away from stream courses. We find that *C. aurantiacum* abundance has negatively affected the regeneration of native *shola* tree species as well as the abundance of native *shola* understorey shrubs. Fifty three percent of invaded plots had no native shrubs present. In plots where both *C. aurantiacum* and native shrubs were present in large enough numbers, we found evidence of negative spatial dependence between stem locations of *C. aurantiacum* and native shrubs. Our findings have important implications for the management and conservation of these mosaics.

KEYWORDS

tropical montane forest, Western Ghats, *shola*, land cover change, invasion, *Cestrum aurantiacum* Lindl., multitype point pattern analysis

1 Introduction

Tropical montane ecosystems occur on all continents across the globe, and are thought to be especially vulnerable to multiple drivers of global change (Loeffler et al., 2011; Salinas et al., 2021). These include climatic changes such as warming and altered precipitation regimes, but also pervasive land-use changes such as the intensification of agriculture,

expansion of silviculture and built-up areas for human habitation (He et al., 2023). With complex topographies that support a diversity of natural vegetation types and multiple interacting change drivers, the responses of these ecosystems to ongoing and future global change are complex and difficult to predict (Loeffler et al., 2011; Salinas et al., 2021). For example, rates of invasion of montane ecosystems have been increasing rapidly across the globe, but the reasons for this remain poorly understood (Iseli et al., 2023), and are likely to vary across regions.

The "sky-islands" of the mountain tops of the Western Ghats in southern India, a global biodiversity hotspot, are a tropical montane ecosystem that typifies the above scenario. These forest–grassland mosaics consist of distinctive stunted evergreen forests (locally known as *sholas*) set in a matrix of grasslands. They are rich in endemic biodiversity and hold great significance, not only from an evolutionary perspective, but also for their provision of critical ecosystem services including climate and hydrological regulation for the entire southern peninsular region (Sukumar et al., 1995; Bose et al., 2016; Joshi et al., 2018). Over the course of the past hundred and fifty years, but accelerating over the past five decades, large sections of these mosaic habitats have been converted to other land uses such as agricultural and silvicultural plantations, mainly at the expense of grasslands (Prabhakar, 1994; Joshi et al., 2018). This has resulted in extensive land-cover change across the region, with more than sixty percent of the grassland habitats converted to exotic tree plantations, and also the widespread invasion of remnant patches of natural habitats (Joshi et al., 2018; Arasumani et al., 2019; Sriramamurthy et al., 2022).

One visible and widely acknowledged effect of the conversion of grasslands to exotic tree plantations has been the increase in invasive alien species in the remnant grasslands (Thomas and Palmer, 2007, *pers. obs.*). While one of main species of exotic plantation trees, *Acacia mearnsii*, itself is a dominant and aggressive invader of the remnant natural grasslands (Thomas and Palmer, 2007; Arasumani et al., 2019), other woody invasive shrubs, including scotch broom *Cytisus scoparius* and common gorse *Ulex europaeus* have also invaded the grasslands extensively in recent years (Sriramamurthy et al., 2022). While these woody invasions of the grasslands have received lot of research attention (Joshi et al., 2018; Arasumani et al., 2019; Sriramamurthy et al., 2020), far less research attention has been paid to the less visible invasions, often in the understoreys, of *shola* forest patches. This is an important knowledge gap, as the patterns and consequences of invasions within *shola* forests are likely to differ from those in grasslands, such that the management of invasives in the *sholas* versus the grasslands, will require different strategies.

Over the past few decades, *shola* forests have witnessed the spread of an exotic woody invader, *Cestrum aurantiacum* Lindl. The genus *Cestrum* is native to Central and South America where it thrives in montane forests (Monro, 2012). The abundant, attractive and fragrant flowers of this genus are the reason it has been introduced as an ornamental plant in many regions, where it has subsequently become naturalized, and in several cases, turned invasive, including in parts of Africa, Asia, Australia and multiple oceanic islands (Henderson, 2007; Harvey et al., 2012; Junaedi, 2012; Gardener et al., 2013; Padmanaba et al., 2017; Makokha, 2018). In the Indian subcontinent, *C. aurantiacum* has been reported across many montane regions including the Himalaya, the Western Ghats and in Sri Lanka (Kunwar, 2003; Sajeev et al., 2012; Wijesundara, 2012; Moktan and Das, 2013; Mandal and Joshi, 2015; Nayak et al., 2020). In general, *Cestrum* spp. are fast-growing and capable of vegetative reproduction (Symon, 1981). *C. aurantiacum* tends to form dense mats which can suppress the regeneration of other plant species (USDA, 2013; Witt and Luke, 2017). However, few studies have investigated the impacts of invasion by *C. aurantiacum* on native forest communities, and there is little primary data on the ecology and impacts of this particular species.

Here, we investigated the correlates and consequences of the invasion of *shola* forest communities by *C. aurantiacum*. Because *C. aurantiacum* was introduced as an ornamental plant in tea plantations, we hypothesized that *sholas* near tea plantations would be more heavily invaded by *C. aurantiacum* than *sholas* further away. We also expected that *C. aurantiacum* abundance within *sholas* would be related to other climatic and habitat factors such as rainfall and local topography, which influence stand structure and soil moisture, and thereby the optimal conditions for this species. Finally, we expected that *C. aurantiacum* invasion has led to reduced native *shola* tree regeneration, as well as reduced abundances of native *shola* understorey shrubs, possibly through negative competitive interactions.

2 Methods

2.1 Study area

The study was conducted across 60 km^2 in the western and southern parts of the Upper Nilgiris Plateau (11.17°N,76.77°E and 11.50°N, 76.43°E), that still hold large areas of natural *shola*–grassland mosaics, dating to at least 40,000 years ago (Caner et al., 2007). Please see Supplementary Figure S1 for a map of the study area. Other dominant land cover types in the region, such as non-native tree plantations and commercial tea plantations, were established relatively recently (Prabhakar, 1994), predominantly through the conversion of natural grasslands (Joshi et al., 2018). The region is rich in endemic plants (Blasco, 1971) and has extraordinary vertical and horizontal physiographic differentiation. Mean annual rainfall ranges from above 2500 mm on the Western side to 1200 mm towards the east (Von Lengerke, 1977; Caner et al., 2007). The dry season lasts for 3–4 months mainly between December and March. Temperature ranges from a mean maximum of 24 °C in April to a mean minimum of 5 °C in December. Frost occurs between November and March and mainly in the valleys rather than the higher hill slopes (Von Lengerke, 1977; Caner et al., 2007). The elevation range covered in this study extends from 1750–2400 m ASL.

2.2 *Cestrum*: a montane forest invasive in the Upper Nilgiris

The genus *Cestrum* in the family Solanaceae has 175 known species of shrubs, vines and small trees (de Rojas and D'Arcy, 1998;

Monro, 2012). The native range for this genus is Central and South America (Monro, 2012). Here most *Cestrum* species occur in montane areas, above 800 m elevation, in cloud forests and conifer and oak forests (de Rojas and D'Arcy, 1998; Monro, 2012). Introduced as ornamentals in various parts of the world, many species of this genus have now become invasive. Most *Cestrum* spp. bear berries with small seeds that remain viable in the seed bank and are bird-dispersed (Marambe et al., 2001; Geldenhuys, 2004; Gardener et al., 2013). They are also shade-tolerant (Geldenhuys, 2004), drought-tolerant, capable of growing on poor soils and have invaded a range of habitats from coastal dunes to savannahs, grasslands, plantations and closed forest (Henderson, 2007). Most are quite toxic to livestock, native mammals and humans (de Rojas and D'Arcy, 1998; Makokha, 2018). For these reasons, they are labelled as noxious weeds with moderate to high invasive potential (Nel et al., 2004; Henderson, 2007). In South Africa and Australia, extensive programs have been undertaken to clear areas of *Cestrum* species (Macdonald and Jarman, 1985; Stockard, 1996; Marais and Wannenburgh, 2008).

C. aurantiacum is an evergreen climbing shrub 1–6 m tall, with thin, unpleasant smelling leaves that are toxic to livestock. It is native to central America (Costa Rica, Guatemala, Honduras, Mexico and Nicaragua; CABI, 2023). In many parts of its invaded range, *C. aurantiacum* occurs in montane forests, between 1500 to above 2000m (Junaedi, 2012; Sajeev et al., 2012; Wijesundara, 2012; Moktan and Das, 2013; Makokha, 2018; Witt et al., 2018). In the Nilgiris, it has successfully invaded native forest fragments and the understorey of tree plantations above 2000 m (Saravanan et al., 2014, Figure 1). It appears to have spread from settled areas and tea plantations, where its abundance is highest (AAD *pers. obs*) and was likely imported as an ornamental plant for the estate managers' bungalows. In its native range, it appears to be well adapted to the cloud forest environment (de Rojas and D'Arcy, 1998; Monro, 2012), which would allow it to thrive in the dense shade of *sholas*.

2.3 Data collection

Shola woody communities were sampled using 0.04 ha plots (n = 87), that were located using a stratified random sampling design based on topography and surrounding land cover. Field data were collected between 2010–2012 (Das et al., 2017). We sampled a total of 52 *shola* forest patches in varying landscape contexts (i.e., natural grassland, tea plantation and non-native tree plantations). Within forest patches, plots were spaced at least 50 m apart. Species identity, height and diameter at breast height (dbh) were recorded for individuals >1 cm dbh. We also recorded the position of individual trees and shrubs within the plot by dividing it into 5m blocks and mapping the location of each stem within each block. Two transects of four 1 × 1 m seedling plots each were laid across each vegetation plot. Seedlings (individuals <50 cm height) of all woody species within these plots were censused. Distance to the nearest forest edge, GPS location of the plot corner, elevation, slope and aspect were also recorded in the field. We confirmed species identities using published flora (Gamble, 1923; Ramesh et al., 2008) and the help of an experienced taxonomist.

2.4 Data analysis

We modelled *C. aurantiacum* presence as a function of distance to the closest tea plantation edge using a GLM with binomial error and a logit link function (McCullach and Nelder, 1989). The results were used to find a threshold distance from tea plantations beyond which the probability of *C. aurantiacum* occurrence approached zero. We used this threshold to identify a subset of study plots within which *C. aurantiacum* presence was likely based on their distance from a tea plantation edge (n = 54). This was done to ensure that subsequent analysis of the correlates of *C. aurantiacum* abundance was free from the issue of zero-inflation (Martin et al., 2005). We used data from these plots to model *C. aurantiacum* abundance as a function of bio-climatic and habitat variables listed as follows: temperature seasonality (standard deviation of monthly temperature averages), mean annual precipitation, CV of precipitation (i.e., variation in monthly precipitation within a year), distance to tea plantation, distance to nearest *shola* edge, distance to stream. Bioclimatic predictors were sourced from Hijmans et al. (2005). This data is derived from interpolations of existing weather station data at a 1 km^2 spatial resolution. The values represent long term averages between 1950 and 2000. Distance from tea plantation was measured using high resolution imagery in Google Earth (Google Earth, 2013). Distance from nearest forest edge was recorded in the field and distance to

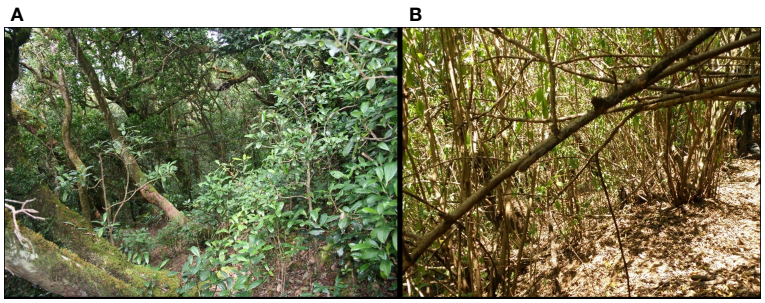

FIGURE 1
(A) *Shola* understorey with native shrubs (*Psychotria* spp.) present. **(B)** *Shola* understorey invaded by *Cestrum aurantiacum* with no native shrubs visible.

stream was calculated in QGIS after deriving a stream network from a DEM with 30m resolution (METI and NASA, 2011). All predictors were checked for collinearity and standardized prior to running the models. A set of competing models using these predictors were compared using Akaike Information Criteria to identify the model that best predicted *C. aurantiacum* abundance.

To assess impacts of *C. aurantiacum* invasion on native woody plants, we tested whether the number of *shola* tree seedlings and native shrubs in the plot were related to *C. aurantiacum* abundance using GLMs with a Poisson error term and a log link function. Analysis of spatial point patterns has been used to assess the presence of competitive interactions between plants (Gray and He, 2009; Pescador et al., 2020). Here, we assessed evidence for competitive interactions between *C. aurantiacum* and native shrub species by testing whether native shrubs (individuals belonging to three genera: *Psychotria*, *Lasianthus* and *Tarenna*) were located farther from *C. aurantiacum* individuals than what would be expected if their distributions were independent at the plot level. As most of the plots invaded by *C. aurantiacum* had no native shrubs present in the understorey, this test was run on only three plots which had sufficient sample size for both *C. aurantiacum* as well as native shrubs. We first tested whether the point pattern of *C. aurantiacum* and native shrubs within the plot conformed to a homogenous Poisson point process by dividing each of the three plots into nine sub plots and conducting a x^2 test to assess whether the point pattern departed from complete spatial randomness. After confirming homogeneity of the observed point pattern, we used the cross-type L-function (Lcross), a linearized version of Ripley's *K* function for multitype point patterns (Baddeley et al., 2016), to assess whether the point locations of native shrubs showed evidence of competitive inhibition relative to a null hypothesis in which their locations were independent of those of *C. aurantiacum* within each plot. The Ripley's *K* function for multitype points quantifies spatial aggregation between points of different types within a circle of radius *r* around a given focal point (Baddeley et al., 2016). The null hypothesis was modelled by splitting the data into the sub-patterns of points of each type and randomly shifting each of these sub-patterns, independently of the other using a toroidal shift and then calculating Lcross for the plot (Baddeley et al., 2016). As we had a square plot (20 × 20 m), we also used a toroidal shift to correct for edge effects while estimating Lcross (Baddeley et al., 2016). We used Monte Carlo simulations to test the significance of Lcross at the α = 0.05 level (Baddeley et al., 2016). All analyses were conducted in QGIS v.3.22 (QGIS Development Team, 2022) and statistical software R v.4.2.1 (R Core Team, 2022) using the packages: 'spatstat' (Baddeley et al., 2016), 'maptools' (Bivand and Lewin-Koh 2022).

3 Results

3.1 Correlates of *C. aurantiacum* abundance

C. aurantiacum was present in 17 of the 87 (19.5%) study plots. In these plots, the number of mature individual *C. aurantiacum* stems ranged from 1–54 (mean of 17.6). The probability of *C. aurantiacum* presence was greatest between 0–2 km from a tea plantation edge and fell to near zero beyond 4 km from a tea plantation edge (Figure 2). Within plots ≤ 4 km from a tea plantation edge (n = 54), *C. aurantiacum* abundance was influenced by both bio-climatic (temperature seasonality and annual precipitation) and habitat factors (i.e., distance to tea edge, distance to *shola* fragment edge, distance to stream; Table 1). The β for seasonality of temperature (0.015 [0.0009]) indicates that *C. aurantiacum* abundance is higher in areas with greater seasonality of temperature. *Cestrum* abundance decreases with mean annual precipitation (−0.004 [0.0005]). Abundance decreases with distance from the *shola* edge (−0.014 [0.002]) and tea plantations (−0.0001 [0.0001]) and increases with distance from stream (0.0003 [0.0007]) (Figure 3).

3.2 Relationship between *C. aurantiacum* abundance and native shrubs and regeneration of native trees

Most of the plots (53%) where *C. aurantiacum* was present did not have any individuals belonging to native shrub genera. The number of individuals of native shrub species in the plot was significantly negatively related to *Cestrum* abundance (β = −0.07 [0.005], $P < 0.001$). *Cestrum* abundance had a significant but weak negative relationship with the number of native *shola* tree seedlings in a plot (−0.009 [0.002], $P < 0.001$; Figure S2). However, the number of *shola* tree saplings in a plot did not show a significant relationship to *C. aurantiacum* abundance (0.00006 [0.0007], $P > 0.1$).

The results of the point pattern analysis indicate support for competitive inhibition of native shrubs by *C. aurantiacum*. The Lcross metric indicates greater separation between native shrub

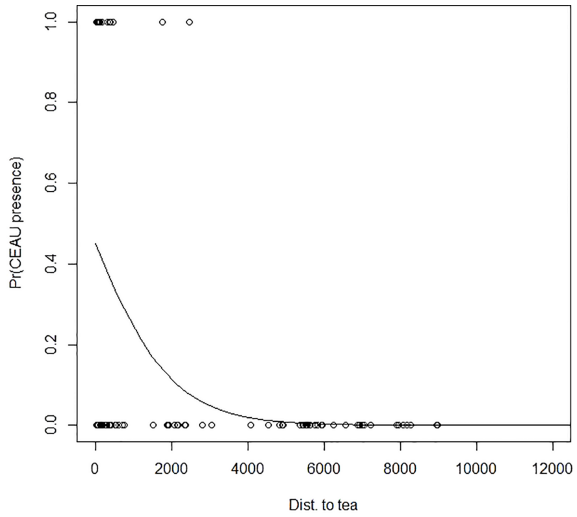

FIGURE 2
Probability of *Cestrum aurantiacum* presence in *shola* forest patches in the Upper Nilgiris modelled as a function of distance from tea plantation edge in meters. Modelled as a GLM with binomial error.

TABLE 1 Results of model selection using GLMs with Poisson error to model *Cestrum aurantiacum* abundance in sholas as a function of bio-climatic and distance variables.

S.no	Model*	AIC	ΔAIC	Mod lik	AIC_Weight
1	tmp.seas+ann.prec+d.tea+d.edge+d.stream	668.69	0	~1	~1
2	tmp.seas+prec.cv+d.tea+d.edge+d.stream	707.52	38.83	~0	~0
3	tmp.seas+d.tea+d.edge+ d.stream	729.67	60.98	~0	~0
4	tmp.seas+ann.prec	918.93	250.24	~0	~0
5	tmp.seas	936.54	267.85	~0	~0
6	prec.cv+d.tea+d.edge+d.stream	952.71	284.02	~0	~0
7	ann.prec+d.tea+d.edge+ d.stream	1105.4	436.71	~0	~0
8	d.tea+d.edge+ d.stream	1107.7	439.01	~0	~0
9	prec.cv	1140	471.31	~0	~0
10	d.stream	1178.2	509.51	~0	~0
11	d.tea+ d.edge	1332.1	663.41	~0	~0
12	d.tea	1345	676.31	~0	~0
13	d.edge	1444	775.31	~0	~0
14	ann.prec	1509.2	840.51	~0	~0

Predictor codes: tmp.seas = temperature seasonality, ann.prec = mean annual precipitation, prec.cv = cv of precipitation, d.tea = distance to tea edge, d.stream = distance to nearest stream, d.edge = distance to nearest shola edge.

locations and *C. aurantiacum* locations than expected under spatial independence, at scales of approximately 1–5 meters in two of the three plots, and some evidence in support of spatial dependence at the 0.5–1.5 m scale in the third plot (Figure 4).

4 Discussion

More than half (53%) of the woody species encountered in this study are endemic to the Western Ghats (Ramesh and Pascal, 1997). Woody invasive shrubs such as *Lantana camara* (< 2000 m; Najar et al., 2019) and *C. aurantiacum* (> 2000m) threaten this unique biodiversity. Here we show that the invasive spread of *C. aurantiacum* in the Upper Nilgiris is associated with the presence of tea plantations, as native *shola* forests embedded within a matrix of tea estates or within 4 km from a tea plantation edge, were more likely to have this species in the understorey, with its abundance increasing in *sholas* closer to tea plantations. Further, we found that increasing *C. aurantiacum* abundance appeared to negatively impact the presence and abundance of dominant native shrub genera *Psychotria*, *Lasianthus* and *Tarenna* as well as *shola* seedling regeneration. A number of studies including Bartuszevige et al. (2006); González-Moreno et al. (2013); Chen et al. (2017); Shiferaw et al. (2019), and the synthetic review by Vilà and Ibáñez

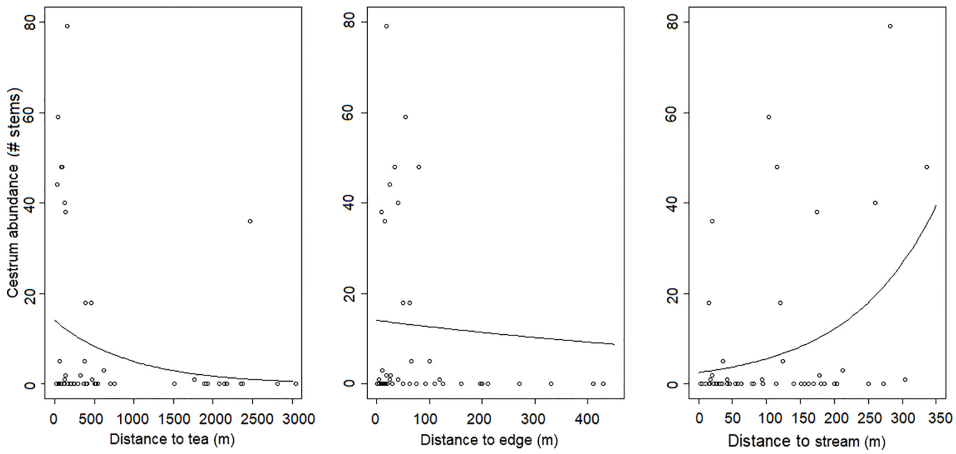

FIGURE 3
Cestrum aurantiacum abundance in *sholas* modelled as a function of distance to tea plantation edge, distance to nearest *shola* fragment edge and distance to stream, modelled using GLMs with Poisson errors.

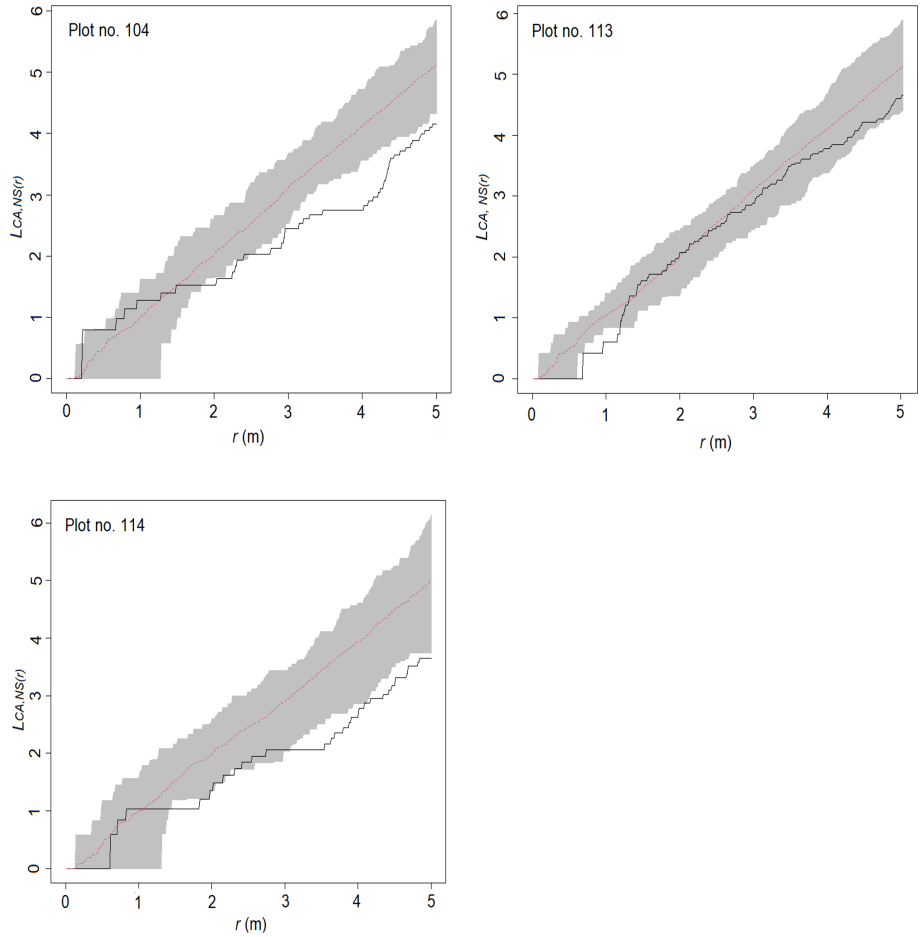

FIGURE 4
Lcross function for point locations of *Cestrum aurantiacum* (CA) and native shrub species (NS) in three plots in the Upper Nilgiris *shola* forests. In each case, the black solid line shows observed value while the red dashed line represents the expectation under complete spatial independence between the locations of CA and NS. Values of $L_{(CA,\ NS)}\ r > r$ indicate spatial aggregation, while $L_{(CA,\ NS)}\ r < r$ indicates spatial regularity. The grey shaded area represents the 95% confidence envelope of the Lcross function under the null expectation of spatial independence, calculated using Monte Carlo simulations.

(2011) have similarly found that landscape attributes play an important role (or a more important role than local site factors) in driving the presence of invasive species or the variation in invasion risk across space, while Milbau et al. (2009) outline a hierarchical framework where "…factors operating at a smaller scale are subordinate to factors operating at a larger scale, but if conditions at higher levels are satisfied, the small-scale factors may become indispensable for making accurate predictions".

4.1 Bioclimatic and site-level factors influencing the spread of *C. arurantiacum* and their links to land cover change

C. aurantiacum abundance was positively related to annual temperature seasonality – which in turn is highly negatively correlated to the elevation gradient in this study, indicating lower bio-climatic suitability at the highest part of the elevation gradient in this study (2200–2400 m). This species is susceptible to frost damage (AAD *pers. obs.*), which could explain why it does not occur in open grasslands (where frost occurs; Joshi et al., 2020) but rather along roads (Nayak et al., 2020) and other edges where some shrub or tree cover is present (Jobin et al., 2023). The conversion of large expanses of native grasslands to timber plantations, tea and other landuses (Prabhakar, 1994; Joshi et al., 2018) may thus have facilitated the spread of this species, by creating connected edge habitats with suitable microclimatic conditions (reduced extent and intensity of frost; Von Lengerke, 1977) across the landscape.

Land cover changes and associated changes in anthropogenic disturbances may also favour the spread of this invasive species through the opening of canopies that increase light availability in the understory (Lozano and MacIsaac, 1997; Iseli et al., 2023). Junaedi (2012) found that *C. aurantiacum* presence was positively related to light intensity. Wijesundara (2012) reports it spreading in montane forest die-back gaps in Sri Lanka. Here we found the species to be more abundant in plots close to *shola*–tea plantation edges, which are more likely to have greater light penetration due to human disturbance. Finally, land cover changes are often associated with changes in the composition of pollinator and disperser communities (Raman, 2006), which in turn can facilitate invasive spread. In the Nilgiris, *C. aurantiacum* seeds are dispersed by common bird species that thrive in anthropogenic habitats, like

the red-whiskered bulbul (AAD *pers. obs.*). In Sri Lanka, its seeds are dispersed by the yellow-eared bulbul (Wijesundara, 2012), while flowers are reported to be pollinated by the Sri Lankan white-eye (*Zosterops ceylonensis;* Wijesundara, 2012).

4.2 Impacts of *C. aurantiacum* on native *shola* woody plant communities

Shola seedling regeneration was found to be lower in *C. aurantiacum* invaded sites. A similar finding has been reported for *Lantana* invaded sites in the Upper Nilgiris (Najar et al., 2019). The negative relationship between *C. aurantiacum* and native seedling regeneration could be due to either direct competitive effects or allelopathic interactions (Callaway and Ridenour, 2004). *Cestrum* spp. are reported to have anti-microbial properties (Prasad et al., 2013), which may lead to altered soil microbial communities in invaded sites (Elgersma and Ehrenfeld, 2011), thereby affecting native seedling regeneration. Alternatively, this association could also arise due to greater human disturbance in *sholas* near tea plantations, leading to lower levels of native species regeneration, while also allowing *C. aurantiacum* to spread faster (Lozano and MacIsaac, 1997). Further research is needed to elucidate the mechanisms behind this observation.

We found a strong negative relationship between *C. aurantiacum* abundance and the dominant native shrubs of the *shola* understorey, with some evidence in support of negative spatial interactions within the plot. There are several factors that could contribute to the impact of *C. aurantiacum* on native shrub populations. For instance, *C. aurantiacum* is native to cloud forest understoreys of central America and may therefore be well adapted to the microclimatic conditions of *shola* forest understoreys. This could enhance its impact within the context of this habitat (Kestrup and Ricciardi, 2009). It also grows in denser stands than native species, which has been associated with stronger impacts (Hejda et al., 2009). The combination of such environmental matching and greater fecundity (discussed below), could lead to large increases in abundance of *C. aurantiacum* in *shola* understories, sufficient to exclude native shrubs in parts of their range (MacDougall et al., 2009; Ricciardi et al., 2013).

While *C. aurantiacum* and native shrubs share common abiotic habitat requirements, they differ phylogenetically and also in key traits linked to growth and resource acquisition (trait divergence or phylogenetic distinctiveness; Ricciardi and Atkinson, 2004). Native *shola* understorey dominants all belong to the family Rubiaceae, while *C. aurantiacum* is a member of Solanaceae. Further, it displays traits associated with fast growth and rapid resource capture in comparison to native shrubs (high specific leaf area (SLA) – thinner, larger, more easily bruised leaves, low stem specific density; AAD *pers. obsv.*). Therefore, *C. aurantiacum* may avoid the effects of competitive interactions with native shrub species (Levine et al., 2003) by being sufficiently different from them in terms of phylogeny and key traits (Sofaer et al., 2018; Pearse et al., 2019).

Finally, *C. aurantiacum* exhibits characteristics associated with greater fecundity compared to native shrubs, i.e., more frequent and profuse flowering and fruiting (AAD *pers. obs.*). A South African study found it had comparable levels of fruit set to *Lantana* (Rambuda, 2001). Further research is required to assess the presence and relative contribution of each of the factors discussed above to the magnitude of *C. aurantiacum* impact on native shrubs.

4.3 Implications for conservation and management of *shola* habitats

Upper montane forests in the tropics and subtropics, like the *sholas*, often occur as relatively small patches (<10 ha), that are separated by native grasslands, tea plantations or non-native timber stands (Wijesundara, 2012; Das et al., 2017). Hence, these habitats may be more vulnerable to impacts of invasion in the same way that islands are, due to their restricted area and isolation (Pyšek et al., 2012). In particular, they may exhibit a different form of the relationship between invader abundance and per capita impact compared to continuous forest ecosystems, with associated implications for the timing and nature of management interventions (Sofaer et al., 2018; Strayer, 2020).

Tea estates constitute approximately 26% of the Upper Nilgiris Plateau above 1400 m ASL (Arasumani et al., 2019) and therefore potentially pose a serious threat to native forests through propagule rain from invasive plants. We observed wide variation in the quality of tea estate (holdings >100 ha) management across the landscape, ranging from abandonment of large areas planted with tea to intensely managed tea plantations. *Shola* patches in Korakundah tea estate, which has numerous certifications for ecological sustainability and fair trade, did not have *C. aurantiacum* in the understorey, indicating that estate management based on best practices could be effective in controlling the spread of this species. The COVID pandemic and related restrictions have probably hampered estate upkeep and management through shortages of tea estate labour and management personnel in areas important for conservation (Bates et al., 2021).

More recent work (Jobin et al., 2023) indicates that *C. aurantiacum* is also growing in the understorey of non-native timber plantations. It is also common in settlements and along road margins (AAD *pers obs*),. Together these landcover types probably contribute massive amounts of seed rain from *C. aurantiacum* across the Upper Nilgiris. Therefore, urgent attention to control of this species (particularly along road margins) in production and forestry landscapes surrounding natural *shola* forests – specifically targeting the interface between *sholas* and the surrounding land cover – is critical to mitigate the impacts of invasion. Experimental studies comparing the relative effectiveness of control methods for this species at different levels of invasion should be prioritized along with the restoration of native *shola* species (Mohandass et al., 2016; Najar et al., 2019).

Data availability statement

The raw data supporting the conclusions of this article will be made available by the authors, without undue reservation.

Author contributions

AAD conceptualized the research, collected the primary field data, ran the analysis and wrote and edited the manuscript. JR helped with conceptualization of the manuscript, and wrote and edited the manuscript. DJ helped with collection and analysis of field data, visualized the results, and edited the manuscript. All authors contributed to the article and approved the submitted version.

Funding

Funding for field data collection was provided by the ATREE-NORAGRIC grant. Further financial support for AAD from the DBT-RA programme in Biotechnology & Life Sciences is gratefully acknowledged.

Acknowledgments

We thank Tamil Nadu Forest Department for granting fieldwork permits, and the management of Korakundah, Royal Valley, Thia Shola and Prospect Tea Estates for field assistance. We thank Uma Ramakrishnan for supporting AAD during her postdoctoral work. We are grateful to K.S. Bawa and T. Ganesh for guidance and support. We also thank Kartik Shanker and Siddharth Krishnan for their assistance with logistics during field data collection and R. Ganesan for taxonomic assistance. Paul Dorai, V. Rathish, Kishore and Thorthai Gooden assisted with field data collection. We are grateful to Mandira Banerji for her support. Finally, we thank the reviewers for their comments on the manuscript.

Conflict of interest

The authors declare that the research was conducted in the absence of any commercial or financial relationships that could be construed as a potential conflict of interest.

Publisher's note

Supplementary material

The Supplementary Material for this article can be found online at: https://www.frontiersin.org/articles/10.3389/fevo.2023.1198085/full#supplementary-material

References

Arasumani, M., Khan, D., Vishnudas, C. K., Muthukumar, M., Bunyan, M., Robin, V. V., et al. (2019). Invasion compounds an ecosystem-wide loss to afforestation in the tropical grasslands of the Shola Sky Islands. *Biol. Conserv.* 230, 141–150. doi: 10.1016/j.biocon.2018.12.019

Baddeley, A., Rubak, E., and Turner, R. (2016). *Spatial point patterns: methodology and applications with R* (Boca Raton, Florida, USA: CRC press).

Bartuszevige, A. M., Gorchov, D. L., and Raab, L. (2006). The relative importance of landscape and community features in the invasion of an exotic shrub in a fragmented landscape. *Ecography* 29, 213–222. doi: 10.1111/j.2006.0906-7590.04359.x

Bates, A. E., Primack, R. B., Biggar, B. S., Bird, T. J., Clinton, M. E., Command, R. J., et al. (2021). Global COVID-19 lockdown highlights humans as both threats and custodians of the environment. *Biol. Conserv.* 263, 109175. doi: 10.1016/j.biocon.2021.109175

Bivand, R., and Lewin-Koh, N. (2022). *maptools: Tools for Handling Spatial Objects. R package version 1.1-6*. Available at: https://CRAN.R-project.org/package=maptools.

Blasco, F. (1971). *Montagnes du Sud de l'Inde: forêts, savanes, écologie* (Pondicherry: Institut Français de Pondicherry. French Institute of Pondicherry).

Bose, R., Munoz, F., Ramesh, B. R., and Pelissier, R. (2016). Past potential habitats shed light on the biogeography of endemic tree species of the Western Ghats biodiversity hotspot, South India. *Journal of Biogeography* 43, 899–910.

CABI (2023). *Cestrum aurantiacum. CABI Compendium* (Wallingford, UK: CAB International).

Callaway, R. M., and Ridenour, W. M. (2004). Novel weapons: invasive success and the evolution of increased competitive ability. *Front. Ecol. Environ.* 2, 436–443. doi: 10.1890/1540-9295(2004)002[0436:NWISAT]2.0.CO;2

Caner, L., Seen, D. L., Gunnell, Y., Ramesh, B. R., and Bourgeon, G. (2007). Spatial heterogeneity of land cover response to climatic change in the Nilgiri highlands (southern India) since the Last Glacial Maximum. *Holocene* 17, 195–205. doi: 10.1177/0959683607075833

Chen, C., Wu, S., Meurk, C. D., Ma, M., Zhao, J., and Tong, X. (2017). Effects of local and landscape factors on exotic vegetation in the riparian zone of a regulated river: Implications for reservoir conservation. *Landscape Urban Plann.* 157, 45–55. doi: 10.1016/j.landurbplan.2016.06.003

Das, A. A., John, R., and Anand, M. (2017). Does structural connectivity influence tree species distributions and abundance in a naturally discontinuous tropical forest formation? *J. Vegetation Sci.* 28, 7–18. doi: 10.1111/jvs.12474

de Rojas, C. B., and D'Arcy, W. G. (1998). The genera cestrum and sessea (Solanaceae: cestreae) in Venezuela. *Ann. Missouri Bot. Garden* 85, 273–351. doi: 10.2307/2992010

Elgersma, K. J., and Ehrenfeld, J. G. (2011). Linear and non-linear impacts of a non-native plant invasion on soil microbial community structure and function. *Biol. Invasions* 13, 757–768. doi: 10.1007/s10530-010-9866-9

Gamble, J. S. (1923). *Flora of the Presidency of Madras* (London, UK: Adlard & Son).

Gardener, M. R., Trueman, M., Buddenhagen, C., Heleno, R., Jäger, H., Atkinson, R., et al. (2013). *A Pragmatic Approach to the Management of Plant Invasions in Galapagos | SpringerLink. Plant Invasions in Protected Areas: Patterns, Problems and Challenges, Invading Nature* (Dordrecht: Springer).

Geldenhuys, C. J. (2004). Concepts and process to control invader plants in and around natural evergreen forest in South Africa1. *Weed Technol.* 18, 1386–1391. doi: 10.1614/0890-037X(2004)018[1386:CAPTCI]2.0.CO;2

QGIS Development Team. (2022). QGIS Geographic Information System. QGIS Association. Available at: http://www.qgis.or.

González-Moreno, P., Pino, J., Carreras, D., Basnou, C., Fernández-Rebollar, I., and Vila, M. (2013). Quantifying the landscape influence on plant invasions in Mediterranean coastal habitats. *Landscape Ecol.* 28, 891–903. doi: 10.1007/s10980-013-9857-1

Google Earth. (2013). *Satellite images for southern India. Data providers: Digital Globe and Cnes/SPOT. Imagery dated 2008-2013*. Available at: www.googleearth.com (Accessed July and August 2013).

Gray, L., and He, F. (2009). Spatial point-pattern analysis for detecting density-dependent competition in a boreal chronosequence of Alberta. *For. Ecol. Manage.* 259, 98–106. doi: 10.1016/j.foreco.2009.09.048

Harvey, K. J., Nipperess, D. A., Britton, D. R., and Hughes, L. (2012). Australian family ties: does a lack of relatives help invasive plants escape natural enemies? *Biol. Invasions* 14, 2423–2434. doi: 10.1007/s10530-012-0239-4

He, X., Ziegler, A. D., Elsen, P. R., Feng, Y., Baker, J. C., Liang, S., et al. (2023). Accelerating global mountain forest loss threatens biodiversity hotspots. *One Earth* 6, 303–315. doi: 10.1016/j.oneear.2023.02.005

Hejda, M., Pyšek, P., and Jarošík, V. (2009). Impact of invasive plants on the species richness, diversity and composition of invaded communities. *J. Ecol.* 97, 393–403. doi: 10.1111/j.1365-2745.2009.01480.x

Henderson, L. (2007). Invasive, naturalized and casual alien plants in southern Africa: a summary based on the Southern African Plant Invaders Atlas (SAPIA). *Bothalia* 37, 215–248. doi: 10.4102/abc.v37i2.322

Hijmans, R. J., Cameron, S. E., Parra, J. L., Jones, P. G., and Jarvis, A. (2005). Very high resolution interpolated climate surfaces for global land areas. *Int. J. Climatol.* 25, 1965–1978. doi: 10.1002/joc.1276

Iseli, E., Chisholm, C., Lenoir, J., Haider, S., Seipel, T., Barros, A., et al. (2023). Rapid upwards spread of non-native plants in mountains across continents. *Nat. Ecol. Evol.* 7, 405–413. doi: 10.1038/s41559-022-01979-6

Jobin, V., Das, A., Harikrishnan, C. P., Chanda, R., Lawrence, S., and Robin, V. V. (2023). Patterns of understory invasion in invasive timber stands of a tropical sky island. *Ecol. Evolution.* 13 (4), e9995. doi: 10.1002/ece3.9995

Joshi, A. A., Ratnam, J., and Sankaran, M. (2020). Frost maintains forests and grasslands as alternate states in a montane tropical forest–grassland mosaic; but alien tree invasion and warming can disrupt this balance. *J. Ecol.* 108, 122–132. doi: 10.1111/1365-2745.13239

Joshi, A. A., Sankaran, M., and Ratnam, J. (2018). 'Foresting' the grassland: Historical management legacies in forest-grassland mosaics in southern India, and lessons for the conservation of tropical grassy biomes. *Biol. Conserv.* 224, 144–152. doi: 10.1016/j.biocon.2018.05.029

Junaedi, D. I. (2012). Invasive plants in mountainous remnant forest: recommendation for choosing best decision for invasive species management of Cestrum aurantiacum Lindl. *Buletin Kebun Raya* 15, 37–47.

Kestrup, Å. M., and Ricciardi, A. (2009). Environmental heterogeneity limits the local dominance of an invasive freshwater crustacean. *Biol. Invasions* 11, 2095–2105. doi: 10.1007/s10530-009-9490-8

Kunwar, R. M. (2003). Invasive alien plants and Eupatorium: Biodiversity and livelihood. *Himalayan J. Sci.* 1, 129–133. doi: 10.3126/hjs.v1i2.213

Levine, J. M., Vila, M., Antonio, C. M. D., Dukes, J. S., Grigulis, K., and Lavorel, S. (2003). Mechanisms underlying the impacts of exotic plant invasions. *Proc. R. Soc. London Ser. B.: Biol. Sci.* 270, 775–781. doi: 10.1098/rspb.2003.2327

Loeffler, J., Anschlag, K., Baker, B., Finch, O. D., Diekkrueger, B., Wundram, D., et al. (2011). Mountain ecosystem response to global change. *Erdkunde* 65, 189–213. doi: 10.3112/erdkunde.2011.02.06

Lozano, J. D., and MacIsaac, H. J. (1997). Biological invasions: are they dependent on disturbance? *Environ. Rev.* 5, 131–144. doi: 10.1139/a97-007

Macdonald, I. A. W., and Jarman, M. (1985). *Invasive alien plants in the terrestrial ecosystems of Natal, South Africa* (National Scientific Programmes Unit: CSIR).

MacDougall, A. S., Gilbert, B., and Levine, J. M. (2009). Plant invasions and the niche. *J. Ecol.* 97, 609–615. doi: 10.1111/j.1365-2745.2009.01514.x

Makokha, J. (2018). Invasion of Cestrum aurantiacum Lindl. in Kenya. *J. Environ. Prot.* 9, 671–690. doi: 10.4236/jep.2018.96042

Mandal, G., and Joshi, S. P. (2015). Estimation of above-ground biomass and carbon stock of an invasive woody shrub in the subtropical deciduous forests of Doon Valley, western Himalaya, India. *J. Forestry Res.* 26, 291–305. doi: 10.1007/s11676-015-0038-8

Marais, C., and Wannenburgh, A. (2008). Restoration of water resources (natural capital) through the clearing of invasive alien plants from riparian areas in South Africa —costs and water benefits. *South Afr. J. Bot.* 74, 526–537. doi: 10.1016/j.sajb.2008.01.175

Marambe, B., Bambaradeniya, C., Kumara, D. P., and Pallewatta, N. (2001). *Human dimensions of invasive alien species in Sri Lanka. The Great Reshuffling: Human Dimensions of Invasive Alien Species* IUCN, Cambridge. 135–144.

Martin, T. G., Wintle, B. A., Rhodes, J. R., Kuhnert, P. M., Field, S. A., Low-Choy, S. J., et al. (2005). Zero tolerance ecology: improving ecological inference by modelling the source of zero observations. *Ecol. Lett.* 8, 1235–1246. doi: 10.1111/j.1461-0248.2005.00826.x

McCullach, P., and Nelder, J. A. (1989). *Generalized Linear Models. 2nd* (NY: Chapman and Hall).

METI and NASA. (2011). *ASTER Global DEM version 2.* Available at: http://gdem.ersdac.jspacesystems.or.jp (Accessed July 12th 2013).

Milbau, A., Stout, J. C., Graae, B. J., and Nijs, I. (2009). A hierarchical framework for integrating invasibility experiments incorporating different factors and spatial scales. *Biol. Invasions* 11, 941–950. doi: 10.1007/s10530-008-9306-2

Mohandass, D., Chhabra, T., Pannu, R. S., and Beng, K. C. (2016). Recruitment of saplings in active tea plantations of the Nilgiri Mountains: Implications for restoration ecology. *Trop. Ecol.* 57, 101–118.

Moktan, S., and Das, A. (2013). Diversity and distribution of invasive alien plants along the altitudinal gradient in Darjiling Himalaya, India. *Pleione* 7, 305–313.

Monro, A. K. (2012). Eight new species of Cestrum (Solanaceae) from Mesoamerica. *PhytoKeys* 8, 49–82. doi: 10.3897/phytokeys.8.2238

Najar, M. U. I., Puyravaud, J.-P., and Davidar, P. (2019). Shola tree regeneration is lower under Lantana camara L. thickets in the upper Nilgiris plateau, India. *J. Threatened Taxa* 11, 14562–14568. doi: 10.11609/jott.4918.11.12.14562-14568

Nayak, R., Verma, A. K., Manika, N., Bargali, K., Pandey, V. N., Behera, S. K., et al. (2020). Alien species in the flora of Sikkim Himalaya, India. *J. Economic Taxonomic Bot.* 4, 119–137.

Nel, J. L., Richardson, D. M., Rouget, M., Mgidi, T. N., Mdzeke, N., Le Maitre, D. C., et al. (2004). A proposed classification of invasive alien plant species in South Africa: towards prioritizing species and areas for management action: working for water. *South Afr. J. Sci.* 100, 53–64. doi: 10.10520/EJC96213

Padmanaba, M., Tomlinson, K. W., Hughes, A. C., and Corlett, R. T. (2017). Alien plant invasions of protected areas in Java, Indonesia. *Sci. Rep.* 7, 1–11. doi: 10.1038/s41598-017-09768-z

Pearse, I. S., Sofaer, H. R., Zaya, D. N., and Spyreas, G. (2019). Non-native plants have greater impacts because of differing per-capita effects and nonlinear abundance–impact curves. *Ecol. Lett.* 22, 1214–1220. doi: 10.1111/ele.13284

Pescador, D. S., de la Cruz, M., Chacón-Labella, J., Pavón-García, J., and Escudero, A. (2020). Tales from the underground: Soil heterogeneity and not only above-ground plant interactions explain fine-scale species patterns in a Mediterranean dwarf-shrubland. *J. Vegetation Sci.* 31, 497–508. doi: 10.1111/jvs.12859

Prabhakar, R. (1994). *Resource, Use, Culture And Ecological Change: A Case Study Of The Nilgiri Hills Of Southern India (PhD Thesis)* (Bangalore: Indian Institute of Science).

Prasad, M., Prabhu, A., Thakur, M. S., and Ruparel, Y. M. (2013). Phytochemical screening, anti-oxidant potential and antimicrobial activities in three species of Cestrum plants. *Int. J. Pharma Bio Sci.* 4, B673–B678.

Pyšek, P., Jarošík, V., Hulme, P. E., Pergl, J., Hejda, M., Schaffner, U., et al. (2012). A global assessment of invasive plant impacts on resident species, communities and ecosystems: the interaction of impact measures, invading species' traits and environment. *Global Change Biol.* 18, 1725–1737. doi: 10.1111/j.1365-2486.2011.02636.x

Raman, T. R. S. (2006). Effects of habitat structure and adjacent habitats on birds in tropical rainforest fragments and shaded plantations in the Western Ghats, India. In: D. L. Hawksworth and A. T. Bull (eds) *Forest Diversity and Management. Topics in Biodiversity and Conservation*, vol 2. Springer, Dordrecht. doi: 10.1007/978-1-4020-5208-8_28

Rambuda, T. D. (2001). *Pollination and breeding systems of alien invasive plants in KwaZulu-Natal in South Africa. (M.Sc. Thesis)* (Pietermaritzburg: University of Natal).

Ramesh, B. R., Ayappan, N., Grard, P., Prosperi, J., Aravajy, S., and Pascal, J.-P. (2008). *BIOTIK: Western Ghats* (Pondicherry: French Institute of Pondicherry).

Ramesh, B. R., and Pascal, J. P. (1997). *Atlas of endemics of the Western Ghats, India*. French Institute of Pondicherry, Pondicherry, India.

R Core Team (2022). *R: A language and environment for statistical computing* (Vienna, Austria: R Foundation for Statistical Computing). Available at: https://www.R-project.org/.

Ricciardi, A., Hoopes, M. F., Marchetti, M. P., and Lockwood, J. L. (2013). Progress toward understanding the ecological impacts of nonnative species. *Ecol. Monogr.* 83, 263–282. doi: 10.1890/13-0183.1

Ricciardi, A., and Atkinson, S. K. (2004). Distinctiveness magnifies the impact of biological invaders in aquatic ecosystems. *Ecology letters* 7, 781–784.

Sajeev, T., Sankaran, K., and Suresh, T. (2012). *Are alien invasive plants a threat to forests of Kerala. KFRI occasional papers*, Forest Health Programme Division Kerala Forest Research Institute, Peechi.

Salinas, N., Cosio, E. G., Silman, M., Meir, P., Nottingham, A. T., Roman-Cuesta, R. M., et al. (2021). Tropical montane forests in a changing environment. *Front. Plant Sci.* 12, 712748. doi: 10.3389/fpls.2021.712748

Saravanan, V., Santhi, R., Kumar, P., Balasubramanian, A., and Damodaran, A. (2014). Influence of forest fire on floral diversity of the degraded shola forest ecosystem. *Int. Res. J. Biol. Sci.* 3 (1), 49–56.

Shiferaw, H., Schaffner, U., Bewket, W., Alamirew, T., Zeleke, G., Teketay, D., et al. (2019). Modelling the current fractional cover of an invasive alien plant and drivers of its invasion in a dryland ecosystem. *Sci. Rep.* 9, 1576. doi: 10.1038/s41598-018-36587-7

Sofaer, H. R., Jarnevich, C. S., and Pearse, I. S. (2018). The relationship between invader abundance and impact. *Ecosphere* 9, e02415. doi: 10.1002/ecs2.2415

Sriramamurthy, R. T., Bhalla, R. S., and Sankaran, M. (2020). Fire differentially affects mortality and seedling regeneration of three woody invaders in forest–grassland mosaics of the southern Western Ghats, India. *Biol. Invasions* 22, 1623–1634. doi: 10.1007/s10530-020-02207-7

Sriramamurthy, R. T., Sankaran, M., and Bhalla, R. S. (2022). *Wildfires and aliens: differenced Normalized Burn Ratios (dNBR) indicate that woody invasive plants increase fire intensities in montane forest-grassland mosaics of the Western Ghats, India, 23 March 2022*, PREPRINT (Version 1) Available at Research Square doi: 10.21203/rs.3.rs-1382178/v1

Stockard, J. D. (1996). Restoration of Wingham brush 1980-1996. In *Eleventh Australian Weeds Conference Proceedings* (ed. R. C. H. Shepherd). Weed Science Society of Victoria Inc., Melbourne, pp. 432–436.

Strayer, D. L. (2020). Non-native species have multiple abundance–impact curves. *Ecol. Evol.* 10, 6833–6843. doi: 10.1002/ece3.6364

Sukumar, R., Suresh, H. S., and Ramesh, R. (1995). Climate change and its impact on tropical montane ecosystems in southern India. *Journal of Biogeography* 22:533–536.

Symon, D. (1981). The solanaceous genera, Browalia, Capsicum, Cestrum, Cyphomandra, Hyoscyamus, Lycopersicon, Nierembergia, Physalis, Petunia, Salpichroa and Withania, naturalised in Australia. *J. Adelaide Bot. Garden* 3, 133–166.

Thomas, S. M., and Palmer, M. W. (2007). The montane grasslands of the Western Ghats, India: Community ecology and conservation. *Community Ecol.* 8, 67–73. doi: 10.1556/ComEc.8.2007.1.9

USDA (2013). *Weed Risk Assessment for Cestrum laevigatum Schltdl. (Solanaceae) – Inkberry* (NC, USA: Raleigh).

Vilà, M., and Ibáñez, I. (2011). Plant invasions in the landscape. *Landscape Ecol.* 26, 461–472. doi: 10.1007/s10980-011-9585-3

Von Lengerke, H. J. (1977). *The Nilgiris: weather and climate of a mountain area in south India* (Wiesbaden, Germany: Steiner).

Wijesundara, S. (2012). *Present Status of Montane Forests in Sri Lanka. The National Red List 2012 of Sri Lanka; Conservation Status of the Fauna and Flora* (Colombo, Sri Lanka: Ministry of Environment).

Witt, A., Beale, T., and Van Wilgen, B. W. (2018). An assessment of the distribution and potential ecological impacts of invasive alien plant species in eastern Africa. *Trans. R. Soc. South Afr.* 73, 217–236. doi: 10.1080/0035919X.2018.1529003

Witt, A., and Luke, Q. (2017). *Guide to the Naturalized and Invasive Plants of Eastern Africa* (UK: CABI; Wallingford).

Frontiers in
Ecology and Evolution

Ecological and evolutionary research into our natural and anthropogenic world

This multidisciplinary journal covers the spectrum of ecological and evolutionary inquiry. It provides insights into our natural and anthropogenic world, and how it can best be managed.

Discover the latest Research Topics

See more →

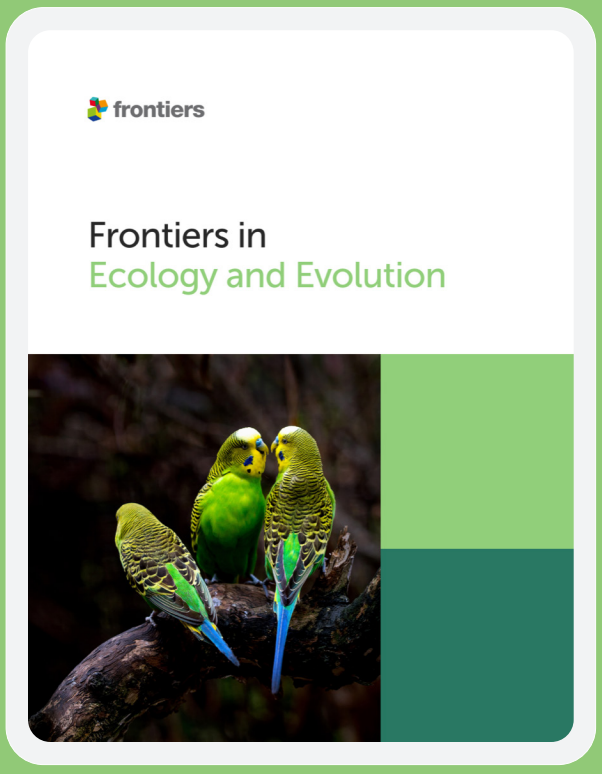

Frontiers

Avenue du Tribunal-Fédéral 34
1005 Lausanne, Switzerland
frontiersin.org

Contact us

+41 (0)21 510 17 00
frontiersin.org/about/contact